N. RUDENKO

MATERIALS HANDLING EQUIPMENT

MATERIALS HANDLING EQUIPMENT

N. RUDENKO

MATERIALS HANDLING EQUIPMENT

PEACE PUBLISHERS
Moscow

TRANSLATED FROM THE RUSSIAN BY A. TROITSKY

EDITED BY NICHOLAS WEINSTEIN

Н. Ф. РУДЕНКО

ГРУЗОПОДЪЕМНЫЕ МАШИНЫ

(На английском языке)

CONTENTS

Introduction 6

PART ONE

GENERAL INFORMATION ON MATERIALS HANDLING EQUIPMENT

Chapter I. Intraplant Transporting Facilities and Handling Equipment 7
1. Types of Intraplant Transporting Facilities 7
2. Principal Groups of Materials Handling Equipment 8
3. Choice of Materials Handling Equipment 9

Chapter II. Types of Materials Handling Equipment 12
1. Hoisting Equipment 12
2. General Characteristics of Hoisting Machines 15
3. Surface and Overhead Equipment 17
4. General Characteristics of Surface and Overhead Transporting Facilities 19
5. Application of Materials Handling Equipment 19

PART TWO

COMPONENTS AND THEORY OF HOISTING EQUIPMENT

Chapter III. Flexible Hoisting Appliances (Chains and Ropes) 22
1. Welded Load Chains 22
2. Roller Chains 23
3. Hemp Ropes 25
4. Steel Wire Ropes 26
5. Calculating the Endurance (Fatigue Strength) of Steel Wire Ropes by Professor Zhitkov's Method 37
6. Fastening of Chains and Ropes 43
7. Load Suspension Appliances 46

Chapter IV. Pulleys, Pulley Systems, Sprockets and Drums 51
1. Pulleys 51
2. Pulley Systems 53
3. Design of Chain and Rope Sheaves and Sprockets 58
4. Chain and Rope Drums 64

Chapter V. Load Handling Attachments 74
1. General 74
2. Forged Standard Hooks 74
3. Forged Ramshorn Hooks 79
4. Solid Triangular Eye Hooks 81
5. Hinged Triangular Hooks 82
6. Appliances for Suspending Hooks 83
7. Crane Grabs for Unit and Piece Loads 94
8. Electric Lifting Magnets 99
9. Grabbing Attachments for Loose Materials 100
10. Methods for Designing Grab Buckets 109
11. Crane Attachments for Handling Liquid Materials 113

Chapter VI. Arresting Gear and Brakes 114
1. Arresting Gear 114
2. Shoe Brakes 121
3. Elements of Shoe Brakes 124
4. Electromagnetic Shoe Brakes 127
5. Thrustor-Operated Shoe Brakes 127

6. Controlled Brakes 139
7. Approximate Static Calculation Method for Shoe Brake Design 143
8. Thermal Calculation of Shoe Brakes 150
9. Precise Methods of Shoe Brake Design 156
10. Band Brakes 165
11. Cone Brakes 178
12. Disk Brakes 182
13. Safety Handles 182
14. Centrifugal Brakes 186
15. Brakes Applied by the Lifted Load 187

Chapter VII. Drives of Hoisting Gear 195
1. Hand Drive and Operating Levers 195
2. Power Drives 198

Chapter VIII. Hoisting Gear 202
1. Hand Power Hoisting Mechanisms 202
2. Hoisting Mechanisms with an Individual Electric Drive 203
3. Hoisting Mechanisms Operating from a Common Motor Drive for Several Mechanisms 204

Chapter IX. Travelling Gear 205
1. Rail Travelling Mechanisms 205
2. Trackless Travelling Mechanisms 226

Chapter X. Slewing, Jib and Luffing Gear 229
1. Slewing Mechanisms 229
2. Jib and Luffing Mechanisms 243

Chapter XI. Operation of Hoisting Gear during Transient Motion 248
1. Dynamic Load 248
2. Selecting the Motor Rating and Determining Braking Torque for Hoisting Mechanisms 254
3. Drive Efficiency 255
4. Selecting the Motor Rating and Determining Braking Torque for Travelling Mechanisms 255
5. Selecting the Motor Rating and Determining Braking Torque for Slewing Mechanisms 256
6. Selecting the Motor Rating and Determining Braking Torque for Jib and Luffing Mechanisms 257

Chapter XII. Crane Frame Structures (Trusses) 260
1. Superstructures of Rotary Cranes with a Fixed Radius 260
2. Superstructures of Rotary Jib Cranes and Rotary Luffing-Boom Cranes 264
3. Superstructures of Cantilever Cranes 267
4. Structures of Overhead Travelling Cranes 270

Chapter XIII. Stability of Cranes 292
1. Stability of Stationary Rotary Cranes with a Fixed Pillar Secured in the Foundation 292
2. Stability of Stationary Rotary Cranes with a Turntable 294
3. Stability of Travelling Rotary Cranes 295
4. Stability of Semigantries 298

PART THREE

ELEVATORS

1. Cage Elevators 299
2. Portable Air-Operated Hoists 311
3. Stackers 311

Appendix 317

INTRODUCTION

Materials handling equipment is an integral part of mechanical equipment in every modern industrial enterprise.

The numerous designs of materials handling equipment are the result of a great variety of the kinds and properties of loads being moved and the abundance of transporting operations without which modern production is unthinkable.

The entire production process in every enterprise essentially depends on a rational choice of the types of materials handling equipment, correct determination of its main parameters and efficient operation. Every mechanical engineer must therefore have a thorough knowledge of the design and operational features of this equipment and the methods of its design and practical application. This textbook is intended for students majoring in the field of general engineering.

The book comprises three parts.

Part One gives general information on materials handling equipment: its role in production and its application in modern engineering practice, and enumerates the main types of materials handling equipment.

Part Two is devoted to the description of the parts and units of hoisting machines: chains, ropes, pulleys, sprockets, drums, grabbing and braking gear, drives, hoisting, travelling, slewing, jib and luffing mechanisms of cranes, and their stability.

General-purpose cranes employed in mechanical engineering include various types of stationary rotary cranes, cantilever and jib cranes, both fixed path and trackless, as well as locomotive, crawler-mounted and bridge-type cranes.

Since these types of machines are also the subjects for practical designing work of the students, the theory and design models are given in their application to general-purpose machines. Special-type cranes are not considered in this textbook and are only mentioned briefly in respective parts of the text.

The last, third, part gives a brief description of elevators (lifts).

PART ONE

GENERAL INFORMATION ON MATERIALS HANDLING EQUIPMENT

CHAPTER I

INTRAPLANT TRANSPORTING FACILITIES AND HANDLING EQUIPMENT

1. TYPES OF INTRAPLANT TRANSPORTING FACILITIES

Materials handling equipment is employed for moving loads in premises or areas, departments, factories and plants, at construction sites, points of storage and reloading, etc.

As distinct from the so-called long-distance transport (railway, automobile, water and air) shipping loads over considerable distances, materials handling equipment moves loads over comparatively short distances. In practice these distances are usually confined to tens or hundreds of metres and reach thousands of metres only occasionally to ensure a constant load transfer between two or several points connected by common production activities.

Handling and loading operations in each enterprise depend on the available external and intraplant transporting facilities. External transporting facilities supply the enterprise with raw materials, semifinished items, fuel, auxiliary materials, etc., and ship ready products and wastes from the enterprise.

The intraplant transporting facilities distribute the loads, which come in, throughout the enterprise, move materials between processing units directly engaged in production and bring finished products and waste to loading points to be loaded and shipped from the enterprise by external transporting facilities.

Transporting processes of this kind are not confined only to shifting loads from place to place but also include *loading and unloading operations*, i.e., delivery of loads to load-carrying machines, unloading the machines at prearranged places, stowing the loads in warehouses and moving them to processing equipment.

For important loading and unloading operations some handling mechanisms are provided with special grabbing devices operated by auxiliary machines and appliances or manually.

The transporting facilities inside the plant are in turn subdivided into interdepartment and intradepartment facilities. At construction sites the transporting facilities can be classified as external, intra-area and intrasection facilities.

Interdepartment transporting facilities move loads between departments, for example, at a mechanical engineering plant, between blank manufacturing, machining and auxiliary departments, as well as between departments and warehouses, loading and unloading points, etc. A diagram illustrating the layout of interdepartment transporting facilities at a mechanical engineering plant is shown in Fig. 1.

Intradepartment transporting facilities move loads between sections, stores, machines, etc., within the limits of one department.

Interoperational transporting facilities which move loads from one processing unit to another and are closely connected with manufacturing operations performed in the department or enterprise as a whole constitute a special kind of transporting facility operating inside and sometimes between departments. These facilities play an especially vital role in mass flow production where they serve as a link between individual processing machines and units and help to time the work of the department or enterprise according to a single schedule and pace.

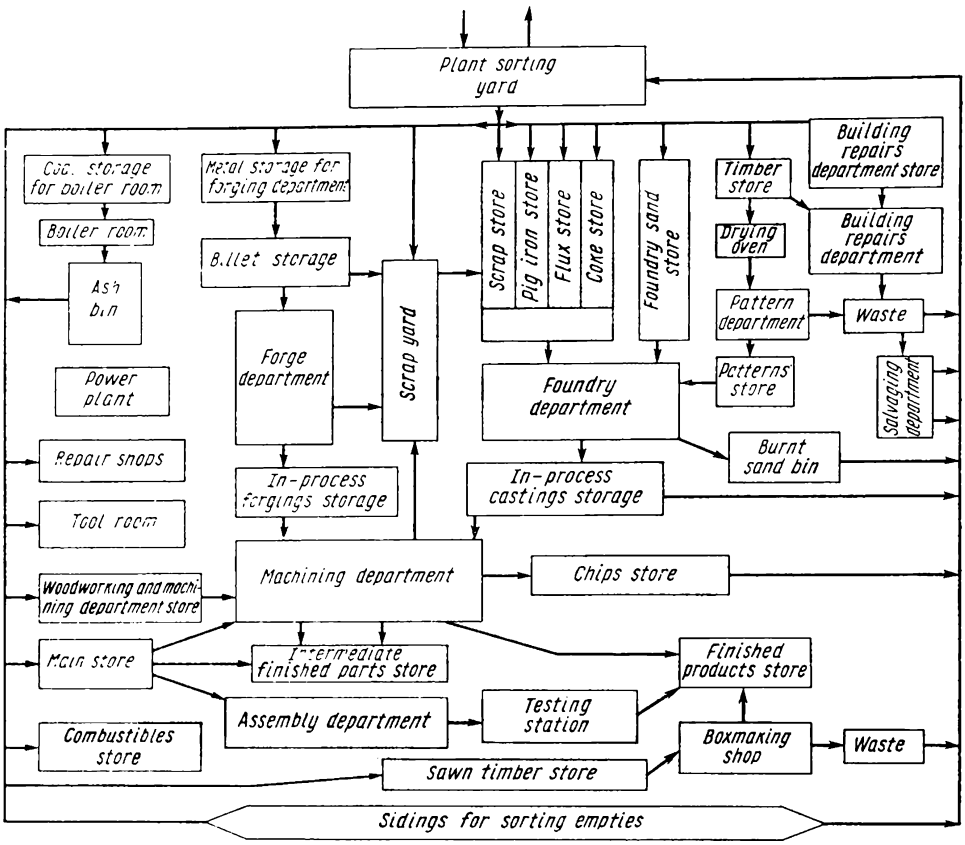

Fig. 1. Layout of interdepartment transporting facilities in a mechanical engineering plant

2. PRINCIPAL GROUPS OF MATERIALS HANDLING EQUIPMENT

The main groups of materials handling equipment classified by their design features are represented in Fig. 2.

Each of these groups of equipment can be defined briefly as follows:

Hoisting equipment is a group of machines with lifting gear intended for moving loads mainly in batches.

Conveying equipment is a group of machines which may have no lifting gear and which move loads in a continuous flow.

Surface and overhead equipment is a group of machines which also may not be provided with lifting gear and which usually handle loads in batches.

Each of these groups of machines is distinguished by a number of special features and by their specific spheres of application. The differences in the design of these groups also depend on the nature of the load they handle, the direction of working movements and the nature of the handling processes.

Loads can be classified as bulk or unit loads.

Materials handled in bulk are composed of a large number of homogeneous particles or lumps, for example: coal, ore, cement, sand, earth, stone, clay, etc.

Unit loads may differ widely in form and weight.

Hoisting machines are intended mainly for unit loads—various parts of machines and whole machines, elements of metal structures, hoppers and ladles, girders, building blocks and materials, etc. Conveyors can be used to handle either only bulk or only unit loads while surface and overhead facilities—both bulk and unit loads.

As a rule, the working movement in hoisting machines is intended either for raising or lowering the load. Some hoisting machines can also travel horizontally,

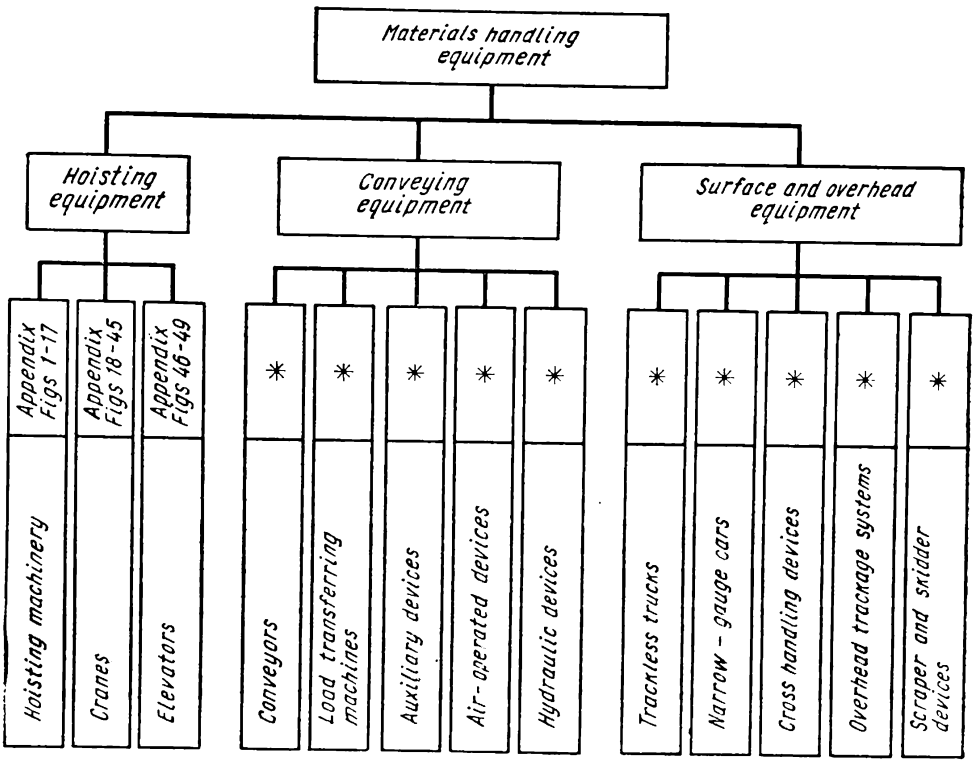

Fig. 2. Main types of materials handling equipment:

Notes: 1. Numbers of drawings indicated for separate groups of machines can be found in the Appendix (at the end of the book)
2. Groups of machines marked by asterisks (*) are not considered in this textbook

turn round, move radially, etc. Most of the transporting facilities shift loads in a horizontal direction although many can also move them at various angles to the horizon or in a vertical direction.

Most hoisting mechanisms are designed to perform controlled individual movements. This mode of performance is typical, for example, of many cranes which lift the load, slew it, hold it at rest, if required, and carry it to its destination.

Many transporting facilities —conveyors, trucks and telphers—move along a fixed path and perform many identical working operations.

Identical working operations and uniform loads that they carry enable the transporting facilities to be highly automatised not only for moving but also for loading and unloading operations. This cannot be achieved in many hoisting mechanisms which require hand servicing not only for controlling the working movements but very often also for loading and unloading, as, for instance, when differently shaped loads are suspended on or removed from a hook.

Such are the characteristic features of the main groups of materials handling equipment. However, in certain types of machines these features are not clearly defined which makes it impossible to classify such machines into any definite groups.

3. CHOICE OF MATERIALS HANDLING EQUIPMENT

Materials handling machines are manufactured in a great variety of designs. For this reason the same operation can be frequently performed by various methods and devices.

The proper choice of a device requires not only a special knowledge of the design and operational characteristics of the mechanism but also a thorough understanding of the organisation of production at the enterprise.

A transporting facility should move loads to their destination in the scheduled time, i.e., loads should be delivered to the department or enterprise in the required amounts. The materials handling equipment should be mechanised to the fullest possible extent so as to employ only a few workers for control, maintenance and auxiliary jobs. At the same time these devices should not damage the loads being moved, or encumber in any way the premises or hamper the production processes. They should be safe in operation and economical both with respect to capital outlay and operational costs.

The following principal technical factors can be pointed out for guidance in the choice of the types of devices which can be expediently employed to mechanise any handling process.

Kind and properties of loads to be handled: for unit loads—their form, weight, convenient bearing surface or parts by which they can be suspended, brittleness, temperature, etc.; for bulk loads—lump size, tendency to cake, volume weight, friability and the amount of crumbling liable to occur during shipment, temperature, chemical properties, etc. These characteristics of loads can essentially narrow down the range of devices which can be applied in each definite case since the different devices are not adapted equally to the various properties of loads.

Required hourly capacity of the unit. A practically unlimited hourly load moving capacity can be easily obtained with certain types of devices as, for instance, with some continuous-action conveyors. On the other hand, there are devices, such as power-driven trucks or overhead travelling cranes following a definite cycle of movements with a return idle run, which can operate efficiently only if they possess an adequately high lifting capacity and speed at strenuous duty.

Direction and length of travel. Various types of devices can carry loads in a horizontal or vertical direction or at an angle to the horizon. Thus, a vertical movement or a movement close to the vertical requires a hoist, crane, bucket or tray elevator; horizontal movement is provided by self-propelled or hand trucks, fixed path facilities, various types of conveyors, etc. Some devices can easily negotiate track curves while others move only rectilinearly, in one direction. The length of path, the location of the load supplying points and the ramification of the load delivery stations are also very important for the correct choice of a transporting facility.

Methods of stacking loads at the initial, final and intermediate points, loading onto vehicles and unloading at their destination differ considerably because some handling machines can be loaded mechanically while others require special auxiliary fixtures or manual power. Thus, for example, bulk loads can be stored either in lot, in a pile, from which they must be scooped up in some way or another, or in a bunker from which they flow by gravity onto the transporting facility.

Unit loads can be stowed directly on the ground or on pallets, stands, racks, trays, etc., from which they are delivered to and removed from the materials handling devices by different methods.

Characteristics of production processes involved in moving loads. This most important factor essentially influences the choice of the type of transporting facility. As a rule, the movements of materials handling equipment are closely linked with and depend on the manufacturing process; sometimes these movements may even be directly involved in the performance of certain processing operations. Such are, for example, special cranes employed in foundry, forging and welding departments, assembly and foundry conveyors, processing conveyors in machining, painting and other departments.

Specific local conditions include the size and shape of the area, type and design of the building, ground relief, possible arrangement of the processing units, dust or humidity conditions in the premises, presence of vapours or gases, temperature, etc.

The choice of devices is also influenced by the considerations of a further expansion of the enterprise, the period it will be in existence (temporary or permanent), the kind of energy available, and problems of sanitation, safety and operational convenience.

After selecting from the great variety of materials handling devices, on the basis of technical factors, those which can be used in definite conditions to mechanise the handling processes, they are compared from the engineering and economic points of vien.

In economic evaluation of various types of devices both the total capital outlay and the operational costs should be taken into consideration.

The capital outlay includes the cost of equipment, the cost of its erection and transporting and construction costs involved in its installation and operation. The difference in the cost of buildings and structures which can be serviced by alternative transporting facilities should also be considered when comparing capital outlay.

Operational costs include:

1) wages and salaries of the personnel plus additions for social services;
2) cost of electric power;
3) cost of lubricating, wiping, rigging and other materials;
4) cost of repairs and maintenance.

Moreover, account should also be taken of losses due to depreciation of the load during handling. Here also belong the expenditures on the maintenance of the materials handling installation, annual deductions for the amortisation of mechanical equipment and the funds assigned for its general overhauls.

In each case the materials handling equipment chosen should satisfy all the requirements of the production processes and ensure at the same time a high degree of mechanisation and the most favourable labour conditions; it should cut the handling cost per unit of load and reduce the term within which the capital investments will pay.

CHAPTER II

TYPES OF MATERIALS HANDLING EQUIPMENT

1. HOISTING EQUIPMENT

The great variety of existing types of hoisting equipment makes their accurate classification extremely difficult. This task is still further complicated by the fact that this classification may be based on various characteristics as, for example, design, purpose, type of movement, etc.

When machines are classified according to the type of movement (kinematic characteristic) the load is assumed to be concentrated at its centre of gravity and the group of the machine is determined by the path made by the load travelling in a horizontal plane.

When machines are classified according to their purpose they are often regarded in their application to specific operating conditions; cranes, for example, are accordingly subdivided into metallurgical, construction, harbour, etc.

The main types of hoisting equipment grouped together according to their design features are tabulated in Fig. 3 and are shown schematically in the Appendix.

These groups of hoisting equipment have the following main distinctive features.

Hoisting machines (Appendix, dwgs 1-17) are a group of periodic-action devices designed as self-lifting gear, or for hoisting and moving loads, or else as independent mechanisms of cranes or elevators.

Cranes (Appendix, dwgs 18-45) are a combination of separate hoisting mechanisms with a frame for lifting or both for lifting and moving loads which can be freely suspended on or secured to them.

Elevators (Appendix, dwgs 46-49) are a group of periodic-action machines intended for raising loads in guideways.

Hoisting equipment can be of a stationary, portable or travelling type; most cranes and elevators are either stationary or travelling.

Of the hoisting equipment represented in Fig. 3 the group of cranes is the most extensive. The main types of cranes are further classified in Fig. 4.

The group of stationary rotary cranes (Appendix, dwgs 18-25) mainly includes fixed cranes with booms and fixed jib cranes swivelling about a vertical axis.

The group of cranes travelling on runway rails (Appendix, dwgs 26-30) comprises primarily cantilever and monorail cranes (both rotary and nonrotary) which move rectilinearly along special tracks.

The group of trackless cranes (Appendix, dwgs 31-35) is made up mainly of pillar cranes mounted on trucks, automobiles or tractors and intended for travelling on dirt, gravel and asphalt roads.

The group of locomotive or crawler-mounted cranes (Appendix, dwgs 36-38) includes more powerful pillar cranes moving on railway tracks, dirt roads and in warehouse areas.

Hoisting equipment

Hoisting machinery	Jacks	Dwgs 1-5
	Pulleys	Dwgs 6-7
	Portable hand hoists	Dwgs 8-9
	Hand trolley hoists	Dwg 10
	Portable power-operated hoists	Dwg 11
	Travelling power-operated hoists	Dwgs 12-13
	Special-purpose monorail telphers	Dwg 14
	Winches	Dwgs 15-16
Cranes	Crane trolleys	Dwg 17
	Stationary rotary cranes	Dwgs 18-25
	Cranes travelling on guide rails	Dwgs 26-30
	Trackless cranes	Dwgs 31-35
	Locomotive and crawler-mounted cranes	Dwgs 36-38
	Bridge-type cranes	Dwgs 39-45
	Cable cranes	*
	Floating cranes	*
Elevators	Cage elevators	Dwg 46
	Portable air-operated hoists	Dwg 47
	Manually propelled stackers	Dwg 48
	Vertical skip elevators	Dwg 49
	Mast-type elevators	*
	Funiculars	*

Fig. 3. Main types of hoisting equipment

Note: Types of machines marked by asterisks (*) have a limited application in the engineering industries and are therefore not considered in this textbook

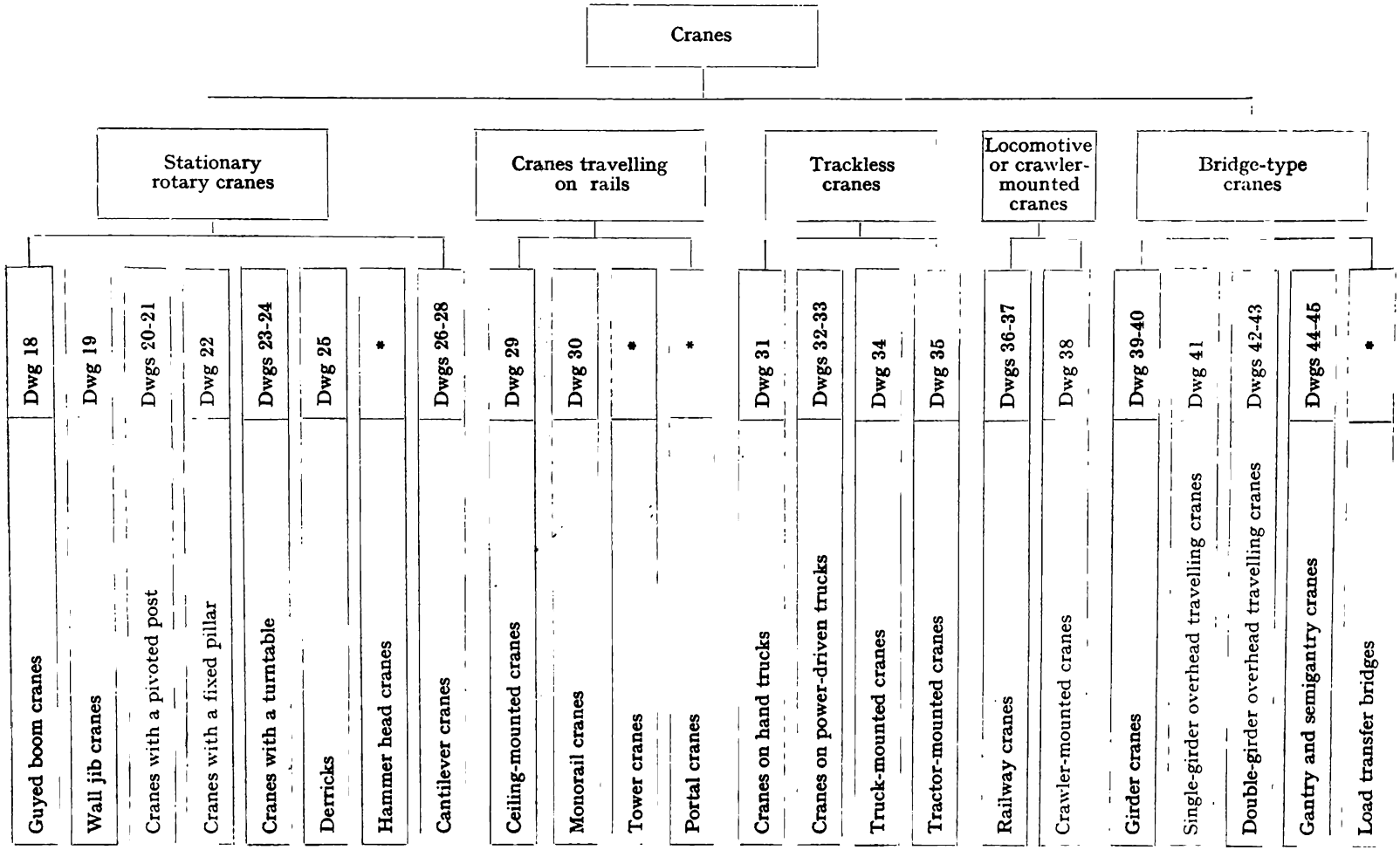

Fig. 4. Main types of cranes

Note: Types of machines marked by asterisks (*) have a limited application in the engineering industries and are therefore not considered in this textbook

The group of bridge-type cranes (Appendix, dwgs 39-45) comprises travelling cranes with a trussed bridge and moving on rail tracks laid on the building walls or on the ground. In the latter case the bridge is provided with high supporting legs which can be arranged on both sides of the bridge (gantries and load transfer bridges) or on one side (semigantries).

The group of hoisting equipment (Figs 3 and 4) also includes special types of machines intended for definite, sometimes very specific, duties. Since their industrial application is extremely limited they will not be considered in this textbook.

2. GENERAL CHARACTERISTICS OF HOISTING MACHINES

The main technical parameters of the hoisting machines are: lifting capacity, dead weight of the machine, speed of various movements, lifting height and geometrical dimensions of the machine (span, outreach, etc.).

All hoisting machines belong to the class of periodic-action devices and their hourly capacity can be expressed by the following formula:

$$Q_{hr} = nQ \text{ t/hr} \tag{1}$$

where n—number of machine cycles per hr;

Q—weight of live load in tons.

When handling unit loads, Q is understood to mean the weight of one piece load in tons, and in handling bulk materials

$$Q = V \psi \gamma \tag{2}$$

where V—capacity of the bucket, grab, etc., in cu m;

ψ—filling factor;

γ—volume weight, in t/m^3.

The total load-lifting capacity of the machine will be

$$Q_{\Sigma} = (Q + G) \text{ tons} \tag{3}$$

where Q—weight of live load, in tons;

G—weight of bucket or grab, in tons.

The number of cycles per hour is

$$n = \frac{3{,}600}{\Sigma t_1} \tag{4}$$

where Σt_1—the total time in seconds expended on individual operations of one cycle which depends on the speed of motion during the various operations, travel and lifting height, the time lost in acceleration and retardation, the degree to which the operations have been combined and the time lost in grabbing and discharging the load.

The hourly capacity of hoisting machines is a constant value only for those machines which operate regularly under full load. For example, when coal is handled by load transfer bridges it can reach 1,500 t/hr and more.

The required number of department hoisting devices is usually estimated from their mean annual productivity assuming average loads, average travel and average speeds of motion; the practical hourly capacity of these devices is a variable value which depends on the factors indicated above.

All types of cranes and hoisting machines can be broken down into four groups in accordance with operating conditions and depending on the combination of the following factors:

1) load on the machine;
2) its annual and daily utilisation;
3) relative duty factor (period during which the mechanism is switched on, DF%);
4) ambient temperature.

There are four operating conditions: light (L), medium (M), heavy (H), and very heavy (VH) duty. Tables 1 and 2 characterise these duties.

Table 1

Characteristics of Duties

Duty	Mean utilisation of mechanism				
	By load K_{load}	By time		Duty factor, DF%	Ambient temperature, °C
		K_{year}	K_{day}		
Light (L)	0.5	0.25	0.33 (one shift)	15	25
Medium (M)	0.5	0.5	0.67 (two shifts)	25	25
Heavy (H)	0.75	0.75	0.67 (two shifts)	40	25
Very heavy (VH)	1.0	1.0	1.0 (three shifts)	40	45

The following notation is used in Tables 1 and 2.

$K_{load} = \frac{Q_{m.load}}{K_{n.load}}$ —mean lifting capacity utilisation.

Here

$Q_{m.load}$ — mean value of load;

$Q_{n.load}$ — nominal (rated) load;

$K_{year} = \frac{h \text{ days}}{365 \text{ days}}$ — mean annual utilisation of the machine;

$K_{day} = \frac{h \text{ hours}}{24 \text{ hours}}$ — mean daily utilisation of the machine;

$DF = \frac{t_{op}}{t_{op} + t_{idle}} 100\%$—relative duty factor, i.e., mean utilisation of the mechanism during one working cycle;

t_{op} — operation time of the mechanism;

t_{idle} — time of idle periods.

These values are determined from mean operational or design data.

The following number of switching-on operations for an electric drive per hour has been accepted for the various duties:

Nominal duty	Light	Medium	Heavy	Very heavy
Number of switching-on operations per hour	60	120	240	300-720

The different mechanisms of a crane may operate at various duties.

Table 2

Permissible Utilisation of Crane Mechanisms at Various Duties

Duty	Mean safe utilisation: By load weight K_{load}	By time: K_{year}	By time: K_{day}	Relative duty factor DF%	Ambient temperature, °C	Type of crane mechanisms and their purpose (typical cases)
	Irregular rare operation 0.75-1.0					Hoisting and travelling mechanisms of maintenance cranes, cranes in motor rooms; travelling mechanisms of load transfer bridges; travelling mechanisms of cable crane towers; electric hoists intended for the repair of machine tools and other department equipment. Rarely operated winches.
L	0.5 0.25 0.1	0.25 0.5 1.0	0.33 0.67 1.0	15		
	1.0	1.0	0.67	15		Hoisting and travelling mechanisms of cranes in machining and assembly departments of medium-lot production plants and cranes employed in mechanical shops. Slewing mechanisms of building cranes. Electric hoists in engineering plants. Slewing and travelling mechanisms of ordinary harbour cranes. Mechanisms of assembly cranes at construction sites. Truck travelling and slewing mechanisms of shipbuilding cranes.
	0.75	0.5	0.33	25		
M	0.5	0.5	0.67	—	25	
	0.25	1.0	1.0	40		
	0.1	1.0	1.0	60		
	1.0	1.0	0.67	25		Mechanisms of processing cranes in machining and foundry departments and warehouses of large-lot production plants. Hoisting and travelling mechanisms of cable crane trucks. Hoisting mechanisms of building cranes. Electric hoists in metallurgical plants. Hoisting and travelling mechanisms of shipbuilding cranes. Mechanisms of magnetic cranes in bedding plants.
	1.0	1.0	0.33	40		
H	0.75	0.75	0.67	40		
	0.5	1.0	1.0	40		
	0.1-0.25	1.0	1.0	60		
	1.0	1.0	1.0	40	45	
	0.75	1.0	1.0	60	25	Mechanisms of processing cranes employed in the metallurgical industry. Iron-ore and coal handlers. Mechanisms of special clamshell and magnetic cranes and warehouse cranes in metallurgical plants.
VH	0.5	1.0	1.0	60		
	0.25	1.0	1.0	60	45	
	0.1	1.0	1.0	60		

3. SURFACE AND OVERHEAD EQUIPMENT

The main types of surface and overhead equipment grouped according to their design features are tabulated in Fig. 5.

The designs listed in Fig. 5 have the following distinctive features.

Trackless trucks are surface wide-area transporting facilities which move loads on the ground.

Narrow-gauge cars are surface transporting facilities which move loads along narrow-gauge railway tracks.

Cross handling devices are surface transporting facilities which shift railway cars within the territory of a single enterprise.

Overhead trackage systems are structures carrying tracks or cable along which loaded trucks travel.

Fig. 5. Main types of surface and overhead equipment

4. GENERAL CHARACTERISTICS OF SURFACE AND OVERHEAD TRANSPORTING FACILITIES

The following are the main technical parameters of surface and overhead mechanisms: hourly capacity, useful load carrying capacity and speed.

The hourly capacity of these machines can be determined from the following general formula:

$$Q_{hr} = \frac{Qn}{1{,}000} \tag{5}$$

where Q—useful lifting capacity of one handling unit, in kg;

n—number of machine cycles per hour (when the line is serviced by one handling unit) or the number of the handling units which pass through the loading point during one hour (when the line is serviced by several units).

5. APPLICATION OF MATERIALS HANDLING EQUIPMENT

Various types and combinations of materials handling equipment are extensively used today in all branches of industry.

At each enterprise a rational organisation of intraplant transporting facilities is just as essential for successful operation as rational organisation of the production processes. Transporting facilities play an extremely important role in mass production where they are organically connected with the production cycle. Intraplant transporting facilities in the metallurgical and engineering industries have a very complex structure.

The role of intraplant transporting facilities is not confined to careful and inexpensive handling of materials, semifinished goods and finished products. The plant transporting facilities, especially those operating between and within departments, should link together and unite the production processes of the individual departments of the plant in a common well-coordinated rhythm and operate quickly and efficiently.

In modern mechanised enterprises the design of many machines depends on the methods by which the materials or semifinished goods are supplied to and moved away from the machine. It can be asserted that the mechanisation of the processes involved in moving loads was the principal stimulus for the outstanding progress attained today in many enterprises. A transporting system organised on rational lines essentially improves the quality of a product, increases labour productivity in the departments, helps to economise labour and improves labour conditions.

The transporting facilities are selected so as to suit the flow of materials which represents the general system of movement of materials, semifinished articles and products in the department or plant. This system reflects the dynamics of the production process and is usually represented graphically on the department or plant layout showing the equipment arrangement. The weight and direction of load movement are represented to scale by lines or stripes of different thickness.

PART TWO

COMPONENTS AND THEORY OF HOISTING EQUIPMENT

The component parts and units of hoisting equipment include:
1) flexible hoisting appliances (chains and ropes);
2) pulleys, pulley systems, sprockets and drums;
3) load handling attachments;
4) stopping and braking devices;
5) drives (motors);
6) transmissions;
7) transmission components (axles and shafts, bearings and step bearings, clutches, etc.);

Materials for Parts

Part	Grade of metal	State of metal	Tensile strength kg/mm²
Travelling wheels of bridges and trolleys, toothed gears and rims of conventional crane transmissions, couplings, brake sheaves, pulleys and drums of heavy metallurgical cranes.	Steel 45Л	—	55
Travelling wheels of bridges and trolleys of heavy and high-speed cranes.	Steel 55Л	Surface hardening of rolling circle	60
Forged driving pinions of gear transmissions.	Steel 6 Steel 45	Structural improvement after rolling	60-7 57
Axles of travelling wheels, pulleys, drums, transmission shafts, shafts of drives.	Steel 5 Steel 45	As rolled —	50-6 60-7
Drums, reduction gear housings, bearings, pulleys and brake drums, couplings, brake shoes, worm wheel hubs of conventional cranes.	Cast iron 15-32 Cast iron 12-28	—	15
Braking weights and counterweights.	Cast iron 00	—	—
Hooks, hook nuts and hook shackles.	Steel 3	As annealed	38-4
Keys and worm screws.	Steel 15	As annealed	40
Tyres of travelling wheels.	Steel 6 Steel 65Г	As rolled Normalised	60-7 75
Bolts and shafts of brakes, brake parts: eyes, lugs, braces, levers, pins, clamps, shackles, cross bars, clutches, installing elements of welded drums, etc.	Steel 3	As rolled	38-4
Yokes, guards, washers and other unimportant parts.	Steel 0	Ditto	32-4
Bushings of reduction gear boxes, bearings of travelling wheels, pulleys and drums.	Silicon-lead brass, grade ЛКС 80-3-3 or ЛМПС 58-2-2; antifriction cast iron СЦЧ-1	— —	25-3 18

Note: Bhn and ultimate strength have the following ratio: a) for steel with Bnh >

8) rails and travelling wheels;
9) machine structures (crane frames);
10) control devices.

In view of the great danger arising from machine breakage (a breakdown of some kind may cause the machine to drop the load being lifted resulting not only in damage to the load but also in human casualties), all the mechanisms and their metal structures should be manufactured from high-quality materials which strictly conform to manufacturing specifications and are selected on the basis of certificates provided by metal suppliers.

The safe stresses recommended by modern engineering practice for various materials will be indicated below in the sections dealing with the methods of designing individual parts of hoisting machines. The technical characteristics of the materials employed are specified by respective State Standards. The main parts of crane mechanisms are manufactured from materials whose quality should not be inferior to the values indicated in Table 3.

of Crane Mechanisms *Table 3*

Mechanical properties				
ıld point, kg/mm²	Fatigue limit, kg/mm²	Relative elongation, %	Brinell hardness number	Notes
28	25	16	170	
30	27	12	180	Hardness of rolling circle and flanges
30	26	12	150-200	Bhn = 280 to 320
32	25	17	210-250	
27	20	—	130-170	
30	26	12	150-200	
—	—	—	163-229	Bending strength 32 and 28 kg/mm²
—	—	—	—	Not tested
22	17	22	95-110	
23	18	23	110-135	
30	26	12	150-200	
40	32	8	240	
22	17	21	110-132	
19	16	18	—	
10-14	6-8	10-15	80-100	Permanent- or sand-mould casting
—	—		170-229	Bending strength 36 kg/mm²

$75\delta_b \approx 0.345$ Bhn; (b) for steel with Bhn $< 175\delta_b = 0.362$ Bhn.

CHAPTER III

FLEXIBLE HOISTING APPLIANCES (CHAINS AND ROPES)

1. WELDED LOAD CHAINS

Welded chains are formed from oval steel links in the sequence shown in Fig. 6.

The main dimensions of the links are (Fig. 7): pitch (t) equal to the inside length of the link, outside width (B) and diameter (d) of the chain bar. Depending on the ratio between the pitch and the diameter of the chain bar, welded chains are classified as short-link ($t \leq 3d$) and long-link ($t > 3d$) chains.

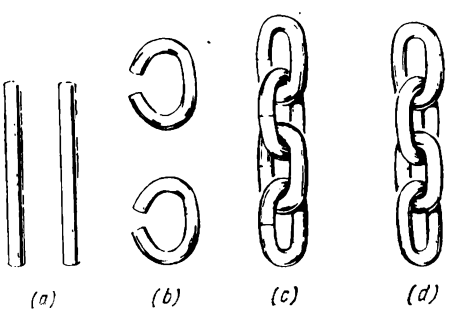

Fig. 6. Stages in the manufacture of welded chains:
(a) blanks of cut steel bar, *(b)* prebent blanks, *(c)* chain assembled prior to welding, *(d)* chain with welded links

Manufacturing accuracy subdivides welded chains into pitched or calibrated chains with permissible deviations from the nominal pitch size within $\pm 0.03d$ and from the outside width within $\pm 0.05d$ and uncalibrated chains

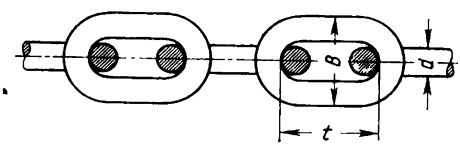

Fig. 7. Main dimensions of a load chain link

with permissible deviations within $\pm 0.1d$ of the nominal size in pitch and outside width.

Welded chains are manufactured from steel 2 and 3.* Links for welded chains are formed by a number of methods. The most widespread of these are hammer (forge) and electric resistance welding. In forge welding a single weld is made in the link. When the electric resistance method is used the link is made from two butt-welded half-links. The welds are made on the straight sides of the link. The resistance welding method produces more accurate chains with increased strength.

As a rule, chains are manufactured in lengths of the required size. These lengths of chain are joined by means of connecting links (Fig. 8).

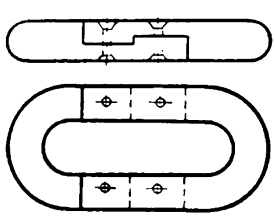

Fig. 8. Connecting link of load chain

When assembling separate lengths of forged links into chains the welded ends of each pair of adjoining links should form one joint to increase the life and strength of the chain. Chains welded by the electric resistance method can be assembled in any manner. After manufacture the chains are annealed. The main dimensions and characteristics of welded chains conform to a State Standard.

* Here and elsewhere, the grades of steel and other materials are designated according to the respective Soviet Standards (GOST). — *Tr.*

Welded chains should be tested under a load equal to one half the breaking load; no permanent set is permitted after the test.

Welded chains are used in low-capacity hoisting machines (hoists, winches, hand-operated cranes, etc.) as the main lifting appliances, especially as slings for suspending the load from the hook or other device.

Welded calibrated chains are likewise employed as hand-drive chains for traction wheels ($d = 5$ to 6 mm at a speed of $v = 0.6$ to 0.75 m/sec).

Welded chains have the disadvantage of heavy weight, susceptibility to jerks and overloads, sudden failure, intensive wear of the links in the joints and low safe speeds of movement.

On the other hand, the chains are distinguished for good flexibility in all directions, possibility of using small diameter pulleys and drums and their simple design and manufacture.

The shortcomings of welded chains limit their application for hoisting purposes; they are used only in some of the hand-operated mechanisms mentioned above on condition that the diameters of drums and pulleys (D) encircled by the chain are not less than $20d$ (where d is the diameter of the chain bar). In power-driven mechanisms the diameters of drums and pulleys should be at least $30d$. When welded chains are used for hoisting purposes preference is given to calibrated types because the considerable disagreement between the pitch of an uncalibrated chain and the pitch of a sprocket or pocket sheave causes frequent jamming and shocks and, hence, rapid failure.

Selecting Load Chains. With respect to external forces the links of welded chains are statically determinate and with respect to internal stresses three-fold statically indeterminate. It is therefore extremely difficult to find the actual stresses, which can be determined only approximately.

As a rule, chains are checked for tension by taking a somewhat reduced safe stress to account for the statically indeterminate feature of the links with respect to stresses and additional bending stresses when the chain runs over pulleys and drums.

The general formula for selecting welded chains in tension is

$$S_s = \frac{S_{br}}{K}$$

where S_s — safe load carried by the chain, in kg;

S_{br} — breaking load, in kg;

K — factor of safety (see Table 4).

The most intensive wear which reduces the chain strength occurs on the internal bent sections of the links acting as joints for a tractive chain.

The intensity of wear depends on the following factors: the ratio between the pitch of the chain and drum or sheave, the tension and speed of the chain, the angle of relative turn of the links as they pass around the sheaves, the environment, etc.

New forge-welded chains always break at the welds. In good-quality electric resistance welded chains breakage of links takes the form of an oblique shear in the sections passing at a small angle to the longitudinal axis of the chain and beginning at the boundary points of the contact surfaces on the jointed links.

We observe an analogous picture in links with various degree of wear.

2. ROLLER CHAINS

Roller chains are composed of plates (Fig. 9) hinge-jointed by pins. Chains for light loads are made with two plates; for heavier weights the number of plates can be increased to 12. The plates can be secured on the pins by upsetting the pin ends (Fig. 10*a*). This method is used for chains designed to handle light loads. In chains which are to handle heavy loads washers are placed under the upset

end of the pin (Fig. 10*b* and *c*). Fastening with cotter pins and washers or only with cotter pins (Fig. 10*d*, *e*, *f*) is applied in chains which have to be frequently disconnected.

Extended roller pins sometimes used in chains (Fig. 11) are intended for collecting the free end of the chain so that it does not interfere with operation.

As hoisting appliances roller chains are used in hand-operated hoists and, when power-driven, for winches and hoisting mechanisms of high load-lifting capacity operating at slow speed if the weight is being lifted in guideways.

At present, however, roller chains are being increasingly replaced in power-driven mechanisms by steel wire ropes.

Roller chains are superior to welded chains in a number of ways. Since the plates are solid the reliability of operation is considerably higher. Roller chains have good flexibility and can therefore be used on sprockets of small diameter and with a small number of teeth. This decreases the size of the mechanism and reduces its cost. Besides, the friction in the joints of such a chain is considerably less than in the joints of a welded chain with the same load-lifting capacity.

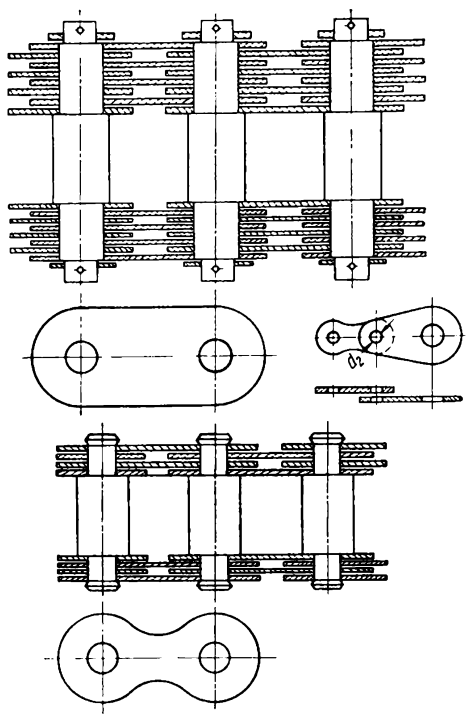

Fig. 9. Roller chains

Roller chains should be not allowed to carry weight acting at an angle to the plane of the rotation of the links since in this case the plates experience a high bending stress which may break the pins. Neither can roller chains be used in dusty premises because their joints are extremely susceptible to abrasive dust. As a result, such chains are never used in winches and cranes operating in the open.

Plates and pins are made of steel 40, 45 and 50. Their size and specifications are established by the respective State Standards.

The maximum speed of roller chains is specified by the Standard and should not exceed 0.25 m/sec.

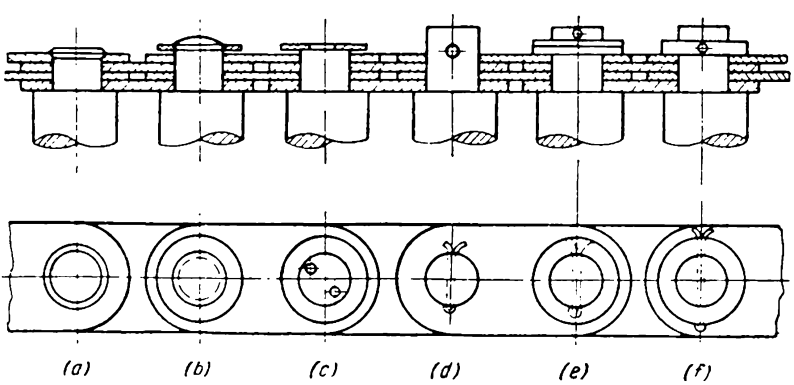

Fig. 10. Fastening the plates on the roller pins

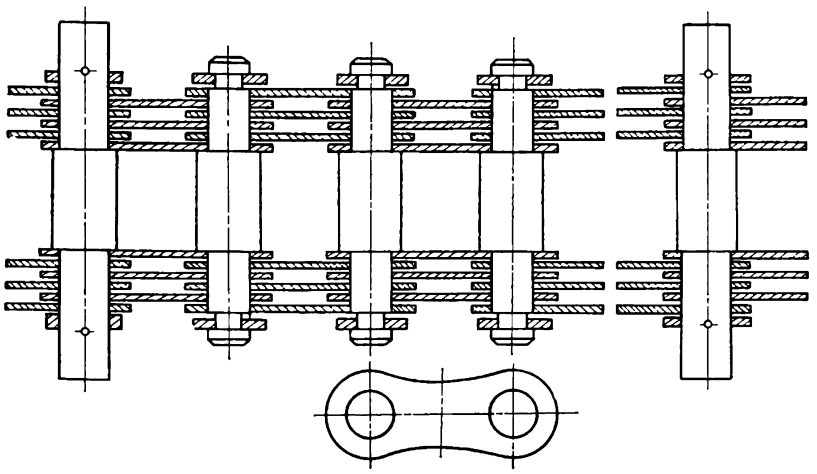

Fig. 11. Roller chains with extended pins

The values of the factor of safety K, the ratio $\frac{D}{d}$ and the number of teeth on the sprockets for welded and roller chains are tabulated below.

Table 4

Data for the Selection of Chains

Chains	Drive	Factor of safety, K	Ratio $\frac{D}{d}$	Minimum number of teeth on sprocket
Welded calibrated and uncalibrated	Hand	3	20	5
	Power	6	30	5
Welded calibrated on a pocket sheave	Hand	4.5	20	—
	Power	8	30	—
Welded uncalibrated (slings) passing around the load	—	6	—	—
Ditto, not passing around the load	—	5	—	—
Roller	—	5	—	8

3. HEMP ROPES

The poor mechanical properties of hemp ropes (rapid abrasion, inadequate strength, rapid damage from sharp objects and atmospheric effects, etc.) make them suitable only for hand-operated hoisting machinery (rope pulleys). The diameters of the sheaves over which the rope runs should be at least $10d$ (where d is the nominal diameter of the rope). Hemp ropes are used predominantly as tie-ropes for lifting tackle (hooks, etc). Hemp ropes conform to State Standards and are formed from three hemp strands and each strand from separate yarns. The twist of the strands is opposite to that of the yarns.

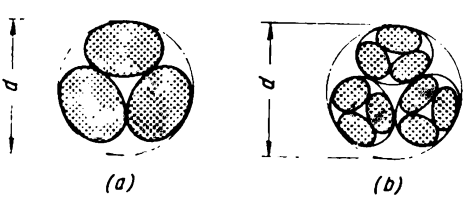

Fig. 12. Cross-sections of hemp ropes

By the mode of manufacture and the number of strands hemp ropes are classified as plain laid (Fig. 12*a*) and cable laid (Fig. 12*b*). The latter are twisted

from three ordinary ropes. Hemp ropes are frequently impregnated with tar to make them rotproof. Although tarred ropes display a better resistance to external effects they are heavier and not sufficiently flexible; moreover, their strength is about 20 per cent less than that of a white rope. The breaking strength of hemp ropes subdivides them into ropes of the 1st and 2nd grades.

In hoisting mechanisms both lifting and tie ropes must be exclusively of the 1st grade.

Selecting Hemp Ropes. Hemp ropes are selected only on the basis of the tension according to the formula

$$S = \frac{\pi d^2}{4} \sigma_{br} \tag{6}$$

where d—diameter, in cm, of a circle circumscribing the strands;

S—load on the rope, in kg.

For hemp ropes used for lifting, the safe conventional breaking stress referred to 1 sq cm of the area of a nominal diameter hemp rope (i.e., diameter d including voids) is $\sigma_{br} = 100$ kg/cm^2 for white rope and $\sigma_{br} = 90$ kg/cm^2 for tarred rope. Hence, for hoisting appliances formula (6) can be transformed as follows:

for white rope

$$S = 0.785d^2; \tag{7}$$

for tarred rope

$$S = 0.705d^2 \tag{8}$$

where d is in mm and S in kg.

4. STEEL WIRE ROPES

Steel wire ropes are extensively used in hoisting machinery as flexible lifting appliances. As compared to chains they have the following advantages:

1) lighter weight;
2) less susceptibility to damage from jerks;
3) silent operation even at high working speeds;
4) greater reliability in operation.

Failure in chains occurs suddenly while in wire ropes the outer wires are subject to more intensive wear and break before the inner wires. As a result, the wire rope becomes fuzzy long before rupture and should be immediately replaced. Wire ropes cost less than chains but they require larger drums which makes the entire hoisting mechanism heavier and more cumbersome.

Wire ropes are manufactured from steel wire with an ultimate strength of $\sigma_b = 130$ to 200 kg/mm^2. In the process of manufacture the wire is subjected to special heat treatment which, combined with cold drawing, imparts high mechanical properties to the wire.

Cranes operating in dry premises utilise ropes made of bright (uncoated) wire. Ropes intended for operation in damp premises are galvanised (zinc-coated) to protect them against corrosion. However, the load-lifting capacity of a rope with galvanised wires is about 10 per cent lower due to the tempering effects of hot zinc coating.

Steel wire ropes are manufactured by special machines: first separate wires are twisted into strands and then the strands are formed into a round rope. Both processes proceed simultaneously: the strands are laid on a core made of hemp, asbestos or a wire of softer steel. An asbestos or wire core is used for ropes subject to the action of radiant heat (for example, in cranes operating near furnaces in hot shops). However, a wire core reduces the flexibility of the rope in view of which metal cores are ordinarily used only when the ropes are subject to high compression as, for example, when being wound on a drum in several layers.

Wire ropes formed from strands are known as double lay ropes. They are the most popular type used in hoisting machinery.

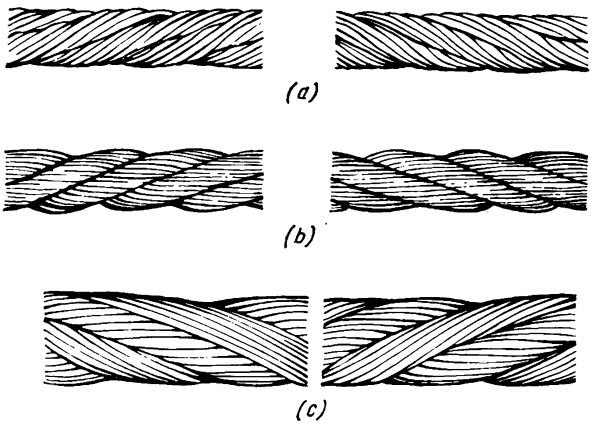

Fig. 13. Lays of steel wire ropes

The lay of ropes classifies them into: 1) cross or regular lay ropes; 2) parallel or Lang lay ropes; and 3) composite or reverse laid ropes.

Regular lay ropes (Fig. 13*a*) find the greatest application. Such ropes are so constructed that the direction of twist of the wires in the strand is opposite to that of the strands in the rope.

In a parallel (Lang) lay rope the direction of twist of the wires in the strand is the same as that of the strands in the rope (Fig. 13*b*). These ropes are more flexible and resist wear more effectively; however, they tend to spin. Parallel laid ropes are employed in lifts and in other hoists with guideways and also as haulage ropes.

In ropes with a reverse lay the wires in two adjacent strands are twisted in the opposite direction (Fig. 13*c*).

Besides, direction of the lay of a rope can be either right-hand or left-hand. Right-hand lay ropes are more frequently used.

General-Purpose Steel Wire Ropes. Wire ropes are manufactured according to State Standards.

The ropes shown in Fig. 13 have an ordinary (one-size-wire) construction in which the strands are twisted of wires of the same diameter (Fig. 14, *A*). In this case the wires in the covering layer will repeatedly cross over the inner wires (Fig. 14*a*) thereby creating zones of increased unit pressure which shortens rope life.

A Warrington compound rope (Fig. 14, *B*) is twisted of strands with wires of various diameters.

The wires of the adjacent layers do not intersect and each outer wire beds in the valley formed by two inner wires (Fig. 14*b*). This sharply reduces unit pressure between the wires and essentially increases the flexibility and life of such ropes as compared to *A*-type ropes.

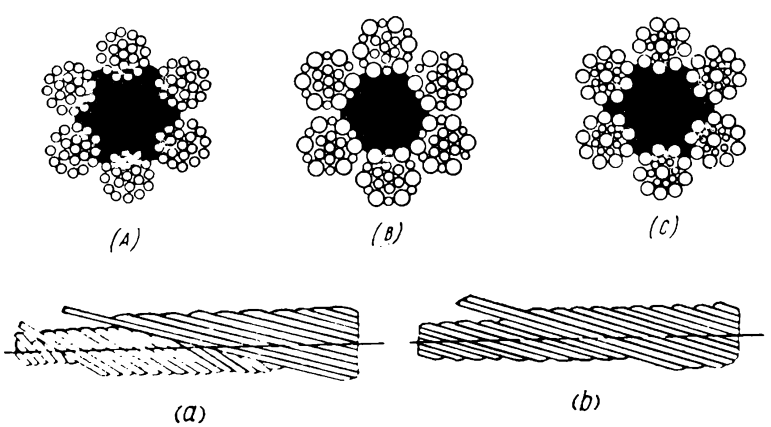

Fig. 14. Construction of steel wire ropes

Compound-construction ropes of the Seale type (Fig. 14, *C*) are distinguished by the fact that the inner and outer layers of each strand are of wires of different diameter, the number of the wires in the layers as well as their size being so selected as to prevent intersection of the wires.

In their operating capacity *C*-type ropes are equivalent to *B*-type ropes and as regards their flexibility they are intermediate between *A*- and *B*-type ropes.

Nonspinning Wire Ropes. A recent development in rope manufacture are the so-called nonspinning ropes. Such ropes are produced at the Odessa Rope Works, etc.

In such ropes each individual wire and each strand before being laid is preformed to correspond to its disposition in the rope. As a result, unloaded wires are not subject to internal stresses.

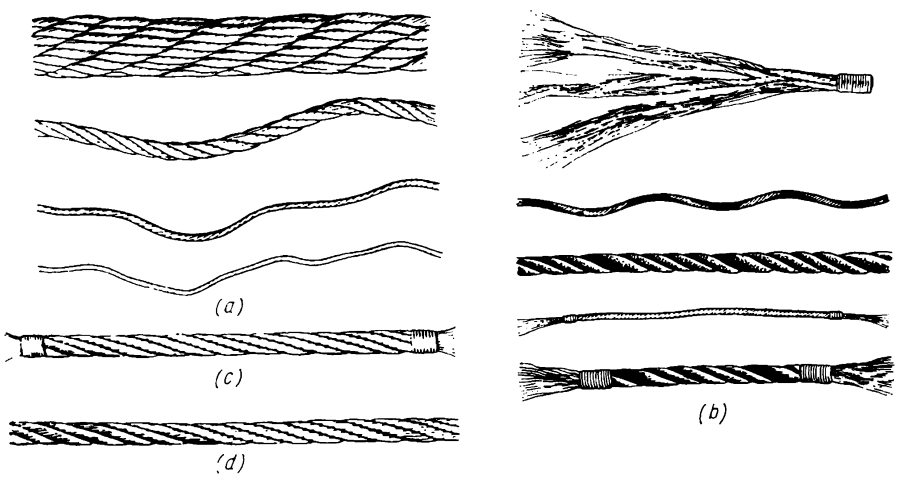

Fig. 15. Nonspinning and ordinary ropes

These ropes do not tend to untwist if the servings around their ends are untied. This facilitates wire rope splicing.

Nonspinning ropes have the following advantages over the usual *A*-type ropes (see Fig. 14):

1) uniform load distribution over the individual wires which reduces internal stresses to a minimum;

2) better flexibility;

3) less wear of the ropes from running over a sheave or coiling on a drum inasmuch as the wires and strands do not project from the rope contour and the outer wires wear uniformly; broken wires remain in their initial position and do not stick out of the rope (longer life);

4) greater operational safety.

Fig. 15*a* shows a nonspinning rope, its individual strands and wires and their original form before building up the rope. In Fig. 15*b* is seen a fuzzy ordinary rope made from straight wires after the servings around its ends have been removed and a nonspinning rope with one strand removed and also without servings. Fig. 15*c* shows a worn ordinary rope and Fig. 15*d* a worn nonspinning rope.

Steel Wire Ropes with Flattened Strands. Crane ropes composed of flattened strands (Fig. 16) are utilised in places where they are subject to intensive abrasion and wear. They are usually made from five flattened strands with a flattened wire core; the strands are laid on a hemp core. Ropes with flattened strands have a larger area in contact with the groove of a pulley or drum than round-strand ropes. Hence, they experience more uniform pressure and wear less. The groove

of the pulley or sheave should be so designed that the rope contacts it on 1/3 of its circumference. Fig. 16 also shows the cross-section of a type *C* rope with flattened strands (see Fig. 14).

Locked-Coil Steel Wire Ropes. Locked-coil wire ropes find application in cableways and cable cranes; they are never met with in hoisting machines of the usual type. They have the advantages of a smooth surface, tightly packed wires and little wear. Their shortcoming is an insufficient flexibility.

A locked-coil rope consists of an outer layer formed of specially shaped wires and an inner single-lay spiral rope (Fig. 17*a*, *b*, *c*). In semilocked-coil ropes the outer layer is combined of shaped and round wires (Fig. 17*d*). The external view of a locked-coil rope is shown in Fig. 17*e*.

Fig. 18 shows the cross-sections of ropes used in materials handling machines.

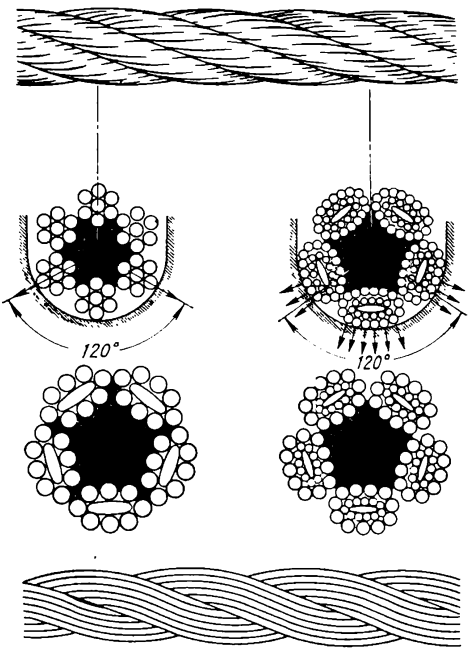

Fig. 16. Ropes with flattened strands

The external diameter of the rope is measured over a pair of opposite strands (Fig. 19).

The rope should be replaced if a definite number of broken outer wires are detected over the length of one lay (or pitch).

The lay (pitch) is found in the following manner. Mark off the surface of any strand and count off, beginning from this place, as many strands along the rope axis as there are in the rope cross-section and place another mark on the strand which comes next after the last strand counted. The distance between the marks will be the pitch of the rope (Tables 5 and 6).

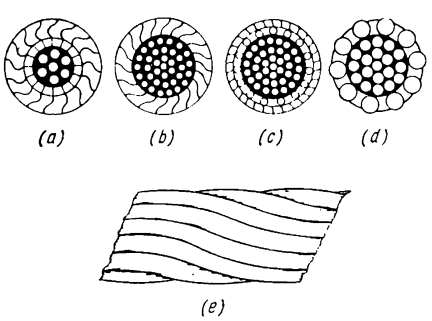

Fig. 17. Locked-coil ropes

Table 5

Ropes for Lifts

Initial factor of safety of rope for tension	Rope construction			
	6 × 19 = 114 + 1c*		6 × 37 = 222 + 1c	
	Cross laid	Parallel laid	Cross laid	Parallel laid
	Number of wire breaks over the length of one pitch after which the rope should be discarded			
up to 9	14	7	23	12
9-10	16	8	26	13
10-12	18	9	29	14
12-14	20	10	32	16
14-16	22	11	35	17
over 16	24	12	38	19

* Six stands of 19 wires in each plus one core.

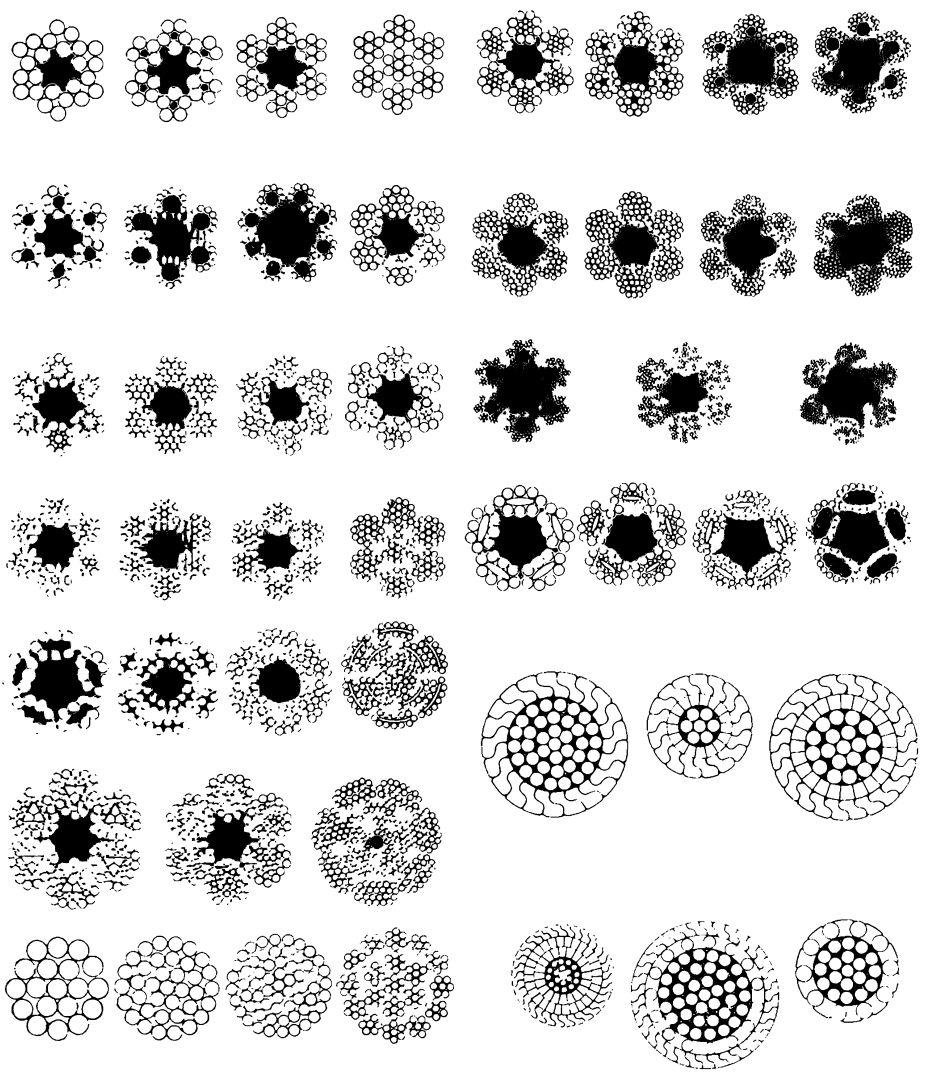

Fig. 18. Wire ropes used in materials handling machinery

Some of the recent constructions of ropes are designed with one bright wire for a definite number of dark wires for easier calculation of the number of broken wires. In such ropes each wire has its own ordinal number which can be easily determined in each cross-section of the rope (Fig. 20).

Selecting Steel Wire Ropes. Extremely complex phenomena are involved in the operation of ropes which in some part are indeterminate. Individual wires in a loaded bent rope experience a complex stress consisting of tension, bending and twisting stresses combined with mutual compression and rubbing of the wires and strands. As a result, the total stress can be determined analytically only to a certain degree of approximation. Besides, as they run over pulleys and drums, the outer wires are subjected to abrasion which, in turn, reduces the total strength of the rope.

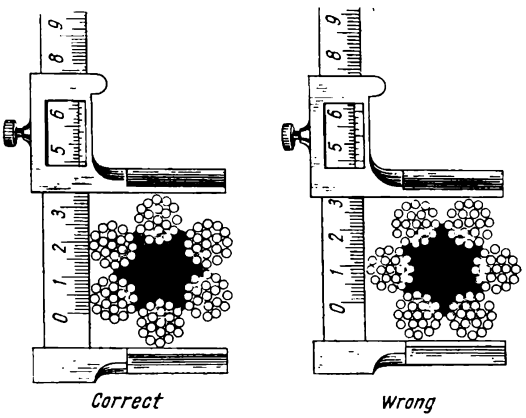

Fig. 19. Measuring the rope diameter

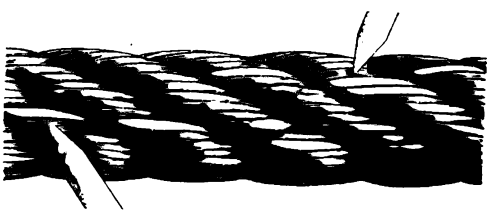

Fig. 20. Rope with a definite number of bright wires

Table 6

Ropes for Cranes and Hoists

Initial factor of safety of rope for tension	Rope construction							
	6 × 19 = 114 + 1c		6 × 37 = 222 + 1c		6 × 61 = 366 + 1c		18 × 19 = 342 + 1c	
	Cross laid	Parallel laid	Cross laid	Parallel laid	Cross laid	Parallel laid	Cross laid	Parallel laid
	Number of wire breaks over the length of one pitch after which the rope should be discarded							
up to 6	12	6	22	11	36	18	36	18
6-7	14	7	26	13	38	19	38	19
over 7	16	8	30	15	40	20	40	20

Experiments have shown that the life of a rope is greatly affected by fatigue. It has been found that each rope can withstand during its life only a definite number of bends after which rapid disintegration sets in.

Depending on the number of bends, the rope life can be found from the ratio $\frac{D_{min}}{d}$ (D_{min} is the minimum diameter of a pulley or drum and d is the diameter of the rope) and $\frac{D_{min}}{\delta}$ (δ — diameter of the wires in the rope).* Investigations have shown that at the same ratio $\frac{D_{min}}{d}$ rope life is approximately inversely proportional to the number of bends. One bend is assumed to mean the transition of the rope from its straight position into a bent one, or from a bent position into

* The question as to which of the ratios $\left(\frac{D_{min}}{d}\right)$ or $\left(\frac{D_{min}}{\delta}\right)$ affects the life of the rope more is as yet controversial.

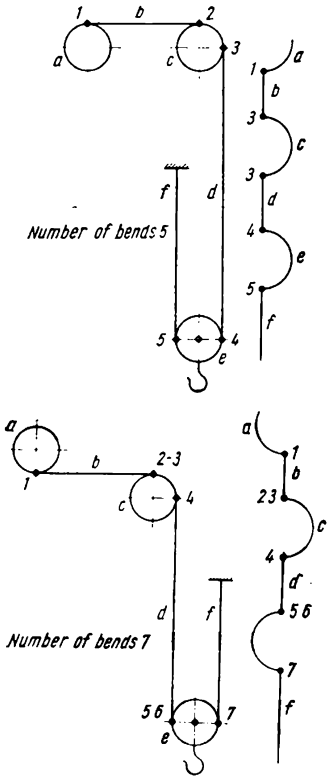

Fig. 21. Determining the number of the rope bends with one movable pulley

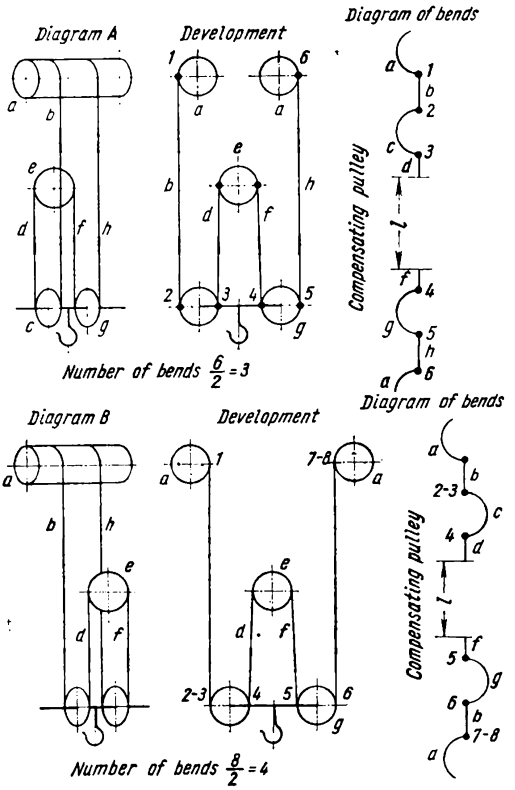

Fig. 22. Determining the number of bends in multiple pulleys

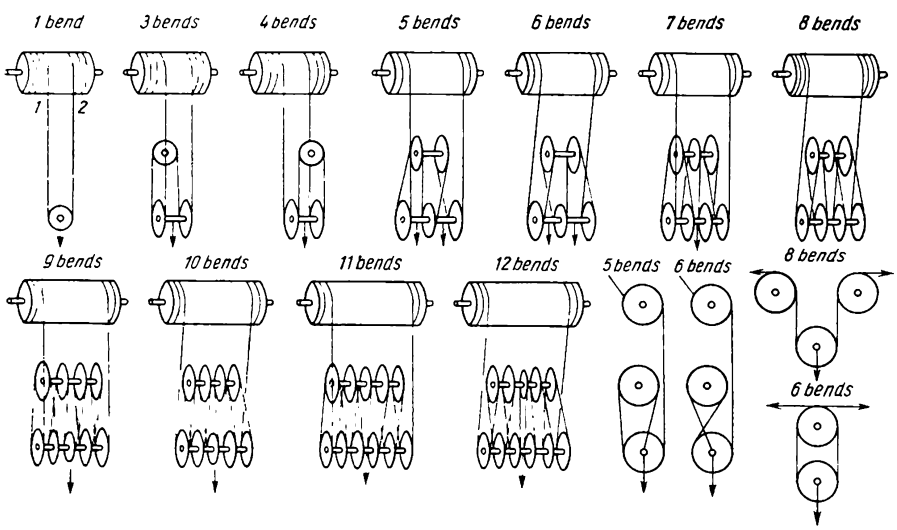

Fig. 23. Number of bends for various modes of load suspension

a straight one. Reverse bending (i. e., towards the side opposite to the preceding bend) reduces the rope life approximately by one half, or it is tantamount to two single bends towards the same side. The number of bends is determined by the number of points (pulleys, drums) where the rope runs on and off, the bends in one direction at these places being tantamount to a single bend and the variable bends to a double bend.

The number of bends can be found with sufficient accuracy if we plot a diagram of the type illustrated in Fig. 21.

Fig. 22 (diagrams *A* and *B*) shows loads suspended on multiple crane pulleys, the number of bends and the methods for their determination. With a diagram of a pulley system available, first construct a development of the mechanism and then a rope bending diagram. In determining the number of bends for multiple pulleys the compensating pulley is not considered since it remains stationary when the load is being raised or lowered.

Since every multiple pulley system can be regarded as a pulley with two independent ropes connected on the compensating pulley, the design number of bends of a multiple pulley rope can be obtained by dividing the total number of points where the parallel parts of the rope run on and off by 2.

For widespread diagrams of load suspension the design number of bends is indicated in Fig. 23.

To obtain the same rope life, the effect of the number of bends should be compensated for by an appropriate change in the ratio $\frac{D_{min}}{d}$. Table 7 illustrates the values of $\frac{D_{min}}{d}$ as a function of the number of bends.

Table 7

Number of bends	$\frac{D_{min}}{d}$	Number of bends	$\frac{D_{min}}{d}$	Number of bends	$\frac{D_{min}}{d}$	Number of bends	$\frac{D_{min}}{d}$
1	16	5	26.5	9	32	13	36
2	20	6	28	10	33	14	37
3	23	7	30	11	34	15	37.5
4	25	8	31	12	35	16	38

Ropes are checked for strength as follows. On the basis of the accepted load suspension method we use Table 7 to find the ratio $\frac{D_{min}}{d}$. Expressing the diameter of the rope by the formula

$$d = 1.5\delta\sqrt{i} \qquad (9)^*$$

we obtain the ratio

$$\frac{D_{min}}{1.5\delta\sqrt{i}}$$

where δ — diameter of one wire;
i — number of wires in the rope.

The stress in a loaded rope in its bent part in tension and bending is

$$\Sigma\sigma = \frac{\sigma_b}{K} = \frac{S}{F} + \frac{\delta E'}{D_{min}} \qquad (10)$$

where σ_b — ultimate breaking strength of the rope wire material, in kg/cm²;
K — rope factor of safety;
S — tension in rope falls in kg;
F — area of useful cross-section of the rope in sq cm;

* This formula holds true only for one-size-wire ropes.

$E' = \frac{3}{8}E$ — corrected rope elastic modulus;

$E' = \frac{3}{8}2{,}100{,}000 \approx 800{,}000$ kg/cm²;

the other notations being as before.

Transforming formula (10) we obtain

$$F = \frac{S}{\frac{\sigma_b}{K} - \frac{\delta}{D_{min}}E'} = \frac{S}{\frac{\sigma_b}{K} - \frac{d}{D_{min}} \cdot \frac{\delta}{d}E'} = \frac{S}{\frac{\sigma_b}{K} - \frac{d}{D_{min}} \cdot \frac{E'}{1.5\sqrt{i}}}. \quad (11)^*$$

After specifying K and selecting the number of wires i depending on the rope construction and at a definite σ_b and $\frac{d}{D_{min}}$ we use formula (11) to find the rope cross-sectional area.

After finding F we select a rope with the nearest characteristics, first checking whether its ultimate strength σ_b corresponds to that accepted in formula (11). The number of wires in the rope is determined by the accepted design.

For the ropes most frequently used in hoisting machinery (excepting compound laid ropes), i. e., for the ropes with 114, 222 and 342 wires, formula (11) assumes the following form:

$$F_{(114)} = \frac{S}{\frac{\sigma_b}{K} - \frac{d}{D_{min}}50{,}000}; \quad (12)$$

$$F_{(222)} = \frac{S}{\frac{\sigma_b}{K} - \frac{d}{D_{min}}36{,}000}; \quad (13)$$

$$F_{(342)} = \frac{S}{\frac{\sigma_b}{K} - \frac{d}{D_{min}}29{,}000}. \quad (14)$$

Multiplying both sides of formulas (12), (13) and (14) by σ_b we obtain other formulas for the selection of the rope by its breaking strength P referred to the total cross-section of the rope, i. e.,

$$P_{(114)} = \frac{S\sigma_b}{\frac{\sigma_b}{K} - \frac{d}{D_{min}}50{,}000}; \quad (15)$$

$$P_{(222)} = \frac{S\sigma_b}{\frac{\sigma_b}{K} - \frac{d}{D_{min}}36{,}000}; \quad (16)$$

$$P_{(342)} = \frac{S\sigma_b}{\frac{\sigma_b}{K} - \frac{d}{D_{min}}29{,}000}. \quad (17)$$

The values of d and δ in the selected rope need not be checked further since the effect of these values is taken fully into account in the design formulas.

* This formula holds true only for one-size-wire ropes.

Formula (10)

$$\frac{\sigma_b}{K} = \frac{S}{F} + \frac{\delta E'}{D_{min}}$$

is based on the following.

The ratio between the moment and the radius of curvature in bending gives

$$\varrho = \frac{EI}{M}$$

where ϱ is the radius of curvature;

E — elastic modulus of the wire;

I — moment of inertia of the wire cross-section;

M — bending moment.

Tension or compression stress in bending a straight wire in its extreme fibre located at a distance of $\frac{\delta}{2}$ from the neutral line, where δ is the wire diameter, equals

$$\sigma = \pm \frac{M}{I} \cdot \frac{\delta}{2} = \pm \frac{EI}{\varrho I} \frac{\delta}{2} = \pm E \frac{\delta}{2\varrho} = \pm E \frac{\delta}{D_{min}}$$

(D_{min} — diameter of the pulley or drum over which the rope runs).

This stress would be developed in a straight wire if it were not a component part of the rope.

Actually, the wire in the rope is a double or triple spiral clamped between the adjacent wires and subject to torsion before being bent. Experiments show that the bending stress will be lower and the formula for σ should be corrected by introducing a special factor which depends on the type and lay of the rope, its operating conditions, etc., and equals approximately 3/8.

By adding the tensile stress over the straight section to the bending stress we shall obtain the previous formula (10), i. e.,

$$\sigma_\Sigma = \frac{S}{F} + \frac{3}{8} E \frac{\delta}{D_{min}} = \frac{S}{F} + \frac{\delta E'}{D_{min}}.$$ *

Ropes should be subjected to only one tensile test according to the formula

$$S = \frac{P}{K}, \tag{18}$$

where S — maximum permissible tension set up in the rope in kg;

P — actual breaking strength of the rope in kg;

K — factor of safety taken from Table 9 depending on the type of mechanism and the conditions of its operation.

The maximum working tension in the rope parts of a load pulley system S_w is found from the formula

$$S_w = \frac{Q}{n \cdot \eta \cdot \eta_1}$$

where Q — weight of the load being raised in kg;

n — number of pulley reeving parts;

η — pulley efficiency (Table 8);

η_1 — efficiency with account taken of the loss due to rope stiffness in coiling on a drum, assumed equal to 0.98.

* This is an approximate calculation of the rope stress which takes into account only static loads; dynamic tests may be dispensed with within the limits of the recommended factors of safety when the rope is not too long.

Table 8

Pulley Efficiency

Single pulley		Multiple pulley		Efficiency	
Number of parts of line	Number of rotating pulleys	Number of parts of line	Number of rotating pulleys	Sliding friction in pulley bushes (resistance factor of one pulley is 1.05)	Rolling friction in pulley bushes (resistance factor of one pulley is 1.031)
2	1	4	2	0.951	0.971
3	2	6	4	0.906	0.945
4	3	8	6	0.861	0.918
5	4	10	8	0.823	0.892
6	5	12	10	0.784	0.873

The minimum permissible diameter of a drum or pulley is found from the formula

$$D \geqslant e_1 e_2 d \qquad (18a)$$

where D — diameter of the drum or pulley over the bottom of the groove, in mm;
d — rope diameter, in mm;
e_1 — factor depending on the type of the hoisting device and its service conditions (Table 9);
e_2 — factor depending on the rope construction (Table 10).

The diameter of the compensating pulley can be 40 per cent less than the diameter of the blocks carrying the load.

Table 9

Minimum Permissible Values of Factors K and e_1

Type of hoisting mechanism	Drive	Operating conditions	Factor K	Factor e_1
I. Locomotive, caterpillar-mounted, tractor- and truck-mounted pillar cranes (including excavators operating as cranes), cranes and hoisting mechanisms at construction sites and temporary jobs.	Hand	Light	4	16
	Power	Light	5	16
	Power	Medium	5.5	18
	Power	Heavy and very heavy	6	20
II. All other types of cranes and hoisting mechanisms.	Hand	Light	4.5	18
	Power	Light	5	20
	Power	Medium	5.5	25
	Power	Heavy and very heavy	6	30
III. Hand-operated winches with a load-lifting capacity of up to 1 ton mounted on various automotive vehicles (automobiles, trucks, etc.).	—	—	4	12
IV. Trolley hoists.	—	—	5.5	20
V. Clamshell mechanisms (except for pulleys in grabs) for hoisting mechanisms of item I.	—	—	5	20
VI. Ditto, for hoisting mechanisms of item II.	—	—	5	30

Notes: 1. The operating conditions of hoisting machinery can be found in Tables 2 and 3.

2. In ropes intended for passenger lifts factor K should be at least 14.

3. Factor K of sling ropes should be at least 10.

4. In determining the minimum permissible diameter of the pulleys in grabs of hoisting machinery, enumerated in items I, II and IV, factor e_1 may be reduced to 18.

5. The factor of safety of ropes for hoisting tackle conveying molten or white hot metal, acids, fire-hazardous, explosive and poisonous substances should equal 6.0 irrespective of the operating conditions.

6. The factor of safety of ropes intended only for supporting crane booms, i.e., used as guys, should be at least 3.5.

Table 10

Values of Factor e_2 Depending on Rope Construction

Rope construction	Factor e_2
Ordinary 6×19 = 114+1 core:	
cross laid	1.00
parallel laid	0.90
Compound 6×19 = 114+1 core:	
a) Warrington:	
cross laid	0.90
parallel laid	0.85
b) Seale:	
cross laid	0.95
parallel laid	0.85
Ordinary 6×37 = 222+1 core:	
cross laid	1.00
parallel laid	0.90

Note: For hand-operated cranes and hoisting mechanisms and also for the ropes not indicated in the table, the factor e_2 can be assumed as unity.

5. CALCULATING THE ENDURANCE (FATIGUE STRENGTH) OF STEEL WIRE ROPES BY PROFESSOR ZHITKOV'S METHOD

Proceeding from the fact that rope failure is caused by the fatigue of the material and that each wire rope can withstand only a definite number of bends many investigators have set themselves the task of finding by experiment the relationship between rope life and the various factors causing wear and of determining in each individual case the number of bends after which rope failure begins.

The method of calculating the endurance of wire ropes should be recognised as the most scientific and perfect. Correct in principle, it is also of great practical importance. In designing hoisting appliances the designer should always bear in mind the dependence of the rope life on the size of drums or pulleys, load, rope construction and other factors.

The method of calculating wire ropes for endurance described below has been developed by summing up the results of many years of research conducted mainly at the Hammer and Sickle Works. Ropes of various construction from 3 to 28 mm in diameter were tested on three special machines to find the metallurgical, production, design and operational factors which affect the strength of ropes.

As the first step, characteristics of rope life were compiled for all tests in the form of graphs which determined the relations

$$z = f_1(\sigma) \qquad \text{and} \qquad z = f_2\left(\frac{D}{d}\right).$$

These data were used to draw a diagram showing the relation $\sigma = f_3\left(\frac{D}{d}\right)$ for various numbers of rope bends (Fig. 24) and to obtain mathematically the following design formula:

$$A = \frac{D}{d} \qquad m\,\sigma\,CC_1C_2 \qquad (19)$$

where $A = \frac{D}{d}$ — ratio between the diameter of drum or pulley and the rope diameter;

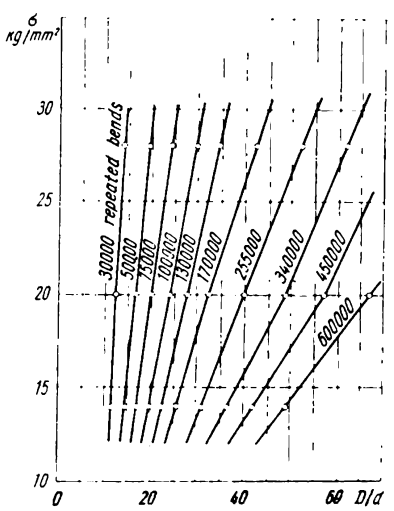

Fig. 24. Diagram for determining the number of rope bends

m — factor depending on the number of repeated bends of the rope z during the period of its wear until it fails (Table 11);
σ — true tensile stress in the rope, in kg/mm²;
C — factor characterising rope construction and the ultimate tensile strength of the wire material (Table 12);
C_1 — factor depending on the rope diameter (Table 13);
C_2 — factor determining the additional production and operational factors not accounted for by factors C and C_1 (the values of C_2 are indicated in (Table 14).

Table 11

Values of Factor m

z in thousands	30	50	70	90	110	130	150	
m	0.26	0.41	0.56	0.70	0.83	0.95	1.07	
z in thousands	170	190	210	230	255	280	310	340
m	1.18	1.29	1.40	1.50	1.62	1.74	1.87	2.00
z in thousands	370	410	450	500	550	600	650	700
m	2.12	2.27	2.42	2.60	2.77	2.94	3.10	3.17

Table 12

Values of Factor C

σ_b, kg/mm²	Rope construction									
	6 × 7 = 42 and one core		6 × 19 = 114 and one core						6 × 37 = 222 and one core	
			Ordinary		Warrington		Seale			
	cross laid	parallel laid	cross laid	parallel laid	cross laid	parallel laid	cross laid	parallel laid	cross laid	parallel laid
130	1.31	1.13	1.08	0.91	0.69	0.61	0.81	0.69	1.12	0.99
160	1.22	1.04	1.00	0.83	0.63	0.54	0.75	0.62	1.06	0.93
180	1.16	0.98	0.95	0.78	0.59	0.50	0.70	0.57	1.02	0.89

Table 13

Values of Factor C_1

Rope diameter	up to 5	5.5-8	8.5-10	11-14	15-17.5	18-19	19.5-24	25-28	30-34.5	37-43.5
C_1	0.83	0.85	0.89	0.93	0.97	1.00	1.04	1.09	1.16	1.24

Table 14a

Values of Factor C_2

Material of rope wire	C_2
Carbon steel: 0.55% C; 0.57% Mn; 0.25% Si; 0.09% Ni; 0.08% Cr; 0.02% S and 0.02% P	1
Carbon steel: 0.70% C; 0.61% Mn; 0.09% Si; 0.021% S and 0.028% P	0.9
Chromium pearlitic steel: 0.40% C; 0.52% Mn; 0.25% Si; 0.2% Ni; 1.1% Cr; 0.025% S and 0.025% P	1.37
Stainless steel: 0.09% C; 0.35% Mn; 0.3% Si; 8.7% Ni; 17.4% Cr; 0.02% S and 0.02 P	0.67
Ordinary open-hearth steel	1
Open-hearth steel smelted of charcoal pig iron and clean scrap	0.63
Wire made from the whole ingot	1
Wire made from the ingot middle zone	0.92

Table 14b

Operation	Treatment			C_1
Drawing	Draught per drawing—25%			1
	Draught per drawing—10%			0.93
	Surface	ordinary		1
		polished		0.89
Heat treatment process	Patenting in a lead bath			1
	Normalising			1.08
	Air hardening			1.1
	Annealing			1.15
Stranding process	Lay pitch			
	Strands in rope	Wires in strands		
		first lay	second lay	
	1.8 *d* of rope	10.2 *d* of strand	12.1 *d* of strand	1
	6.7 *d* of rope	10.2 *d* of strand	12.1 *d* of strand	1.13
	8.8 *d* of rope	10.2 *d* of strand	12.1 *d* of strand	1.06
	8.8 *d* of rope	12.0 *d* of strand	14.0 *d* of strand	0.91
	6.7 *d* of rope	8.3 *d* of strand	7.9 *d* of strand	1.18
	6.9 *d* of rope	25.0 *d* of strand	6.9 *d* of strand	0.72
	One-strand core	Impregnated with grease	Hemp	1
			Cotton	1.11
			Manila	0.82
			Sisal	0.82
			Steel	1.36
	One-strand core	Not impregnated with grease	Hemp	1.15
			Cotton	1.46
			Manila	1.0
			Sisal	0.82
			Steel	1.36
	Three-strand core	Impregnated with grease	Hemp	1.06
			Sisal	0.74
	Additional processing	Straightening of wires and rope		0.89
		Prestretching of rope		0.93

Table 14c

Operational factors	Indices	C_2
Pulley material	Iron casting	1
	Duralumin	0.92
	Laminated fabric	0.80
Pulley groove radius	0.52 *d* of rope	1
	0.75 *d* of rope	1.16
	R = ∞	1.27
	40° V-groove	1.26
Nature of rope bend	One-side bend	1
	Multiple bend	1.4
Angle of contact of rope on pulley	180	1
	90	1.14
	45	1.27

Table 14c, continued

Operational factors	Indices	C_t
Angle of deflection of rope relative to a plane normal to the axis of the pulley or drum (fleet angle)	0°	1
	1°30′	1.09
	3°	1.16
	5°	1.22
Ambient temperature	+20° C	1
	0° C	0.9
	—20° C	0.83

After specifying the rope life we can find the diameters of the drum or pulleys by formula (19). If the stress σ, ratio $\frac{D}{d}$ and the operating conditions of the hoisting mechanism are known we can determine the life of ropes of various construction.

When calculating the endurance of a rope we must know the permissible number of bends during the period of its operation.

In different hoisting mechanisms one and the same rope can withstand different numbers of bends depending on the number of guiding pulleys encircled by the rope and the height to which the load is raised (which is not always the same) as well as the ratios between the full and mean working loads.

To obtain more accurate data on the number of the working cycles, the number of rope bends and the rope loads, certain enterprises and construction sites carried out long-term observations and timing of the work of various hoisting machines. Table 15 has been compiled on the basis of these data.

Table 15

Values of a, z_2 and β

Operating conditions of hoisting mechanisms		Daily operation, hrs	Working days per month	Mean number of working cycles per day	a	Mode of load suspension		z_2	Height h of load lifting in m at the maximum number of rope bends per cycle for $l_1 = 1$ m and $l_2 = 2$ m	β
Hand-driven		8	25	16	400	Simple suspension		2	—	0.7
Power-driven	Light duty	8	25	40	1,000	Suspension with one movable pulley		4	2	0.5
	Medium duty	16	25	136	3,400	Multiple pulley with ratio:	2×2	3	2	0.4
							2×2	5	3	0.3
	Heavy and very heavy duty	24	30	320	9,600		2×4	7	4	0.25
							2×5	9	5	0.2

If we know the operating conditions of the hoisting mechanism, after specifying the rope life we can find the permissible number of bends z_1 from the formula

$$z_1 = az_2 N \beta \tag{20}$$

where N — rope life, in months;

a — average number of working cycles per month;

z_2 — number of repeated bends per cycle (raising and lowering) at the full lifting height and one-sided bending;

β — factor of change in the endurance of the rope due to lifting the load to less than the full height and to lifting less than the full load.

The values of a, z_2 and β are given in Table 15 which also specifies the height h of load lifting at which the rope will be bent on all the pulleys. In a suspension with one movable pulley (Fig. 25) the point v of the rope on fixed pulley *1* will reach the lower movable block *2* when the hook housing is lowered by a height $h = 1$. In cranes with booms the section of the rope passing over pulleys *1* and *2* will never reach the drum and pulley *3*.

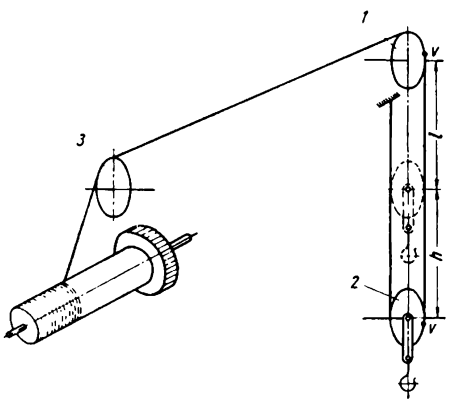

Fig. 25. Suspension with one movable pulley

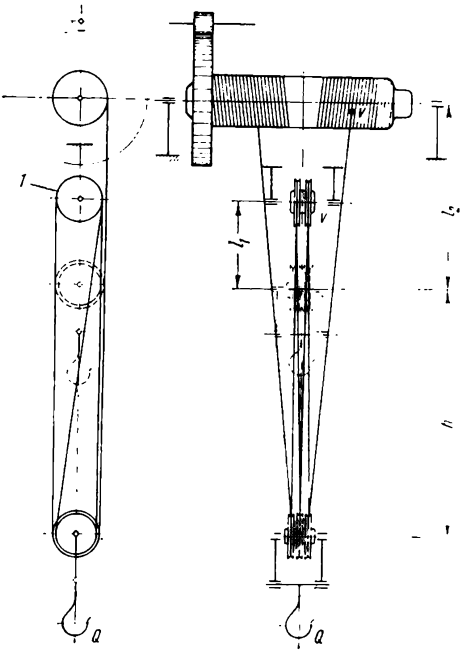

Fig. 26. Suspension on a multiple pulley system

In a multiple pulley system (Fig. 26) point v of the rope on the drum will reach pulley *1* when the hook housing is lowered by the height

$$h \geqslant l_1 (i - 2) + l_2$$

where l_1 — distance from the hook housing to the fixed pulleys;

l_2 — distance from where the rope runs off the drum to the movable housing;

i — one half of the number of parts in the line.

In this way, only if the load is lowered by a height h, will the section of the rope running off the drum run over all the pulleys; when the height of lowering is less than h the number of rope bends will be less than the maximum; the same occurs when the rope raises the load.

Using the results of tests (Fig. 27), obtained in determining the rejection norms of worn steel wire ropes, and bearing in mind that there is a direct relationship between the number of bends and the number of breaks in the rope we can accept the relation

$$\varphi = \frac{z}{z_1} = 2.5.$$

In this case we mean that the line "rejection norm" divides the curves of the rope endurance to the ratio 1:1.5 (approximately), i. e., the rope life is 0.4 of its durability.

The number of repeated bends which cause the rope to fail is found from the formula

$$z = z_1 \varphi = a z_2 N \beta \varphi. \qquad (21)$$

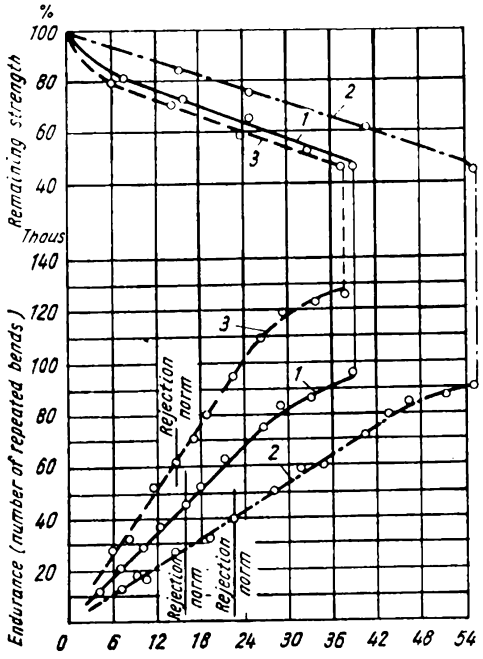

Fig. 27. Dependence of load-lifting capacity and the rope endurance on the number of broken wires over the length of one rope pitch:
1—cross laid rope 6×19, *2*—cross laid rope 6×37, *3*—parallel laid rope 6×37

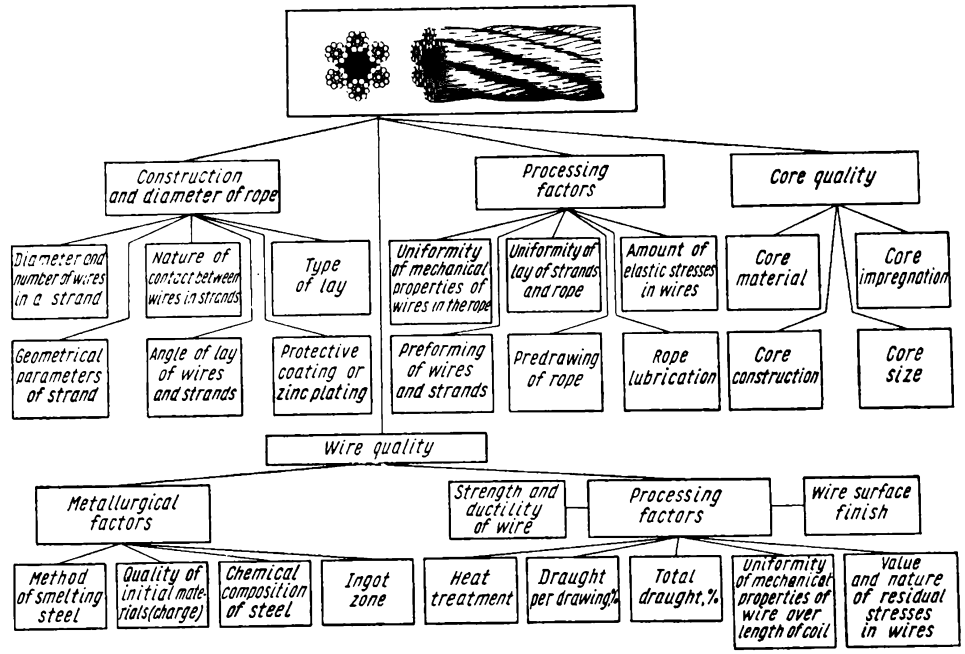
Construction and diameter of rope
Processing factors
Core quality
Diameter and number of wires in a strand
Nature of contact between wires in strands
Type of lay
Uniformity of mechanical properties of wires in the rope
Uniformity of lay of strands and rope
Amount of elastic stresses in wires
Core material
Core impregnation
Geometrical parameters of strand
Angle of lay of wires and strands
Protective coating or zinc plating
Preforming of wires and strands
Predrawing of rope
Rope lubrication
Core construction
Core size
Wire quality
Metallurgical factors
Strength and ductility of wire
Processing factors
Wire surface finish
Method of smelting steel
Quality of initial materials (charge)
Chemical composition of steel
Ingot zone
Heat treatment
Draught per drawing, %
Total draught, %
Uniformity of mechanical properties of wire over length of coil
Value and nature of residual stresses in wires

Fig. 28. Main factors affecting the quality of a steel wire rope

The method of calculating the endurance of ropes makes it possible to estimate the working capacity of the rope under various operating conditions. This method is superior to other methods in that it provides the designer and mechanic with a clear picture as to rope life.

Fig. 28 illustrates the main factors affecting the quality of a steel wire rope.

6. FASTENING OF CHAINS AND ROPES

The ends of chains and ropes are secured by various methods some of which will be discussed below.

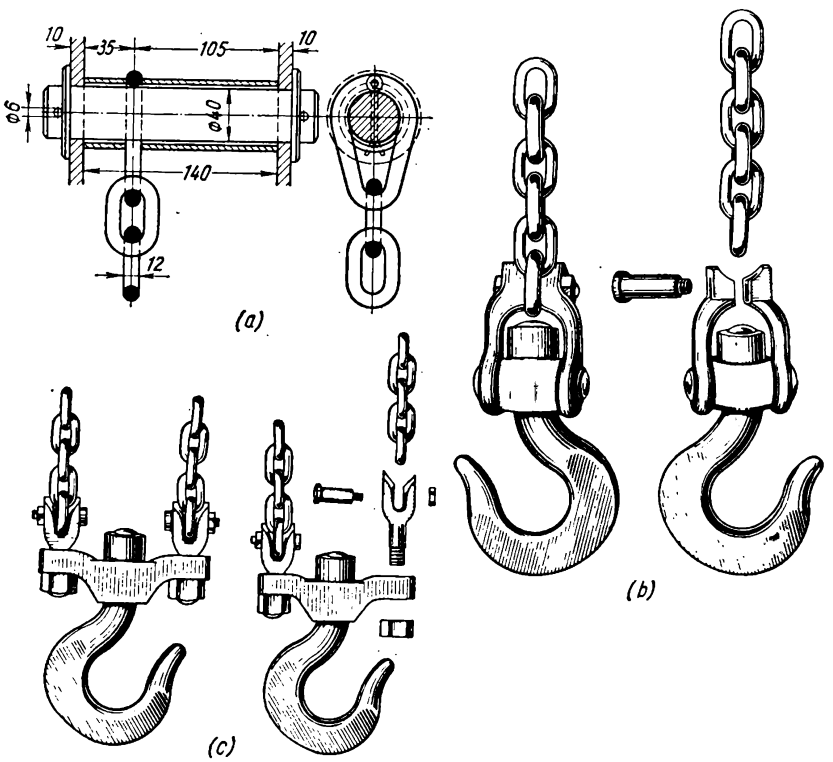

Fig. 29. Methods of fastening welded load chains

Fastening Welded Load Chains. Fig. 29*a* shows how the end of a hoisting chain is attached to a trolley frame. A welded shaped end link is placed on a shaft secured in the side plates of the trolley frame. On both sides of the link are distance pieces to locate the chain.

Fig. 29*b* shows how the end of a chain is attached to a hook with the help of a split yoke and a bolt. The fastening of a hook to two chain strands with the help of a crosspiece and forked eyes is illustrated in Fig. 29*c*. The shank of each fork is fastened with a nut directly to the hook crosspiece.

Fastening of Roller Chains. Fig. 30 shows how a roller chain is connected to the trolley frame by means of a special end link with a large bolt hole d_1 and having a longer pitch l_1 than ordinary links. End links of roller chains conform to a State Standard depending on the main pitch l and the load-lifting capacity of the chain.

Fastening of Hemp Ropes. Hemp ropes are usually joined together by splicing or with the help of eyelet thimbles (Fig. 31). All other methods are inadequate because of the comparatively low strength of hemp ropes.

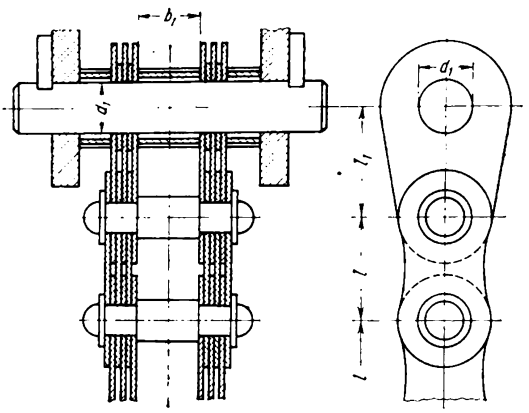

Fig. 30. Fastening of load roller chains

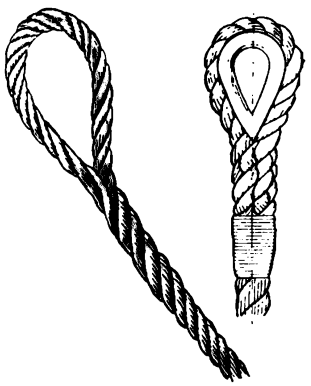

Fig. 31. Fastening of hemp ropes

Fastening of Wire Ropes. The following methods are used to attach the ends of steel wire ropes to a winch frame, the boom of a rotary crane or any other part of a hoisting mechanism.

Tapered wire-rope socket. The rope is secured in a tapered socket (Fig. 32) in the following sequence of operations.

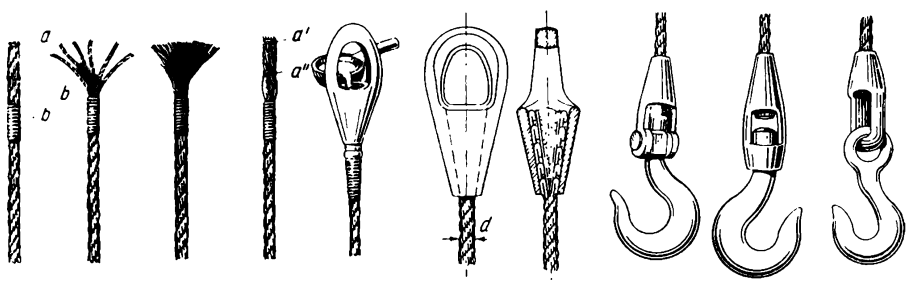

Fig. 32. Fastening of a wire rope in a tapered socket

1. The end of the rope is first served securely with soft wire at points *a* and *b* whose position depends on the length of the steel socket. The lower serving *b* should be wider than the upper one.
2. The upper serving *a* is then removed and the strands opened.
3. The wires are broomed out in each strand and the hemp core is cut out.
4. The wires are then bound together at two points with temporary seizings *a'* and *a''*.
5. The end of the rope is pushed into the socket, the wires are bent in a hook-like manner and melted lead is poured into the socket.

Fig. 32 shows various wire-rope sockets for suspending the hook.

Approximate checking for the strength of a tapered socket involves the following:

Lateral pressure on the socket walls (Fig. 33) is

$$P = \frac{Q}{2 \sin \alpha}$$

where Q — load on the rope.

At the same time

$$P = \frac{pF}{2}$$

where p — unit pressure on the socket walls;

F — bearing area in contact equal to

$$F = \frac{l(d_1 + d_2)\pi}{2}.$$

Hence

$$P = \frac{Q}{2\sin\alpha} = \frac{pl(d_1 + d_2)\pi}{2 \cdot 2}.$$

Substituting

$$l = \frac{r_1 - r_2}{\sin\alpha} = \frac{d_1 - d_2}{2\sin\alpha}$$

we have

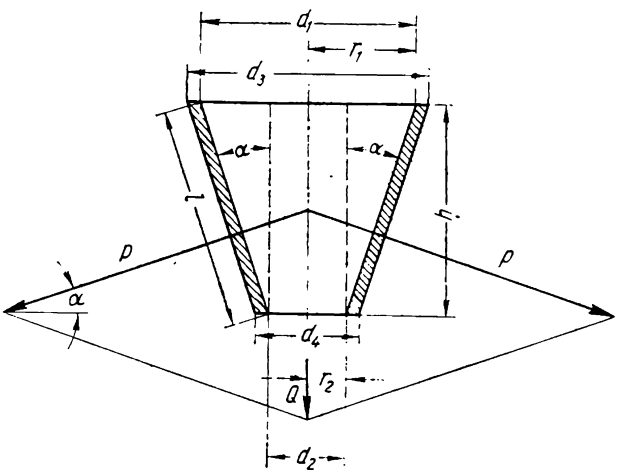

Fig. 33. Diagram for calculating the strength of a tapered wire-rope socket

$$\frac{Q}{2\sin\alpha} = \frac{p(d_1 - d_2)(d_1 + d_2)\pi}{2 \times 2 \times 2\sin\alpha}$$

and simplifying we obtain

$$Q = \frac{p(d_1^2 - d_2^2)\pi}{4}$$

whence

$$p = \frac{4Q}{(d_1^2 - d_2^2)\pi}, \tag{22}$$

i. e., unit pressure between the inner walls of the socket and the lead filling is equal to the unit pressure on the horizontal projection of the bearing area.

When $d_2 \approx d$ (d — rope diameter)

$$d_1 = \sqrt{\frac{4Q}{p\pi} + d^2}. \tag{23}$$

Unit pressure p should not exceed 115 kg/cm².

The height of the socket h is determined by checking the lead filling for shear

$$h = \frac{Q}{\pi d [\tau]_{sh}} \tag{24}$$

where $[\tau]_{sh} = 125$ kg/cm².

The thickness of the socket walls, considered as a cylinder with internal pressure, is found from the following general formula

$$d_{ex} = d_{in}\sqrt{\frac{\sigma_{br} + 0.4p}{\sigma_{br} - 1.3p}}$$

where d_{ex} and d_{in} — external and internal diameters;

σ_{br} — safe breaking stress, in kg/cm² (for steel castings $\sigma_{br} = 400$ to 700 kg/cm²);

p — internal pressure found from formula (22).

Since the lead filling does not contact the walls uniformly the value of p should be doubled for more reliability. The following equations will hold for the broadest and narrowest sections of the socket:

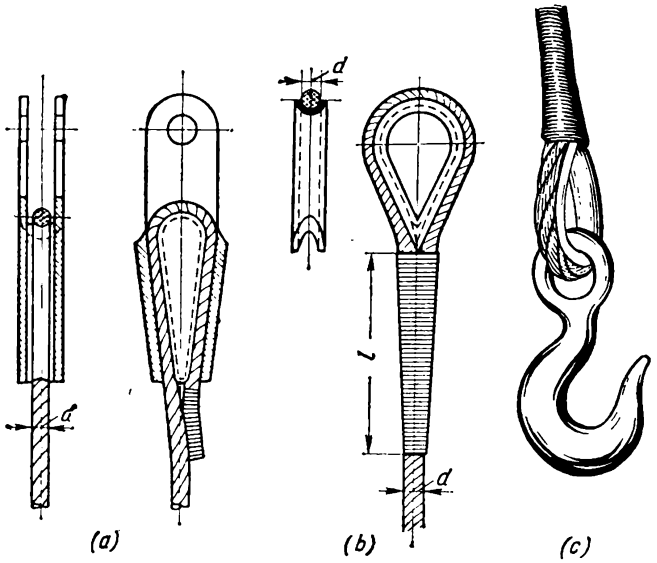

Fig. 34. Wedge-socketing of a rope (*a*) and fastening by means of an eyelet thimble (*b*, *c*)

for the broad section

$$d_3 = d_1 \sqrt{\frac{\sigma_{br} \pm 0.4 \times 2p}{\sigma_{br} - 1.3 \times 2p}}. \quad (25)$$

for the narrow section

$$d_4 = d_2 \sqrt{\frac{\sigma_{br} + 0.4 \times 2p}{\sigma_{br} - 1.3 \times 2p}}. \quad (26)$$

Wedge-sockets. A rope is passed around a steel grooved wedge (Fig. 34*a*) and placed together with the wedge into a flat socket of a corresponding shape made of cast steel. The load pulls the rope into the socket and reliably clamps it there.

Eyelet thimble. A rope is passed around a steel eyelet thimble (Fig. 34*b*) and its free end is spliced with the main part of the rope. The length of splicing is $l > 15d$ but not less than 300 mm.

Fig. 34*c* shows a hook attached to a rope eyelet thimble. This mode of fastening has extremely widespread application. Instead of splicing, the thimble can be secured by fitting special bull-dog clips or clamps on the wire rope (Fig. 35). The minimum number of clamps is three. Fig. 36 illustrates a rope eyelet thimble in which the rope is clamped by means of plates and bolts.

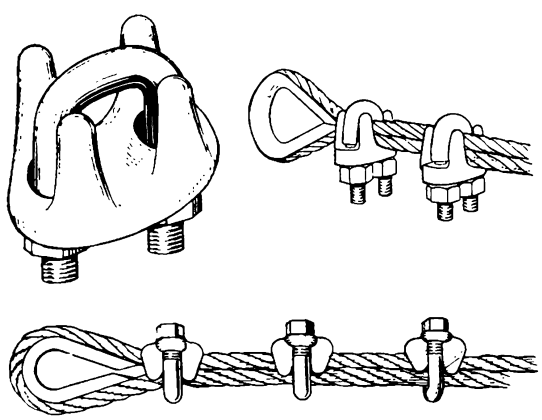

Fig. 35. Bull-dog clamps

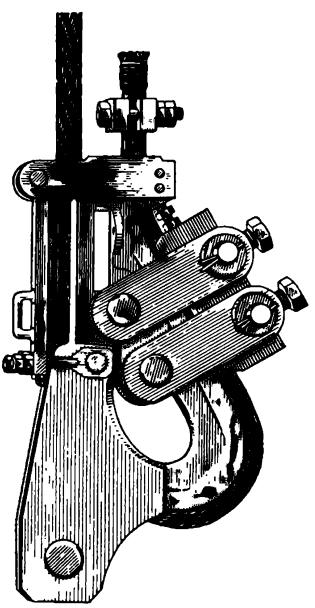

Fig. 36. Rope eyelet thimble with plates and bolts

7. LOAD SUSPENSION APPLIANCES

Unit piece loads are carried by chain or rope slings attached to hooks or iron grips.

Permissible Included Angles Between Sling Legs. In Fig. 37*a* we have a

load suspended from two legs of a sling. If we denote the weight of the load being lifted by Q the tension in each leg of the sling will be

$$S = \frac{Q}{2\cos\alpha}. \tag{27}$$

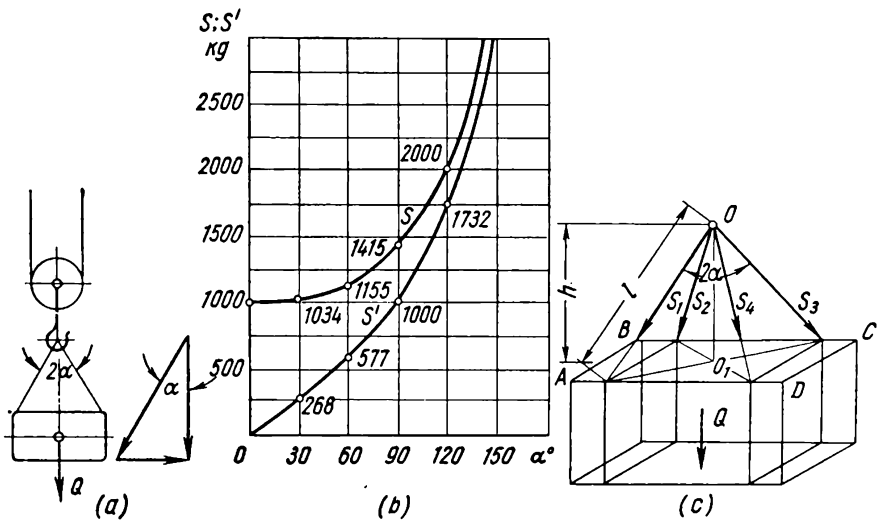

Fig. 37. Determining the forces acting in sling legs

The horizontal component of the tension S is

$$S' = \frac{Q}{2}\tan\alpha.$$

If we determine the forces S and S' for a load $\frac{Q}{2} = 1{,}000$ kg and with an included angles from $2\alpha = 0°$ to $2\alpha = 180°$, the relation between S and S' will be expressed by the curves shown in Fig. 37*b*. These curves show that larger included angles lead to greater tension in the chain or rope sling legs as well as to a greater compressive or bending force acting on the load being lifted. Hence, as the included angle increases the useful load on the sling legs diminishes.

If the load is suspended symmetrically on four chains (Fig. 37*c*) it can be assumed that the weight will be equally distributed between the four legs of the sling. In this case the tension in the sling legs will be

$$S = S_1 = S_2 = S_3 = S_4 = \frac{Q}{4\cos\alpha}. \tag{28}$$

But since

$$\cos\alpha = \frac{O_1O}{OA} = \frac{h}{l}$$

the final formula will take the following form:

$$S = \frac{Q}{4}\frac{l}{h}. \tag{29}$$

If the weight of the load Q is known the tension in each leg will be

$$S = \frac{1}{\cos\alpha}\frac{Q}{m} = k\frac{Q}{m} \tag{30}$$

where m — number of legs in the sling;
α — angle between the legs and the vertical.
If $\alpha = 0°$, 30°, 45° and 60°, then $k = 1$, 1.15, 1.42 and 2, respectively.

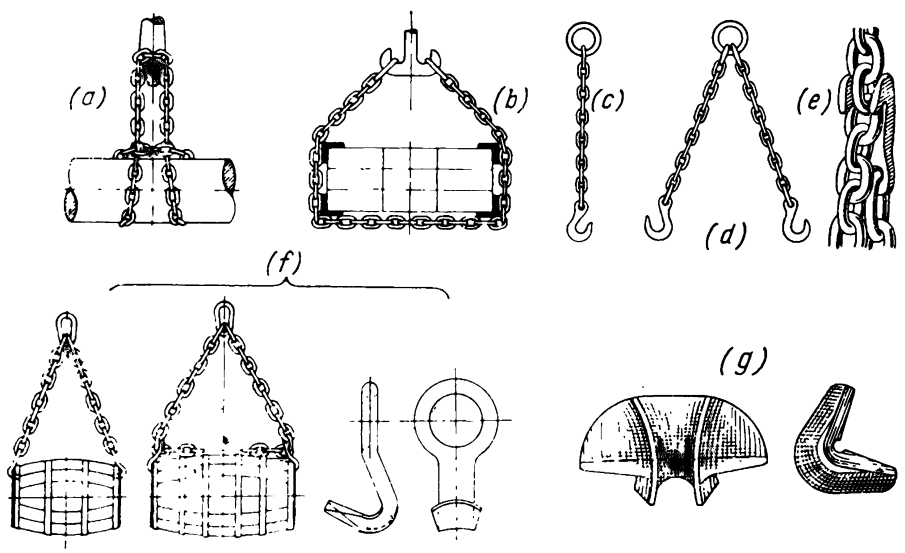

Fig. 38. Chain slings

Chain slings. These slings are made from ordinary uncalibrated welded chains with eyes and hooks for suspension or with tong-shaped grips for the object being lifted. Use is also made of endless chains and free chains with rings at the ends. Such chain is passed under the load or is passed several times around the hook while the end rings or the free part of the chain is hung on the crane hook.

Fig. 38*a* shows an endless chain, Fig. 38*b*—a free chain with rings, Fig. 38*c*—a chain with a hook and a ring, Fig. 38*d*—two-leg chain sling, Fig. 38*e*—a claw-shaped grip for making a loop in the chain.

Fig. 38*f* shows barrels suspended on chain slings by tong-shaped grips which fit the bevelled edges of the barrels. Chain slings are used predominantly for heavy-duty service, and always in cases of large temperature variations or a permanent high temperature. Unless special soft metal protective pads are used (Fig. 38*g*), chain slings are likely to damage the corners of the commodities being handled. Similar pads are also used for rope slings.

The tension of chain slings can be found from formulas (28) and (30) and k is assumed: for either endless or free chains passed around the load $k \geqslant 6$ (Fig. 38*a* and *b*), for chains that do not encircle the object $k \geqslant 5$ (see Fig. 38*c*, d and *f*).

Hemp Rope Slings. Rigidly twisted white hemp ropes find extensive application for suspending loads on crane hooks. They are much inferior in strength to steel wire ropes but possess better flexibility and can be easily tied into knots. Hemp ropes are easily damaged by sharp edges of the commodities being handled and should be protected with soft pads (see Fig. 38*g*) or special protective devices (corner pieces).

Methods of tieing hemp ropes are illustrated in Fig. 39.

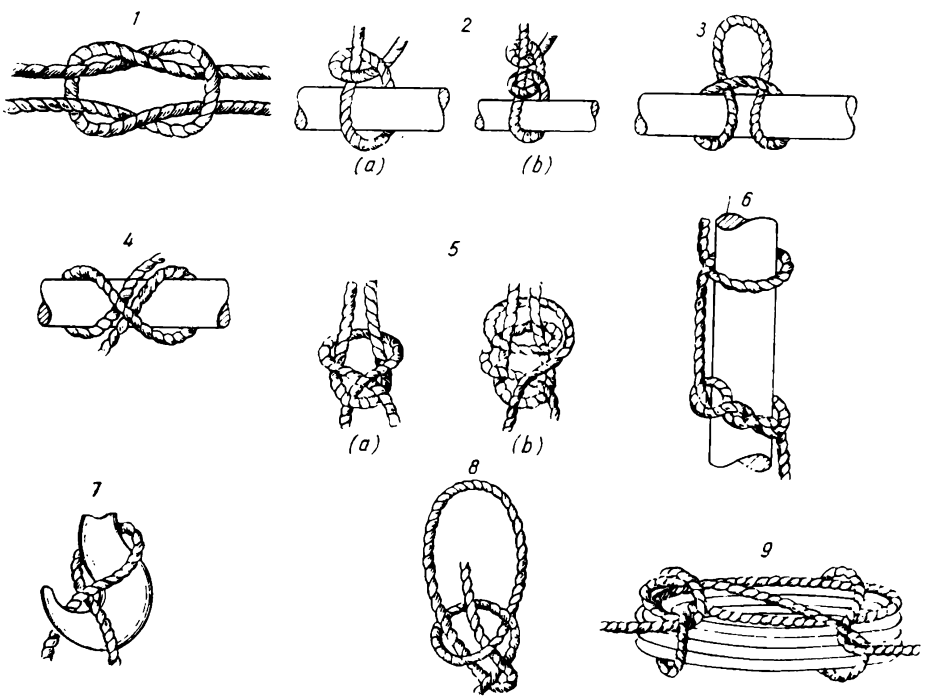

Fig. 39. Knots and slings of hemp rope:

1—square knot; *2*—(a) half hitch, (b) two half hitches; *3*—sling; *4*—clove hitch; *5*—(a) sheet bend, (b) double-sheet bend; *6*—timber and half hitch, the upper loop retains timber in vertical position; *7*—single blackwall hitch; *8*—bowline knot; *9*—sheep shank. All knots are loose

Hemp ropes are selected by formula (6) and the tensions in the sling legs are checked by formulas (28)-(30). The breaking stresses are: for white rope $\sigma_{br} = 50$ kg/cm²; for tarred rope $\sigma_{br} = 45$ kg/cm².

Steel Wire Rope Slings. Heavy loads are frequently handled by wire rope slings. As compared to chains they weigh less but are too rigid and tend to twist. Besides, when handling commodities with sharp edges they bend excessively and wear out rapidly. They are also very susceptible to high temperatures.

Fig. 40*a* shows a one-leg wire rope sling and Fig. 40*b* two- and four-leg wire rope slings.

Steel wire rope slings are calculated by formula (11) and their tension is determined by formulas (28), (29) and (30); $k \geqslant 10$ for slings passed around the load (see Fig. 40*a*) and $\geqslant 6$ for slings which do not encircle the load (see Fig. 40*b*).

Loads hoisted by chain or rope slings should be reliably secured so that they may not alter the position in the sling during its movement.

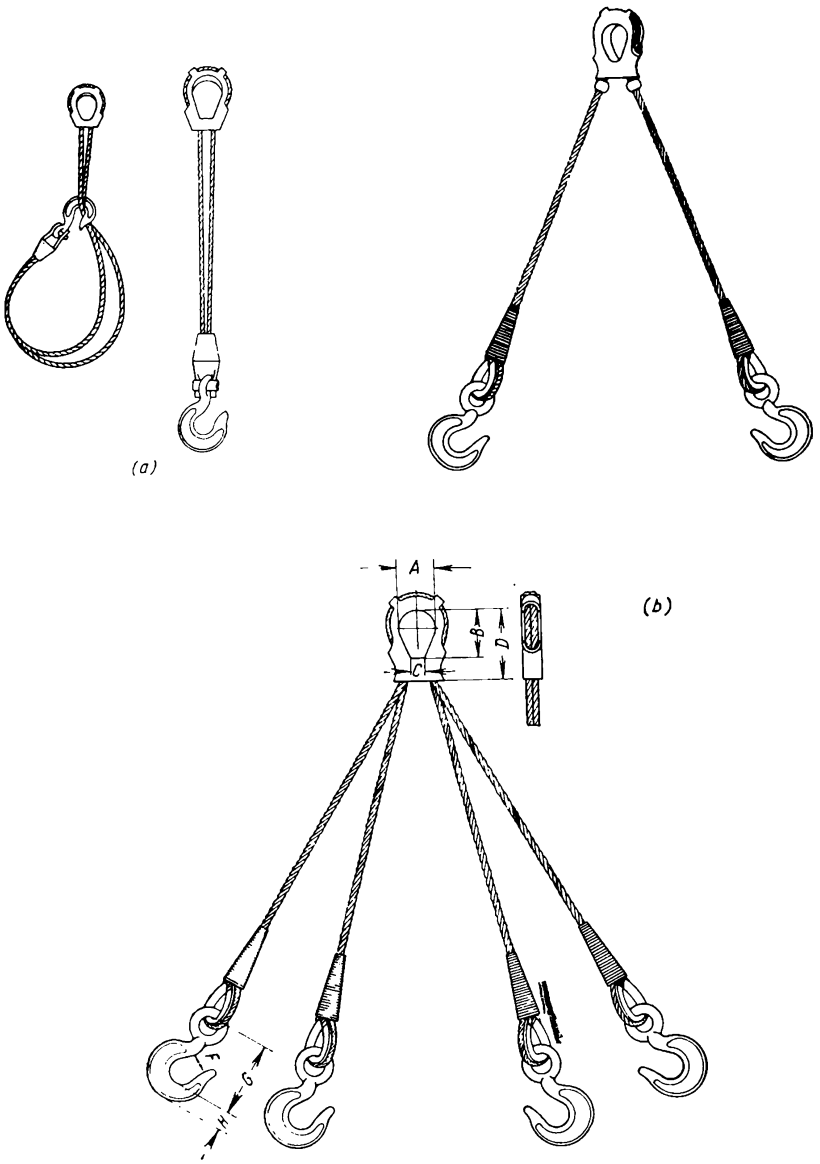

Fig. 40. Steel wire rope slings

CHAPTER IV

PULLEYS, PULLEY SYSTEMS, SPROCKETS AND DRUMS

1. PULLEYS

Pulleys are manufactured in fixed and movable designs. Pulleys with fixed axles are also called guiding because they change the direction of the flexible hoisting appliance.

Fixed Pulleys

Fig. 41*a* and *b* shows diagrams of fixed pulleys. One end of the rope passin. around the pulley is loaded with weight Q and the other with the pulling force Z The path of pulling force S is equal to the height h to which the load is raised Disregarding the resistance in the pulley the pulling force Z_0 equals Q.

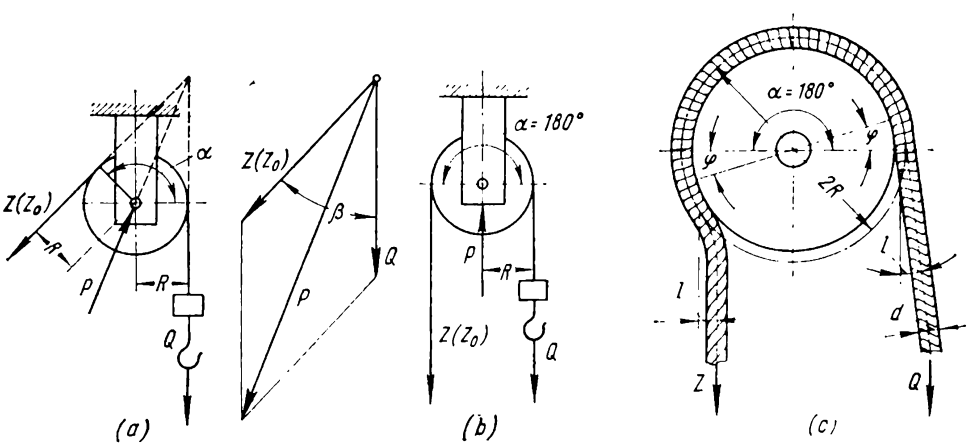

Fig. 41. Single fixed pulleys

In actual fact $Z > Q$ because of the resistance in the pulley (resistance of the flexible parts to bending and frictional resistance in the bearings).

The property of rigidity in the ropes passing over the pulley manifests itself in the fact that the rope running onto the pulley does not begin to follow its circumference at once but is at first deflected by the amount e towards the outside (Fig. 41*c*); and conversely, when running off the pulley it deflects approximately by the same amount towards the inside. This increases the arm of force Q when the rope runs on and decreases the arm of force Z when the rope runs off. In a state of equilibrium $Z\ (R\cos\varphi - e) = Q\ (R\cos\varphi + e)$ and then we shall have the following relationship between the pull values:

$$\frac{Z}{Q} = \frac{1 + \dfrac{e}{R\cos\varphi}}{1 - \dfrac{e}{R\cos\varphi}}. \tag{31}$$

Hence, after division, and neglecting small magnitudes

$$Z \approx Q\left(1 + \frac{2e}{R\cos\varphi}\right). \tag{32}$$

The frictional resistance in the bearings is

$$W = \sum (Q + Z_0)\,\mu\,\frac{d'}{2R} \approx Q\,\mu\,\frac{d'}{R} \tag{33}$$

where d' — diameter of the pulley axle;
μ — coefficient of friction.

The resultant force P on the pulley is easily determined by graphical methods as shown in Fig. 41*a*. At $\alpha = 180°$ the two parts of the rope will be parallel and

$$\Sigma (Q + Z_0) \approx Q + Z_0 \approx 2Q = P.$$

The pulling force will be

$$Z \approx Q\left[1 + \frac{2e}{R\cos\varphi} + \mu\frac{d'}{R}\right]. \tag{34}$$

The magnitude $\varepsilon = \dfrac{Z}{Q}$ is called the pulley factor of resistance and

$$\varepsilon = \frac{1}{\eta}$$

where η — pulley efficiency.
Therefore

$$\varepsilon = \frac{1}{\eta} = 1 + \frac{2e}{R\cos\varphi} + \mu\frac{d'}{R}.$$

The value $\dfrac{2e}{R\cos\varphi}$ — rigidity of the ropes — can be found only experimentally.

Experiments conducted in the U.S.S.R. have shown that the following average value can be assumed for ropes:

$$\frac{2e}{R\cos\varphi} = 0.1\,\frac{d}{D - 10}$$

where d — rope diameter, in cm;
D — pulley diameter, in cm.

Apart from the rigidity of the ropes the factor of resistance in pulleys also depends on the type of bearings and the lubricants used for the pulley axles. When grease ($\mu \approx 0.1$) is used to lubricate chain and rope sheaves the following average values can be taken: $\varepsilon \approx 1.05$ and $h \approx 0.95$. For pulleys with ball or roller bearings friction in the axles is usually disregarded and an average of $\varepsilon \approx 1.02$ and $\eta \approx 0.98$ is assumed.

Movable Pulleys

These pulleys have movable axles to which either a load or force (effort) is applied. Accordingly, there are pulleys for a gain in force and pulleys for a gain in speed.

Pulleys for a Gain in Force. For the pulley shown in Fig. 42*a* the distance travelled by the point of the rope where the effort is applied is equal to twice the height to which the load is raised:

$$\left.\begin{aligned} s &= 2h; \\ c &= 2v, \end{aligned}\right\} \qquad (35)$$

where c — speed of the applied force;
v — speed of the load.

With regard to the resistance in the pulley

$$\left.\begin{aligned} Z + S_0 &= Q;\ Z = \varepsilon S_0 = \varepsilon (Q - Z); \\ Z &= \frac{\varepsilon}{1+\varepsilon} Q;\ \eta = \frac{Z_0}{Z} = \\ &= \frac{Q}{2} \cdot \frac{1+\varepsilon}{\varepsilon Q} = \frac{1+\varepsilon}{2\varepsilon}. \end{aligned}\right\} \qquad (36)$$

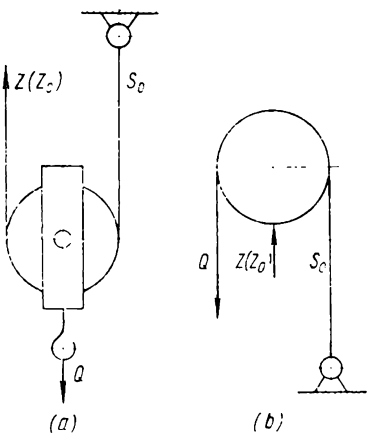

Fig. 42. Simple movable pulleys for a gain in force and speed

When $\varepsilon \approx 1.05, \eta \approx 0.975$, i.e., the efficiency of a movable pulley is somewhat higher than that of a fixed pulley.

Pulleys for a Gain in Speed. For the pulley shown in Fig. 42*b* the distance travelled by the point where the force is applied is equal to half the height to which the weight is raised:

$$\left.\begin{aligned} s &= \frac{h}{2}; \\ c &= \frac{v}{2}. \end{aligned}\right\} \qquad (37)$$

With regard to the resistance in the pulley

$$\left.\begin{aligned} Z &= Q + S_0 = Q + Q\varepsilon = Q(1+\varepsilon); \\ \eta &= \frac{Z_0}{Z} = \frac{2Q}{Q(1+\varepsilon)} = \frac{2}{1+\varepsilon}. \end{aligned}\right\} \qquad (38)$$

When $\varepsilon \approx 1.05$, $\eta \approx 0.975$, i. e., in this case too, the efficiency of a movable pulley is higher than that of a fixed pulley.

2. PULLEY SYSTEMS

A pulley system is a combination of several movable and fixed pulleys or sheaves. There are systems for a gain in force and for a gain in speed. Hoisting devices employ pulleys for a gain in force predominantly and only rarely, as for example, in hydraulic or pneumatic lifts, pulleys for a gain in speed. As independent lifting appliances pulley systems are of secondary importance; they are mainly used for power transmission in winches and cranes.

Pulley Systems for a Gain in Force. These are designed: *a*) with the rope running off a fixed pulley and *b*) with the rope running off a movable pulley.

Designs with the Rope Running off a Fixed Pulley. If we denote by z the number of pulleys (Fig. 43*a*) then the number of the parts of the line on which the weight is suspended will also equal z.

The transmission ratio $i = z$.

Neglecting harmful resistance, the effort on the running-off part of the rope will be

$$Z_0 = \frac{Q}{z}.$$

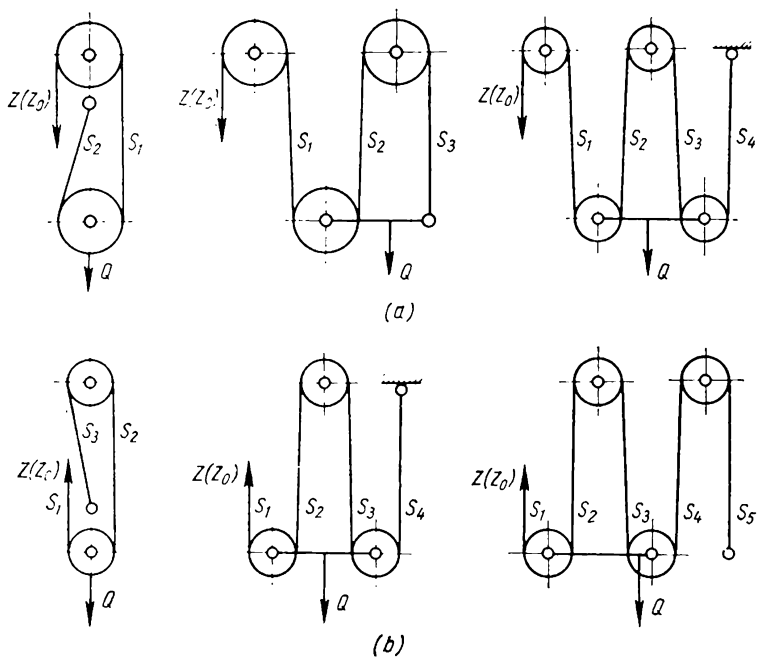

Fig. 43. Pulley systems for a gain in force

The actual effort is

$$Z = \frac{Q}{\eta_\Sigma z} = \frac{Q\varepsilon_\Sigma}{z}$$

where η_Σ and ε_Σ — resultant efficiency and factor of the pulley system resistance.

The total tension in all parts of a flexible rope will be

$$Q = S_1 + S_2 + S_3 + S_4 + \ldots + S_n = S_1 + \frac{S_1}{\varepsilon} + \frac{S_1}{\varepsilon^2} + \frac{S_1}{\varepsilon^3} + \ldots$$

$$+ \frac{S_1}{\varepsilon^{n-1}} = S_1\left(1 + \frac{1}{\varepsilon} + \frac{1}{\varepsilon^2} + \ldots + \frac{1}{\varepsilon^{n-1}}\right) = S_1 \frac{1}{\varepsilon^{n-1}}$$

$$(\varepsilon^{n-1} - \varepsilon^{n-2} + \varepsilon^{n-3} + \ldots + \varepsilon + 1).$$

The addends in the brackets are the series of a geometrical progression where the common ratio $q = \varepsilon$, first term $a = 1$ and last term $u = \varepsilon^{n-1}$; as is known, the sum of the terms of this series equals

$$\frac{qu - a}{q - 1} = \frac{\varepsilon\varepsilon^{n-1} - 1}{\varepsilon - 1} = \frac{\varepsilon^n - 1}{\varepsilon - 1},$$

hence

$$Q = S_1 \frac{1}{\varepsilon^{n-1}} \frac{\varepsilon^n - 1}{\varepsilon - 1},$$

or

$$S_1 = \frac{Q}{\frac{1}{\varepsilon^{n-1}} \frac{\varepsilon^n - 1}{\varepsilon - 1}}.$$

Since $Z = S_1\varepsilon$ and $n = z$ the resultant efficiency of the pulley system will be

$$\eta_\Sigma = \frac{Q}{Zz} = \frac{Q}{\frac{Q}{\frac{1}{\varepsilon^{n-1}} \frac{\varepsilon^n - 1}{\varepsilon - 1} \varepsilon z}} = \frac{1}{\varepsilon^{n-1}} \frac{\varepsilon^n - 1}{\varepsilon - 1} = \frac{1}{\varepsilon^z} \frac{\varepsilon^z - 1}{\varepsilon - 1}. \tag{39}$$

The pulling force (effort)

$$Z = S_1 \varepsilon = \frac{Q\varepsilon}{\frac{1}{\varepsilon^{n-1}} \frac{\varepsilon^n - 1}{\varepsilon - 1}} = Q\varepsilon^n \frac{\varepsilon - 1}{\varepsilon^n - 1} = Q\varepsilon^z \frac{\varepsilon - 1}{\varepsilon^z - 1}. \tag{40}$$

The path of the applied effort for the given pulley system is

$$s = zh$$

and the speed of the rope

$$c = zv,$$

where h — path and v — speed of the load.

Designs with the Rope Running off a Movable Pulley. With z pulleys (Fig. 43*b*) the number of parts of the rope on which the load is suspended will be $z + 1$.

The transmission ratio

$$i = z + 1.$$

The ideal effort on the running off part of the rope is

$$Z_0 = \frac{Q}{z + 1}.$$

The actual effort is

$$Z = \frac{Q}{\eta_\Sigma (z + 1)}.$$

Employing the expression obtained previously we have

$$S_1 = \frac{Q}{\frac{1}{\varepsilon^{n-1}} \frac{\varepsilon^n - 1}{\varepsilon - 1}}.$$

For $Z = S_1$ we shall have

$$\eta_\Sigma = \frac{Q}{Z(z + 1)} = \frac{Q}{\frac{Q}{\frac{1}{\varepsilon^{n-1}} \frac{\varepsilon^n - 1}{\varepsilon - 1} (z + 1)}} = \frac{1}{z + 1} \frac{1}{\varepsilon^{n-1}} \frac{\varepsilon^n (\varepsilon - 1)}{\varepsilon - 1}. \tag{41}$$

Since in this case $n = z + 1$ the final formulas will have the following form:

$$\eta_\Sigma = \frac{1}{\varepsilon^z (z + 1)} \frac{\varepsilon^{z+1} - 1}{\varepsilon - 1}; \tag{42}$$

$$Z = Q\varepsilon^z \frac{\varepsilon - 1}{\varepsilon^{z+1} - 1}; \tag{43}$$

$$s = h(z + 1); \quad c = v(z + 1).$$

This case is met with most frequently in hoisting machinery.

With a factor of resistance $\varepsilon = 1.05$, the efficiency curve for various numbers of pulleys is shown in Fig. 44.

Approximate Determination of Tension in the Individual Rope Parts of a Pulley System. The tension in the rope will be minimum in the first part and maximum in part $(z + 1)$ (Fig. 45) where z is the number of pulleys. It can be assumed approximately that

$$\left.\begin{aligned} S_1 = \frac{Q}{z+1};\ S_2 = \varepsilon S_1 = \varepsilon \frac{Q}{z+1};\ S_3 = \varepsilon S_2 = \varepsilon^2 \frac{Q}{z+1};\ \\ S_{z+1} = \varepsilon S_z = \varepsilon_z \frac{Q}{z+1} = Z. \end{aligned}\right\} \quad (44)$$

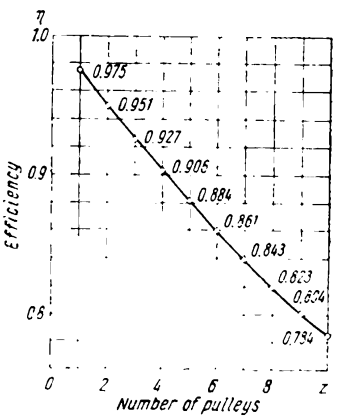

Fig. 44. Efficiency of pulley systems

In hoisting mechanisms of winches and cranes the pulling force (effort) $Z = S_{z+1}$ usually equals the tension of the rope coiled around the drum.

Multiple Pulley Systems. The following shortcomings due to direct suspension of loads from the rope end or from employing simple pulleys for a gain in force in hoisting appliances can be pointed out:

1) the rope parts are in one plane and this may cause the load to sway;

2) large diameters of ropes and pulleys;

3) the load being lifted moves in a horizontal direction because a rope coiling on a drum moves along its length.

These shortcomings can be avoided, especially in the hoisting mechanisms of winches and cranes with an electric drive, by using multiple pulley systems which raise the load in a strictly vertical direction and keep it more stable. These systems carry the load with twice as many parts as a similar simple pulley system.

Moreover, one of the main reasons for the use of multiple pulleys is dictated by

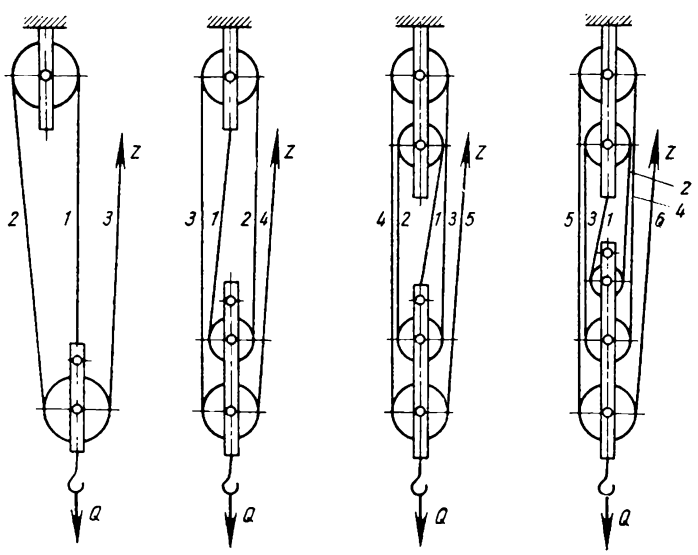

Fig. 45. Pulley systems for a gain in force

the necessity to reduce the load acting on the ropes enabling thinner, less expensive ropes and pulleys and drums with smaller diameters to be employed. This reduces the size and weight of the entire mechanism.

Fig. 46 illustrates multiple crane pulley systems for a gain in force. They are designed by combining simple pulleys with the two ends of the rope secured on a drum or on drums with right- and left-hand helical grooves. The rope passes from

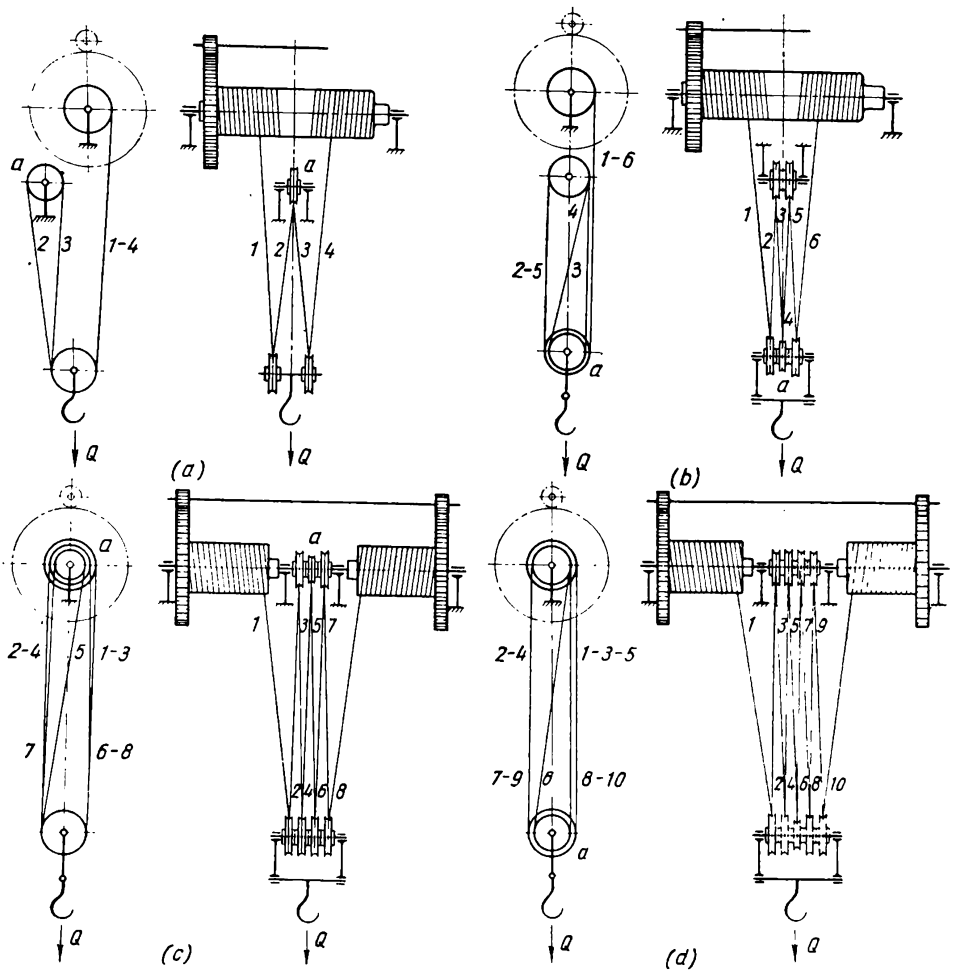

Fig. 46. Multiple pulley systems

one half of the pulley system to the other by means of a compensating pulley *a* which simultaneously equalises the lengths of the rope parts when they stretch nonuniformly.

A multiple pulley system with four parts (Fig. 46*a*) is used to carry loads of up to 25 tons. The transmission ratio i equals 2. The length of the rope being wound around each half of the drum $l = 2h$ (h — lifting height). The rope speed is $c = 2v$ and the efficiency $\eta \approx 0.94$.

A multiple pulley system with six parts (Fig. 46*b*) is used less frequently. In it $i = 3$; $l = 3h$; $c = 3v$ and $\eta \approx 0.92$.

A multiple pulley system with eight parts (Fig. 46*c*) usually carries loads weighing up to 75 tons. It has $i = 4$; $l = 4h$; $c = 4v$ and $\eta \approx 0.9$.

A multiple system with ten parts (Fig. 46*d*) lifts up to 100 tons. Here $i = 5$; $l = 5h$; $c = 5v$ and $\eta \approx 0.87$.

To raise loads over 100 tons use is made of pulley systems with twelve carrying parts.

In the general case, the ratio of a multiple pulley equals

$$i = \frac{z}{2}$$

where z—number of the carrying rope parts in the pulley system.

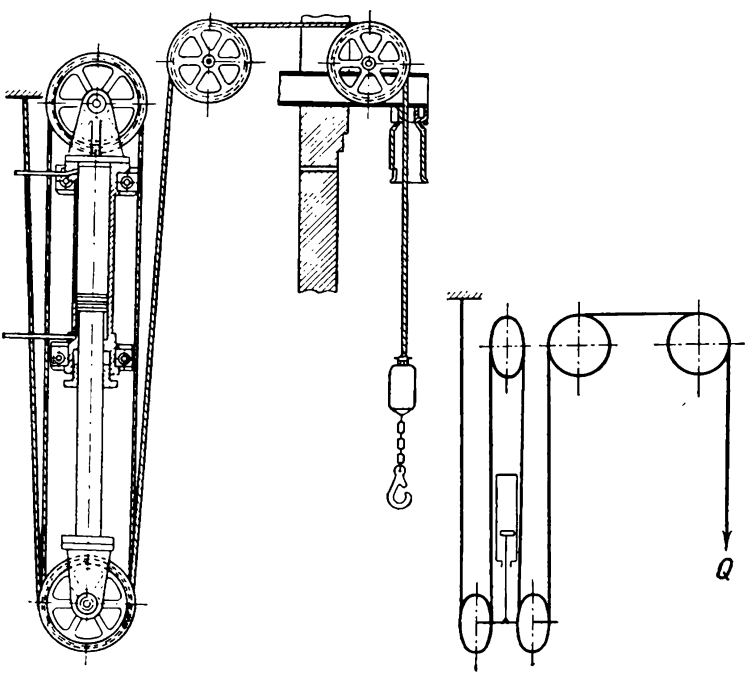

Fig. 47. Pulley system for a gain in speed

Pulley Systems for a Gain in Speed. As has been noted above, pulley systems for a gain in speed are used mainly in hydraulic and pneumatic lifts to move the load faster than the piston. Fig. 47 shows a general view and line diagram of a hydraulic lift pulley. Its ratio is

$$i = \frac{1}{4}.$$

3. DESIGN OF CHAIN AND ROPE SHEAVES AND SPROCKETS

Sheaves for Welded Chains. These sheaves of movable or fixed design are mainly used in hand-driven hoists and winches although sometimes they are employed for power-driven devices. The grooved rim, ordinarily of cast iron, is either flanged or flat (Fig. 48*a*). Since the rim is not machined the chain fits in the groove with a clearance. The diameter of a chain sheave for hand-driven mechanisms is selected from the ratio $D \geqslant 20d$ where d is the diameter of the chain bar.

For a power drive $D \geqslant 30d$.

The sheaves are usually mounted freely on their axles. Due to the low speed, sheave hubs are designed without bronze bushing.

The efficiency of a chain sheave is equal to $\eta \sim 0.95$.

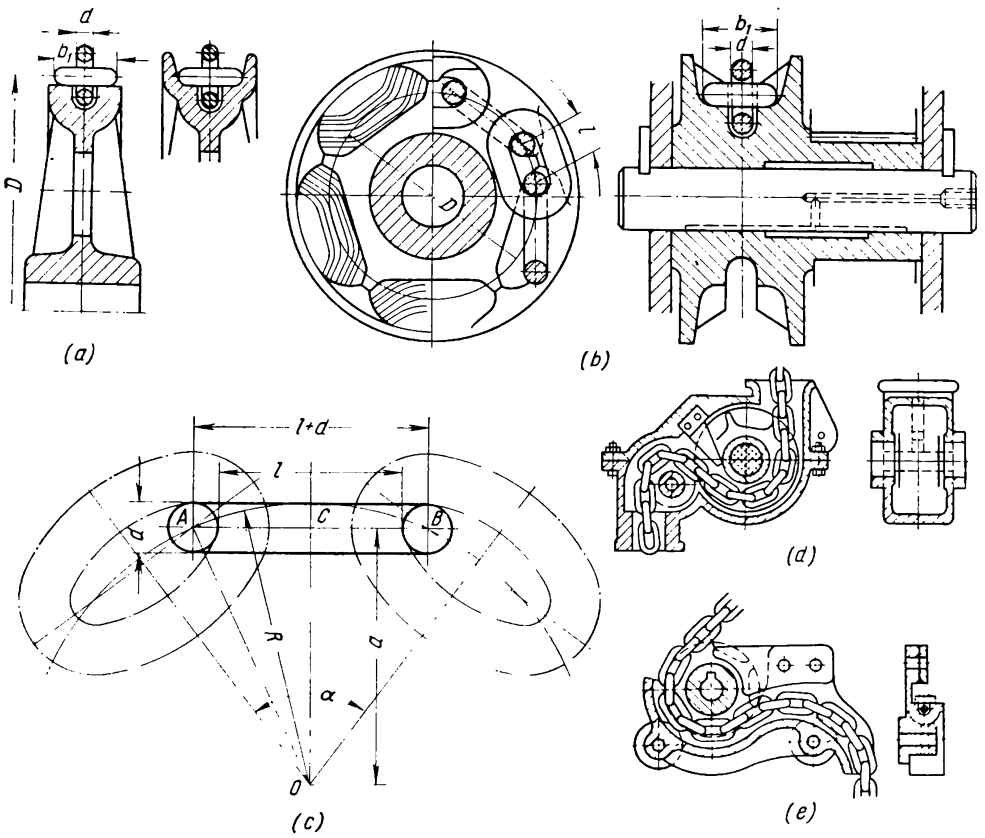

Fig. 48. Sheaves and sprockets for welded chains

The resistance of welded chains running over sheaves to bending is ordinarily determined from the formula:

$$W = Q \frac{d}{R} \mu \tag{45}$$

where R — radius of the sheave;
μ — coefficient of friction in the link joints ($\mu \approx 0.1$ to 0.2);
Q — tension in the chain.

Sprockets for Welded Chains. They are used as driving chain wheels of hand-operated hoists and winches. Sprockets for welded chains (Fig. 48*b*) are grey iron castings moulded to precise patterns (only in special cases are they made of steel castings). Around the periphery the sprockets are provided with pockets which fully conform in shape and size to the oval links of the chain. The sprocket catches the running-on chain and the links seat in the pockets, thereby preventing the chain from slipping off the rim. As a rule, sprockets are manufactured with a small number of teeth and are small in size ensuring compactness and low cost of the driving mechanism.

Considerable frictional resistance is observed when the chain runs over the sprocket. This decreases the efficiency and leads to wear of the chain and sprocket. Both chain and sprocket should therefore be regularly greased.

The efficiency is $\eta \approx 0.93$. The resistance to bending of the chain is determined in the same way as for chain sheaves, according to formula (45), taking a somewhat higher coefficient of friction μ.

The diameter of the sprocket can be found as follows.

From triangle AOC (Fig. 48*c*):

$$AO = \sqrt{CO^2 + AC^2}$$

or

$$R = \sqrt{a^2 + \left(\frac{l+d}{2}\right)^2}.$$

The angle $\alpha = \frac{360^\circ}{z}$ where z is the number of teeth.

Expressing the value of a through α, l and d, and after algebraic transformations, we obtain

$$2R = D = \sqrt{\left(\frac{l}{\sin\frac{90^\circ}{z}}\right)^2 + \left(\frac{d}{\cos\frac{90^\circ}{z}}\right)^2} \qquad (46)$$

where l — inside length of the link;
d — diameter of the chain bar;
z — number of sprocket teeth; the minimum number of teeth $z = 4$.

To protect chains against rapid wear provision should be made for as many teeth as possible.

If the number of teeth is large ($z > 9$) and the diameter of the chain bar is sufficiently small ($d = 16$ mm) the second term under the radical in formula (46) can be neglected and the diameter of the sprocket determined from the formula:

$$D \approx \sqrt{\left(\frac{l}{\sin\frac{90^\circ}{z}}\right)^2} = \frac{l}{\sin\frac{90^\circ}{z}}. \qquad (47)$$

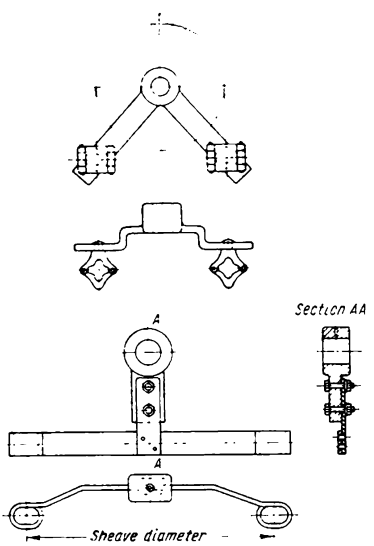

Fig. 49. Guide straps for welded chains

Sprockets with high flanges (Fig. 48*b*) are the most popular type. Usually a sprocket is freely mounted on the axle and the driving gear or worm wheel is keyed on its elongated hub. The arc of contact between the sprocket and chain should be at least 180°. If the arc is less the device is provided with a chain guide (Fig. 48*d*) or a guide block (Fig. 48*e*). Special guide straps are often used for hand-driven traction chains (Fig. 49) which are freely mounted on an axle and prevent the chain from slipping off the sprocket.

Sprockets for Roller Chains. These sprockets are used as driving chain wheels for hand-operated hoists and winches with a lifting capacity over 10 tons. Depending on the design of this type of mechanism the sprockets are either fitted on a shaft or made integral with the shaft or else they are freely mounted on a fixed axle (Fig. 50).

Sprockets are manufactured from cast iron, forged steel or steel castings. The sprocket teeth are always milled. The efficiency with regard for the friction in the bearings is $\eta \approx 0.95$.*

* Resistance of roller chains on sprockets to bending is determined from the formula $W = Q \frac{\delta}{R} \mu$ where δ — diameter of the roller pins; μ — coefficient of friction ($\mu \approx 0.08$ to 0.1) and R — radius of the sprocket.

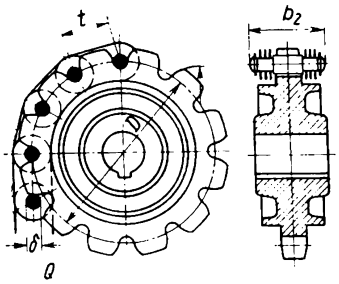

If we denote by z the number of teeth and by t the chain pitch then the diameter of the pitch circle can be determined as follows:

From the triangle AOC (Fig. 50) we have

$$\overline{AO} = \frac{\overline{AC}}{\sin\frac{\alpha}{2}};\quad 0.5D = \frac{0.5t}{\sin\frac{\alpha}{2}} \text{ but } \alpha = \frac{360^\circ}{z};$$

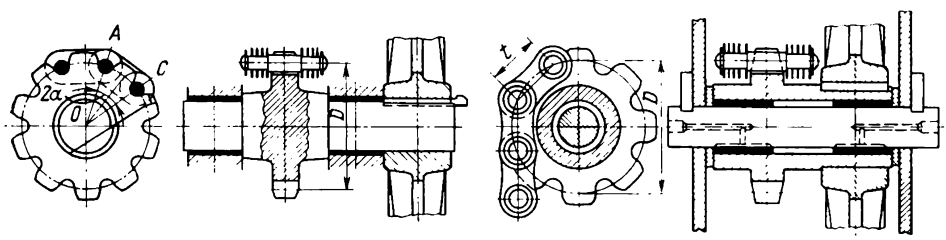

Fig. 50. Sprockets for roller chains

therefore

$$0.5\,D = \frac{0.5t}{\sin\frac{180^\circ}{z}}$$

or

$$D = \frac{t}{\sin\frac{180^\circ}{z}}. \tag{48}$$

Contrary to toothed gears the pitch is measured here along a chord. The minimum number of teeth is usually $z = 8$.

To ensure safe operation, sprockets for roller chains are sometimes enclosed in special housings (Fig. 51) which serve as guides and prevent the chain from slipping off. In hoists and hand winches with a small lifting height the free end of the chain is fastened to their frames. This reduces by one half the length of the hanging part of the chain when the load is in the extreme upper position. If the load is to be raised very high the winches are equipped with a special chain collector (Fig. 52). For this purpose pins with elongated journals are inserted into the chain at definite intervals; when the chain runs off, the extended pins rest on inclined guideways made from two angles and uniformly collect the long end of the chain.

Rope Sheaves. Rope sheaves may be of a fixed, movable and compensating design. They are usually made in the form of a casting (grey iron or steel) or weldment.

The efficiency is $\eta \approx 0.96$ to 0.97 with account taken of friction in the bearings.

The diameter of sheaves for hemp ropes should not be less than $10d$ where d is the diameter of the rope. For wire ropes the minimum diameter of the sheaves is determined from formula (18a). The periphery of the rim should be such that the rope does not jam in the groove and can deviate sufficiently from the central plane of the sheave.

In order to provide for rope run-off at a tangent to the side of a deep groove without a sharp bend (fleet angle α), the central point ε of the rope cross-section should be inside the groove (Fig. 53). The permissible fleet angle α is found from the formula

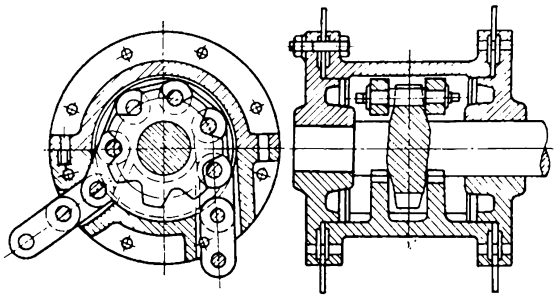

Fig. 51. Housing for the sprockets of roller chains

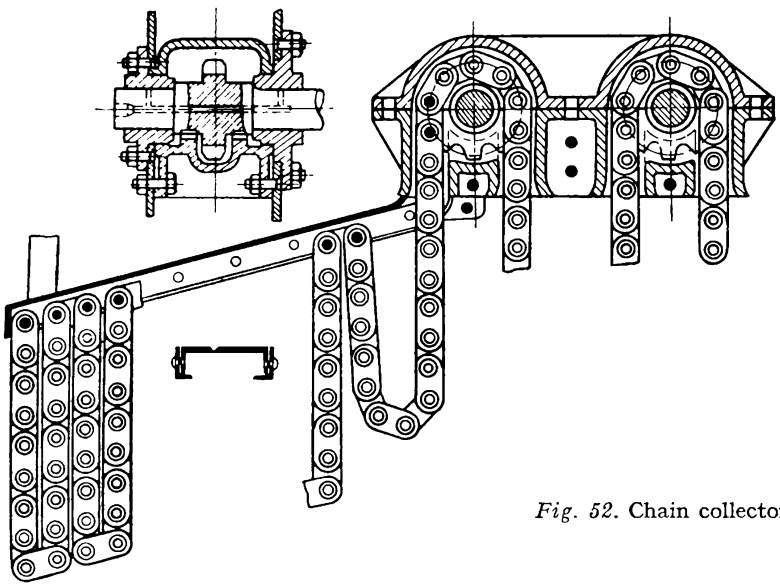

Fig. 52. Chain collector

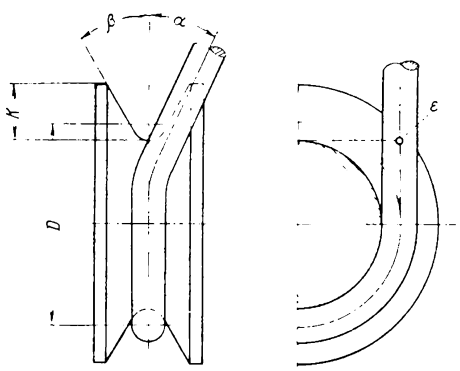

Fig. 53. Fleet angle of a running-off rope

$$\tan \alpha_{max} < \frac{2 \tan \beta}{\sqrt{1 + \frac{D}{0.7k}}}. \tag{49}$$

The cross-section of sheave rims for steel wire ropes as specified by Soviet Standards is illustrated in Table 16.

Table 16

Grooves of Sheaves for Steel Wire Ropes, mm

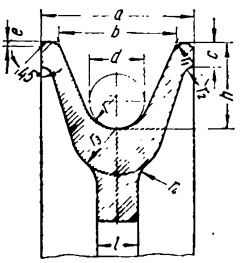

Rope dia	*a*	*b*	*c*	*e*	*h*	*l*	*r*	r_1	r_2	r_3	r_4
4.8	22	15	5	0.5	12.5	8	4.0	2.5	2.0	8	6
6.2	22	15	5	0.5	12.5	8	4.0	2.5	2.0	8	6
8.7	28	20	6	1.0	15.0	8	5.0	3.0	2.5	9	6
11.0	40	30	7	1.0	25.0	10	8.5	4.0	3.0	12	8
13.0	40	30	7	1.0	25.0	10	8.5	4.0	3.0	12	8
15.0	40	30	7	1.0	25.0	10	8.5	4.0	3.0	12	8
19.5	55	40	10	1.5	30.0	15	12.0	5.0	5.0	17	10
24.0	65	50	10	1.5	37.5	18	14.5	5.0	5.0	20	15
28.0	80	60	12	2.0	45.0	20	17.0	6.0	7.0	25	15
34.5	90	70	15	2.0	55.0	22	20.0	7.0	8.0	28	20
39.0	110	85	18	2.9	65.0	22	25.0	9.0	10.0	40	30

Small sheaves are usually cast in one piece without ribbing. Large sheaves are provided with ribs and holes or with cross-shaped spokes (Fig. 54*a*).

Fig. 54*b* shows a welded rope sheave.

As a rule, sheaves are freely mounted on fixed axles on antifriction bearings or bronze bushings. If several sheaves are mounted on a single axle each sheave should be provided with a separate lubricating facility.

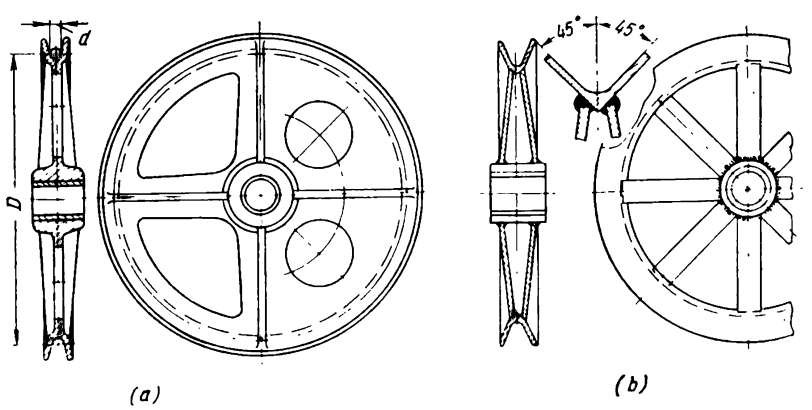

Fig. 54. Rope sheaves

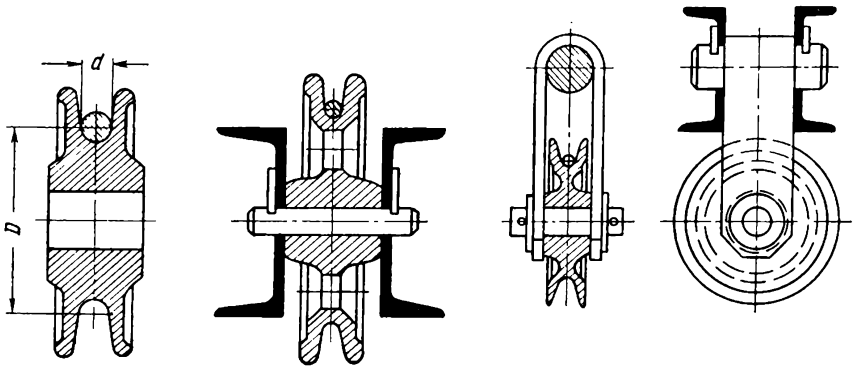

Fig. 55. Compensating sheaves

The diameters of compensating sheaves (Fig. 55) may be taken 40 per cent smaller than the diameters of the sheaves carrying the load. The ratio between the hub length and the diameter of the axle of working sheaves is usually taken within the range: $\frac{l}{d} = 1.5$ to 1.8.

Lubricant should be fed to the unloaded part of the bearing surface in the sheave. The bushings of the sheaves can be checked for unit pressure by the formula

$$p = \frac{Q}{ld} \tag{50}$$

where l — length of the bushing;
d — diameter of the sheave axle;
Q — acting load.

Depending on the peripheral velocity of the sheave hub hole surface, unit pressures should not exceed the following values:

v in m/sec	0.1	0.2	0.3	0.4	0.5	0.6	0.7	0.8	0.9	1.0	1.1	1.2	1.3	1.4	1.5
p in kg/cm²	75	70	66	62	60	57	55	54	53	52	51	50	49	48	47

4. CHAIN AND ROPE DRUMS

Chain Drums. These drums are used only in exceptional cases for hand-operated rotary cranes with a lifting capacity of up to 5 tons. Taking into account the friction in the bearings, the efficiency of the drum is $\eta = 0.94$ to 0.96. The material is cast iron. The diameter of the drum $D \geqslant 20d$ (d — diameter of the chain bar).

As a rule, drums for welded chains are provided with helical grooves (Fig. 56*a*) to guide the chain in coiling. The pitch of the groove $s = b + (2 \text{ to } 3)$ mm where b is the outside width of the chain link. The width of groove $c \approx 1.2d$. The number of threads is determined by the length of the chain being wound. To relieve the fastening of the chain end (Fig. 56*b*) provision should be made for at least 1½ holding turns.

The chain (or rope) during operation should not deflect from the direction of the helix by more than 1:40 for a plain drum and 1:10 for a drum with a helical groove. The height of the side flanges l should not be less than the width of link b.

Since during rotation of the drum the chain either runs on or off, the value of harmful resistances due to bending can be assumed 100 per cent less than in sheaves (where both running on and off takes place) and formula (45) assumes a somewhat different form

$$W = Q \frac{d}{2R} \mu. \tag{45a}$$

The wall thickness of a cast-iron chain drum can be found from the following empirical formula:

$$w = (0.75 \text{ to } 1.3)d \text{ cm}$$

where d — diameter of the chain bar.

The wall thickness at the weakest place should not be less than 15-20 mm.

Rope Drums. Drums for hemp ropes are usually of the plain type with high flanges to enable the rope to be wound in several layers. This enables the length of the drum to be reduced considerably. The drum diameter is selected from the same ratios as the diameter of sheaves: $D \geqslant 10d$.*

Drums for steel wire ropes are made of cast iron, more rarely of steel castings or weldments. With regard to friction in the bearings the efficiency is $\eta \approx 0.95$. The drum diameter depends on the diameter of the rope. With a power drive the drum should always be provided with helical grooves so that the rope winds up uniformly and is less subject to wear (Fig. 57*a*). The radius of the helical grooves should be selected so as to prevent jamming of the rope. Table 17 lists the dimensions of standard and deep grooves for drums.

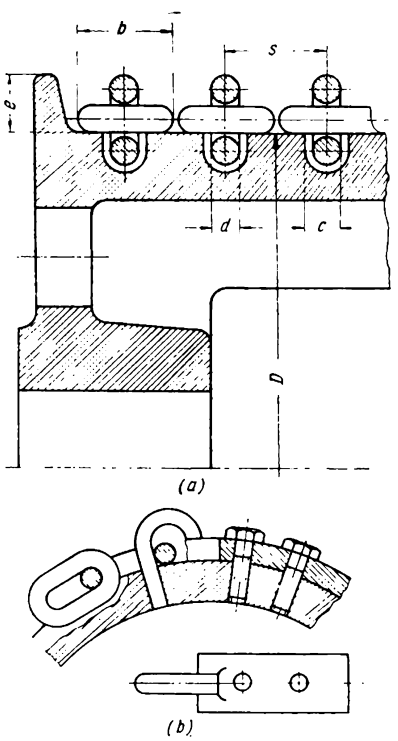

Fig. 56. Chain drum

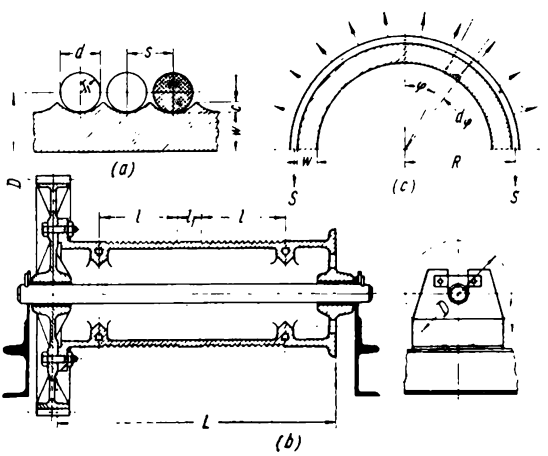

Fig. 57. Helical grooves in rope drums

Drums with one coiling rope have only one helix — right-hand; drums designed for two rope members (Fig. 57*b*) are provided with two helices — right-hand and left-hand. The number of turns on the drum for one rope member is

$$z = \frac{Hi}{\pi D} + 2 \tag{51}$$

where i — ratio of the pulley system;

D — drum diameter;

H — height to which the load is raised; the figure 2 is added to account for the holding turns.

This standard is applied to cast crane drums.

* In multi-layer winding the flanges of the drum should extend above the upper layer of rope by at least one rope diameter.

Table 17

Dimensions of Drum Grooves (in mm)

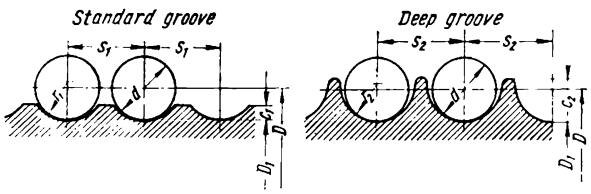

Rope dia d	r_1	Standard groove		Deep groove			Rope dia d	r_1	Standard groove		Deep groove		
		s_1	c_1	s_2	c_2	r_2			s_1	c_1	s_2	c_2	r_2
4.8	3.5	7	2	9	4.5	1.0	19.5	11.5	22	5	27	13.5	2.0
6.2	4.0	8	2	11	5.5	1.5	24.0	13.5	27	6	31	16.0	2.5
8.7	5.0	11	3	13	6.5	1.5	28.0	15.5	31	8	36	18.0	2.5
11.0	7.0	13	3	17	8.5	1.5	34.5	19.0	38	10	41	22.0	3.0
13.0	8.0	15	4	19	9.5	1.5	39.0	21.0	42	12	50	24.5	3.5
15.0	9.0	17	5	22	11.0	2.0							

The length of the helix on the drum

$$l = zs$$

where s — pitch.

Leaving a length of about $5s$ for holding the rope and for both side flanges we obtain the full length of the drum

$$L = \left(\frac{Hi}{\pi D} + 7\right)s. \tag{52}$$

If two rope members are coiled on the drum (multiple pulley system) the full length of the drum will be

$$L = \left(\frac{2H_i}{\pi D} + 12\right)s + l_1 \tag{53}$$

where l_1 is the space in the middle of the drum, between the right- and left-hand helices, dictated by the design. Since space for two holding turns should be provided on each side, and taking $4s$ for the rope fastening on each side and for the side flanges, we shall obtain $12s$ for both sides. This feature has been taken into account in formula (53).

The wall thickness of a cast-iron drum can be found approximately from the following empirical formula:

$$w = 0.02D + (0.6 \text{ to } 1.0) \text{ cm} \tag{54}$$

where D — drum diameter.

During operation the drum is subject to the combined action of torsion, bending and compression. The first two strains produce an appreciable stress only in very long drums.

The effect of compression is much larger and for this reason it should be checked first.

Let us assume that we separate from the body of the drum a half-ring with a thickness w (Fig. 57*c*) and with a width equal to the rope pitch s. The effect of the separated half-ring will be replaced by the tension forces of the rope $2S$.

The force bearing on an element of area $dF = Rd\varphi s$ amounts to

$$dS = Rd\varphi sp$$

where p is normal pressure on a unit of drum surface.

The sum of the projections of all elementary forces on a vertical plane will be

$$2S = 2\int_0^{\frac{\pi}{2}} Rd\varphi sp \cos\varphi = 2Rsp\int_0^{\frac{\pi}{2}} \cos\varphi\, d\varphi = 2Rsp$$

whence

$$p = \frac{S}{Rs} = \frac{2S}{Ds}.$$

Since the surface of the drum is subject to the action of uniformly distributed forces with the intensity p, the drum can be likened to a cylinder with an external pressure in whose walls the stress is determined from the well-known Lamé formulas.

The stress at the inner surface of a cylinder according to Lamé is

$$\sigma_{in} = p_{in}\frac{D^2 + d^2}{D^2 - d^2} - 2p_{out}\frac{D^2}{D^2 - d^2}$$

and at the outer surface

$$\sigma_{out} = 2p_{in}\frac{d}{D^2 - d^2} - p_{out}\frac{D^2 + d^2}{D^2 - d^2}.$$

When $p_{in} = 0$, $p_{out} = p$ and $d = D - 2w$, we can obtain, after appropriate transformations, the maximum compressive stress at the inner surface of the drum

$$\sigma_{max} = \frac{SD}{(D - w)ws}.$$

Assuming the fraction $\frac{D}{D-w} \approx 1$ we obtain a formula ordinarily used for the calculations

$$\sigma_{comp} = \frac{S}{ws}. \qquad (55)$$

The permissible value of σ_{comp} for grade 15-32 cast iron is up to 1,000 kg/cm²; for steel castings — up to 1,600 kg/cm²; for welded drums (steel 3 and 5) — up to 1,800 kg/cm².

When calculating the drum for complex stresses due to the joint action of bending and torsion, the permissible stress σ_{bend} can be taken for grey iron castings at not over 230 kg/cm², for steel castings not over 1,200 kg/cm² and for welded drums not over 1,400 kg/cm².

Fastening Ropes on Drums. Fastening by means of set screws is shown in Fig. 58*a*. A cored opening is provided in the body of the cast drum for the end of the rope. Inserted in this opening is plate *b* with a lug and with a semicircular groove on the inner side shaped to conform with the cross-section of rope *a*. The plate is drawn tight with two screws *c*.

This adjustable fastening enables the rope to be quickly replaced. When two ropes are being coiled on the drum the fastening is duplicated for safety (Fig. 57*b*).

A wedge fastening is shown in Fig. 58*b*. Rope *a* is passed around steel wedge *b* and inserted together with it into the opening in the drum body. The opening should be tapered from both sides to the middle so that the wedge can be inserted from either side.

Fastening with the aid of plates is performed according to State Standards. This most widespread method of fastening is extremely reliable and convenient. A steel plate is provided on the inner side with two grooves for the rope and, in between, with a hole for a screw or stud.

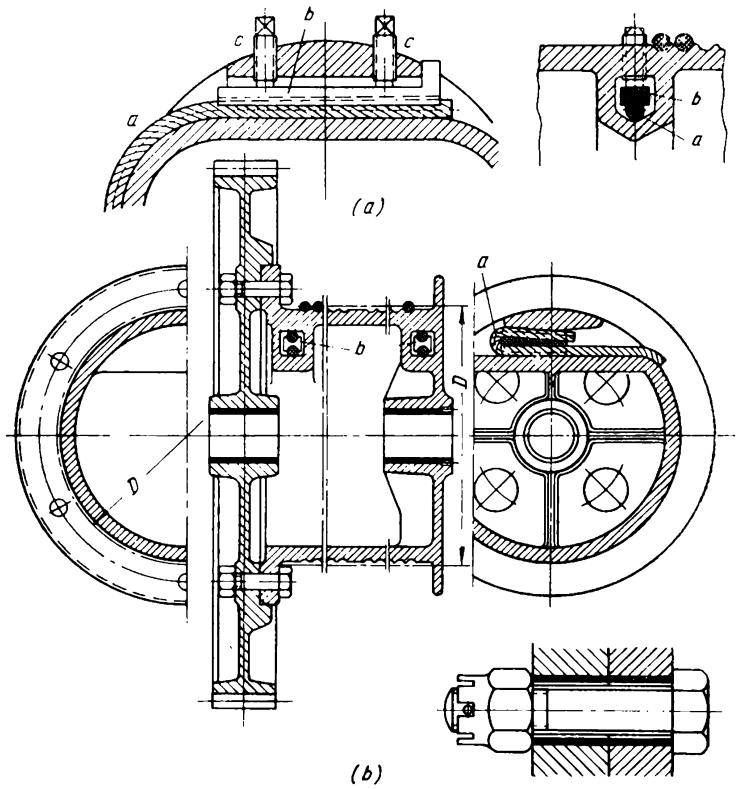

Fig. 58. Fastening ropes on drums

The crest of the groove for the fastening screws is made over half the circumference. The rope is secured with two plates as shown in Table 18.

Friction Drums for Ropes. Friction drums are rope driving drums in which motion is transmitted to the rope by friction between the rope and drum.

Friction drums have the advantage of being able to raise loads to great height. They can also be used with winches to move railway cars and whole trains.

Fig. 59*a* shows a simple friction drum and Fig. 59*b*—a drive with two friction drums. Simple friction drums are provided with helical grooves for the rope which coils around them in one or several turns. In a double-drum drive the rope usually beds in annular grooves. The ratio between the tensions of the oncoming and running-off parts of the rope in a simple drum (Fig. 59*a*) is expressed by Euler's formula

$$S_1 : S_2 = e^{\mu 2\pi n} \tag{56}$$

where S_1—tension in the oncoming part of the rope;
S_2—tension in the running-off part of the rope;
n—number of the rope turns;
e—base of Napierian logarithms;
μ—coefficient of friction. For wire ropes and cast-iron drums it can be taken approximately as $\mu = 0.15$.

The peripheral force on the drum is

$$P = S_1 - S_2. \tag{57}$$

In a simple friction drum (Fig. 59*a*) the rope shifts along the drum axis. The number of grooves and, hence, the width of the drum should correspond to the axial shift of the rope.

Table 18

Soviet Standards for Fastening Steel Wire Ropes to Drums

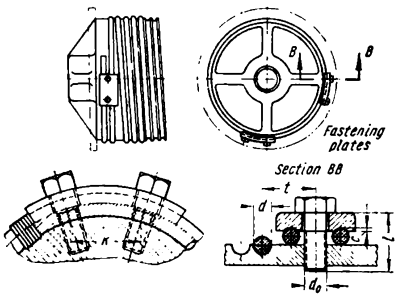

Rope dia, mm	Locating dimensions, mm		Screw size		Plate		Rope dia, mm	Locating dimensions, mm		Screw size		Plate	
	k	*t*	d_0	*l*	*c*, mm	Number of fastenings		*k*	*t*	d_0	*l*	*c*, mm	Number of fastenings
4.8 6.2	28	19	8	20	2	1	19.5 20.5 21.5	58	53	22	60	8	1
7.7 8.7	34	25	10	30	4	1	23 24 26	78	60	22	60	10	1
11 13	52	35	16	45	5	1							
15 17.5 18	53	43	18	50	7	1	28 28.5 30 31	78	70	27	75	12	1
							32.5 33.5 34.5 36	100	85	30	100	14	2

Simple friction drums are employed for the drives of trucks in rotary cranes with a variable radius (usually two turns), load transfer bridges, cable cranes, etc.

In a double-drum friction drive (Fig. 59*b*) the rope is wound several times around two parallel drums revolving in the same direction and actuated by a single motor. The tension in the parts of the rope is:

$$S_2 = \frac{S_1}{e^{\mu\alpha}\eta_1}\ ;\ S_3 = \frac{S_1}{e^{\mu 2\alpha}\eta_1^2};\ \ldots S_{n+1} = \frac{S_1}{e^{\mu n\alpha}\eta_1^n} \qquad (58)$$

where S_1—tension in the oncoming part of the rope;
S_2, S_3—tension in intermediate parts of the rope;
S_{n+1}—tension in the running-off part;
α-π—arc of contact of the rope on one drum;
n—bearing areas in contact between the rope and both drums;
η_1—efficiency taking into account the rigidity of the rope in one encirclement (disregarding losses in the bearings); $\eta_1 \approx 0.995$.

The total peripheral force of both drums is

$$P = S_1 - S_{n+1}.$$

The load on drum shaft *I* is

$$Q_1 = S_1 + S_2 + S_3 + \ldots S_n.$$

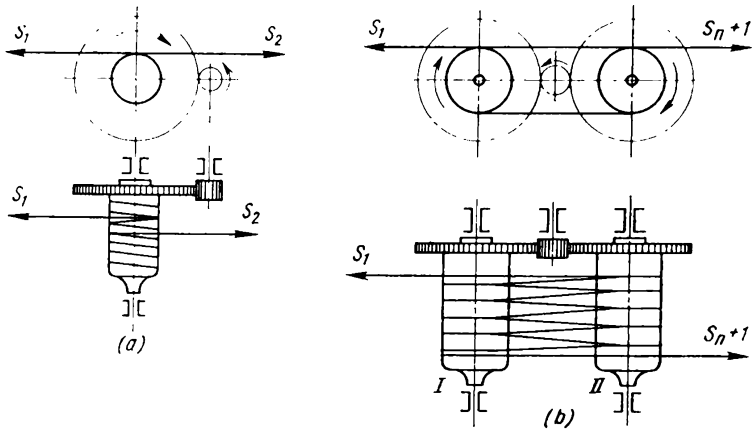

Fig. 59. Friction drums

The load on drum shaft *II* is

$$Q_2 = S_2 + S_3 + \ldots S_{n+1}.$$

Losses in the bearings are

$$W = (Q_1 + Q_2)\mu_1 \frac{d}{D}$$

where μ_1—coefficient of friction in the bearings;
d—diameter of the bearing journal;
D—drum diameter.

The total efficiency of the drive is

$$\eta = \frac{S_1}{P + W}.$$

The axles of friction drums can be relieved from high radial pressures by means of special rims which run on rollers carrying these radial forces.

Capstans. In electric capstans used to move railway cars the barrels are usually arranged vertically. The rope is attached to the car by means of a hook. During operation the rope winds around the capstan barrel which revolves to take on the rope. The effort in the running-off part of the rope held by the operator (Fig. 60*a*) is

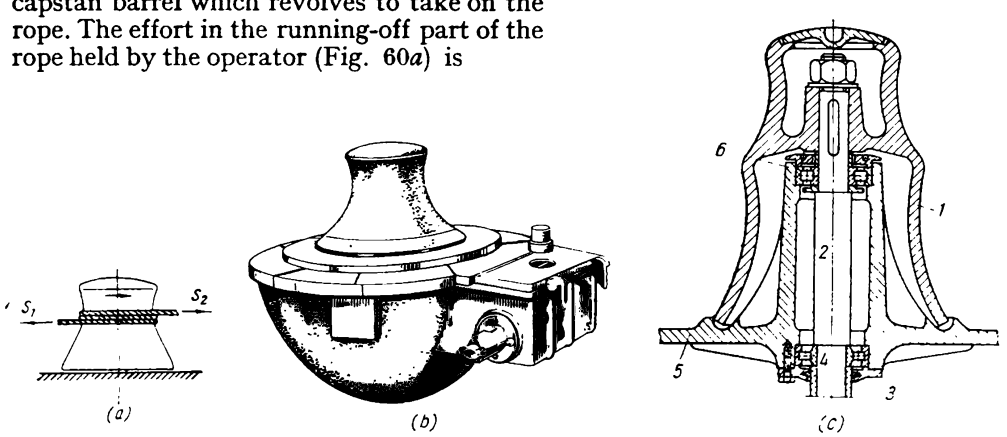

Fig. 60. Capstans:
1—barrel, *2*—shaft, *3*—felt sealing ring, *4*—roller bearing (self-aligning), *5*—housing cover, *6*—radial-thrust roller bearing

$$S_2 = \frac{S_1}{e^{\mu 2\pi n}}$$

where n is the number of turns.

The coefficient of friction is $\mu = 0.1$ to 0.3. The peripheral force is $P = S_1 - S_2$.

The barrel (Fig. 60*b*) is fitted onto a vertical shaft running in bearings and actuated by a drive motor through gearing.

The overhang of the shaft is reduced by a special casting made integral with the housing cover and inserted into the barrel. This casting accommodates bearings supporting the shaft (Fig. 60*c*).

Since the walls of the capstan barrel are inclined, an axial downward force always arises. It is carried by a thrust bearing. The design of the drum provides therefore for a self-aligning lower roller bearing and a flanged upper bearing carrying both radial and axial forces.

When two speeds of the rope movement are required use is made of drums with a double barrel (Fig. 60*c*).

Below are given several examples of rope selection calculations.

Example 1. Select by calculations the ropes, pulleys and drum required for an electric overhead travelling crane with a lifting magnet.

Given: Lifting capacity $Q = 5{,}000$ kg, lifting height $H = 8$ metres, medium service duty, weight of the lifting magnet $G = 2{,}000$ kg, number of rope parts $z = 4$.

1. The maximum tension in the rope. In a multiple pulley system with two movable sheaves and four parts of the rope (Fig. 46*a*) the tension in one part will be

$$S = \frac{(Q + G + G_0)}{z\eta_p}$$

There G_0—weight of the lifting tackle, 120 kg;
η_p—efficiency of the pulley system, 0.94, i.e.,

$$S = \frac{(5{,}000 + 2{,}000 + 120)}{4 \times 0.94} \sim 1{,}900 \text{ kg.}$$

Since the lifting height is small we disregard the weight of the rope.

2. The number of rope bends and the ratio $\frac{D_{min}}{d}$. According to Fig. 23 the number of bends for a pulley system in diagram *A* will equal $n = 3$. From Table 7 and with $n = 3$ $\frac{D_{min}}{d} = 23$.

3. The rope cross-section. Taking the design of the rope with the number of wires $i = 222$, we obtain from formula (13)

$$F_{(222)} = \frac{S}{\frac{\sigma_b}{\varphi} - \frac{d}{D_{min}} \times 36{,}000} = \frac{1{,}900}{\frac{1{,}500}{4} - \frac{1}{23} \times 36{,}000} \approx 0.87 \text{ sq cm.}$$

Breaking strength $\sigma_b = 15{,}000$ kg/cm², safety factor for overhead travelling cranes—according to Table 9 is $\varphi = 4$.

4. Choice of rope. According to Soviet Standards the nearest value of the cross-sectional area F for a rope with 222 wires is 0.85 sq cm.

Therefore: rope diameter $d = 15$ mm; wire diameter $\delta = 0.7$ mm; weight of one linear metre of the rope $g = 0.77$ kg; breaking strength $\sigma_b = 15{,}000$ kg/cm²; breaking load of the rope $P = 10{,}500$ kg.

The rope should be checked by formula (18). The maximum permissible tension in the rope should not exceed

$$S = \frac{P}{K} = \frac{10{,}500}{5.5} = 1{,}910 \text{ kg;}$$

in our case the maximum tension is 1,900 kg, hence the choice of the rope was correct.

The following notation can be used for ordering the rope:
$6 \times 37 + 1$—15 — 150 (Soviet Standard).

5. Diameters of the drum and lower pulleys in the block frame. $D = 23d = 23 \times 15 = 345$ mm. From Table 9 the minimum diameter of pulleys and drums should equal $D = 25d$ or $D = 25 \times 15 = 375$ mm. We take $D = 400$ mm.

6. Diameter of the compensating pulley $D_1 = 0.6D$; $D_1 = 0.6 \times 400 = 240$ mm. We take $D_1 = 250$ mm.

7. Radius of grooves on the drum. In Table 18 a standard groove has $r_1 = 9$ mm.
8. Pitch of the groove helix on the drum. In Table 18 the pitch is $s = 17$ mm.
9. Number of turns on each side of the drum [formula (51)]

$$z = \frac{Hi}{\pi D} + 2 = \frac{8 \times 2}{3.14 \times 0.4} + 2 = 15 \text{ turns.}$$

10. Full length of the drum (formula 53)

$$L = \left(\frac{2Hi}{\pi D} + 12 \right) s + l_1 = [2(z - 2) + 12] s + l_1 = [2(15 - 2) + 12] \times 17 + 100 = 746 \text{ mm}$$

where l_1—free space between the right- and left-hand grooves (equal approximately to the distance between the lower pulleys of the block frame). We take $l_1 = 100$ mm.

11. The wall thickness of a cast-iron drum (formula 54) is
$w = 0.02D + 1$ cm $= 0.02 \times 40 + 1 = 1.8$ cm $= 18$ mm.
Test for compression stress (formula 55)

$$\sigma_{comp} = \frac{S}{ws} = \frac{1{,}900}{1.8 \times 1.7} = 620 \text{ kg/cm}^2,$$

which is permissible.

12. Choice of plates for fastening the rope ends to the drum. With a rope diameter of $d = 15$ mm the diameter of the holes for studs, according to Table 18, equals $d_0 = 18$ mm. The type of studs—M18 × 50. The other dimensions are also taken from Table 18.

Example 2. Select a wire rope for a travelling crane with a lifting capacity $Q = 10$ tons assuming the rope life equal to 12 months. The load is suspended on four rope parts. Medium service duty.

The tension P in one part of the rope is found from the formula

$$P = \frac{Q}{4\eta} = \frac{10{,}000}{4 \times 0.95} = 2{,}640 \text{ kg}$$

where η is the efficiency of the pulley system—equal to 0.95.

The magnitude of the full breaking load of the rope S can be found from the equation

$$S = PK = 2{,}640 \times 6 = 15{,}800 \text{ kg}$$

where K is the permissible factor of safety depending on the type of the lifting appliances and their duty. For the given case we take $K = 6$ ($K_{min} = 5.5$).

We choose the rope according to the State Standard: $6 \times 19 = 114$; it is a cross laid rope with $\sigma_b = 160$ kg/mm², $d = 17$ mm and $F = 108$ sq mm.

The actual tensile stress in the rope will be

$$\sigma = \frac{P}{F} = \frac{2{,}640}{108} = 24.4 \text{ kg/mm}^2.$$

The number of repeated bends z of the rope prior to its failure is found from formula (21):

$$z = az_2 N\beta\varphi = 3{,}400 \times 3 \times 12 \times 0.4 \times 2.5 = 122{,}400 \text{ bends}$$

where N—number of months the rope has been in operation (12); the values of a, z_2 and β are taken from Table 15.

The ratio $A = \frac{D}{d}$ is found from formula (19):

$$A = \frac{D}{d} = m\sigma CC_1C_2 + 8 = 0.905 \times 24.4 \times 1 \times 0.97 \times 1 + 8 = 29.4.$$

The values of factors m, C, C_1 and C_2 are taken from Tables 11 to 14, incl.
The drum diameter $D = 25d = 29.4 \times 17 = 500$ mm.

Example 3. Determine the life of a rope selected in Example 2 if the ratio $\frac{D}{d} = 27$.

We have from formula (19)

$$m = \frac{A - 8}{\sigma CC_1C_2} = \frac{27 - 8}{24.4 \times 1 \times 0.97 \times 1} = 0.8.$$

From Table 11 we find the number of repeated bends $z = 105{,}000$.
The rope life is found from formula (21)

$$N = \frac{z}{az_2\beta\varphi} = \frac{105{,}000}{3{,}400 \times 3 \times 0.4 \times 2.5} = 10.3 \text{ months.}$$

Example 4. Find the life of a Warrington-type rope, cross laid, with d = 17.5 and F = 104 sq mm rigged on a crane with a lifting capacity of Q = 10 tons, when $\frac{D}{d} = 27$.

The actual stress

$$\sigma = \frac{2{,}640}{104} = 26.4 \text{ kg/mm}^2;$$

$$m = \frac{A - 8}{\sigma C C_1 C_2} = \frac{27 - 8}{26.4 \times 0.63 \times 0.97 \times 1} = 1.17.$$

Hence, according to Table 11, $z = 168{,}000$ bends.
The rope life is

$$N = \frac{z}{a z_2 \beta \varphi} = \frac{168{,}000}{3{,}400 \times 3 \times 0.4 \times 2.5} = 16.5 \text{ months.}$$

Example 5. Determine the size of the rope and the diameter of the drum for an overhead travelling crane with a lifting capacity Q = 20 tons operating on heavy duty. The trolley ratio is 2×3; the rope life—8 months. The 6×37 rope is cross laid with a core made of Manila hemp and impregnated with grease

$$\sigma_b = 180 \text{ kg/mm}^2.$$

The tension in one rope member

$$P = \frac{Q}{6\eta} = \frac{20{,}000}{6 \times 0.9} = 3{,}700 \text{ kg.}$$

The breaking load on the rope as a whole is

$$S = PK = 3{,}700 \times 7 = 25{,}900 \text{ kg}$$

where K—safety factor equal to 7 (for heavy duty $K_{min} = 6$).
The rope is selected from the State Standard: $d = 21.5$ mm and $E = 174$ sq mm.
The safe stress is

$$\sigma = \frac{P}{F} = \frac{3{,}700}{174} = 21.2 \text{ kg/mm}^2.$$

The number of repeated bends z of the rope prior to failure is found from formula (21)

$$z = a z_2 N \beta \varphi = 9{,}600 \times 5 \times 8 \times 0.3 \times 2.5 = 288{,}000 \text{ bends.}$$

The ratio $\frac{D}{d}$ is found from formula (19)

$$A = \frac{D}{d} = m \sigma C C_1 C_2 + 8 = 1.8 \times 21.2 \times 1.02 \times 1.04 \times 0.82 + 8 = 41.2.$$

The drum diameter is

$$D = 41.2d = 41.2 \times 21.5 = 885 \text{ mm.}$$

Example 6. Find the life of a rope, parallel laid, for the same conditions as in Example 5.
From formula (19)

$$m = \frac{A - 8}{\sigma C C_1 C_2} = \frac{41.2 - 8}{21.2 \times 0.89 \times 1.04 \times 0.82} = 2.06.$$

Referring to Table 11 for the value of $z = 355{,}000$ we find the rope life

$$N = \frac{z}{a z_2 \beta \varphi} = \frac{355{,}000}{9{,}600 \times 5 \times 0.3 \times 2.5} = 9.9 \approx 10 \text{ months.}$$

CHAPTER V

LOAD HANDLING ATTACHMENTS

1. GENERAL

On general-purpose cranes which carry loads of various shape the load is handled by means of chain or rope slings attached to hooks. Standard (single) and ramshorn hooks are the two most popular designs used for this purpose.

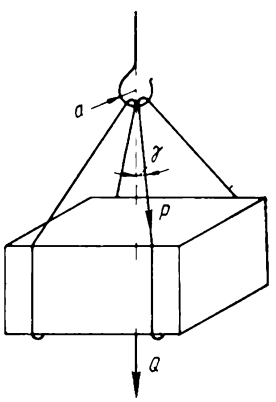

Fig. 61. Suspension of a load from a hook

Sometimes use is made of solid and built-up triangular hooks. Standard and ramshorn hooks may be flat-die or closed-die forged or else made of a series of shaped plates. One-piece forged hooks are used for lifting loads weighing up to 100 tons (single hooks—up to 50 tons, ramshorn hooks—beginning from 25 tons and upwards), while triangular and laminated hooks can be employed to carry over 100 tons.

All types of hooks are made of steel 20.

After the forging and machining operations hooks are carefully annealed and cleaned from scale. The inner diameter of hooks should be sufficient to accommodate two strands of chain or rope which carry the load.

As a rule, the load is suspended on a four-leg sling with two loops over the saddle of the hook (Fig. 61)

$$P = \frac{\frac{Q}{4}}{\cos\gamma} = \frac{Q}{4\cos 45^\circ} \approx 0.35Q.$$

More often than not hooks have a trapezoidal section, made wider on the inside. A trapezoidal section makes for a better utilisation of the material and less complicated design. On top, the hook ends in a round shank operating only in tension. The upper part of die-forged hooks is threaded for suspension from crosspieces of load carrying devices.

2. FORGED STANDARD HOOKS

Fig. 62*a* shows a simple forged standard hook. The diameter *a* and the overall proportions of standard and ramshorn hooks can be found in appropriate State Standards. In the process of designing, the proportions of a hook are assumed tentatively on the basis of these standards; subsequently, the hook is checked for strength and all its proportions are finally established.

Calculating Hook Dimensions. The hook shank is checked for the tensile stress in the threaded portion (minor diameter d_1). The unit tensile stress is

$$\sigma_t = \frac{Q}{\frac{\pi d_1^2}{4}}. \tag{59}$$

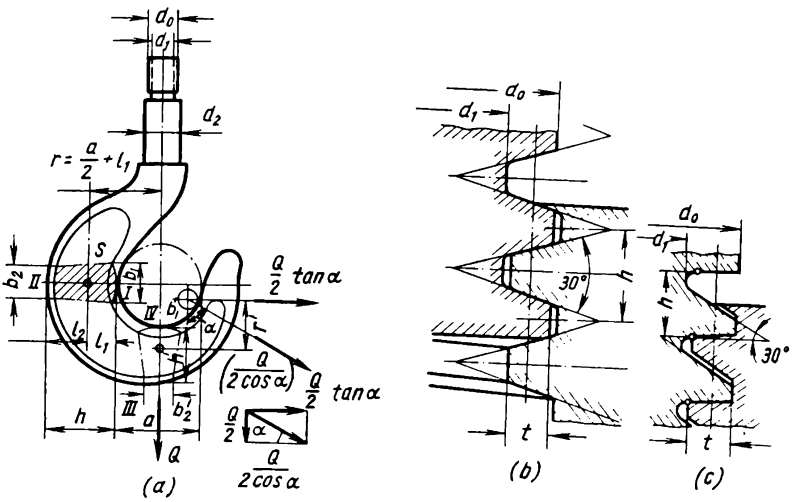

Fig. 62. Forged standard hook

The safe unit stress σ_t should not exceed 500 kg/cm² for steel 20. The minimum height of the hook nut is determined from the permissible compressive stresses in the thread according to the following formula:

$$H = \frac{4Qt}{\pi (d_0^2 - d_1^2) p} \tag{60}$$

where t—thread pitch;

d_0—major diameter and d_1—minor diameter of the thread.

The safe unit compression stress p (steel on steel) is taken as

$$p = (300 \text{ to } 350) \text{ kg/cm}^2.$$

Hooks of small lifting capacity are provided with a normal metric vee thread. In hooks intended to carry from 5 tons and more preference is given to a trapezoidal (Fig. 62*b*) or buttress (Fig. 62*c*) thread. Buttress thread offers greater advantages theoretically since a hook is loaded only in one direction.

The unit stress in the saddle of the hook can be found from the formula

$$\sigma = \frac{Q}{F} + \frac{M}{Fr} + \frac{M}{Fr} \cdot \frac{1}{\varkappa} \cdot \frac{y}{r} \tag{61}$$

where σ—unit stress for the fibre at a distance y from the neutral axis;

Q—load on the hook;

F—area of critical cross-section;

r—radius of curvature of the neutral axis at the critical cross-section;

$\varkappa$—factor depending on the shape of the cross-section and the curvature of the beam;

y—distance from the fibre to the neutral axis; it has a negative value if the fibre is between the centre of a curvature and neutral axis and a positive value for all the fibres on the other side of the neutral axis.

The bending moment M is assumed to be positive if it causes the hook curvature to increase (its radius decreases) or negative if the curvature decreases. Since a load tends to open the hook the moment is negative (Fig. 62*a*):

$$M = -Qr = -Q(0.5a + e_1).$$

The value of $\varkappa$ is found from the relation

$$\varkappa = -\frac{1}{F}\int_{e_1}^{e_2}\frac{y}{y+r}\,dF$$

which for a trapezoid with sides b_1 and b_2 and with height h will be as follows:

$$\varkappa = -1 + \frac{2r}{(b_1 + b_2)\,h}\left[\left\{b_2 + \frac{b_1 - b_2}{h}(e_2 + r)\right\}\ln\frac{r + e_2}{r - e_1} - (b_1 - b_2)\right]. \qquad (62)$$

It can be assumed with an accuracy sufficient for practical purposes that in normal type hooks the centre of curvature of the neutral axis at the critical section coincides with the geometrical centre of the hook mouth so that $r = 0.5a + e_1$.

If we take $h = a$, i.e., $\frac{h}{a} = 1$ and $\frac{b_1}{b_2} = n$, formula (62) after transformations will have the following form:

$$\varkappa = \frac{5n + 7}{3(n + 1)^2}\left[(1.5n - 0.5)1.09861 - (n - 1)\right] - 1 \qquad (63)$$

since, neglecting the displacement of the neutral axis relative to the centroid of the section, we have

$$e_1 \approx \frac{n + 2}{n + 1}\frac{h}{3}.$$

Under these conditions formula (63) can be used to find $\varkappa$ for any value of $\frac{b_1}{b_2}$.

Substituting in formula (61) the values: $M = -Q(0.5a + e_1)$, $r = 0.5a + e_1$, $y = -e_1$ (for the stretched extreme inner fibre) and $y = e_2$ (for the compressed extreme outer fibre) we shall obtain the unit stress in the cross-section between points I and II.

Since
$$\sigma = \frac{Q}{F} - \frac{Q(0.5a + e_1)}{Fr} - \frac{Q(0.5a - e_1)}{Fr}\,\frac{1}{\varkappa}\,\frac{y}{y + r} =$$

$$= \frac{Q}{F}\left[1 - \frac{0.5a + e_1}{r}\left(1 + \frac{1}{\varkappa}\,\frac{y}{y + r}\right)\right] = \frac{Q}{F}\left[1 - \frac{0.5a + e_1}{r}\right.$$

$$\left.\left(1 - \frac{1}{\varkappa}\,\frac{e}{r - e_1}\right)\right] = \frac{Q}{F}\,\frac{1}{\varkappa}\,\frac{2e_1}{a},$$

the maximum unit tensile stress of the inner fibres of the section is

$$\sigma_I = \frac{Q}{F}\,\frac{1}{\varkappa}\,\frac{2e_1}{a} < \sigma_{safe}. \qquad (64)$$

The maximum unit compressive stress of the outer fibres is found in the same way:

$$\sigma_{II} = -\frac{Q}{F}\,\frac{1}{\varkappa}\,\frac{e_2}{\frac{a}{2} + h} \leqslant \sigma_{safe}. \qquad (65)$$

Here, the minus sign shows compressive stress.

If $h \leqslant a$ (standardised hooks) the value of $\varkappa$ for these cases can be found more easily by graphical methods.

Methods of Graphical Determination of Factor $\varkappa$. To find the centroid of the section to the accepted scale a cross-section of the hook should be drawn first (Fig. 63). After this a system of coordinates LGK is set up. The axis of abscissas GK is divided into an arbitrary number of parts from which vertical lines are drawn through the cross-section of the hook. The verticals may be randomly spaced. Areas $S = xy$ are plotted vertically on the diagram.

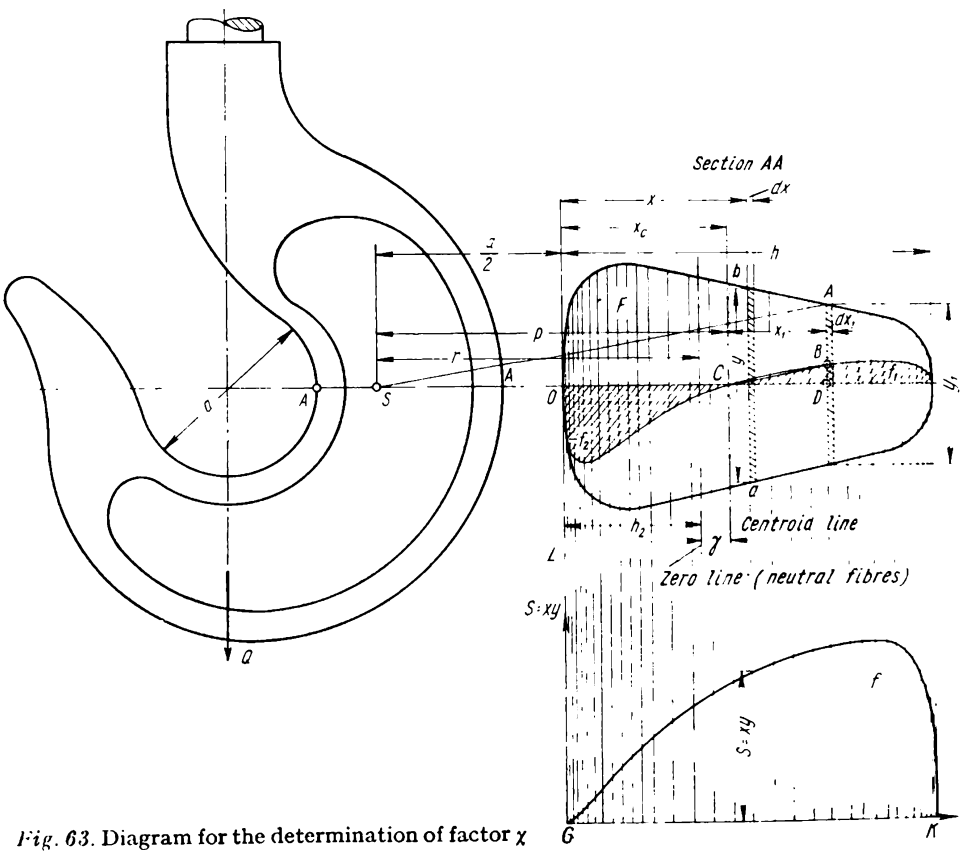

Fig. 63. Diagram for the determination of factor χ

The value of x is the distance from point O to the corresponding vertical lines; y is the respective length of the vertical lines inside the section. The extremities of the ordinates are connected by a continuous line. The abscissa of the section centroid is determined from the following formula:

$$x_c = \frac{\int_0^h yxdx}{\int_0^h ydx} = \frac{f}{F} \tag{66}$$

where f—area bounded by the curve;
F—area of the hook cross-section.

The areas f and F are determined with a planimeter.

To find the auxiliary areas f_1 and f_2 a straight line SA is drawn from the centre of curvature S, and through point C a parallel line CB is drawn which cuts off the sought-for line DB on the vertical DA. Continuing the same procedure for

all the verticals we shall obtain a number of points and if we connect them by a continuous curve we shall be able to find areas f_1 and f_2 which join at point C. The difference f_1—f_2 will always be a negative value.

The areas f_1 and f_2 are determined with a planimeter.

The factor $\varkappa$ will equal

$$\varkappa = -\frac{1}{F}\int_{e_1}^{e_1}\frac{e_2}{y+r}\,dF = -\frac{2(f_1-f_2)}{F}. \tag{67}$$

The distance between the zero line (neutral fibres) and the centroid line is

$$\gamma = \frac{\varrho\varkappa}{1+\varkappa} \tag{68}$$

where ϱ is the radius of centroid curvature.

Table 19 gives the principal design values for standard single hooks.

Table 19

Principal Design Values for Single Hooks

Lifting capacity Q, tons	Area of critical section F, sq cm	Distance between centroid and inner contour x_c, cm	Radius of mouth $\frac{a}{2}$, cm	Radius of hook curvature ϱ, cm	Design area in sq cm		Factor $\varkappa = \frac{2(f_1-f_2)}{F}$	Distance between zero line and centroid $\gamma = \frac{\varrho\varkappa}{1+\varkappa}$	Distance between zero line and inner contour $h_2 = x_c - \gamma$
					f_1	f_2			
0.25	3.44	1.13	1.5	2.63	0.138	0.278	0.081	0.196	0.934
0.5	5.87	1.56	2.0	3.56	0.227	0.488	0.089	0.292	1.268
1.0	10.26	1.98	2.5	4.48	0.437	0.919	0.094	0.384	1.596
1.5	17.52	2.63	3.0	5.63	0.760	1.578	0.0935	0.481	2.149
2.0	28.7	3.30	3.5	6.80	1.381	2.800	0.098	0.610	2.690
3.0	41.1	3.96	4.0	7.96	1.690	3.970	0.110	0.787	3.173
5.0	58.0	4.61	4.75	9.36	2.930	5.720	0.0961	0.820	3.790
7.5	77.8	5.40	5.5	10.90	3.551	7.730	0.108	1.060	4.340
10.0	104.0	6.28	6.5	12.78	4.250	10.500	0.120	1.185	5.095

Safe Stresses. The unit stresses determined from formulas (64) and (65) should not exceed 1,500 kg/cm² for steel 20.

Section *III-IV* is checked for strength at the maximum permissible angle $2\alpha = 120°$ in the same way as section *I-II* (Fig. 62*a*).

Neglecting the shearing force $\frac{Q}{2}$ calculations are made for the force $\frac{Q}{2}\tan\alpha$ using the same method as above taking instead of $\frac{a}{2}$ the value of r' and the corresponding dimensions of the section.

The cylindrical portion of the hook shank entering the hole in the crosspiece is subject to tension. However, accidental misalignment may cause bending forces to arise as well and for this reason the value of the permissible stress is deliberately reduced (Fig. 62*a*).

$$\sigma_t = \frac{Q}{\frac{\pi d_2^2}{4}} \leqslant 500 \text{ kg/cm}^2.$$

Example. Checking a forged single hook.

Given: Useful load-lifting capacity of the crane G = 5,000 kg; weight of the hook with grabbing tongs G_0 = 1,000 kg.

1. Full load on the hook $Q = G + G_0 = 5{,}000 + 1{,}000 = 6{,}000$ kg.

2. Stress in the thread. We take a standard hook with a lifting capacity of 5 tons for a power drive and check its dimensions for strength. The hook shank is provided with a metric vee thread having a major diameter of 48 mm (M = 48). According to formula

(59), the stress is

$$\sigma_t = \frac{Q}{\frac{\pi d_1^2}{4}} = \frac{6{,}000}{13.23} \approx 455 \text{ kg/cm}^2,$$

which is permissible.

3. The minimum height of the hook nut [formula (60)] is

$$H = \frac{4Qt}{\pi (d_0^2 - d_1^2) p} = \frac{4 \times 6{,}000 \times 0.5}{3.14 (4.8^2 - 4.1^2) \times 150} = 4 \text{ cm}.$$

4. Checking stresses in the hook saddle. From graphic construction we obtain (Table 19) the area of the critical section of the hook found with a planimeter, $E = 58$ sq cm.

The area formed by the curve in coordinates LGK (Fig. 63), is $f = 266.5$ cu cm.

The abscissa of the centroid is

$$x_c = \frac{f}{F} = \frac{266.5}{58} = 4.61 \text{ cm}.$$

The auxiliary areas obtained with a planimeter are

$$f_1 = 2.93 \text{ sq cm and } f_2 = 5.72 \text{ sq cm}.$$

Factor $\varkappa$ [formula (67)] is

$$\varkappa = \frac{2 (f_1 - f_2)}{F} = \frac{2 (2.93 - 5.72)}{58} = 0.0961 \text{ (Table 20)}.$$

The distance between the zero line and centroid from formula (68) is

$$y = \frac{\varrho \chi}{1 + \chi} = \frac{9.36 \times 0.0961}{1 + 0.0961} = 0.82 \text{ cm}.$$

The distance between the extreme inner fibres and zero line (Fig. 63) is

$$e_1 = h_2 = x_c - y = 4.61 - 0.82 = 3.79 \text{ cm}.$$

The maximum unit tensile stress in the inner fibres according to formula (64) is

$$\sigma_I = \frac{Q}{F} \times \frac{1}{\varkappa} \times \frac{2e_1}{a} = \frac{6{,}000}{58} \times \frac{1}{0.0961} \times \frac{2 \times 3.79}{9.5} = 860 \text{ kg/cm}^2$$

where $a = 95$ mm.

The maximum unit compression stress in the outer fibres according to formula (65) is

$$\sigma_{II} = -\frac{Q}{F} \times \frac{5}{\varkappa} \times \frac{e_2}{\frac{a}{2} + h} = \frac{6{,}000}{58} \times \frac{1}{0.0961} \times \frac{6.71}{4.75 + 10.5} = -475 \text{ kg/cm}^2$$

where $h = 105$ mm.

Both unit stresses are below the safe value.

The unit stresses in section *III-IV* are determined in the same way.

3. FORGED RAMSHORN HOOKS

Ramshorn hooks (Fig. 64) are designed with smaller saddles than single hooks of the same lifting capacity. The dimensions of the smooth and threaded portions of the shank are almost the same as in single hooks and the threaded part of the shank is checked by the same methods of calculation.

In principle, the curved portion of a ramshorn hook is checked in the same way as for single hooks. However, because of asymmetric suspension, the specified tension of the sling should be somewhat increased (approximately by 1/3).

Due to the force $\frac{1}{3} \times \frac{Q}{2} = \frac{2}{3} Q$ acting on one horn, the tension in the sling acting at an angle of α to the vertical (usually $\alpha \approx 45°$) will be $P = \frac{2Q}{3 \cos \alpha}$.

The force normal to section *I-II* is:

$$P_1 = \frac{2Q \sin (\alpha + \beta)}{3 \cos \alpha} \tag{69}$$

where β –angle of inclination of the section to the vertical.

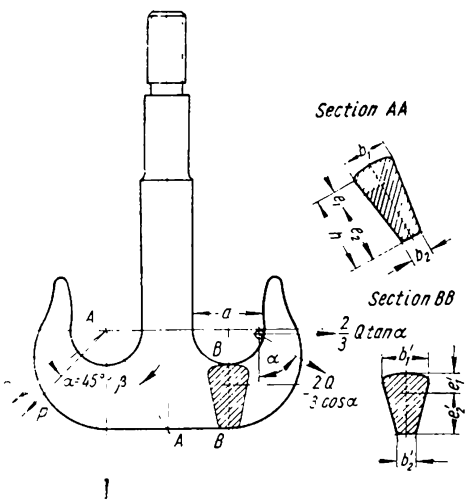

Fig. 64. Ramshorn hook

As in a single hook, the section of a ramshorn hook is a rounded-off trapezoid with height h and bases b_1 and b_2.

Disregarding the shearing force, the unit stresses in the extreme fibres will be

$$\sigma_I = \frac{P_1}{F} \times \frac{1}{\varkappa} \times \frac{2e_1}{a}, \qquad (70)$$

$$\sigma_{II} = -\frac{P_1}{F} \times \frac{1}{\varkappa} \times \frac{e_2}{\frac{a}{2} + 2e_1 + e_2} \qquad (71)$$

where a—hook diameter;
e_1 and e_2—distance between the neutral line and the extreme fibres;
F—area of the critical cross-section.

The value of factor $\varkappa$ is usually determined graphically (see Fig. 63).

Since the forces in the sling act at an angle, it is necessary to check section *III-IV* assuming the largest angle $2\alpha=120°$. As in the case of a single hook, the calculations are done for the normal force $\frac{2}{3} Q \tan \alpha$ neglecting the shearing force $\frac{2}{3} Q$.

The stresses are assumed to be the same as in single hooks.

The operating rules for cranes prohibit suspension of the load on one horn only; this is quite possible, however. Let us assume that half the load is suspended on one horn. In this case the main shank will be overloaded, the maximum unit stress in which can be determined (Fig. 65) proceeding from the following considerations (critical section *V-VI*):

$$P_t = \frac{Q}{2} \cos \beta; \quad P_{sh} = \frac{Q}{2} \sin \beta; \quad \sigma_t = \frac{P_t}{F} \text{ and } \tau_{sh} = \frac{P_{sh}}{F}.$$

The bending stress σ_{bend} arises from the moment

$$M_{bend} = -P_t \left(\frac{a+d}{2} \right).$$

Hence

$$\sigma_\Sigma = \sqrt{(\sigma_t + \sigma_{bend})^2 + 3\tau^2}. \qquad (72)$$

Example. Checking the stresses in the curved portion of a forged ramshorn hook.
Given: Lifting capacity 15 tons; dimensions as in Fig. 66.
1. Full load Q = 15 tons.
2. Force normal to the section [formula (69)]

$$P_1 = \frac{2Q \sin (\alpha + \beta)}{3 \cos \alpha} = \frac{2 \times 15{,}000 \times \sin 77°}{3 \cos 45°} = 13{,}750 \text{ kg}.$$

3. Factor $\varkappa$.
Cross-sectional area F = 115.8 sq cm.
Auxiliary area f = 789 cu cm. The centroid abscissa is

$$x_c = \frac{f}{F} = \frac{789}{115.8} = 6.8 \text{ cm}.$$

The auxiliary areas are f_1 = 5.71 sq cm and f_2 = 11.7 sq cm.
Thus, the factor

$$\varkappa = \frac{2(f_1 - f_2)}{-F} = \frac{2(5.71 - 11.7)}{-115.8} = 0.104.$$

The distance between the zero line and centroid is

$$\gamma = \frac{\varrho\varkappa}{1+\varkappa} = \frac{13.8 \times 0.104}{1+0.104} = 1.29 \text{ cm}.$$

The distance between the extreme inner fibres and zero line is

$$e_1 = x_c - \gamma = 6.8 - 1.29 = 5.51 \text{ cm}.$$

4. Unit stresses are

$$\sigma_I = \frac{P_1}{F} \times \frac{1}{\varkappa} \times \frac{2e_1}{a} = \frac{13{,}750}{115.8} \times \frac{1}{0.104} \times \frac{2 \times 5.51}{14} =$$

$$= 900 \text{ kg/cm}^2;$$

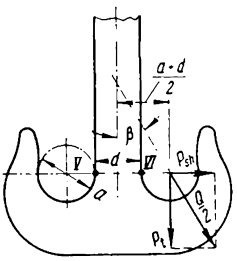

Fig. 65. Ramshorn hook with a load suspended on one horn

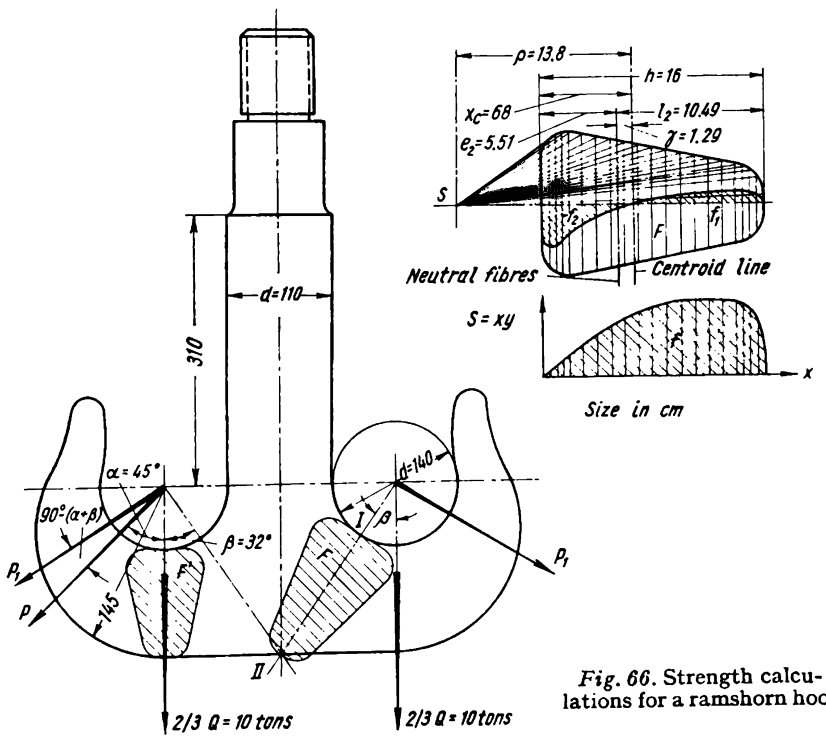

Fig. 66. Strength calculations for a ramshorn hook

$$\sigma_{II} = -\frac{P_1}{F} \times \frac{1}{\varkappa} \times \frac{e_2}{\frac{a}{2} + e_1 + e_2} = -\frac{13{,}750}{115.8} \times \frac{1}{0.104} \times \frac{10.45}{\frac{14}{2} + 16} = -520 \text{ kg/cm}^2.$$

Both values are permissible.

4. SOLID TRIANGULAR EYE HOOKS

Solid triangular eye hooks (Fig. 67) are usually employed in cranes with a high lifting capacity (over 100 tons), and occasionally in medium-power cranes. The shortcoming of such hooks is that the slings carrying the load must be passed through the eye. Solid triangular hooks are forged in one piece.

From the viewpoint of external forces a solid hook is statically determinate and with respect to internal stresses threefold statically indeterminate. Since the bow is made integral with the sides and is subject to bending forces it also causes bending in the sides.

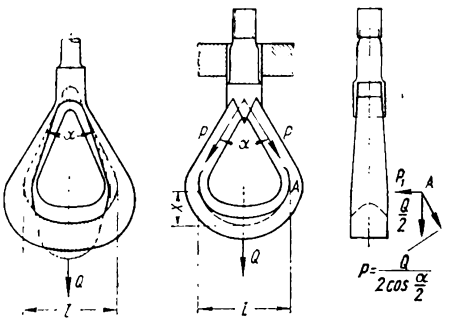

Fig. 67. Solid triangular eye hook

Fig. 67 illustrates a tentative bending moment diagram. According to investigations, the bending moment in the bow will be

$$M_1 \approx \frac{Ql}{6}.$$

The bending moment where the sides adjoin the bow is

$$M_2 = \frac{Ql}{13}.$$

The tensile force acting on the sides is

$$P = \frac{Q}{2\cos\frac{\alpha}{2}}$$

where α—angle between the inclined sides;
Q—load:
l—bow span measured along the neutral line of the sections.

The junctions between the bow and the sides as well as between the shank and the sides should be gradual and without sharp corners.

The maximum unit stress in the bow (Fig. 67) can be also found from the formula

$$\sigma = \frac{M_{bend}}{W} + \frac{P_1}{F}$$

where

$$M_{bend} \approx \frac{Ql}{6} + P_1 x;$$

$P_1 = \frac{Q}{2}\tan\frac{\alpha}{2}$ —compressive force acting on the bow, in kg;
W—moment of resistance;
F—area of bow cross-section.

The safe unit stress for steel 3, according to Soviet Standards, is $\sigma_{safe} = 800$ kg/cm².

5. HINGED TRIANGULAR HOOKS

The manufacture of solid triangular eye hooks encounters a number of production difficulties. For this reason in handling heavy loads preference is given to built-up hinged triangular hooks. Fig. 68*a* shows a built-up hinged hook with one joint and Fig. 68*b*—a built-up hook with three joints.

The unit stress in the links of three-joint built-up hooks is

$$\sigma_t = \frac{Q}{4\cos\frac{\alpha}{2}F} \tag{73}$$

(when the bow is suspended on four links).

The permissible value is

$$\sigma_t = 1{,}200 \text{ kg/cm}^2.$$

The unit stress in the bow is determined as a stress in a curved beam:

$$\sigma = \frac{P_1}{F} + \frac{M}{FR} + \frac{M}{\varkappa FR}\frac{e_1}{R-e_1} \tag{74}$$

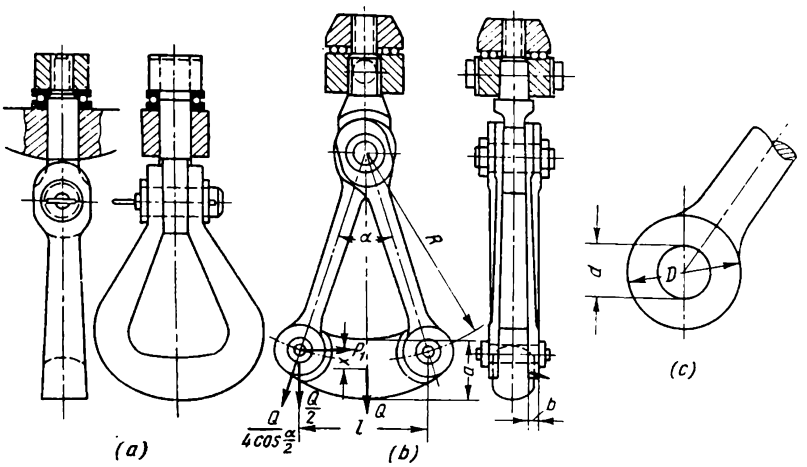

Fig. 68. Built-up hinged triangular hooks

where

$$M = \frac{Ql}{4} + P_1 x;$$

$$P_1 = \frac{Q}{2} \tan \frac{\alpha}{2}$$

where F—cross-sectional area;

e_1—distance between the neutral axis and the fibres carrying the greatest load.

The factor $\varkappa$ for an ellipse is expressed by the formula:

$$\varkappa = \frac{1}{4}\left(\frac{a}{R}\right)^2 + \frac{1}{8}\left(\frac{a}{R}\right)^4 + \frac{5}{64}\left(\frac{a}{R}\right)^6 \qquad (75)$$

where a—major axis of the ellipse or the diameter of a circle.

The shank eye stress is checked by the Lamé formula (Fig. 68*b* and *c*)

$$\sigma_t = \frac{p(D^2 + d^2)}{D^2 - d^2}$$

where $p = \frac{Q}{4 \cos \frac{\alpha}{2} bd}$ (unit pressure);

b—width of the eye.

6. APPLIANCES FOR SUSPENDING HOOKS

Hook Weights. For raising light loads (≈up to 5 tons) hooks are very often attached directly to a flexible lifting tackle. However, in these cases the hook

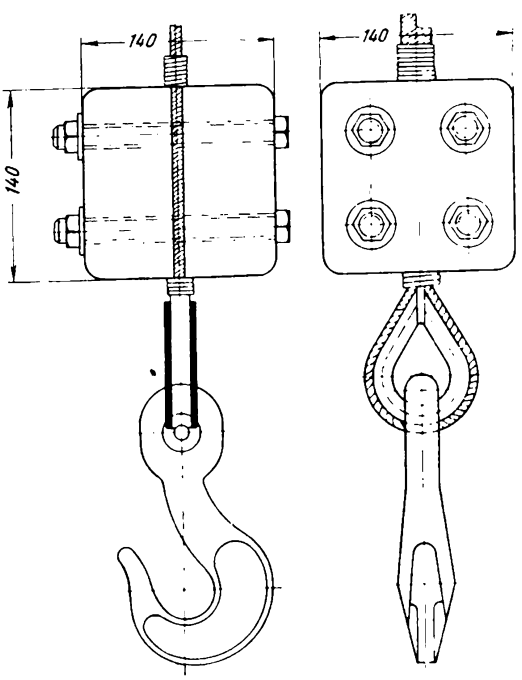

Fig. 69. Hook with additional weight

is too light to overcome friction in the lifting mechanism during lowering. For this reason an additional weight has to be added to the hook (Fig. 69). To dampen the shocks the hook weight is sometimes provided with springs. They are extremely important in cranes servicing forging hammers.

Hook Bearings. Ball thrust bearings allow a loaded hook to turn easily in handling loads over 3 tons. Mounted on crosspieces they support the hook nuts. The best design is that of a self-aligning bearing with a spherical seating ring, since it does not require a spherical surface in the crosspiece.

The recess for the seating ring is made to a depth of from 3 to 10 mm depending on the size of the bearing. The bearings should be enclosed in a housing to protect them against dust and moisture.

Table 20 gives sizes and loads for self-aligning thrust bearings for hooks carrying from 5 to 75 tons.

Hook nuts should be provided with locking devices (Table 20) to prevent their unscrewing.

Table 20

Sizes of Ball Thrust Bearings for Hooks, mm

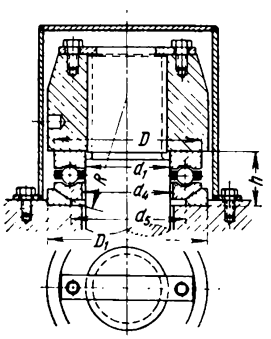

Lifting capacity Q, tons	d_1	d_4	d_5	D	D_1	h	R	r	Limiting working load, tons
5	50	52	75	92	100	36	75	1.5	7.5
7.5	60	62	85	106	115	41	85	2	9.0
10	70	72	95	120	130	44	95	2	11.6
15	80	82	110	136	145	50	110	2	15.8
20	90	93	125	155	165	57	125	2	20.6
25	100	103	140	172	185	64	140	2	26.0
30	115	120	160	200	215	74	160	3	35.5
40	125	130	175	220	220	79	175	3	41.5
50	130	135	185	240	250	101	185	3.5	58.0
60	150	155	205	260	270	106	205	4	67.4
75	170	175	230	285	300	111	230	4	77.5

Crosspieces for Hooks. A hook crosspiece is pivoted in the side plates of casings usually reinforced with straps or shackles made of plate steel. This enables the hook to be turned in two mutually perpendicular directions. The crosspiece is forged from steel and provided with turned trunnions at the ends. The diameter of the hole for the hook shank should be somewhat larger than the shank itself. Some designs of crosspieces are shown in Fig. 70.

The maximum bending moment is

$$M_1^{max} = \frac{Q}{2} \times \frac{l}{2} - \frac{Q}{2} \times \frac{d_1}{4} = \frac{Q}{4}(l - 0.5\,d_1) \qquad (76)$$

where d_1—outside diameter of the bearing seating ring.

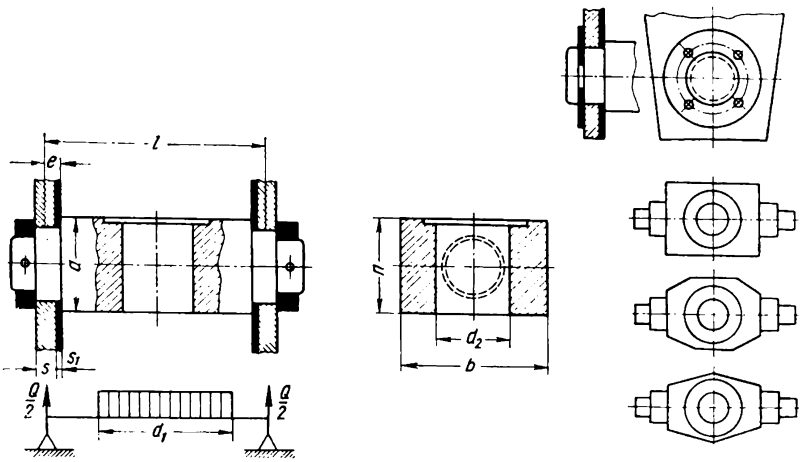

Fig. 70. Crosspieces for hooks

The moment of resistance

$$W \approx \frac{1}{6}(b - d_1)h^2. \tag{77}$$

Safe bending stress

$$\sigma_{bend} = 600 \text{ to } 1{,}000 \text{ kg/cm}^2.$$

The bending moment for the crosspiece trunnions

$$M_2 = \frac{Q}{2} \times \frac{s + s_1}{2}. \tag{78}$$

Unit pressure between the trunnion and the casing

$$p = \frac{Q}{2d\,(s + s_1)} \tag{79}$$

where s—shackle thickness;
s_1—side plate thickness;

$$l = \frac{s + s_1}{2}.$$

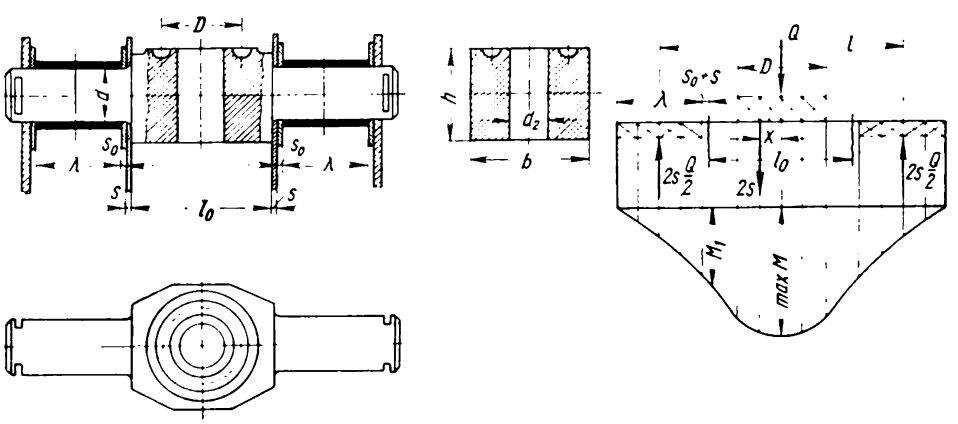

Fig. 71. Crosspiece for mounting two rope sheaves

The trunnions of the crosspiece should have no axial shift but they should be able to turn. Fastening can be done either by adjusting rings secured by taper pins or by means of a split ring inserted into a slot of the trunnion and attached with screws to the straps or shackles (Fig. 70). This mode of fastening is most widely used.

Fig. 71 shows a crosspiece with trunnions for mounting two rope sheaves. The forces of the ropes acting on the sheaves are regarded during calculations as uniformly distributed loads acting on the trunnions. The bending moment in the middle of the crosspiece is

$$M_1^{max} = \frac{Q}{2}\left(\frac{\lambda}{2} + s_0 + s - \frac{l_0}{2} + \frac{D}{2}\right). \tag{80}$$

The bending moment in the trunnions is

$$M_2 = \frac{Q}{2}\left(\frac{\lambda}{2} + s_0 + s\right). \tag{81}$$

The moment of resistance is determined from formula (77).

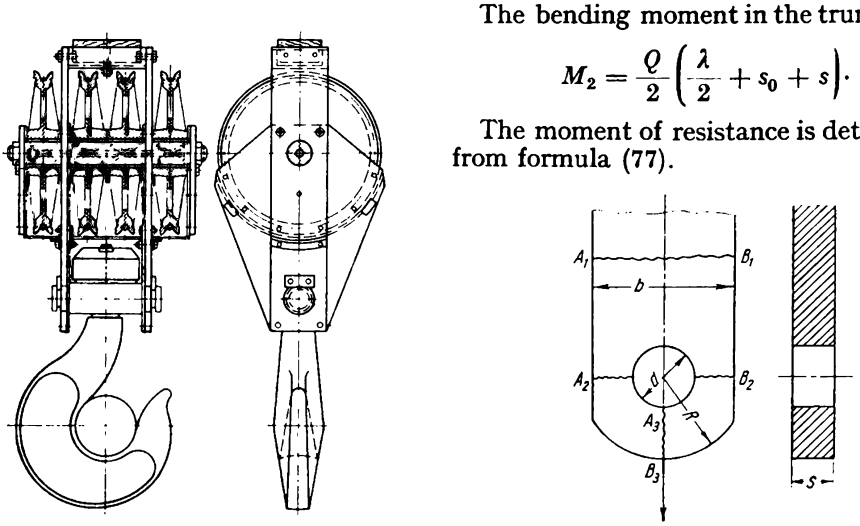

Fig. 72. Crosspiece with shackles for a four-sheave casing

As has been said above the crosspiece is secured in the side plates which are strengthened with shackles or straps (Fig. 72). As a rule, only shackles are checked for strength neglecting the plates in view of their relatively small thickness. The shackles are checked as follows:

In section A_1B_1 (Fig. 72)

$$\sigma_t = \frac{Q}{2bs}.$$

In section A_2B_2

$$\sigma_t = \frac{Q}{2(b-d)s}.$$

For section A_3B_3 use is made of the Lamé formulas

The unit pressure is

$$p = \frac{Q}{2ds}.$$

The unit stress at the inner surface is

$$\sigma_{A_3} = \frac{p[(2R)^2 + d^2]}{(2R)^2 - d^2}.$$

The unit stress at the outer surface is

$$\sigma_{B_3} = \frac{p2d^2}{(2R)^2 - d^2}.$$

The maximum stress will be at the inner surface, i.e.,

$$\sigma_{A_1} = \frac{Q\,(4R^2 + d^2)}{2ds\,(4R^2 - d^2)}$$

whence

$$s = \frac{Q}{2d\sigma_t} \times \frac{4R^2 + d^2}{4R^2 - d^2}. \tag{82}$$

Accurate Strength Calculations of Crosspieces by the Method Developed by A. A. Staroselsky

If the crosspiece is designed with a seat for an antifriction bearing the pressure on the contact surface of the loaded area can be assumed as distributed over a half-cylinder according to the following law:

$$p_c = p \cos \varphi.$$

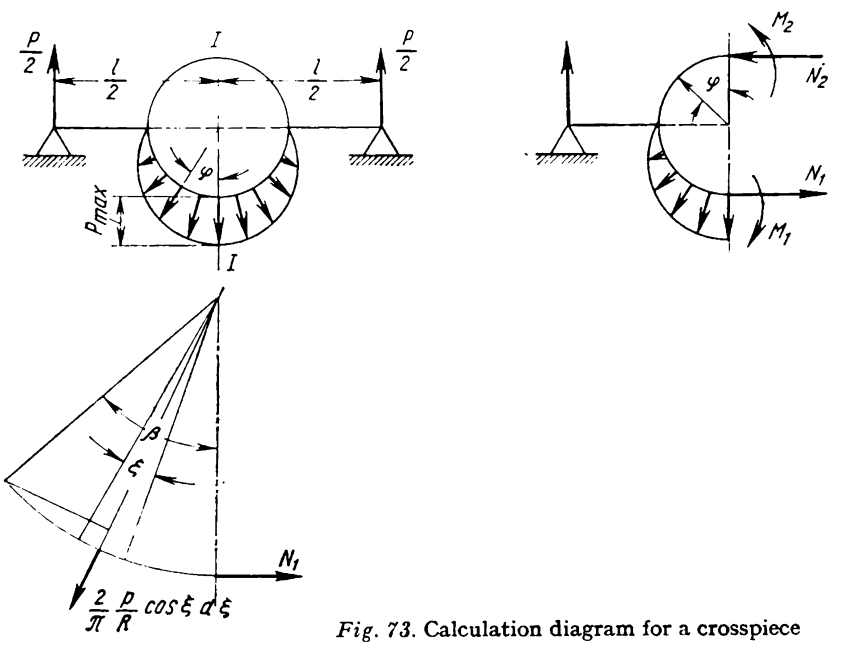

Fig. 73. Calculation diagram for a crosspiece

Let p be the resultant pressure on the axle. Then we find from the equation

$$p = \frac{2}{\pi} \times \frac{P}{R} \text{ kg/cm}. \tag{83}$$

Passing a section mentally through *I-I*, eliminating the right-hand side and denoting the elastic forces over the ring sections as shown in Fig. 73 we can set down the equation for equilibrium of the left-hand side:

$$N_1 - N_2 - \frac{2}{\pi} P \int_0^{\frac{\pi}{2}} \cos\varphi \sin\varphi d\varphi = 0; \tag{84}$$

$$\frac{Pl}{4} + M_1 - M_2 - (N_1 + N_2)R = 0. \tag{85}$$

As extra unknowns we take M_1 and N_1.

From equation (84) we find N_2:

$$N_2 = N_1 - \frac{P}{\pi}. \tag{86}$$

After substituting N_2 in equation (85) we shall have

$$M_2 = M_1 - 2N_1 R + \left(\frac{1}{4} \times \frac{l}{R} + \frac{1}{\pi}\right) PR. \tag{87}$$

The bending moment in an arbitrary section of the lower half-ring will be

$$M_\varphi = M_1 - N_1 R_1 (1 - \cos\varphi) + \frac{2}{\pi} PR \int_0^\varphi \cos\xi \sin(\varphi - \xi)\, d\xi$$

or

$$M_\varphi = M_1 - N_1 R (1 - \cos\varphi) + \frac{1}{\pi} PR\varphi \sin\varphi;$$

$$\frac{\partial M_\varphi}{\partial M_1} = 1; \quad \frac{\partial M_\varphi}{\partial N_1} = -R(1 - \cos\varphi).$$

The bending moment in an arbitrary section of the upper half-ring will be

$$M_\beta = M_2 + N_2 R (1 - \cos\beta).$$

Using relationships (86) and (87) we can reduce the expression for M_β to the following form:

$$M_\beta = M_1 - N_1 R (1 + \cos\beta) + P\left(\frac{l}{4} + \frac{R}{\pi}\cos\beta\right); \tag{88}$$

$$\frac{\partial M_\beta}{\partial M_1} = 1; \quad \frac{\partial M_\beta}{\partial N_1} = -R(1 + \cos\beta).$$

The total potential energy of deformation in the crosspiece is equal to the sum of three addends: potential energy of the rectilinear part (U_1), of the lower half-ring (U_2) and the upper half-ring (U_3).

$$U = U_1 + U_2 + U_3.$$

Since U_1 is not a function of M_1 and N_1, then, according to the principle of least work, we shall have

$$\frac{\partial (U_2 + U_3)}{\partial M_1} = 0; \tag{89}$$

$$\frac{\partial (U_2 + U_3)}{\partial N_1} = 0. \tag{90}$$

The potential energy due to the action of the normal and shearing forces can be neglected because it is very small as compared with the potential energy of the bending moment which is determined from the following equations:

$$U_2 = \int_0^{\frac{\pi}{2}} \frac{M_\varphi^2}{EI} R d\varphi; \tag{91}$$

$$U_3 = \int_0^{\frac{\pi}{2}} \frac{M_\beta^2}{EI} R d\varphi, \tag{92}$$

where I is the equatorial moment of inertia of the ring cross-section.

The expanded equations (89) and (90) can be written as follows:

$$\int_0^{\frac{\pi}{2}} \left[M_1 - N_1 R (1 - \cos\varphi) + \frac{1}{\pi} PR\varphi \sin\varphi \right] d\varphi +$$

$$+ \int_0^{\frac{\pi}{2}} \left[M_1 - N_1 R (1 + \cos\beta) + P\left(\frac{l}{4} + \frac{R}{\pi}\right) \cos\beta \right] d\beta = 0;$$

$$\int_0^{\frac{\pi}{2}} \left[M_1 - N_1 R (1 - \cos\varphi) + \frac{1}{\pi} PR\varphi \sin\varphi \right] (1 - \cos\varphi)\, d\varphi +$$

$$+ \int_0^{\frac{\pi}{2}} \left[M_1 - N_1 R (1 - \cos\beta) + \frac{1}{\pi} P\left(\frac{l}{4} + \frac{R}{\pi} \cos\beta\right) \right] (1 + \cos\beta)\, d\beta = 0.$$

For the sake of convenience we subtract the first equation from the second term by term, integrate the result and make appropriate transformations to obtain a system of equations:

$$4\pi N_1 R - P(R + 2l) = 0;$$

$$\pi M_1 - \pi N_1 R + P\left(2\frac{R}{\pi} + \frac{\pi}{8} l\right) = 0.$$

Solving them we find

$$N_1 = \frac{1}{4\pi}\left(1 + 2\frac{l}{R}\right) P; \tag{93}$$

$$M_1 = \left(-0.12 + 0.034\frac{l}{R}\right) PR. \tag{94}$$

If the outer ring of the bearing is press-fitted into the crosspiece it will take part in the operation of the crosspiece, increasing its rigidity; this has been neglected in the calculations.

When the ring part of the crosspiece is an element of a sliding couple then, due to the fit clearance, contact with the journal is over an arc less than 180° and the distribution law deviates from the cosine curve law. However, we deem it possible also in this case to utilise the above solution as a first approximation.

Example 1. Calculating the strength of a hook crosspiece (Fig. 74).

We shall use the same data as in the example for a single hook.

1. Strength calculations of the crosspiece (Fig. 74). According to formula (76), the maximum bending moment is

$$M_1^{max} = \frac{Q}{4}(l - 0.5d_1) = \frac{6{,}000}{4}(22 - 0.5 \times 11) \sim$$
$$\sim 24{,}750 \text{ kg-cm}.$$

The moment of resistance [formula (77)] is

$$W = \frac{1}{6}(b - d_1)h^2 = \frac{1}{6}(14 - 5)\, 6^2 \sim 54 \text{ cu cm}.$$

The unit stress in the crosspiece is

$$\sigma_{bend} = \frac{24{,}750}{54} \sim 460 \text{ kg/cm}^2,$$

which is permissible.

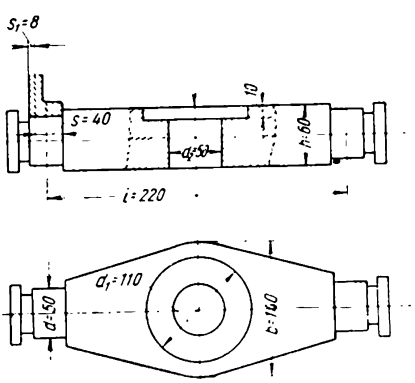

Fig. 74. Crosspiece of a hook

2. Checking the crosspiece trunnions. The bending moment for checking the trunnions by formula (78) is

$$N_2 = \frac{Q}{2}\frac{s+s_1}{2} = \frac{1}{2}\ 6{,}000\frac{4.8}{2} \approx 7{,}200 \text{ kg-cm}.$$

The unit stress in the trunnions is

$$\sigma_{bend} = \frac{M_2}{W_{tr}} = \frac{7{,}200}{0.1\times 5^3} \approx 576 \text{ kg/cm}^2,$$

which is permissible.

The unit pressure on the trunnions [formula (79)] is

$$p = \frac{Q}{2d\,(s+s_1)} = \frac{6{,}000}{2\times 5\times 4.8} \approx 125 \text{ kg/cm}^2,$$

i. e., quite negligible.

Example 2. Determining unit stresses in section I-I of the crosspiece (Fig. 75): $l = 800$ mm, $P = 2{,}200$ kg.

The section is represented in Fig. 76; here, $b = 6$ cm, $h = \frac{25-15}{2} = 5$ cm, $R = \frac{25+15}{4} = 10$ cm.

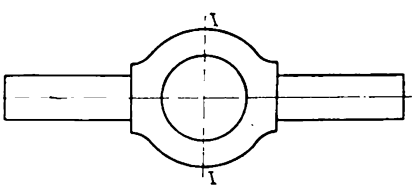

Fig. 75. Diagram for calculating stresses in the crosspiece

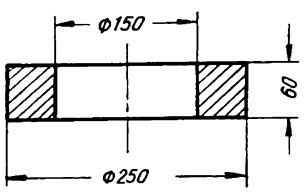

Fig. 76. Critical section of the crosspiece

The cross-sectional area of the ring is

$$F = bh = 6\times 5 = 30 \text{ sq cm}.$$

The equatorial moment of resistance is

$$W = \frac{bh^2}{6} = \frac{6.5^2}{6} = 25 \text{ cu cm}.$$

The normal force acting on the lower section, according to formula (93), is

$$N_1 = \frac{1}{4\pi}\left(1+2\frac{l}{R}\right)P = \frac{1}{4\pi}\left(1+2\frac{80}{10}\right)2{,}200 = 3{,}000 \text{ kg}.$$

The normal force acting on upper section is

$$N_2 = N_1 - \frac{P}{\pi} = 3{,}000 - \frac{2{,}200}{\pi} = 2{,}300 \text{ kg}.$$

The bending moment in the section of the lower half-ring is [formula (94)]

$$M_1 = \left(-0.12+0.034\frac{l}{R}\right)PR = \left(-0.12+0.034\frac{80}{10}\right)2{,}200\times 10 = 3{,}340 \text{ kg-cm}.$$

The bending moment in the section of the upper half-ring is

$$M_2 = M_1 - 2N_1R + \left(\frac{1}{4}\times\frac{l}{R}+\frac{1}{\pi}\right)PR = 3{,}340 - 2\times 3{,}000\times 10 +$$

$$+\left(\frac{1}{4}\times\frac{80}{10}+\frac{1}{\pi}\right)2{,}200\times 10 = -5{,}700 \text{ kg-cm}.$$

The maximum absolute value of the normal unit stress is

$$\sigma_{max} = \frac{M_2}{W}+\frac{N_2}{F} = \frac{5{,}700}{25}+\frac{2{,}300}{30} = 304 \text{ kg/cm}^2.$$

Using the conventional approximate methods of calculation we find the bending moment in the middle of the crosspiece.

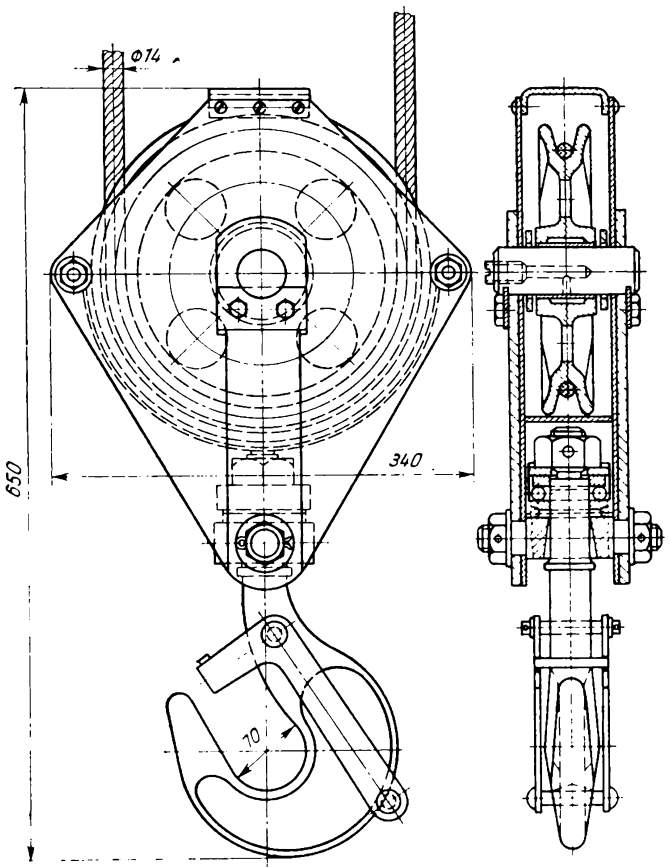

Fig. 77. Ordinary single-sheave hook casing

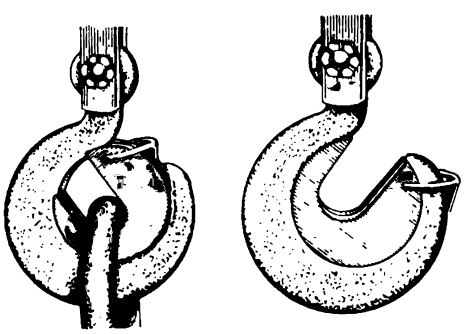

Fig. 78. Hook with a safety clamp

$$M = \frac{Pl}{4} = \frac{2{,}200 \times 80}{4} = 44{,}000 \text{ kg-cm.}$$

The equatorial moment of resistance in the critical cross-section is

$$W_0 = \frac{6(25^3 - 15^3)}{6 \times 25} = 490 \text{ cu cm;}$$

then

$$\sigma_{\substack{max \\ min}} = \pm \frac{M}{W_0} = \pm \frac{44{,}000}{490} = \pm 90 \text{ kg/cm}^2.$$

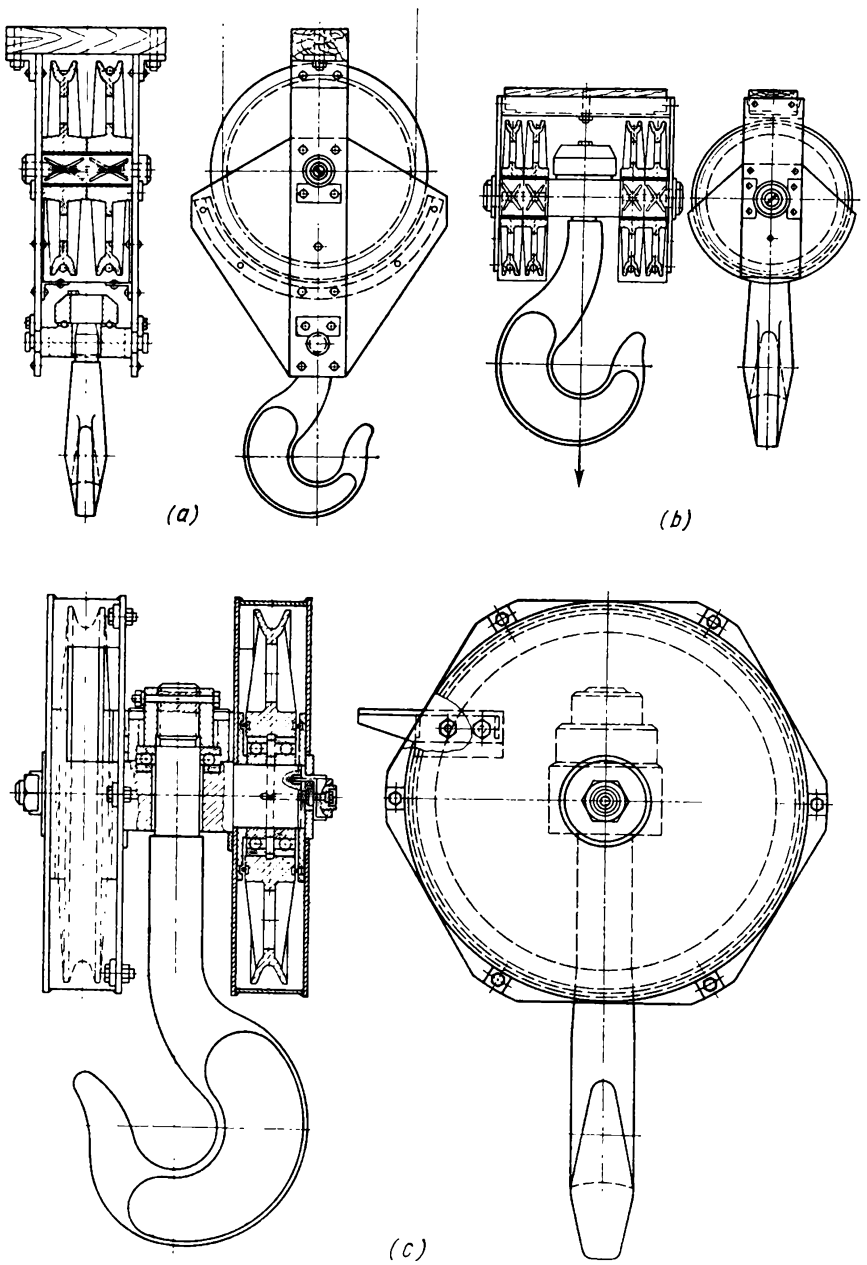

Fig. 79. Hook casings

Casings for Hooks. A casing is the entire suspension tackle which includes: carrying devices (hooks), crosspiece, lower sheaves and casing plates with shackles in which the axles of the sheaves and the trunnions of the crosspiece are secured. Fig. 77 shows a casing with one sheave and an appliance which prevents the rope from slipping off.

When the load being lowered tends to pull the sling chains or ropes out from the hook the latter is provided with safety locks as shown in Fig. 77. The clamp in Fig. 78 is an extremely ingenious device which reliably secures the rope.

Casings for multiple pulleys are designed with either a normal or reduced height. In a normal casing the lower sheaves are mounted on an axle secured in the side plates of the casing (Fig. 79*a*). The shortcoming of this design is an excessive height of the suspension gear. Normal casings with two sheaves (weighing approximately from 32 to 565 kg) are used to hoist loads of from 1 to 30 tons. The elongated plates on top of such casings carry a wooden block to cushion accidental

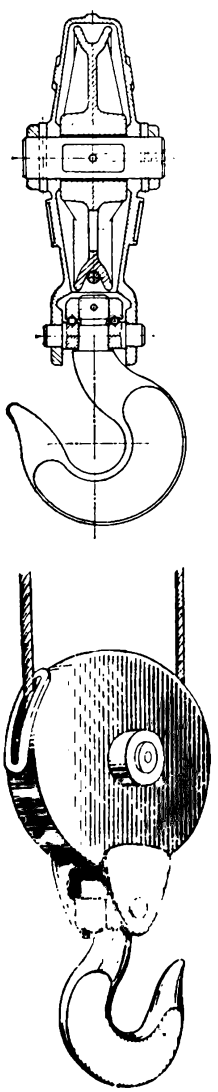

Fig. 80. Casings for electric hoist hooks

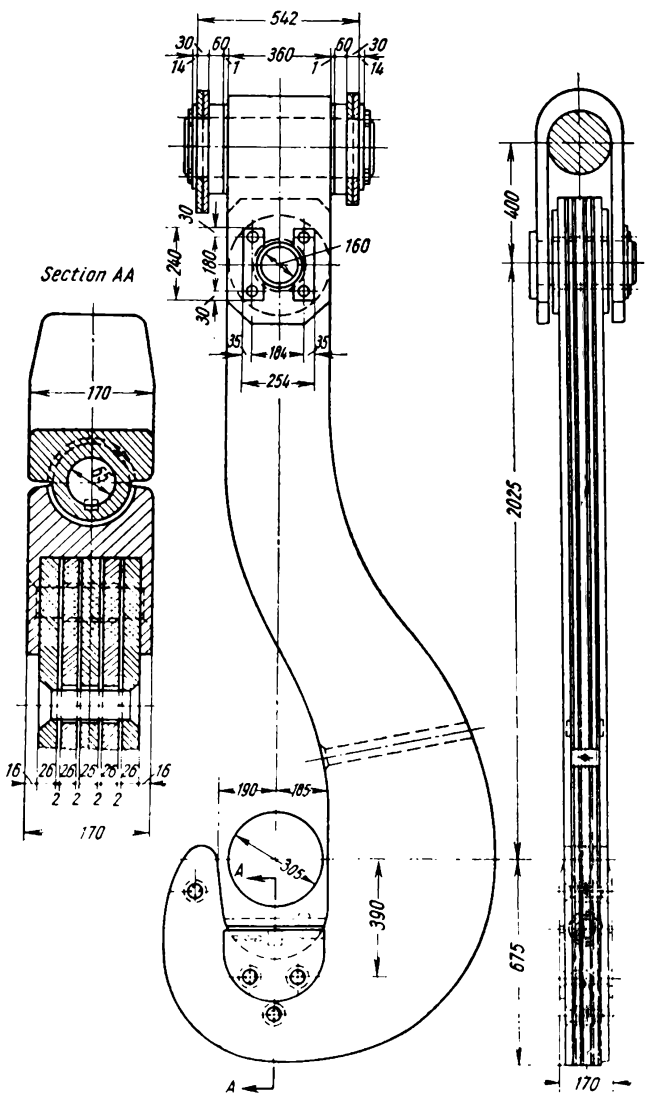

Fig. 81. Suspension of a laminated hook to the side plates of the casing

blows of the casing against the drum or crane frame and also serve to support a lever-actuated limit switch.

Grease cups for lubricating the sheave axles are now being replaced by plugs which close the lubricating hole because projecting grease cups are liable to become damaged during operation. The recess behind the plug is made equal in capacity to the grease cup necessary for the given diameter of axle (Fig. 79*a*). The plugs are periodically screwed in with a special wrench.

In a shortened casing the sheaves are arranged on elongated trunnions of the crosspiece. The lifting capacity of such casings with four sheaves (Fig. 79*b*) ranges from 24 to 100 tons and their weight is from 425 to 2,200 kg. Shortened casings with two sheaves (Fig. 79*c*) can carry from 2 to 25 tons and weigh from 48 to 450 kg. Shortened casings allow a greater lifting height to be obtained and weigh less.

Recently developed casings are of welded construction with bolts used only for assembly.

In the latest designs of electric hoists the casings are usually cast of steel and enclose the sheaves, slits being provided for the rope (Fig. 80). Cast casings are more compact, of elegant shape and devoid of protruding parts. They protect the ropes and sheaves from the action of heat when the hoist operates near furnaces or cupolas.

Suspension of a single laminated hook of a foundry crane to the side plates of the casing is illustrated in Fig. 81. The lifting capacity of such a crane (manufactured by the Novo-Kramatorsk Works, U.S.S.R.) is 125 tons. The hook is made up of a series of shaped steel plates riveted together at the bottom and connected on top by an axle secured by span pieces. The hook is fitted with two steel pads—lower and upper. The sides of the lower pad are attached to the plates of the hook; it carries a section of a steel tube which serves as a joint for the upper pad. The latter is provided with a groove to accommodate the hoop strap of the ladle and can swivel on the lower pad joint through a small angle.

Both single and ramshorn laminated hooks find wide application at present in cranes servicing metallurgical works and in special cranes with a high lifting capacity. They are easier to manufacture and more dependable in operation than ordinary solid forged hooks because the plates never rupture simultaneously.

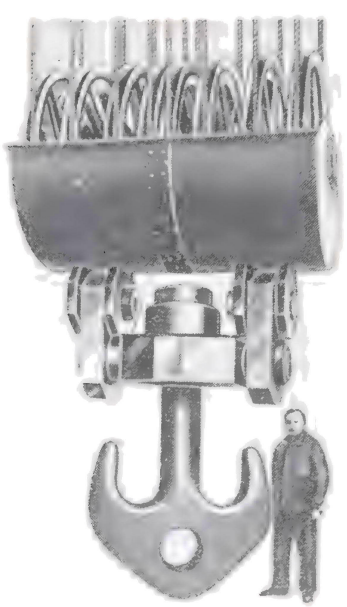

Fig. 82. Suspension gear for a 300-ton crane

Fig. 82 shows the suspension gear of a 300-ton crane for forging presses. It is 4.5 metres high and weighs 17 tons. The hole in the middle of the hook is designed to hold a manipulator.

7. CRANE GRABS FOR UNIT AND PIECE LOADS

A higher utilisation factor and handling capacity of lifting appliances depend directly on the time required to suspend and remove the load. This time is reduced by special grabbing attachments which should:

1) conform with the shape and properties of loads;
2) quickly grab and release them;
3) possess adequate mechanical strength and reliability;
4) meet safety requirements;
5) not damage the load;
6) have a minimum weight;
7) be convenient in operation.

Loads handled at industrial enterprises can be subdivided into the following five groups:

1. Unit loads, as a rule cumbersome, for example boilers, assembled machines, metal structures, etc.
2. Mass piece loads: steel billets, medium-size castings, forgings, machine parts, rolled steel, sheets and plates, boxes, barrels, bales, etc.
3. Mass small-size piece loads: small castings, forgings, machine parts, pigs, bolts, rivets, etc.
4. Loose materials: coal, coke, cinder, sand, metal chips, etc.
5. Liquid materials: cast iron, steel and other molten metals.

The first three types of load are handled by the following special grabbing attachments: carrier beams and clamps, load platforms and side-dump buckets, ordinary and self-closing tongs.

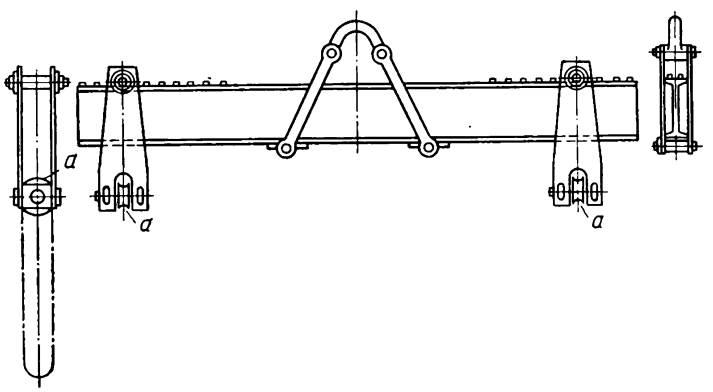

Fig. 83. Carrier beam for a foundry crane for holding and dumping mould flasks

Carrier Beams. These devices are employed to move long, cumbersome and heavy loads, such as locomotives, railway cars, boilers, long rolled stock, sheet and plate steel, etc. Fig. 83 shows a carrier beam of a foundry crane for suspending and dumping mould flasks. The mould flasks are suspended on chains from shackles which are adjustable along the beam and register in grooves on the upper face of the beam. The rollers *a* which allow the mould flask to be dumped add to the operating convenience of the device.

Crane Grabs and Clamps. Similar parts, as for example, wheel pairs, axles, sheet and plate steel, paper rolls, wire coils, etc., are handled by grabs which conform to the shape of the load. The type of grab for wheel pairs, axles and shafts depends on their length and the number of parts being handled simultaneously.

Fig. 84 shows grabs of the carrier type for short and long shafts. In grabs with claws for long shafts the ends of claws are turned slightly upwards to prevent

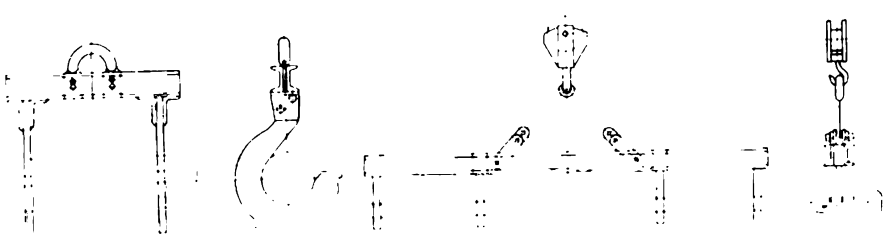

Fig. 84. Grabs for short and long shafts

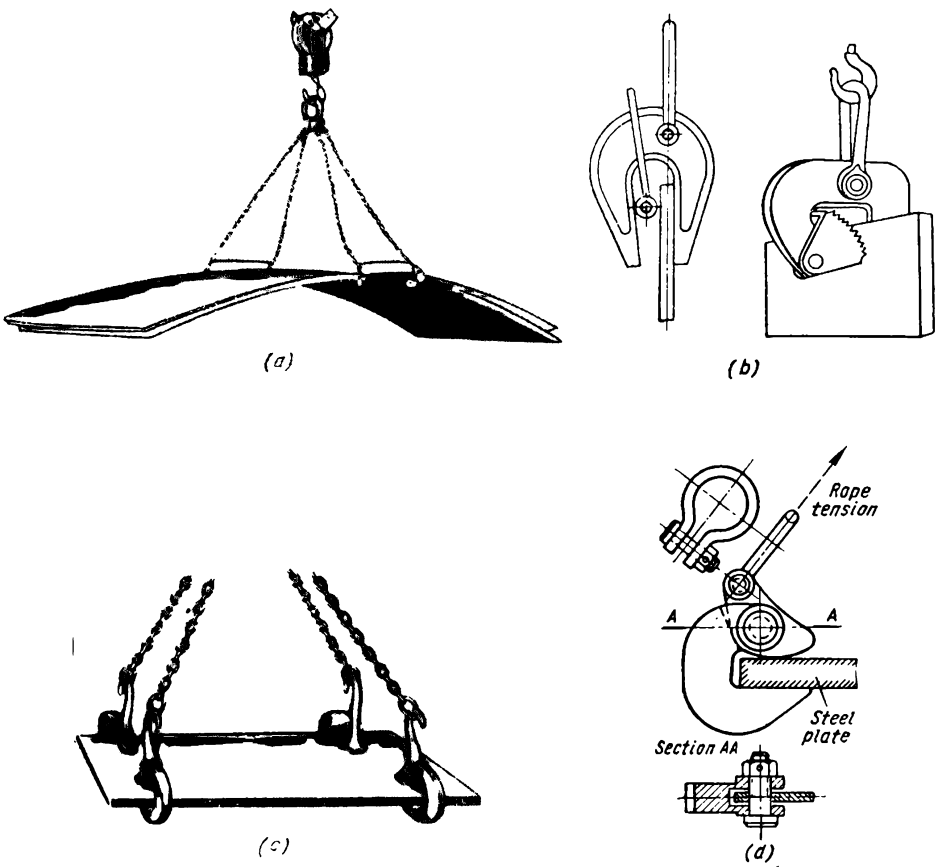

Fig. 85. **Lifting clamps for sheet and plate steel**

the shafts from rolling off. The type of grab for sheet and plate steel depends on the thickness and length of the sheets, their number in the lot and on the mode of handling—horizontal or vertical. Preference is usually given to horizontal handling but the sheets should not be permitted to sag excessively (Fig. 85*a*).

Thick plates are moved vertically by the devices shown in Fig. 85*b* in which the plates are gripped by the action of their own weight. Plates are moved horizontally with the aid of clamps suspended on a four-leg chain sling (Fig. 85*c* and *d*). Large numbers of plates are usually handled by lifting magnets (see below). Fig. 86 shows different types of grabbing devices.

Load Platforms and Side-Dump Buckets. These appliances are used for batch handling of piece loads (boxes, bales, bar steel, machine parts, etc.) and also of small-size loads (briquettes, bricks, pigs, small cast-iron parts). To avoid casualties small loads should never be conveyed on open-type platforms and buckets.

The contents of platforms and buckets can be emptied by cranes onto flat railway cars. They are often of a detachable or dumping type. A typical side-dump bucket is shown in Fig. 87.

Load platforms and buckets are simplified versions of containers employed by railway and other modes of transportation. These are large-size boxes intended to accommodate any load. They are convenient in that they can be placed onto flat cars, trucks, etc., without removing their contents, or taken off just as simply. A railway container is shown in Fig. 88; its characteristics and dimensions can be found in appropriate State Standards.

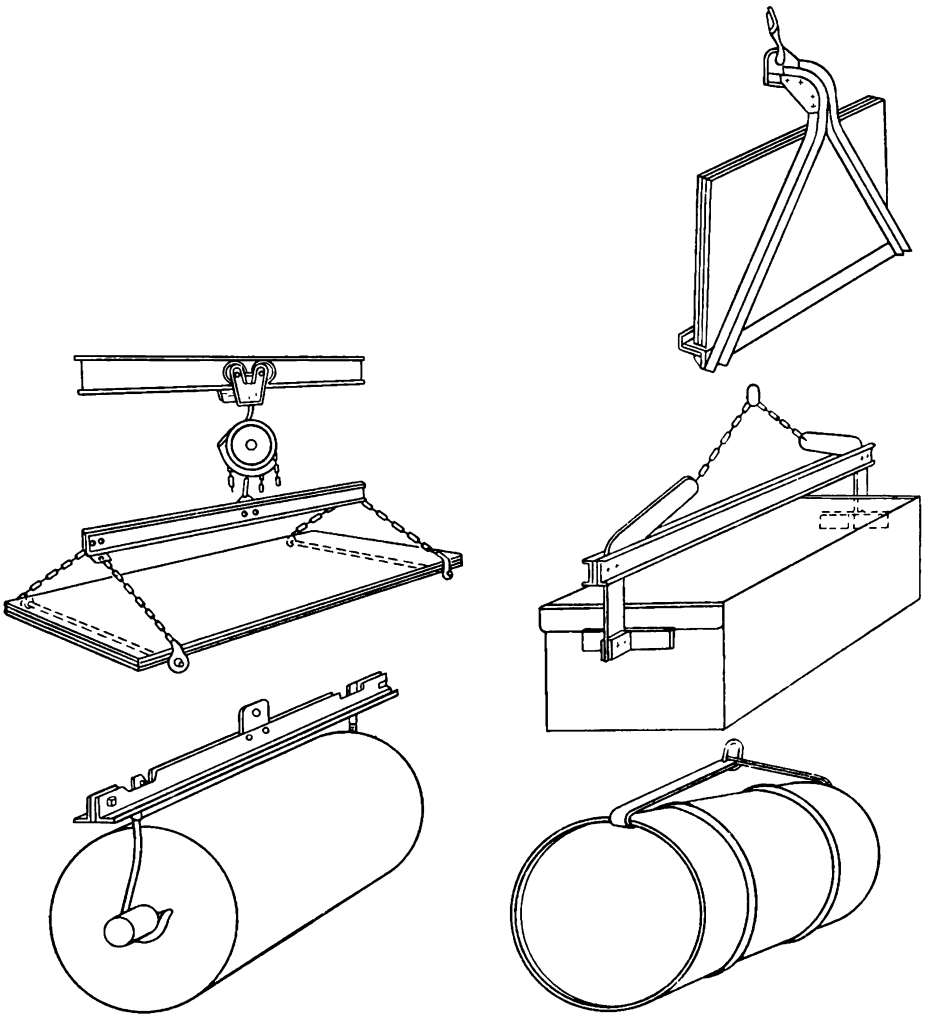

Fig. 86. Various types of grabbing devices

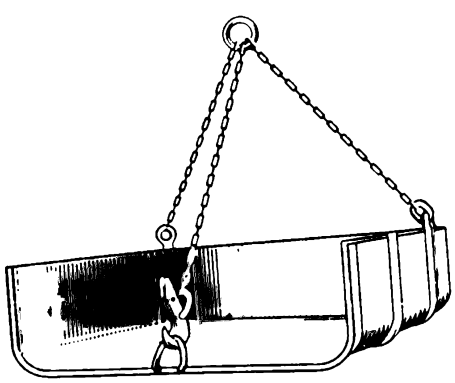

Fig. 87. Side-dump bucket

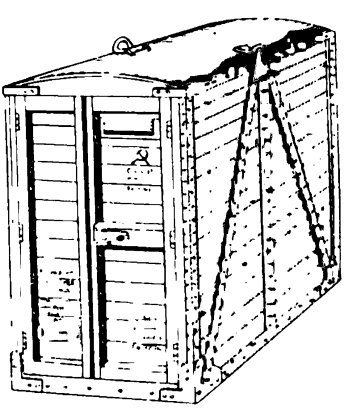

Fig. 88. Container

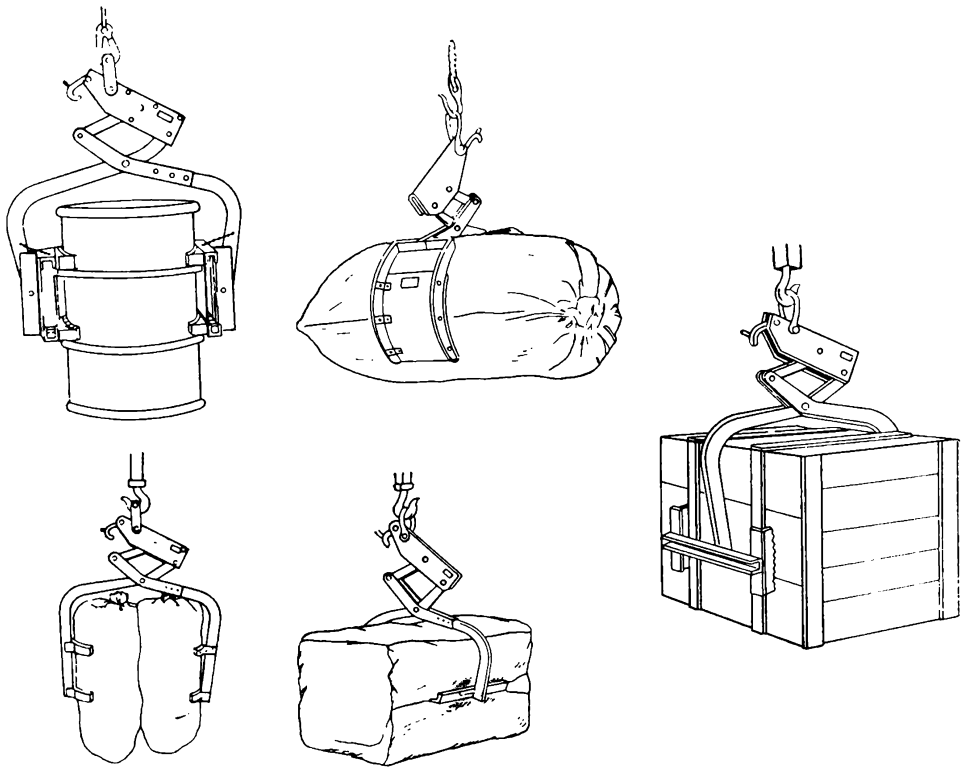

Fig. 89. Self-closing tongs

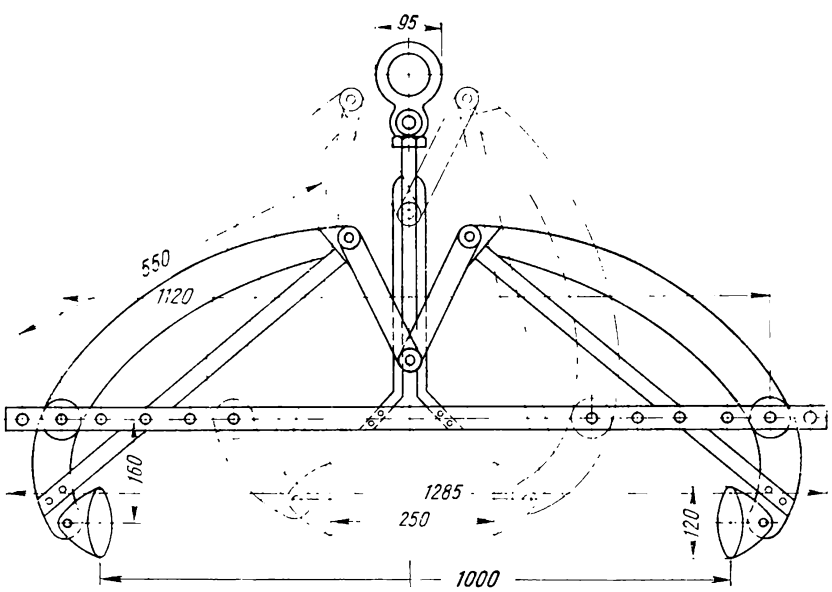

Fig. 90. Tongs for handling concrete slabs and large stones

Ordinary and Self-Closing Tongs. The tendency to reduce the amount of manual labour in handling piece loads to the minimum has led to the development of various types of tongs and other automatic grabs. As a rule, the tongs are made self-closing, i.e., they close under the action of the load being handled. The tongs are opened manually by means of a special lever.

Fig. 89 shows self-closing tongs for handling bales, boxes, barrels, etc.; they are suspended from a crane hook and are held open by an automatic dog as they are lowered onto the load. As soon as the dog is released the tongs are closed by the tension of the lifting ropes.

Fig. 90 illustrates tongs for handling concrete slabs and large stones.

8. ELECTRIC LIFTING MAGNETS

Lifting magnets are used to handle magnetic materials of diverse form (ingots, beams, rails, steel sheets and plates, pipes, scrap, metal chips, pigs, boxes containing steel articles, etc.). Lifting magnets have found especially widespread application in metallurgical and mechanical engineering works. Their principal advantage lies in the fact that they eliminate the need for manual suspension of loads and drastically reduce the time required for this operation.

Lifting magnets have the disadvantage of a certain reduction in the useful lifting capacity due to the weight of the electric magnet.

However, lifting magnets can cope with a considerable amount of load in minimum time and substantially increase the efficiency of the lifting devices. This also allows a more rational utilisation of storage floorspace where the height of stacks can be increased without applying manual labour.

Personnel should keep away from the zone of the magnet action as sudden failure of current will drop the load.

Lifting magnets operate on direct current. The lifting capacity of the same magnet varies within a wide range depending on the form, size, chemical composition and temperature of the objects being lifted. The magnet develops the maximum lifting power when massive objects with a smooth surface are being raised. If the load has an irregular shape and is composed of small articles the lifting capacity of the magnet drops sharply (Table 21).

Table 21

Specifications of Lifting Magnets Manufactured by the Dynamo Works

Type	External dia, mm	Height of suspension tackle, mm	Size of eye bolt, mm		Generator rating, kw	Current with hot coil, a	Weight, kg	Lifting capacity, kg			
			height	width				Ingot or plate	Scrap	Pigs	Steel chips
M-21	785	825	175	100	3.5	8.6	460	6,000	180	200	80
M-31	1,000	925	200	120	5.5	15	820	9,000	300	250	110
M-41	1,170	1,165	250	140	11.0	30	1,670	16,000	500	600	200
	Length	Width									
ПМ-1	1,000	420	—	—	1.5	4.9	700	—	—	—	—
ПМ-3	2,000	420	—	—	3.0	9.7	1,300	—	—	—	—

The lifting capacity of the magnet drops as the magnetic properties of the load being lifted weaken, as for example, when the load contains admixtures of manganese and nickel. An increase in the temperature of the object being lifted to 200 -300 C does not change its magnetic properties and the lifting capacity of the magnet is retained. At temperatures above 300 C the lifting power of the magnet decreases. Electric lifting magnets can be used to handle loads with a temperature of up to 600 C if they have thermal insulation. When the load temperature is 700 C and over the lifting capacity of the magnet drops to zero. The Dynamo Works in Moscow manufactures circular (type M) and rectangular

(type M) lifting magnets. Rectangular magnets are used for handling regularly shaped objects such as beams, ingots, pipes, sectional and sheet steel, etc. Since many loads require a relatively small area of attraction the electromagnet is small in width but long.

Circular magnets usually handle loads of diverse form and size.

The electric lifting magnet should possess a high mechanical and electric properties and retain its operating efficiency under heavy service. The magnet should be able to withstand heavy blows from the massive loads it attracts and shocks caused by falling onto the load being raised.

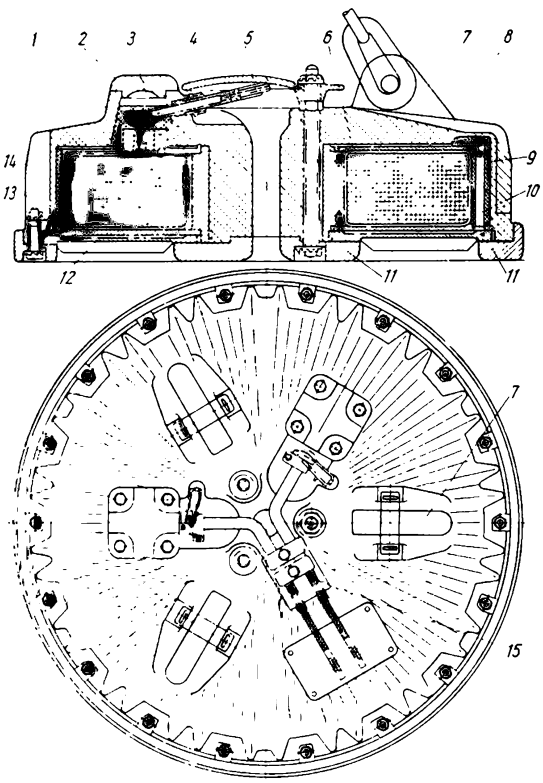

Fig. 91. Electric lifting magnet

1—coil terminal, *2*—cover, *3*—hatch, *4*—insulated copper stud, *5*—cable, *6*—coil, *7*—lugs for lifting the magnet, *8*—body, *9*—steel bush, *10*—stud, *11*—pole shoes, *12*—nonmagnetic plate, *13*—lower brass spacer plate, *14*—fins, *15*—springs

Fig. 91 shows an electric magnet, type M, manufactured at the Dynamo Works. The current is supplied by an insulated double-core flexible cable in a rubber hose. When the magnet is raised the cable winds up on a special take-up drum mounted on the crane truck.

Electric lifting magnets with large masses of magnetic steel have quite a large residual magnetism and continue to hold all light objects even after the magnets are deenergised. To eliminate residual magnetism and release the attracted objects a reverse current is passed through the magnet coil. This demagnetising current should be much weaker than the operating current, otherwise the magnet will be magnetised again.

9. GRABBING ATTACHMENTS FOR LOOSE MATERIALS

Tubs. Self-dumping tubs are suspended on a crane hook by a bale; they turn over on horizontal trunnions. The centre of gravity of a loaded tub should be so selected as to enable the tub to retain its vertical position during movement with the aid of a trip bar. When the trip bar is released the tub tilts over and discharges its contents. Since the centre of gravity of an empty tub is behind the trunnions the tub returns to the vertical position after the load has been dumped.

Fig. 92 shows a self-dumping tub with a sloping front wall. This form permits the tub to be brought to the pile in such a manner that most of the material runs into it by gravity and only a small amount has to be loaded by shovels.

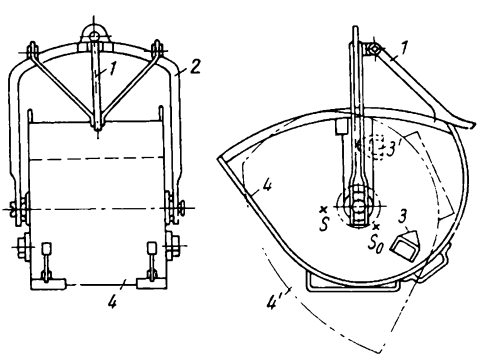

Fig. 92. Self-dumping tub

1—locking lever, *2*—bail, *3*—tilt-limiting stop, *4*—tub, *S*—centre of gravity of loaded tub, S_0—centre of gravity of empty tub

Self-dumping tubs have a capacity of 0.25 to 3 cu m. They are used chiefly for charging bunkers.

Side-Dump and Bottom-Dump Tubs. Tubs of this type are used to handle gravel, sand, earth, etc., with the help of cranes. They are superior to the tilting tubs in that they do not scatter much of the material in dumping.

A bottom-dump tub is shown schematically in Fig. 93*a*. Attached to lifting ropes *1* is a cross-member with pipe *3* connected to body *8* of the tub. Hinged doors *5* of the bottom are linked by rods *6* with central rod *4*, the upper end of which is attached to dumping rope *2*. The closed tub hangs on rope *2* with its doors held against stops *7*; ropes *1* are only slightly tensioned. At the moment of dumping, ropes *1* retain their former position and rope *2* is released; the weight of the material opens the doors.

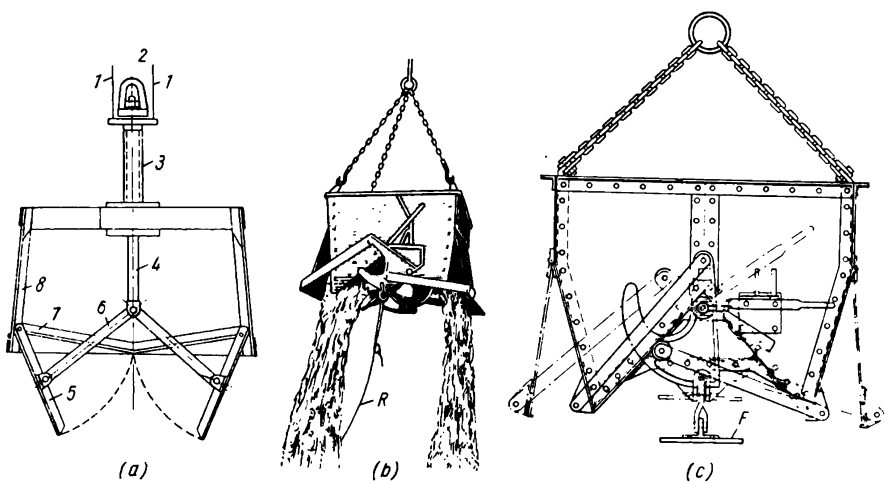

Fig. 93. Bottom-dump and side-dump tubs

Fig. 93*b* shows a side-dump tub. The tub can be dumped at any height by pulling on rope *R*. On top of a pile it can be dumped automatically by means of pad *F* (Fig. 93*c*).

Side-dump and bottom-dump tubs have a capacity ranging from 0.3 to 2 cu m.

Tubs with Scoops. These tubs have a capacity of 1 to 3 cu m and for special purposes up to 8 cu m. They comprise two hinge-jointed scoops with a rounded bottom.

One such tub is shown in Fig. 94. During loading and movement it hangs from cross-member *c*, frame *g* and holding ropes *m*. The tub is opened by levers *h* linked to movable cross-member *f* and dumping ropes *n*. As the latter are pulled up, the levers *h* grip hooks *i* and open the tub. The holding and dumping ropes (*m* and *n*) wind up on separate drums of a hoisting winch.

When the capacity of such tubs is not large and the service is not severe special double-drum winches can be dispensed with. For this purpose the holding and dumping ropes *m* and *n* are suspended on an ordinary hook of a hoisting device. In this case the tub is raised with hooks *d* and *e* linked together. To open the tub these hooks should be disengaged and the tub suspended on levers *h* engaged to hooks *i*.

In these and similar designs the cross-member for opening the tub is part of the hoisting device and the tubs themselves are but temporary containers for the load in which it is conveyed by various modes of transport.

Tubs with scoops are frequently used to collect chips for which purpose they are installed in special pits. Filled tubs are lifted from the pits and conveyed by a crane to the storehouse for chips and scrap.

Grab Buckets. The designs of tubs discussed above have an automatic dumping process but they require manual labour and mechanisms for loading. Some of the designs require operating personnel even during dumping. These shortcomings make the application of tubs irrational when large amounts of loose material have to be handled. Instead, use is made of special buckets which mechanically grab and automatically dump the material.

The available designs of grab or clamshell buckets can be subdivided into the following four types: double-rope, single-rope, motor-driven and special.

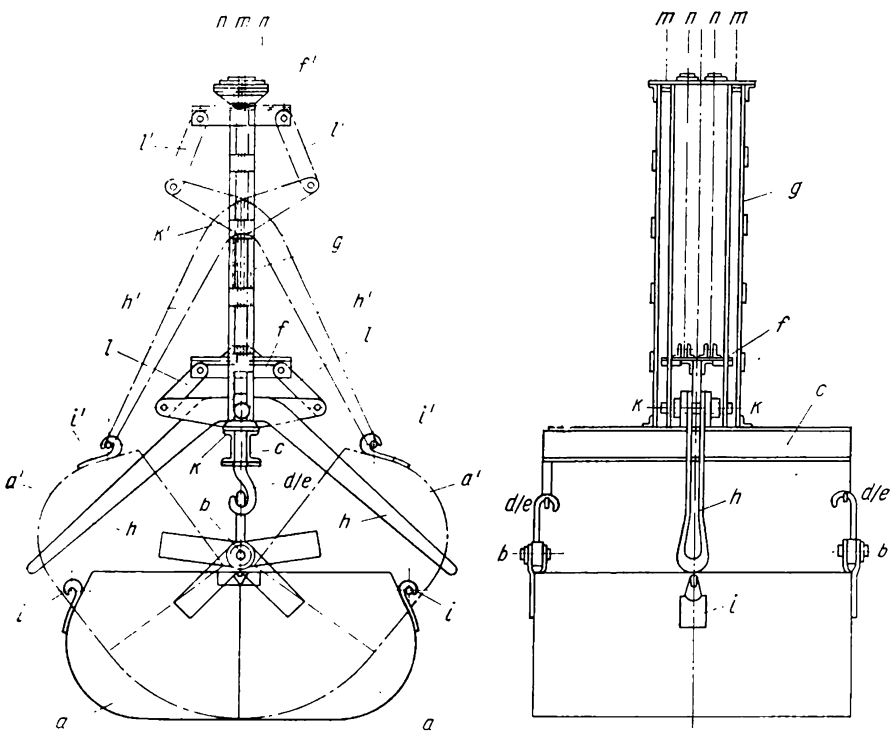

Fig. 94. Tub with scoops

a—scoops, *b*—shaft, *c*—lifting cross-member, *d* and *e*—hooks, *f*—movable cross-member, *g*—guiding frame, *h*—tong-type levers *i*—scoop hooks, *k*—lever pin, *l*—rods between *f* and *h*, *m*—holding ropes, *n*—dumping ropes

Double-Rope Grab Buckets. These are grab buckets in which the lifting operation is effected by one group of ropes (or one rope) called the hoisting or holding rope and the opening and closing by another group of ropes (or one rope) called the closing rope.

Double-rope grab buckets can be dumped at any height but this requires a special double-drum winch.

A general view of a symmetric or centre-pull double-rope grab bucket is illustrated in Fig. 95. Two scoops with rounded bottoms are hung from four rods outside and from a cross-member inside. The rods are provided with upper joints in the cross-member to which the hoisting ropes are attached. The upper and lower cross-members accommodate sheaves for the closing ropes. The grab bucket hangs on hoisting and closing ropes and is opened or closed by slacking or tensioning the closing ropes. The principle of operation of a double-rope grab bucket is shown in Fig. 96.

An opened bucket (Fig. 96*a*) is lowered as follows. Both drums a_1 and a_2 revolve for descent, i. e., clockwise. The grab bucket goes down until its scoops engage the material to be handled.

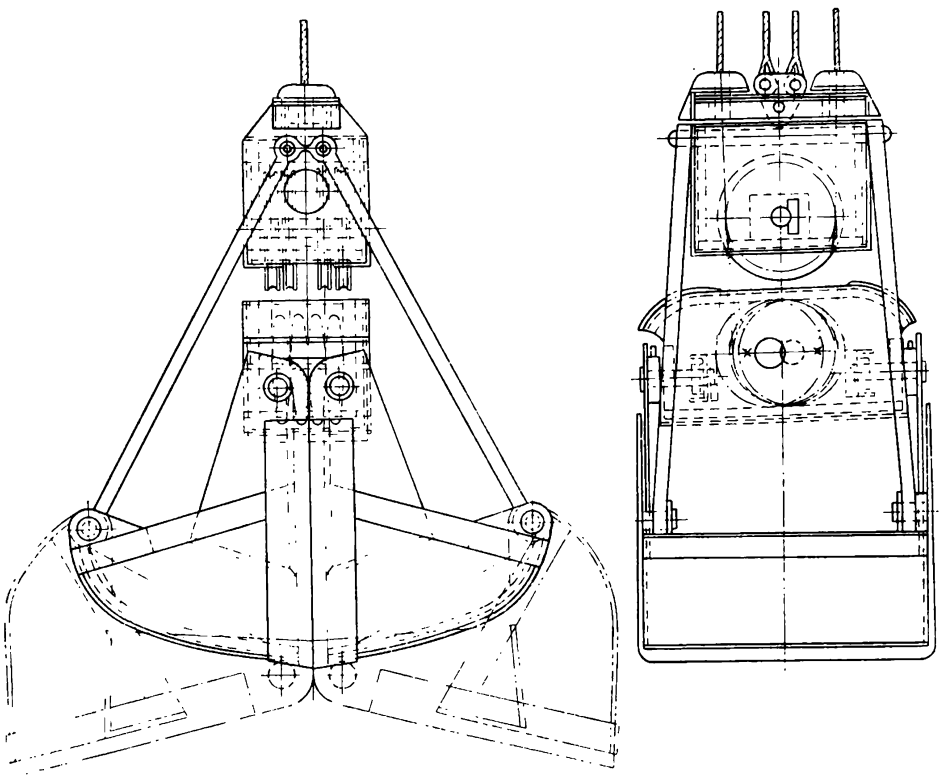

Fig. 95. Double-rope symmetric or centre-pull grab bucket

The grab bucket is closed as follows (Fig. 96*b*). The closing drum a_1 rotates fo lifting, i. e., counterclockwise while the hoisting drum a_2 is immobile. The closing rope S_1 is tightened, the movable cross-member goes upwards and the scoops cut into the material as they are gradually brought together until their edges are tightly compressed. In raising (Fig. 96*c*) both drums rotate clockwise.

To dump the grab bucket (Fig. 96*d*) the hoisting drum is braked and the closing drum revolves for descent (clockwise); this causes the bucket scoops to open under the action of their own weight and that of the material and the contents are dumped.

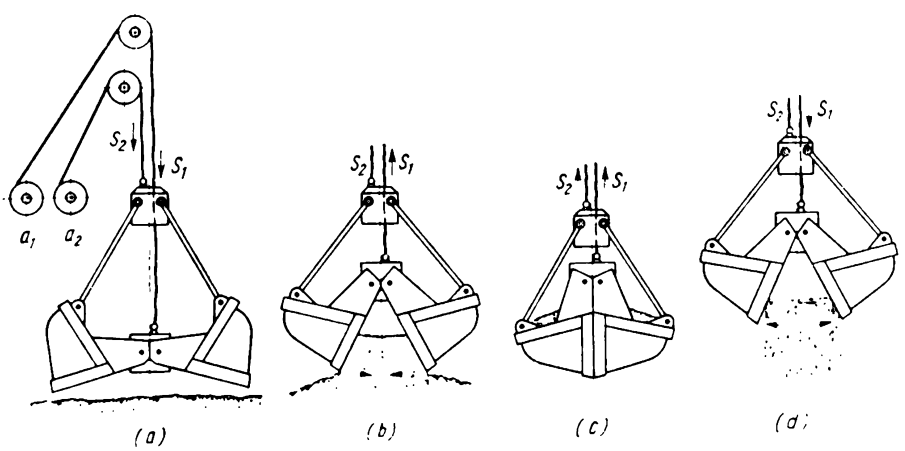

Fig. 96. Principle of operation of a double-rope grab bucket

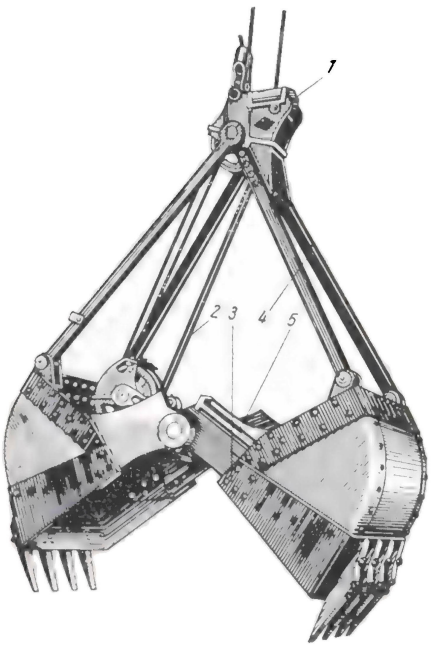

Fig. 97. Asymmetric or lever-arm grab bucket

Depending on the kind of the material the edges or lips of the scoops are either smooth or provided with teeth. The pulley for the closing rope is usually a system for a gain in force between the tension of the closing rope and the cutting force on the scoops edges. The transmission ratio of the pulley system depends on the material and ranges from 4 to 6 in the grab buckets handling coal and ore.

Depending on the material for which they are intended grab buckets are manufactured in three designs:

light-duty (for handling coal, not very hard and small-lump coke, fine ore, salt, etc.);

medium-duty (for handling hard large-lump coal, ore of medium specific weight, clinker, sand, gravel, etc.);

heavy-duty (for handling large-lump ore, hard rocks and other loose materials with similar properties).

Another modification is the asymmetric or lever-arm grab bucket. Such grab buckets (Fig. 97) consist of cross-member *1*, pulley system for closing rope *2*, scoops *3*, four rods *4*, rocker arm 5 and hoisting and closing ropes. This grab bucket is distinguished for a more advantageous position of its centre of gravity as compared with symmetric-type buckets, by comparatively simple assembly and smaller overall size. Besides, the presence of a rocker arm produces a large closing force on the scoop edges. This makes it possible to reduce the number of sheaves and simplify the design of the cross-members.

The Tauber Double-Rope Grab Bucket (Fig. 98) comprises a bell formed by two parallel longitudinal walls connected on top by horizontal plates, a cross-member connected to the bell, an upper cross-member, two knife scoops, rods and a pulley system.

To grab the material an opened bucket is lowered onto the material in the position shown in Fig. 99*a*. Dropping at high speed the side walls of the grab cut into the material. When the winch drum begins to wind the closing rope the upper and lower cross-members are drawn together and the knife scoops bite into the material pushing it into the space between the walls of the bell. When the scoops are completely closed they will form together with the side walls of the bell the bucket shown in Fig. 99*b*. This new modification has appreciable advantages over other designs.

Single-Rope Grab Buckets. These are buckets in which both working operations (hoisting or lowering, closing or opening) are performed by one pulling device, usually a rope. Such grabs are used where the same lifting device is employed for handling piece and loose loads, for example in foundry shops to handle moulding sand, at construction sites, in cinder ditches when cleaning locomotives, etc. In other words, single-rope grab buckets are employed for short-term jobs after termination of which they are removed from the crane hook (if thus hung) or are replaced by a lifting hook (when the bucket is attached directly to the hoisting ropes of a winch).

There are single-rope self-dumping grab buckets (bell grabs) and grab buckets which are dumped by means of a separate rope or chain.

Grab buckets of the first type are obsolete and find very limited application

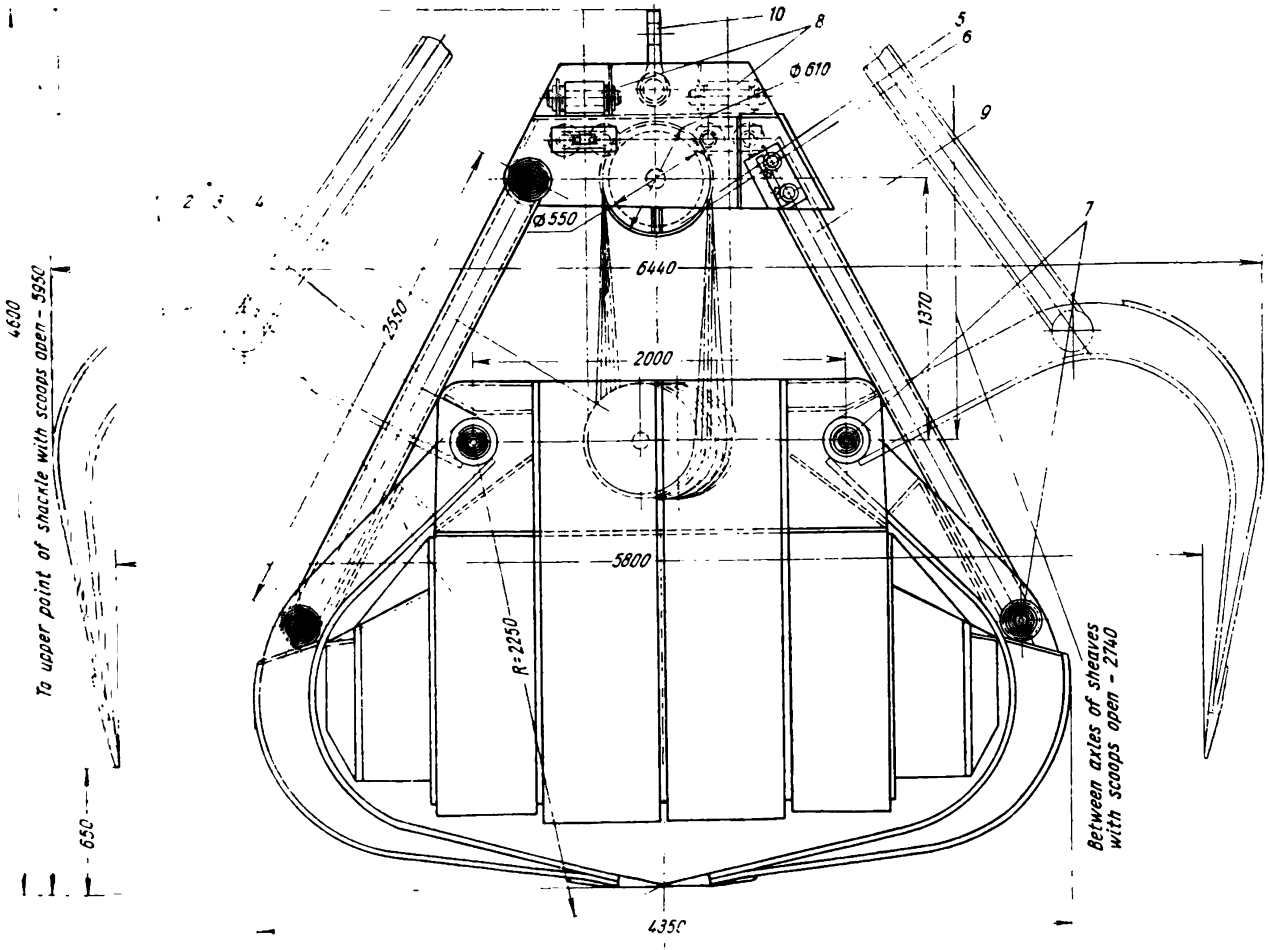

Fig. 98. Tauber double-rope grab bucket

1—scoop, *2*—bell, *3*—movable rod, *4*—lower sheaves, *5*—head, *6*—upper sheaves, *7*—ball-type oilers, *8*—guiding rollers, *9*—fixed rod, *10*—shackle

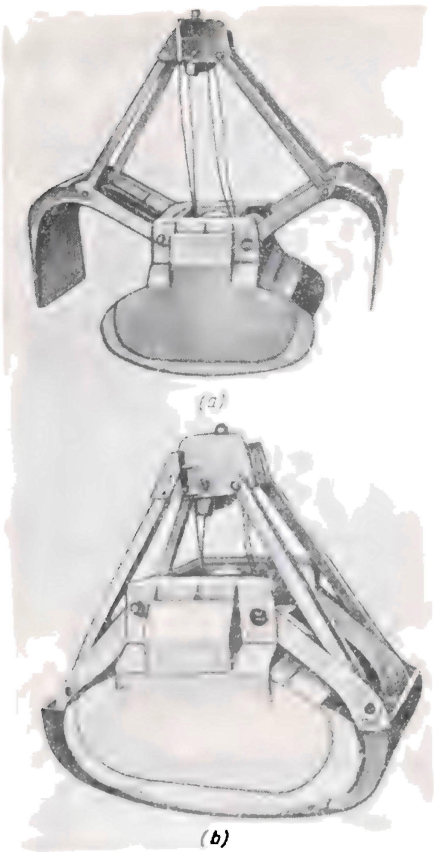

Fig. 99. Tauber double-rope grab bucket in operation

today. Hand-operated grab buckets are free from the shortcomings inherent in self-dumping grabs and are quite widespread in a variety of improved versions. Fig. 100 shows the construction of a single-rope grab bucket, hand-operated by means of a chain.

Motor-Driven Grab Buckets. In motor-driven grab buckets the scoops are closed and opened, as a rule, by a chain or rope driven by a motor installed on the frame of the grab. A motor-driven grab bucket which closes independently from the crane winch can be suspended on the hook of any crane without the use of a special double-drum winch. Therein lies its essential advantage, since the crane can be used for handling both piece and loose loads. Moreover, a motor-driven grab can open to any amount within the limits of the scoop span which is very important in many cases.

In foundry shops motor-driven grabs can be used both for handling loose materials (coke, sand) and for cleaning casting pits. Since the grab bucket can be easily removed from the crane the latter can be at any time adapted for conveying mould flasks, patterns and castings.

A motor-driven grab can be dumped at any height and grab the material carefully because the opening of the scoops can be adjusted as desired. Smooth operation of a motor-driven grab bucket helps to prolong the service life of the means of conveyance (railway cars, etc.).

Motor-Driven Grab Bucket with an Electric Hoist. This design (Fig. 101) comprises an ordinary lever-type grab bucket with one central shaft for scoops that are closed by an electric hoist. The scoops are controlled by the pulley ropes whose sheaves are secured on the lower cross-member. To prevent accidents and breakdown in case the motor has not been switched off for some reason or other with the grab closed, a special safety clutch is provided between the motor and the hoist mechanism.

Special Grab Buckets. These are buckets with specially shaped scoops to conform with the kind of operation and the material to be handled. The closing mechanism and the upper part of the grab are usually designed along conventional lines.

Multi-Blade Grab Bucket. An extremely important feature in grab buckets handling lump material is the degree to which its capacity is utilised and the ability to hold the load; besides, such grabs should not crush the material thereby often deteriorating its quality. Ordinary grab buckets in which both scoops swing in one plane are not very effective in handling lump material. An adequate filling is easily achieved only in a multi-blade grab in which the scoops are located in different planes. Such grabs are known as orange-peel buckets. Thanks to their tong-like form the scoops, or rather blades, of such devices (from 3 to 8) easily

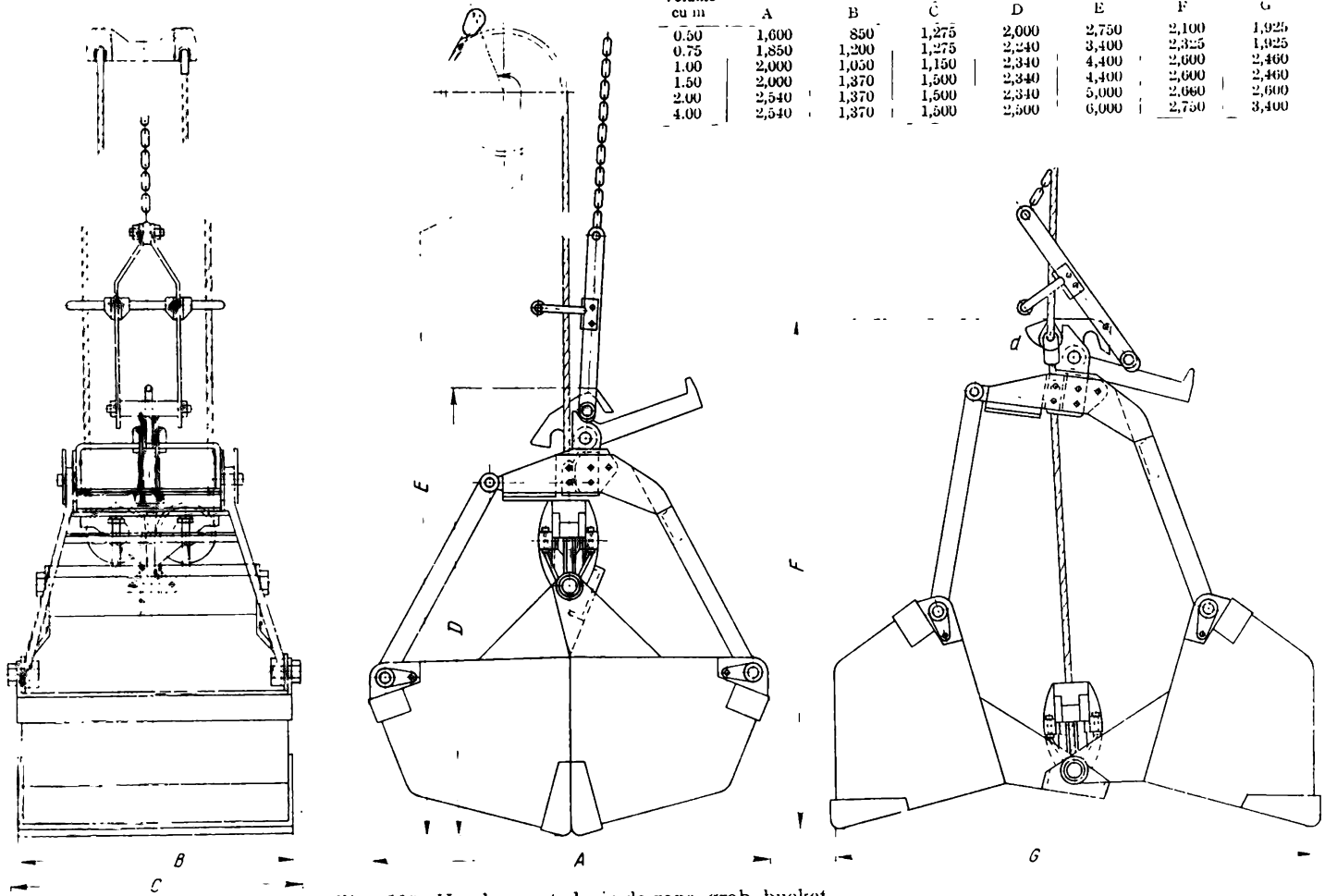

Volume cu m	Main dimensions						
	A	B	C	D	E	F	G
0.50	1,600	850	1,275	2,000	2,750	2,100	1,925
0.75	1,850	1,200	1,275	2,240	3,400	2,325	1,925
1.00	2,000	1,050	1,150	2,340	4,400	2,600	2,460
1.50	2,000	1,370	1,500	2,340	4,400	2,600	2,460
2.00	2,540	1,370	1,500	2,340	5,000	2,660	2,600
4.00	2,540	1,370	1,500	2,500	6,000	2,750	3,400

Fig. 100. Hand-operated single-rope grab bucket

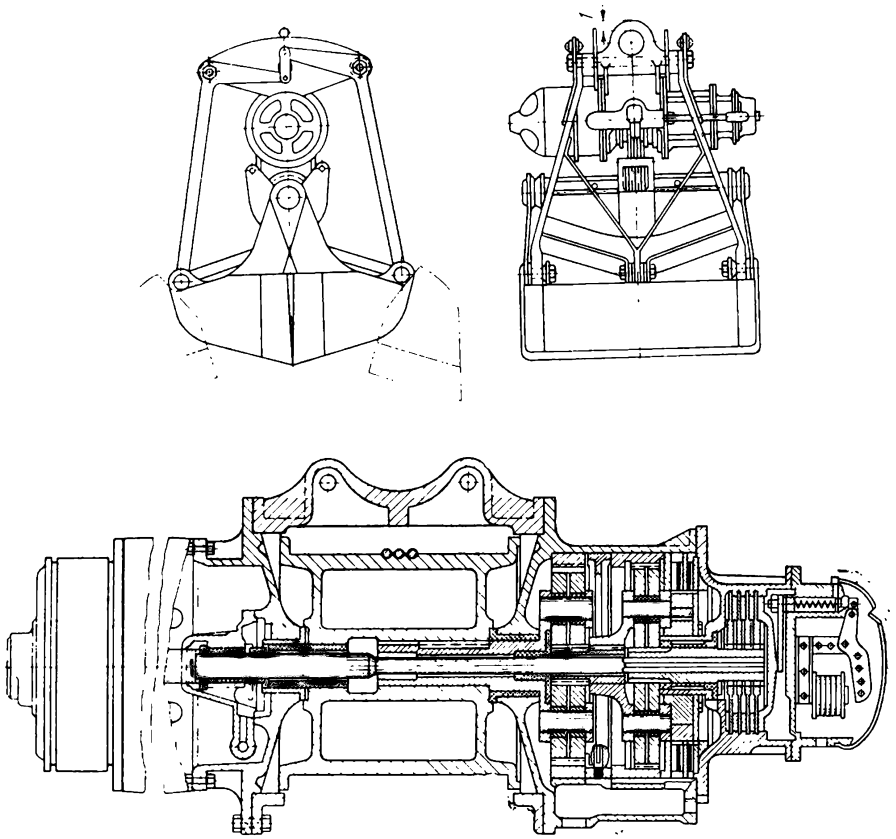

Fig. 101. **Motor-driven grab bucket with an electric hoist**

engage the mass of lumpy material causing only an insignificant damage to its integrity. As the blades of an orange-peel bucket penetrate into a porous material they encounter various resistance and for this reason the operation of the grab will be more effective if its blades move independently from each other. Indeed, in an eight-blade orange-peel bucket, for example, when four of the blades bear against the material, the other four penetrate into its mass; hence, these four blades can penetrate into the material only if the design of the bucket allows them to advance in front of the other blades, i. e., if they move independently.

The design of a six-blade orange-peel bucket is shown in Fig. 102*a*. The scoops of the grab are connected by rods with the head and the closing rope and not through the bottom cross-member as in ordinary grab buckets. Each blade is provided with a sheave for the closing rope which consecutively encircles the sheaves of the head and the blades making for independent movement of the latter. In this way, the bucket is a combination of separate mechanisms operating similarly to the human hand.

When an orange-peel bucket closes, a definite force is developed in each blade. Uniform distribution of forces in the blades is achieved because the closing rope consecutively encircles the sheaves in the head and in the blades and passes through compensating sheaves. For this purpose the sheaves in the head have a star-like construction.

The external movement of the scoops is limited by the size of the rings which connect them. The blade sheaves are protected by casings which simultaneously protect the closing rope against wear. The hoisting ropes are fastened in the grab head by wedge clamps. A general view of an orange-peel can be seen in Fig. 102*b*. Fig. 102*c* and *d* shows the bucket handling a stone.

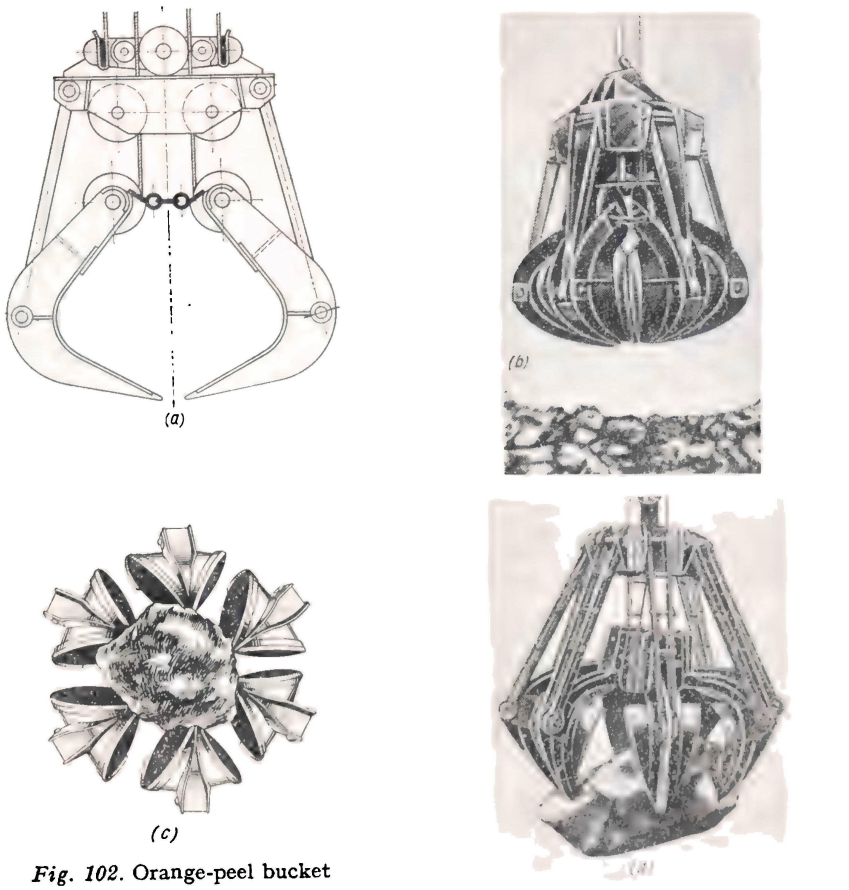

Fig. 102. Orange-peel bucket

A grapple for handling metal chips is shown in Fig. 103. Its scoops are made in the form of separate steel tines. A multiple-tine grapple for stones (Fig. 104) is a variety of a multi-blade grab adapted for handling large-lump material.

10. METHODS FOR DESIGNING GRAB BUCKETS

So far we have scarse knowledge of the phenomena arising during the operation of various types of grabs, scoops, buckets, scrapers, etc., which automatically grab diverse loose materials because we know very little of the physical properties of these materials. However, for normal operation of such devices as grabs, the knowledge of the physical properties of the loads is a primary requisite.

The following properties of loose materials affect the parameters of grabs: size and form of lumps, their moisture content, viscosity, internal friction, bulk weight, degree of resist-

Fig. 103. Grapple for metal chips

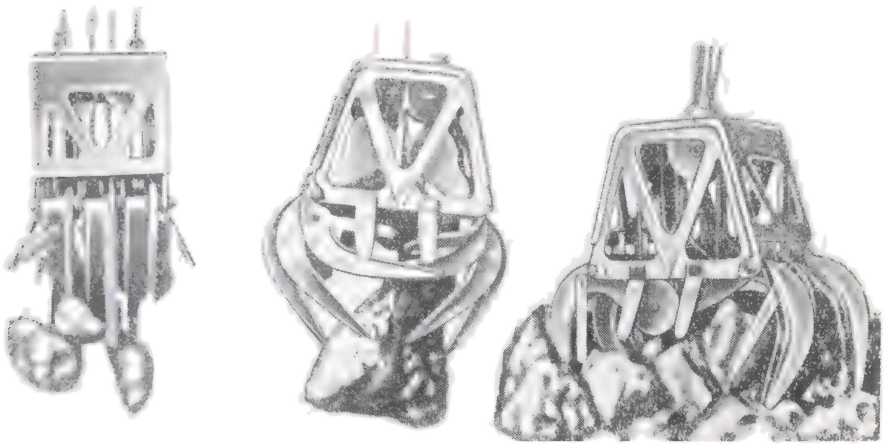

Fig. 104. Multiple-tine grapple for handling stones

ance of the material to the penetration of alien bodies, etc. The methods of designing grabs on the basis of physical properties of loose materials could be called ideal. Unfortunately, these methods do not yet exist.

Grabs are designed by the following methods.

The type of grab and its weight are selected on the basis of experimental data and the kind of the material being handled.

The dependence between the weight and capacity of a grab can be expressed by the following ratios:

(a) for a light-duty grab

$$G_{gr} = 0.8V + 0.5;$$

(b) for a medium-duty grab

$$G_{gr} = 1.5V + 0.5;$$

(c) for a heavy-duty grab

$$G_{gr} = 2.3V + 0.5;$$

(d) for a very heavy-duty grab

$$G_{gr} = 3V + 0.5$$

where G_{gr}—weight of the grab, in tons;
V—grab capacity, in cu m.

The size of the grab scoops is found from the given capacity and standardised main dimensions.

Using a dimensioned gearing diagram of the grab mechanisms and data on the weight of its parts we can find the forces acting in its parts on the basis of statics.

Experimental data recommend the following weight relationships:

$$G_1 = 0.2G_{gr};$$

$$G_2 = 0.5G_{gr};$$

$$G_3 = 0.3G_{gr}$$

where G_1—weight of the lower cross-member with counterweights;
G_2—weight of the scoops;
G_3—weight of the upper cross-member with rods.

The determined forces are used to check the strength of the grab parts.

Finally, we determine the force needed to close the scoops.

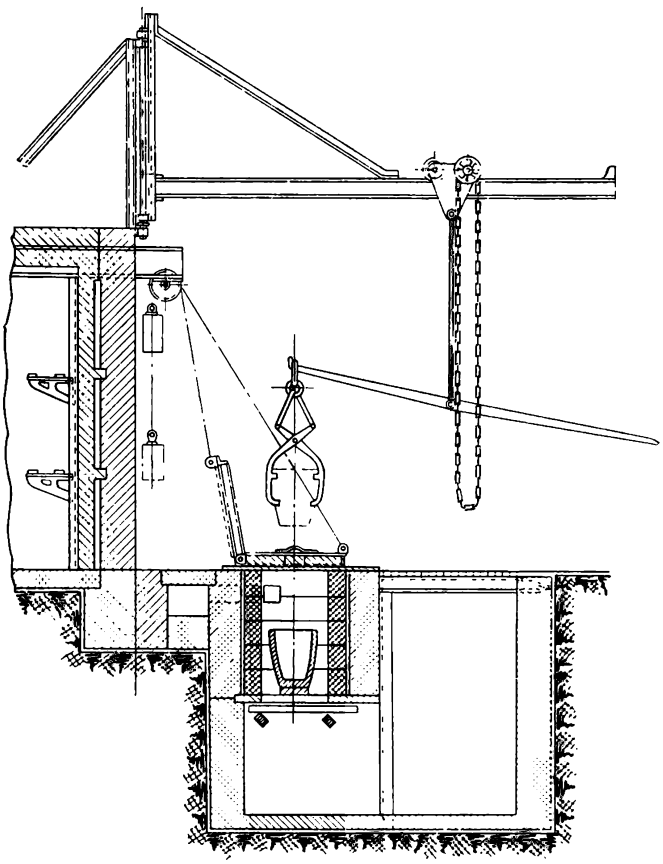

Fig. 105. Rotary jib crane with crucible tongs

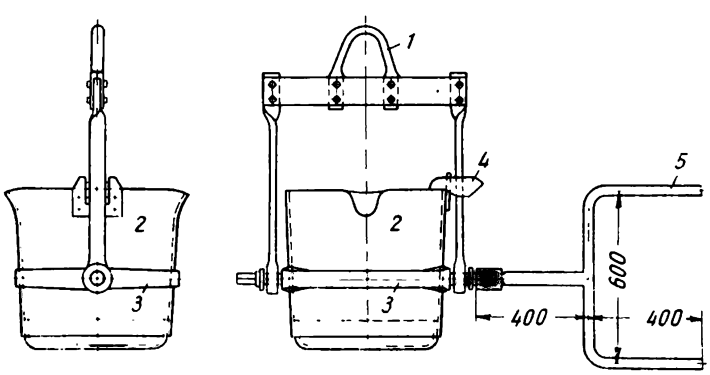

Fig. 106. Crane ladle

1—bail, *2*—ladle, *3*—ring with trunnions, *4*—stop, *5*—tilting fork

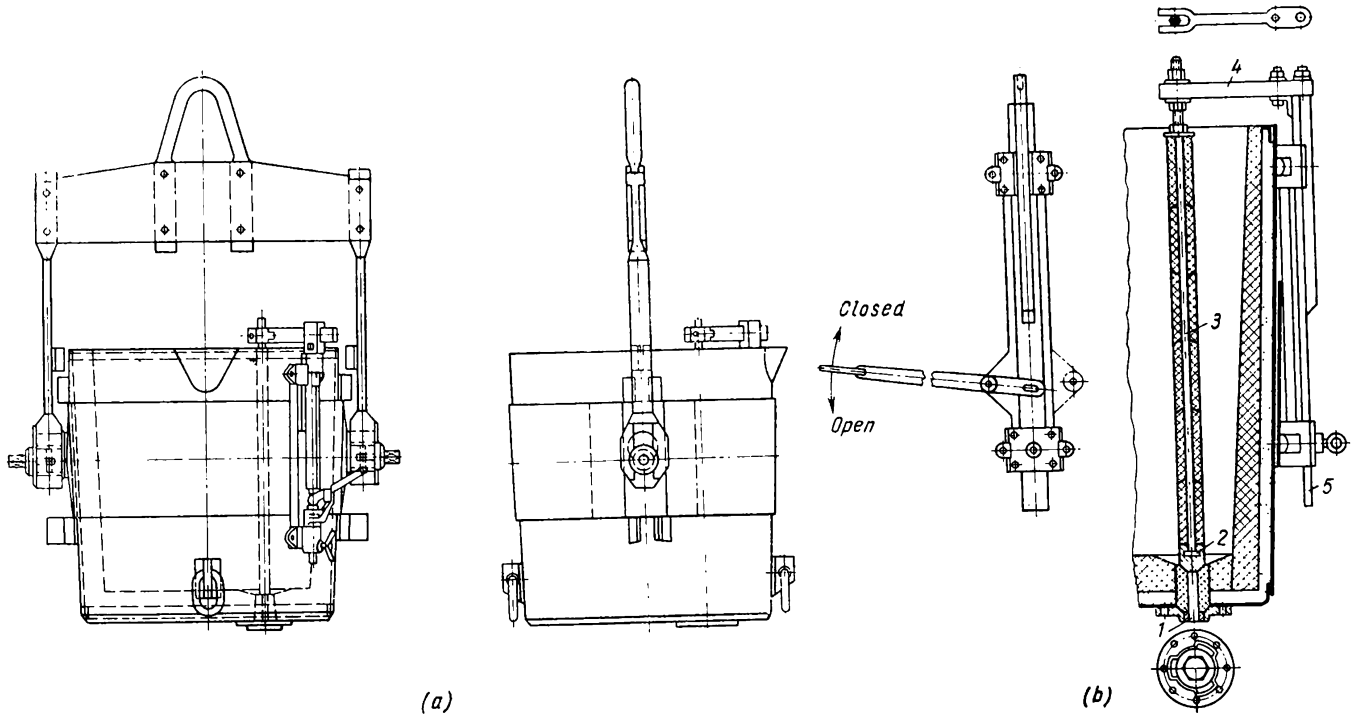

Fig. 107. Bottom-pour ladle:

a—ladle, *b*—stopper device: *1*—taphole, *2*—stopper, *3*—refractory-covered stopper rod, *4*—lever, *5*—handle

11. CRANE ATTACHMENTS FOR HANDLING LIQUID MATERIALS

Crucibles (for melting copper alloys, steel and other metals) are manufactured of refractory materials; they can hold from 40 to 300 kg of metal.

Crucibles are removed from furnaces and conveyed by fork tongs. They do not damage the walls of the crucibles which lose much of their strength due to the high temperature.

Fig. 105 shows a rotary jib crane with a lever and tongs for handling crucibles.

Ladles for handling liquid metal are made of plate steel and have a refractory lining. Ladles of small capacity are handled manually. Large ladles are conveyed by narrow-gauge cars or monorails or by means of cranes. They are suspended on the crane hook from special tilting bails.

Small capacity crane ladles are tilted manually by means of lever forks (Fig. 106); self-tilting is prevented by a special stop. To pour medium-size ladles use is made of a special tilting device actuated by a handwheel. Large ladles are tilted with the aid of a special mechanism mounted on the crane trolley. Bottom-pour ladles (Fig. 107) are provided with a taphole in the bottom which is closed by a stopper fitted onto a movable rod. The rod is actuated by a system of hinge-jointed levers whose design should take into account the temperature expansion of the metal.

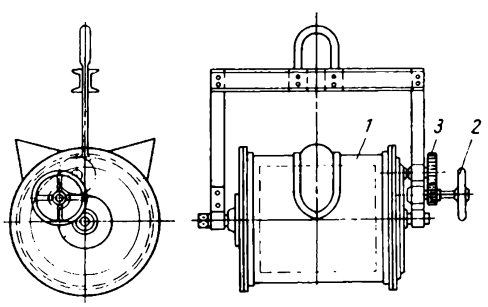

Fig. 108. Drum ladle
1—drum with refractory lining, *2*—handwheel for tilting the ladle, *3*—gearing

Drum ladles with a capacity of 0.5 to 5 tons (Fig. 108) are employed in foundries; they are moved around on trucks along narrow-gauge tracks or by means of cranes.

Safe and easy servicing (the personnel is better protected against heat radiation than in servicing ordinary ladles) and insignificant heat losses due to radiation (because the drums are closed) make the application of drum ladles highly effective.

A drum ladle can be tilted more easily than an ordinary ladle of equal capacity because in the former only the friction of the molten metal against the walls of the drum and the friction in the journals need be overcome whereas an ordinary ladle must be raised somewhat to pour metal. For the repair of linings of drum ladles their detachable walls can be easily removed. Since drum ladles are subject to the same stresses over their entire surface they have a much longer life than other designs of ladles.

CHAPTER VI

ARRESTING GEAR AND BRAKES

1. ARRESTING GEAR

Arresting gear is used to hold the load lifted by winches.

Ratchet Gearing. This type of gearing comprises a ratchet wheel and a pawl. Ratchet teeth can be arranged external or internal to the wheel or at its side. The teeth are so shaped that the ratchet runs free when the load is being raised.

Fig. 109*a* shows the most widespread design of ratchet gearing with teeth on the outside of the wheel. Best engagement is obtained at a point of contact between the tangent passing through the pawl pivot and the outside diameter of the ratchet wheel. In this case pressure on the pawl is directed along the peripheral force.

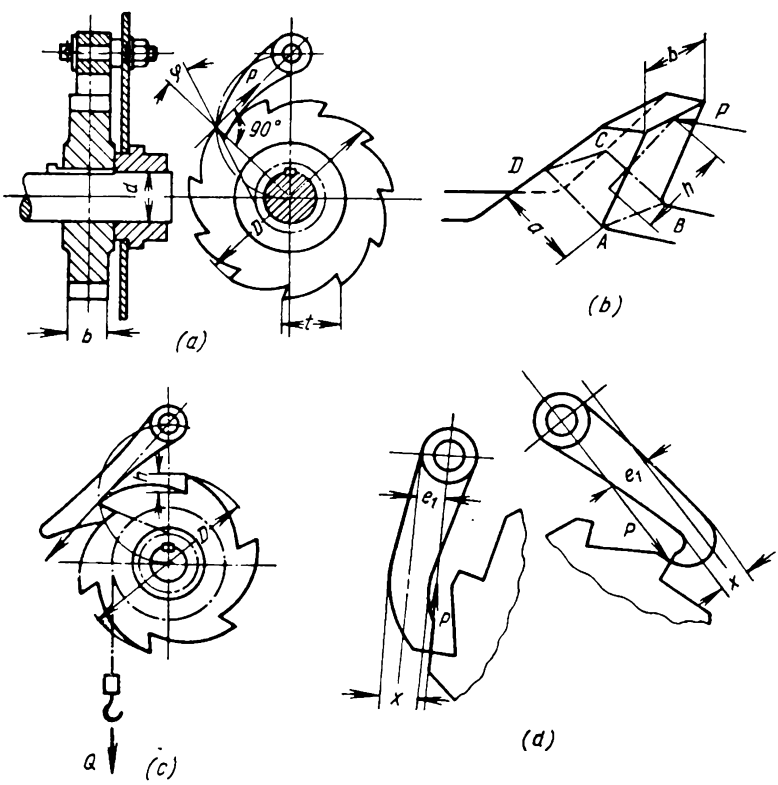

Fig. 109. Ratchet gearing with external teeth

Depending on its purpose a ratchet wheel can be designed with different numbers of teeth:

$z = 6$ to 8 for rack-and-pinion jacks, ratchets and brakes applied by the lifted load (worm hoists);

$z = 12$ to 20 for independent ratchet arresters;

$z = 16$ to 25 and more for ratchet-type brakes.

The length of the teeth (width of the pawl bearing area) is selected with account taken of linear unit pressure

$$b = \frac{P}{p}$$

where P—peripheral force;

p—linear unit pressure.

Unit pressure is taken as $p = 50$ to 100 kg/cm for a steel pawl and a cast-iron ratchet wheel and $p = 150$ to 300 kg/cm for a steel pawl and a steel ratchet wheel.

The teeth of a ratchet with external engagement are checked for bending by the formula

$$m \approx 2\sqrt[3]{\frac{M}{z\psi\,[\sigma_{bend}]}} \tag{95}$$

where m—module equal to the pitch on the outside diameter divided by π;

M—transmitted torque in kg-cm;

z—number of teeth; $\psi = \frac{b}{m} = (1.5 \text{ to } 3.0)$;

$[\sigma_{bend}]$—safe bending stress.

Formula (95) (see Fig. 109*b*) is derived as follows:

Let $ABCD$ be the tooth fracture area.

The strength equation for bending will be

$$Ph = \frac{a^2 b}{6}[\sigma_{bend}].$$

Usually $a = m$ and $h = 0.75$ m; $b = \psi m$; $P = \frac{2M}{D}$ and $D = zm$.

Then

$$\frac{2M}{zm}\,0.75m = \frac{m^2 \psi m\,[\sigma_{bend}]}{6}$$

and

$$m \approx 2\sqrt{\frac{M}{z\psi\,[\sigma_{bend}]}}.$$

The peripheral speed of the ratchet wheel is directly proportional to its diameter. Since the force of impact between the pawl and tooth increases in proportion to the square of the velocity, a harmful increase in peripheral speed should be avoided.

Impact at high speeds is lessened by employing smaller teeth and pitch; use can also be made of two or several pawls whose points of engagement are shifted by a corresponding fraction of the pitch. In independent ratchet gearing or ratchet-type brakes the ratchet wheel is always fixed on the shaft.

The ratchet pawl can be designed as in Fig. 109*a* or have the shape of a catch shown in Fig. 109*c*.

The pawl is checked either for eccentric compression or eccentric tension:

$$\sigma = \frac{M_{bend}}{W} + \frac{P}{F}$$

where $M_{bend} = Pe_1$;

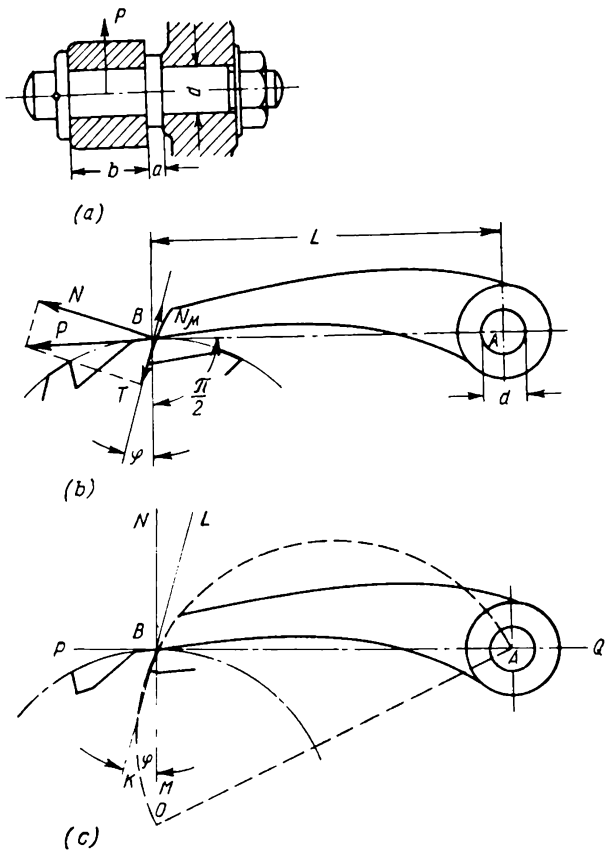

Fig. 110. Diagrams for designing ratchet pawls

$W = \dfrac{bx^2}{6}$ is the minimum moment of resistance (Fig. 109*d*).

The pawl pin (Fig. 110*a*) is usually considered as a cantilever beam subject to bending.

The strength equation is

$$Pl = 0.1d^3\,[\sigma_{bend}].$$

For $l = \dfrac{b}{2} + a$ and $P = \dfrac{2M}{zm}$ we have

$$d = 2.71\sqrt[3]{\frac{M}{zm\,[\sigma_{bend}]}\left(\frac{b}{2} + a\right)}. \tag{96}$$

In view of impact load application the pin is usually made of steel 45 taking a somewhat reduced safe bending stress:

$$[\sigma_{bend}] = (300 \text{ to } 500) \text{ kg/cm}^2.$$

The best conditions for a pawl sliding over the ratchet teeth are obtained when $\varphi > \varrho$ where ϱ is the angle of friction (Fig. 110*b*). The force $T = P \sin\varphi$ tends to push the pawl towards the root of the tooth while the friction forces $N\mu$ (where $N = P\cos\varphi$) and the friction forces in the pawl pin $P\mu_1$ oppose this movement.

When $\Sigma M_A = 0$ we obtain

$$(T - N\mu)\,L\cos\varphi - P\mu_1\frac{d}{2} = 0.$$

Substituting the values for T and N and cancelling $\cos^2 \varphi$ we have

$$PL(\tan \varphi - \mu) - \frac{1}{\cos^2 \varphi} P\mu_1 \frac{d}{2} = 0$$

and

$$\tan \varphi - \mu = \frac{\frac{d}{2}\mu_1}{L \cos^2 \varphi}.$$

But $\mu = \tan \varrho$, then

$$\tan \varphi - \tan \varrho = \frac{\frac{d}{2}\mu_1}{L \cos^2 \varphi}.$$

Since the right-hand side of the equation is a positive value, $\tan\varphi - \tan\varrho > 0$; hence $\varphi - \varrho > 0$, or φ should be larger than ϱ.

Table 22 gives data for the construction of tooth profiles for ratchet wheels with external and internal engagement.

Table 22

Construction of Tooth Profiles for Ratchet Wheels

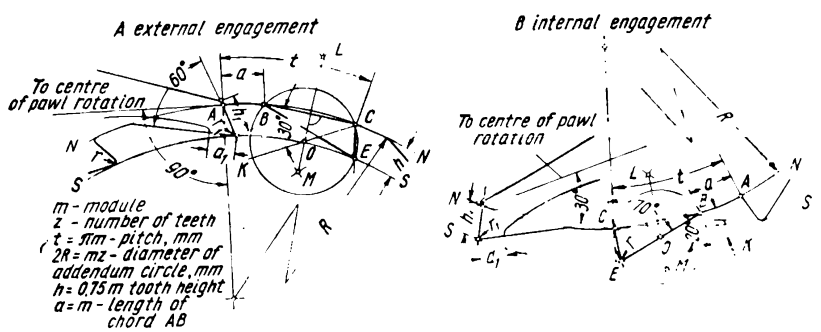
A external engagement
B internal engagement
To centre of pawl rotation
To centre of pawl rotation
m - module
z - number of teeth
t = πm - pitch, mm
2R = mz - diameter of addendum circle, mm
h = 0,75m tooth height
a = m - length of chord AB

	m	6	8	10	12	14	16	18	20	22	24	26	30
Ratchet wheel	z	From 6 to 30 inclusive											
	t	18.85	25.13	31.42	37.70	43.98	50.27	56.55	62.83	69.12	75.40	81.68	94.25
	h	4.5	6	7.5	9	10.5	12	13.5	15	16.5	18	19.5	22.5
	a	6.0	8	10	12	14	16	18	20	22	24	26	30
	r	1.5	1.5	1.5	1.5	1.5	1.5	1.5	1.5	1.5	1.5	1.5	1.5
Pawl	h_1	6	8	10	12	14	14	16	18	20	20	22	25
	a_1	4	4	6	6	8	8	12	12	14	14	14	16
	r_1	2	2	2	2	2	2	2	2	2	2	2	2

The following sequence is accepted for constructing the profile of external teeth (see dwg in Table 22). We first describe addendum circle NN and dedendum or root circle SS. Circle NN which is also the pitch circle is divided by pitch t into equal parts. From any of the division points we lay out chord $AB = a$. On chord BC we construct an angle of 30° from point C.

Then perpendicular LM is erected from the middle of chord BC to its intersection with side CK at point O. From point O we describe a circle with the radius OC.

Point E, which is the point of intersection of this circle with circle SS, is the vertex of a 60° angle.

The profiles of internal teeth are constructed as follows. We first describe addendum circle NN and dedendum circle SS. Circle NN is divided by pitch t into equal parts. From any of the division points we plot chord $AB = a$. On chord BC we construct an angle of 20° from point C. Then perpendicular LM is erected from the middle of chord BC to its intersection with side CK at point O. From point O we describe a circle with the radius OC. Point E which is the point of intersection of this circle with circle SS is the vertex of a 70° angle.

The pawl pivot axis is found from the following construction (Fig. 110*c*).

The centre-to-centre distance OA (between the centres of the pawl and ratchet wheel) is taken as the diameter of a half circle whose intersection at point B with the addendum circle of the wheel will give us the position of the tooth which engages with the pawl and section BA will be the length of the pawl.

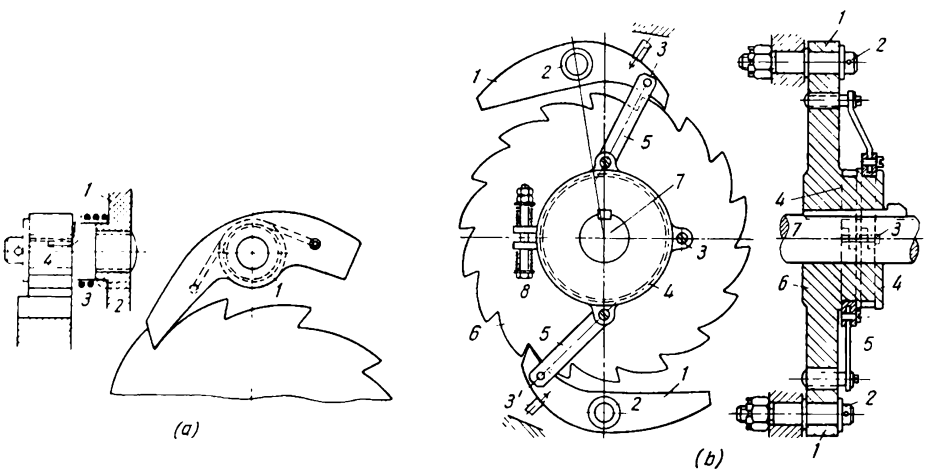

Fig. 111. Pawls operated by springs and friction rings

a: *1*—torsion spring connected to the brake disk and pawl, *2*—brake disk; *b*· *1*—pawl, *2*—pawl pivot, *3*—pin limiting upward movement of the pawl, *4*—friction ring with pivot, *5*—levers connecting the pawls and ring, *6*—ratchet wheel, *7*—brake shaft, *8*—bolts with springs for tightening the ring

Line BA will be perpendicular to the ratchet radius OB from geometrical considerations. The length of the pawl BA is usually taken equal to $2t$. Pawls which do not engage with the teeth under the action of their own weight are additionally weight- or spring-loaded (Fig. 111*a*).

When a load is being raised the teeth of a ratchet wheel slip under the pawl and produce an unpleasant clicking noise (especially when the shafts rotate at a high speed). The noise is eliminated by employing so-called noiseless pawls operated by means of a friction ring (Fig. 111*b*). Such pawls find application only in brake ratchets.

Ratchet wheels with inside teeth are used exclusively to brake ratchet wheels. Their teeth are cast on the inner rim of the brake drum mounted freely on a shaft. One or two pawls are mounted on a lever secured to the shaft and operated by friction rings (Fig. 112). The number of teeth ranges from $z = 16$ to 30.

Teeth on the inside of a ratchet wheel are much stronger than those provided on the outside. For this reason their strength equation has a somewhat different form:

$$m = \sqrt[3]{\frac{M}{z\psi\,[\sigma_{bend}]}}. \qquad (97)$$

The letters denote the same values as in formula (95).

Friction Arresters. As compared to toothed arresting gear, friction arresters offer certain advantages: they operate noiselessly and without jerks. However, in

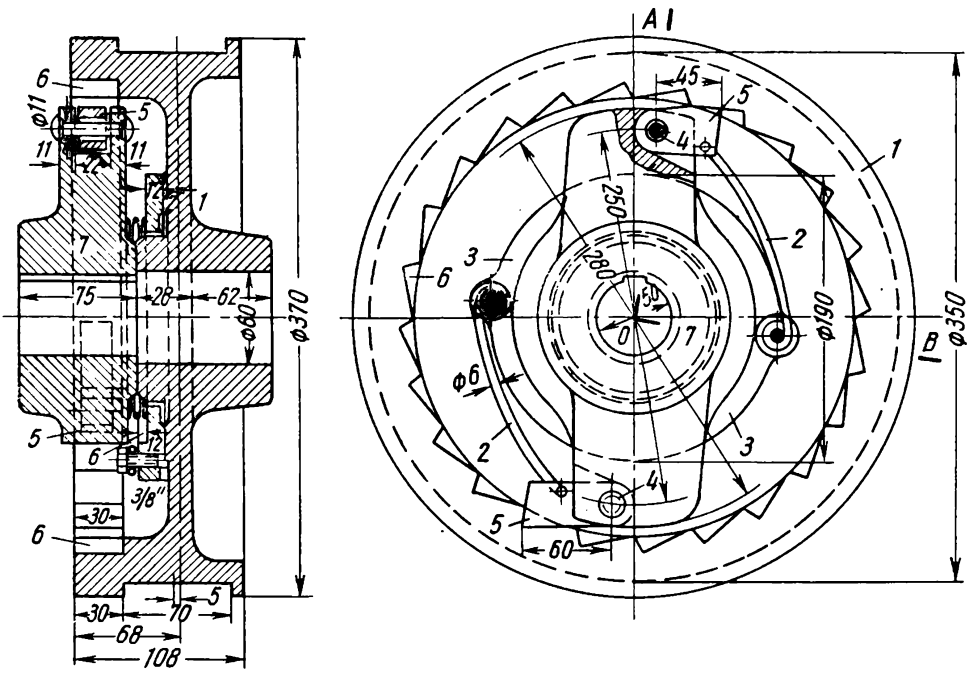

Fig. 112. Ratchet wheel with inside teeth

1—brake drum, *2*—retracting springs hinge-jointed to the ring and pawls, *3*—friction ring, *4*—pawl bolts, *5*—pawls hinge-jointed to lever *7*, *6*—ratchet teeth cast on the inner rim of drum *1*, *7*—double-arm lever keyed on the shaft

these arresters the pressure on the pawl pivot and shaft is considerably higher. For this reason they have a very limited application and always in combination with brakes.

Fig. 113 illustrates a friction arrester with an inside wedge-shaped engagement gear. The angle of the wedge is taken equal to $2\alpha \approx 45°$ to $50°$. The coefficient of friction is $\mu \approx 0.1$. The angle φ is 15° on the average. To avoid unidirectional action the arrester is always provided with two pawls arranged at diametrically opposite points. The pressure on the pawl pivot is

$$P_0 = \frac{P}{\tan \varphi}$$

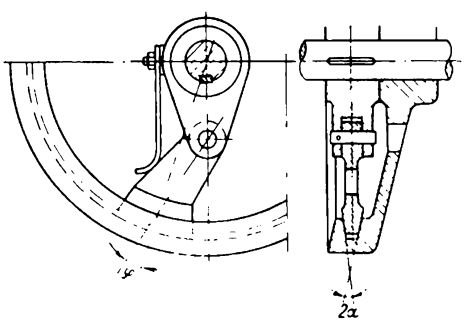

Fig. 113. Friction arrester

where P—peripheral force.

The brake disk should be strengthened with ribs to take up the load due to the pawl pressure.

Roller Ratchets. The extensively used roller ratchets are usually employed in combination with brakes. Fig. 114*a* shows a roller ratchet in a separate housing. Such ratchet gearing operates as follows.

Shaft *1* which is to be stopped carries bush *2* provided with recesses for rollers *3*. Ring *6* is fitted on key *5* in body *4*. Rollers *3* do not hamper counterclockwise rotation of bush *2* together with shaft *1*. As shaft *1* begins to rotate clockwise under the action of the load (shaft *1* carries a drum around which the ropes lifting the load are wound) the rollers become wedged in the recesses of bush *2* and are

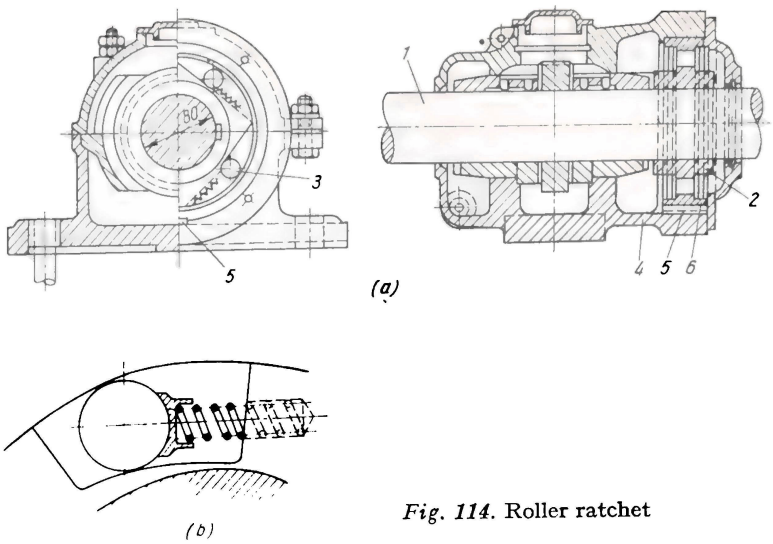

Fig. 114. Roller ratchet

forced against fixed ring *6*. In order to prevent the rollers from dropping into the recesses by their own weight they are provided with retaining springs as shown in Fig. 114*b*. Fig. 115 demonstrates various designs of roller ratchets.

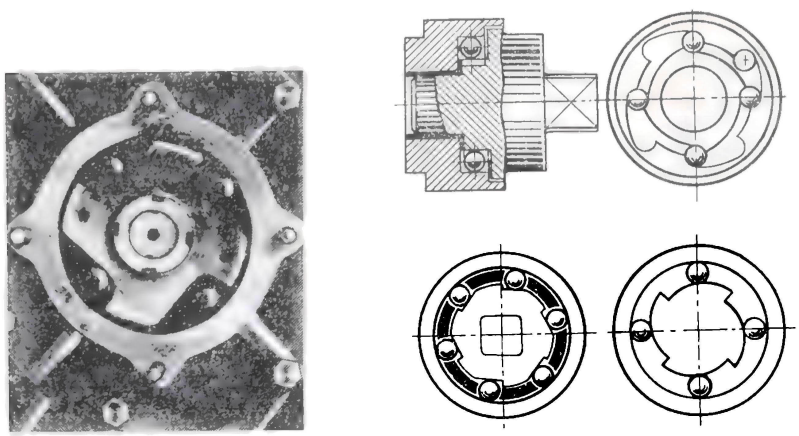

Fig. 115. Designs of roller ratchets

Design of Roller Ratchets (Fig. 116). A roller wedged between the follower and driver is subject to the action of normal forces N_1 and N_2 and tangential friction forces $\mu_1 N_1$ and $\mu_2 N_2$. With the roller in equilibrium the resultant force $R_1 = R_2$.

The transmitted torque is

$$M = z\mu N \frac{D}{2}$$

where z—number of rollers (usually $z = 4$). The coefficient of friction $\mu \approx 0.06$.

When $\mu = \tan\varrho > \tan\frac{\alpha}{2}$ we obtain

$$N < \frac{2M}{zD \tan\frac{\alpha}{2}} \quad (N = N_1 = N_2).$$

However, for greater reliability, the force acting on one roller is assumed as

$$N \approx \frac{2M}{zD \tan \frac{\alpha}{2}}. \qquad (98)$$

The length of roller $l \approx \frac{N}{p}$

where $p \approx 450$ kg/cm if the operating elements have been manufactured from quality steel and properly hardened.

Table 23 lists the main dimensions of roller ratchets with a Rockwell hardness of the operating surfaces $R_C = 58$ to 61.

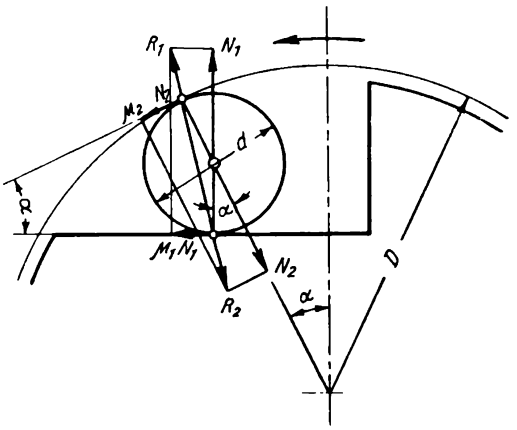

Fig. 116. Design diagram of a ratchet roller

Table 23

Main Dimensions of Roller Ratchets

Transmitted power at 100 rpm N_{100}, hp	Bush diameter D, mm	Roller diameter d, mm	Roller length l, mm	Number of rollers z	Angle of wedge $\alpha°$
0.25	102	12.7	19.0	4	7
0.5	127	15.9	23.8		
1.0	152	19.0	29.4		
1.5	178	22.2	33.3		
2.0	203	25.4	38.1		

The material used is casehardened steel 15.

Roller ratchets are selected using the following formula:

$$N_{safe} = \frac{100\, N_{100}}{nK}$$

where n—actual rpm;

K—safety factor, taken from 1.5 to 2.

2. SHOE BRAKES

In hoisting machinery brakes are intended for controlling the speed of load lowering or for holding the suspended load at rest. Brakes are also used to absorb the inertia of moving masses (truck, crane, load, etc.). Depending on their purpose the brakes can be classified as parking (holding), lowering and combined types, the latter type serving both for stopping the load and controlling the speed of descent.

There are operated and automatic brakes. The operated brakes include: shoe or block, band, cone, disk and ratchet brakes and brakes with safety handles.

Among the automatic brakes are centrifugal brakes (to control speed) and brakes applied by the weight of the lifted load.*

Shoe, or block, brakes are designed either with external or internal shoes. External shoe brakes are a regular feature of hoisting machinery while the use of internal shoes is confined to servicing truck-mounted cranes.

The Principle of Brake Operation. To understand the principle of operation of a shoe brake let us examine the diagrams of single shoe brakes shown in Fig. 117.

* Hydraulic, pneumatic and electric braking is not considered in this textbook.

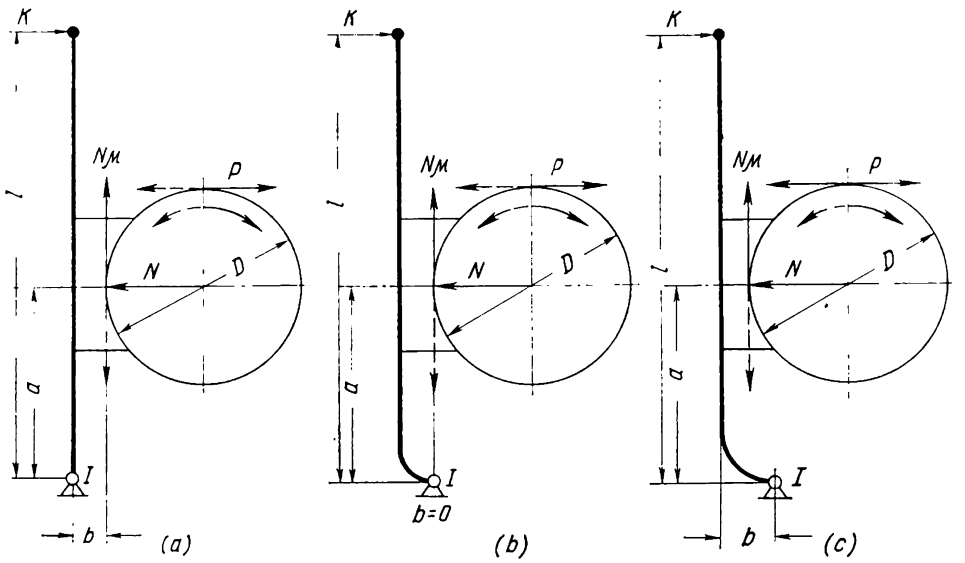

Fig. 117. Diagrams of single shoe brakes

Since the unidirectional action of a single shoe causes bending strain in the brake shaft, single shoe brakes are employed only for retarding small torques in a hand drive when the diameter of the shaft does not exceed 50 mm. Pressure exerted by a cast-iron shoe on the brake wheel should be such that the friction force produced on the surface of the wheel* counterbalances the peripheral force

$$N\mu \geqslant \frac{2M}{D} = P.$$

The friction force $N\mu$ acts relative to the brake wheel in a direction opposite to the peripheral force P (for a given direction of rotation) and, relative to the shoe, in the direction of wheel rotation.

Force K at the end of the brake lever depends on the position of pivot I and will equal (Fig. 117*a*)

$$K = \frac{N}{l}(a \pm \mu b) = \frac{P}{l}\left(\frac{a}{\mu} \pm b\right) \tag{99}$$

(the upper sign refers to clockwise wheel rotation and the lower sign to counter-clockwise rotation).

From Fig. 117*b*

$$K = N\frac{a}{l} = \frac{Pa}{\mu l} \tag{100}$$

(force K in this diagram is the same for both directions of rotation).

From the diagram in Fig. 117*c*

$$K = \frac{N}{l}(a \pm \mu b) = \frac{P}{l}\left(\frac{a}{\mu} \pm b\right) \tag{101}$$

(the upper sign refers to the clockwise wheel rotation and the lower sign to counter-clockwise rotation).

* This generally accepted idea is only approximately true since actually the friction force is applied on a greater arm than the radius of the brake wheel.

For rotation in both directions the diagram in Fig. 117*b* theoretically offers greater advantages; here force K is the same for both directions of rotation.

When $\frac{a}{\mu} = b$ (Fig. 117*a*—counterclockwise rotation, Fig. 117*b*—clockwise rotation), force $K = 0$ and the brake becomes an arrester operating in one direction. In actual brake designs this self-braking effect should be avoided.

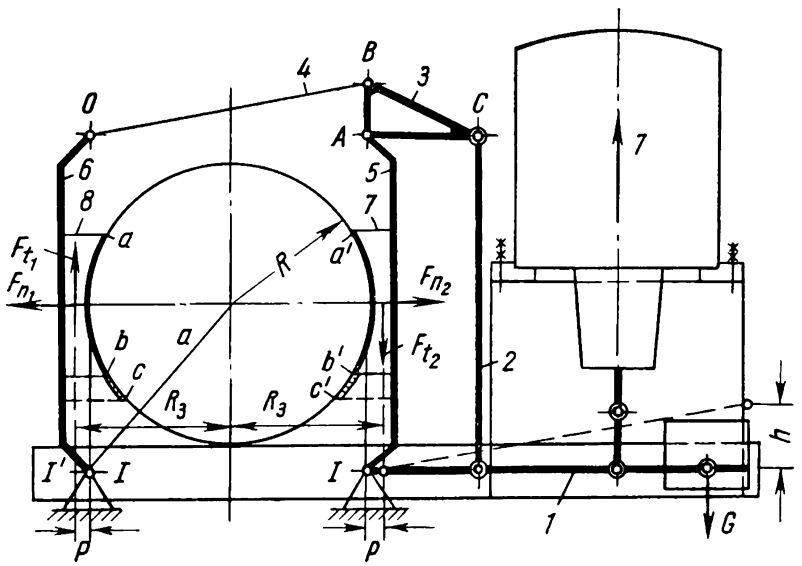

Fig. 118. Diagram of a double shoe brake

Double shoe brakes (Fig. 118) are extensively used in hoisting, travelling and slewing mechanisms of cranes and, as distinct from single shoe brakes, produce no bending strain in the brake shaft. Electrically driven winches and cranes are designed almost exclusively with double shoe brakes. The brake is applied by weight G and released by an electromagnet. Hence, the permanently applied brake is released only when the magnet is switched on. The electric circuit usually provides for interlocking the motor and magnet which automatically produce braking action even in case of accidental stoppage of the motor.

A double shoe brake (Fig. 118) operates on the following principle. Weight G causes lever *1* to go down together with pull-rod *2*. Rod *2* turns rigid triangle *3* to which it is hinge-jointed at point C. Let us assume that point A is stationary, then point C moves down; in this case point B will shift to the right. This motion will be transmitted to pull-rod *4* and lever *6* which will force shoe *8* against the brake wheel. When shoe *8* is drawn up tight point B will become stationary and triangle *3* will rotate about it. Due to this, point A will shift to the left and will apply shoe *7* through lever *5*.

In actual designs of the brake shown in Fig. 118, lever *1* is composed of two parts linked together by a turnbuckle to provide for adjustment of the brake.

Other diagrams of double shoe brakes are shown in Fig. 119.

Brake (Fig. 119) application by a weight secured on the brake lever entails the following essential shortcomings. After the current is switched off and the weight drops the latter oscillates together with the lever, decreasing and increasing pressure of the shoe on the wheel and changing accordingly the intensity of the braking torque. This periodic change in the braking torque is a very undesirable phenomenon both in hoisting and travelling mechanisms. Springs are more reliable in this respect since they operate more gently and make possible more accurate adjustments within a wider range.

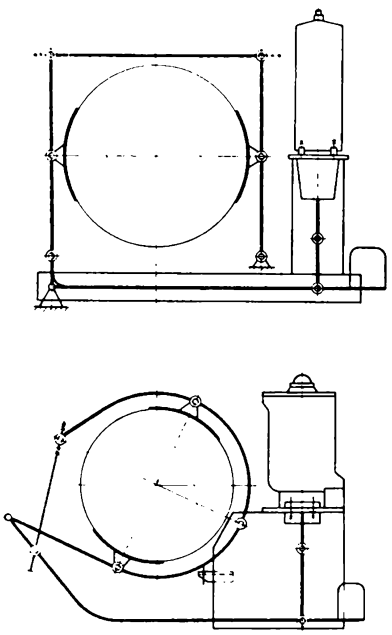

Fig. 119. Diagrams of double shoe brakes

Fig. 120 shows a design in which the brake is applied by a spring.

3. ELEMENTS OF SHOE BRAKES

Brake Wheels. Hand-operated hoisting machinery is usually designed with cast-iron wheels and those employing power drives with cast steel wheels of a grade not below

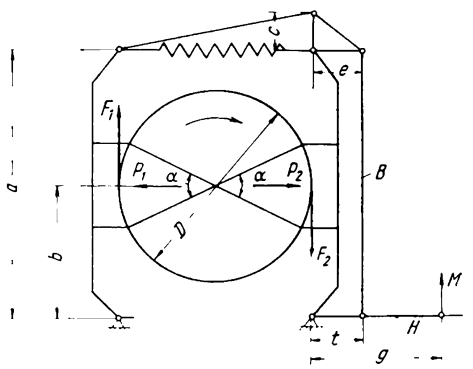

Fig. 120. Diagram of a brake applied by a spring

55 JI, group III, or else die-forged of steel not below grade 45 according to Soviet Standards with a minimum hardness of the rubbing surfaces of Bhn 280. Truck travelling mechanisms may employ cast-iron brake wheels. Brake wheels should be dynamically balanced. The width of the wheel should exceed that of the shoe by 5 to 10 mm. Brake wheels should be always finned for better heat dissipation and provided with holes between the fins for more rapid air circulation and to dissipate the heat more effectively into the atmosphere. If the brake is mounted on a flexible coupling it is installed in the half which faces the driving mechanism.

Brake Shoes. Wooden brake shoes are manufactured from maple or poplar and are attached to the lever by means of bolts. For a mechanical drive the shoes are made of cast iron (permanent-mould casting, grade СЧ 12-28) and provided with special brake linings (Fig. 121*a*). The linings may be secured with rivets (Fig. 121*b*) or with countersunk screws.

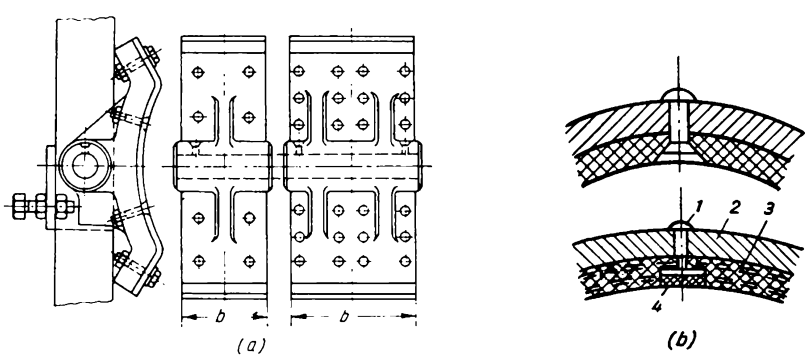

Fig. 121. Fastening of linings to brake shoes by rivets:
1—rivet, *2*—brake band or shoe, *3*—lining, *4*—plug

Brake Linings. Brake linings should satisfy the following requirements:
(a) have a high coefficient of friction;
(b) retain braking capacity at temperatures up to 300°C;
(c) effectively resist wear at the highest speeds, unit pressures and temperatures;
(d) easily yield to treatment;
(e) have a low cost.

Today, almost everywhere use is made of rolled band. Rolled band is produced on rolling machines from cheap nontextile asbestos and rubber with an addition of sulphur for subsequent vulcanisation. Rolled band is manufactured up to 8 mm thick and up to 100 mm wide. It is very elastic and can be curved as desired. It possesses a high and stable coefficient of friction which ranges between 0.42 and 0.53 and can withstand temperatures up to 220°C. Experiments recommend the following average coefficients of friction for various unlubricated materials: cast

Table 24

Maximum Permissible Unit Pressures for Shoe Brakes

Materials of rubbing surfaces	Unit pressure, kg/cm²	
	Holding brake	Lowering brake
Cast iron on cast iron	20	15
Steel on cast iron	20	15
Steel on steel	4	2
Asbestos brake band on metal	6	3
Rolled band on metal	6	4

Table 25

Characteristics of Friction Materials

Name	Coefficient of friction on dry surface	Permissible temperature, °C	Safe unit pressure, kg/cm²	Specific gravity	Notes
Asbestos brake lining with interwoven brass wires	0.45-0.35	350	p = 2 to 6 p_{max} = 12	1.55	Normal brake lining
Asbestos brake lining without brass wires	0.45-0.35	200	p = 1 to 4 p_{max} = 6	1.55	For less intensive duty
Fibre brake lining of wood pulp without brass wires	0.55-0.4	150-200	p_{max} = 10	1.25	Normal brake lining
Hydraulically compressed asbestos composition with brass wires	0.43-0.4	300	p = 2 to 12 p_{max} = 15	1.6	For clutches
Brake shoes of asbestos composition with brass wires; compacted by a hydraulic press (design A)	0.5-0.35	300	p = 2 to 6 p_{max} = 12	1.5	As brake lining
Brake shoes of special composition without metal wires (design S)	0.5-0.2	110	p = 1 to 3 p_{max} = 12	1.3	For less intensive duty
Linings of braking fibre	0.55	110	p = 8 to 10	1.25	For rope drive pulleys; lining by application on a washer

iron on cast iron—0.15, steel on cast iron—0.15, type A asbestos brake band on cast iron or steel—0.37, type B asbestos brake band on cast iron or steel—0.35, rolled band on cast iron or steel —0.42, wood on cast iron—0.30, wood on steel—0.25, leather on cast iron—0.20, leather on steel—0.20, bronze on cast iron—0.17, bronze on steel—0.16, bronze on bronze—0.18, steel on laminated fabric—0.15 and steel on fibre—0.17.

The maximum permissible unit pressures for shoe brakes are listed in Table 24.

Table 25 gives characteristics of friction materials of the German firm "Mick".

A new development are sintered metal linings which do not contain organic matter and therefore their coefficients of friction are only slightly altered in heating. They possess a relatively high resistance to wear.

The coefficient of friction of sintered linings varies from 0.6 to 0.76. At a speed of 20 m/sec they withstand a unit pressure of 8 kg/cm^2. Among the new Soviet-made friction materials on a rubber and pitch base is "Retinax", prepared with brass chips, which can sustain a high temperature, a very important factor, and possesses an adequate coefficient of friction.

Brake Levers and Pull-Rods. Brake levers are manufactured from die-forged or cast steel. The safe bending stress of levers with account taken of braking shocks is taken from 400 to 800 kg/cm^2 depending on the brake size.

Steel cast levers are more expensive but they possess greater rigidity and have less lost motion in the pivots.

In the brake shown in Fig. 118, upper pull-rod *4* is made adjustable and is of round bar steel. The safe unit tensile stress in the pull-rod section is 300 to 500 kg/cm^2. The cross-member is subject to bending from the effort acting on the rod and is checked in the same manner as the crosspiece of a hook. Fig. 122 shows the most widespread designs of adjustable pull-rods.

The end lever of the brake is usually manufactured from one or several pieces of forged steel.

The braking weight is made of cast iron in a round or square form. The weight is secured on the end lever of the brake by a hinge or with a bolt.

Fastening Parts of a Brake Magnet. Electromagnets are employed almost exclusively to obtain a releasing effect. To enable the brake end lever to deflect, the rods of the magnet armature are connected with the lever (Fig. 123*a*) by means of a hinged shackle. In d-c brake magnets the armature is made turnable which allows the body of such a magnet to be fixed in any position relative to its axis. In three-phase magnets the armatures cannot be turned and for this reason the rod is provided with two holes at 90° from each other (Fig. 123*a*). Three-phase magnets can therefore be secured only in two positions.

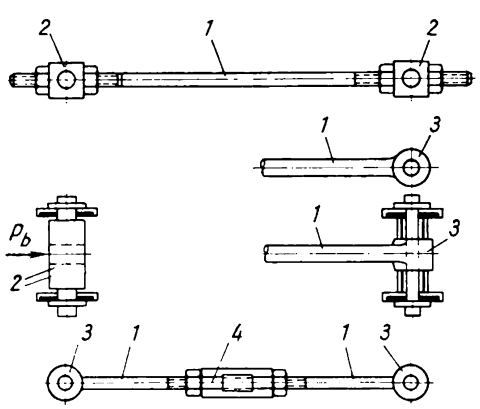

Fig. 122. Parts of shoe brakes
1—pull-rod, *2*—cross-member, *3*—eye, *4*—turnbuckle

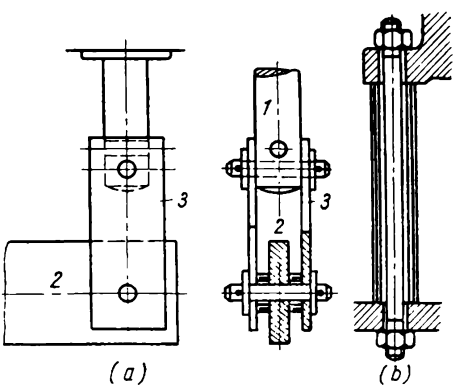

Fig. 123. Fastening parts of an electromagnet
a—lever system; *1*—magnet armature pull rod, *2*—brake end lever, *3*—pivoted shackle; *b*—element of the magnet fastening

Since the magnets do not experience the action of any lateral forces they are frequently fastened by bolts with spacing tubes (Fig. 123*b*).

4. ELECTROMAGNETIC SHOE BRAKES

A great variety of designs of shoe brakes which differ mainly by the arrangement of their lever systems are employed in materials handling equipment. For the most part they are double shoe designs with shoes connected to the brake levers rigidly or pivoted. Rigidly connected shoes lead to unequal wear of the brake linings and develop forces which may bend the brake shaft. Therefore, brakes with pivoted shoes have found wide application. Electromagnetic shoe brakes can be classified into four groups.

The first group includes brakes with long-stroke plunger-type electromagnets in which the lever system is linked to the electromagnet plunger at the bottom. The design of such brakes is characterised by many joints and low rigidity of the brake levers. The following shortcomings may be noted: (1) rapid wear of the pivots, (2) excessive initial lost motion and (3) slow application and release of the brake. Fig. 124 shows one such brake for two positions of a three-phase electromagnet.

In the second group are brakes with short-stroke electromagnets and with long-stroke magnets in which the lever system is attached to the electromagnet plunger on top (Fig. 125). This group of brakes is distinguished by the following features: (1) rigid levers, (2) fewer pivots and (3) brake application by a compressed spring.

The third group comprises brakes with short-stroke clapper-type electromagnets operating from d. c. (Fig. 126). In these brakes the electromagnet acts directly on the brake lever. Brakes of this type are designed with the minimum number of pivots, operate quickly and can be easily adjusted. The brake is applied by a spring.

In the fourth group are brakes with electromagnets secured directly on the brake lever and operating both from alternating and direct current (Figs 127 and 128).

Brakes of this group are light in weight and small in size which makes them very popular.

A three-shoe brake (Fig. 129) holds a place of its own. The brake comprises a magnet, spring and three shoes with friction linings. When the current is switched on, armature *1* of the electromagnet turns lever *6* downwards. As a result, shoe *2* will be retracted from the brake wheel until it contacts bolt *3* of lever *9*. Simultaneously, upper shoe *5* will also be retracted until the middle shoe reaches bolt *8*. The brake can be easily adjusted by turning bolts *8* and *7* and by moving the nuts on pull-rod *4*.

Electromagnetic shoe brakes with straight-line shoe movement. This type of brake is frequently employed in mine hoists. In general-purpose materials handling appliances such brakes have not yet been used. Fig. 130*a* and *b* shows two versions of brakes designed by Professor S. P. Gomellya with straight-line shoe movement. In these brakes rocking levers have been replaced by a frame which moves together with the shoe in rigid guideways. Uniform wear of the linings constitutes an advantage of such brakes.

5. THRUSTOR-OPERATED SHOE BRAKES

A thrustor-operated brake is a recent development in brake design techniques. The device has the following advantages:

(1) constant pressure;

(2) gentle application and release of brake without jerks and shocks;

(3) large number of switching-in operations per hour (up to 600) which can never be obtained with electromagnets.

An electrohydraulic thrustor is an independent mechanism which requires neither clutches nor external piping (Figs 131 and 132). The thrustor cylinder accommodates a centrifugal pump and a piston with two push-rods extending out-

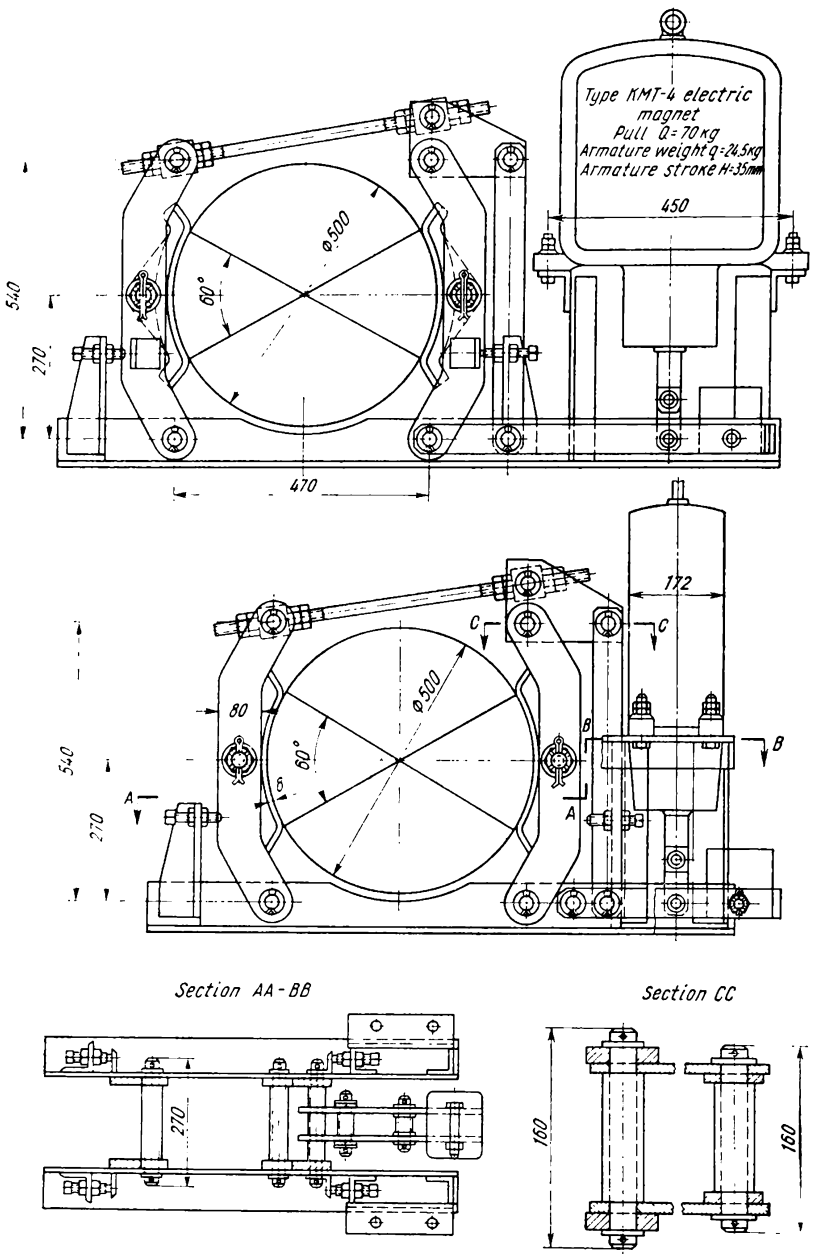

Fig. 124. Double-shoe brake

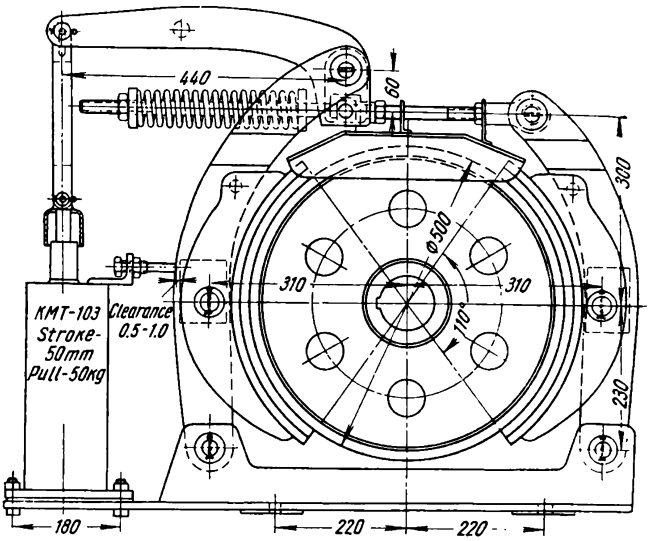

Fig. 125. Brake with an a-c magnet and plunger attached on top

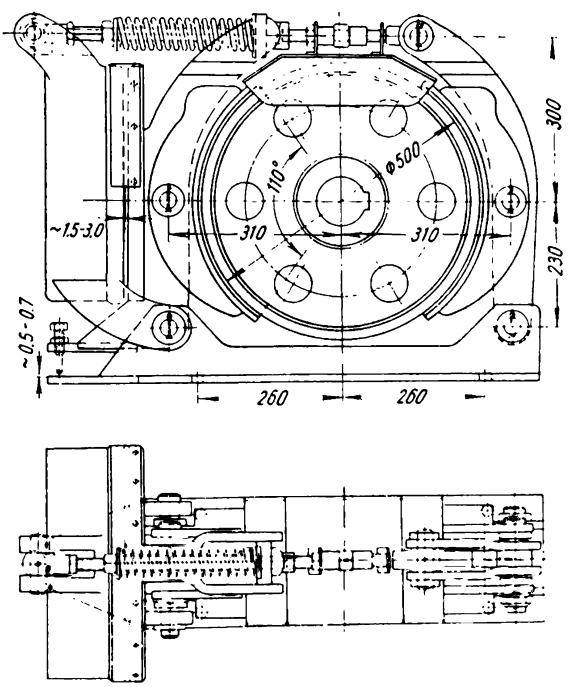

Fig. 126. Brake with a type A d-c short-stroke electromagnet

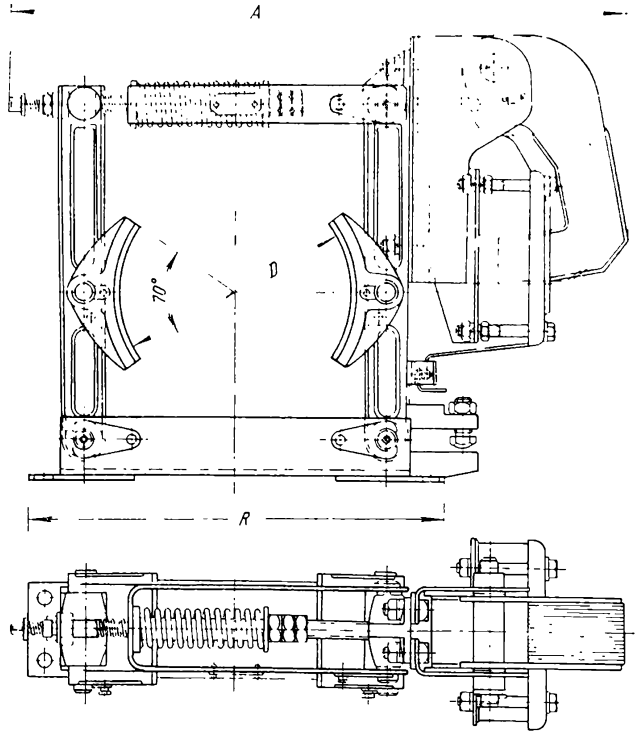

Fig. 127. Brake with a type MO-Б a-c electromagnet

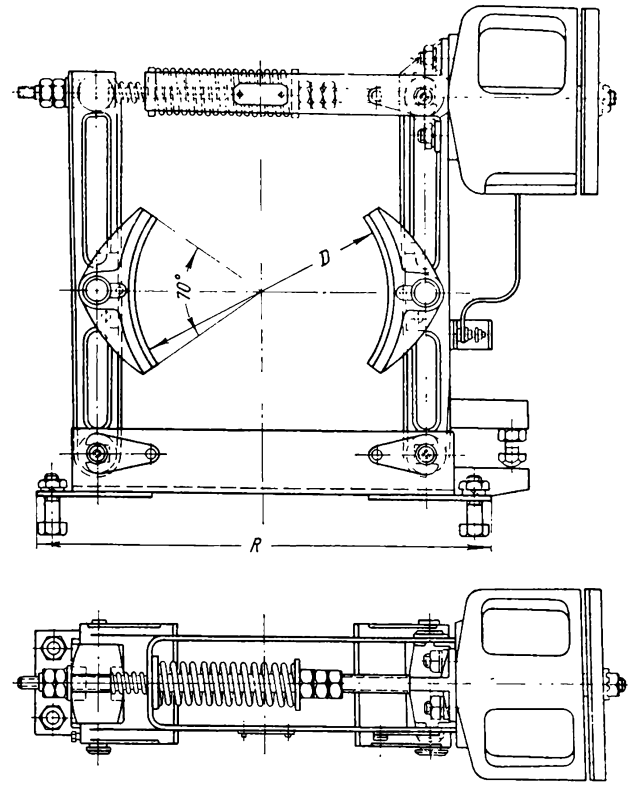

Fig. 128. Brake with a type MII d-c electromagnet

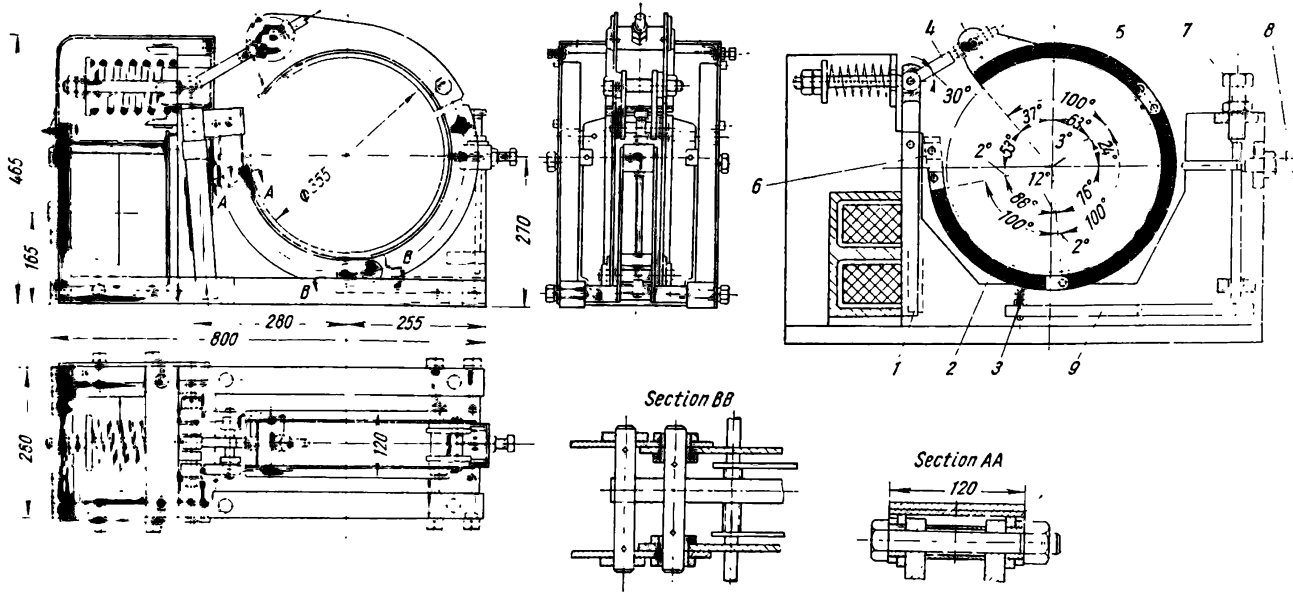

Fig. 129. Spring-operated three-shoe brake with a short-stroke electromagnet

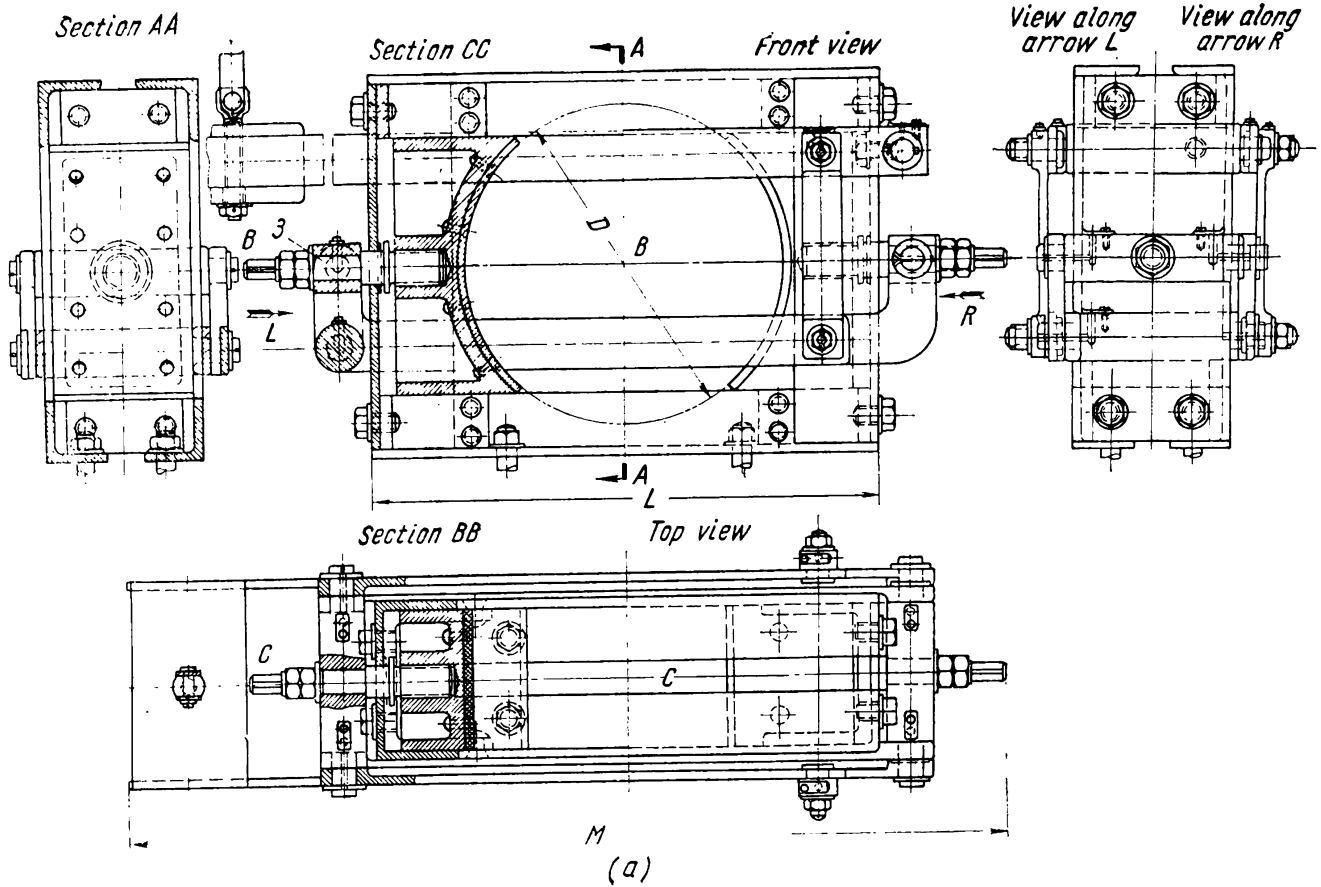
Section AA
Section CC
A
Front view
View along arrow L
View along arrow R
B
3
L
D
B
R
A
L
Section BB
Top view
C
C
M

(a)

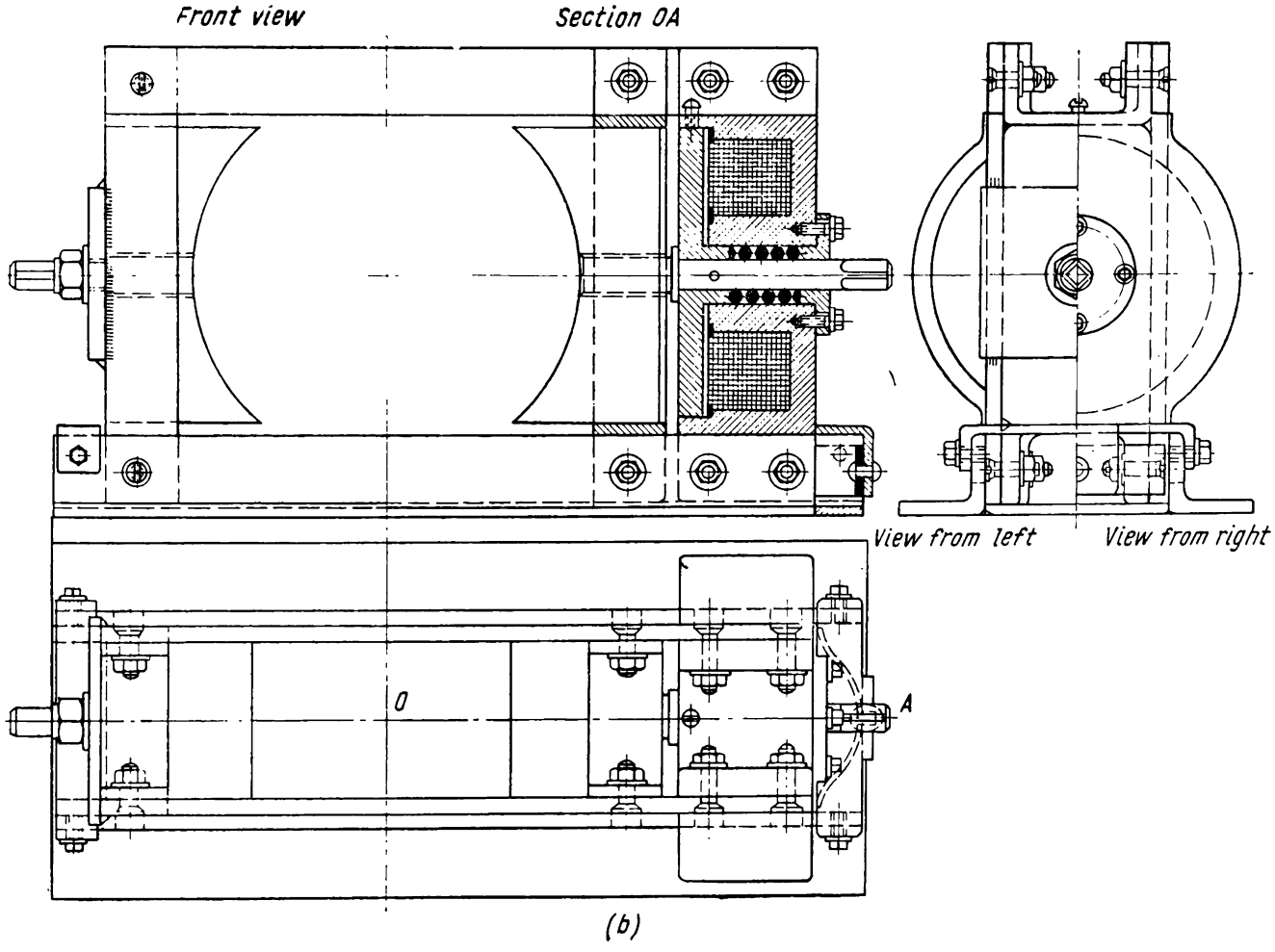
Front view
Section OA
View from left
View from right
O
A
(b)

side through the thrustor cover and transmitting effort to the brake. The pump impeller is connected with the shaft of a flange-mounted electric motor on the thrustor cover (Fig. 132) or with a specially designed shaft made in one piece with the cover (Fig. 131).

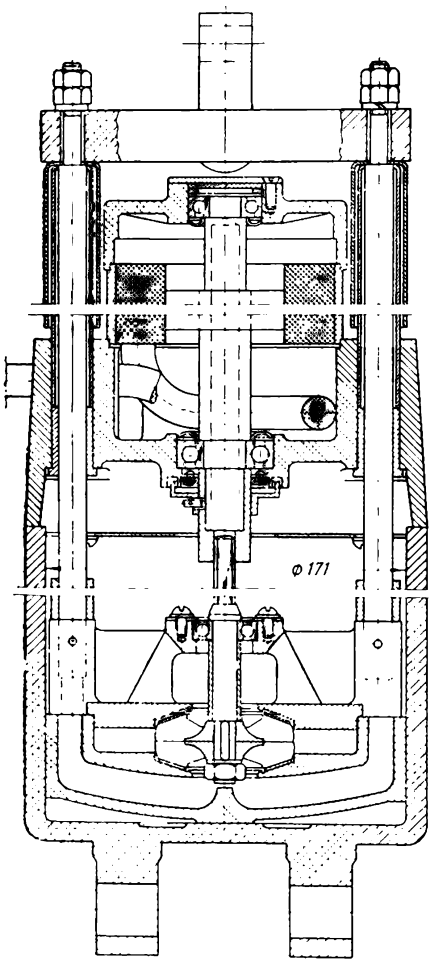

Fig. 131. Electrohydraulic thrustor with the pump mounted on the piston

There are two distinctive designs of thrustors depending on the arrangement of the pump in the thrustor and connection of the motor shaft with the shaft of the centrifugal pump. In one of these designs the pump is secured to the piston and moves together with it when the thrustor operates. This design employs a sliding linkage between the shafts of the impeller and motor. To achieve this linkage a square bronze shaft of the pump is usually fitted telescopically to the hollow shaft of the motor provided with a corresponding square hole (Fig. 131).

In the other design (Fig. 132) the pump is separate from the piston and is mounted on the bottom of the cylinder. This makes it possible to dispense with a telescopic shaft and to make use of an ordinary flanged motor. Moreover, this design allows a much easier adjustment of the hole for fluid discharge and, hence, makes it possible to change the time required for the upward and downward strokes of the piston.

Fig. 132 shows the thrustor with the motor switched off and with piston *1* in the extreme lower position. When the current is switched on impeller *2* begins to rotate and creates surplus pressure in valve chest *3* which raises valve *4*, compresses spring *5* and admits the fluid through the valve ports into the cylinder under the piston. At this moment the fluid is pumped from the space above the piston into the space under the piston and piston *1* under the action of surplus pressure goes upward overcoming the resistance of the external load.

The amount by which the valve hole is opened and the time required for upward movement of the piston are regulated by adjusting screw *6* provided in the thrustor cover. The nut of this screw limits the travel of rocker arm *7* and, consequently, the upward travel of the valve. When the piston reaches the extreme upper position the pump continues to rotate and maintains a constant pressure under the piston. When the current is switched off the impeller stops and the piston descends under the action of the external load and its own weight causing the fluid to flow back to the space above the piston. In this case the surplus pressure of the fluid, maintained under the piston and in the valve chest, compresses spring *5* and the valve ports remain open. When the piston reaches the extreme lower position and the external load no longer creates surplus pressure in the fluid, spring *5* will force valve *4* downwards and close the valve ports. The amount by which the valve ports are closed during the downward stroke is regulated by adjusting screw *8* whose end bears against rocker arm *7* when the valve moves down.

Thus, by adjusting screws *6* and *8* we can obtain the required rate of fluid flow when the piston travels upwards and downwards and, hence, the time required for its stroke. The thrustor is not susceptible to mechanical overloads because if external load exceeds the lifting force of the thrustor its piston will remain stationary while the pump will continue to operate building up normal working

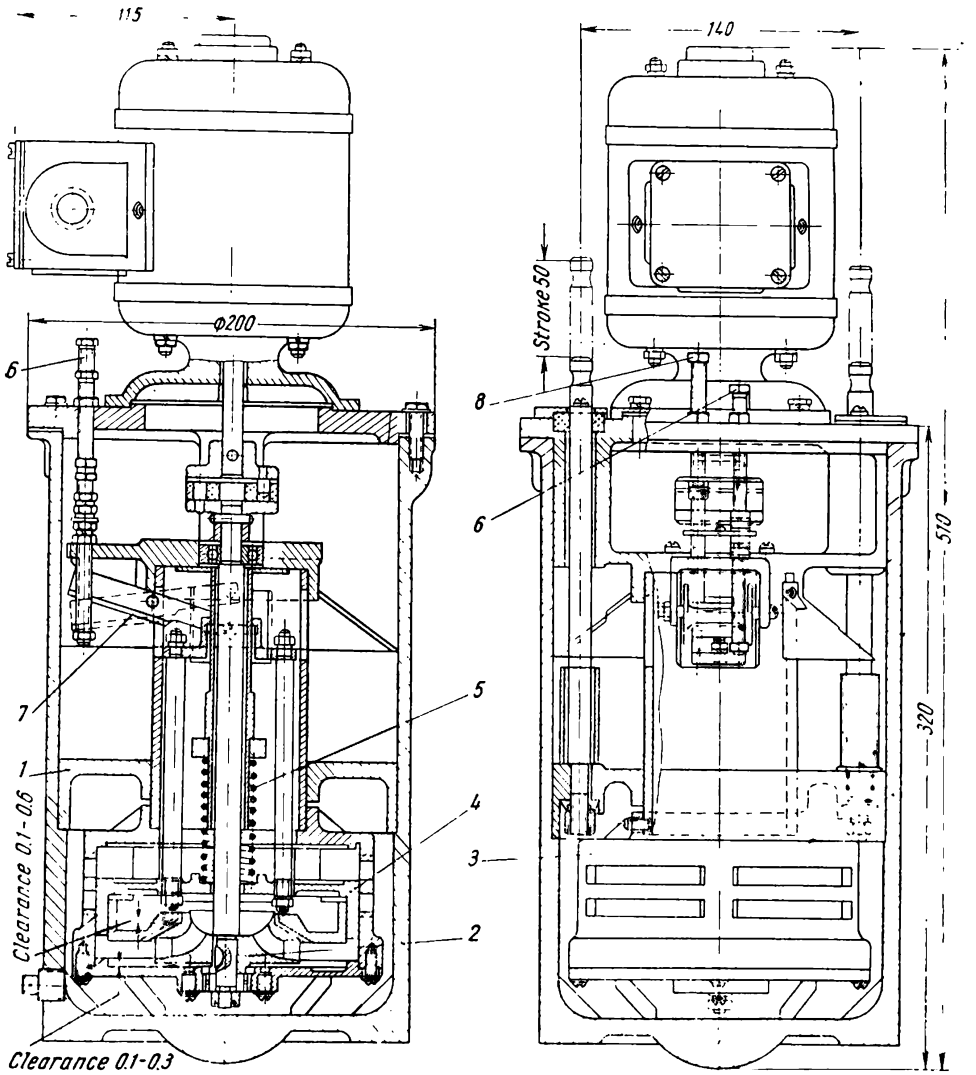

Fig. 132. Electrohydraulic thrustor with the pump mounted in the cylinder

pressure of the fluid under the piston. This gives rise neither to excessive currents in the motor nor to excessive stresses in the thrustor elements. The thrustor has also the advantage of its stroke being limited arbitrarily both for raising and descent involving no change in the lifting force or additional consumption of electric power.

The thrustor shown in Fig. 131 has no adjusting valves although there exist designs of thrustors of the same type provided with valves *1* (Fig. 133*a* and *b*). This thrustor is designed so that access to adjusting screws *2* is difficult since these screws are arranged inside the thrustor cylinder.

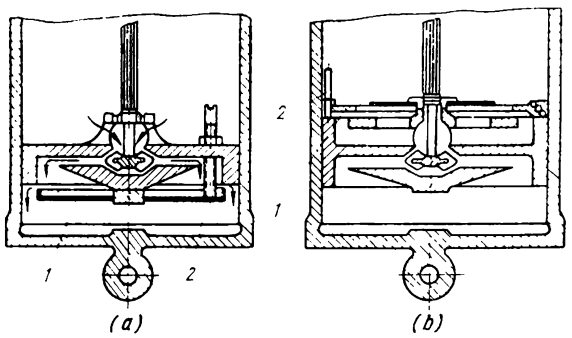

Fig. 133. Two methods of adjusting a thrustor with the pump mounted on the piston

Apart from the size of the port for fluid flow, the time required for the piston stroke is also affected by the load borne by the thrustor. The greater is the external load the more time is needed to raise the piston and less time to lower it.

As a rule, thrustors are filled with low-viscosity oil. At a lower temperature and higher viscosity the time of upward travel increases. For the processes involving low temperatures the oil is heated either by an idle run for a certain time (the oil is warmed up by the operating pump) or by installing a heater in the thrustor housing having an independent electric power supply. In winter use can be made of a mixture of oil and kerosene (1:1) with a low freezing point.

Analysis of operation of electromagnetic and electrohydraulic brakes confirmed beyond all doubt the indisputable advantages offered by electrohydraulic thrustors used instead of electromagnets. Only thrustor-operated brakes make it possible to develop similar designs for the entire range of the required braking torques for direct and alternating current operation. The only difference lies in installing the appropriate electric motor on the thrustor.

Fig. 134 shows a hydraulic thrustor. The main characteristics of the experimental lot of thrustors of this type are listed in Table 26.

Table 26

	T-I		T-II		
Rated force, kg	60		160		
Maximum stroke, mm	55	75	55	85	135
Time of maximum upward travel, sec	0.5	0.73	0.65	1.0	1.5
Rated work, kg-m	3.3	4.8	9.6	14.4	22.4
Motor rpm	2,840				
Electric motor power, kw	0.144		0.326		
Oil pressure, kg/cm²	0.306		0.303		
Piston area, sq cm	196.35		528.38		
Piston diameter, cm	170		270		
Pump delivery, l/sec	2.16		4.93		
Thrustor weight (without oil), kg	40.5		70.3		

These thrustors are so designed that two types can service brakes with wheel diameters from 400 to 800 mm. One design of thrustor-operated brakes is shown in Fig. 135.

In designing the thrustors the principal attention has been given to developing reliable construction with the maximum unification of its elements. The pull-rods of the thrustor are enclosed in telescopic housings; the spherical bottom of the thrustor body is provided with a detachable tray with a lug which allows the thrustor to be secured by various methods depending on the design requirements. In brakes with 600, 700 and 800-mm wheels the thrustor is mounted on the lug and in brakes with 400 and 500-mm wheels it is mounted on the spherical part. The latter is accomplished by means of adjusting bolts which prevent lateral movement of the thrustor.

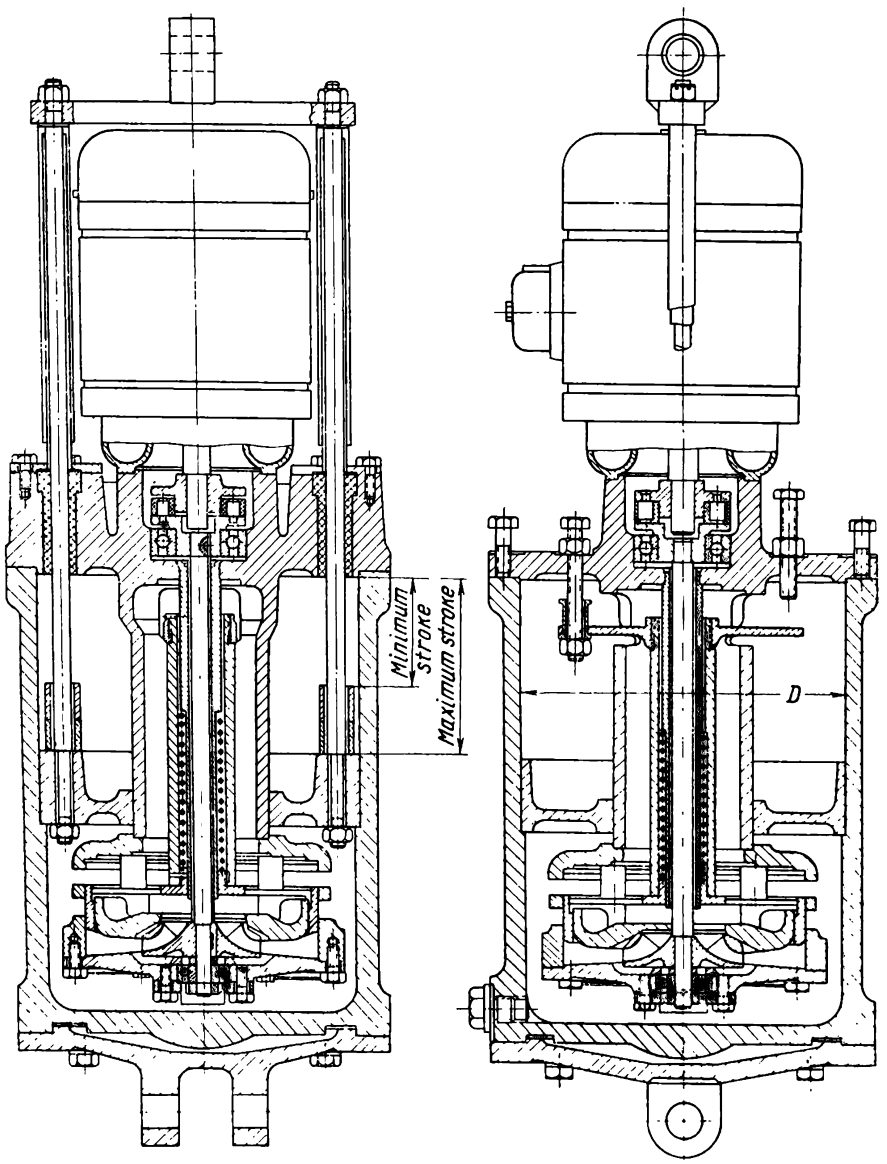

Fig. 134. Electrohydraulic thrustor

The rated stroke of each type of thrustor can be changed, retaining the same tractive force, by means of sleeves fitted on the rods (inside the body) which limit piston travel.

The thrustor and the brake are so adjusted as to reserve about 1/3 of the stroke for compensation of the wear of the brake linings. When, in the course of lining wear, the thrustor stroke nears the rated value the brake should be readjusted and the thrustor travel reduced. Otherwise, in case of excessive wear, the thrustor piston will bear on the shoulders of the body and will prevent the brake from being applied.

The brake is applied by the tension of two compressed springs mounted vertically between the thrustor and the brake lever.

The thrustor rods are connected with the brake by means of an angle lever. As the piston travels upwards the angle lever turns, pushes the brake rod and com-

presses the brake spring. Simultaneously, the brake lever on the other side of the wheel is retracted. The brake lever at the thrustor begins to move when the first lever reaches the stop on the brake base member.

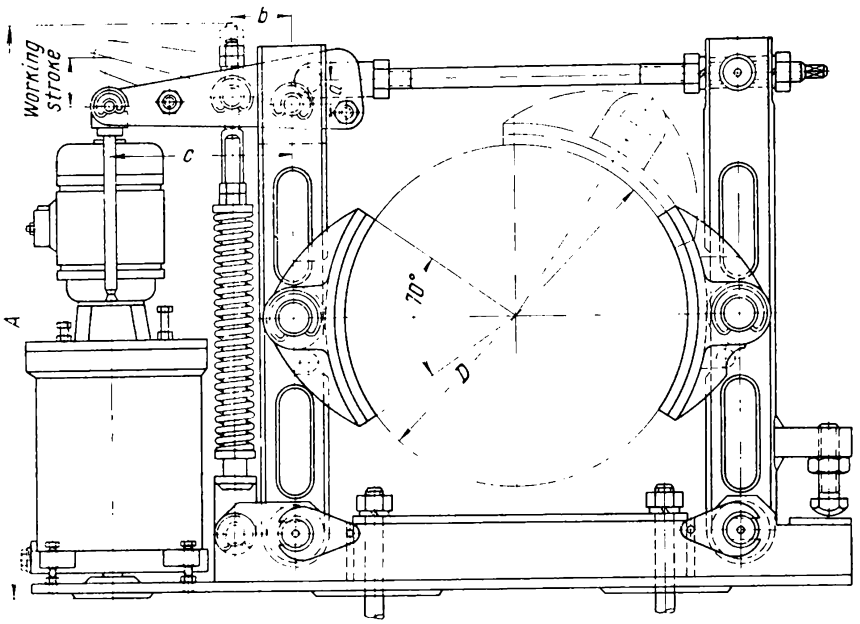

Fig. 135. Thrustor-operated brake

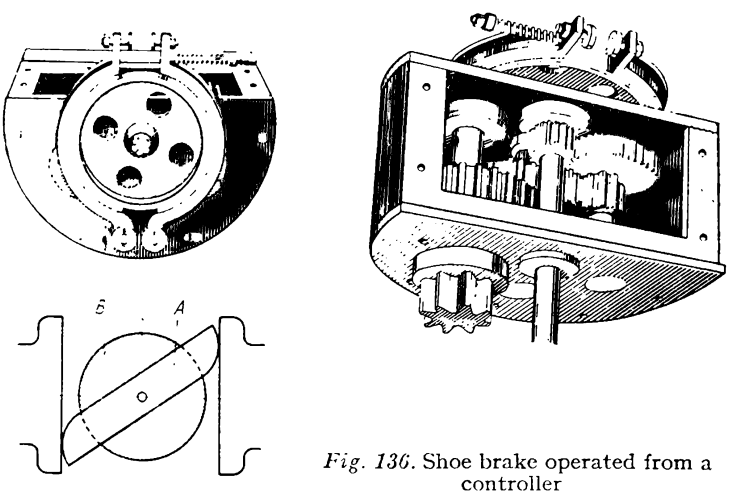

Fig. 136. Shoe brake operated from a controller

Shoe Brakes Operated from a Controller. In electric hoists shoe brakes are frequently operated from a controller. One such design is shown in Fig. 136. Two levers lined with ferrodo encircle almost the whole of the brake wheel. On top they are provided with two cups between which pin *A* is secured on shaft *B* of the hoist controller. As the motor is started the shaft turns together with pin *A* and, overcoming the tension of the spring, releases the brake. To stop the motor the controller is turned in the opposite direction and the spring applies the brake.

6. CONTROLLED BRAKES

Electromagnetic and thrustor-operated brakes applied automatically when the current is switched off are designed to brake mechanisms with a rated load. For this reason lighter weights or mechanisms carrying no load are stopped faster than with a load which leads to added strain on the elements and causes rapid wear of the mechanism.

The crane operator can control the braking process only with the aid of controlled brakes which enable him to decelerate gradually and come to a smooth accurate stop. This improves the efficiency and operating conditions of the elements in the mechanism.

Controlled brakes find widespread application in travelling and slowing mechanisms. In hoisting mechanisms where the braking torque is needed not only for stopping the load but also for holding it at rest controlled brakes are employed only in small-capacity hoists for controlling load descent. In this case use can be made only of normally applied brakes, i. e., brakes in which the rated braking torque is created by the weight of the load or the tension of a spring and manual control serves for releasing the brake wheel.

In travelling and slewing mechanisms of cranes, in addition to normally applied brakes use is also made of normally released and combined brakes. In normally released brakes without effort applied to the pedal or control lever the brake is in the released position. An effort applied to the pedal produces a braking effect.

Ordinarily, the brake is released by a compressed spring whose tension should be sufficient to overcome resistance in the elements of the brake system when the brake is released.

During the whole period of crane operation combined brakes are held in the released position by the force of an electromagnet (designed for continuous duty). Braking is effected by means of a pedal; the value of the braking torque, as in normally released brakes, is proportional to the pressure exerted on the pedal and can therefore be varied within a wide range.

The use of combined brakes is stipulated by safety rules according to which travelling mechanisms of cranes and trucks should be provided with braking devices applied automatically at the extreme positions of the crane and also in case of temporary failures of electric current. The kinematics of a combined brake is designed to ensure independent action of the controlled drive and automatic application when the electromagnet is switched off.

A great variety of designs of controlled brakes are employed for materials handling equipment. They differ mainly in their principle of operation and the type of control.

In overhead travelling cranes with the cabs mounted on the bridge the brake of the travelling mechanism is controlled by a foot pedal and the brake is installed in the middle of the bridge. The effort is transmitted by means of a rope, lever or hydraulic system.

The size of pedal-controlled brakes can be established according to the following empirical rule: the crane operator should stop a loaded crane travelling at normal speed at a distance (in m) equal to 10 per cent of the value of this speed (in m/min) without skidding of the wheels.

Fig. 137 shows a diagram of a pedal-controlled shoe brake with a rope transmission. An identical system of rope transmission for a bridge crane with a cab moving together with the crane trolley is illustrated in Fig. 138.

The hydraulic brake control system (Fig. 139*a*) comprises master cylinder *1* in which fluid pressure is created, hydraulic cylinder *2* acting on the lever system of the shoe brake and operating from the pressure built up by the master cylinder, supply tank *3* containing a sufficient amount of fluid for filling the entire system, copper tubing *4*, pressure hose, joints and clamps.

The master cylinder is provided with a piston as is the hydraulic cylinder on the brake. Both pistons are equipped with special cup seals which prevent fluid leakage and enable pressure to be built up.

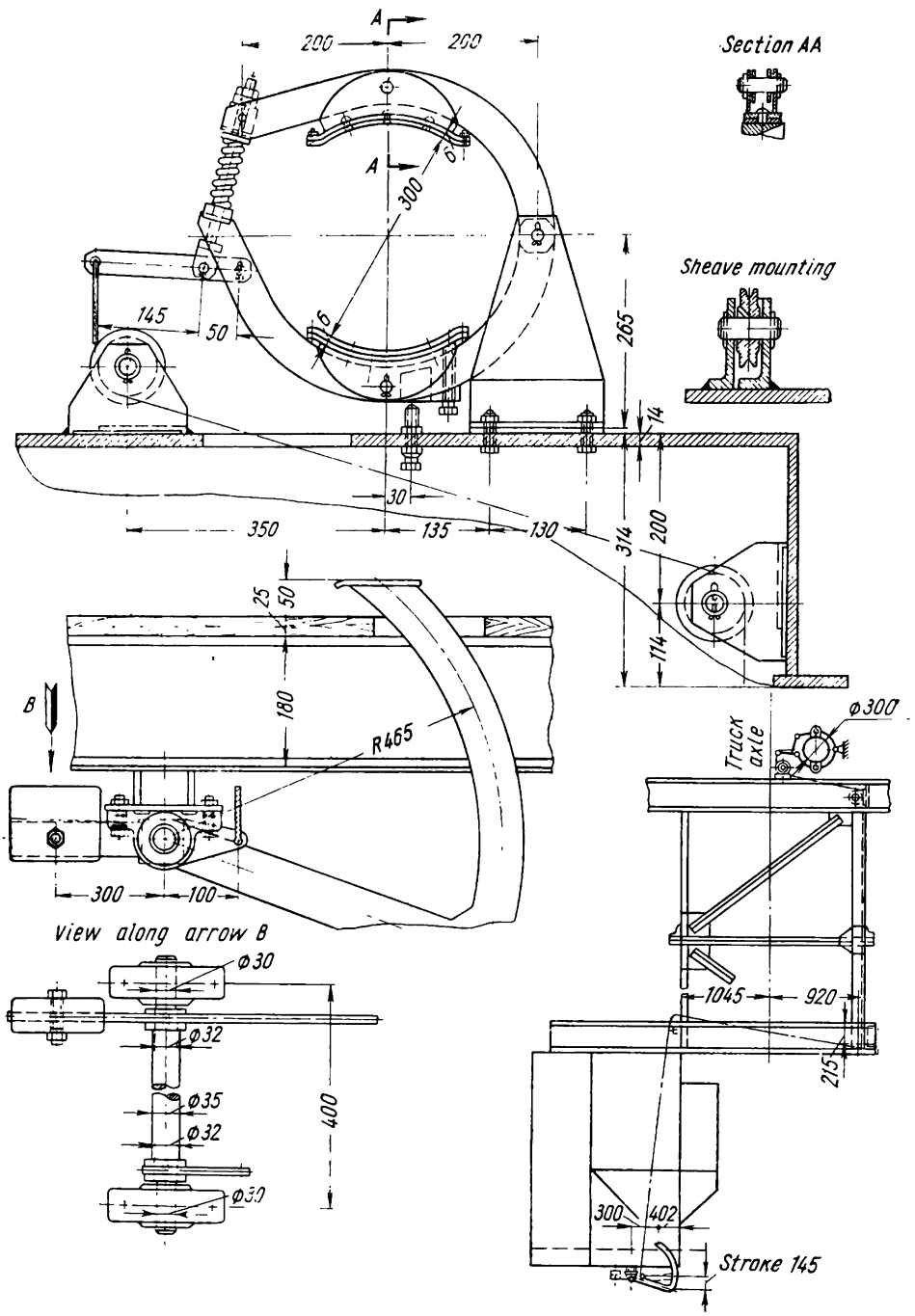

Fig. 137. Rope transmission of a pedal-controlled shoe brake

The piston of the master cylinder is controlled by a braking pedal. The fluid forced from the master cylinder by the moving piston is directed along the tubing into the hydraulic cylinder, presses against its piston and, acting on the lever system, produces the braking effect. Increased pressure on the pedal of the master cylinder correspondingly increases pressure on the brake shoes.

When no force is exerted on the pedal the brake shoes are released by means of a spring which also acts on the piston of the hydraulic cylinder, forcing out the fluid and returning it along the tubing to the master cylinder.

Fig. 139*b* shows a master cylinder unit comprising a supply tank, master cylinder *E* with piston *L*, inner lever *A*, outer lever *F* with a pedal and a brake shaft.

Master cylinder *E* is installed into compensating tank *B* which accumulates the fluid and stores its surplus and also protects the master cylinder against dirt, air and water.

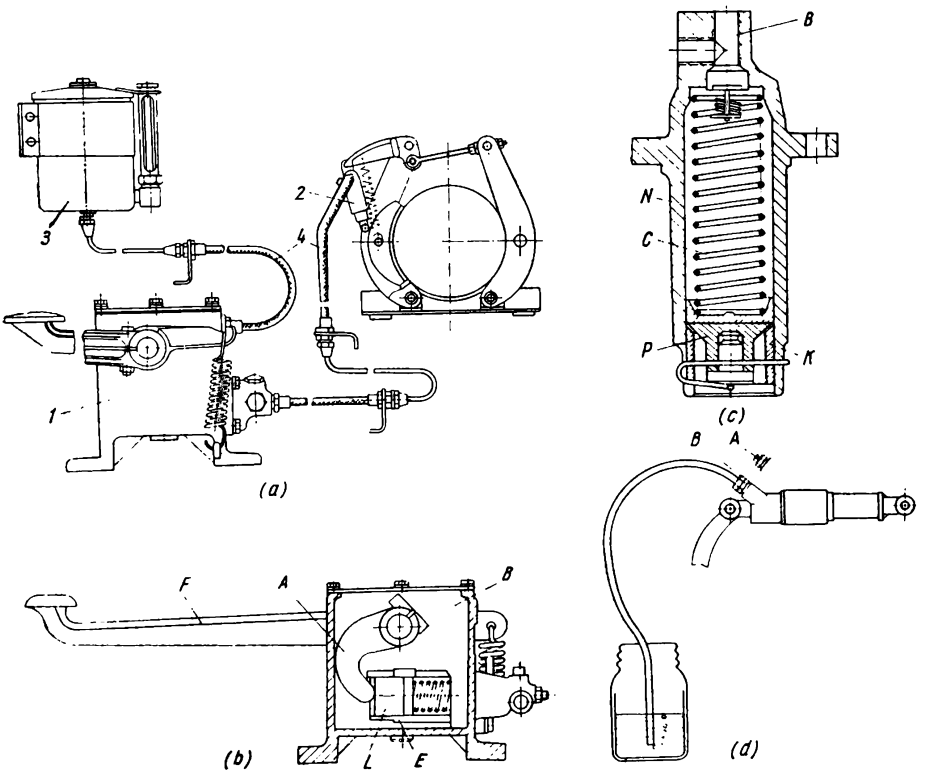

Fig. 139. Hydraulic system of a pedal-controlled shoe brake

The compensating properties of tank *B* are intended to maintain a constant volume of fluid during the entire period of operation irrespective of the reduced volume of the fluid due to temperature variations. Secondly, it continuously and immediately refills the system upon possible fluid losses.

The hydraulic cylinder (Fig. 139*c*) consists of body *N* with moving piston *P*, piston cup and spacer spring *C*.

The hydraulic cylinder is filled with oil from the supply tank through upper hole *B* while the vacuum formed by the piston stroke is eliminated by air entering through holes *K* in the piston.

The brake pedal is pushed back by a return spring. In this case the piston of the hydraulic cylinder is pushed into the cylinder by the brake spring and the braking fluid is forced out of the cylinder back into the system. At the same time the nonreturn valve (external in a double valve) opens under the pressure from the returning fluid and admits the fluid into the master cylinder. The return flow of the fluid is also facilitated by the vacuum which is set up in the master cylinder when its piston returns to the initial position.

If the foot pedal is quickly released the piston of the master cylinder may move so quickly that it sets up a vacuum in the cylinders and the tubing and air may

force back the cup of the hydraulic cylinder piston and penetrate into the system. This may essentially interfere with operation. To prevent this the tension of the return spring of the pressure cylinder piston, which is also the spring of the nonreturn valve, is so selected that when the pressure of fluid in the system drops below 0.42-0.56 kg/cm² the nonreturn valve closes and a certain surplus pressure is maintained in the hydraulic control system. This keeps air out of the tubing. The time during which surplus pressure is retained in the system depends on the air-tightness of the joints. After the nonreturn valve has been closed the vacuum set up in the master cylinder is compensated for by the inflow of fluid from the supply tank through the corresponding holes.

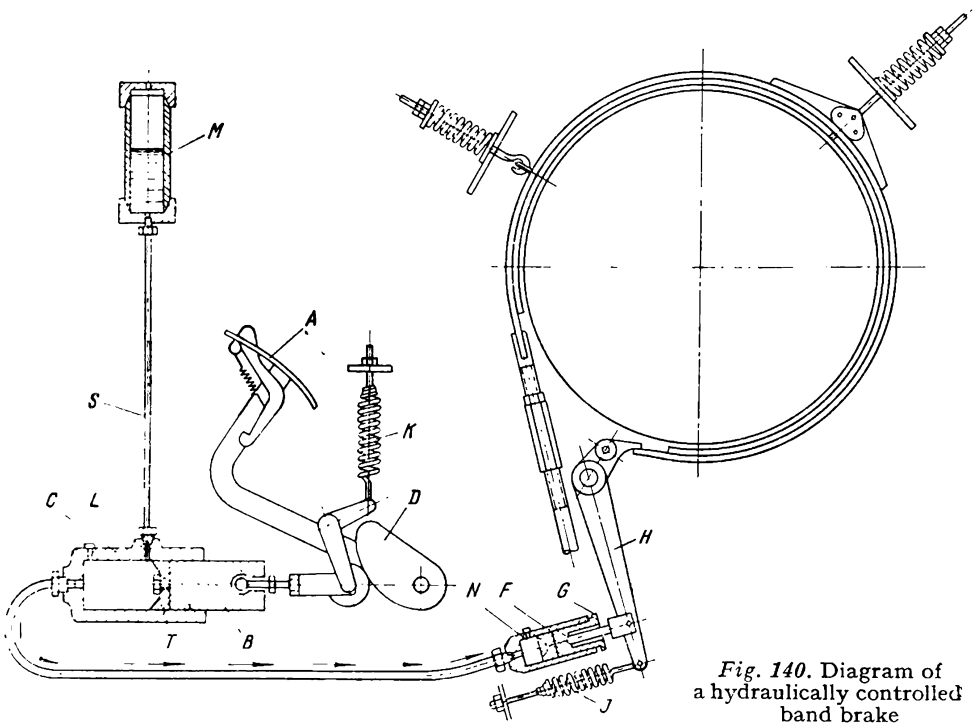

Fig. 140. Diagram of a hydraulically controlled band brake

In filling the hydraulic control system with fluid air should be thoroughly excluded since its presence in any part of the system may lead to failure of the brakes. The presence of air in the system is indicated by a resilient (the pedal springs back) or jerky (the pedal sinks) stroke of the pedal. Air can penetrate into the system if the level of fluid in the supply tank is too low or through faulty joints.

The air is bled from the system by pumping. With this aim in view the master cylinder is filled with braking fluid and plug *A* (Fig. 139*d*) for air bleeding is screwed out of the hydraulic cylinder and connection *B* with a rubber tube is screwed on instead. The end of the rubber tube is submerged into a vessel with braking fluid so that it is below the fluid level. Then the system is pumped through by slowly depressing the brake pedal all the way down. Repeated depressing and release of the pedal will force the air from the system in the form of bubbles together with the braking fluid through the end of the rubber tube. Pumping should be continued until a uniform stream of braking fluid without bubbles begins to flow from the system. Then plug *A* is screwed in again. During and at the end of pumping the level of fluid in the tank should not drop below half the height of the tank.

Fig. 140 shows a diagram of a hydraulic band brake of a modern travelling boom crane. Pressure in the master cylinder *C* is produced by means of pedal *A*

cam *D* and piston *B*. Braking fluid flows along a tube into hydraulic cylinder *F* whose piston *G* acts on lever arm *H* of the drum band brake. When pedal *A* is released spring *J* returns lever *H* to its initial position.

The fluid returned by piston *G* into the master cylinder acts on piston *B* and pedal *A*.

When the pedal is released spring *K* retracts piston *B* and opens hole *L* which communicates the fluid in the system with the fluid in tank *M* through tube *S*. In this way all losses of fluid in the system due to worn cups *N* and *T* or leakage in the tubing joints are automatically replenished.

Hydraulic braking systems are filled with a braking fluid of homogeneous composition and uniform physical properties. It must possess a stable viscosity, little affected by temperature variations, and have no detrimental chemical effect on rubber and metal parts.

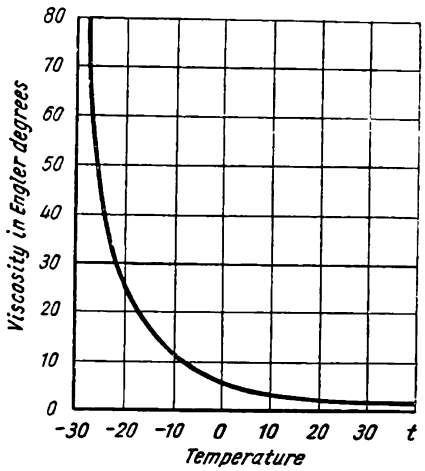

Fig. 141. Change in the viscosity of braking fluid with variations in temperature

There exist at present over ten grades of different braking fluids all of which are distinguished by the absence of mineral oils, kerosene, petrol, sugar, glucose and water, as well as solid mineral impurities.

By composition braking fluids are divided into two main groups: (a) fluids containing castor oil as their viscous base (main group of fluids) and (b) fluids containing glycerine as the viscous base.

Fig. 141 illustrates changes in viscosity of grade БСК Soviet-made braking fluid depending on the temperature.

7. APPROXIMATE STATIC CALCULATION METHOD FOR SHOE BRAKE DESIGN

A shoe brake applied by a weight of a type still used in cranes of old designs is shown in Fig. 142.

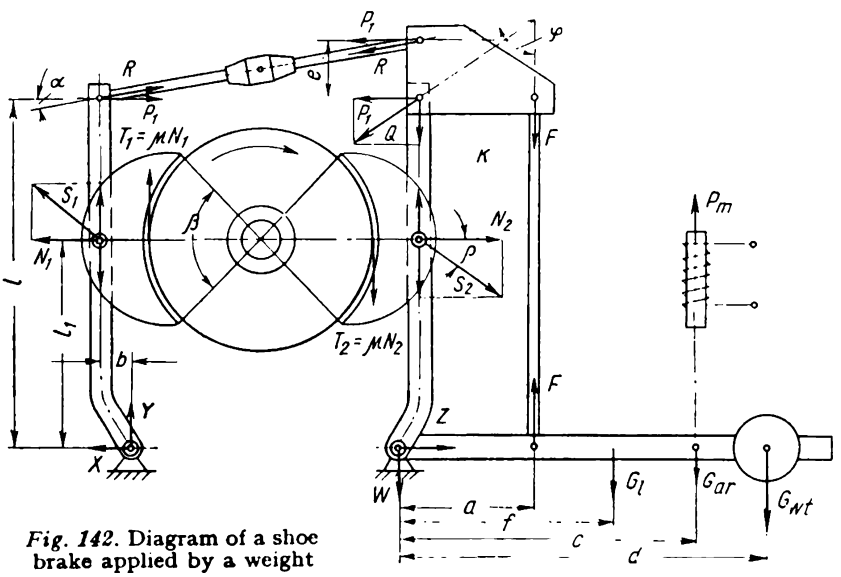

Fig. 142. Diagram of a shoe brake applied by a weight

The total peripheral braking force produced by both shoes on the rubbing surface is

$$T = \frac{2M_{br}}{D}$$

The weight required to apply the brake is

$$P_1 = \frac{M_{br}}{\mu D\eta} \frac{i_1^2 - \mu^2 b^2 *}{l l_1} . \qquad (102)$$

The normal pressure on the shoe of the left lever with the wheel rotating as shown in Fig. 142 is

$$N_1 = \frac{P_1 l}{l_1 - \mu b} = \frac{M_{br}(l_1 + \mu b)}{\mu D l_1 \eta}$$

Unit pressure between the wheel and the shoe of the left lever is

$$p = \frac{N_1}{F} < p_{safe} .$$

Normal pressure on the shoe of the right lever is

$$N_2 = \frac{P_1 b}{l_1 + \mu b} = \frac{M_{br}(l_1 - \mu b)}{\mu D l_1 \eta}$$

Since $N_2 < N_1$ the unit pressure on the right shoe is not checked.

In developing equilibrium equations for vertically mounted brake levers (see Fig. 142) and determining the forces acting on the shoe, the moment from the unbalanced weight of the levers is not taken into account for the following reasons:

(1) in ordinary designs of shoe brakes this moment is extremely small and has no practical significance;

(2) unbalanced weight of one lever is taken over by the pull-rod above the wheel by the other brake lever and the action of their weights is thus mutually compensated for.

If the levers are arranged horizontally, their weight and the weight of the shoes should be always taken into consideration.

In examining the equilibrium of forces acting during braking on the brake lever with a shoe which pivots on a hinge pin two forces of equal magnitude T and directed opposite to each other are applied in the centre of the pivot.

In this way the lever is acted upon by forces N and T and the shoe by a couple T on an arm equal to the distance from the centre of the pivot to the rubbing surface of the wheel at the middle of the shoe. In ordinary designs this arm has a minimum value. In this case the moment of forces T tending to turn the shoe and changing the uniform distribution of unit pressures over the shoe length is very small and can be disregarded in equilibrium equations.

Since the normal pressures N_1 and N_2 acting on the wheel are not equal the brake shaft is subject to the action of a bending force

$$\Delta S = S_1 - S_2 .$$

Expressing the forces S through normal pressures and making appropriate transformations we obtain

$$\Delta S = \frac{2M_{br}}{Dl_1} \sqrt{1 + \mu^2} \times b .$$

* The value of $\mu^2 b^2$ is usually neglected.

The vertical component of the bending force is

$$\Delta S_v = T_1 - T_2 = \frac{2M_{br}\mu b}{Dl_1}.$$

The horizontal component of the bending force is

$$\Delta S_h = N_1 - N_2 = \frac{2M_{br}b}{Dl_1}.$$

It follows therefore that with a given braking torque the bending force will be determined by the length of arm b. In straight levers when $b = 0$ the bending effort theoretically equals zero.

To eliminate completely the forces bending the brake shaft the design of shoe brakes should meet the following requirements:

(1) the axes of the shoes should be aligned with the centre of the wheel;

(2) the shoes should be symmetric with respect to the line which connects their axes;

(3) the pivots of the levers should be arranged at equal distances from the wheel centre.

The forces acting in the rods of the brake system are

$$R = \frac{P_1}{\cos\alpha}; \quad F = P_1\frac{l}{k};$$

$$Q = \sqrt{R^2 + F^2 + 2RF}\sin\alpha.$$

The forces in the supporting pivots of the braking levers:

$$Y = T_1 + P_1\tan\alpha;$$

$$X = N_1 - P_1; \quad Z = N_2 - P_1;$$

$$W = T_2 + P_1\left(\frac{l}{k} + \tan\alpha\right).$$

The weight applying the brake G_{wt} is

$$G_{wt} = \frac{P_1\frac{la}{\eta k} - (G_l f + G_{ar}c)\eta}{d}$$

where G_l—weight of the braking lever;

G_{ar}—weight of the magnet armature;

η—efficiency of the brake lever system; with good quality pivots it can be taken as 0.9 to 0.95.

Analysis of a spring-applied shoe brake, type TK, with a short-stroke electromagnet (Fig. 143).

Irrespective of the type of brake actuator (electromagnet or thrustor), the resultant force P_1^* of the main and auxiliary springs, which acts equally on both levers at the given braking torque M_{br}, is found from the equation

$$P_1 = \frac{M_{br}}{\mu D\eta}\frac{l_1}{l}$$

where μ—coefficient of friction;

* The auxiliary spring is not used in a thrustor-operated brake.

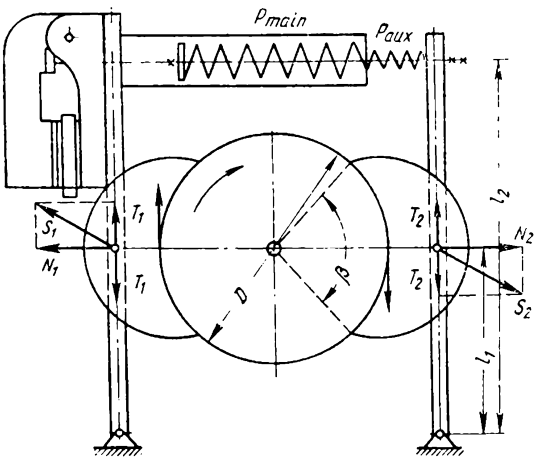

Fig. 143. Diagram of a shoe brake applied by a spring

η—efficiency of the brake lever system, i. e., ratio of the actual pressure exerted by the shoes on the wheel to the total tension of the springs acting on the brake rod and referred to the centre of the shoes; for a brake with good quality pivots and adequate lubrication η = = 0.9 to 0.95.

The effort of the auxiliary spring P_{aux} intended only for tilting back the nonmagnetic lever ranges from 2 to 8 kg depending on the size of the brake.

The effort of the main spring

$$P_{main} = P_1 - P_{aux} .$$

When using a short-stroke a-c electromagnet (type МО-Б) account should be taken of the moment due to the weight of the magnet armature (indicated in the respective catalogues) which reduces the operating effort of the main spring, and the rated force P_{main} should be duly corrected.

The total normal pressure between the shoe and the wheel is

$$N = \frac{M_{br}}{\mu D} .$$

We can disregard the effect of the unbalanced weight of type МП and МО-Б lever-mounted electromagnets on the value of normal pressure exerted by the shoe on the wheel because normal pressure is changed negligibly.

The mean unit pressure between the shoe and wheel is

$$p = \frac{N}{F} < p_{safe}$$

where F—design bearing area between the shoe and wheel which can be found from the formula

$$F = \frac{\pi D}{360} B\beta$$

where B—width of the shoe; the width of the wheel is usually taken 5 mm larger than that of the shoe to ensure full contact of the friction lining;

β—angle of contact between the wheel and shoe; in shoe brakes of various designs this angle may range from 60° to 120°.

The safe unit pressure p_{safe} is taken from Table 24. The maximum permissible clearance between the shoe and wheel is

$$\varepsilon = h_1 \frac{l_1}{2l} .$$

In this formula h_1 is half of the maximum permissible stroke of the brake pull-rod determined by the stroke of the magnet armature; the other half of the magnet stroke is used to compensate for wear and deformation of the linings and deflection of the levers.

The clearance between the shoe and wheel is established depending on the amount of runout of the braking wheel, the deflection of the braking shaft, the amount of wheel expansion due to heating in operation, the deflections of the braking levers and the elasticity of the friction material.

The following values of radial adjusting clearances between the shoe and wheel have been accepted for type TK brakes:

Wheel diameter D, mm	100	200	300	400	500	600	700	800
Adjusting clearance ε, mm	0.6	0.8	1.0	1.25	1.25	1.5	1.5	1.75

The rigidity of the lever system should be checked by calculations. The total deformation of the system should not exceed 10 per cent of the rated stroke of the magnet. Braking lever stresses are determined for bending moment M due to force P_1 in the critical cross-section of the lever:

$$\sigma = \frac{M}{W} d$$

where W—moment of resistance, in cu cm, to bending of the lever section being checked;

d—dynamic factor accounting for the nature of force application when the brake is being applied.

Braking levers are made of steel. Safe bending stresses should not exceed $0.4\sigma_s$. In checking the strength of the pivot pins the safety margin relative to the yield point and with regard to the dynamic load should be at least 1.5.

The unit pressure in the pivot pins should not exceed 30 kg/cm^2. The pins are manufactured from steel 45, 50 or 60 hardened to Bhn = 300 to 350.

Analysis of Combined Controlled Shoe Brakes. Since the effort of the main spring of combined controlled brakes is completely taken up by the electromagnet the brake application system, when the magnet is deenergised, is designed in the same way as for noncontrolled brakes with an electromagnetic actuator.

The designs of the control systems of normally released and combined brakes do not differ in principle and involve calculations for the effort needed to develop the rated braking torque. Calculations are performed in the same way both for shoe and band brakes, the only difference being in the magnitudes of the forces and strokes.

A calculation diagram for a normally released brake with hydraulic control is shown in Fig. 144, diagrams of combined brakes in Figs 145 and 146. The relationship between the braking torque M_{br} and the effort applied to the pedal P_{ped} is found as follows:

$$M_{br} = \mu N D \frac{P_{ped} h \mu D \eta_0}{2\varepsilon}.$$

Hence we can find clearance ε:

$$\varepsilon = \frac{P_{ped} h \mu D \eta_0}{2M_{br}}.$$

Since the ratio $\frac{h}{\varepsilon}$ equals the total transmission ratio of the lever and hydraulic system the effort P_{ped} applied to the pedal and needed to develop the braking torque M_{br} in a normally released brake (in Fig. 144) and in a combined brake (in Fig. 146) will be

$$P_{ped} = \left(\frac{M_{br} l_1}{\mu D l} + P_{aux} \right) \frac{a}{b} \frac{n}{m} \left(\frac{D_{mas}}{D_{hyd}} \right)^2 \frac{1}{\eta_0}; \qquad (103)$$

for the other combined brake (in Fig. 145)

$$P_{ped} = \left(\frac{M_{br} l_1}{\mu D l} + P_{aux} \frac{l_2}{l} \right) \frac{b}{c} \frac{n}{m} \left(\frac{D_{mas}}{D_{hyd}} \right)^2 \frac{1}{\eta_0} \qquad (104)$$

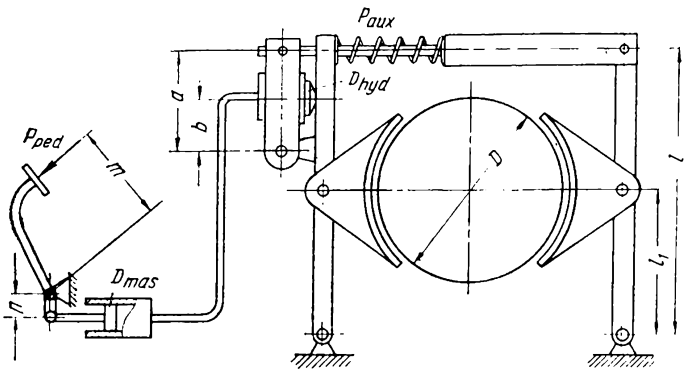

F g. 144. Diagram of a normally released shoe brake

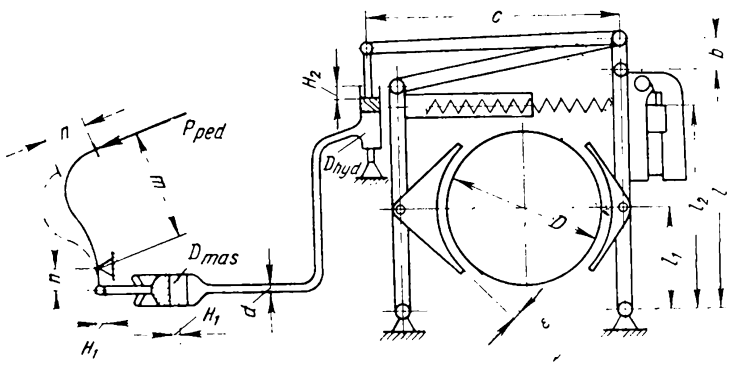

Fig. 145. Diagram of a combined shoe brake with a long-stroke piston

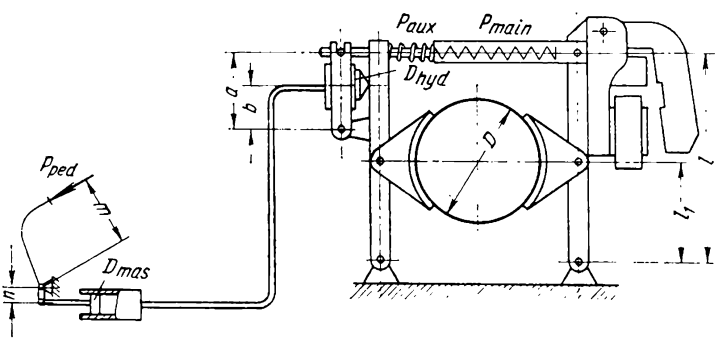

Fig. 146. Diagram of a combined shoe brake with a short-stroke piston

For a simple normally released band brake (in Fig. 140) the effort P_{ped} on the pedal can be found from the formula

$$P_{ped} = \left[\frac{2M_{br}}{D(e^{\mu\alpha} - 1)^*} + P_{aux}\frac{c+d}{c}\right]\frac{b}{c}\frac{n}{m}\left(\frac{D_{mas}}{D_{hyd}}\right)^2\frac{1}{\eta_0}. \quad (105)$$

In these formulas: P_{aux} is the effort of the auxiliary spring in kilogrammes. This effort should be minimal and at the same time sufficient to overcome residual pressure in the hydraulic system and the moment of friction in the pivots of the brake lever system when the brake is released and also to return the piston of the hydraulic cylinder to the initial position. Tests conducted on controlled brakes of various designs have shown that the effort developed by the auxiliary (releasing) spring should be between 10 and 20 kg.

η_0— the total efficiency of the hydraulic control system of the brakes and the lever system of the brake and pedal. The tests establish the total efficiency η_0 at 0.65 to 0.75. The losses for the friction in the cups and pistons are evaluated from the efficiency of the pipeline as 0.8 to 0.87.

In formulas (103), (104) and (105) D_{mas} and D_{hyd} are the diameters of the master and hydraulic cylinders;

l_1, l_2, l, a, b, c, d, m, n—arms of the lever system;

D—diameter of the brake wheel.

The maximum pedal stroke should not exceed 250 mm and that of the control lever—400 mm. In a newly readjusted brake 50 per cent of the stroke is reserved to compensate for the wear of the brake linings and pivots and for the elastic deformation of the lever system. Hence, calculations are carried out for a pedal stroke of 125 to 150 mm and lever stroke of 200 to 250 mm. The angle of the pedal or lever turn for maximum stroke should not exeed 60°.

The total transmission ratio of the brake control system can be represented in the following form:

$$i_t = i_l i_h i_p$$

where i_l—ratio of the brake lever system;

i_p—ratio of the pedal arms;

i_h—ratio of the hydraulic system.

Then for the systems in Figs 144 and 146

$$i_t = \frac{l}{l_1}\frac{b}{a}\left(\frac{D_{hyd}}{D_{mas}}\right)^2\frac{m}{n};$$

for the system in Fig. 145 (106)

$$i_t = \frac{l}{l_1}\frac{c}{b}\left(\frac{D_{hyd}}{D_{mas}}\right)^2\frac{m}{n};$$

and for the system in Fig. 140

$$i_t = \frac{m}{n}\left(\frac{D_{hyd}}{D_{mas}}\right)^2\frac{c}{b}. \quad (107)$$

In distributing transmission ratios between the different elements of the control mechanism the following recommendations based on experimental research should be taken into consideration:

1. Full stroke of the master cylinder piston should not exceed 40-45 mm.
2. Full stroke of the hydraulic cylinder piston should not exceed 40 mm.

The ratios between the diameters of the hydraulic and master cylinders cannot be selected arbitrarily; they should conform to the values of the adjusting clearance between the lining and the wheel, the operating stroke of the pedal and

* Euler's number ($e^{\mu\alpha}$) is explained in Sec. 10 of this chapter.

the transmission ratios of the brake lever system. Proceeding from the equality of the volumes of fluid flowing from the master cylinder into the hydraulic cylinder and back again and from the data of experimental research the following diameter ratios have been obtained for systems in Figs 144 and 146:

$$D_{hyd} = (1.8 \text{ to } 3)\, D_{mas};\ i_h = 3 \text{ to } 9$$

and for the system in Fig. 145

$$D_{hyd} = (1.0 \text{ to } 1.5)\, D_{mas};\ i_h = 1 \text{ to } 1.3.$$

8. THERMAL CALCULATIONS OF SHOE BRAKES

Determining the Size of Brake Wheels. The required size of brake wheels depends mainly on the amount of energy absorbed by the brake in the course of one hour because this directly determines the wear of the wheel and linings and also the heating of the wheel.

At the same time unit wear per hp-hr also depends on a number of other factors as, for example, the material of the wheel and linings, unit pressure, peripheral speed and, to a very large degree, on the temperature of the brake wheel.

The combination of these numerous factors makes all the methods of calculating the wear of brake wheels highly unsatisfactory although they can still be used for a tentative estimation of the expected brake life.

For this reason the experimentally established values of pv and $pv\mu$, where p is unit pressure on the working surface and v—peripheral speed of the brake wheel, continue to be employed as initial data for such calculations. These experimental data are resorted to because we lack more exact methods for heat calculation. The greatest shortcoming of these data is that they take into account neither operating conditions of the brakes nor the purpose for which they are intended (lowering, holding or travelling).

In view of all this it is more expedient to determine the size of brake wheels by calculating the amount they are heated. It is assumed further that the brake wheel is mounted on a shaft rotating at the highest speed, i.e., on the motor shaft, thereby ensuring optimal conditions of heat dissipation and minimum size of the brake.

Lowering Brakes. All heat generated by the energy of a falling load must be dissipated by the brake wheel into the atmosphere by radiation and heat exchange with enveloping streams of air.

The amount of heat dissipated by radiation during one hour equals approximately

$$Q_1 = [C_1 S_1 + C_2 S_2]\left[\left(\frac{273 + t_1}{100}\right)^4 - \left(\frac{273 + t_2}{100}\right)^4\right] \text{ kcal/hr} \qquad (108)$$

where S_1—area, in sq m, of a smoothly polished surface of the brake wheel rim (not enveloped by shoes);

C_1—radiation constant for a smoothly polished steel surface (assumed equal to 1.3);

S_2—area, in sq m, of the two side surfaces of the brake wheel*;

C_2—radiation constant for a dull (oxidised) steel surface (assumed equal to 4.3);

t_1—maximum permissible temperature of the brake wheel in °C allowed by the material of the linings;

t_2—temperature in the premises in °C.

In considering heat exchange with a stream of air we must distinguish between natural and forced air circulation. Natural circulation takes place when the brake

* Since the inner surface of the brake wheel cannot radiate heat in all directions and, besides, has some of its parts covered by adjacent design elements hindering radiation, it is neglected in our calculations.

wheel is idle and forced circulation during operation. In this case the operating time corresponds to the relative switching-in period, or duty factor (DF), for the given unit.

We take the operating time of the brake equal to 0.15 of the entire cycle for light duty, 0.25 for medium (normal) duty and 0.40 for heavy duty.

The amount of heat dissipated during one hour due to heat exchange with natural air circulation will be approximately

$$Q_2 = \alpha_1 S_3 (t_1 - t_2) (1 - \mathrm{DF}) \text{ kcal/hr} \tag{109}$$

where α_1—coefficient of heat transfer with natural air circulation (5 kcal/m² hr°C);

S_3—total surface, in sq m, of the brake wheel except for the parts wrapped by the shoes;

t_1 and t_2—temperatures of the brake wheel and the premises, in °C, respectively.

As the brake wheel rotates the coefficient of heat transfer substantially increases due to higher relative speed of the wheel and the ambient air.

According to Nusselt, the following relation is approximately true between the relative speed of the wheel v_0 in m/sec and the coefficient of heat transfer α_2:

$$\alpha_2 = 6.14 v_0^{0.78}. \tag{110}$$

On the rim of the brake wheel, the sum of the outer and inner surface of which will be denoted by S_4 in sq m, this speed (v_0) is approximately equal to the peripheral speed of the wheel

$$v_0 = \frac{\pi D n}{60} \text{ m/sec}$$

where D—wheel diameter, in m;

n—wheel rpm.

For further calculations the side surface of the wheel may be represented as separate circular areas s_1, s_2, s_3, etc., for which certain mean values of speeds v_1, v_2, v_3, etc., will hold true.

The total amount of heat dissipated during one hour due to heat exchange with forced air circulation will be

$$Q_3 = \mathrm{DF}\,(t_1 - t_2)\, 6.14 \left[S_4 v_0^{0.78} + 2s_1 v_1^{0.78} + 2s_2 v_2^{0.78} + \ldots + 2s_n v_n^{0.78}\right] \text{ kcal/hr.} \tag{111}$$

The total amount of heat dissipated during one hour is

$$Q_{tot} = Q_1 + Q_2 + Q_3 \text{ kcal/hr} \tag{112}$$

and should equal the amount of heat liberated during absorption of the kinetic energy in lowering the load. We shall use the following notation:

G_1—mean weight of the loads being lowered, in kg;

h—mean height of load lowering, in m;

η—efficiency of the hoisting mechanism;

z—number of lowering operations per hr;

$A = \frac{1}{427}$ — mechanical equivalent of heat, in kcal/kg-m.

Then the heat liberated in one hour will be

$$Q_{tot} = G_1 hz\eta A \text{ kcal/hr.} \tag{113}$$

These calculations presuppose an exact knowledge of the crane operating conditions.

If such data are not available a tentative estimation may be made from the power rating N, in hp, of the motor actuating the hoisting mechanism.

If a load being lifted comprises $X\%$ of the total load-lifting capacity of the crane then the average mean power in lowering will be

$$N_{low} = N\eta^2 X \text{ hp.}$$

If the lowering and hoisting speeds are the same, the time of lowering will account for $\frac{DF}{2}$ of the total operation time since the height of lowering equals approximately the height of hoisting.

The total amount of heat liberated during one hour, i.e., during 3,600 sec is equal to

$$Q_{tot} = N\eta^2 X \times 3{,}600 \frac{DF}{2} \times \frac{75}{427} = 316 N\eta^2 DFX \text{ kcal/hr.} \quad (114)$$

It follows from this formula that when the lowering speed is higher than the hoisting speed the power increases in the same proportion in which the time of lowering decreases relative to the time of raising.

Formulas (112) and (114) can be used to check the size of brake wheels for permissible heating during braking.

In normal climatic conditions the maximum temperature in the premises is assumed to be 35°C.

The permissible temperature of the brake wheel depends on the material of the linings. For an asbestos brake lining, with or without interwoven metal mesh, $t_1 = 200°$ to 300°C. However, these limiting values cannot be recommended for calculations; account should be taken of possible temperature peaks in lowering to ensure reliable operation of the brake.

The lower the temperature of the brake wheel, the longer will be the life of the linings and wheel. For this reason preference should be given to designs with cooling fins to attain more effective heat dissipation.

The size of wheels employed in lowering brakes can be selected from Table 27 which indicates respective power ratings for various brake wheels of hoisting mechanism motors for medium duty (mean weight of the load being lowered is 50 per cent of the total lifting capacity, DF = 0.25, $\eta = 0.85$ and $t_1 = 100°$C).

Table 27

Size of Wheels for Lowering Brakes Depending on Hoisting Mechanism Motor Power

Brake wheel					Motor power in raising, in hp, at n rpm*		
Diameter D, mm	Width B, mm	Weight, kg	Moment of gyration, kg-m²	Moment of inertia, kg-m/sec²	$n = 570$	$n = 730$	$n = 960$
250	80	16	0.7	0.018	7(197)	8(219)	9(248)
320	100	29	1.96	0.05	12(330)	13(370)	15(426)
400	125	53	5.5	0.14	21(610)	24(688)	28(790)
500	160	90	15.7	0.40	37(1,055)	42(1,195)	50(1,383)
630	200	135	43.2	1.1	67(1,925)	77(2,196)	—(2,570)
800	250	203	86.4	2.2	212(3,486)	144(4,011)	—(4,730)

* The figures in brackets indicate the amount of heat in kcal/hr dissipated at 100° C.

At lower values of efficiency these ratings may be increased by $\left(\frac{0.85}{\eta}\right)^2$ times.

For other mean weights of loads being lowered the tabulated data should be corrected by a ratio inversely proportional to the weights.

Travelling Brakes. These brakes are classified as brakes intended for stopping a crane or trolley at full speed and brakes for travelling mechanisms provided with electric braking gear.

Brakes of the second type should absorb a smaller part of the energy of motion and stop the crane; such brakes can be calculated in the same way as holding brakes of hoisting mechanisms.

Brakes of the first type should be designed in the same way as lowering brakes, i.e., from heating considerations.

The amount of heat liberated during one hour for z braking operations is

$$Q_{tot} = z\left[\frac{G}{g}\frac{v^2}{2} - Wf\frac{vt_{br}}{2}\right]\eta\frac{1}{427} \text{ kcal/hr} \qquad (115)$$

where G—weight of the crane or truck, in kg;
$g=9.81$—acceleration due to gravity, in m/sec²;
Wf—resistance to motion, in kg;
t_{br}—braking time, in sec;
η—actuator efficiency.

The size of the brake wheel should be so assigned that the total amount of heat that can be dissipated by the brake—$Q_1+Q_2+Q_3$—is equal to or exceeds the amount of the liberated heat Q_t.

Table 28 will be useful in selecting wheel sizes for travelling brakes. It is compiled for 80-100 braking operations per hour for a travelling mechanism mounted on sliding friction bearings.

Table 28

Wheel Sizes for Travelling Brakes Depending on the Power of the Travelling Mechanism

Brake Wheel		Motor power in hp at								
Diameter D	Width B	n = 570 rpm and travelling speed, m/min			n = 730 rpm and travelling speed, m/min			n = 960 rpm and travelling speed, m/min		
mm		90	120	180	90	120	180	90	120	180
250	80	18	13	9	20	15	10	22	17	11
320	100	29	23	15	33	26	17	37	29	19
400	125	50	40	27	56	45	30	65	52	35
500	160	80	65	45	90	73	50	105	85	59
630	200	130	110	80	150	125	90	—	—	—
800	250	210	180	138	250	210	160	—	—	—

Travelling brakes which operate at speeds in the order of 60 m/min should be designed in the same way as holding brakes of hoisting mechanisms.

Holding Brakes. The amount of heat absorbed and dissipated by holding brakes into the atmosphere is calculated by the same procedure as for travelling or lowering brakes when the number of braking operations per hour is known.

Differentiation should be made between braking the whole mechanism and the load at full speed or (as, for example, in electric braking) at a very low speed.

Since holding brakes operate under more stable duty than lowering and travelling brakes their sizes can be selected with a sufficient degree of accuracy from the available experimental data.

In general, for holding brakes provided with ferrodo linings

$$pv = 15 \text{ to } 30 \text{ kg-m/sec-cm}^2$$

where p—unit pressure on the brake shoe, in kg/cm², calculated from the torque on the motor shaft M, kg-cm:

$$p = \frac{2M}{D\mu}\frac{1}{2bl} \text{ kg/cm}^2$$

where b and l—width and length of the lining, in cm;
v—peripheral speed of the brake wheel, in m/sec.

Larger values should be taken for light duty and an average number of switching-in operations whereas for heavy duty the value of pv should never exceed 15.

The rpm of the brake wheel is also very important. For instance, at 1,000 rpm we can take larger values of pv than at 600 rpm because of better heat dissipation. In electrical braking larger values of pv can likewise be taken.

For normal operating conditions the size of wheels for holding brakes can be tentatively selected from Table 29.

Table 29

Brake wheel		Power of hoisting mechanism motor in hp at n rpm		
Diameter, mm	Width, mm	$n = 570$	$n = 730$	$n = 960$
160	50	9	10	11
200	65	13	15	16
250	80	19	21	24
320	100	31	35	40
400	125	52	59	67
500	160	85	96	112
630	200	135	156	—
800	250	220	260	—

In hoisting mechanisms employing electric braking the power of the motor (corresponding to the wheel size) can be increased by 20 per cent and for light duty (small number of switching-in operations and rare full loads) by another 12 per cent.

However, at heavy duty (large number of switching-in operations and almost exclusively full loads) these power ratings of the electric motors should be reduced by at least 20 per cent.

Calculating the Durability of Linings. The life of brake linings can be approximately estimated from the following formula:

$$y = \frac{\Delta G}{qA} \tag{116}$$

where y—life (number of braking operations);

ΔG—wear of the lining, in cu cm;

q—permissible wear of linings, in cm³/hp-hr;

A—work done during one braking operation, in hp-hr.

For ferrodo-type linings operating with dry friction on a smooth steel wheel at moderate temperatures q may equal approximately 0.2 cm³/hp-hr.

Design of the Spring and Selection of the Electromagnet. In present-day practice the brake is applied almost always by springs which provide much smoother performance than a weight.

If the required force on the brake shoes is P the required tension of the spring in conventional brake designs will be

$$K = P\frac{b}{a} - V\frac{l}{c}. \tag{117}$$

Since the brake must hold the load with a definite degree of reliability the design braking torque is assumed larger than the moment developed by the load being lowered.

If we denote the nominal moment of the hoisting mechanism motor by M and the actuator efficiency by η, the braking moment with the wheel mounted on the motor shaft will be

$$M_{br} = \nu M\eta^2. \tag{118}$$

For ordinary holding brakes the safe braking factor may be taken as $\nu = 2$ to 3 while for travelling brakes it may range from 0.5 to 1.5.

The pressure required to apply a double shoe brake is calculated from the braking torque:

$$P = \frac{M_{br}}{D\mu} = \frac{\nu M\eta^2}{D\mu}. \tag{119}$$

The unit pressure on the shoes is

$$p = \frac{P}{bl}. \tag{120}$$

The coefficient of friction depends on the material of the linings (see Table 25).

When M_{br} and μ are known we can easily determine all the required data for calculating the initial tension of the spring.

It should be taken into account that, in releasing, the spring extends and the load on it increases somewhat.

At a small helix angle this additional load can be made comparatively light. This is very important for increasing the life of the spring which depends, mainly, on the difference between the loads exerted on the spring when the brake is released or applied.

When the difference between these loads is small the safe stress for the spring material can be taken as $[\tau]=4{,}000$ kg/cm² without fear of failure.

In general, springs should operate in compression in brakes and so as to prevent the dropping of the load if the spring suddenly breaks.

Braking magnets should provide adequate releasing effect.

If:

λ—departure of the shoes from the wheel, in cm;

η'—efficiency of the brake lever system,

then the work performed by the magnet on releasing will be

$$A' = \frac{2P\lambda}{\eta'} \text{ kg-cm.} \tag{121}$$

When

$$P = \frac{\nu M\eta^2}{D\mu} \tag{122}$$

and

$$\eta' \approx 0.9$$

then

$$A' = 2.2\frac{\nu M\eta^2}{D\mu}\lambda \text{ kg-cm.} \tag{123}$$

The departure of the shoes λ should be large enough to avoid contact with the wheel when the brake is released.

The amount of the shoe departure can be reduced in proportion to the accuracy of the brake, particularly, to the reduction in the clearances of the lever pivots. The following values of λ can be taken for ordinary designs of crane brakes depending upon the diameters of the wheels.

Diameter of sheave, mm	160; 200; 250	320; 400; 500	630; 800
Shoe departure λ	0.1-0.15	0.15-0.20	0.18-0.25

The type of the electromagnet is selected from the appropriate catalogues on the basis of the work required in releasing A', the pull of the magnet being taken 25 per cent larger than that required by the design.

The magnet armature stroke should be sufficient to compensate for the wear of the linings.

Thus, only 80 per cent of the stroke indicated in the catalogues should be utilised. However, the permissible pull of the magnet as stipulated by the catalogues should be fully utilised. In case of three-phase magnets this is compulsory, otherwise the magnet will operate in jerks and frequently fail in operation.

9. PRECISE METHODS OF SHOE BRAKE DESIGN

The existing method of designing shoe brakes is based on the hypotheses of constant force exerted by the shoe on the wheel and constant coefficient of friction. This method proceeds from static equilibrium equations of the brake levers. It is assumed that the braking force is applied to the wheel statically and no distinction is drawn between the design of a shoe brake with a shoe rigidly fastened to the brake lever and a brake w th a pivoted shoe.

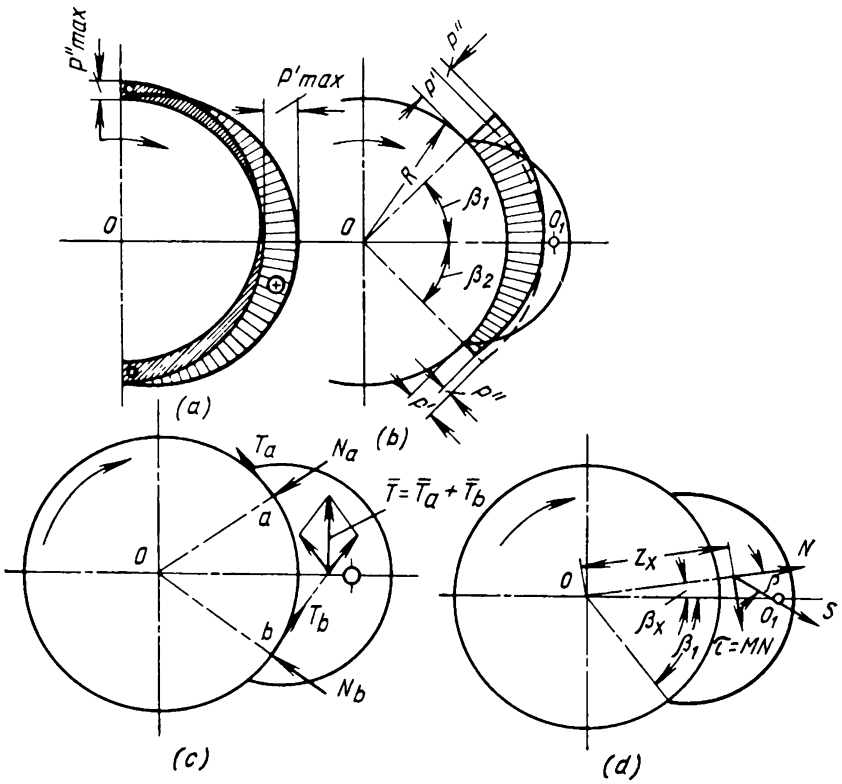

Fig. 147. Distribution of unit pressures and forces in braking

Further assumption concerns the positioning of the point of application of the resultant force of normal pressure of the shoe on the wheel and friction forces at the intersection of the wheel circumference with the line which connects the wheel and shoe centres. It is also assumed that the resultant of these forces does not pass through the shoe pivot which disagrees with the actual conditions of its equilibrium when the shoe is pivoted on the lever.

This method of shoe brake design, based on a great many assumptions and suppositions, by no means corresponds to the actual physical phenomena of the braking process and misrepresents actual force distribution over the various elements of the brake.

If we examine the geometry of motion of the lever with the shoe and the motion of the shoe relative to its pivot we shall see that unit pressures are distributed over the length of the shoe according to the sine and cosine law (Fig. 147*a*) with the greatest unit pressures on the oncoming part of the shoe and the minimum on the running-off part (Fig. 147*b*). The point of application of the resultant of the friction forces T and normal forces N always lies beyond the circumference of the wheel irrespective of the law of distribution of unit pressures over the length of the shoe and of whether friction occurs on the inner or outer surface of the

brake wheel. Indeed, if we take any two points a and b on the surface of the wheel (Fig. 147*c*) we see that elementary friction forces T_a and T_b are applied at these points and $T_a=\mu N_a$ and $T_b=\mu N_b$. Since the elementary friction forces are directed at a tangent the resultant of these forces T will be always applied beyond the friction circumference of the wheel. This holds true for any points of contact between the wheel and shoe irrespective of all other factors and also of whether the shoe is fastened rigidly or pivoted. Therefore, the resultant of all the tangential forces should be applied at the point located beyond the circumference of the wheel.

The direction of the resultant of the normal forces is determined by angle β_x (Fig. 147*d*) in which case

$$\tan \beta_x = \mu \left(1 - \frac{R}{\overline{OO_1}} \frac{4 \sin \beta_1}{2\beta_1 + \sin \beta_1}\right).$$

In this way the direction of the resultant is determined not only by the design of the brake but also by the coefficient of friction.

The resultant of the normal and tangential forces is inclined to the resultant of the normal forces by the angle of friction ϱ in the direction of wheel rotation ($\tan \varrho=\mu$) and passes through the axis of the shoe.

The point of application of the resultant of the normal and tangential forces is beyond the brake wheel at a distance L_x from the centre and

$$L_x = \overline{OO_1}\left(\cos\beta_x - \frac{1}{f} \sin \beta_x\right).$$

Angle β_x is always positive, i.e., it is constructed to the side where the shoe runs onto the wheel or, which is the same, counter to wheel rotation.

The theory of shoe brakes which accounts for nonuniformity in the distribution of unit pressures on the shoes more comprehensively reveals the phenomena attending the braking process.

Below are given some examples of shoe brake design.

Example 1. Design a brake applied by a weight and having a long-stroke magnet (see Fig. 142).
Calculations are done for M_{br} = 1,200 kg-cm.
We take a brake with a 250-mm wheel.
The total peripheral braking effort is

$$T = \frac{2M_{br}}{D} = \frac{2 \times 1{,}200}{25} = 96 \text{ kg}.$$

We specify the arms ratio as $\frac{l}{l_1} = \frac{27}{14}$; arm b = 3 cm.

The condition for brake application is

$$P_1 = \frac{M_{br}}{\mu D \eta} \frac{l_1^2 - \mu^2 b^2}{l l_1} = \frac{1{,}200}{0.4 \times 25 \times 0.95} \frac{14^2 - 0.4^2 \times 3^2}{14 \times 27} \approx 65 \text{ kg}.$$

The normal maximum pressure is

$$N_1 = \frac{P_1 l}{l_1 - \mu b} = \frac{65 \times 27}{14 - 0.4 \times 3} = 138 \text{ kg}.$$

The normal minimum pressure is

$$N_2 = \frac{P_1 l}{l_1 + \mu b} = \frac{65 \times 27}{14 + 0.4 \times 3} = 115 \text{ kg}.$$

The area of the lining for B = 75 mm and β = 90° is

$$F = \frac{\pi D}{360} B\beta = \frac{\pi 25}{360} 7.5 \times 90 = 147 \text{ sq cm}.$$

The unit pressure is

$$p = \frac{N_1}{F} = \frac{138}{147} = 0.97 \text{ kg/cm}^2 < p_{safe}.$$

The bending force is

$$\Delta S = \frac{2M_{br}}{Dl_1}\sqrt{1+\mu^2 b} = \frac{2\times 1{,}200}{25\times 14}\sqrt{1+0.4^2\times 3} = 22 \text{ kg.}$$

The vertical component is

$$\Delta S_v = \frac{2M_{br}\mu b}{Dl_1} = \frac{2\times 1{,}200\times 0.4\times 3}{25\times 14} = 8.3 \text{ kg.}$$

The horizontal component is

$$\Delta S_h = \frac{2M_{br}b}{Dl_1} = \frac{2\times 1{,}200\times 3}{25\times 14} = 20.5 \text{ kg.}$$

Let us now determine the required size of the type KMT long-stroke a-c braking electromagnet

$$P_m h k_1 = N\varepsilon\frac{1}{\eta};$$

$$P_m h = N\varepsilon\frac{1}{k_1\eta} = 138\times 0.1\,\frac{1}{0.8\times 0.9} = 19.2 \text{ kg-cm.}$$

The adjusting clearance is taken as $\varepsilon = 1$ mm. We take a type KMT-101 braking magnet in which the pull is 10 kg, maximum stroke 40 mm and the armature weight 2.8 kg.

In the process of designing and after determining the approximate location of the applying weight and magnet as dictated by the design we find the approximate magnitude of the weight which should be subsequently specified more accurately since the arms and weight of the lever may be changed.

$$G_{wt} = \frac{P_1\frac{al}{\eta k} - [G_l f + G_w c]\,\eta}{d}.$$

For our design we take in cm: $l = 4$, $a = 16$, $k = 13$, $f = 23$, $c = 40$ and $d = 40$.

With regard for the vertical rod the lever weight is $G_l = 3$ kg. The required magnitude of the applying weight will be

$$G_{wt} = \frac{65\frac{4\times 16}{13\times 0.95} - (3\times 23+2.8\times 40)\,0.95}{40} = 4.1 \text{ kg.}$$

Then we check whether the magnet armature stroke corresponds to the departure of the shoes. The maximum departure of the shoe is

$$\varepsilon_{max} = \frac{h_m l_1 l a}{2lkc} = \frac{40\times 14\times 4\times 16}{2\times 27\times 13\times 40} = 1.28 \text{ mm.}$$

With a departure of $\varepsilon = 1$ mm the magnet stroke will be

$$h'_m = \frac{2\varepsilon lkc}{l_1 l a} = \frac{2\times 0.1\times 27\times 13\times 40}{14\times 4\times 16} = 3.13 \text{ cm.}$$

In this way when the brake is set up for the first time we use 78 per cent of its stroke the rest being reserved to compensate for the wear of the linings, lost motion and elastic deformations of the lever system.

We then check the magnet as to its pull:

$$P_m c \geqslant G_l f + G_{wt} d + G_w c,$$

i.e., $10\times 40 > 2.5\times 23+4.2\times 40+2.8\times 40$ and $400 > 388$.

Hence, the magnet is also suitable as concerns the pull it develops.

Example 2. Design a spring-applied brake with a type MO-Б electric magnet (Fig. 143). The braking torque developed by a type TK-300 brake is $M_{br} = 5{,}000$ kg-cm.

The aim of these calculations is to check the brake.

The resultant application force of both springs is

$$P_1 = \frac{M_{br}}{\mu D\eta}\frac{l_1}{l} = \frac{5{,}000}{0.4\times 30\times 0.95}\,\frac{19}{43} = 194 \text{ kg.}$$

Type TK brakes employ rolled friction linings with a coefficient of friction of 0.4. The tension of the auxiliary spring is taken as 6 kg. The brake is provided with a type MO-300Б electromagnet which at a DF = 40 per cent develops a torque equal to 1,000 kg-cm. The

moment due to the armature weight is 22 kg-cm. The arm of the magnet action on the brake rod is $j = 46$ mm. The tension of the main spring required to overcome the moment due to the armature weight in releasing is

$$P_2 = \frac{92}{4.6} = 20 \text{ kg}.$$

The tension of the main spring with account taken of the action of the auxiliary spring and the weight of the magnet armature is

$$P_{main} = P_1 + P_{aux} + P_2 = 194 + 6 + 20 = 220 \text{ kg}.$$

The effort on the rod developed by the electromagnet is

$$P_m = \frac{M_m}{j} = \frac{1{,}000}{4.6} = 217 > 194 \text{ kg}.$$

Hence, the magnet will operate normally utilising practically all of the available moment. The stroke of the electromagnet armature is $L = 5.5$ mm which corresponds to a stroke of the brake rod $h = 4.4$ mm.

The maximum departure of the shoe from the wheel is

$$\varepsilon = h\frac{l_1}{2l} = 4.4\,\frac{19}{2 \times 43} = 0.975 \text{ mm}.$$

The initial clearance should equal half the maximum clearance, i. e., $\varepsilon_1 = 0.5$ mm.

The normal pressure exerted by the shoe on the wheel is

$$N = \frac{M_{br}}{\mu D} = \frac{5{,}000}{0.4 \times 30} = 417 \text{ kg}.$$

The area of the friction lining is

$$F = \frac{\pi D}{360} B\beta = \frac{\pi 30}{360}\, 14 \times 70 = 255 \text{ sq cm}.$$

The unit pressure is

$$p = \frac{N}{F} = \frac{417}{255} = 1.64 \text{ kg/cm}^2$$

which is considerably less than the safe pressure (such a small value of unit pressure is taken to ensure long life of the friction lining).

Brake levers for type TK brakes are die-forged from steel 5 and are of a double-T section. The moment of bending resistance of the type TK-300 brake lever is $W = 24.1$ cu cm.

The bending moment in the critical cross-section is

$$M'_{bend} = 194 \times 21 = 4{,}070 \text{ kg-cm}.$$

The bending moment with regard to dynamic phenomena is

$$M_{bend} = M'_{bend}\, d = 3.5 \times 4{,}070 = 14{,}250 \text{ kg-cm}.$$

Here d—dynamic factor assumed as 3.5 in type TK brakes

$$\sigma = \frac{M_{bend}}{W} = \frac{14{,}250}{24.1} = 590 \text{ kg/cm}^2.$$

The moment of the cross-section inertia is

$$I = Wh_s = 24.1 \times 3.2 = 77 \text{ cm}^4.$$

The braking lever is a beam loaded on the cantilever portion by the tension of the spring and bearing in its middle part against the shoe pivot. The deflection of the cantilever can then be found from the formula

$$y = \frac{P_1 l_1}{EI}\left(\frac{al}{4} + \frac{a^2}{3}\right) = \frac{194 \times 19}{2.1 \times 10^6 \times 77}\left(\frac{19 \times 24}{4} + \frac{19^2}{3}\right) = \frac{0.535}{100} = 0.00535 \text{ mm}$$

where a and l are the lever arms.

Example 3. Design a combined controlled brake.

The brake is of the TKT-300Y type. The braking torque is $M_{br} = 50$ kg-m. A diagram of the brake is shown in Fig. 146.

The type MO-300B electric magnet develops a torque of 400 kg-cm at a DF = 100 per cent. On the basis of this moment we select the tension of the springs and determine the braking torque developed by the brake when the current is switched off.

To force the fluid as quickly as possible from the hydraulic cylinder back into the master cylinder when the brake is released the tension of the auxiliary spring is taken somewhat larger than for ordinary holding brakes.

For a type TKT-300Y brake the tension of the auxiliary spring P_{aux} is 12 kg.

The force exerted by the magnet on the brake rod when the magnet is energised is

$$P_m = \frac{M_m}{j} = \frac{400}{4.6} = 87 \text{ kg}.$$

The effort on the rod due to the armature weight is

$$P_{ar} = \frac{M_{ar}}{j} = \frac{92}{4.6} = 20 \text{ kg}.$$

The force of the main spring is

$$P_{main} = P_m + P_{aux} + P_{ar} = 87+12+20 \sim 120 \text{ kg}.$$

The torque developed by the brake upon switching off is

$$M_{br} = \frac{P_m l}{l_1} \mu D = \frac{87 \times 43}{19} 0.4 \times 30 = 2{,}350 \text{ kg-cm}.$$

The master braking cylinder from a type GAZ-51 auto truck has a diameter $D_{mas} = 32$ mm, and a piston area $F_{mas} = 8$ sq cm.

In the hydraulic cylinder $D_{hyd} = 70$ mm and $F_{hyd} = 38.5$ sq cm.

In travelling cranes the compensating tank is mounted at the height of the hydraulic cylinder and there will be therefore no pressure drop.

The brake control pedal is counterbalanced by a special spring and the weight of the pedal has no effect on the fluid pressure.

According to formula (103), the effort applied to the pedal is

$$P_{ped} = \left(\frac{M_{br} l_1}{\mu D l} + P_{aux}\right) \frac{a}{b} \frac{n}{m} \left(\frac{D_{mas}}{D_{hyd}}\right)^2 \frac{1}{\eta_0}.$$

The total efficiency is $\eta_0 = 0.7$ and then

$$P_{ped} = \left(\frac{5{,}000 \times 19}{0.4 \times 30 \times 43} + 12\right) \frac{24}{17} \frac{6}{27} \left(\frac{3.2}{7}\right)^2 \frac{1}{0.7} = 17 \text{ kg}$$

which is normal for this type of control mechanisms.

The designed maximum stroke of the pedal is 200 mm

$$\varepsilon = \frac{P_{ped} h \mu D \eta_0}{2 M_{br}} = \frac{17 \times 20.0 \times 0.4 \times 30 \times 0.7}{2 \times 5{,}000} = 0.28 \text{ cm}.$$

In this case the designed departure of the shoes $\varepsilon = 1$ mm is obtained when the stroke of the pedal is much shorter.

The total transmission ratio of the control system is

$$i_t = \frac{l}{l_1} \frac{b}{a} \left(\frac{D_{hyd}}{D_{mas}}\right)^2 \frac{m}{n} = \frac{43}{19} \times \frac{17}{14} \left(\frac{7}{3.2}\right)^2 \frac{29}{6} = 37.$$

The full stroke of the master cylinder for a pedal stroke of $h = 200$ mm is

$$H_{mas} = h \frac{n}{m} = 200 \frac{6}{29} = 41.5 \text{ mm}.$$

The stroke of the hydraulic cylinder for full stroke of the pedal is

$$H_{hyd} = h \frac{n}{m} \left(\frac{D_{mas}}{D_{hyd}}\right)^2 = 200 \frac{6}{29} \left(\frac{3.2}{7}\right)^2 = 8.7 \text{ mm}.$$

In emergency braking the effort on the pedal may become equal to the weight of the operator (80 kg); in this case the pressure in the system should not exceed 50-60 kg/cm²:

$$p = P_{ped} \frac{m}{n} \frac{4}{\pi D^2_{mas}} = 80 \frac{29}{6} \frac{4}{\pi 3.2^2} = 50.4 \text{ kg/cm}^2.$$

The velocity of the fluid flow in the tubing should not exceed 1-1.2 m/sec.

The volume of the fluid passing through the tubing for releasing the brake on the working stroke of the pedal is

$$V = \frac{H_{mas}}{2} \frac{\pi D^2_{mas}}{2} = \frac{4.15}{2} \frac{\pi 3.2^2}{4} = 16.5 \text{ cu cm}.$$

The velocity of fluid flow when the time of the brake release is $t = 0.6$ sec is

$$v = \frac{V}{tF_t} = \frac{16.5}{0.6 \times 0.27 \times 100} = 1.02 \text{ m/sec}$$

where F_t is the cross-sectional area of the tubing; with an inner diameter of $d_t = 6$ mm, $F_t = 0.27$ sq cm.

Example 4. Design a lowering brake for a crane (for unit loads) with a lifting capacity of 3 tons and a lifting height of 27 m.

The size of the brake wheel should be assigned in conformity with the permissible heating under the following unfavourable conditions:

Mean weight of the load being lowered equals 2/3 of the full load—$G_1 = 2{,}000$ kg;
Mean height of lowering, equal to raising, is 3/4 of the full height of raising—$h = 20$ m;
Number of switching-in operations per hour—$z = 40$;
Switch-in period for the hoisting mechanism—DF = 40 per cent;
Efficiency of the hoisting mechanism—$\eta = 0.85$;
Lowering speed equals the lifting speed—$v = 66$ m/min;

Power of the hoisting mechanism motor—$N = \frac{3{,}000 \times 66}{4{,}500 \times 0.85} = 52$ hp;

Motor rpm—$n = 570$ rpm.

From Table 27 we select a brake wheel with the following dimensions: diameter—600 mm and width—200 mm.

Checking for the heating of the brake.

1. The amount of heat liberated during one hour is found from equation (43).

$Q_{tot} = G_1 hz\eta A = 2{,}000 \times 20 \times 40 \times 0.85 \frac{1}{427} = 3{,}180$ kcal/hr or from equation (114)

$Q_{tot} = 316N\eta^2 \text{DF}X = 316 \times 52 \times 0.85^2 \times 0.40 \times 0.67 = 3{,}170$ kcal/hr.

2. The amount of heat dissipated by the wheel at the accepted maximum temperature of the wheel $t_1 = 135°$C and a temperature in the premises $t_2 = 35°$C:

(a) By radiation

$$Q_1 = [c_1 S_1 + c_2 S_2] \left[\left(\frac{273+t_1}{100}\right)^4 - \left(\frac{273+t_2}{100}\right)^4\right].$$

With an angle of contact $\alpha = 70°$ (for two shoes $2 \times 70° = 140°$), the surface of the wheel rim not embraced by the linings equals

$$S_1 = 0.63\,\pi\,0.20\,\frac{360-140}{360} = 0.242 \text{ sq m}$$

and

$$S_2 = 2 \times 0.63^2 \frac{\pi}{4} = 0.625 \text{ sq m}.$$

$$Q_1 = [1.3 \times 0.242 + 4.3 \times 0.625] \left[\left(\frac{273+135}{100}\right)^4 - \left(\frac{273+35}{100}\right)^4\right]; \; Q_1 \approx 570 \text{ kcal/hr}.$$

(b) By heat transfer at rest according to equation (109)

$$Q_2 = \alpha_1 S_3 (t_1 - t_2)(1 - \text{DF});$$

$$S_3 = S_1 + S_2 + 0.6\,\pi \times 0.16 = 0.242 + 0.625 + 0.3 = 1.167 \text{ sq m};$$

$$Q_2 = 5 \times 1.167\,(135-35)\,(1-0.4) = 350 \text{ kcal/hr}.$$

(c) By heat transfer in motion (by convection) from equation (111)

$$Q_3 = \text{DF}\,(t_1 - t_2)\,6.14 \left[S_4 \left(\frac{\pi Dn}{60}\right)^{0.78} + 2S_1 v_1^{0.78} + 2S_2 v_2^{0.78} + \ldots + 2S_n v_n^{0.78}\right]$$

where S_4—whole surface of the rim;

S_1, S_2, S_n —surfaces of the circular areas;

v_1, v_2, v_n —respective mean peripheral speeds of these areas.

For the sake of simplicity we can divide the side surface of the wheel into two areas S_1 and S_2.

$$S_4 = \pi\,(0.63 \times 0.2 + 0.6 \times 0.16) = 0.7 \text{ sq m};$$

$$S_1 = \frac{\pi}{4}\,(0.6^2 - 0.4^2) = 0.157 \text{ sq m};$$

$$S_2 = \frac{\pi}{4}\,0.4^2 = 0.125 \text{ sq m};$$

$$\frac{\pi Dn}{60} = \frac{\pi 0.63 \times 570}{60} = 18.8 \text{ m/sec};$$

$$v_1 = \frac{\pi 0.5 \times 570}{60} = 14.9 \text{ m/sec};$$

$$v_2 = \frac{\pi 0.2 \times 570}{60} = 6 \text{ m/sec}.$$

Whence:

$$Q_3 = 246\,(6.9+2.59+1.01) = 2{,}580 \text{ kcal/hr}.$$

The total amount of heat that can be dissipated during one hour is

$$Q_1+Q_2+Q_3 = 570+350+2{,}580 = 3{,}500 \text{ kcal/hr}.$$

This is even somewhat more than the amount of heat liberated in braking.

$Q_{wt} = 3{,}180$ kcal/hr, so that the maximum temperature of the sheave will be somewhat below 135°C.

Since for ferrodo lining the safe temperature is 200°C, the selected brake sheave will satisfy the operating requirements.

3. Checking the life of the brake linings.

The work of one braking operation is

$$A = \frac{2{,}000 \times 20 \times 0.85}{270{,}000} = 0.126 \text{ hp-hr}.$$

The wear of the lining is

$$\Delta G = 2lb\Delta h = 2 \times 19 \times 38.5 \times 0.6 = 880 \text{ cu cm}.$$

The service life or permissible number of braking operations is

$$y = \frac{\Delta G}{qA} = \frac{880}{0.2 \times 0.126} = 35{,}000.$$

The service life in hours for 40 braking operations per hour is

$$\frac{35{,}000}{40} = 875.$$

The service life in days for an eight-hour working day is

$$\frac{875}{8} = 109.$$

Example 5. Design a double-shoe holding brake for the hoisting mechanism of a 10-ton travelling crane with a lifting speed of 30 m/min.

The crane operates on heavy duty (150 braking operations per hour) with electric braking.

The efficiency of the hoisting mechanism is $\eta = 0.8$.

The motor power is $N = \frac{10{,}000 \times 30}{4{,}500 \times 0.8} = 83.5$ hp.

The motor speed is $n = 570$ rpm.

1. The brake wheel is selected from Table 29.

Under normal operating conditions a 500-mm diameter brake wheel corresponds to a 85-hp motor.

For heavy duty the motor power will be 20 per cent less, but with electric braking its power can be also reduced by 20 per cent.

Therefore, the selected brake wheel is of ample size.

2. Checking the pv value.

The torque on the motor shaft is

$$M = 71{,}620 \frac{83.5}{570} = 10{,}500 \text{ kg-cm}.$$

The coefficient of friction for ferrodo lining (Table 25) is $\mu = 0.45$.

The size of the linings is $b = 15$ cm and $l = 29$ cm.

Unit pressure is

$$p = \frac{M}{D\mu} \frac{1}{bl} = \frac{10{,}500}{50 \times 0.45} \frac{1}{15 \times 29} = 1.07 \text{ kg/cm}^2.$$

The peripheral speed is

$$v = \frac{\pi D \times 570}{60} = 14.9 \text{ m/sec},$$

then: $pv = 1.07 \times 14.9 = 16$ kg-m/cm^2-sec, i. e., permissible.

3. Checking the life of the brake lining (disregarding electric braking).

The work of one braking operation is

$$A = M_{br}\frac{\pi n}{30}t_{br}\frac{1}{2}.$$

The time of braking is different in raising and lowering.
In raising

$$t'_{br} = \frac{\Sigma I\omega}{M_{br} + M_{wt}};\ \Sigma I = 1.4\ \text{kg-m/sec}^2$$

where M_{wt}—moment due to the weight equal to 67 kg-m.
Then

$$\omega = \frac{\pi n}{30};$$

$$M_{br} = \nu M\mu^1 = 2.5 \times 10{,}500 \times 0.64 = 168\ \text{kg-m};$$

$$t'_{br} = \frac{1.4\frac{\pi 570}{30}}{168+67} = 0.355\ \text{sec}.$$

In lowering

$$t''_{br} = \frac{\Sigma I\omega}{M_{br}-M_{wt}} = \frac{1.4\times 59.5}{101} = 0.82\ \text{sec}.$$

The mean value is

$$t_{br} = \frac{t'_{br} + t''_{br}}{2} = \frac{0.355 + 0.82}{2} = 0.59\ \text{sec}.$$

The work of braking is

$$A = 168\times 59.5\times 0.59\times 0.5 = 2{,}980\ \text{kg-m};$$

$$A = \frac{2{,}980}{270{,}000} = 0.011\ \text{hp-hr}.$$

The permissible wear of the lining in volume is

$$\Delta G = 2bl\Delta h = 2\times 15\times 29\times 0.5 = 435\ \text{cu cm}.$$

The service life or permissible number of braking operations is

$$y = \frac{\Delta G}{qA} = \frac{435}{0.2\times 0.011} = 198{,}000.$$

The life in hours for 150 braking operations per hour is

$$\frac{198{,}000}{150} = 1{,}320.$$

The life in days for an eight-hour working day is

$$\frac{1{,}320}{8} = 165.$$

4. Checking for heating (disregarding electric braking).
The amount of heat liberated in one braking operation is

$$\frac{2{,}980}{427} = 7\ \text{kcal}.$$

The total amount of heat liberated per hour for 150 braking operations is 1,050 kcal/hr.
The amount of heat that can be dissipated per hour at 100°C (from Table 27) is 1,055 kcal/hr.
In this way, even disregarding electric braking, the brake wheel will not be heated to more than 100°C.
5. Selection of the braking magnet.
The force required is

$$P = \frac{M_{br}}{D\mu} = \frac{16{,}800}{50\times 0.45} = 745\ \text{kg}.$$

The departure of the shoes is assumed to equal $\delta = 0.20$ cm.
The work performed by the magnet is

$$A' = 2.2\frac{\nu M\eta^2}{D\mu}\delta = 330\ \text{kg-cm}.$$

With regard for wear the work performed by the magnet should be 25 per cent greater than required which will amount to

$$330 \times 1.25 \approx 420 \text{ kg-cm.}$$

The selected magnet has a stroke $h = 5$ cm and its armature weighs $G_{ar} = 22$ kg. The pull is

$$\frac{420}{5} = 84 \text{ kg.}$$

6. Calculation of the transmission ratio of the brake levers.

With a magnet stroke of $0.8 \times 5 = 4$ cm the brake shoes should depart to a distance of $2e = 0.2 \times 2 = 0.4$ cm.

In this case the total transmission ratio of the lever system should amount to

$$i = \frac{g}{f} = \frac{l}{c}\frac{a}{b} = \frac{4}{0.4 \times 1.1} = 9.1$$

(coefficient 1.1 takes into account the lost motion of the levers).

The following dimensions can be assigned for the given brake: $a = 515$ mm; $b = 270$ mm; $c = 60$ mm; $l = 205$ mm and $f = 260$ mm. Hence, the length of the lever q to the point of linkage with the magnet armature is

$$g = 9.1 \frac{270}{515} \times \frac{60}{205} \times 260 = 363 \text{ mm.}$$

7. Selection of the spring. The force P is created by the tension of the spring as well as by the weight of the magnet armature and the brake levers.

$$P = K\frac{a}{b} + V\frac{l}{c}\frac{a}{b}.$$

The weight of the armature and the levers as referred to rod V will be

$$V = (G_{ar} + G_l)\frac{g}{f} = (22+3)\frac{363}{260} = 35 \text{ kg.}$$

Hence

$$K = P\frac{b}{a} - V\frac{l}{c};$$

$$K = 745\frac{270}{515} - 35\frac{205}{60} = 271 \text{ kg.}$$

We select a spring with a wire diameter of $\delta = 12$ mm, with a mean radius of $r = 3.6$ cm and a number of active coils $n = 12$.

The elongation of the spring, pretensioned with a force of 271 kg, will be

$$f = \frac{64nr^3}{\delta^4}\frac{K}{G} = \frac{64 \times 12 \times 3.6^3}{1.24}\frac{271}{850{,}000} = 5.5 \text{ cm.}$$

Additional elongation of the spring in releasing the brake is

$$f_1 = 2e\frac{a}{b} = 2 \times 0.2\frac{515}{270} = 0.8 \text{ cm.}$$

Thus, the total elongation of the spring will be 6.3 cm and the maximum force extending the spring $271\frac{6.3}{5.5} = 310$ kg.

At $[\tau] = 4{,}000$ kg/cm^2, the lifting capacity of the spring is

$$K_{max} = \frac{\pi\delta^3}{16r}4{,}000 = \frac{\pi 1.2^3}{16 \times 3.6}4{,}000 = 377 \text{ kg.}$$

Therefore, the spring dimensions have been assigned correctly.

10. BAND BRAKES

General Theory of Band Brakes. Band brakes are designed as simple, differential and additive-action types. The brake consists of a drum about which is wrapped a flexible steel band usually lined with some friction material (ferrodo, etc.). The resistance of friction due to all the friction forces acting on the surface of contact with the drum is equal to the difference in the forces S_{on} and S_{off} on the band ends. Since this must equalise the peripheral force P

$$P = S_{on} - S_{off}.$$

The relationship between the forces on the band ends is expressed by the well-known Euler's equation

$$S_{on} = S_{off} e^{\mu\alpha} \tag{124}$$

whence

$$S_{on} = \frac{P e^{\mu\alpha}}{e^{\mu\alpha} - 1}; \tag{125}$$

$$S_{off} = \frac{P}{e^{\mu\alpha} - 1} \tag{126}$$

where S_{on}—tension of the oncoming end of the band;
S_{off}—tension of the running-off end of the band;
e—base of Napierian (natural) logarithms;
μ—coefficient of friction;
α—angle of the drum subtended by the band in radians;
P—peripheral force on brake drum rim.

For ordinary brakes the arc of contact α is taken from 180° to 270°. The coefficient of friction μ is selected from Table 30 which lists values of $e^{\mu\alpha}$.

Table 30

Values of $e^{\mu\alpha}$

$\frac{\alpha_{rad}}{2\pi} = \frac{\alpha^\circ}{360^\circ}$	μ						
	0.2	0.25	0.3	0.35	0.4	0.45	0.5
0.1	1.13	1.17	1.21	1.25	1.29	1.33	1.37
0.2	1.29	1.37	1.46	1.56	1.65	1.76	1.87
0.3	1.45	1.6	1.76	1.93	2.13	2.34	2.57
0.4	1.65	1.87	2.18	2.41	2.73	3.1	3.51
0.425	1.7	1.95	2.23	2.55	2.91	3.33	3.8
0.45	1.76	2.03	2.34	2.69	3.1	3.57	4.11
0.475	1.82	2.11	2.45	2.84	3.3	3.83	4.45
0.5	1.87	2.19	2.57	3.00	3.51	4.11	4.81
0.525	1.93	2.28	2.69	3.17	3.74	4.41	5.2
0.55	2.0	2.37	2.82	3.35	3.98	4.74	5.63
0.6	2.13	2.57	3.1	3.74	4.52	5.45	6.59
0.7	2.41	3.0	3.74	4.66	5.81	7.24	9.02
0.8	2.75	3.51	4.52	5.81	7.47	9.6	12.35
0.9	3.1	4.11	5.45	7.24	9.6	12.74	16.9
1.0	3.51	4.81	6.59	9.02	12.35	16.9	23.14

To find the relation between the tensions S_{on} and S_{off} let us consider an elementary arc (Fig. 148*a*) subtended by the angle $d\varphi$ where φ is the angle corresponding to the distance over the arc from the point being considered to the point where the band leaves the drum.

Due to the tangential friction forces the tension of the strap over the sections of the elementary arc will be $S + dS$ and S.

The projection of forces on the direction dN is

$$(S + dS) \sin \frac{d\varphi}{2} + S \sin \frac{d\varphi}{2} - dN = 0.$$

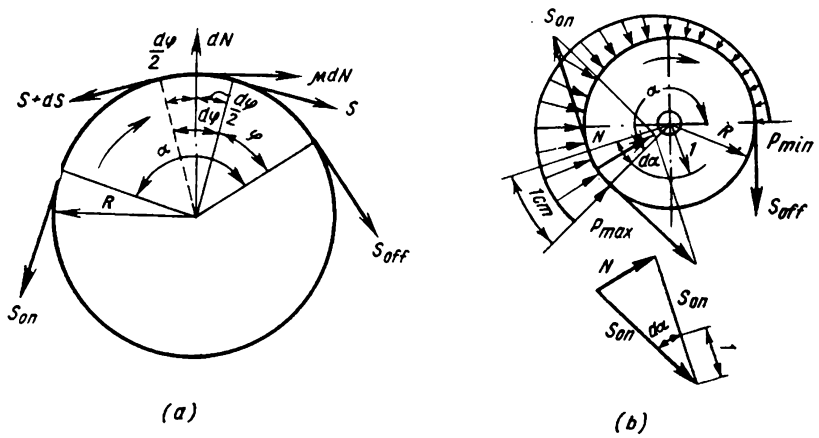

Fig. 148. Diagrams for determining tension in the band and unit pressures on the drum

The projection of forces on the tangent is

$$(S + dS)\cos\frac{d\varphi}{2} - S\cos\frac{d\varphi}{2} - \mu dN = 0.$$

We assume that

$$\sin\frac{d\varphi}{2} \approx \frac{d\varphi}{2} \quad \text{and} \quad \cos\frac{d\varphi}{2} \approx 1.$$

Neglecting the higher-order infinitesimal ($dSd\varphi$) we obtain

$$Sd\varphi = dN; \quad dS = \mu dN$$

whence the ratio

$$\frac{dS}{Sd\varphi} = \mu$$

or

$$\frac{dS}{S} = \mu d\varphi.$$

Integrating this equation we obtain

$$\int\frac{dS}{S} = \int \mu d\varphi \text{ or } \ln S = \mu\varphi + C.$$

For $\varphi=0$ when $S=S_{off}$, $\ln S_{off}=C$ or, finally,

$$\ln S = \mu\varphi + \ln S_{off}; \ \ln S - \ln S_{off} = \mu\varphi; \ \ln\left(\frac{S}{S_{off}}\right) = \mu\varphi.$$

whence $\frac{S}{S_{off}} = e^{\mu\varphi}$ or $S = S_{off}e^{\mu\varphi}$.

For the oncoming end $S_{on} = S_{off}\, e^{\mu\varphi}$, i.e., the relation (124) where φ is the arc of contact in radians; e—base of Napierian logarithms, equal to 2.718 . . . .

The maximum unit pressure between the band and the brake drum arises at the point of application of the tension S_{on} of the band (Fig. 148*b*); decreasing gradually it reaches its minimum value at the point of application of tension S_{off}. If we assume that $S_{on} + dS_{on} \approx S_{on}$ then the normal pressure N at the point of application of tension S_{on} and $S_{on} + dS_{on}$ (per unit surface 1 cm long and b cm

wide) can be approximately found from the following equations (Fig. 148*b*):

$$\frac{d\alpha}{1} = \frac{1}{R} \text{ and } \frac{d\alpha}{N} = \frac{1}{S_{on}}$$

whence

$$N = S_{on}\, d\alpha = S_{on} \frac{1}{R} . \tag{127}$$

Consequently, the maximum unit pressure is

$$p_{max} = \frac{S_{on}}{Rb} \tag{128}$$

and the minimum pressure is

$$p_{min} = \frac{S_{off}}{Rb} . \tag{129}$$

If the length of contact between the band and drum is

$$l = 2\pi R \frac{\alpha^\circ}{360^\circ}$$

then the rubbing surface is

$$F = b\pi 2R \frac{\alpha^\circ}{360^\circ} .$$

If $p = \frac{p_{max} + p_{min}}{2}$ kg/cm² denotes the mean unit pressure, then the braking power will be

$$N_{br} = Fpv_{cr}\mu$$

where v_{cr}—critical slipping speed;
μ—coefficient of friction, whence the *unit* braking power will be

$$N_{un} = pv_{cr} = \frac{N_{br}}{F\mu} . \tag{130}$$

The value of pv_{cr} may be taken the same as for shoe brakes. To avoid excessive wear of the band or lining at the oncoming end, the maximum unit pressure p_{max} should not exceed the values indicated in Table 31.

Table 31

Safe Unit Pressures p_{safe} in Band Brakes in kg/cm²

Type of brake	Material of the rubbing surfaces			
	Steel band on cast-iron or steel drum	Asbestos brake band on steel or cast-iron drum	Rolled, press-formed and shaped friction material on metal drum	Wood on cast-iron drum
Holding	15	6	8	6
Lowering	10	3	4	4

Simple Band Brakes

In a simple band brake (Fig. 149) the oncoming end of the band is fixed (maximum tension S_{on}) and the brake lever experiences only force S_{off} which creates the moment $S_{off}a$. From what has been said above [formula (126)]

$$S_{off} = \frac{P}{e^{\mu\alpha} - 1} ;$$

where a—length of arm from the fixed pivot to the point where the band is fastened to the lever (running-off end).

The peripheral force is $P = \frac{2M_{br}}{D}$ where M_{br} is the actual braking torque.

As in shoe brakes, the magnitude of the weight on the braking lever (Fig. 149) is

$$G = \frac{S_{off}a - G_{ar}l}{l_1}. \quad (131)$$

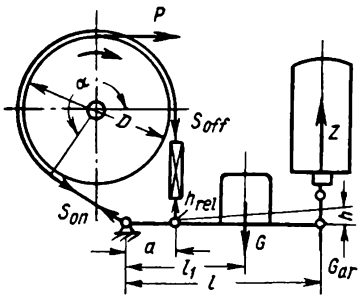

Fig. 149. Diagram of a simple band brake

When the brake drum rotates in the opposite direction the tension forces S_{on} and S_{off} change places and the weight G required for braking increases. This circumstance makes the application of a simple band brake unsuitable for slewing and travelling mechanisms (two-way braking).

The transmission ratio of the lever $i = \frac{l}{a}$ is usually assumed within 3 to 6 (sometimes the lower limit reaches 10). The band tension S_{off} should be applied, as far as possible, at an angle of 90° to the pivot of the brake lever. If this cannot be achieved the end of the straight lever should be bent.

A double-shoe design relieves the shaft of large bending forces. In band brakes the shaft is subject to additional force from band tension which can be determined by the following formulas:

resultant force on the shaft

$$Q = \sqrt{V^2 + H^2} \quad (132)$$

where V—vertical force and H—horizontal force;

$$V = S_{on_y} + S_{off_y}; \quad (133)$$

$$H = S_{on_x} \pm S_{off_x}. \quad (134)$$

Here S_{on_y}, S_{on_x}, S_{off_y} and S_{off_x} are vertical and horizontal components of the tensions S_{on} and S_{off}, respectively (the plus sign when the tensions S_{on_x} and S_{off_y} act in the same direction and the minus sign when they act in opposite directions).

Distance of release. The radial departure of the band from the drum is usually within 0.8-1.5 mm. The distance of release at the running-off end linkage is

$$h_{rel} = [2(R + \varepsilon)\pi - 2\pi R]\frac{\alpha}{2\pi} = \varepsilon\alpha. \quad (135)$$

Brake lever travel at the linkage with the electromagnet armature is

$$h = \varepsilon\alpha\frac{l}{a} \quad (136)$$

where α is in radians.

The required pull of the magnet is

$$Z = S_{off}\frac{a}{l}. \quad (137)$$

The efficiency of the lever system in band brakes may be neglected since they have only two hinged joints.

The work performed by the electromagnet will be

$$A = \frac{1}{0.75}Zh.$$

The coefficient 0.75 accounts for the utilisation of the armature stroke.

In most cases hand-operated winches may be provided with an unlined steel band coated slightly with grease. The effort G applied by the operator to the brake handle should not exceed 10-20 kg. In hand-operated winches a band brake is designed not only to hold the load at rest but also to control the lowering speed.

Multi-wrap Band Brakes

An arc of contact of $\alpha=270°$ in a simple band brake is insufficient for large torques. In such cases use is made of multi-wrap band brakes which allow a much larger angle, up to 650°. The band has the form of a fork (Fig. 150*a*).

The large angle of wrap is obtained by passing one end of the strap through the forked space of the other end. The forked end is usually the oncoming end because its cross-section is increased to obtain greater strength.

A multi-wrap brake is designed along the same lines as a simple band brake. The magnitude of the braking weight in this design is insignificant even for large braking torques. The distance of release is calculated from equations (135) and (136) and is 2 or 3 times longer than in a simple brake.

Fig. 150*b* shows a multi-wrap band brake employed in electric hoists manufactured by the Lenin Works. It has an angle of wrap of 630°. A cast-iron lever is cast integral with the weight.

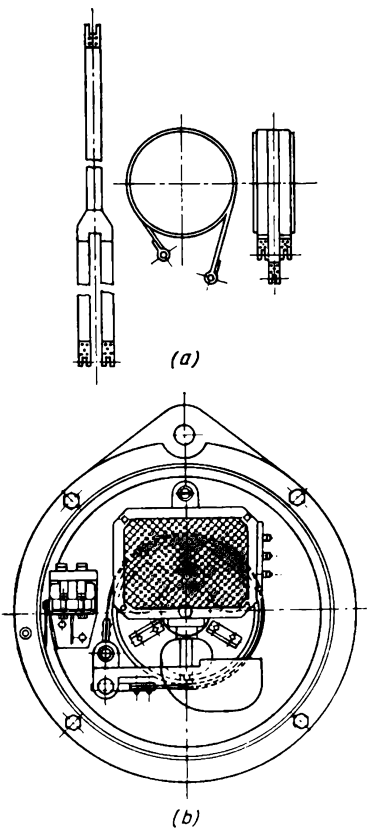

Fig. 150. Multi-wrap band brake

Differential Band Brakes. In these brakes (Fig. 151*a*) both ends of the band are attached to the braking lever. They are called differential because their braking torque is determined by the difference in the moments caused by the tension of the band ends relative to the pivot axis of the braking lever.

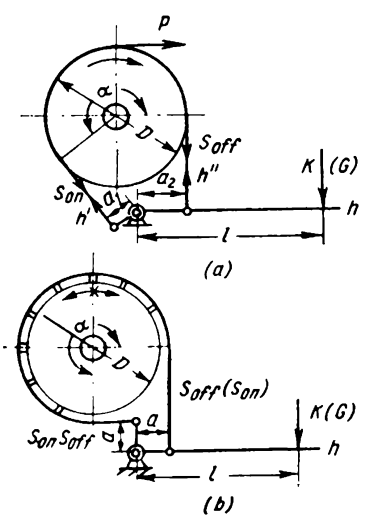

Fig. 151. Diagrams of differential and additive-action band brakes

The equation of moments relative to the pivot axis of the lever will be

$$Kl - S_{off}a_2 + S_{on}a_1 = 0$$

whence the braking effort is

$$K = \frac{S_{off}a_2 - S_{on}a_1}{l}. \qquad (138)$$

Replacing the tensions S_{on} and S_{off} by the peripheral force P we obtain

$$K = \frac{P}{l}\,\frac{a_2 - a_1 e^{\mu\alpha}}{e^{\mu\alpha} - 1} \qquad (139)$$

When $a_2 < a_1 e^{\mu\alpha}$ the effort K will be a negative value and the brake will become an automatically operating arrester. When the rotation of the brake drum is reversed the tensions S_{on} and S_{off} will change places and the force K (or weight G) must be $e^{\mu\alpha}$ times larger.

Travel of the Brake Lever. If h' and h'' are the arms of the levers a_1 and a_2 the difference h_0 between them will equal the elongation of the band in releasing

$$h_0 = h'' - h' = \varepsilon\alpha. \tag{140}$$

From the ratio

$$\frac{h'}{a_1} = \frac{h''}{a_2} = \frac{h}{l}$$

we obtain

$$h' = a_1 \frac{h}{l} \text{ and } h'' = a_2 \frac{h}{l}.$$

Substituting these values in equation (140) we obtain the travel of the lever at the point of application of force K

$$h = h_0 \frac{l}{a_2 - a_1} = \varepsilon\alpha \frac{l}{a_2 - a_1} \tag{141}$$

where ε has the same value as in a simple brake.

Additive-Action Band Brakes. In this brake (Fig. 151*b*) both ends of the band are fastened to the brake lever on arms equal in size ($a_1 = a_2 = a$). The equation of moments for the pivot of the brake lever is

$$Kl - S_{on}a - S_{off}a = 0.$$

The force on the brake lever

$$K = \frac{a}{l}(S_{on} - S_{off}) \tag{142}$$

is the same for both directions of rotation since in a brake with equal arms the tensions S_{on} and S_{off} change places. In an additive-action brake the braking effort on the lever is $(e^{\mu\alpha} + 1)$ times larger than in a simple band brake. The brake drum is stopped in this type of brake by the tension of both ends of the band.

The travel of the brake lever at the point of application of force K is the same as above:

$$h = \frac{\varepsilon\alpha l}{2a}. \tag{143}$$

It has been pointed out above that an additional load on the brake shaft is the main shortcoming of all the examined types of band brakes. For this reason they are comparatively seldom used in hoisting machinery while a differential brake is a very rare feature of mechanisms with mechanical drives.

Construction of Band Brakes. To ensure a tight contact with the drum the width of the band b should not exceed 150 mm for drum diameters of $D > 1{,}000$ mm and 100 mm for $D < 1{,}000$ mm. For brakes of hand-operated winches use can be made of ordinary plain steel bands of the following sizes:

Width b, mm	25-30	40-60	80	100	140-200
Thickness s, mm	3	3-4	4-6	4-7	6-10

Power-driven mechanisms require steel bands with brake linings. Wooden shoes are made of hornbeam or poplar. They are attached to the band by two or four wood screws. A gap of 4-6 mm should be left between the shoes.

The brake lining* is fastened to the strap with countersunk copper rivets or screws (Fig. 152*a*).

* One method of fastening a rolled brake lining to a steel band is shown in Fig. 152*b*.

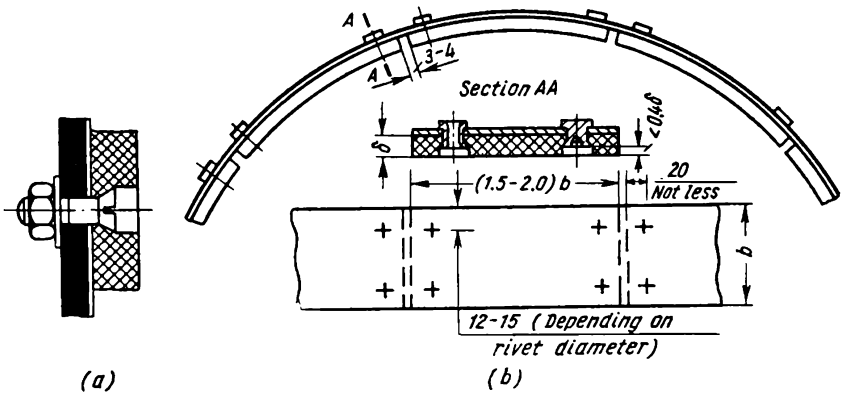

Fig. 152. Recommended sizes for fastening linings made of rolled friction material to a steel braking band
a—section at the point of fastening, *b*—method of fastening

Brake bands are checked for tensile rupture from the maximum tension S_o with due regard for the two rivet holes weakening the cross-section. The stress will be

$$\sigma = \frac{S_{on}}{(b - 2d)s}. \tag{144}$$

For steel 3 or 4 the safe stress ranges from 500 to 800 kg/cm²;
here b—width of the band;
s—thickness of the band;
d—diameter of the rivet.

As a rule, the oncoming end of the strap is fixed rigidly (Fig. 153*a*) and the running-off end is made adjustable (Fig. 153*b*). The diameter of the rivets may be taken from $d=8$ to $d=13$ mm; usually, the number of rivets is not below $n=4$. The rivets should be checked for shear and compression.

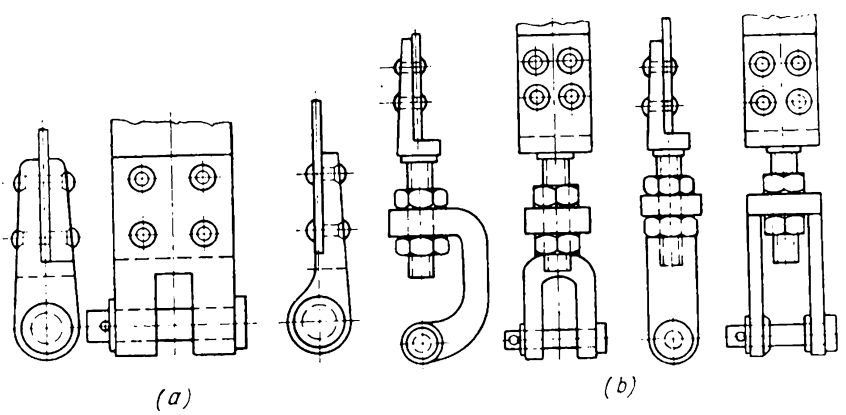

Fig. 153. Band fastening devices

The shearing stress is

$$\tau = \frac{S_{on}}{n_1 n \frac{\pi d^2}{4}} \tag{145}$$

where n_1—number of shearing planes.

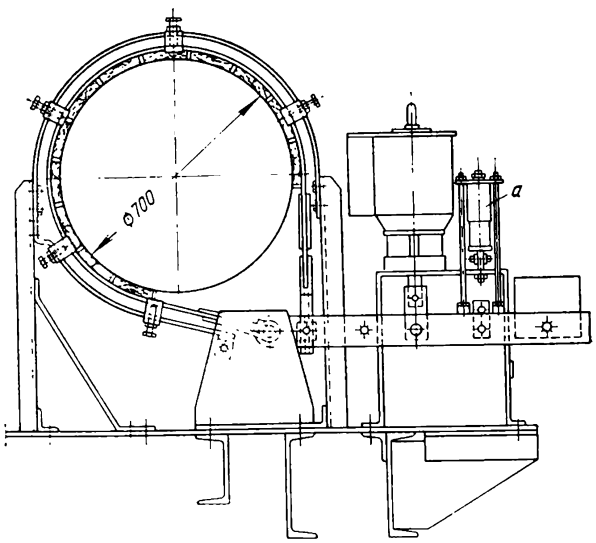

Fig. 154. Design of a simple band brake with a damping device (*a*)

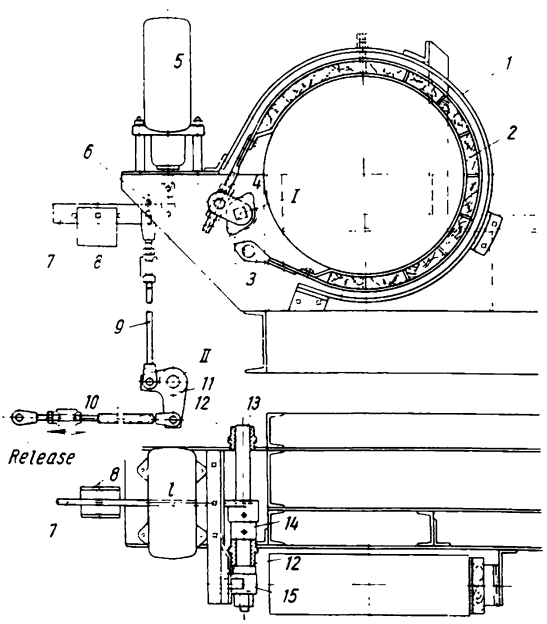

Fig. 155. Band brake of a rotary bucket crane

1—bar with adjusting screws, *2*—brake band with wooden shoes, *3*—fixed pivot, *4*—adjustable pivot, *5*—braking electromagnet, *6*—fork, *7*—brake lever secured on axle *13* with a pin, *8*—braking weight, *9*—pull-rod, *10*—pull-rod for hand release from the operator's cab, *11*—angle lever, *12*—flanged bearings of axle *13*, *13*—pivot axle of the brake lever, *14*—adjusting ring, *15*—fork for fastening the band

The compression stress is

$$\sigma_{com} = \frac{S_{on}}{nds}. \qquad (146)$$

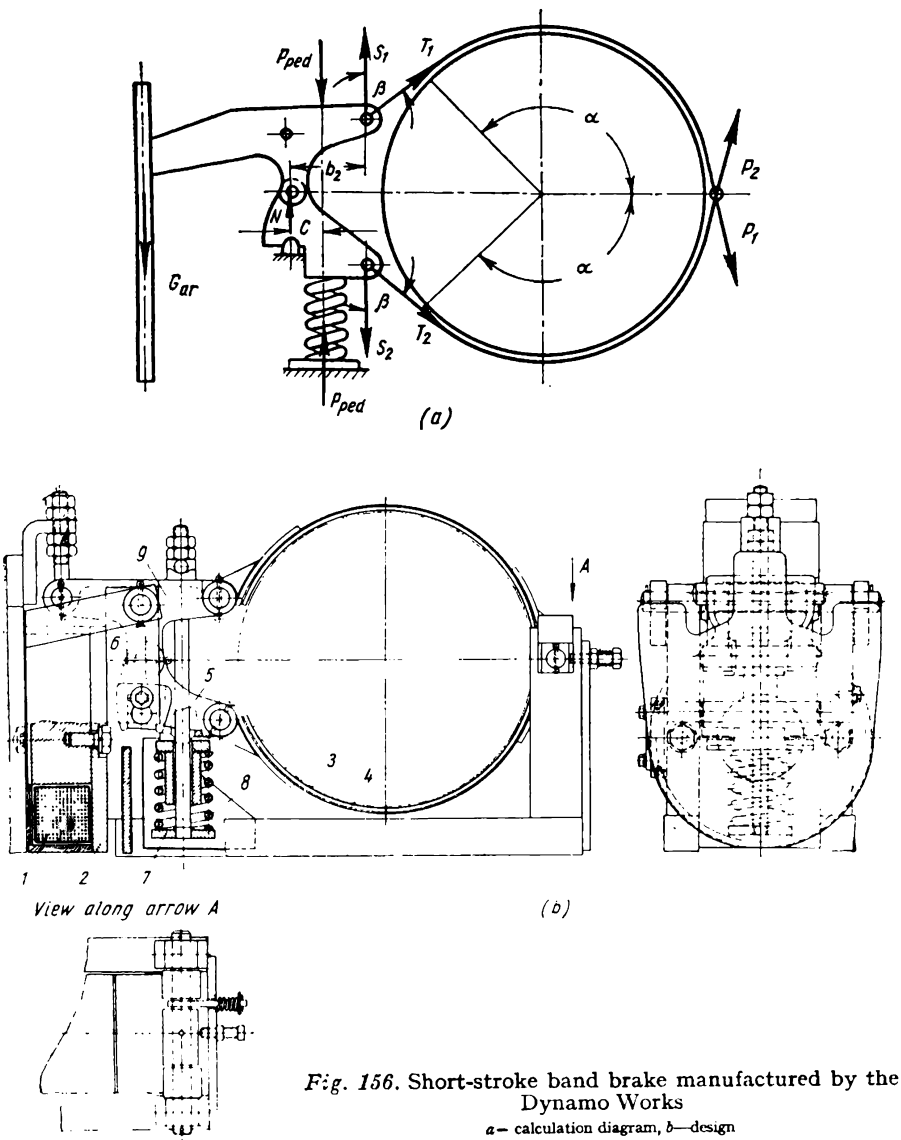

Fig. 156. Short-stroke band brake manufactured by the Dynamo Works
a— calculation diagram, *b*—design

Accounting for possible jerks during brake operation the safe shearing stress is somewhat reduced: for steel $2\,[\tau] = 300$ to 400 kg/cm². The safe compression stress is $[\sigma_{com}] = 2\,[\tau]$.

In order that the band may withdraw uniformly from the drum, band brakes should have a bent bar (Fig. 154) made of flat steel and fitted round the outside of the band with adjusting screws spaced at definite intervals to adjust the band departure.

Fig. 155 shows a band brake for a rotary bucket crane with a lifting capacity of 6 tons. The brake can be operated both by an electromagnet and a hand drive (in lowering).

One shortcoming of band brakes controlled by long-stroke electromagnets accrues from large overall dimensions due to large brake levers.

This shortcoming is avoided in so-called short-stroke electromagnetic brakes (Fig. 156). They are provided with a magnet designed as an ordinary solenoid coil *1* enclosed in housing *2*.

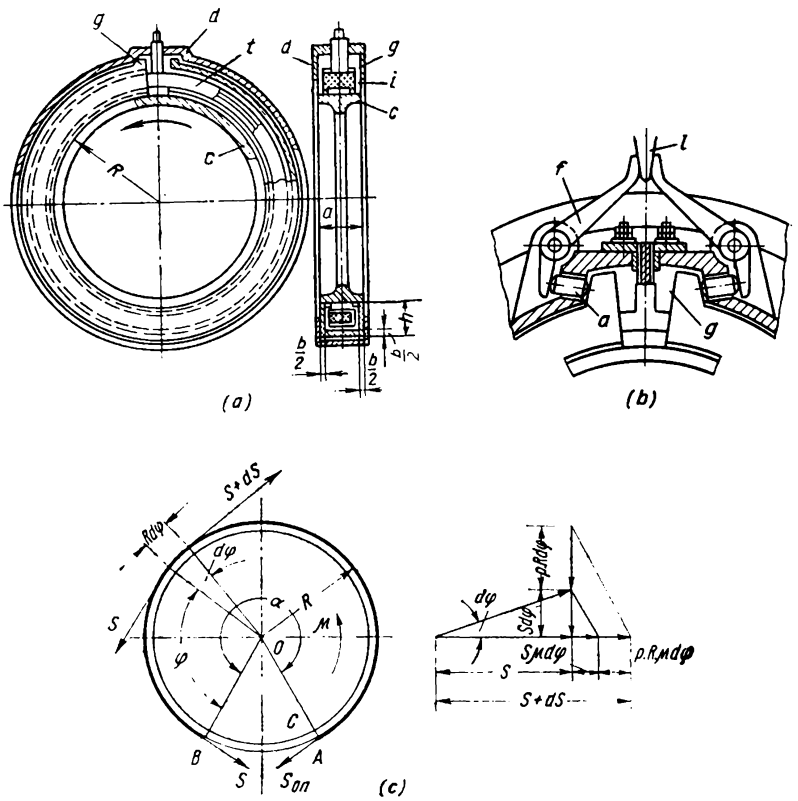

Fig. 157. Electromagnetic band brake

Brake drum *3* in enveloped by bands *4* (with ferrodo linings) whose ends are connected to rocker arm *5* and shackle *9*. Armature arms *7* are connected to rocker arm pivot *6*. The brake is applied by spring *8* which causes armature *7* to turn around pivot *6* and depart from the magnet. When current is passed through coil *1* the armature is pulled in and the brake operates.

Fig. 157*a* shows a new type of an electromagnetic band brake. A ferromagnetic brake drum *c* is embraced over almost 360° by a box-shaped magnetic band *g* fitted loosely into housing *d*. The band accommodates coil *i* rigidly secured to housing *d* and provided with terminals for the connection to the power supply. Band *g* is inserted into housing *d* compressed and is provided at the ends with shoulders entering the respective recesses in housing *d* to limit the departure of the band from the brake drum.

The brake operates as follows. As current flows through coil *i* the magnetic lines of force pass through the sides of band *g* and brake drum *c* causing the band to compress and seize drum *c*.* When the current is switched off the elastic band overcomes the force of residual magnetism, expands and releases the brake drum.

* As soon as the band is attracted by the magnetic lines of force to the drum it will turn together with the drum until it bears against housing *d* which stops the drum.

The releasing process takes a fraction of a second. More rapid release of the brake is achieved by installing a spring between the ends of the band but experiments show that this is not always necessary.

In this type of brake, apart from the mechanical action of the band (as in an ordinary band brake), use is made of the magnetic force acting over the entire length of the band which makes it possible to increase the braking torque substantially. The band of this brake can also be applied by means of a lever system (Fig. 157*b*). In this case the ends of the brake band *g* are drawn together by means of pins *a* and double-arm levers *f* which are forced apart by wedge *l*.

Let us now derive the basic equations for the design of such a brake and compare it with an ordinary band brake. Let us assume that brake drum *c* is acted upon by moment $M=PR$ in a counterclockwise direction (Fig. 157*c*). The magnetic band embraces the drum over arc α, between points *A* and *B*. If an elementary length $Rd\varphi$ (length of arc) is cut from the band it will be acted upon by the following forces: tension *S* in the band, acting on the element from the left; tension $S+dS$ acting on it from the right; normal pressure $Sd\varphi$; friction force $S\mu d\varphi$; normal magnetic pressure equal to $pRd\varphi$ and friction force produced by it $pR\mu d\varphi$ where *p* is the force of magnetic attraction in kg per 1 cm of the band width.

It follows from the equilibrium condition of the separated element of the band that

$$dS = S\mu d\varphi + pR\mu d\varphi = (S + pR)\,\mu d\varphi \tag{147}$$

whence

$$\mu d\varphi = \frac{dS}{S + pR}\,.$$

Integrating this equation in the limits from 0 to α we obtain

$$\int_0^{\alpha} \mu d\varphi = \int_{S_{off}}^{S_{on}} \frac{dS}{S + pR}\,;$$

$$\mu\alpha = \ln \frac{S_{on} + pR}{S_{off} + pR} \quad \text{or} \quad (S_{on} + pR) = (S_{off} + pR)e^{\mu\alpha}. \tag{148}$$

For $p=0$, i.e., when the magnet takes no part in operation, we obtain the well-known Euler's formula (124), i.e.,

$$S_{on} = S_{off}\, e^{\mu\alpha}\,.$$

If the tension in the running-off end of the band is $S_{off}=0$ which corresponds to brake operation without mechanical engagement, formula (148) will take the form

$$S_{on} = pR\,(e^{\mu\alpha} - 1)\,. \tag{149}$$

To compare an ordinary band brake with a brake provided with a magnetic band let us compare the expressions for peripheral forces of both brakes for the same tension S_{off} in the running-off end of the band. For an ordinary brake

$$P_0 = S_{on} - S_{off} = S_{off}\,(e^{\mu\alpha} - 1) \tag{150}$$

and for a brake with a magnetic band

$$P_{mag} = S_{on} - S_{off}\,.$$

Substituting here the value of S_{on} from formula (148) we have

$$P_{mag} = (S_{off} + pR)\,(e^{\mu\alpha} - 1). \tag{151}$$

When S_{off} is constant for both brakes the peripheral force of the brake with a magnetic band will be

$$P_{mag} = P_0 + pR\,(e^{\mu\alpha} - 1), \tag{152}$$

i.e., larger than in an ordinary band brake by the value $pR\,(e^{\mu\alpha}-1)$.

Let us take a numerical example. We take $S_{off}=50$ kg, $\mu=0.3$, $\alpha=270°$, $R=30$ cm and $p=20$ kg/cm.

For an ordinary band brake

$$P_0 = S_{off}\,(e^{\mu\alpha} - 1) = 50\,(4.1 - 1) = 155 \text{ kg};$$

for a brake with a magnetic band

$$P_{mag} = P_0 + pR\,(e^{\mu\alpha} - 1) = 155 + 20 \times 30\,(4.1 - 1) = 2{,}015 \text{ kg}.$$

Hence, with these numerical values, the braking force increases $\frac{2{,}015}{155} \approx 13$ times as compared with an ordinary band brake due to the force of magnetic attraction.

This example shows that in this design the braking effect is created mainly by the action of the electric magnet while the action of the mechanical tensioning of the band (from force S_{off}) is insignificant.

The design of a brake with a magnetic band has the advantage of small size and absence of levers. This brake can be very effective in many mechanisms of materials handling equipment. It cannot be used for load lifting mechanisms since it operates under current (an accidental failure of current may drop the load). In travelling and slewing mechanisms, especially for large braking torques, the small size and constant torque with different directions of drum rotation make this brake by no means inferior to electromagnetic disk brakes.

This mechanism can also be used as a friction clutch where it operates as a safety device against motor overloads.

Band Brakes with Ratchet Wheels. When hand-operated, these brakes can be used for controlling load descent and for holding loads at rest. It is therefore a combination of a lowering and a holding brake.

Fig. 158 shows a band brake with a ratchet wheel. It has the following design. Ratchet wheel *a* is keyed to the load shaft whereas brake drum *b* is mounted freely on the shaft. The brake is applied by weight *G* and released by pulling up the brake lever. Pawl *d* is mounted on pivot *l* secured in the brake drum and is retained in engagement with the ratchet wheel by spring *f*.

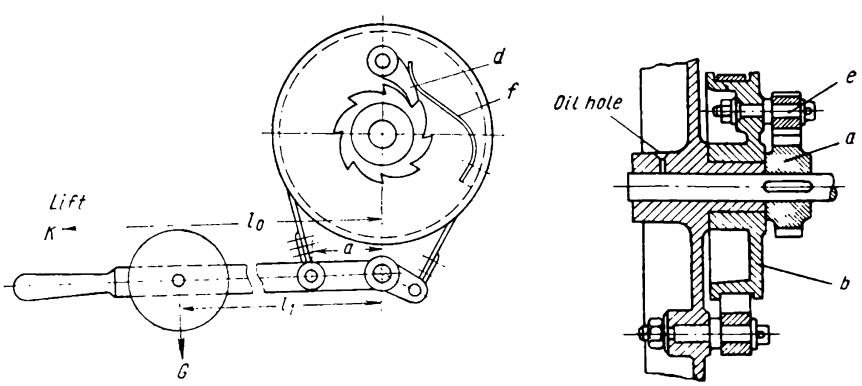

Fig. 158. Band brake with ratchet gearing

Operation of the Brake

Hoisting. The brake is applied by the weight and its drum is stationary. The driving force causes the shaft with the ratchet wheel to rotate clockwise while the wheel teeth slip under the pawl.

Holding. The load causes the brake shaft to turn for lowering until the nearest tooth on the ratchet wheel is engaged by the pawl. Since the brake is applied, the load is held at rest.

Lowering. The brake lever is pulled up by the operator. Since the band is loosened the ratchet wheel and brake drum rotate together with the shaft for lowering (counterclockwise). The speed of lowering is adjusted by raising the lever to various heights.

A brake with a ratchet wheel does not ensure full safety of operation. Inexpert handling may considerably increase the load speed. For this reason a brake with a ratchet wheel is very often used in conjunction with a centrifugal brake. The pawls are displaced relative to each other by half the pitch of the teeth. This improves the dependability of the brake operation and reduces pawl slip by one half.

The unpleasant clicking noise in lifting the load is eliminated by means of controlled pawls. The braking gear can be recommended in the form of an ordinary band brake. If the drum diameter of hand-operated winches is limited by lack of space and the braking weight which has to be lifted is too heavy, a differential brake is sometimes resorted to instead of a simple one. However, the former has a very small release distance and this complicates the adjustment of the load lowering speed.

Example. Design a simple band brake with a ratchet wheel for a hand-operated winch.

Given: Actual braking torque, with account taken of the braking coefficient (β), $M_{br} = 1{,}500$ kg-cm; diameter of the brake drum $D = 30$ cm; unlined steel band ($\mu = 0.15, \alpha = 225°$, $e^{\mu\alpha} = 1.8$); width of band $b = 50$ mm.

1. The peripheral force on the surface of the brake drum is

$$P = \frac{2M_{br}}{D} = \frac{2 \times 1{,}500}{30} = 100 \text{ kg}.$$

2. The tension in the running-off end [formula (126)] is

$$S_{off} = \frac{P}{e^{\mu\alpha} - 1} = \frac{100}{1.8 - 1} = 125 \text{ kg}.$$

3. The magnitude of the weight on the brake lever [formula (131)] is

$$G = \frac{S_{off} a}{l_1} = \frac{125 \times 50}{700} \approx 10 \text{ kg}$$

where the lever arms are assumed to equal $a = 50$ mm; $l_1 = 700$ mm.

4. The effort applied by the operator on the brake lever when $l_0 = 800$ mm is

$$K = G \frac{l_1}{l_0} = 10 \frac{700}{800} = 8.75 \text{ kg},$$

which can be easily accomplished.

5. The travel of the brake lever (at full release) at the point of fastening of the running-off end [formula (135)]:

$$h_{rel} = e\alpha = 1.25 \frac{2\pi \times 225°}{360°} = 5 \text{ mm}$$

and at the point where the operator's effort is applied (see Fig. 158), according to formula (136), is

$$h = h_{rel} \frac{l_0}{a} = 5 \frac{800}{50} = 80 \text{ mm}.$$

6. The tension in the oncoming end of the band [formula (124)] is

$$S_{on} = S_{off} e^{\mu\alpha} = 125 \times 1.8 = 225 \text{ kg}.$$

7. In checking the brake for maximum unit pressure [formula (128)]:

$$p_{max} = \frac{S_{on}}{Rb} = \frac{225}{15 \times 5} = 3 \text{ kg/cm}^2$$

which is much below the safe limit (for a lowering brake—up to 15 kg/cm²).

8. The unit tensile stress in the band ($b = 50$ mm, $s = 3$ mm, $d = 8$ mm), according to formula (144), is

$$\sigma = \frac{S_{on}}{(b-2d)s} = \frac{225}{(5-2\times 0.8)0.3} = 220 \text{ kg/cm}^2$$

which is permissible for steel 3.

9. Checking the strength of the band fastenings. The unit shearing stress in the rivets [formula (145)] is

$$\tau = \frac{S_{on}}{n_1 n \frac{\pi d^2}{4}} = \frac{225}{2 \times 3 \frac{3.14 \times 0.8^2}{4}} = 75 \text{ kg/cm}^2$$

(number of shearing planes $n_1 = 2$, and the number of rivets $n = 3$).

The unit compressive stress on the rivets [formula (146)] is

$$\sigma_{com} = \frac{S_{on}}{nds} = \frac{225}{3 \times 0.8 \times 0.3} = 315 \text{ kg/cm}^2.$$

Both stresses are below the safe limits for steel 2.

10. Module of the ratchet wheel. Because of the small diameter of the brake drum the number of teeth can be taken as $z = 16$. The module is found from formula (95). When $\psi = 2.5$ and $[\sigma_{bend}] = 300$ kg/cm² for steel 3:

$$m = 2\sqrt[3]{\frac{M_{br}}{z\psi [\sigma_{bend}]}} = 2\sqrt[3]{\frac{1,500}{16 \times 2.5 \times 300}} = 10 \text{ mm}.$$

11. The peripheral force on the outside diameter of the ratchet wheel is

$$P_{per} = \frac{2 M_{br}}{D_z}.$$

The ratchet wheel diameter is $D_z = zm = 16 \times 10 = 160$ mm, therefore

$$P_{per} = \frac{2 M_{br}}{D_z} = \frac{2 \times 1,500}{16} = 190 \text{ kg}.$$

12. Pressure on a unit length of the ratchet wheel tooth. The tooth width is $b_z = \psi m = 2.5 \times 10 = 25$ mm, consequently

$$p = \frac{P_{per}}{b_z} = \frac{190}{2.5} = 75 \text{ kg/cm}$$

which is insignificant for steel 3.

13. The diameter of the ratchet wheel pawl pivot is found from formula (96) for $[\sigma_{bend}] = 300$ kg/cm² (steel 45) and $a = 5$ mm (see Fig. 110)

$$d_{pawl} = 2.71\sqrt{\frac{M_{br}}{zm [\sigma_{bend}]}\left(\frac{b_z}{2} + a\right)} = 2.71\sqrt{\frac{1,500}{16 \times 1 \times 300}\left(\frac{2.5}{2} + 0,5\right)} = 22 \text{ mm}.$$

11. CONE BRAKES

Cone brakes are employed either as independent systems with electromagnetic or motor control or in combination with ratchet gearing which constitutes an essential component of brakes operated by a raised weight.

Fig. 159 shows a diagram of a cone brake and its principle of operation. The moment of friction developed by the brake is

$$M_{fr} = PR = N\mu R = S\frac{\mu}{\sin\gamma}R.$$

The angle γ ranges from 15° to 25°.

The width of the taper b is determined from the safe unit pressure:

$$p = \frac{N}{b2R\pi}$$

where

$$N = \frac{S}{\sin\gamma}\ ; \quad b = \frac{R_1 - R_2}{\sin\gamma}\ .$$

The mean speed of sliding on the rubbing surfaces is

$$v_{mean} = \frac{2\pi \dfrac{R_1 + R_2}{2}\, n}{60} = \frac{\pi (R_1 + R_2)\, n}{60} \text{ m/sec}$$

where n—rpm of the brake shaft;
R—mean radius, in m.

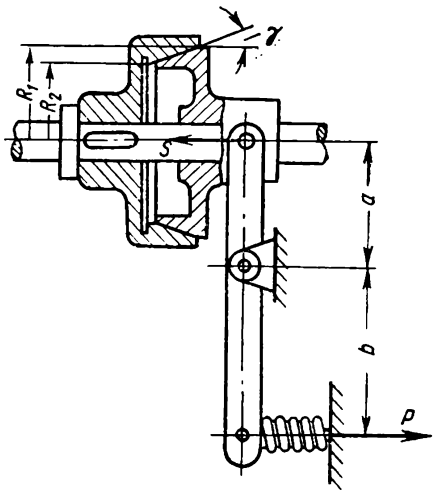

Fig. 159. Diagram of a cone brake

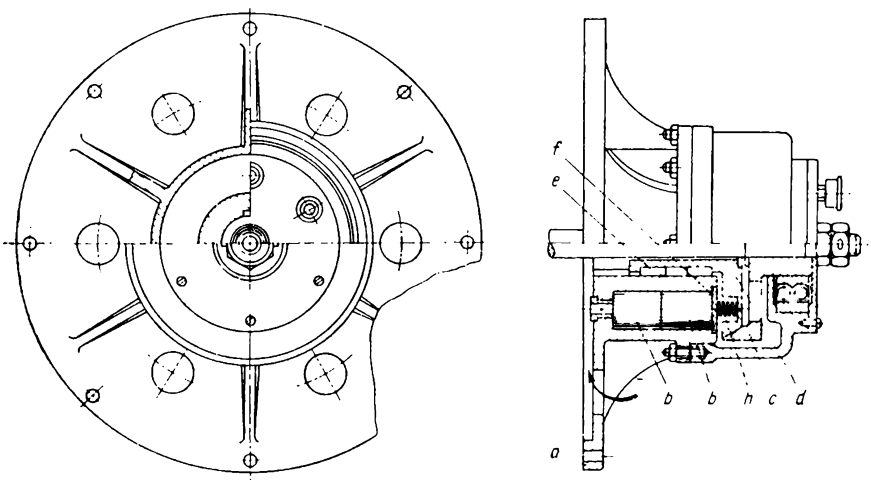

Fig. 160. Cone brake with electromagnetic control

The unit braking power pv_{mean} is taken 30 to 50 per cent less than for shoe brakes (due to the less favourable conditions of heat dissipation).

Fig. 160 illustrates an electromagnetic brake for an electric hoist designed by the author. Flange *a* of the brake is bolted to the hoist fram and also serves as a housing for an electromagnet which accommodates two solenoid coil sections *b*. External friction disk *c* is secured on the end of the hoisting mechanism shaft while internal disk *d* with an elongated hub and two keys *e* can be shifted into the magnet housing. The annular recess for the coil sections is covered with bronze disk *f* to direct the magnetic lines of force more effectively and prevent their leakage. Disk *f* supports six helical springs *h* entering recesses in disk *d*. The electromagnet housing is cooled by air passing through holes provided in cover *a*.

This brake is applied by springs and released by a solenoid.

The brake solenoid shown in Fig. 160 is designed as follows. The force of magnetic attraction is

$$F = \frac{B^2 S}{8\pi} \text{ dynes}$$

where S—cross-sectional area of the magnet poles, in sq cm;
B—flux density in the air gap, in gausses.

The relation between the number of ampere-turns (iw), required to overcome the resistance of the air gap (δ cm) with the brake released, and the flux density is as follows:

$$B = \frac{0.4\pi\ (iw)}{\delta}$$

whence

$$F = \frac{0.16\pi^2\ (iw)^2}{8\pi\delta^2} S \frac{1}{981{,}000} \text{ kg}$$

or

$$F = \frac{6.4}{10^8} (iw)^2 \frac{S}{\delta^2}$$

whence

$$iw = 1{,}250\delta \sqrt{\frac{10F}{S}}. \tag{153}$$

If we denote the diameter of bare wire by d, the length of winding by L in m, resistivity by ϱ in ohm mm^2/m and voltage by E, then the current (in a) will be

$$i = \frac{E}{\varrho L} \frac{\pi d^2}{4} \text{ a}. \tag{154}$$

Since

$$L \approx \frac{\pi D_{mean} w}{1{,}000}$$

where D_{mean}—mean diameter of the coil in mm and w—number of turns, then

$$i = \frac{1{,}000\ E}{\varrho \pi D_{mean} w} \frac{\pi d^2}{4}$$

or

$$iw = \frac{1{,}000\ E d^2}{4\varrho D_{mean}} = 250 \frac{E}{\varrho} \frac{d^2}{D_{mean}}$$

and we finally obtain

$$\frac{d^2}{D_{mean}} = \frac{5\varrho}{E} \delta \sqrt{\frac{10F}{S}}. \tag{155}$$

The selected value of D_{mean} is used to determine d. The number of turns w is calculated from the permissible current in the wire [formula (154)].

Fig. 161 shows the hoisting mechanism of an electric hoist with a motor-controlled cone brake (without an electromagnet). This ingenious system operates on the following principle. A motor enclosed in a drum is provided with a tapered rotor whose right shaft end carries a cone brake disk. When idle, the rotor is always braked by a spring against the fixed cover of the housing. When the motor is started the rotor is pulled in due to its tapered shape; it overcomes the resistance of the spring and thus releases the brake.

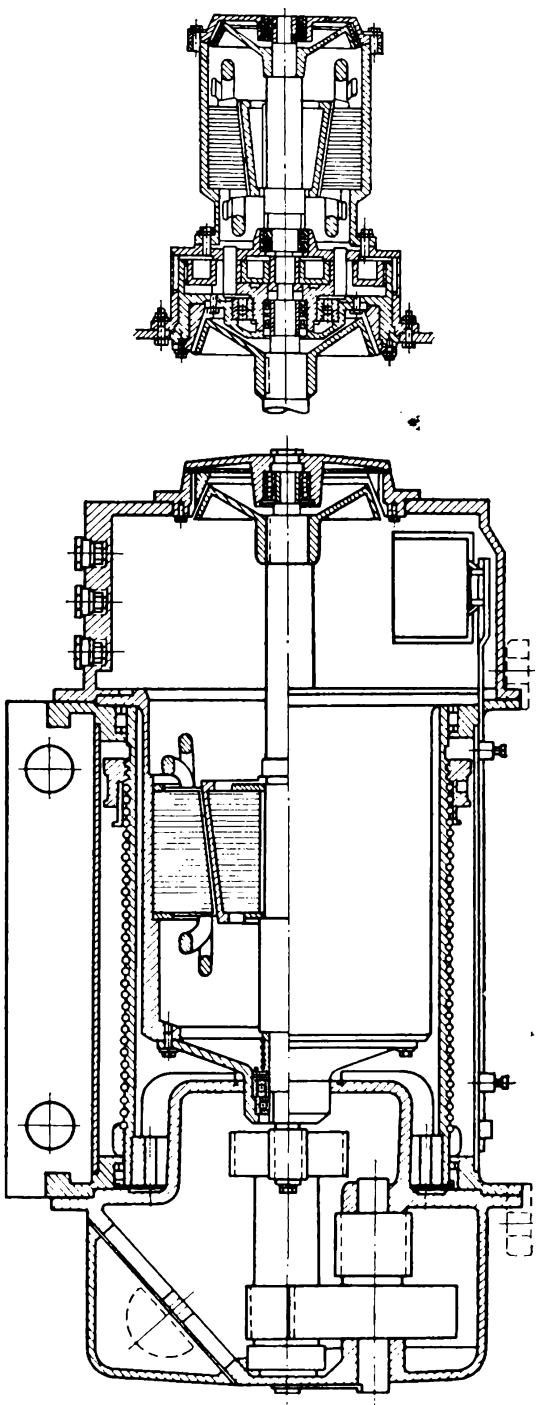

Fig. 161. Cone brake of an electric hoist controlled by the tapered rotor of the motor

12. DISK BRAKES

Multi-disk brakes depend for their action upon the friction between sets of fixed and rotating disks (Fig. 162). Disks *2* enclosed in a stationary housing *1* are keyed in the housing while disks *3* are keyed on the shaft and rotate together with it. Under the action of axial force S of the shaft the disks are pressed together and the friction between them develops the braking effect.

If we denote by z the number of contact surfaces, then the moment of friction produced by the axial force S of the shaft will be

$$M_{fr} = PR = zS\mu R. \qquad (156)$$

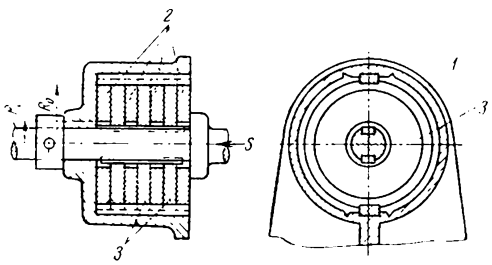

Fig. 162. Disk brake

The number of contact surfaces in a disk brake equals $z=2n$ where n—total number of rotating disks.

The disks are alternately of steel and bronze. Ample lubrication and good surface finish are essential for the successful operation of this brake ($\mu \approx 0.1$). Instead of bronze, the rotating steel disks are frequently lined on both sides with ferrodo.

The unit pressure is

$$p = \frac{S}{F}$$

where F—annular braking surface of one disk.

The permissible unit pressure is selected from Table 32.

Table 32

Safe Unit Pressure

Material of friction surfaces	p, kg/cm²		
	dry	greased	in oil bath
Metal on metal	2-3	3-4	6-8
Woven or braided friction material on metal	2-3	4-6	6-8
Pressed, rolled or shaped friction material on metal	4-6	6-10	10-12

If a disk brake is used in combination with a ratchet or any other arrester and operates as a lowering brake, it should be immersed in an oil bath. In this case $\mu \sim 0.04$ and $p=3$ kg/cm².

If $v_{mean} = \frac{2R\pi n}{60}$ is the sliding speed on the mean radius then the safe unit braking power is taken 30 to 50 per cent less than for shoe brakes (due to less favourable conditions of heat dissipation).

One design of a disk brake is the holding brake of the electric hoist described below (Fig. 171).

13. SAFETY HANDLES

Lowering of loads by hand-operated winches equipped with spur gearing presents a certain hazard for the operator. Therefore, rack jacks and winches with spur gearing should be always provided with easily serviced safety handles.

The safety handle shown in Fig. 163 has very much in common with a variable pressure lowering brake operated by the lifted load (see below). The weight of

the load acts on the driving gear secured on shaft *a* of the handle and produces an axial thrust in the screw thread which makes the handle, ratchet wheel and shaft rotate together because the handle screws onto the threaded bushing of the shaft and engages the disk brake.

When the load is being lifted the parts locked together by the friction force revolve clockwise and the teeth on the ratchet wheel pass freely under the pawl. If the handle is released the load turns the ratchet wheel slightly in the opposite direction which stops as soon as the nearest tooth is engaged by the pawl. The load is held stationary.

To lower the load the handle is rotated counterclockwise, i.e., for lowering; in this case, it turns on its thread and shifts to the right by an adjustable amount. This relieves the pressure on the disks and the load is free to descend. As soon as the angular speed of the shaft tends to exceed the angular speed of the handle, the latter screws on again and presses against the stationary ratchet wheel, thereby producing a braking effect and decelerating the shaft until the angular speeds of the handle and shaft are equalised.

A good braking effect in lowering can be easily achieved since when the shaft gains on the handle the nut moves automatically relative to the screw and brakes the shaft. The moment of friction in the thread should be therefore much smaller than the moment due to the weight of the handle. The handle in a design of this type should never be balanced.

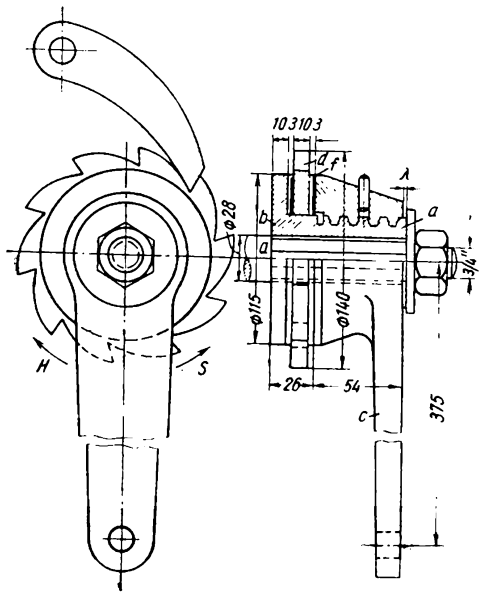

Fig. 163. Safety braking handle

Another design of a safety handle for more rapid lowering of the load is shown in Fig. 164. Here, the brake applied by springs is released by pushing the handle in the lowering direction and the load descends under the action of its own weight. In this case the lowering speed is controlled by the force applied to the handle. This feature may lead to accidents if the winch is operated by unskilled personnel; to avoid this hazard the handles of this type are often provided with an additional centrifugal lowering brake.

This handle can be secured on either end of the shaft.

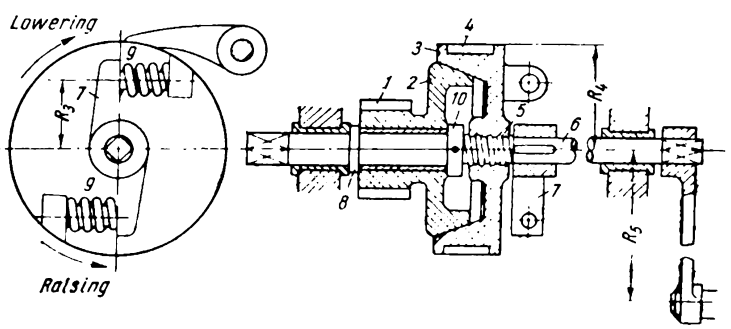

Fig. 164. Safety handle for rapidly lowering a load

Tapered disk *2* with driving gear *1* is mounted freely on shaft *6* and tapered disk *3* with ratchet wheel *4* is screwed on the threaded portion of shaft *5*. Double-arm lever *7*, under the action of two springs *9* bearing against lugs in disk *3*, is keyed to the same shaft.

Shaft *6* has shoulder *8* and thrust ring *10* to limit the axial shift of disk *3*.

With the load suspended from the hoisting gear, springs *9* turn disk *3* relative to shaft *6* by means of lever *7* causing the disk to move on the thread to the left and bear against the tapered disk thereby engaging the friction cones.

The ratchet wheel retains disk *3*, and hence disk *2* and gear *1*, and the load is held at rest. In raising the load the entire system (lever *7*, disks *2* and *3* and gear *1*) revolves together with shaft *6* and the pawl does not impede the motion. To lower the load the handle should be turned in a direction opposite to lifting and the thread will retract disk *3* to the right (compressing springs *9*), disengage it from disk *2* and the latter will revolve under the action of the load being lowered together with gear *1*.

Let us denote the torque on shaft *6* created by the weight of the load by M'; then the moment of friction, with regard to the friction on the shoulder, will be

$$M_{fr} = S\frac{R_1 + R_2}{2}\frac{\mu}{\sin\gamma} + S\frac{d + d_1}{4}\mu_1 \qquad (157)$$

where S—axial thrust;
R_1 and R_2—maximum and minimum radii of the taper;
d and d_1—diameters of shaft a at the shoulder and of the shoulder m;
γ—half-angle of the cone;
μ and μ_1—coefficients of friction in the taper and on the shoulder m.

The moment developed by the springs is

$$M_{sp} = 2R_3F$$

where F—force of each spring; in this case the moment M_{sp} cannot be more than the effort P_{op} applied by the operator on the handle, i.e.,

$$M_{op} = P_{op}R_5.$$

The moment developed by the springs M_{sp} should equal the moment required to turn the nut on the screw, i.e.,

$$S_1 \tan(\alpha + \varrho)\, r_0 = 2R_3F$$

where α—angle of the thread helix;
ϱ—angle of friction in the thread;
r_0—pitch radius of the screw;
S_1—axial thrust due to moment M_{sp}.

Hence

$$S_1 = \frac{2R_3}{r_0}\frac{F}{\tan(\alpha + \varrho)}.$$

The force required to overcome friction on the ratchet teeth in pulling in is

$$S_2 = \frac{M'}{R_4}\mu_2$$

where M'—moment due to the suspended load;
μ_2—coefficient of friction of the pawls on the ratchet wheel teeth.

The force producing engagement in the taper is

$$S = S_1 - S_2 = \frac{2R_3}{r_0}\frac{F}{\tan(\alpha + \varrho)} - \frac{M'}{R_4}\mu_2.$$

Substituting the value of S into formula (157) we obtain

$$M_{fr} = \left(\frac{R_3}{r_0}\frac{F}{\tan(\alpha+\varrho)} - \frac{M'}{2R_4}\mu_2\right)\left[\left(R_1+R_2\right)\frac{\mu}{\sin\gamma} + \frac{d+d_1}{2}\mu_1\right]. \quad (158)$$

To obtain a braking effect, M_{fr} should be larger than M'.

The axial thrust for a cone brake will be

$$S = \frac{2M_{fr}\sin\gamma}{(R_1+R_2)\mu}.$$

Substituting this value into the formula for unit pressure for cone brakes we obtain

$$p = \frac{S}{\pi(R_1^2-R_2^2)} = \frac{2M_{fr}\sin\gamma}{\mu\pi(R_1+R_2)^2(R_1-R_2)}$$

whence

$$(R_1+R_2)^2(R_1-R_2) = \frac{2M_{fr}\sin\gamma}{\pi p_{safe}\mu}. \quad (159)$$

To avoid jamming, the angle γ should be larger than the angle of friction in the taper ϱ_1 ($\tan\varrho_1=\mu$).

Example. Design a safety handle (Fig. 164). Given: Torque created by the load on the handle shaft is $M' = 850$ kg-cm; safe unit pressure is $p_{safe} = 2.5$ kg/cm^2; coefficient of friction in the taper is $\mu = 0.12$; diameter of the shaft at the shoulder $m - d = 4.5$ cm; angle of the cone is $2\gamma = 25°$.

1. Taking the actual braking torque M_{br} 25 per cent higher than the load torque (braking coefficient 1.25), the radii of the cone R_1 and R_2 are obtained from formula (159):

$$(R_1+R_2)^2(R_1-R_2) = \frac{2M_{fr}\sin\gamma}{\pi p_{safe}\mu} = \frac{2\times1.25\times850\times0.216}{3.14\times2.5\times0.12} = 485.$$

Taking the value of

$$R_1-R_2 = 2 \text{ cm}$$

we have

$$R_1+R_2 = \sqrt{\frac{485}{2}} = 15.6 \text{ cm}.$$

Substituting here the value of $R_1 = R_2+2$ cm we have

$$R_1+R_2 = R_2+2 \text{ cm} + R_2 = 2R_2+2 \text{ cm} = 15.6 \text{ cm}$$

whence

$$R_2 = \frac{15.6-2}{2} = 6.8 \text{ cm and } R_1 = R_2+2 \text{ cm} = 6.8+2 = 8.8 \text{ cm}.$$

We take $R_1 = 9$ cm and $R_2 = 7$ cm, then

$$(R_1+R_2)^2(R_1-R_2) = 256\times2 = 512,$$

i.e., we have a certain reserve.

2. The force exerted by each spring F. From considerations of design we take $R_3 = 6$ cm, $R_4 = 11$ cm, $d_1 = 5.5$ cm, $r_0 = 2$ cm, $\alpha = 12°$, $\varrho = 4°$, $\tan(\alpha+\varrho) = 0.287$, $\mu_1 = 0.12$ and $\mu_2 = 0.15$.

From formula (158) we have

$$M_{fr} = \left(\frac{6}{2}\times\frac{F}{0.287} - \frac{850}{2\times11}0.15\right)\left(16\,\frac{0.12}{0.216} + \frac{4.5+5.5}{2}0.12\right) = 1.25\times850$$

or

$$(10.45F-5.8)(8.9+0.6) = 1{,}062$$

whence $F = 11.2$ kg is the force for calculating the tension of each spring.

3. The moment M_{sp} developed by both springs is

$$M_{sp} = 2R_3F = 2\times6\times11.2 = 135 \text{ kg-cm}.$$

4. The effort P_{op} applied to the handle in lowering the load depends on the speed of load lowering and at the point of full release the moment from force P_{op} will equal the moment M_{sp} developed by the springs, i.e.,

$$M_{op} = M_{sp}; \text{ but } M_{op} = P_{op} R_h \text{ whence}$$

$$P_{op} = \frac{M_{op}}{R_h} = \frac{M_{sp}}{R_h} = \frac{135}{35} = 4 \text{ kg}$$

(handle length $R_h = 35$ cm is assigned from considerations of convenience in operating the handle).

5. The force P_{op} applied to the handle in lifting the load is

$$P_{op} = \frac{M}{R_h} = \frac{850}{35} = 24.3 \text{ kg},$$

which is permissible only for short-term operation.

14. CENTRIFUGAL BRAKES

Centrifugal brakes find application in hoisting mechanisms not incorporating self-braking properties. They are designed to control the speed of load lowering automatically when the holding brake is completely released. Centrifugal brakes are therefore in the class of automatic lowering brakes. The most widespread type of centrifugal brake is shown in Fig. 165. It operates as follows.

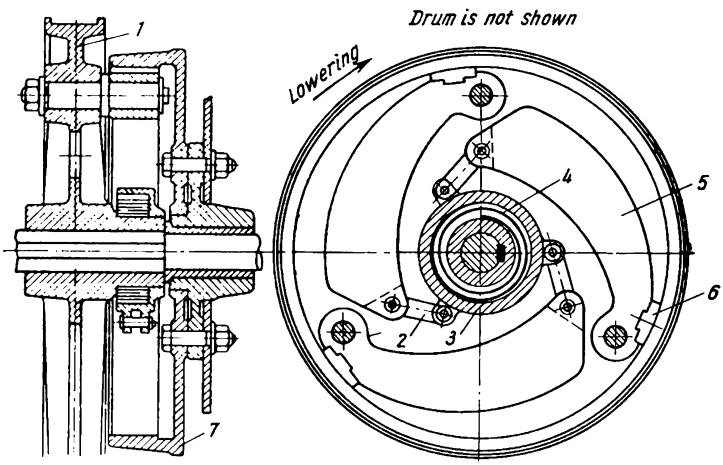

Fig. 165. Centrifugal brake with internal shoes

To drum *1* of the holding band brake, keyed on the mechanism shaft, are attached pivots of three weighted slippers whose ends are connected to adjusting bush *3* by links *2*. Spiral spring *4* fastens bush *3* to the hub of pulley *1*. Slippers *5* are fastened to friction lugs *6*. Fixed rim *7* acts as the second rubbing surface.

The brake operates as follows. When pulley *1* reaches a certain speed slippers *5* are spread apart by centrifugal force and, overcoming the tension of spring *4*, are pressed against the inner rim. The spring is designed for a force which keeps the brake released at low speed.

Fig. 166 shows another design of centrifugal brake. On shaft *1* is keyed disk *2* on whose hub another disk *3* is fitted on splines. Spring *4* which bears against bushing *5*, whose position is adjusted by screws, tends to spread disks *2* and *3* apart whereas weights *6* under the action of the centrifugal force tend to draw them closer together by means of angle levers. As the disks approach each other they clamp fixed disk *7* which may be designed as a ratchet wheel retained against rotation for lowering by a pawl. At a steady speed there should be equilibrium between the load torque which tends to accelerate the shaft and the torque due to friction between the disks which tends to stop the shaft.

If G is the magnitude of one weight, k—number of weights, P—spring tension, r—distance from the axis of rotation to the centres of gravity of the weights at the given speed and v—peripheral speed at radius r; we have

$$v = \frac{\pi r n}{60}$$

and the centrifugal force for one weight will be

$$F = \frac{mv^2}{r} = \frac{G\pi^2 r^2 n^2}{gr \times 30^2}.$$

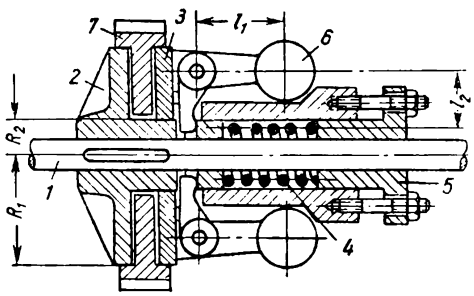

Fig. 166. Centrifugal disk brake

Since $\frac{\pi^2}{g} \approx \frac{1}{100}$ (g—in cm/sec²) we shall have

$$F = Gr\left(\frac{n}{300}\right)^2.$$

The force transmitted to disk b_2 will be

$$P_2 = F\frac{l_1}{l_2} = \frac{l_1}{l_2} Gr\left(\frac{n}{300}\right)^2.$$

Since disk b_1 is additionally under the action of pressure P from the spring which acts opposite to force P_2, the resultant axial thrust S (taking into account the action of all the weights) will be

$$S = kP_2 - P = \frac{l_1}{l_2} kGr\left(\frac{n}{300}\right)^2 - P.$$

With two friction surfaces the actual braking torque M_{fr} from formula (156) will be

$$M_{fr} = 2S\mu\frac{R_1 + R_2}{2} = S\mu(R_1 + R_2). \tag{160}$$

At steady speed

$$M_{fr} = M'$$

whence the total force will be equal to

$$P = \frac{l_1}{l_2}\left(\frac{n}{300}\right)^2 rkG - \frac{M'}{\mu(R_1 + R_2)}. \tag{161}$$

The speed n is assigned from considerations of safety and operating convenience while the other values are dictated by the design.

15. BRAKES APPLIED BY THE LIFTED LOAD

These brakes belong to the class of automatic lowering brakes.

Depending on their principle of operation they are further classified as:

(a) constant-force brakes (with the same load);

(b) variable-force brakes (also with the same load).

Brakes of the first category are not released when the load is lowered while those of the second category are released.

Load-Operated Constant-Force Brakes. The braking action is obtained in these brakes from axial and thrust forces. These brakes are employed only in winches and hoists with irreversible worm gearing.

In worm gearing the peripheral force of the worm wheel due to the action of the suspended load tends to shift the worm shaft axially. This force is used to develop a frictional resistance which balances the moment due to the load. When the load is lowered the surplus of braking resistance (i. e., braking resistance minus the force from the load) is overcome by a drive (usually hand-operated).

One design of such a device is the cone brake with a ratchet arrester shown in Fig. 167. It comprises tapered disk *1* secured on the worm shaft and disk *2* with a tapered recess, ratchet teeth and a ball journal by which it bears on step bearing *3* of fixed housing *4* of the worm drive. The pivot of ratchet pawl *5* is secured in the fixed housing. The ratchet teeth are so directed as to enable disk *1* to rotate freely in lifting the load and to stop it in lowering. As has been noted above, the suspended load produces axial force S which presses tapered disk *1* into the ratchet wheel.

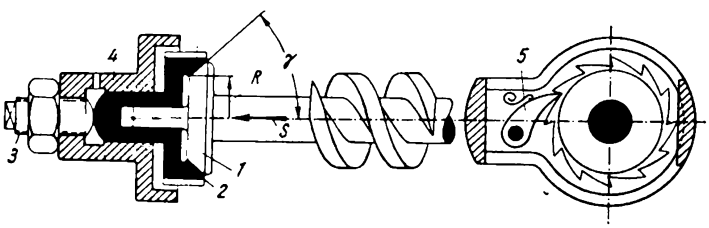

Fig. 167. Load-operated constant-force cone brake

When the load is being raised both disks rotate together and the pawl slips over the ratchet teeth. On stopping, tapered disk *1* is retained in the ratchet wheel by friction due to the axial force and the ratchet wheel by pawl *5*. To lower the load it is necessary to apply a torque to the worm shaft which together with the torque due to the load must overcome the friction torque produced by the tapered surfaces. The latter will in this case slip relative to each other.

Axial force S produces braking torque M_{br} which, as for all brakes, is determined from the formula

$$M_{br} = S \frac{\mu}{\sin\gamma} R.$$

On the other hand, the torque from the load which tends to turn the worm shaft is

$$M' = S \tan(\alpha - \varrho) r_p \tag{162}$$

where α—helix angle of the worm;
ϱ—angle of friction;
r_p—pitch radius of the worm.

Hence, for normal operation of the brake, M_{br} should be larger than M, or

$$R > r_p \frac{\sin\gamma \tan(\alpha - \varrho)}{\mu}. \tag{163}$$

Introducing the braking coefficient β we have

$$R = r_p \beta \frac{\sin\gamma \tan(\alpha - \varrho)}{\mu}. \tag{164}$$

Disk brakes are frequently used instead of cone brakes. In this case

$$M_{br} = zS\mu R$$

whence, respectively,

$$R > r_p \frac{\tan(\alpha - \varrho)}{z\mu}; \tag{165}$$

$$R = r_p \beta \frac{\tan(\alpha - \varrho)}{z\mu}. \tag{166}$$

The following parameters of the brake can be recommended for hand-operated hoists: coefficient of braking $\beta \approx 1.2$ to 1.35; $\alpha \approx 22°$; $\varrho \approx 7°$; $\mu \approx 0.8$ (cast iron on steel); $\gamma \approx 21°$; and number of friction surfaces in a disk brake $z = 2$.

Load-Operated Variable-Force Brakes. These brakes are extensively used in hoists, winches and cranes. Their principle of operation is shown in Fig. 168*a*.

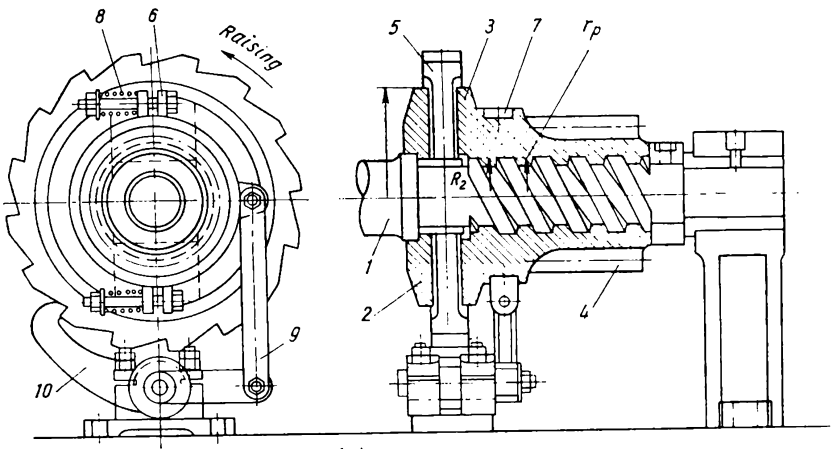

(a)

Disk *2* is keyed on driving shaft *1*. Disk *3*, made integral with gear *4* which transmits rotation to the drum shaft, is mounted on coarse thread of shaft *1*. Ratchet wheel *5* is mounted freely between disks *2* and *3*. The hand of the thread on shaft *1* is such that when the shaft rotates for raising the load, disk *3* shifts to the left, closer to disk *2*, and clamps ratchet wheel *5*. These two disks and the ratchet wheel rotate together since the pawl does not engage the ratchet teeth. The controlled pawl operates on the following principle. As the load is lifted the friction force tends to rotate collars *6* (pressed against bush *7* of disk *3* by springs *8*) and through a system of levers *9* raises pawl *10* above the teeth of wheel *5* and the ratchet stops clicking. On stopping (at the beginning of reverse motion) the same friction force reverses the system, the pawl engages the teeth of the ratchet wheel and stops rotation because the ratchet wheel is engaged due to the weight of the lifted load by a friction force with disk *2*, thus preventing rotation of gear *4*. In this case the moment of friction in the thread should be considerably smaller than the moment due to the inertia forces of the revolving parts of the driving mechanism; otherwise the load may descend. To lower the load, shaft *1* is rotated in the reverse direction. As soon as disk *3* begins to shift to the right, pressure on ratchet wheel *5* decreases. This continues until the moment of friction between the disks becomes insufficient to prevent disk *3* and gear *4* from rotation. As soon as the driving shaft accelerates it tends to increase its angular speed relative to the speed of disk *3*. At this point, gear *4*, due to its thread, shifts again to the left and retards the rotation of the shaft against the fixed disk (held by the pawl) of the ratchet wheel.

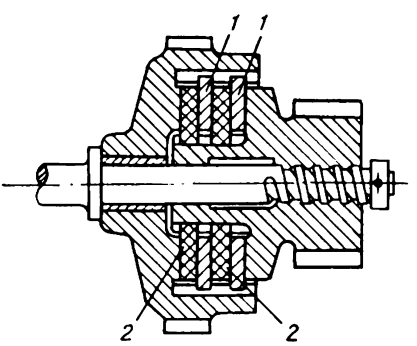

(b)

Fig. 168. Load-operated variable-force disk brake

As a result of these displacements which are gradually transformed into continuous slipping of disks *2* and *3* on the disk of ratchet *5*, gear *4* will rotate at a speed not exceeding that of the driven shaft and the load will be lowered at the assigned speed.

If the driving shaft is stationary the load torque will be equalised in this brake by the moments of friction in the screw and between disks *2* and *3*, i. e.,

$$M' = Sr_p \tan(\alpha + \varrho) + S\mu \frac{R_1 + R_2}{2} \tag{167}$$

where S—axial thrust;
r_p—pitch radius of the screw thread;
α—helix angle of the thread;
ϱ—angle of friction in the thread;
R_2 and R_1—inner and outer radii of the friction surfaces.
Hence,

$$S = \frac{M'}{r_p \tan(\alpha + \varrho) + \mu \dfrac{R_1 + R_2}{2}} . \tag{168}$$

This axial thrust due to the load which compresses the two friction surfaces will produce a moment of friction between disks *2* and *3* (actual braking torque) of

$$M_{br} = S\mu \frac{R_1 + R_2}{2} 2 = S\mu (R_1 + R_2) . \tag{169}$$

Reliable operation of the brake requires that M_{br} be larger than M'. Consequently, the main condition for the normal operation of the brake may be expressed by the following inequality:

$$\frac{R_1 + R_2}{2} > r_p \frac{\tan(\alpha + \varrho)}{\mu} . \tag{170}$$

Denoting the ratio between the braking torque M_{br} and the load torque M' by the braking coefficient $\beta > 1$ we shall obtain for two friction surfaces

$$R_1 + R_2 = \beta 2 r_p \frac{\tan(\alpha + \varrho)}{\mu} . \tag{171}$$

At large braking torques two friction surfaces may not be enough. In such cases, instead of one pair of disks, several disks *1* and *2* are employed (Fig. 168*b*) of which disks *1* are connected to the ratchet wheel and disks *2* to the gear.

Fig. 169 shows the reduction gear of the hoisting mechanism in a newly designed electric hoist with a load-operated variable-force lowering brake.

A modification of the variable-force brakes is the mechanical brake of the Sheppard electric hoist.

A section through the hoisting mechanism is shown in Fig. 170; diagram of the planetary reducer with a mechanical brake in Fig. 171*a* and a modified version of its lever system in Fig. 171*b*.

The hoisting mechanism is provided with two brakes—holding brake *A* (Fig. 170) controlled by an electromagnet and lowering brake *B* controlled by the weight of the lifted load (mechanical brake). If brake *A* fails, brake *B* becomes a holding brake and stops the load.

It can be seen from the cross-section of the reduction gear (Fig. 170) that holding brake *A* is mounted on the motor shaft. It is an ordinary disk brake and operates only when the motor is switched off. It is designed for the full braking torque necessary to hold the load. The brake is released by a single-phase magnet and applied by a spring.

The second (mechanical) brake *B* is applied by the load being lifted and released by the motor. This is a disk-type brake in combination with a roller ratchet. It serves to hold the load at rest and to maintain a constant lowering speed at a definite motor speed.

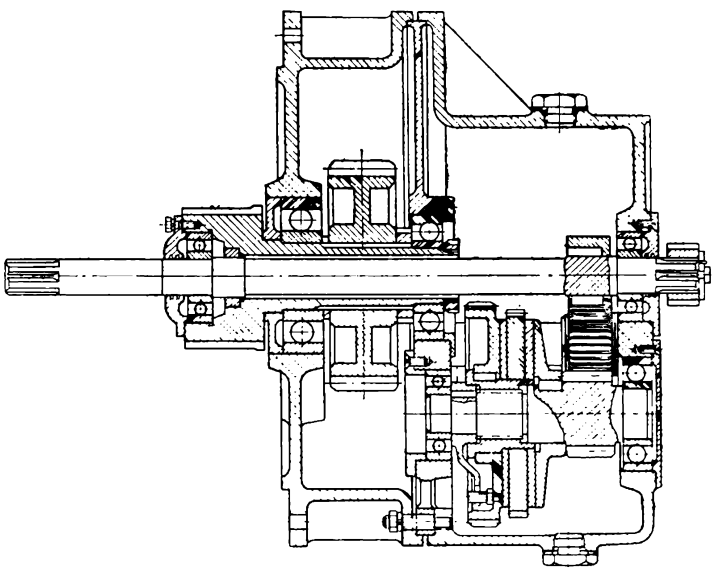

Fig. 169. Load-operated variable-force disk brake in the hoisting mechanism reduction gear

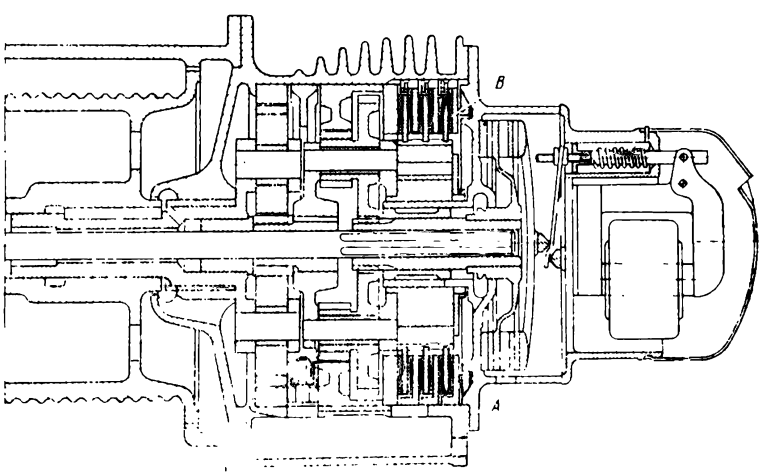

Fig. 170. Mechanical brake of the Sheppard electric hoist

Fig. 171 will be helpful in understanding the principle of operation of the mechanical brake.

Lifting the load. The shaft of motor *1* with gear *1* (Fig. 171*a*) in its clockwise (for example) rotation rotates planet pinions *2* and *3* which roll around internal gear *4*, stationary during load lifting, and rotate arm *5*.

The internal gear is mounted freely in housing *6* and is provided on one side with straps *7* secured at three points and having inclined working surfaces

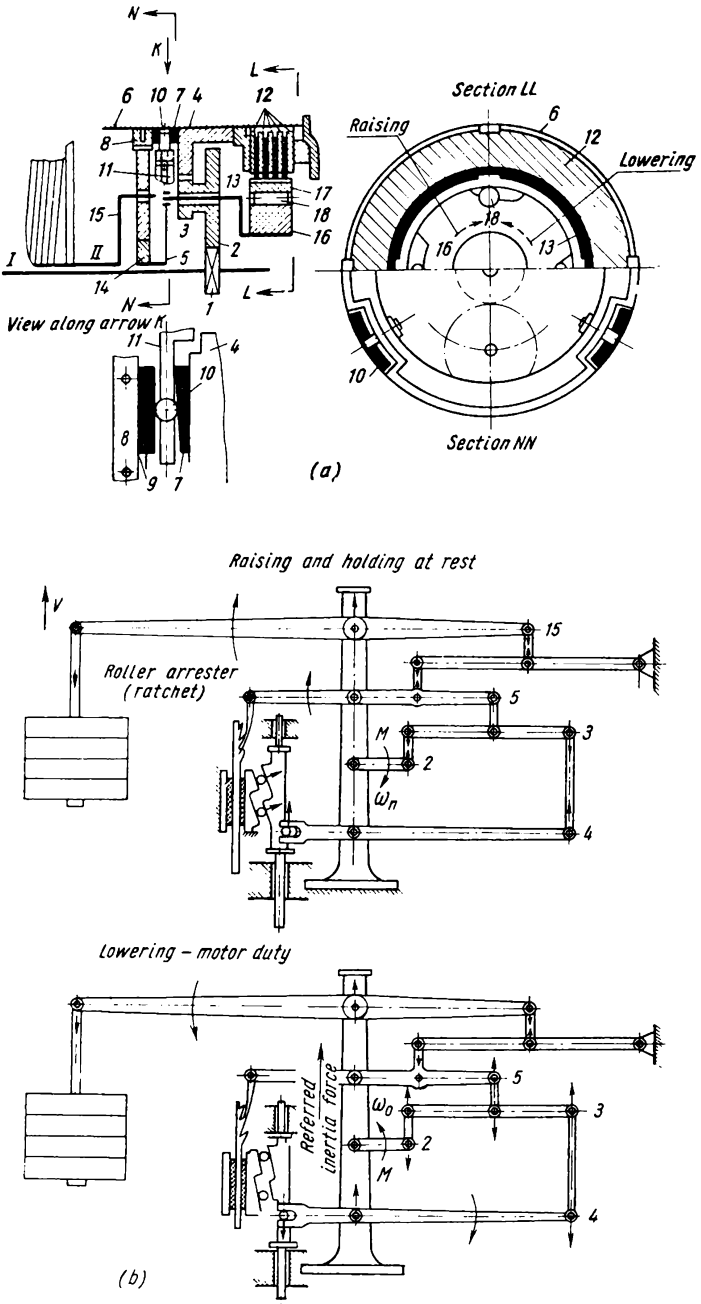

Fig. 171. Operation of mechanical brake in an electric hoist

Rollers *10* are provided between straps *7* and *9* (the latter secured on the side of fixed internal gear *8*). The three rollers are arranged at an angle of 120° to each other on pins secured in cage *11*.

Due to the action of the load, planet pinion *3* tends to turn internal gear *4* counterclockwise. As a result, straps *7* and rollers *10* will force together plates *12* and *13* of the mechanical brake to which the reaction from internal gear *4* is transmitted since the latter remains stationary during lifting. Consequently, arm *5* with gear *14* will be rotated as mentioned above. Since internal gear *8* of the second stage is fixed, arm *15* of the second stage to which the lifting drum *11* is secured will be also rotated. The other end of arm *5* carries the inner member *16* of the roller ratchet which runs free in outer member *17* when the load is being raised. The speed with which the load is raised depends on the transmission ratio of the mechanism and the speed of the motor.

Stopping the load. The holding brake is applied as the current is switched off. When the load stops, the direction of the forces does not change since the direction of the torque from the holding brake on the motor shaft coincides with the direction of torque of the motor in raising. The direction of the torque applied to the drum by the load also remains the same during hoisting, holding and lowering.

In this way, the direction of the forces remains constant in all the links so that internal gear *4* tends to rotate in the same direction as in lifting, i. e., counterclockwise, and thereby retains its initial position. Rollers *18* of the ratchet run free because the drum does not rotate in the reverse direction.

Lowering the load. In lowering the load holding brake *A* is released and the motor is reversed (Fig. 171*b*).

The forces acting on the double-planet pinion are reversed (see arrows in Fig. 171*b*). Internal gear *4* shifts away from the stop and releases the mechanical brake.

The direction of the forces on the double-planet pinion can be reversed only when its angular acceleration, due to the load being lowered and in the presence of retarding resistances in the mechanism, is less than the acceleration imparted by the motor. Otherwise, mechanical brake *B* will not be fully released.

High increase in the speed of the load shifts the asynchronous motor over from motor to generation action.

This will again reverse the forces on the double-planet pinion, the plates of the mechanical brake will be forced together again and the speed of load descent will be reduced.

When the load is being lowered members *16* and *17* of the roller ratchet will revolve together in the counterclockwise direction (Fig. 171*a*) because, if the mechanical brake is released, rollers *18* are jammed slightly.

In this design, if the power is switched off during load lifting and the electromagnetic brake fails due to spring breakage, the rollers will be wedged, thereby engaging the mechanical brake which will stop the load.

Design of the mechanical brake. It has been mentioned above that a hoisting mechanism is provided with two brakes—holding (on the motor shaft) and lowering. The latter becomes an automatic holding brake if the first brake fails in operation. This leads to more reliable operation of the hoisting mechanism.

To stop the load with a mechanical brake provision should be made for a self-braking effect in conformity with the following conditions.

The moment on internal gear *4* from the weight of the load being lifted is

$$M' = Sr_{mean} [\tan (\alpha + \varrho) + \mu] . \tag{172}$$

Moment of friction in the mechanical brake M_{br} (actual braking torque) is

$$M_{br} = zS'\mu_1 R . \tag{173}$$

For self-braking M_{br} should be larger than M'; or

$$zS\mu_1 R > Sr_{mean} [\tan (\alpha + \varrho) + \mu]$$

whence

$$z > \frac{r_{mean}[\tan(\alpha+\varrho)+\mu_1}{R\mu_1}. \quad (174)$$

Here S—axial thrust of internal gear *4*;

r_{mean}—mean radius of internal gear *4* at the places where inclined straps *7* are secured;

α—angle of strap *t* inclination;

ϱ—angle of friction (resistance in rollers *u*) determined from the equation $\tan\varrho = \frac{\mu_2 d + 2f}{D_r}$ (here d—diameter of the roller journal *u*; μ_2—coefficient of friction in the journals; f—coefficient of rolling friction of the roller; D_r—diameter of the roller);

μ—coefficient of friction at the end faces of internal gear *4*;

μ_1—coefficient of friction of the brake disks;

R—mean radius of the brake disks;

z—number of friction surfaces of the mechanical brake, equal to $z = n^{-1}$ (where n is the total number of operating disks)..

Example. Determine the dimensions of a load-operated variable-force disk-type lowering brake for a hand-operated winch (see Fig. 168*a*).

Given: Torque due to the load on the brake shaft $M' = 2{,}500$ kg-cm; radius (pitch) of the screw thread $r_p = 3$ cm; thread helix angle $\alpha = 22°$; the disks are lined with ferrodo, $\mu = 0.3$.

1. Radii of the disks—R_1 and R_2. We take the angle of friction in the thread as $\varrho = 6°$; and the braking coefficient for a hand-operated mechanism $\beta = 1.3$. With two friction surfaces we have from formula (171):

$$R_1+R_2 = \beta 2 r_p \frac{\tan(\alpha+\varrho)}{\mu} = 1.3\times 2\times 3\frac{0.532}{0.3} = 13.85 \text{ cm}.$$

From design considerations, we assume $R_2 = 4$ cm and obtain

$$R_1 = 13.85 - R_2 = 9.85 \text{ cm}.$$

We take $R_1 = 10$ cm and $R_2 = 4$ cm.

2. The actual braking torque M_{br} is equal to

$$M_{br} = M'\beta = 2{,}500\times 1.3 = 3{,}250 \text{ kg-cm}.$$

3. Axial thrust S for two friction surfaces is found from the formula

$$S = \frac{M_{br}}{\mu(R_1+R_2)} = \frac{3{,}250}{0.3(10+4)} = 775 \text{ kg}.$$

4. Checking the brake for unit pressure (for wear). The circular braking surface of one disk is

$$F = \pi(R_1^2 - R_2^2) = 3.14(10^2 - 4^2) = 264 \text{ sq cm}$$

and the unit pressure will be

$$p = \frac{S}{F} = \frac{775}{264} \approx 2.95 \text{ kg/cm}^2$$

which is permissible for a lowering brake.

CHAPTER VII

DRIVES OF HOISTING GEAR

1. HAND DRIVE AND OPERATING LEVERS

A hand drive can be employed in mechanisms with a low lifting capacity, or where the load has to be moved a short distance, or for occasional lifts. For this reason hand drives find application only in winches with a small lifting height (wall-bracket and erection type), in jacks (rack-and-pinion, screw and lever), hoists and sometimes in travelling overhead and gantry cranes and in light-duty rotary cranes.

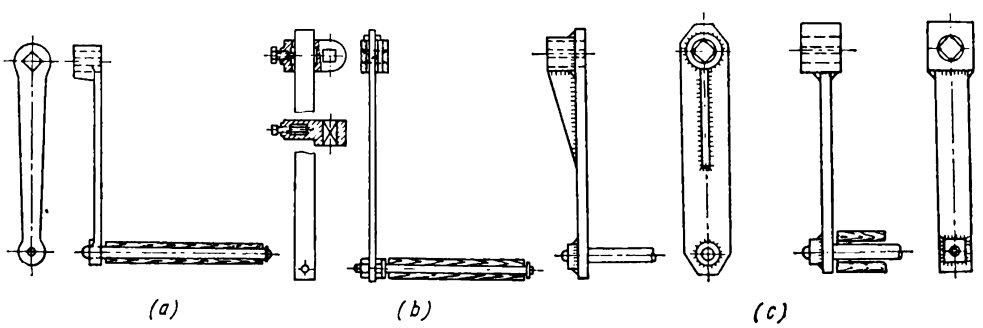

Fig. 172. Crank handles of winches

The principal components of a hand drive are crank handles, ratchets and operating wheels with chains.

Limited power constitutes the most essential shortcoming of hand drives. If we assume that one operator applies a force of 20 kg to the crank handle at a maximum speed of 1 m/sec, then the maximum power of such a drive handled by one operator will be 20 kg-m/sec, i. e.,~0.25 hp. However, even this power cannot be developed for a long time. One unit cannot be serviced by more than four operators at a time, for otherwise they will hinder each other. Consequently, the power of a hand drive is limited to a value of 1 hp.

The lifting capacity of hand lifting gear does not exceed 15,000 kg.

Crank Handles. Hand-drive crank handles are used in rack-and-pinion and locomotive jacks, wall-bracket and erection winches, hand rotary cranes as well as in electrically driven lifting tackle in which a hand drive is provided for an emergency. The principal dimensions of crank handles are given in Table 33. The most widespread design (Fig. 172*a*) has the arm forged of steel and fitted on the square shank of the driving shaft. A loose wooden handle grip is fitted on a round rod, one end of which is riveted over on the side of the arm. The other end carries a safety washer.

Table 33

Principal Dimensions of Hand Drive Crank Handles

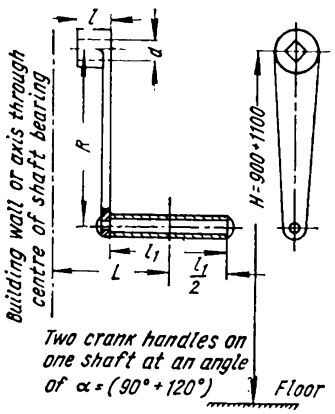

Size, mm

Number of operators	Diameter of handle bushing	Bushing length *l*	Grip length l_1	Length of handle arm *R*
1	(1.8-2.0)*d*	(1-1.5)*d*	250-350	300-400
2	(1.8-2.0)*d*	(1-1.5)*d*	400-500	300-400

Adjustable crank handles (Fig. 172*b*) are intended primarily for worm-drive winches; an arm of adjustable length enables light loads or an unloaded hook to be more rapidly lifted. The forged steel crank handle is secured by an adjusting screw or wing nut in a cast-iron holder fitted on to the square shank of the shaft. When the screw is loosened the handle is retained by a tapered pin in its upper end.

For wall-mounted winches the distance from the crank handle axle to the building wall should not be less than 500 mm. Fig. 172*c* shows crank handles of welded design.

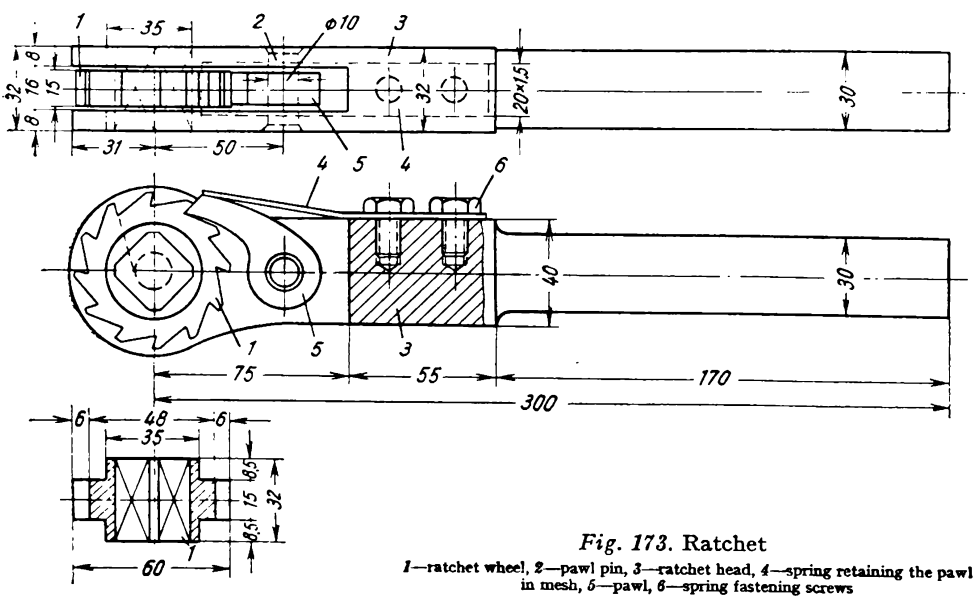

Fig. 173. Ratchet

1—ratchet wheel, *2*—pawl pin, *3*—ratchet head, *4*—spring retaining the pawl in mesh, *5*—pawl, *6*—spring fastening screws

The efforts which may be applied to crank handles are given in Table 34.

Ratchets. Ratchets serve as hand drives of screw jacks. They are lighter than crank handles and are very easy to operate.

Fig. 173 shows one such ratchet. The handle which can be lengthened by a piece of gas pipe is swung alternately back and forth together with the arresting pawl through a small angle. On the backward movement the pawl slips over the teeth of the ratchet wheel linked to the driving shaft. On the reverse movement (forward) the pawl bears against a tooth of the ratchet wheel and the driving shaft turns a certain amount in conformity with the angle of turn of the lever. To make

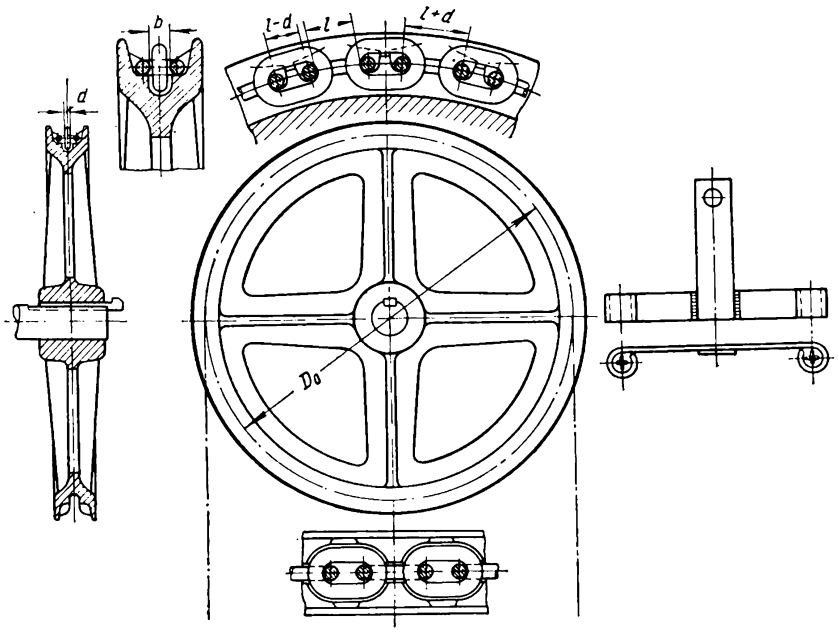

Fig. 174. Operating wheel

the shaft rotate in the reverse direction the ratchet is simply turned over on the square shank of the shaft. Reversible ratchets with shifting pawls are also extremely widespread. The length of the ratchet lever (together with the fitted gas pipe) is taken from 800 to 1,000 mm. The operator may apply up to 30 kg.

Operating Wheels. Operating wheels or sheaves are employed when the shafts to be rotated are high above floor level as, for example, in chain hoists, hand-propelled overhead cranes, etc. In design, operating wheels (Fig. 174) resemble chain sprockets with the only difference that they have a larger number of teeth and their chains are of smaller bar diameter. The shaft of an operating wheel is brought into motion by pulling the right or left part of an endless chain.

The pull on a hand operating chain may be larger than on a crank handle (see Table 34) because this effort can be complemented with the weight of the operator. The distance travelled by the chain on one pull of the operator equals approximately 1 metre. The operating speed is $v = 0.6$ m/sec which with an average pull of 25 kg develops a power of $N \sim 15$ kg-m/sec.

For operating chain use is made of calibrated types with a chain bar diameter of 5-6 mm. The inside length of the chain link is $l \approx 18.5$ mm; the inside width is $b \approx 8$ mm. The pitch diameter D_0 of an operating wheel is found from formulas (46) or (47). The chain should be long enough for its lower end to be from 600 to 800 mm above floor level. The chain is prevented from jumping off during oper-

ation by guide straps made of plate steel. They are attached to the winch frame or else fitted loosely on the shaft of the operating wheel. The strap is designed so that the centres of the loops coincide with the centres of the chain.

Operating Levers and Pedals. Various types of levers and pedals are used to operate hoisting mechanisms.

Levers are usually employed for hand control of gearboxes, clutches and hand brakes, and pedals for foot control of brakes and friction clutches.

In designing mechanisms actuated by man's muscular power the following main rules should be adhered to.

1. In hand hoisting mechanisms the maximum effort by one operator on crane control levers and pedals should not exceed the figures indicated in Table 34 depending on the period of operation.

Table 34

Maximum Effort per Man, kg

Period of operation	On drive handle	On pull chain	On control pedal	On control lever
Continuous operation	12	20	25	18
Operation not exceeding 5 min ...	25	40	35	20

2. The average speed of movement of the operator's hand on a hand drive should not exceed:

(a) 1 m/sec on a crank handle;

(b) 0.6 m/sec on a pull chain.

3. The power developed by one operator is assumed as:

(a) 10.0 kg-m/sec in continuous operation;

(b) 15.0 kg-m/sec for short-term operation up to 5 min.

4. When several operators power a hand drive simultaneously, the simultaneity factor φ of their efforts should be taken into account:

(a) for two operators $\varphi=0.8$;

(b) for four operators $\varphi=0.7$.

5. The stroke of the operating levers should not exceed:

(a) crank handles—400 mm;

(b) pedals—250 mm.

The angle of the lever turn should not exceed 60°.

The total lost motion of the crank handle or pedal should not exceed 10 per cent of the working stroke.

6. Hinged shafts and the holes provided for them in operating levers are to be machined to the 3rd grade of accuracy (running fit). To reduce wear of the joints we recommend low unit pressures and heat treatment of their operating parts.

7. The rotating axle of the crank handle should be arranged at a height of 0.9 to 1.1 metres from the operator's platform and the arm (radius) of the crank handle should not exceed 400 mm (see Table 33).

2. POWER DRIVES

Various designs of power drives are employed in regularly operating winches and cranes and in machines conveying loads over considerable distances or for handling heavy loads in quantity.

Electric drives have the leadership among the various power drives available today. Electrically driven cranes are designed to handle up to 2,000 tons.

Other types of power drives have more or less limited application.

Hydraulic Drive. Hydraulic drives are used where a small lift (100-300 mm) of heavy loads (200-600 t) is required. Such drives actuate heavy-duty jacks.

Hydraulic jacks operate on the principle of hydraulic presses. They have a working pressure of 100-500 atm. Pressure is usually produced with the aid of a small plunger pump equipped with a hand lever.*

Hydraulic devices help to solve a variety of problems of adapting the characteristics of standard motors to that of the work they are to perform. Hydraulic devices ensure excellent speed adjustment of operating gear—both controlled and automatic. Moreover, these devices are small in size, easy in servicing, simplify the control of the machine, increase its life, simplify repair and give greater operational safety. The combination of these factors has extended the sphere of application of such devices, particularly, in load lifting tackle. The great variety of machines and the specific requirements made to them are responsible for their versatile use. A classification of these machines is given below.

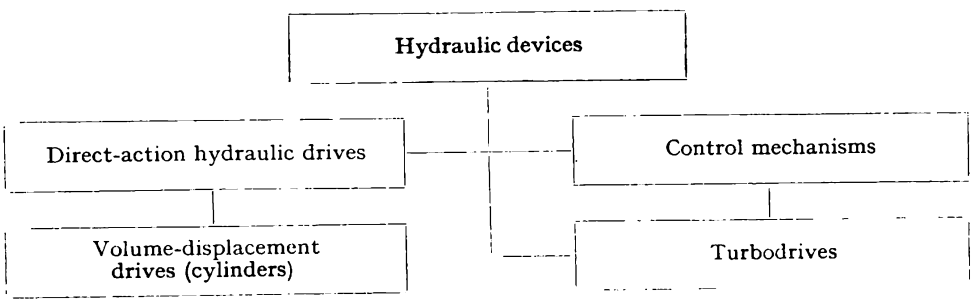

Pneumatic Drive. Pneumatic power is fairly widely applied in small suspended air hoists and pneumatic pulley blocks operating in explosion-hazard premises where it supercedes even electric drives. A pneumatic drive offers the advantage of a large number of switching-in operations per unit of time which cannot be achieved with an electric drive and the possibility of trouble-free operation with heavy overloads. Among its shortcomings are: complex design of air distribution system, smaller distance of horizontal travel due to the air supply hose, and the necessity of precise manufacture and assembly of its parts.

Pneumatic hoists and lifting devices are extensively used in foundry shops, at iron and steel works and for special production purposes.

Steam Drives. Steam drives still continue to retain their importance among the many other types of power drives. They find application mainly in the travelling mechanisms of locomotive cranes for general service on railway sidings, around works and shipyards. These cranes have a good manoeuvrability and do not depend on a stationary source of power supply.

A steam drive has the following shortcomings:

1) it is not always ready to operate for it requires from 1 to 1.5 hours to raise steam;

2) fuel is consumed in keeping up steam between the lifts;

3) fire and sanitary hazards (sparks, smoke);

4) large size and weight;

5) low efficiency (a shortcoming characteristic of all steam drives).

The advantages of a steam drive which still make steam a paying proposition in its competition with other types of drives are as follows:

1) high operational reliability;

2) simple servicing and maintenance requiring less qualified personnel than internal combustion engines;

3) simple repairs.

A steam boiler and steam engine are the main units of every steam installation.

* Hydraulic jack drives with a hand pump are classed among power drives conditionally. In essence they are devices for transforming the muscular power of man.

Internal Combustion Engine Drives. An internal combustion engine offers the following advantages:

1) always ready for starting up;
2) no fuel is consumed while the crane is standing;
3) it can be employed in premises where sparks and smoke are ruled out;
4) no need for a stationary power supply which is especially important for travelling hoisting and handling devices at construction sites, reloading stations, warehouses, etc.;
5) smaller in size than a steam drive;
6) higher efficiency than in a steam drive.

The shortcomings of an internal combustion engine are the following:

1) it cannot be started under load and requires a friction clutch connecting the engine and the drive mechanism;
2) cannot operate with frequent overloads;
3) complex servicing requiring highly qualified personnel.

A recent development is the airless-injection oil engine which operates on heavy liquid fuel. As compared to carburettor engines it possesses the following advantages:

1) less fuel consumed per hp-hr;
2) safer storing of fuel (no combustible gases form in petroleum at normal temperatures);
3) better utilisation of heat;
4) slower speed which is especially important for the life of the diesel engine.

Internal combustion engines are employed in cranes travelling on roads (truck-mounted cranes, automobile- and tractor-mounted cranes) as well as in railway and crawler cranes.

One shortcoming of a drive from an independent internal combustion engine is that to obtain several different working movements of the crane the transmission shaft should be provided with several clutches and separate operating levers. This can be avoided by utilising a diesel-electric drive. The diesel powers a d-c generator which supplies power to individual electric motors servicing each working movement of the crane.

A diesel-electric drive, however, is cumbersome and very expensive.

Among the advantages are less complex mechanical units, more flexible controls, etc.

Fluid transmissions can essentially mollify the shortcomings characteristic of internal combustion engines.

Electric Drives. An electric drive is distinguished by a centralised and simple power supply. It is always ready for starting up, extremely safe in operation and easy and convenient to control. The speed of the load being handled can be adjusted within a wide range. Since the power consumption depends on the power capacity of the unit, an electric drive is superior to all other types of drives from the viewpoint of economy.

The drive may be supplied with direct current at 110, 220, 440 and 500 v or with three-phase current at 380, 500 and 550 v (usually 50 cps). Both kinds of current are almost equivalent in operation.

The following advantages are derived from the application of direct current:

1) power used is always in proportion to load, i.e., light loads can be handled faster than heavy loads and the motor can withstand considerable overloads;
2) large initial torque at a relatively low power consumption;
3) simple switching-in operations;
4) simple and cheap power supply;
5) power can be stored in batteries.

A three-phase current has the following advantages: the electric motor is simple in design (no commutator is used) and is cheaper than a d-c motor. Moreover, transmission and distribution of a-c current over large distances is much simpler and costs less.

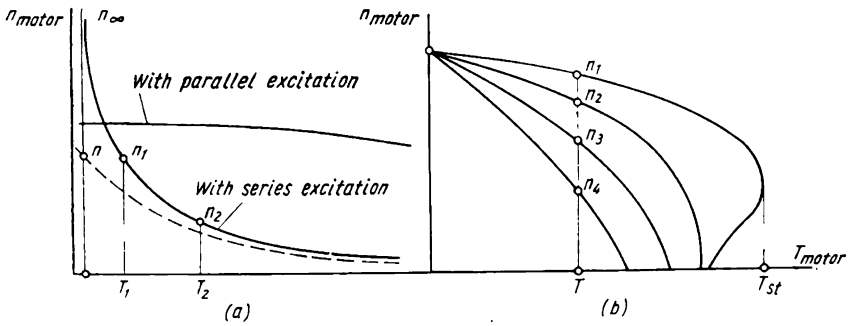

Fig. 175. Characteristics of d-c and a-c electric motors

In addition to direct and three-phase current, use is made sometimes of a single-phase current where the electric motor can be operated without a controller (by shifting the brushes).

The characteristics of a series-wound d-c electric motor are represented in Fig. 175*a*. These motors are self-regulating in the sense that the motor speed drops as the load increases. At slow speed they can develop considerable torque required for starting the mechanism.

Fig. 175*b* shows the characteristics of an asynchronous a-c motor. Here too, the rotor speed drops somewhat when the torque is increased (slip) but to a much lesser degree than in series-wound d-c motors. As compared to d-c motors, three-phase motors are smaller in size and weight, require much less copper, are simpler in design and possess higher efficiency.

CHAPTER VIII

HOISTING GEAR

The load hoisting mechanism is the main element in each lifting device. Irrespective of design, it incorporates the following components:

1) motor or a hand drive (crank handle, ratchet, operating wheel);
2) transmission between the driving and driven shafts (including any types of spur, worm or other gearing together with their parts—shafts, bearings and clutches);
3) drum or sprocket for collecting the rope or chain in hoisting (frequently with additional pulleys);
4) flexible hoisting element (rope or chain);
5) load handling attachment;
6) brake;
7) frame or base structure supporting the hoisting mechanism.

Hoisting mechanisms are subdivided into three groups having:

1) hand power drives;
2) individual (usually electric) power drives;
3) a common motor drive for several mechanisms.

1. HAND POWER HOISTING MECHANISMS

A diagram of one such mechanism is shown in Fig. 176*a*. Motion is transmitted from crank handle shaft *I* through three pairs of spur gears to a drum fitted on shaft *IV* with a radius *R* on which the hoisting rope winds when load *Q* is being raised.

The efficiency of the mechanism is the ratio between the useful lifting work and all the work done. The useful work obtained is

$$A_0 = Qh \tag{175}$$

where *Q*—weight of the load;
h—distance travelled by the load, in m.

The work done is

$$A = Ks \tag{176}$$

where *K*—actual effort applied by the operator to the crank handle;
s—path of force *K* corresponding to path *h*.

Therefore, the efficiency of the mechanism will be

$$\eta = \frac{Qh}{Ks} = \frac{Qv}{Kc} = \frac{K_0}{K} = \frac{K_0}{K_0 + W} \tag{177}$$

where *v*—hoisting speed;
c—speed of the point of application of the driving effort (*c*=30 to 45 m/min);
K_0—ideal effort on the crank handle disregarding friction losses;
W—total resistance due to friction in the mechanism.

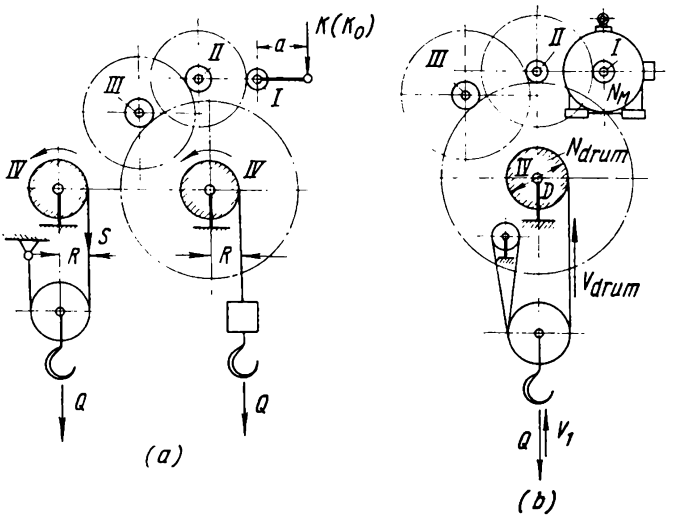

Fig. 176. Diagrams of hoisting mechanisms
a—hand drive, *b*—electric drive

The effort applied by the operator to the crank handle for raising the load is

$$K = \frac{Qh}{\eta S} = \frac{Qv}{c\eta}. \tag{178}$$

This effort should not exceed the values indicated in Table 34.

The total efficiency of the mechanism (for the diagram in Fig. 176*a*) is

$$\eta = \eta_{pul}\,\eta_{drum}\,\eta^3_{gear}$$

where η_{pul} —pulley efficiency;
η_{drum}—drum efficiency;
η_{gear} —efficiency of one pair of gears.

The total transmission ratio of the mechanism can be obtained from the following ratios:

$$i = \frac{\text{moment of load}}{\text{moment of force} \times \eta} = \frac{M_Q}{M_K} = \frac{QR}{\eta K a}. \tag{179}$$

With a pulley available the weight of the load Q should be replaced by the rope tension $S = \frac{Q}{2}$ (Fig. 176*a*).

The speed at which the load is lifted will be

$$v = \frac{\eta K S}{Q}. \tag{180}$$

2. HOISTING MECHANISMS WITH AN INDIVIDUAL ELECTRIC DRIVE

Power is transmitted from the electric motor (Fig. 176*b*) (shaft *I*) through three pairs of spur gears to the drum (shaft *IV*) on which the hoisting rope is being wound.

At a constant lifting speed (v=const) (steady uniform motion) the power developed by the electric motor will be

$$N = \frac{Qv}{75\eta}\ \text{hp} \tag{181}$$

where v—load lifting speed in m/sec.

The torque on the motor shaft is

$$M' = 71{,}620 \frac{N}{n_m} \text{ kg-cm.} \tag{182}$$

The transmission ratio between the motor and drum is

$$i = \frac{\text{motor speed}}{\text{drum speed}} = \frac{n_{motor}}{n_{drum}}.$$

The speed of the rope on the drum is

$$V_{drum} = v i_{pul}$$

where i_{pul}—pulley transmission ratio (in pulley systems for a gain in force $i_{pul} > 1$).

The drum speed in rpm is

$$n_{drum} = \frac{v_{drum}}{\pi D} \text{ rpm}$$

where v_{drum}—speed of the rope on the drum in m/min;
D—drum diameter in m.

3. HOISTING MECHANISMS OPERATING FROM A COMMON MOTOR DRIVE FOR SEVERAL MECHANISMS

These mechanisms are designed for truck- and tractor-mounted cranes, railway and crawler cranes as well as in derrick cranes and grab winches.

A steam engine or an internal combustion engine is the principal actuator used for all these hoists except for those intended for grab winches.

Let us consider, by way of example, a diagram of an automobile-mounted crane manufactured by the Odessa Works and shown in Fig. 177. From the engine motion is transmitted to three crane mechanisms (luffing, hoisting and slewing). From power take-off box *12* motion is transmitted through reversing box *1* to shaft *3* by cardan shaft *2*. Through reduction gear *4*, shaft *3* drives main transmission shaft *7* from which motion is transmitted, by means of clutches and worm drives *5* and *6*, to drum *8* (for boom luffing) or drum *9* (for hoisting). Besides, clutch *10* can transmit motion to worm drive *11* of the slewing gear.

Therefore, in this diagram, transmission shaft *7* is the driving shaft of the hoisting gear.

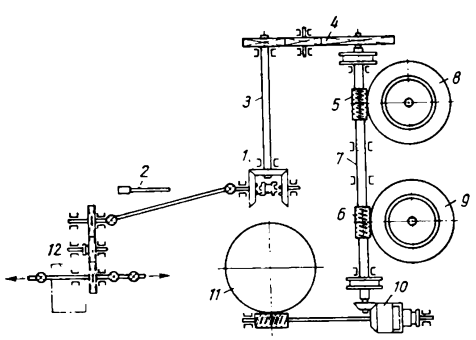

Fig. 177. Diagram of automobile-mounted crane mechanisms

The power on driving shaft *f* for hoisting is

$$N_f = \frac{Qv}{75\eta}$$

where η—efficiency of the mechanism between the shaft of drum *i* and shaft *f*.

Torque on the driving shaft is

$$M_f = 71{,}620 \frac{N_f}{n_f}$$

and the transmission ratio is

$$i = \frac{n_f}{n_i}.$$

CHAPTER IX

TRAVELLING GEAR

These devices are classified into travelling mechanisms for moving trolleys and cranes on runway rails and mechanisms for trackless, rubber-tyred and crawler cranes.

1. RAIL TRAVELLING MECHANISMS

Travelling Mechanisms of Crane Trolleys. Travelling mechanisms of crane trolleys can be subdivided into three groups: hand-operated, with an individual (usually electric) power drive and with a rope power drive.*

Irrespective of design, any travelling mechanism of a trolley incorporates the following elements:

1) motor or operating wheel in a hand drive;
2) transmission between the driving and driven shafts of the trolley wheels;
3) wheels travelling on runway rails;
4) frame (body) of the trolley accommodating the travelling and hoisting mechanisms.

Hand Trolleys. Fig. 178 shows diagrams of hand-operated crane trolleys. Motion is transmitted from the operating wheel (shaft *I*) through two pairs of spur gears to the travelling wheels (shaft *III*).

Determining the wheel load. For four-wheeled trolleys with symmetric suspension of the load and approximately uniform weight distribution on all the four wheels (Fig. 178*a*) the force exerted on the wheels is

$$P_{max} = \frac{Q + G_0}{4} \qquad (183)$$

where Q—weight of the load;
G_0—weight of the trolley.

When the load is suspended asymmetrically in trolleys with two hoists (main Q and auxiliary Q') (Fig. 178*b*) the force exerted on the wheels is approximately equal to**

$$P_{max} = A \approx \frac{G_0}{4} + \frac{Q}{2}\cdot\frac{b_2}{b}; \qquad (184)$$

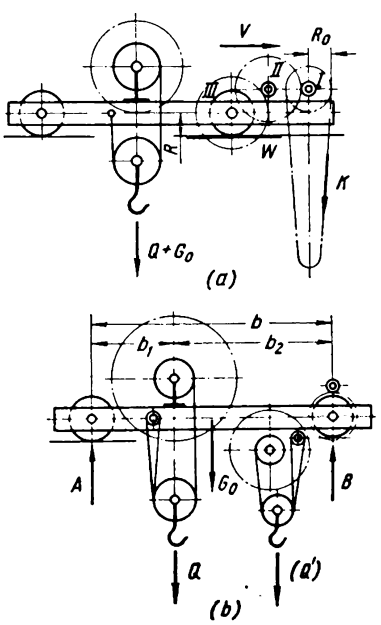

Fig. 178. Travelling mechanisms of crane trolleys

* This group is considered in the Section "Tib and Luffing Mechanisms".
** When only the main hoist is in operation.

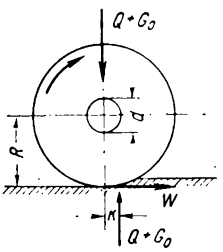

Fig. 179. Diagram for determining resistance to motion

$$P_{min} = B \approx \frac{G_0}{4} + \frac{Q}{2}\frac{b_1}{b}. \tag{185}$$

Resistance to motion. If we denote by W the resistance to motion in a horizontal direction which is to be overcome by the moving loaded trolley (mentally we imagine the resistance as acting on the circumference of a travelling wheel), then the moment of resistance relative to the axle of the wheel at steady motion will be

$$M = WR = (Q + G_0)\,\mu\frac{d}{2} + (Q + G_0)\,k = (Q + G_0)\left(\mu\frac{d}{2} + k\right) \tag{186}$$

where d—diameter of the wheel journal, in cm;
μ—coefficient of friction in the journals;
k—coefficient of rolling friction, in cm.

In equation (186) the first term is the moment of friction in the bearings of the wheel axle and the second term—the moment of rolling friction (Fig. 179). We determine from this equation

$$W = \frac{Q + G_0}{R}\left(\mu\frac{d}{2} + k\right). \tag{187}$$

The coefficient of friction μ in the bearings of the wheels has the following mean values: 0.1 for sliding friction bearings, 0.01 for ball and roller bearings and 0.015 for flexible roller bearings (in rolling friction bearings μ is the referred coefficient of friction). The coefficient of rolling friction k is assumed as $\sim$0.05 cm. After transforming equation (187) we obtain

$$\frac{W}{Q_1 + G_0} = \frac{\mu d + 2k}{D} = w \tag{188}$$

where D—diameter of the travelling wheel;
w—coefficient of resistance to motion or traction factor.

In a general case the traction factor w is the ratio of the forces of harmful resistance to the weight of the load being handled.

To make the determination of the resistance during the movement of a loaded trolley more convenient we take the weight $Q+G_0$ in tons. Then, if $\mu=0.1$ and $k=0.05$ the traction factor in kg per ton of the load being handled is

$$w = \frac{W \times 1{,}000}{(Q + G)_{tons}} = \frac{(0.1d + 2 \times 0.05)1{,}000}{D}$$

if d and D are in cm.

The values of w (with accepted values of μ and k) for various diameters of the axle (journal) and the wheel are given in Fig. 180. Small circles show traction factors for various sizes of wheels and axles.

The values of the traction factors [formula (188)] account only for the friction forces in the bearings and the resistance to rolling. However, the movement of the trolley is associated with yet another additional resistance, due to friction between the wheel flanges and the rails. It depends to a large degree on the state of the track rails and can be approximately accounted for by coefficient β. Hence, the final formula for determining resistance will be

$$W = \beta\,(Q + G_0)_{tons} w. \tag{189}$$

The following values of β can be recommended: 1.25-1.4 if the wheels run on sliding friction bearings and 2.5-5.2 for roller friction bearings.

A hand travelling mechanism is usually driven from a chain and operating (pocket) wheel. The transmission ratio between the driving and driven shafts is

$$i = \frac{M}{\eta M_0} \qquad (190)$$

where $M = WR$—moment of resistance to motion;
η—total efficiency of the mechanism;
$M_0 = KR_0$—torque on the shaft of the operating wheel (see Fig. 178*a*).

For our diagram the mechanism efficiency η is equal to

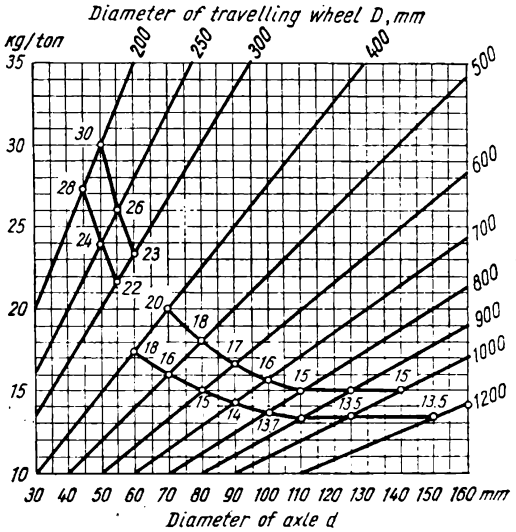

Fig. 180. Values of traction factors (coefficients of resistance to motion)

$$\eta = \eta_0 \eta_{gear}^2 \eta_{t\text{-}w} \qquad (191)$$

where η_0 —efficiency of the operating wheel ~ 0.93;
η_{gear} —efficiency of one pair of gears;
$\eta_{t\text{-}w}$ —efficiency of the travelling wheel bearings.

The values of $\eta_{t\text{-}w}$ are as follows: ~ 0.97 for greased bearings and ~ 0.99 for ball and roller bearings.

The travelling speed is

$$v = \frac{60\eta K c R_0}{M} \text{ m/min} \qquad (192)$$

where c—mean peripheral speed of the operating wheel which, accounting for the favourable effect exerted by inertia forces on the travelling mechanism, may be assumed as 0.8-1 m/sec;
K—effort applied by the operator on the operating (pull) chain, in kg (see Table 34);
R_0—crank handle radius, in cm;
M—moment of resistance to motion referred to the shaft of the travelling wheel, in kg-cm.

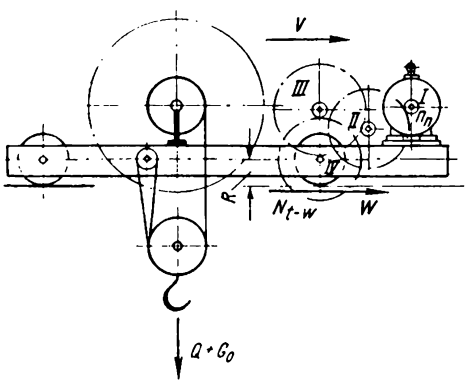

Fig. 181. Diagram of the travelling mechanism of an electrically driven crane trolley

Crane Trolleys with an Individual Electric Drive

A diagram of an electrically driven travelling mechanism is illustrated in Fig. 181. Motion is transmitted from the electric motor (shaft *I*) through three pairs of spur gears to the travelling wheel (shaft *IV*). At steady motion the power developed by the motor will be

$$N = \frac{Wv}{75\eta} \text{ hp} \qquad (193)$$

where v—travelling speed, in m/sec;
η—total efficiency of the mechanism;
W—resistance to motion, in kg, found from formula (189).

The transmission ratio is

$$i = \frac{\text{motor speed}}{\text{travelling wheel speed}} = \frac{n_{mot}}{n_{t\text{-}w}}. \tag{194}$$

The speed of the travelling wheel is

$$n = \frac{v}{\pi D} \tag{195}$$

t-w where v—speed, in m/min;
D—wheel diameter, in m.

Travelling Mechanisms of Overhead Travelling and Gantry Cranes

Hand-Propelled Overhead Travelling Cranes. Fig. 182*a* shows a diagram of the travelling mechanism of a hand-propelled overhead travelling crane. The components of such mechanisms are generally designed on the same lines as for crane trolleys. Motion is transmitted from the operating wheel mounted on the main transmission shaft through two parallel gear trains to two travelling wheels of the crane. They are secured in the cross girders of the frame.

The wheel loads of overhead travelling cranes are variable magnitudes which depend on the position of the trolley. In an ordinary four-wheeled crane the maximum force acting on the wheels arises when the loaded trolley is located in the so-called dead section e of the span (Fig. 182*b*) where e is the distance between the axis of the lifting hook in its extreme position and the axis of the crane runway rails. If we denote by G the weight of the crane (without the trolley) and by G_0 —the weight of the trolley, then the maximum force acting on

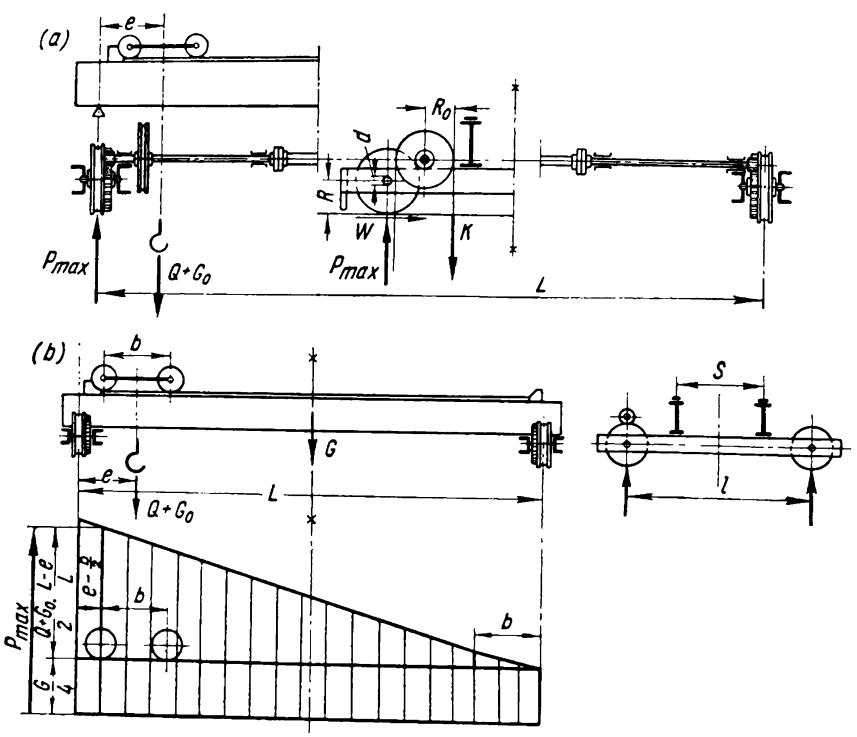

Fig. 182. Travelling mechanism of a hand-propelled overhead travelling crane

a travelling wheel of a four-wheeled crane can be determined with sufficient accuracy from the following formula (Fig. 182*b*)

$$P_{max} \approx \frac{G}{4} + \frac{Q + G_0}{2} \frac{L - e}{L}. \qquad (196)$$

The resistance to motion, transmission ratio and speed for the travelling mechanisms of hand overhead cranes can be found from formulas (189) to (192), inclusive, as for hand crane trolleys. The only thing necessary is to replace $(Q + G_0)$ by $(Q + G_0 + G)$ in formula (189); in this case coefficient β can be taken on an average equal to $\beta = 1.4$ to 1.6.

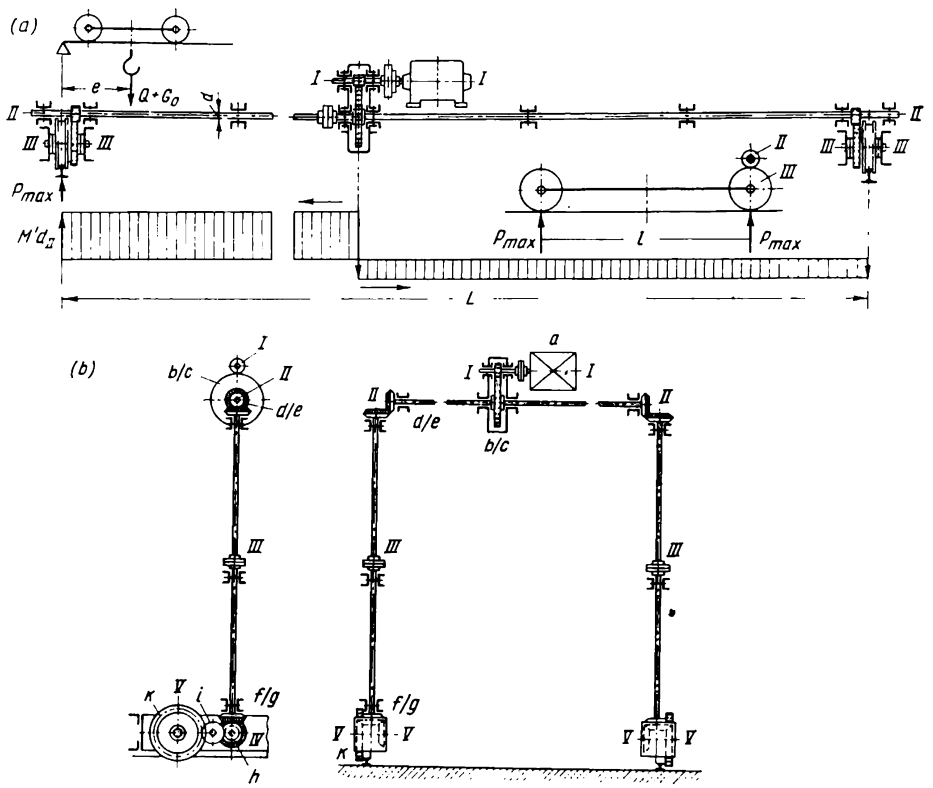

Fig. 183. Diagrams of travelling mechanisms
a—overhead travelling crane, *b*—gantry crane

Electrically Driven Overhead Travelling Cranes. The diagram of the travelling mechanism of an electrically driven overhead crane is represented in Fig. 183*a*.

The wheel load in a four-wheeled crane is determined from formula (196) as for hand-operated cranes.

Cranes with large lifting capacity and a wide span are usually provided with eight and more travelling wheels. In this case they are mounted in pivoted trucks which are equalised in pairs to eliminate a statically indeterminate system when finding the wheel load.

Resistance to motion can be determined as for hand cranes, by the formula

$$W = \beta (Q + G_0 + G)w. \qquad (197)$$

Formula (197) disregards resistance to motion due to a head wind. This resistance should be taken into account in designing cranes which are to operate in the open.

The power developed by the motor at steady motion, transmission ratio and the speed of the travelling wheels can be found from the formulas used for the travelling mechanisms of crane trolleys (193), (194) and (195). The maximum moment for the calculation of the drive of travelling wheels arises when the loaded trolley is in the dead section of the span. In a four-wheeled crane it equals part of the moment of resistance to motion acting on this side, i. e.,

$$M'_{dII} = \beta \left| \frac{G}{2} + \frac{Q + G_0}{L} (L - e) \right| wR . \tag{198}$$

To eliminate slipping of the driving wheels of travelling mechanisms of cranes and trolleys the design should be checked for adhesion. The adhesive force between the wheels and rails can be found from the formula

$$Z = \Sigma P f \tag{199}$$

where ΣP—sum of the minimum forces acting simultaneously on the driving wheels;

f—coefficient of adhesion of wheels with rails.

The mean values of f are as follows: for dry rails $f \leqslant 0.15$ to 0.2 and for damp rails $f \leqslant 0.1$ to 0.12.

The adhesive force should be higher than the resistance forces in motion minus the friction forces in the bearings of the driving wheels:

$$W - \Sigma P \mu \frac{d}{D} < Z . \tag{200}$$

The friction force $\Sigma P \mu \frac{d}{D}$ in the bearings of the driving wheels will not be actually applied on the periphery of the wheel since it is absorbed before that in the bearings, as are other losses in the drive. For this reason the given term is introduced into formula (200) with a minus sign.

Equation (200) can be written in the following form:

$$Z = \alpha W \tag{201}$$

where α is the adhesive force safety factor. The recommended value of α is about 1.3.

In checking crane trolleys for adhesive force, G (weight of the crane) should be omitted in the expression ΣP; the resistance to motion W should also be calculated without G.

Gantry Cranes. The travelling mechanisms of these cranes are more complex in design than those used in overhead travelling cranes. They are provided additionally with two vertical shafts having bevel gear drives (see Fig. 183*b*) for driving the travelling wheels mounted in the supporting legs of the crane. Semigantries are designed with only one vertical shaft.

The travelling mechanism is designed, the wheel loads are determined and the adhesive force is checked in the same way as for overhead travelling cranes.

Travelling Mechanisms of Cantilever and Monorail Cranes

Cantilever Cranes. The maximum force acting on the vertical travelling wheels (Fig. 184) is

$$P_{ver}^{max} = \frac{V}{2} = \frac{Q + G_0 + G}{2} \tag{202}$$

where V—vertical thrust;

Q—weight of the load;

G—weight of the crane (without trolley);

G_0—weight of the trolley.

The maximum force acting on the horizontal rollers is

$$P_{hor}^{max} = \frac{H_1}{2} = \frac{(Q + G_0)a + Ge_1}{2h_1} \quad (203)$$

where H_1—horizontal thrust.

Resistance to motion. In cantilever cranes the resistance to motion of the vertical travelling wheels is complemented with the resistance to motion of the top and bottom horizontal bearing rollers. If we denote the radius of the vertical travelling wheels by R_1, the radius of the horizontal rollers by R_2 and the diameters of their axles by d_1 and d_2, in conformity with formulas (187), (202) and (203), we obtain the total resistance to motion as

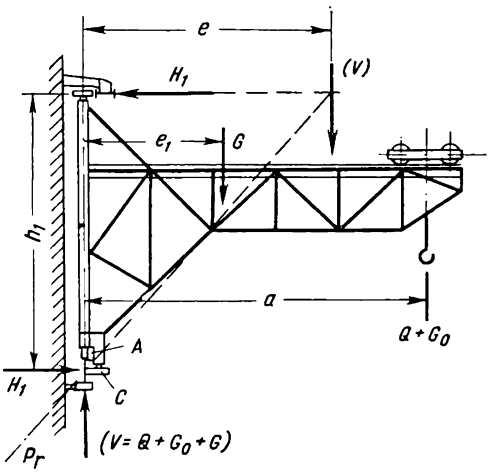

Fig. 184. Diagram of a cantilever crane

$$W = \frac{Q + G_0 + G}{R_1}\left(\mu\frac{d_1}{2} + k\right) + 2\frac{(Q + G_0)a + Ge_1}{R_2 h_1}\left(\mu\frac{d_1}{2} + k\right). \quad (204)$$

The power developed by the motor, transmission ratio and the speed of the travelling wheels can be found from formulas (193), (194) and (195). Check-up for adhesive force is done in conformity with formulas (199), (200) and (201).

Monorail Cranes. A diagram of a monorail crane is given in Fig. 185.

Bearing reactions. If the boom is aligned with the direction of motion then its vertical bearing reactions will be

$$V = Q + G_1 + G_g \quad (205)$$

where Q—weight of the load;

G_1—weight of the revolving superstructure of the crane (without counterweight);

G_g—counterweight.

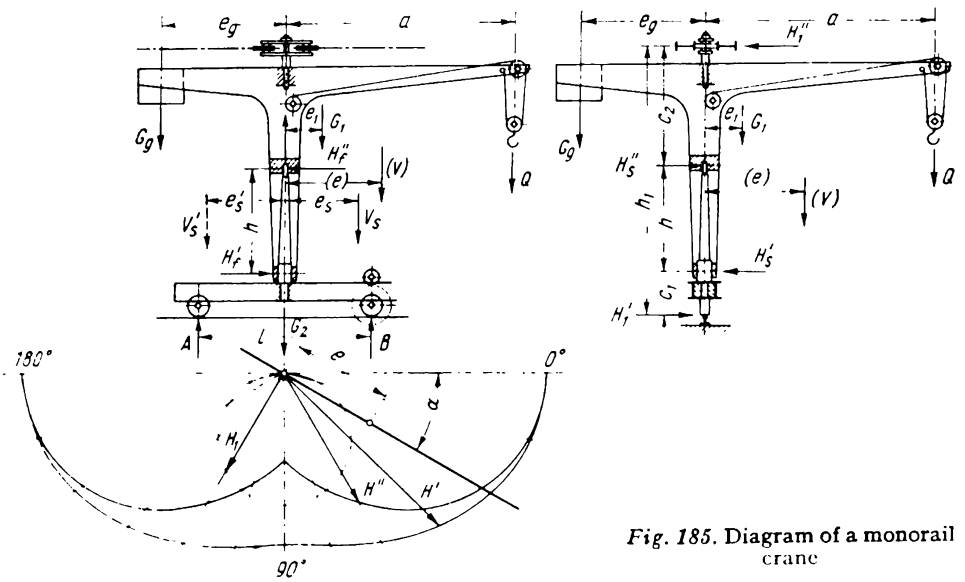

Fig. 185. Diagram of a monorail crane

The horizontal bearing reactions of the post are

$$H_f' = H_f'' = \frac{Q_a + G_1 e_1 - G_g e_g}{h} = V \frac{e}{h} . \tag{206}$$

The moment due to the weight of the crane is fully balanced by the counterweight while the moment due to the load is equalised only by one half.

If the boom is perpendicular to the track rails and the vertical bearing reactions are the same as when the boom is aligned with the direction of motion then the horizontal bearing reactions on the top and bottom runway rails will be

$$H_1' = H_1'' = \frac{Q_a + G_1 e_1 - G_g e_g}{c_1 + h + c_2} = V \frac{e}{h} \tag{207}$$

and the horizontal reactions of the post will be

$$H_s'' = H_1' \frac{c_1}{h} \text{ and } H_s' = H_1' \frac{c_1 + h}{h} . \tag{208}$$

The horizontal bearing reactions of the post and rails vary with the slew angle α of the boom. During transition from H_f' to H_s' (H') and from H_f'' to H_s'' (H'') these changes as well as the changes in H_1' and H_1'' (H_1) from zero to the maximum value can be represented as a polar diagram (Fig. 185).

Wheel loads. Vertical forces on wheels A and B vary with the position of the boom (Fig. 185). For a boom positioned at an angle of α we obtain

$$A = \frac{G_2}{2} + V \frac{\frac{l}{2} - e \cos \alpha}{l} \tag{209}$$

and

$$B = \frac{G_2}{2} + V \frac{\frac{l}{2} + e \cos \alpha}{l} . \tag{210}$$

When $\alpha = 90°$ the boom is perpendicular to the direction of motion and

$$A = B = \frac{1}{2} (V + G_2) . \tag{211}$$

When a boom carrying full load is aligned with the direction of motion ($\alpha = 0°$), the maximum vertical force will be

$$P_{ver}^{max} = B = \frac{G_2}{2} + V \frac{\frac{l}{2} + e}{l} \tag{212}$$

and the minimum vertical force will be

$$P_{ver}^{min} = A = \frac{G_2}{2} + V \frac{\frac{l}{2} - e}{l} \tag{213}$$

where G_2—weight of the bottom truck together with the post.

The maximum force acting on the horizontal rollers ($\alpha = 90°$) is

$$P_{hor}^{max} = H_1 \frac{1}{n} = V \frac{e}{h_1 n} \tag{214}$$

where n—number of rollers.

When $\alpha = 0°$, $P_{hor}^{min} = 0$.

The vertical travelling wheels run along a track rail. The upper horizontal runway comprises two channe or I-beams. In light monorail cranes the bottom bearing rollers are absent and the horizontal force H_1 is carried by the rail through the flanges of the vertical travelling wheels.

Resistance to motion. In monorail cranes, as in cantilever cranes, the resistance to motion depends on the resistance of the vertical travelling wheels and the top and bottom horizontal rollers. We denote: by R_1—radius of the vertical wheels, d_1—diameter of their axles, R_2 and d_2 and also R_3 and d_3—radii of the top and bottom horizontal rollers and the diameters of their axles; then if the boom is perpendicular to the direction of motion the maximum resistance to motion will be

$$W = \frac{V + G_2}{R_1}\left(\mu_1 \frac{d_1}{2} + k\right) + V\frac{e}{h_1}\left[\frac{1}{R_2}\left(\mu\frac{d_2}{2} + k\right) + \right.$$

$$\left. + \frac{1}{R_3}\left(\mu\frac{d_3}{2} + k\right)\right] = (V + G_2)_{tons}\, w_1 + V_{tons}\frac{e}{h_1}(w_2 + w_1). \qquad (215)$$

The traction factors per ton of load w_1, w_2 and w_3 are taken from Fig. 180.

The power developed by the motor, transmission ratio and speed of the travelling wheels can be found from formulas (193), (194) and (195).

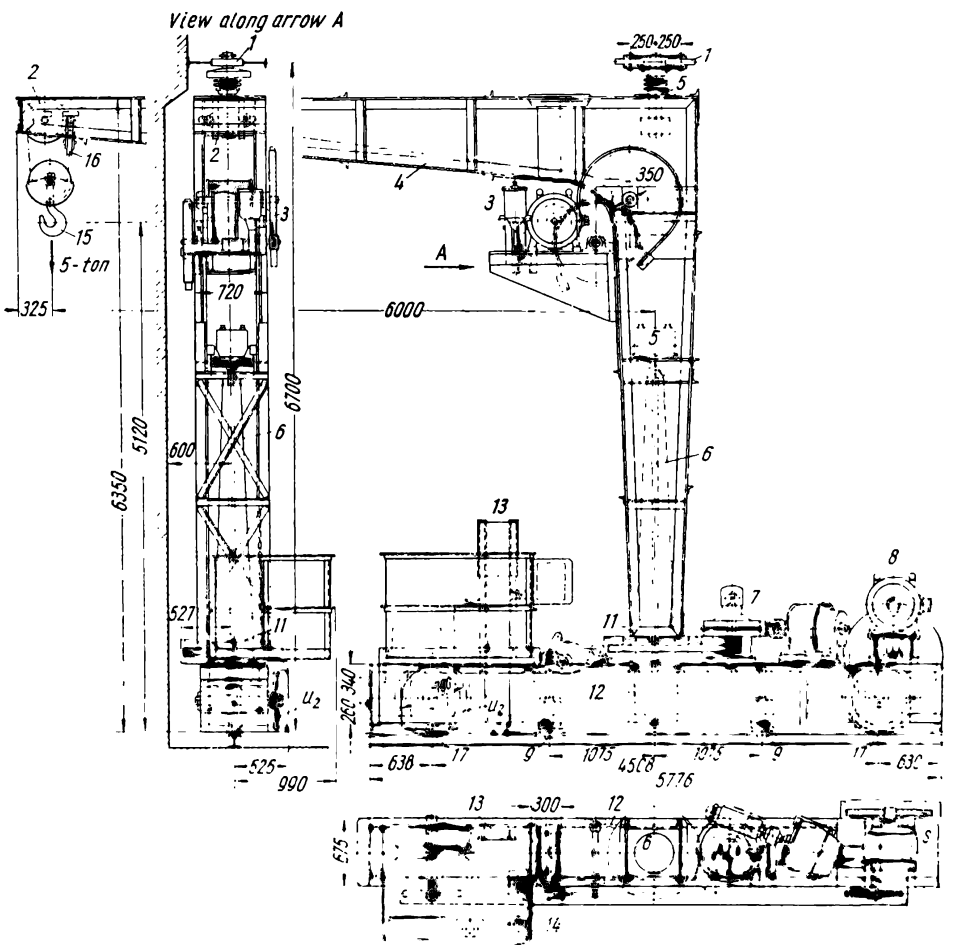

Fig. 186. Monorail crane

1—top horizontal bearing rollers, *2*—guiding pulleys, *3*—hoisting mechanism, *4*—boom, *5*—slip rings, *6*—pillar secured in the truck, *7*—slewing mechanism, *8*—counterweight, *9*—bottom horizontal bearing rollers, *10* and *11*—top and bottom horizontal bearing rollers on the boom, *12*—bottom horizontal bearing rollers on the truck, *13*—distribution box, *14*—controllers, *15*—hook, *16*—counterbalancing pulley, *17*—travelling wheels. Crane operating speeds: hoisting 10.2 m/min, slewing 3.2 rpm, travelling 46.5 m/min.

Checking the adhesive force. When the fully loaded boom is aligned with the direction of motion and is above the first travelling wheel B (see Fig. 185) then one left driving wheel A is subjected to minimum load P_{ver}^{min}. To start the crane without slipping the following condition should be observed: $P_{ver}^{min} f > W_{min}$ or

$$\left(\frac{G_2}{2} + V \frac{\frac{l}{2} - e}{l} \right) f > (V + G_2)_{tons} w_1 . \tag{216}$$

If $P_{ver}^{min} f < W_{min}$, the driving wheel is not loaded sufficiently to engage with the rail and then both wheels should be driving.

The travelling mechanism of a monorail crane (Fig. 186) is designed as follows. Motion is transmitted from the motor through gearing to the right wheel which drives the left wheel by means of a chain.

The chain drive is sometimes replaced by a transmission shaft with two bevel gear drives such as used in travelling mechanisms of cantilever cranes.

In this case it is very important that both bevel pinions are arranged either to the right or left of the driven bevel gears, otherwise the driving wheels will rotate in opposite directions. This requirement holds true both for monorail and cantilever cranes.

Travelling mechanisms of monorail trolleys and hoists. Pulleys suspended from trolleys, monorail hoists and monorail trolleys run along special monorails, sometimes around curves, through switches and turntables. The design of the travelling mechanisms of these devices differs somewhat from those considered earlier due to certain specific features of the trackage.

A hand-pushed trolley is shown in Fig. 187. A hoist trolley propelled by an operating wheel is represented in Fig. 188 while Fig. 189 illustrates a motor-propelled trolley.

Trolley Hoists and Hand-Pushed Trolleys. As has been said above, the friction force in the journals of the travelling wheels as referred to the wheel rim is equal to

$$W_1 = (Q + G_0)\, \mu \frac{d}{D} \tag{217}$$

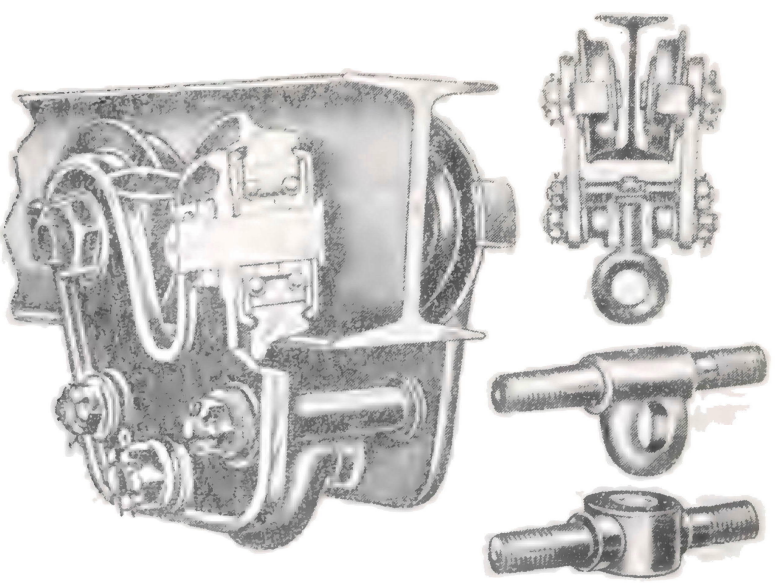

Fig. 187. Hand-pushed trolley

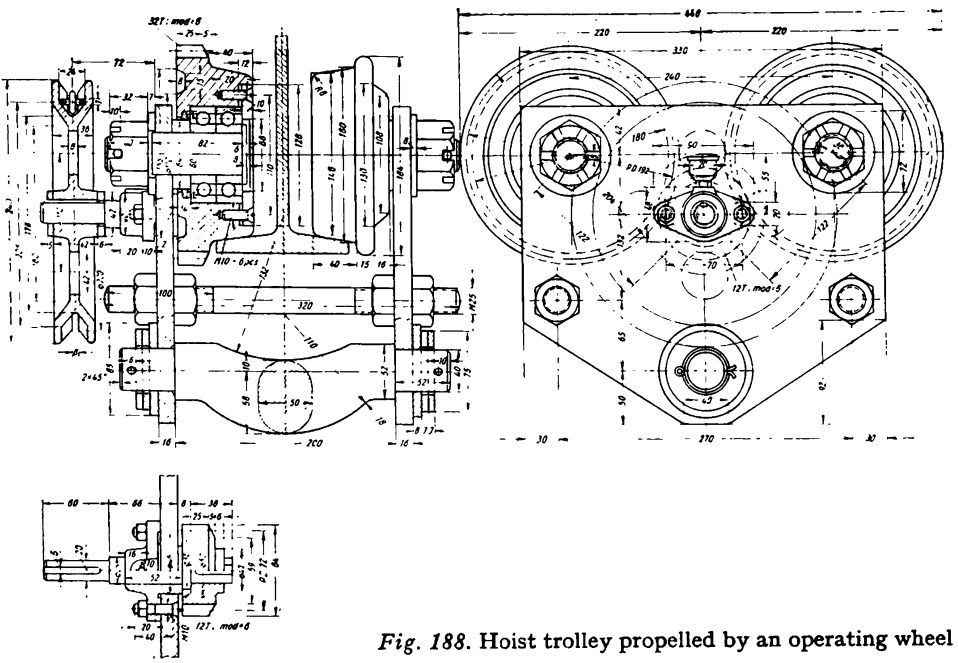

Fig. 188. Hoist trolley propelled by an operating wheel

where Q—weight of the load;
G_0—weight of the trolley and hoist;
d—axle diameter;
D—diameter of the wheel at the mean circle of rolling contact;
μ—coefficient of friction in the wheel bearings.

As indicated above, the friction force on the rim of the wheels due to resistance to rolling on a straight horizontal path is

$$W_2 = (Q + G_0)\frac{2k}{D} \tag{218}$$

where k—coefficient of rolling friction.

Resistance due to cocking of the trolley and to travelling around sharp curves. In travelling around sharp curves and also when the trolley is cocked on a straight track the travelling wheel tends to slip off the rail. To prevent this the wheels are provided with flanges.

In cocking of the trolley the wheel runs as shown schematically in Fig. 190*a*, i. e., one flange contacts the rail thereby producing additional friction. After one full revolution the wheel assumes position *II*. In this case the plane of rotation passing through the point of contact of the rail and flange takes the position O_2O_2. Consequently, cocking is accompanied by lateral slip of the wheel. During one turn this slip equals $\pi D \sin \gamma$ where γ is the angle between the plane of rotation O_2O_2 and the axis of the rail and depends on the distance between the flanges, wheel base and the effective width of contact on the rail.

Resistance due to lateral slip is

$$W_3 = (Q + G_0)\,\mu_1 \sin \gamma\,. \tag{219}$$

Coefficient μ_1 is taken within 0.15-0.2.

On a straight path the angle γ depends on the amount of clearance between the rails and the wheel flanges. Approximately it can be assumed that $\sin \gamma \approx \frac{\delta}{D}$ where δ is the amount of bilateral clearance.

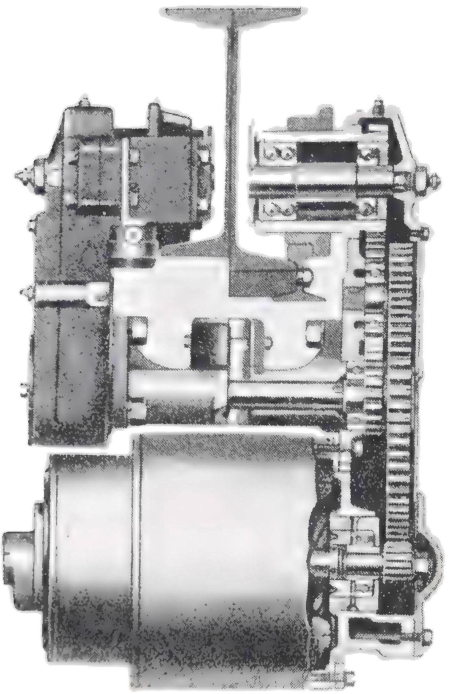

Fig. 189. Motor-propelled truck

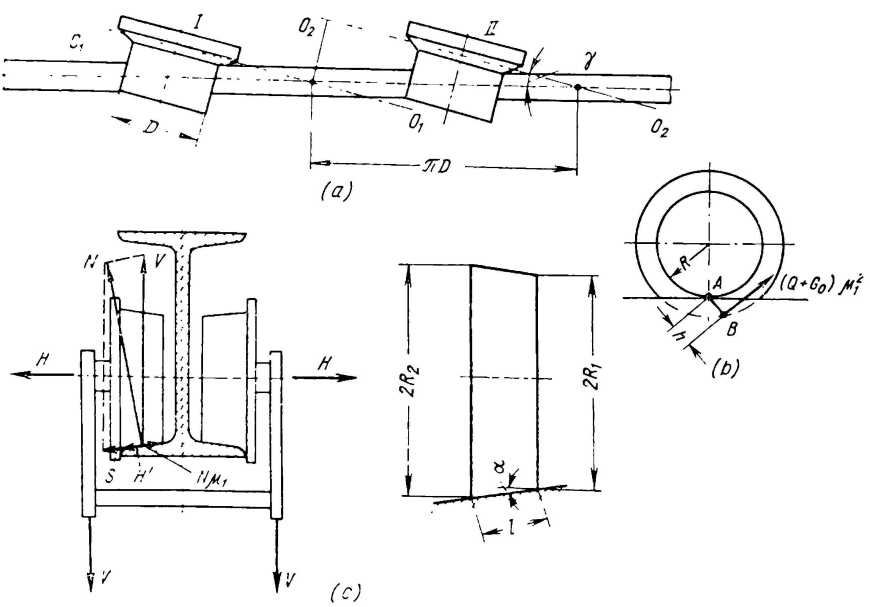

Fig. 190. Diagrams for calculating the resistance of a travelling monorail trolley

Consequently, for a straight path

$$W_3^{st} = (Q + G_0)\,\mu_1 \frac{\delta}{D}. \tag{220}$$

For trolleys having a rigid base the resistance on curves will be

$$W^{cur} = (Q + G_0)\,\mu_1 \frac{l}{2R_s} \tag{221}$$

where l—rigid base of the trolley;
R_s—radius of curvature.

Usually, to reduce the resistance in travelling around curves the ratio $\frac{l}{R_s}$ is taken within the range of $\frac{1}{15}$ to $\frac{1}{20}$ (radius $R_s = 2$ to 3 m).

In addition to the resistance due to lateral slip there will also be losses caused by friction between the flange and the rail. The force with which the flange is pressed to the rail can be assumed equal to $(Q + G_0)\mu_1$; therefore, the friction force will be $(Q + G_0)\mu_1^2$.

The wheel flange contacts the rail at point B (Fig. 190*b*); hence, the friction force applied to this point creates on arm h, relative to the turning point of wheel A, the following moment of resistance to motion:

$$M = (Q + G_0)\,\mu_1^2\, h = W_4^{fl} R.$$

Whence the resistance due to friction of the flanges is

$$W_4^{fl} = (Q + G_0)\,\mu_1^2 \frac{h}{R}. \tag{222}$$

According to engineer V. K. Baranov, the ratio $\frac{h}{R}$ can be taken on an average as $\frac{h}{R} = 0.4$ to 0.7.

In this way the resistance from friction of the flanges is quite appreciable. The amount of resistance can be reduced by replacing the flanges by horizontal rollers which run on the side edges of the runway girder and then

$$W_4^{roll} = (Q + G_0)\,\mu_1 \left(\mu_0 \frac{r'}{R'} + \frac{k'}{R'} \right) \tag{223}$$

where μ_0—coefficient of friction in the journals of the horizontal rollers;
r'—journal radius;
R'—roller radius;
k'—coefficient of rolling friction of the horizontal rollers on the side edges of the beam.

This resistances W_4^{roll} is considerably less than the resistance due to friction of the flanges W_4^{fl}. Fig. 191 shows a monorail trolley with horizontal guiding rollers.

Resistance due to taper of the travelling wheels. When the rail flange is inclined at an angle of α to the horizontal (Fig. 190*c*) the vertical force acting on the wheel $V = \frac{Q + G_0}{2}$ causes the normal reaction $N = V \cos \alpha$ and slipping force $S = V \sin \alpha$ directed along the rail flange.

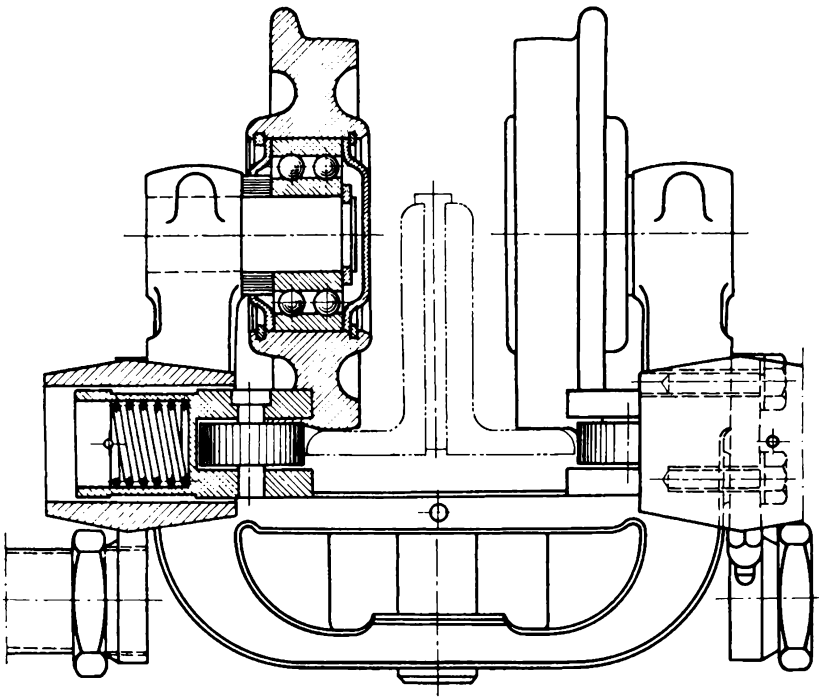

Fig. 191. Monorail trolley with guiding rollers

Slipping will be opposed by friction force $N\mu_2$, which also acts along the rail flange but in the opposite direction. The difference between these forces will give force $H' = S - N\mu_1$ whose horizontal component H forces the wheel hub against the trolley frame:

$$H = H'\cos\alpha = (S - N\mu_1)\cos\alpha = (V\sin\alpha - V\cos\alpha\mu_1)\cos\alpha = \\ = V\cos^2\alpha\,(\tan\alpha - \mu_1).$$

If $\mu_1 \approx 0.17$ and $\alpha \approx 8°$ (standard rolled sections), $H \approx 0$ because $\mu_1 > \tan\alpha$. For this reason friction in the hub from force H is usually neglected.

At large angles of α, in addition to friction in the hub, there also occurs slipping of the travelling wheels on the rail because of their variable diameter. The path of slip for the elementary width dl per revolution of the wheel is

$$\pi(D + 2dl\sin\alpha) - \pi D = 2\pi\sin\alpha\,dl.$$

We take unit pressure as

$$p = \frac{Q + G_0}{l} = \text{const and } R_2 = R_1 + l\sin\alpha.$$

Then the work of slipping per one revolution if it occurs on one of the extreme circles of the wheel will be

$$\int_0^{2\pi} p\mu_1 2\pi\sin\alpha dl = 2\,(Q + G_0)\mu_1\pi\sin\alpha.$$

Hence the resistance due to the taper of the wheels will be

$$W_5 = \frac{2\,(Q + G_0)\,\mu_1\pi\sin\alpha}{2\pi R_{mean}} = (Q + G_0)\frac{\mu_1\sin\alpha}{R_{mean}}. \qquad (224)$$

For $\mu_1 = 0.17$ and $\alpha = 8°$

$$W_5 = 0.024 \frac{Q + G_0}{R}. \tag{225}$$

When the diameter of the wheels is small these resistances are quite appreciable and a spherical-shaped tyre will be more effective than a taper; in this case $W_5 = 0$. A good practice is to incline the wheels (perpendicular to the rolling surface).

In designing trolleys their side plates should be made sufficiently rigid, bearing in mind that a horizontal force $H = (Q + G_0)\mu_1$ which tends to bend or warp the plates may appear when the truck is cocked or travels around curves. If the side plates lack adequate strength, cocking of the wheels may jam the truck completely on sharp curves and large loads may lead to deformation of the rolled rail. This takes place because the wheels no longer bear uniformly on the entire width of the rail thereby overloading the edges.

The total resistance to motion over a horizontal straight path with flanged tapered wheels is

$$W_\Sigma = \Sigma W = (Q + G_0)\left[\mu \frac{d}{D} + \frac{2k}{D} + \mu_1 \frac{\delta}{D} + \mu_1^2 \frac{h}{R} + \frac{0.024}{R}\right]\beta'. \tag{226}$$

For overhead monorail travelling mechanisms the coefficient of resistance to motion will be

$$w = \left[\mu \frac{d}{D} + \frac{2k}{D} + \mu_1 \frac{\delta}{D} + \mu_1^2 \frac{h}{R} + \frac{0.024}{R}\right]\beta' \tag{227}$$

where β'—coefficient accounting for the increase in resistance when travelling through switches and turntables ($\beta' \approx 1.2$).

The transmission ratio and travelling speed for an operating wheel hand drive are determined by formulas (190) and (192).

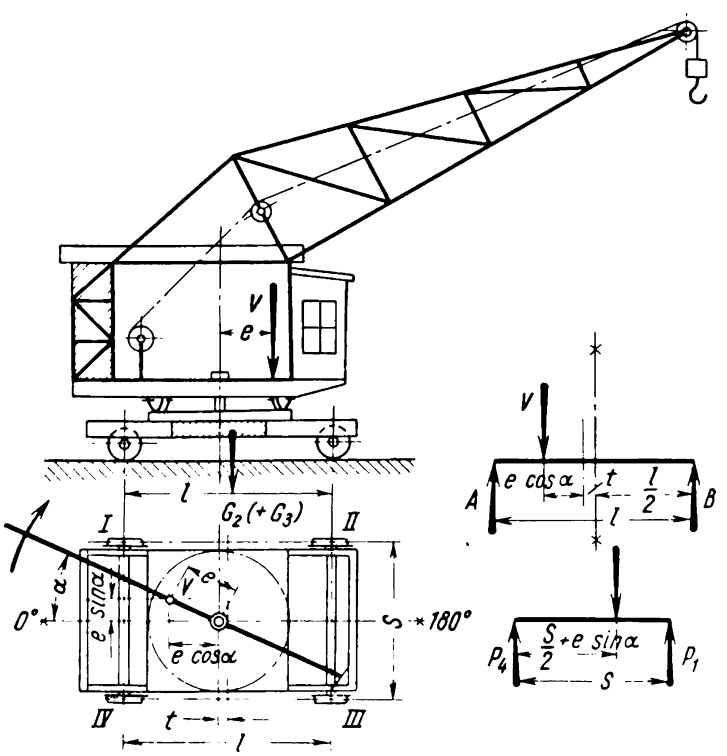

Fig. 192. Diagram of a railway crane

Motor-Propelled Trolley Hoists and Trolleys. The resistance to motion of monorail motor-propelled trolleys and trolley hoists can be found from formula (226); the motor power required for steady motion, transmission ratio and speed of the travelling wheels—from formulas (193), (194) and (195). Adhesion check-up is performed according to formulas (199) and (200).

Travelling mechanisms of railway cranes. A diagram of a railway crane is shown in Fig. 192 and its general view in Fig. 193.

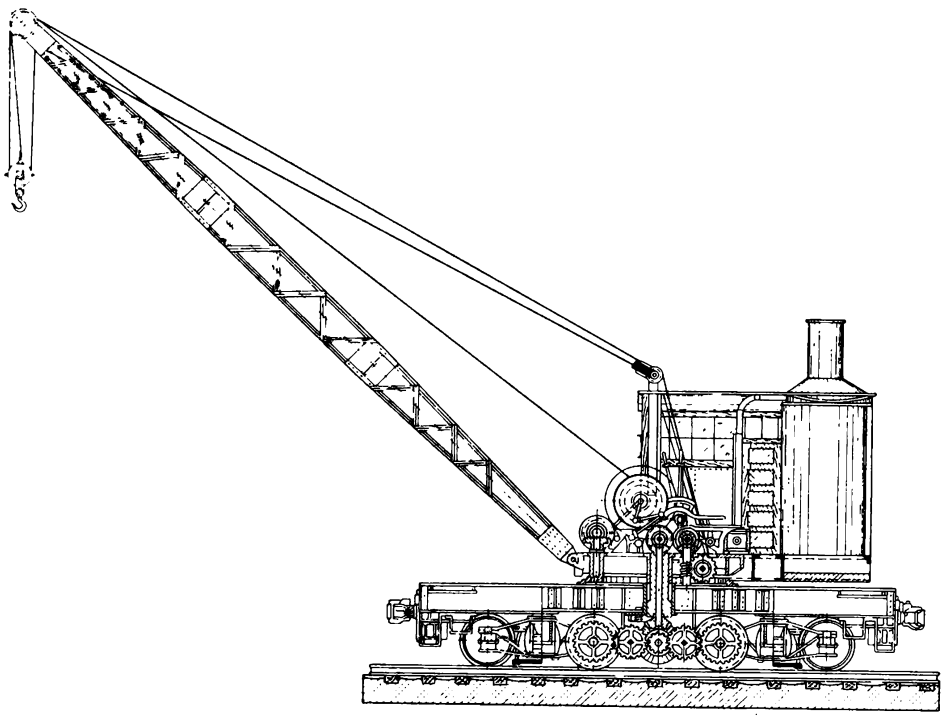

Fig. 193. Railway crane

Wheel loads. The weight of the lower truck G_2 including the weight of the additional counterweight G_3 (if one is used) can be assumed as uniformly distributed over the four travelling wheels (Fig. 192). Consequently, the force exerted on the wheels by the weight of the bottom truck will be

$$P' = \frac{G_2 + G_3}{4}. \tag{228}$$

The force acting on the wheels of a fully loaded crane varies with the position of the boom. For cranes with a turntable (Fig. 192) the force acting on the four driving wheels due to the weight of the revolving superstructure will have the following values:

$$\left.\begin{aligned} P_1 &= \frac{V}{4}\left(1 + 2\frac{e\cos\alpha + t}{l}\right)\left(1 + 2\frac{e\sin\alpha}{S}\right);\\ P_2 &= \frac{V}{4}\left(1 - 2\frac{e\cos\alpha - t}{l}\right)\left(1 + 2\frac{e\sin\alpha}{S}\right);\\ P_3 &= \frac{V}{4}\left(1 - 2\frac{e\cos\alpha - t}{l}\right)\left(1 - 2\frac{e\sin\alpha}{S}\right);\\ P_4 &= \frac{V}{4}\left(1 - 2\frac{e\cos\alpha - t}{l}\right)\left(1 - 2\frac{e\sin\alpha}{S}\right). \end{aligned}\right| \tag{229}$$

In these equations V—resultant of all vertical forces acting on the crane from the loaded revolving structure;

α—slew angle of the boom;

l—distance from the point of application of the resultant force to the slewing axis;

t—distance from the centre of the bottom truck to the turntable axis if the axes of the truck and turntable do not coincide;

$V = Q + G_1 + G_{cw}$ (Q—weight of the load, G_1—weight of the revolving structure, G_{cw}—counterweight).

Equations (229) hold true for any angle from 0 to 360° and for any value of e and t. These formulas are derived from the assumption of a rigid nondeforming platform according to the usual laws of statics.

The maximum force acting on the wheels is

$$P_{\Sigma}^{max} = P^{max} + P' \tag{230}$$

where P^{max}—maximum force exerted by the weight of the fully-loaded revolving structure.

This pressure is complemented with loads due to the wind force which act on the vertical surface of the crane and which can be found in the same way as forces acting on the bearing rollers of live-ring (turntable) cranes.

Force acting on the axle. The force acting on the axle depends on the weight of the bottom truck and the resultant of all the upper forces. The maximum and minimum forces act on the axles when the boom is aligned with the direction of motion (Fig. 192) (over axle *I-IV*), i. e.,

$$\left.\begin{aligned} P_{1\text{-}4}^{max} &= 2P' + A \approx \frac{G_2 + G_3}{2} + V\,\frac{\frac{l}{2} + e + t}{l}; \\ P_{2\text{-}3}^{min} &= 2P' + B \approx \frac{G_2 + G_3}{2} + V\,\frac{\frac{l}{2} - e + t}{l} \end{aligned}\right\} \tag{231}$$

This method for determining the forces acting on the wheels and axles of railway cranes with a turntable gives practically acceptable but only approximate values; precise calculation is extremely difficult because of the elastic strains in the bottom truck. Equations (229) can be used only for a tentative determination of force exerted on the wheels.

If the design wheel load exceeds the safe load, eight travelling wheels, instead of four, are mounted in standard railway trucks (Fig. 193).

Resistance to motion. The total weight of the moving crane can be expressed by the following formula:

$$Q + G_{cr} = Q + G_1 + G_{cw} + G_2 + G_3 \tag{232}$$

where Q—weight of the load;

G_{cr}—weight of the crane.

At established speed the total resistance to motion of a railway crane will be

$$W_{tot} = (Q + G_{cr})\,(w_{fr} + w_w + w_R + w_{gr}) \tag{233}$$

where w_{fr}—unit resistance due to friction forces, in kg/t;

w_w—unit resistance due to head wind, in kg/t;

w_R—unit resistance on curves, in kg/t;

w_{gr}—unit resistance due to gradient, in kg/t.

The following mean values of unit resistance can be taken for steady motion: $w_{fr} = 2$ kg/t; $w_w = 3$ kg/t; $w_R = 5$ kg/t; $w_{gr} = 12$ to 20 kg/t (standard gradient $i = 1.2\%$; gradient of 2% is maximum for local-gauge tracks).

The power developed by the motor is determined for steady motion from the maximum assigned speed.

Checking for adhesive force. This check-up is performed by formulas (199) and (201) for $f = 0.15$. If these formulas fail to give adequate values, either the adhesive weight of the crane should be increased or the design grade of the track reduced.

Runway Rails

Depending on their purpose runway rails for cranes can be classified into the following groups:

1. Rails for trolleys of overhead travelling cranes and for travelling mechanisms of hand-propelled overhead cranes (beams or bars). They are manufactured from flat steel with rounded or chamfered corners and with convex rolling surfaces.

Standard dimensions of rails made of flat steel are given in Table 35.

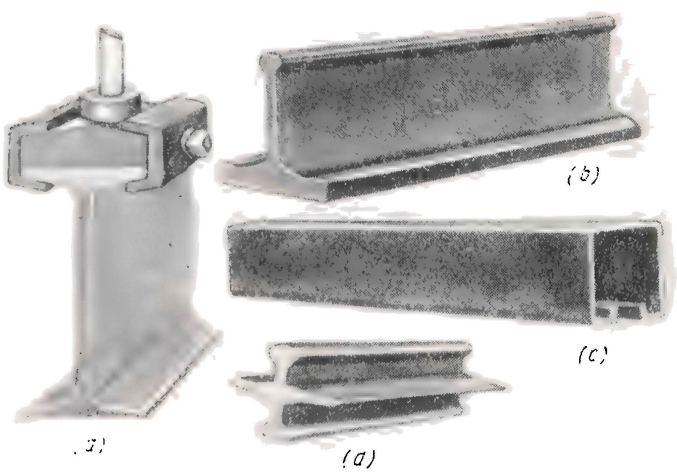

Fig. 194. Monorails

2. Special runway rails for overhead travelling cranes are provided with a broad base and are small in height. They possess a comparatively large moment of inertia. The dimensions and characteristics of these rails are listed in Tables 36 and 37.

3. Rails for monorail, railway, gantry and other types of cranes.

4. Monorails for travelling hoists and trolleys. These rails are designed in a a variety of sections: I-section (Fig. 194*a*), special T-section (Fig. 194*b*), box section (Fig. 194*c*), X-section (Fig. 194*d*), etc. I- and T-profiles are the most popular types.

Travelling Wheels

Travelling Wheels for Monorails. Wheels which travel on the upper flanges of I-beams are employed only in hand-propelled trolleys (Fig. 195*a*); driving wheels are cast integral with a toothed gear.

Wheels which travel on the lower inclined flanges of I-beams (Fig. 194*b*) are always mounted in pairs; for a vertical position they are made with a tapered (slightly convex) tread to conform to the slope angle of the flanges (14%). The wheel tread is inclined at $\sim 8°$ to the horizontal.

Recent practice is to mount travelling wheels at an angle to obtain full bearing with the I-beam flanges. This arrangement avoids additional slipping otherwise caused by the variable diameter of the tapered wheels. The cylindrical rolling surface of a wheel mounted at an angle is also made slightly convex.

Table 35

Rails of Flat and Square Steel for Overhead Travelling Cranes

1. Runway girder.

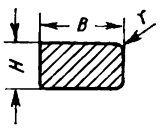

Designation of a runway girder 100×85 mm in cross-section and 5,000 mm long:

Runway girder 100×85; l = 5,000 to 8,000 mm

B	*H*	*r*	Weight per running metre, kg	Length, m	
				minimum	maximum
100	85	15	65.5	5	8
120		14	78.79		

2. Rail of flat steel.

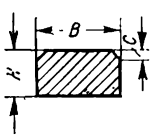

Designation of flat steel 80×40 in cross-section and 5,000 mm long: ⊠ 80×40, l = 5,000

B	*H*	*C*	Weight per running metre, kg	Length, m	
				minimum	maximum
80	40	5	25	5	8
90	50		35		

3. Rail of square steel.

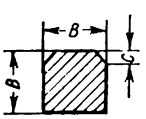

Designation of square steel 40×40 in cross-section: ⊠ 40×40, l = 5,000

B	*C*	Weight per running metre, kg	Length, m	
			minimum	maximum
40	3	12.6		
50		19.6		
			5	7
60	4	28.3		
70		38.5		
80	5	50.3		
90		63.6		
			5	6
100	6	78.5		

Table 36

Special Rails for Overhead Travelling Cranes

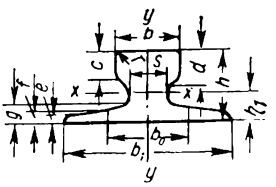

Shape No.	Size, mm											Weight per running metre, kg
	h	*b*	*c*	*d*	*s*	*r*	b_1	b_0	*e*	*f*	*g*	
1	55	45	20	23.5	24	3	125	54	8	11	14.5	22.5
2	65	55	25	28.5	31	4	150	66	9	12.5	17.5	32.2
3	75	65	30	34.0	38	5	175	78	10	14.0	20.0	43.8
4	85	75	35	39.5	45	6	200	90	11	15.5	22.0	57.0

Table 37

Characteristics of Rail Cross-Sections and Maximum Permissible Load on Wheels

Shape No.	Cross-sectional area *F*, sq cm	Distance to centre of gravity η, mm	Moments of inertia		Moments of resistance		Maximum wheel load P_{max}, kg at k*			Diameter of travelling wheel *D*, mm
			I_x, cm⁴	I_y, cm⁴	W_x, cm³	W_y, cm³	40	50	60	
1	28.7	22.7	94.05	182.4	29.12	29.18	6,240	7,800	9,360	400
2	41.01	26.8	180.4	352.6	47.2	47.0	11,280	14,100	16,920	600
3	55.8	30.6	328.6	646.12	74.0	73.8	17,600	22,000	26,400	800
4	72.6	35.2	523.4	988.7	105.1	98.87	25,200	31,500	37,800	1,000

* Here k is the unit pressure which depends on the travelling speed and the operating conditions. For a cast steel wheel k = 40 to 60 kg/cm², for a cast-iron wheel k = 15 to 40 kg/cm².

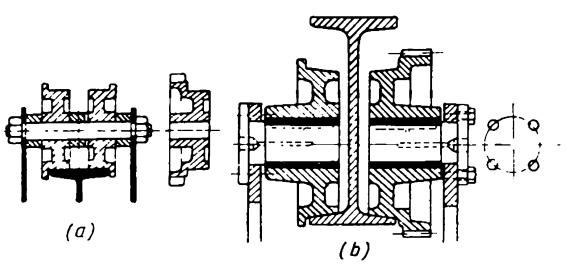

Fig. 195. Monorail trolleys travelling on upper and lower flanges of I-beams

Travelling wheels are usually mounted freely on axles secured in the side plates of a trolley and run either on bronze bushings or rolling friction bearings. The side plates of the truck are subject to bending and tension and should therefore be sufficiently strong. The plates can be manufactured from thick plate steel, from cast iron or steel castings. For hand trolleys use can be made of cast-iron wheels without bronze bushings; a power drive requires wheels made of steel castings and provided with bearings.

For special T-section rails the wheels are also made with a slightly convex tread.

Travelling Wheels for Flat Steel Rails, and for Crane and Railway Rails. Wheels for power-driven cranes are made of steel castings or with shrink-fitted forged steel tyres. Cast-iron wheels can be used with all hand cranes; their application in power-driven cranes is limited to wheel loads of 5 tons and a maximum travelling speed of 30 m/min.

Travelling wheels may be fixed on an axle or revolve freely on it on bronze bushings or rolling friction bearings. All types of cranes (cantilever, overhead, gantry, etc.), except cranes travelling on standard gauge railway tracks and also crane trucks, should be provided with double-flanged wheels allowing for a certain clearance on each side (for truck wheels minimum 10 mm and for crane wheels 10-20 mm). The profile of the wheel inner flange of a rotary railway crane is designed in the same way as for standard railway car wheels. As a rule, wheels with such flanges are rigidly mounted on axles of which one (and sometimes both) are driving.

If the diameter of the driving wheel $D<300$ mm the driving gear is rigidly mounted directly on its hub. Driving wheels of a larger diameter have the gear attached by bolts, which are protected against shear by means of relieving rings. The gear should be located on the travelling wheel by means of shoulders or recesses. The axles of the travelling wheels are usually secured in the channels of the frame by axle holders. Since in this case the wheel hubs should not be in direct contact with the channel webs or gusset plates they are separated by spacer sheets. Travelling wheels for heavy-duty cranes are provided with shrink-fitted steel tyres.

In recent years wheels with axle boxes bolted to the steel structure are being widely employed. This design is much simpler in servicing and facilitates easy wheel removal which is especially convenient in repairing the crane travelling gear.

At present the axles of travelling wheels are often designed with rolling friction bearings instead of bronze bushings.

Runners (Flangeless Track Wheels). Such runners are employed when the wheel is not subject to any (even occasional) lateral loads. They are used in monorail and cantilever cranes, overhead travelling cranes with a jib, in rotary cranes with a turntable, etc. As a rule, runners rotate on bronze bushings or rolling friction bearings mounted on the axles and their tread is slightly convex.

Design of Travelling Wheels. Travelling wheels are checked for strength and wear, according to the theory of contact stresses, in the following sequence.

In determining the diameter of a travelling wheel we should proceed from the local unit compressive stress determined by the following formulas:

(a) for wheels with parallel treads running on flat-head rail:

1) for a steel wheel

$$\sigma_{1max} = 600 \sqrt{\frac{Pk}{br}} \text{ kg/cm}^2; \tag{234}$$

2) for a cast-iron wheel (cast iron 35-56)

$$\sigma_{1max} = 400 \sqrt{\frac{Pk}{br}} \text{ kg/cm}^2; \tag{235}$$

(b) for wheels with tapered treads running on convex-head rail:

1) for a steel wheel

$$\sigma_{2max} = 4{,}000 \sqrt[3]{Pk\left(\frac{1}{r_1} + \frac{1}{r_2}\right)^2} \text{ kg/cm}^2; \tag{236}$$

2) for a cast-iron wheel

$$\sigma_{2max} = 2{,}500 \sqrt[3]{Pk\left(\frac{1}{r_1} + \frac{1}{r_2}\right)^2} \text{ kg/cm}^2. \tag{237}$$

In both cases the working width of the rail should not be less than the width obtained for wheels of the given diameter and load on the assumption that the rail is flat and the wheel has a parallel tread.

In the above formulas:
P—load acting on the wheel, in kg;
b— width of the working face of a flat-head rail, in cm;
r_1 and r_2—radii of parallel and tapered tread wheels, in cm (for a tapered tread wheel r_2—radius at the central part of the rim);
r_1—radius of the rail head, in cm;
k— coefficient accounting for the rolling speed of the wheel determined from the formula $k = (1 \text{ to } 0.2)v$ where v is the rolling speed of the wheel, in m/sec.

The local compression stresses obtained from formulas (234) to (237), inclusive, should not exceed the values indicated in Table 38.

Table 38

Characteristics of Materials for Travelling Wheels

Materia				Safe local unit compressive stress, kg/cm²	
Grade and condition	Ultimate strength, kg/cm²	Yield point, kg/cm²	Bhn	Parallel tread wheel on flat-head rail	Tapered tread wheel on convex-head rail
Cast iron 35-56	7,200	—	170-230	3,500	9,500
Steel 55Л	6,000	3,000	170	6,000	16,500
Steel 3	3,800-4,500	2,200	110-130	4,000	10,500
Steel 5	5,000-6,000	2,900	130-170	5,250	14,000
Hardened steel 3	6,800-8,200	4,500	220-260	7,600	18,000
Steel 6	6,000-7,000	3,400	150-200	6,000	16,000
Hardened steel 6	8,000-9,500	5,000	240-260	8,000	20,000
Steel 65Г	6,000-7,000	4,200	165-200	7,000	17,000
Hardened steel 50Г2	12,000	10,000	350	8,500	24,000

The following values of Brinell hardness for the rolling surfaces of the travelling wheels can be recommended depending on the operational duty of the cranes:
(a) for light-duty cranes—170-200;
(b) for medium- and heavy-duty cranes—240-350.

Operational practice has shown that wheels with parallel treads are subject to rapid wear when used in heavy-duty cranes. Best performance is obtained with tapered travelling wheels.

2. TRACKLESS TRAVELLING MECHANISMS

Crawler Mechanisms

Crawler mechanisms are used in travelling rotary cranes and various loaders. Fig. 196 shows the crawler travelling mechanism of rotary cranes.

Crawler tread (Fig. 196) comprises separate cast links hinge-jointed with pins. The load due to the weight of the crane is transmitted through roller trucks directly to the crawler treads (to their inner surface) resting on the ground.

As the crawler chain moves the roller trucks run over it so that it acts as a continuous rail track. A crawler crane is turned round by braking one crawler chain, i. e., by reducing its speed or by stopping it completely. Due to their large adhesive force crawler travelling mechanisms can negotiate larger gradients than rail transport.

Safe unit pressures on the ground depending on its features and condition vary for crawler cranes from 0.8 to 15.0 kg/cm².

Rubber-Tyred Mechanisms

A general view of a rubber-tyred crane is shown in Fig. 197. The most frequently employed tyre design is a solid rubber rim fitted onto the wheel spider. This is dictated both by specific operation conditions of cranes and high loads exerted on the wheels. A recent innovation is tubeless low-pressure tyres (1.7-2 atm).

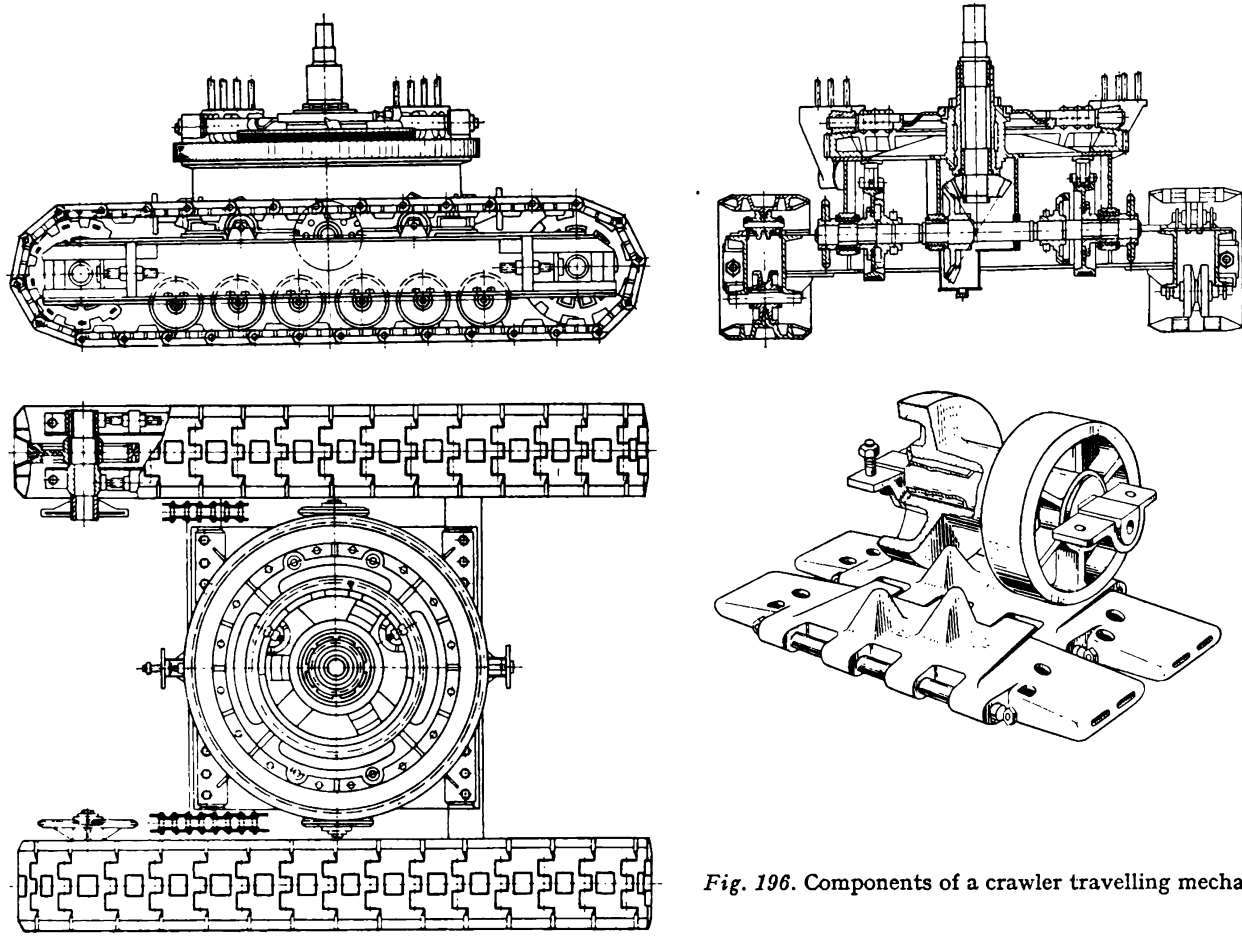

Fig. 196. Components of a crawler travelling mechanism

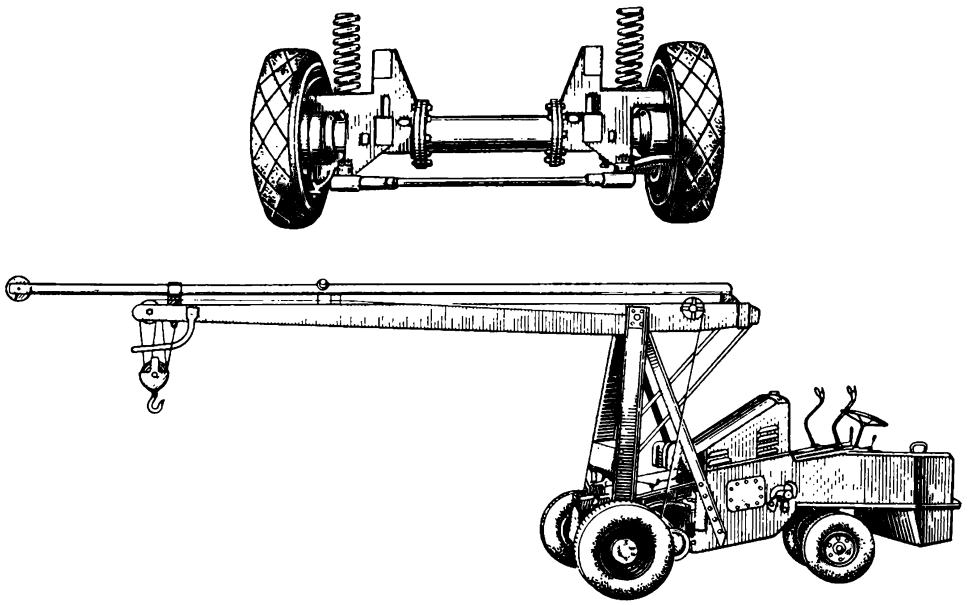

Fig. 197. Rubber-tyred crane

The resistance which arises during the travel of a rubber-tyred crane (disregarding head wind) can be determined by the following formula:

$$W = G\,(\cos \alpha w \pm \sin \alpha) \tag{238}$$

where G—full weight of the crane;
w—coefficient of resistance to motion;
α—terrain gradient; plus sign is for ascent, minus sign for descent.

The adhesive force is found from the formula

$$Z = k_1\, G_0 \cos \alpha \tag{239}$$

where G_0—adhesive weight of crane applied to the driving wheels;
k_1—coefficient of adhesion of the wheels with the ground.

The load on the crane wheels due to the weight of the revolving structure can be found from formula (229); to obtain full load the weight of the truck should be added to the obtained values.

The values of coefficients w and k_1 are as follows:

	w	k_1 for solid rubber tyres	k_1 for pneumatic tyres
Concrete road	0.0135	0.5 -0.6	0.6 -0.75
Asphalt road	0.015	0.25-0.35	0.35-0.45
Cobblestone road	0.04	0.35-0.4	0.45-0.55

For pneumatic tyres the value of w should be reduced by 10-15 per cent.

CHAPTER X

SLEWING, JIB AND LUFFING GEAR

1. SLEWING MECHANISMS

Depending on the design of the supporting members crane slewing mechanisms may be classified into the following three groups.

1. The crane superstructure turns together with the pillar or post in bearings usually erected on a foundation or attached to building columns.

2. The crane superstructure turns about a pillar fixed on a foundation or in the crane truck.

3. The crane turns around a central pivot shaft secured in its nonrevolving part; the turntable of the crane rests on a number of rollers running on a rail bent into a circle and erected on a foundation or on the crane truck.

Slewing Mechanisms of Cranes with a Rotary Pillar. Fig. 198 shows a crane with a rotary pillar. The upper support, fastened to the building column, is provided with a radial bearing and the bottom support, erected on a foundation, with a radial and thrust bearing. This crane is usually slewed by hand by pushing on the load. However, loads from 5 tons and up require an electric motor for slewing.

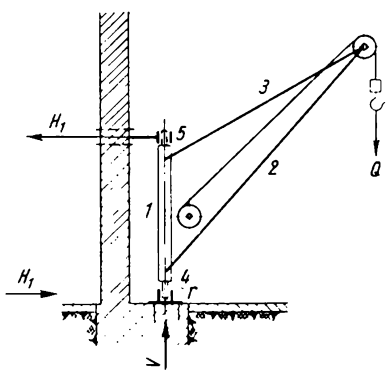

Fig. 198. Diagram of a crane with a rotary pillar

1– pillar, *2* – boom, *3*– guy, *4*– lower support, *5*– upper support

Pillar supports. The top and bottom pivot pins of the pillar are usually secured in holders. One design of a bottom pivot pin (journal) is shown in Fig. 199*a*. This journal is subjected to bending by the horizontal force H_1 and to compression by the vertical force V.

The bending moment in the critical cross-section is

$$M_1 = H_1 y_1 .$$

The bending moment below the shoulder is

$$M = H_1 y$$

where

$$H_1 = \frac{1}{h}(Qa + G_e); \quad V = Q + G$$

(Q –weight of the load; G –weight of the crane).

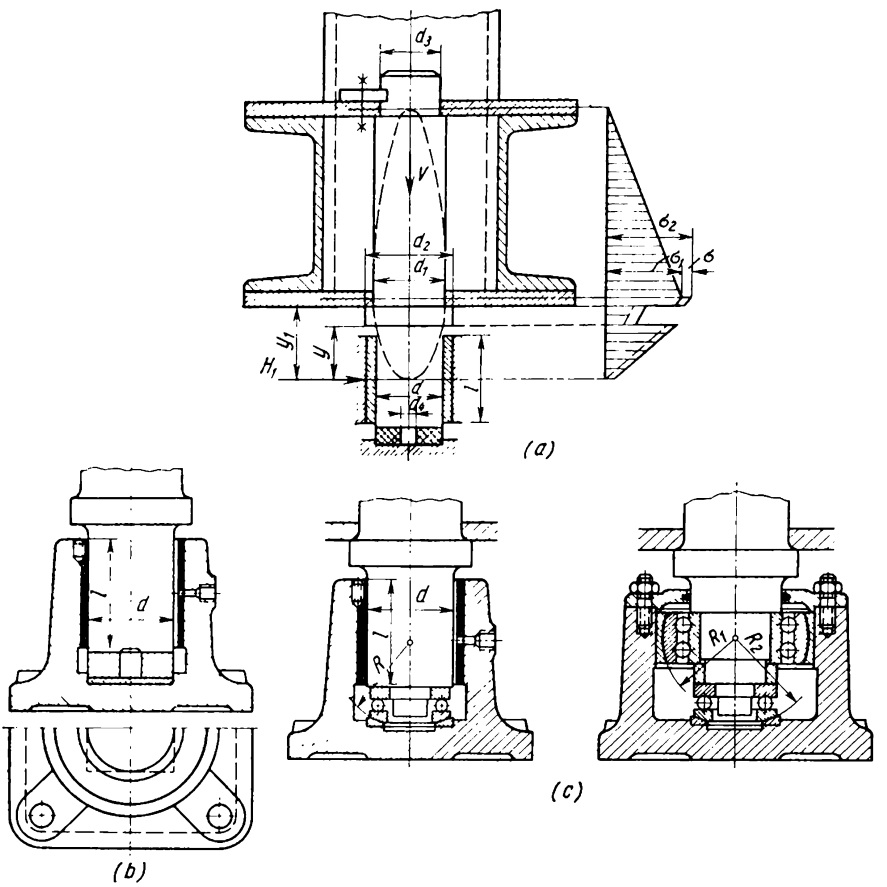

Fig. 199. Design of the bottom support of a rotary pillar

The resultant stress will be

$$\sigma_{\Sigma} = \pm \sigma_{bend} - \sigma_{com} = \pm \frac{H_1 y_1}{\frac{\pi}{32} d_1^3} - \frac{V}{\frac{\pi}{4} d_1^2} \leqslant [\sigma_{com}] . \qquad (240)$$

The lower plate should also be checked for unit pressure between the journal and the plate (pressure on the walls of the hole from force H_1 and the vertical pressure between the journal shoulder and plate from force V).

The design of a bottom sliding friction support is shown in Fig. 199*b* (radial sliding friction bearing). Fig. 199*c* shows other designs of bottom supports with rolling friction bearings.

The design of a top radial bearing is illustrated in Fig. 200*a* and welded bearing housings in Fig. 200*b*.

Resistance to slewing. The moment of resistance due to friction forces relative to the slewing axis is

$$M = Wa = V\mu_1 \frac{2}{3} r + H_1 \mu_2 r + H_1 \mu_3 r_1 . \qquad (241)$$

Here $M = M_1 + M_2 + M_3$ (M_1—moment from the resistance in the thrust bearing; M_2 and M_3—moments from the resistance in the bottom and top journals). The formula includes moment $M_1 = V\mu_1 \frac{2}{3} r$ for an unrecessed thrust bearing. In a

thrust bearing with an annular bearing surface (see Fig. 199*a*) the moment of resistance due to friction is equal to

$$M_1 = V\frac{2}{3}\mu_1\frac{\left(\frac{d}{2}\right)^3-\left(\frac{d_0}{2}\right)^3}{\left(\frac{d}{2}\right)^2-\left(\frac{d_0}{2}\right)^2} \qquad (242)$$

and in a step bearing with a ball for the bearing surface to

$$M_1' = Vr\mu_0\,. \qquad (243)$$

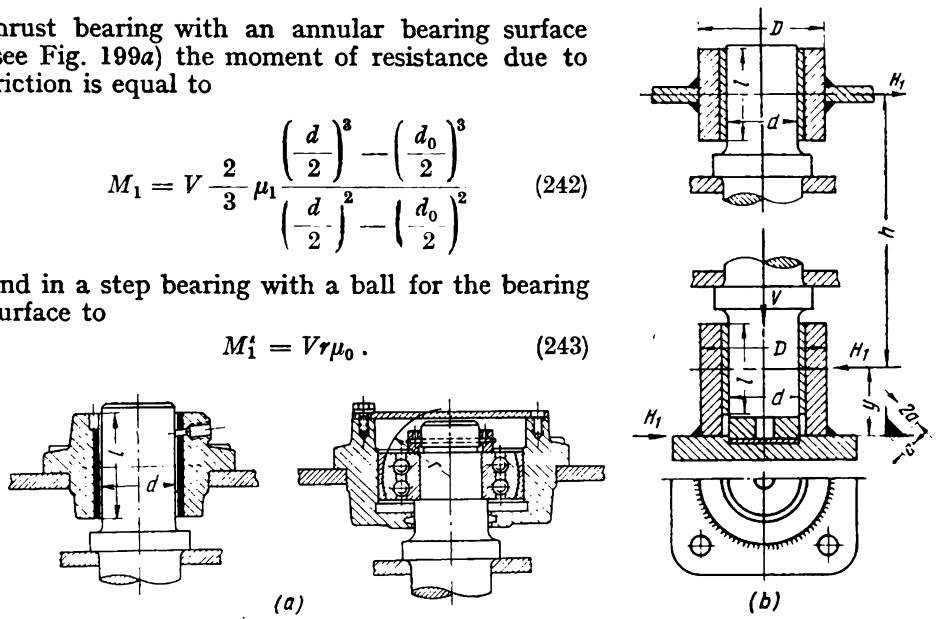

Fig. 200. Design of the upper support of a rotary pillar

In these formulas:

W—resistance to slewing at the end of the boom;

a—boom outreach;

$r=\frac{d}{2}$—radius of the pivot;

μ_1—coefficient of sliding friction in the thrust bearing;

$V=Q+G$—vertical force due to the weight of the load and crane;

d—diameter of the bottom journal;

d_0—inner diameter of the annular thrust bearing (or diameter of the recess);

H_1—horizontal reaction in the supports;

μ_2 and μ_3—coefficients of friction in the bottom and top radial bearings;

r_1—radius of the top journal;

μ_0—coefficient of friction in the ball-type step bearing as referred to the journal diameter.

Formula (241) disregards the resistance to slewing W_w due to wind pressure. This resistance should be taken into account for cranes which are to operate in the open.

Slewing mechanism drive. In hand slewing the effort applied by the operator to turn the crane is

$$P = \frac{W}{\sin\alpha}$$

where α—deflection of the pull rope from the vertical in slewing (α is taken up to 45°);

W—resistance to slewing acting at the end of the boom.

With a power drive and at steady motion the power developed by the motor will be

$$N = \frac{Wv}{75\eta}\ \text{hp}$$

where v—speed at the end of the boom, in m/sec;

η—drive efficiency.

The transmission ratio between the motor and the revolving structure of the crane is

$$i = \frac{n_{mot}}{n_{cr}}; \quad n_{cr} = \frac{60v}{2\pi a}$$

where n_{mot}—rpm of the motor;
n_{cr}—rpm of the crane revolving structure;
a—outreach of the crane boom.

Slewing Mechanisms of Cranes with a Fixed Pillar. Let us examine by way of example a monorail crane (see Fig. 186). In this crane fixed pillar *6* is secured in the bottom truck; the crane boom bears against this pillar which carries all vertical and horizontal forces arising during crane operation and transmits them to the rails and foundation through the bottom truck. The top journal of the pillar is provided with radial and thrust bearings secured in a special girder of the crane frame. The lower horizontal force is transmitted from the radial roller bearing to a special cylindrical projection of the pillar where it is built into the truck.

Crane pillar. The pillar (Fig. 201) is manufactured from forged open-hearth steel, has a conical shape and is provided on the top with a cylindrical journal and at the bottom with a tapered end which is fitted into the foundation plate (stationary rotary cranes) or into the frame of a truck (for example, a monorail crane). The pillar is subject to bending from the moment $H_f h$ and to compression from vertical force V. Forces V and H_f are determined from formulas (205) and (206). The critical section of the pillar is at the built-in end. The length of the pillar between the top journal and the bottom cylindrical projection for the roller bearing is not machined.

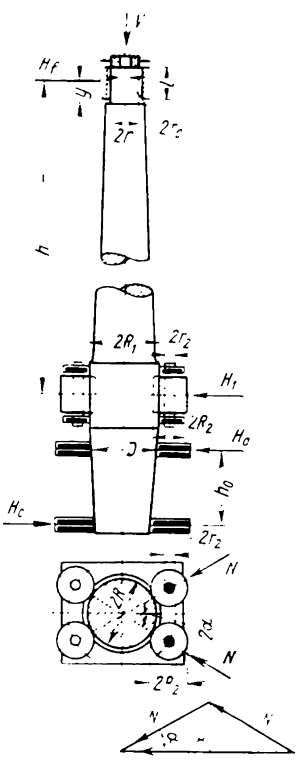

Fig. 201. Fixed pillar of a crane

The diameter D of the pillar at the critical cross-section is found from the required moment of resistance for bending since the compressive force V is so small here that it can be neglected.

$$W = \frac{M_{max}}{\sigma_{bend}} = \frac{Qa + G_1 l_1 - G_g l_g}{\sigma_{bend}} = \frac{\pi d^3}{32} \text{ cu cm} \qquad (244)$$

where Q—weight of the load;
a—crane outreach;
G_1—weight of the crane revolving structure;
l_1—arm of the resultant of weight G_1;
G_g—counterweight;
l_g—counterweight arm relative to the slewing axis.

The resultant stress in the top journal (Fig. 201) is

$$\sigma\Sigma = \pm \sigma_{bend} - \sigma_{com} = \pm \frac{H_f y}{\frac{\pi d^3}{32}} - \frac{Q + G_1 + G_g}{\frac{\pi d^2}{4}} < [\sigma_{com}] \qquad (245)$$

where $d = 2r$.

Inasmuch as the theoretical shape of the pillar between the points of application of the upper and lower horizontal forces H_f will be a cubic parabola it should be constructed before proceeding to design the pillar.

Fig. 202 shows diagrams of the moments and stresses for checking calculations of the pillar cross-sections. The following method can be adopted for graphically determining the maximum deflection of the pillar at the point of application of the upper horizontal force H_f. In determining deflections, due to the variable section of the

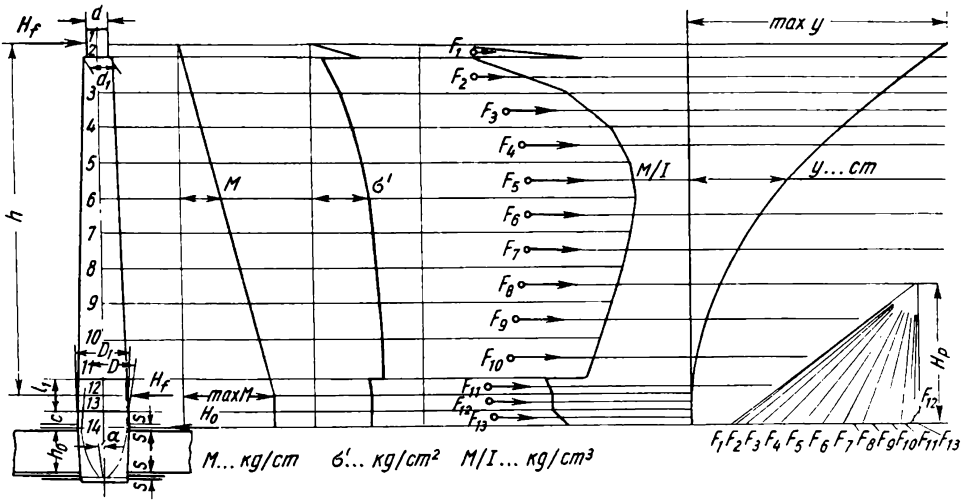

Fig. 202. Graphical solution of a fixed pillar

pillar, a $\frac{M}{I}$ diagram should be plotted first and this fictitious load applied to a fixed beam. The area of $\frac{M}{I}$ is divided into a number of sections F_1-F_{13} with the loads concentrated in their centres of gravity. Individual sections of the diagram are regarded as fictitious forces and the elastic line is constructed as a funicular curve. The maximum deflection will occur at the point of intersection of the last line or string and the upper horizontal force H_f.

The maximum deflection will be

$$\delta_{max} = \frac{1}{E\ (\text{kg/cm}^2)} \left[H_p\ (\text{cm}) b \left(\frac{\text{kg/cm}^2}{\text{cm}} \right) \right] \left| y_{max}\ (\text{cm}) \times a_1\ (\text{cm/cm}) \right| \qquad (246)$$

where E—modulus of elasticity ($E \approx 2{,}100{,}000$ kg/cm²);

H_p—pole distance;

b—scale of stresses, in $\frac{\text{kg/cm}^2}{\text{cm}}$;

y_{max}—maximum ordinate of the elastic line, in cm;

a_1—length scale.

The recommended scales are: $H_p = 10$ cm; $b = 1{,}000$ $\frac{\text{kg/cm}^2}{\text{cm}}$ and $a_1 = 10$ cm/cm.

The following ratio of the maximum deflection of the pillar to the crane outreach is permissible:

$$\frac{\delta_{max}}{a} = \frac{1}{400} \text{ to } \frac{1}{300}.$$

Disregarding the change in the shape and length of the frame girders the approximate deflection value at the end of the boom will be

$$\delta_a = \delta_{max} \frac{a}{h}$$

The lower conical end of the pillar has a taper of tan $\alpha = 0.04$ to 0.07.

The horizontal reaction at the built-in end (Fig. 201) is

$$H_0 \quad H_f \frac{h}{h_0}$$

Pillar crosspiece. The crosspiece (Fig. 203*a*) transmits to the bearing journal of the pillar the weight of the load being raised and the weight of the crane revolving structure as well as the upper horizontal force. As a rule, crosspieces are made of steel and are attached on side trunnions to the crane framework. They are subject to bending from vertical force V and horizontal force H_f (see Figs 201 and 203*b*). The critical section is in the middle of the crosspiece. The maximum bending

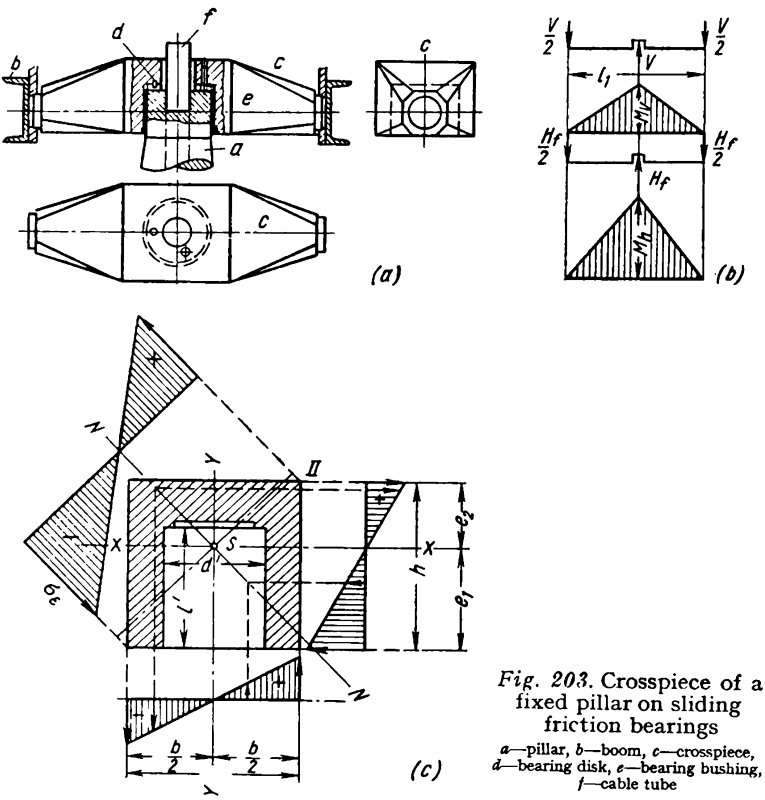

Fig. 203. Crosspiece of a fixed pillar on sliding friction bearings
a—pillar, *b*—boom, *c*—crosspiece, *d*—bearing disk, *e*—bearing bushing, *f*—cable tube

moment is $M_v = V \frac{l_1}{4}$ in a vertical plane and $M_h = H_f \frac{l_1}{4}$ in a horizontal plane.

The shape of the critical cross-section is shown in Fig. 203*c*.

After determining the distance to the extreme fibres e_1 and e_2, moments of inertia I_x and I_y and moments of resistance

$$W_1 = \frac{I_x}{e_1}; \; W_2 = \frac{I_x}{e_2} \text{ and } W_y = \frac{I_y}{\frac{b}{2}}, \tag{247}$$

the bending stresses σ_v and σ_h in both loaded planes should be determined as well as the resultant stress $\sigma\Sigma$. The maximum unit compression stress will be on fibres I:

$$\sigma_{com} = -\frac{M_v}{W_1} - \frac{M_h}{W_y}. \tag{248}$$

The maximum unit tensile stress will be on fibres II:

$$\sigma\Sigma = +\frac{M_v}{W_2} + \frac{M_h}{W_y}. \tag{249}$$

The compression stress has the larger value.

Fig. 203*c* shows the distribution of the resultant stresses $\sigma\Sigma$ relative to axis *NN* plotted through the points of intersection of the directions of the respective stresses σ_v and σ_h.

The crosspiece trunnions are checked for bending due to one half of the resultant pressure $P=\overline{H_f}+\overline{V}$ and are checked for unit pressure as well. Fig. 204 shows a fixed pillar crosspiece on rolling friction bearings.

Bottom radial bearing. Small cranes employ roller bearings with one roller mounted on the side of the boom. Large cranes are provided with two front bearing rollers and, if they have a counterweight, with two pairs of rollers at the front and rear (Fig. 205) mounted in a special box on the lower end of the boom. If we denote by H_f the horizontal bearing pressure [formula (206)] and by 2α—the angle between the two bearing rollers (usually equal to 60°) then the force exerted by each roller on the pillar will be

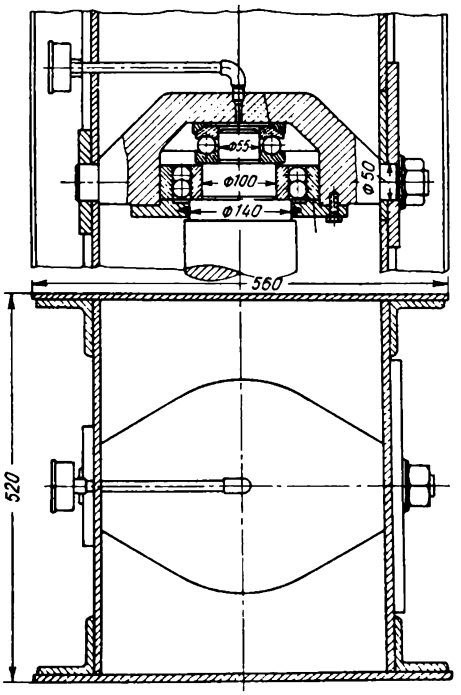

Fig. 204. Crosspiece of a fixed pillar on rolling friction bearings

$$N=\frac{H_f}{2\cos\alpha}.$$

Depending on the load they are to carry rollers are made either of steel or cast iron in the smallest possible sizes and with a convex periphery. They should revolve freely on pins secured in the box by holders. The tentative diameter of the roller is $D_2\approx(2.5\text{ to }3)\,d_2$ where d_2 is the diameter of the roller pin. In heavy-duty rotary cranes with a latticed pillar the bottom support is usually designed with six rollers.

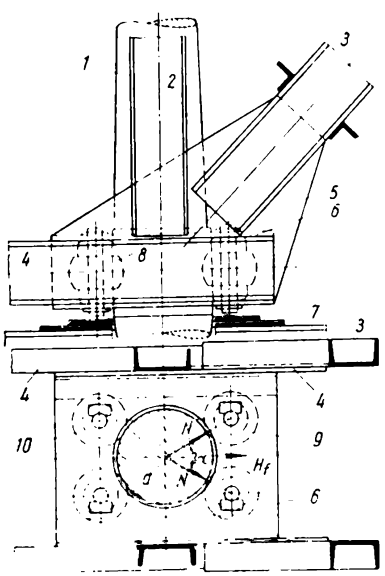

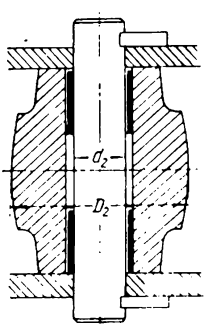

Fig. 205. Bottom roller bearing of a fixed pillar

1 pillar, *2, 3, 4* boom braces, *5*—gusset plate, *6*—roller box, *7*—foundation plate, *8, 9, 10*—rollers

Resistance to slewing. The moment of resistance due to the friction force relative to the slewing axis can be found from the formula

$$M=W_a=$$

$$=V\mu_1\frac{2}{3}\frac{r^3-r_0^3}{r^2-r_0^2}+$$

$$+H_f\mu_2 r+2N\mu_3\times R_1\frac{r_2}{R_2}+$$

$$+2Nk\frac{R_1+R_2}{R_2}\qquad(250)$$

where μ_1, μ_2 and μ_3—respective coefficients of friction in the thrust bearing, top journal and in the pins of the bottom bearing rollers;

k—coefficient of rolling friction of the bottom bearing rollers;
W—resistance to slewing acting at the end of the boom;
a—boom outreach.
The other designations are given in Fig. 198.

For cranes operating in the open account should also be taken of the resistance to slewing W_w due to wind pressure.

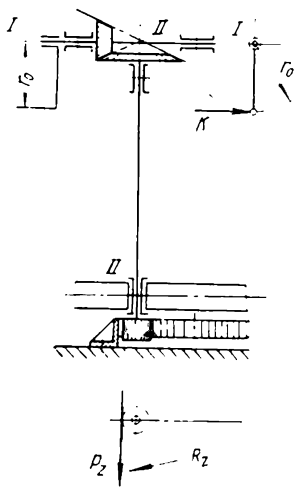

Fig. 206. Hand drive of a crane slewing mechanism

Slewing mechanism drive. The effort applied by the operator to turn the crane by pushing on the load is determined in the same way as for cranes with a rotary pillar. If greater force is required use is made of a hand drive actuated by a crank handle (Fig. 206). Its transmission ratio is

$$i = \frac{1.25M}{\eta M_{op}} \tag{251}$$

where η—drive efficiency;
$M_{op} = Kr_0$—moment created by the operator on the crank handle (operator's effort K—see Table 34);
M—moment of resistance to slewing;
1.25—safety factor.

A hand drive is arranged on the revolving parts of the crane. A usual design comprises a crank handle, a pair of bevel gears and one spur planetary gear train with a fixed ring gear. The force acting on one tooth of the rim is

$$P_z = \frac{M}{R} = W\frac{a}{R}$$

where W—resistance to slewing and a—boom outreach.

The ring gear may be either of the external or internal type. When a large transmission ratio is required another pair of spur gears is arranged between the bevel and planetary gearing.

If $n_{c.h}$ denotes the number of revolutions of the crank handle (an average of 10-12 rpm), the number of revolutions of the crane revolving structure will be

$$n_{cr} = \frac{n_{c.h}}{i}.$$

and the slewing speed at the end of the boom

$$v = 2a\pi n_{cr} \text{ m/min.}$$

The power required from the motor (at steady motion) and the transmission ratio are determined in the same way as for cranes with a rotary pillar.

An electric drive for the slewing mechanism can be designed in one of the following two versions:

1. The motor is mounted on the fixed part of the crane or on a foundation, the driven gear being attached to the revolving structure.
2. The motor is installed on the revolving structure; in this case the last gearing unit should be of the planetary type with the ring gear fixed on the stationary part of the crane or on a foundation (Fig. 207).

Slewing Gear of Cranes with a Turntable

A diagram of a crane with a turntable is shown in Fig. 208. In this crane the load is transmitted from the revolving structure through bearing (slew) rollers

to a circular track secured on a foundation or on the bottom truck of the crane. Aligned with the turning axis is a central pillar or pivot fixed in the stationary part of the crane. When the crane operates the central pivot carries both horizontal and vertical forces.

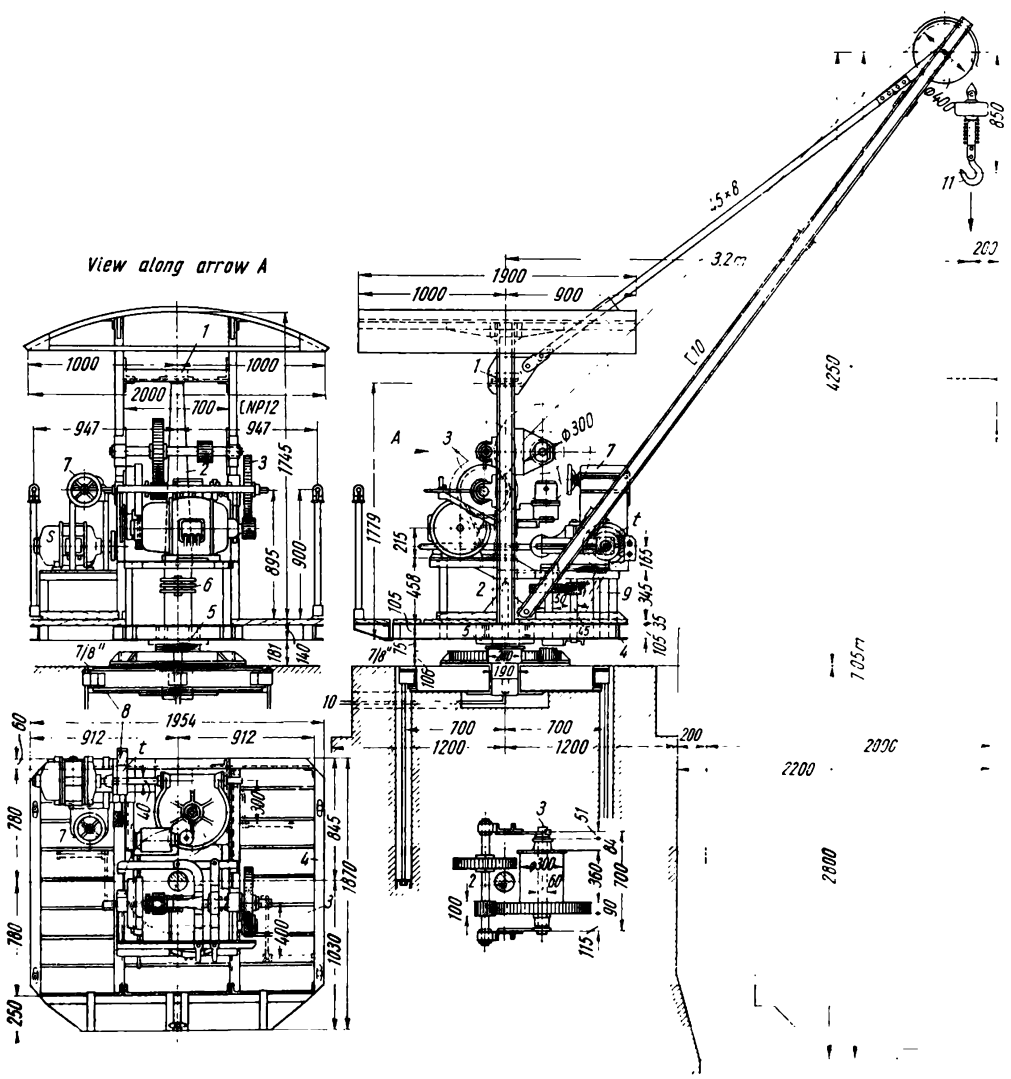

Fig. 207. Rotary crane with a fixed pillar

1 stop support of the revolving structure, *2* pillar, *3* hoist, *4* revolving structure platform, *5* bottom support of the revolving structure, *6* slip rings, *7* controllers, *8* slewing gear, *9* slewing gear brake pedal, *10* power supply cable, *11* hook. Crane operating speeds: hoisting—11.5 m/min, slewing—2 rpm

Resistance to slewing. First case. The centre of gravity of the revolving structure (including the load) is outside its bearing circle (circular track). Here load is applied to the front rollers and the central pivot (the pivot is in tension).

The moment of resistance from the friction forces relative to the slewing axis is

$$M = W_a = P_p \mu_1 \frac{2}{3} \frac{r^3 - r_0^3}{r^2 - r_0^2} + (P_2 + P_3)\left(\mu \frac{d}{2} + k\right) \beta' \frac{R_s}{R} + M_0 \qquad (252)$$

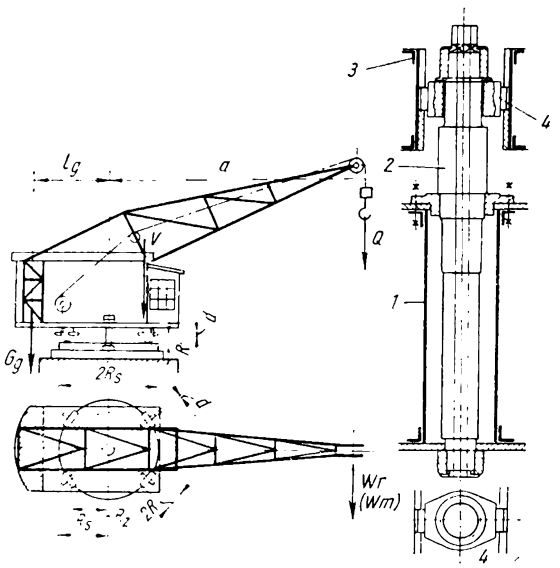

Fig. 208. Diagram of a crane with a turntable and central pivot

1—fixed part, *2*—central pivot, *3*—rotary upper structure, *4*—crosspiece of the central pivot

where W—resistance to slewing at the end of the boom;
a—boom outreach;
P_p—vertical reaction of the central pivot;
μ_1—coefficient of friction in the thrust bearing of the central pivot;
r and r_0—outer and inner radii of the thrust bearing surface on the central pivot;
P_2 and P_3—forces acting on the front slew rollers;
μ—coefficient of sliding friction in the journals of the slew rollers;
d—diameter of the journals on the slew rollers;
k—coefficient of rolling friction of the slew rollers;
R—radius of the slew rollers;
R_s—radius of the circular track;
$\beta' = 1.2$ to 1.3—factor accounting for additional resistance due to friction of the hubs (for tapered rollers) or resistance due to lateral sliding of the rollers on the track (for cylindrical rollers) and taken equal to 1.2-1.3;
M_0—additional moment of friction found from formula (260).

The reaction on the central pivot P_p and force exerted on slew rollers P_2 and P_3 (disregarding wind pressure) can be found from the formulas:

$$P_p = \frac{1}{R_s \cos\beta}(Qa + G_1 l_1 - G_g l_g) - (Q + G_1 + G_g), \tag{253}$$

$$P_2 = P_3 = \frac{1}{2R_s \cos\beta}(Qa + G_1 l_1 - G_g l_g). \tag{254}$$

Here β—half of the angle between adjacent rollers;
Q—weight of the load;
G_1—weight of the revolving structure;
G_g—counterweight; the other designations as in Fig. 208.

In our case the central pivot is subject to tension. The critical cross-section is at the minor diameter of the thread. The top and bottom nuts of the central pivot should be provided with locking devices to prevent unscrewing. The thread is usually of a buttress type.

Second case. The centre of gravity of the entire revolving system is within its bearing circle. Here load is applied to all the rollers. The central pivot is not subject to vertical forces. The moment of resistance to slewing due to the friction forces is

$$M = (Q + G_1 + G_g)\left(\mu\frac{d}{2} + k\right)\beta'\left(\frac{R_s}{R} + M_0\right). \tag{255}$$

Third case. The centre of gravity of the entire system is within the bearing circle. The load is borne by rollers in a cage (Fig. 209) arranged between two rings, of which one is fixed and the other attached to the revolving structure of the crane. The central pivot is not subject to vertical forces. The moment of resistance to slewing due to the friction forces is

$$M = (Q + G_1 + G_g)\, k \frac{R_s}{R} \beta' + M_0 . \qquad (256)$$

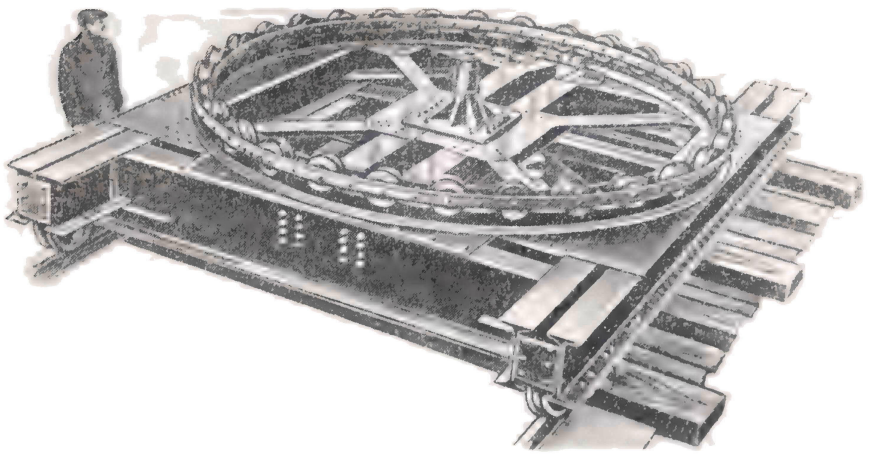

Fig. 209. Bearing rollers for a turntable

Determining the additional moment of friction M_0. Besides the above friction moments, all three cases also involve an additional moment of friction occurring in the radial bearing of the central pivot. It is due to the force exerted on the pivot by the last gear of the planetary train of the slewing mechanism and to the effect produced by the tapered shape of the rollers of the crane revolving structure.

The large ring gear concluding the planetary drive is secured in the fixed part of the crane. The planetary gear in its rotation runs around the ring gear and turns the crane by means of the bearings of its shaft since these bearings are secured in the turntable.

The planetary drive may be designed with either an external or internal ring gear (Fig. 210*a*).

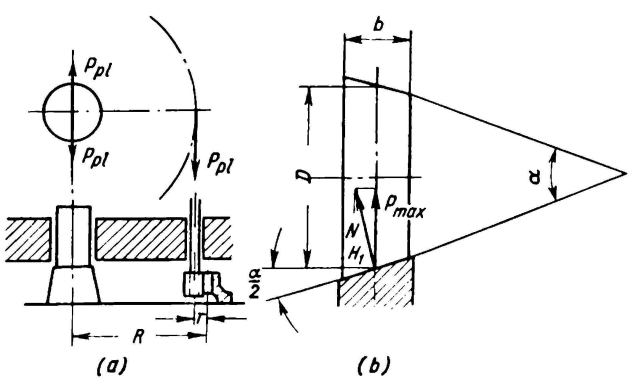

Fig. 210. Diagrams for determining additional moment of friction in the central pivot of the turntable

In internal mesh the horizontal force on the bearings of the driving gear and on the central pivot is

$$P_{pl} = \frac{M_\Sigma}{R - r}; \tag{257}$$

in external mesh

$$P_{pl} = \frac{M_\Sigma}{R + r} \tag{258}$$

where M_Σ—total moment of resistance to slewing (for established motion).

Unequal load on tapered slew rollers produces an additional horizontal force acting on the central pivot. Let us denote by P_{max} the maximum force on one of the tapered rollers on the side of the load and by α the taper angle of the roller (Fig. 210*b*). Since the rollers are tapered this force will give the horizontal component

$$H_1 = P_{max} \tan \frac{\alpha}{2}.$$

On the opposite roller we shall have

$$H_2 = P_{min} \tan \frac{\alpha}{2}.$$

Bearing in mind that wind pressure can be considered only for two rollers in a four-roller design (in the most unfavourable case of force acting on the rollers), the horizontal components H' and H'' of the other two rollers are to be determined disregarding the wind pressure. Then, the horizontal force acting on the central pivot, due to the taper of the rollers, will equal the difference between the resultant forces which act on the opposite pairs of rollers:

$$P_{tap} = [(H_1 + H') - (H_2 + H'')] \cos \beta$$

or

$$P_{tap} = [(P_{max} + P') - (P_{min} + P'')] \tan \frac{\alpha}{2} \cos \beta \tag{259}$$

where P_{max} and P_{min}—maximum load on the front and minimum load on the rear roller with regard to the wind pressure determined by formulas (263) and (264);

P' and P''—load on the front and rear rollers disregarding the wind pressure;

α—taper angle of the roller;

β—half of the angle between adjacent rollers.

Hence, the additional moment of friction in the central pivot will be

$$M_0 = (P_{pl} + P_{tap})\, \mu_2\, r_2 \tag{260}$$

where μ_2—coefficient of friction in the radial bearing of the central pivot;

r_2—pivot journal radius.

The total moment of resistance to slewing (for steady motion) is the sum of the moment due to friction forces and the moment of resistance to slewing offered by the wind M_w

$$M_\Sigma = M + M_w. \tag{261}$$

The moment from the wind pressure can be found from the formula

$$M_w = P_w\, S_{load}\, a + P_w\, S_{cr}\, l_1 - P_w\, S_{cw}\, e_g \tag{262}$$

where P_w—wind pressure, in kg/m²;

S_{load}, S_{cr}, S_{cw}—areas subject to wind pressure at the load, at the crane revolving structure and at the counterweight, in sq m.

Load on the slew rollers of the turntable. A turntable for small and medium cranes is usually designed with four slew rollers (Fig. 211). The maximum load on the front roller of a loaded crane, taking into account the wind pressure, is

$$P_{max} = \frac{\beta}{2} = \frac{V}{2}\frac{e+e_r}{2e_r} + P_w S \frac{e_s}{2e_r}. \quad (263)$$

The minimum load on the rear roller of a loaded crane is

$$P_{min} = \frac{A}{2} =$$

$$= \frac{V}{2}\frac{e_r - e}{2e_r} - P_w S \frac{e_s}{2e_r}. \quad (264)$$

The maximum load on the rear roller of an unloaded crane is

$$P_{max} = \frac{A_0}{2} =$$

$$= \frac{V_0}{2}\frac{e_0 - e_r}{2e_r} - P_w S \frac{e_s}{2e_r}. \quad (265)$$

The minimum load on the front roller of an unloaded crane is

$$P_0^{min} = \frac{B_0}{2} =$$

$$= \frac{V_0}{2}\frac{e_r - e_0}{2e_r} - P_w S \frac{e_s}{2e_r}. \quad (266)$$

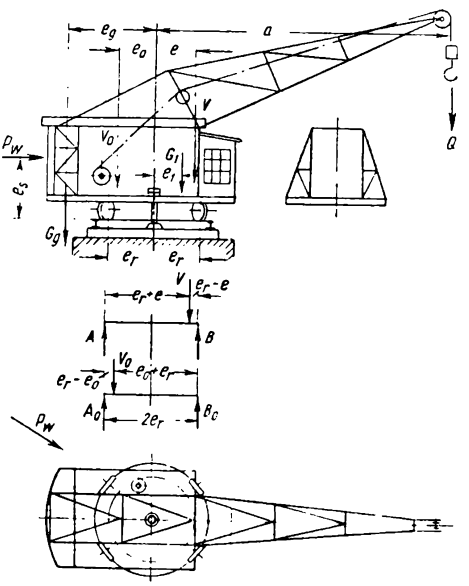

Fig. 211. Diagram for determining the load on the turntable bearing rollers

In these formulas:

P_w—wind pressure on the operator's cab in kg/m²;

S—pressure area in sq m;

V and V_0—weight of the revolving structure of a loaded and unloaded crane ($V=Q+G_1+G_g$; $V_0=G_1+G_g$); the other designations as in Fig. 211.

This method can also be used for determining the vertical reaction P_p of the central pivot, taking into account the wind pressure, when the centre of gravity of the revolving structure is outside its bearing circle.

The circular rail for slew rollers has a standard shape with butt welded ends.

Slewing Mechanism Drive. The power developed by the motor at steady motion is

$$N = \frac{(M + M_w)\, n_{cr}}{71{,}620\eta} \text{ hp} \quad (267)$$

where η—drive efficiency;

n_{cr}—rpm of the crane revolving structure.

Cogwheel Drive. Cogged gearing is employed in crane slewing mechanisms handling heavy loads and also in luffing mechanisms. Both external and internal engagement is used. A cogwheel drive is shown in Fig. 212. The large cog ring is a channel bent into a circle fitted with driving pins which act as teeth. A cogwheel drive has the advantage of a lower cost at large transmission ratios, as well as convenient erection, maintenance and operation.

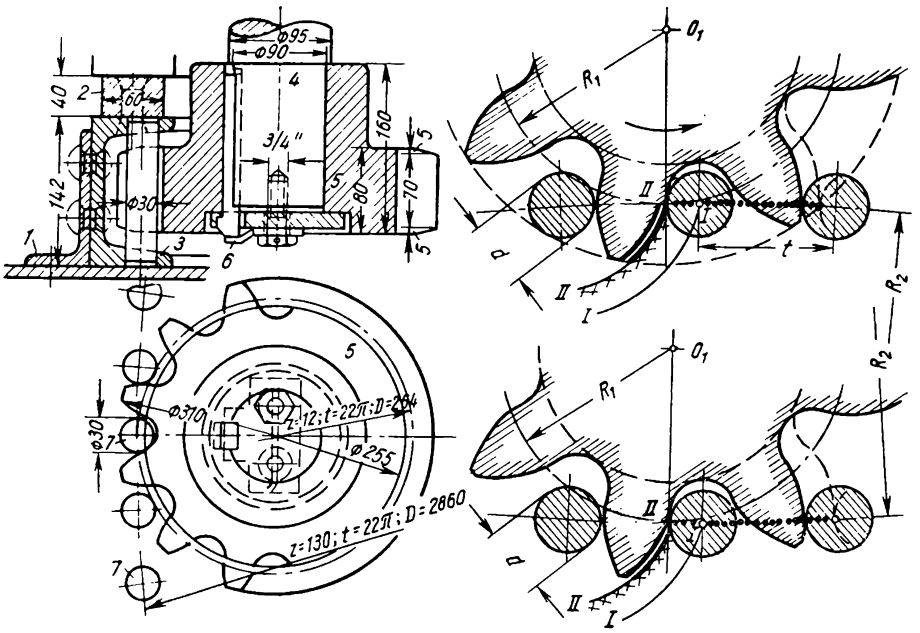

Fig. 212. Cogwheel drive

1—butt knee, *2*—circular runway rail, *3*—cog ring, *4*—driving shaft, *5*—driving pinion, *6*—safety washer for key, *7*—pins: *I-I*—external mesh epicycloid and internal mesh pericycloid, *II-II*—equidistant curve of the epicycloid and pericycloid

The cogwheel is usually made fixed with the pinion running around it (planetary drive). The transmission ratio is $i=8$ to 16. The thickness of the tooth or the diameter of the pin $d=0.475t$; face width of tooth $b=(2 \text{ to } 3)d=\beta d$; minimum number of teeth in the pinion $z=10$ to 13. Here, t is the pitch and β—tooth width factor. The size of the cogged gearing is determined from wear and strength factors.

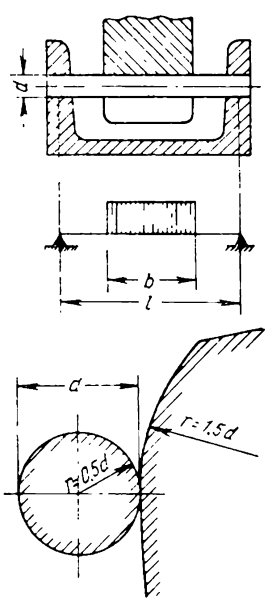

Fig. 213. Diagram for cogwheel calculations

In mesh are always two cylindrical surfaces (Fig. 213) with radii $r_1=0.5d$ and $r_2\approx1.5d$. Using Herz's formula we obtain

$$\sigma_{com}^2 = 0.35 \frac{E_1 E_2}{E_1 + E_2} \frac{P}{\beta d} \frac{0.5d + 1.5d}{0.5d \times 1.5d} = 0.934 \frac{E_1 E_2}{E_1 + E_2} \frac{P}{\beta} \frac{1}{d^2}. \quad (268)$$

For a steel pinion and a steel cog pin the modulus of elasticity $E_1=E_2=2{,}200{,}000$ kg/cm², hence

$$\sigma_{com}^2 = 10{,}274{,}000 \frac{P}{\beta d^2}$$

and

$$d = \frac{1{,}015}{[\sigma_{com}]} \sqrt{\frac{P}{\beta}} \quad (269)$$

where P—peripheral force;

σ_{com}—unit compression stress. At the safe stress $[\sigma_{com}]=8{,}200$ kg/cm² (slow speed).

$$d = 0.124 \sqrt{\frac{P}{\beta}}. \quad (270)$$

For the cogwheel pin load diagram shown in Fig. 213 the unit bending stress will be

$$\sigma_{bend} = \frac{P}{0.4d^3}\left(l - \frac{b}{2}\right) \leqslant [\sigma_{bend}]\,. \qquad (271)$$

Example. Design a cogwheel drive for the slewing mechanism of a crawler tractor.
Given: Diameter of the cogwheel $D = 260$ cm; transmitted torque $M = 160{,}000$ kg-cm.
1. Peripheral force

$$P = \frac{2M}{D} = \frac{2 \times 160{,}000}{260} = 1{,}230 \text{ kg}.$$

2. Diameter of the pin, based on the wear factor [formula (270)]

$$d = 0.124\sqrt{\frac{P}{\beta}} = 0.124\sqrt{\frac{1{,}230}{2.5}} \approx 2.8 \text{ cm}$$

(tooth face width factor $\beta = \frac{b}{d}$ is taken as 2.5).

3. Tooth pitch

$$t = \frac{d}{0.475} = \frac{2.8}{0.475} = 5.9 \text{ cm}.$$

4. Face width of the pinion

$$b = \beta d = 2.5 \times 2.8 = 7 \text{ cm}.$$

5. Checking the bending strength of the pin. Taking $l = 13$ cm, from formula (271), we have

$$\sigma_{bend} = \frac{P}{0.4d^3}\left(l - \frac{b}{2}\right) = \frac{1{,}230}{0.4 \times 2.8^3}\left(13 - \frac{7}{2}\right) = 1{,}330 \text{ kg/cm}^2.$$

The safety factor for pins made of steel 45 with an ultimate strength of 6,000 kg/cm² will be

$$n = \frac{1{,}600}{1{,}330} = 4.5$$

which is permissible at slow speed.
6. Number of pins

$$z = \frac{\pi D}{t} = \frac{3.14 \times 260}{5.9} = 138.44.$$

We take $z = 139$.
7. Actual diameter of the cogwheel

$$D = \frac{zt}{\pi} = \frac{139 \times 5.9}{3.14} = 261 \text{ cm}.$$

2. JIB AND LUFFING MECHANISMS

Mechanisms for changing the crane outreach can be classified into two groups:
1) jib mechanisms changing the outreach by a trolley travelling along a horizontal or inclined girder;
2) luffing mechanisms which raise or lower the boom.
A trolley can be moved by power or manually by a rope drive.

Jib Mechanisms. A rotary (jib) crane with a variable outreach is shown in Fig. 214. Trolley *a* carries an endless length of rope or chain *b* actuated by rope driving sheave *c* or by a drum (by friction force) or else by a chain sprocket (by positive mesh). The sheave or sprocket is rotated by operating wheel *d* through gearing or from an individual electric motor. The lifting rope *e* encircles sheaves *f* on the trolley and movable sheave *h* in the hook casing. One end of the rope is attached to the outer end (*g*) of the boom and the other is wound on the hoisting drum.

The hoist is an independent unit and can raise the load irrespective of whether the trolley moves or is at rest.

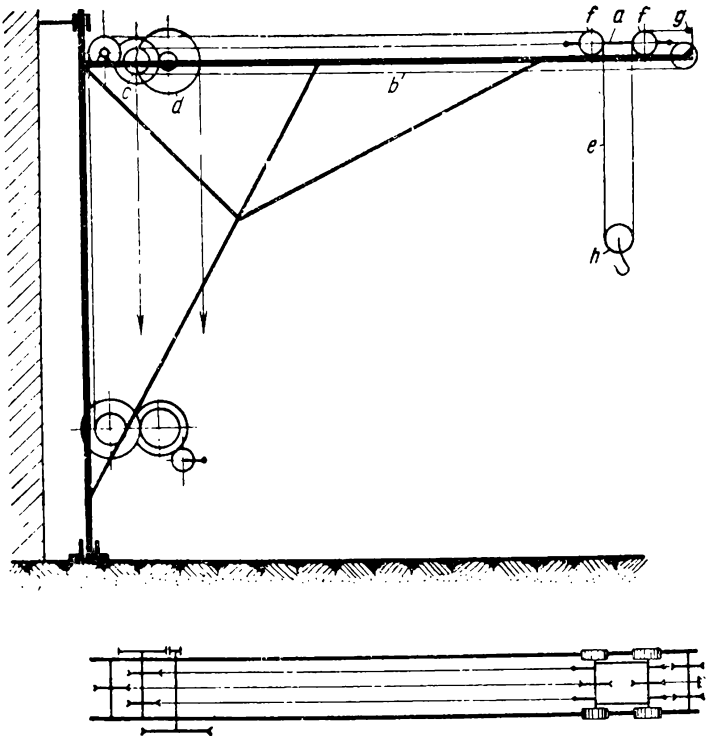

Fig. 214. Diagram of a rotary jib crane with a rope-driven trolley

The resistance to the travel of the trolley at steady motion can be found as follows.

The total resistance to trolley movement is

$$W = W_1 + W_2 \tag{272}$$

where W_1 and W_2—resistances in the travelling wheels and in the lifting rope sheaves.

The resistance from friction in the trolley travelling wheels is

$$W_1 = (Q + q + G_0)\,\beta\left(\frac{\mu d + 2k}{D}\right) \tag{273}$$

where Q—weight of the load;

q—weight of the load-supporting tackle;

G_0—weight of the trolley (excluding the weight of the load-supporting tackle);

β—coefficient accounting for the friction in the flanges of the travelling wheels ($\beta \sim 1.2$ to 1.3 for sliding friction bearings and $\beta \sim 1.8$ to 2.5 for rolling friction bearings);

μ—coefficient of friction in the wheel bearings;

d—diameter of the wheel axles;

k—coefficient of rolling friction of the wheels;

D—wheel diameter.

The resistance in the sheaves of the lifting rope (when the loaded trolley travels, the sheaves revolve) is

$$W_2 = S_{on} - S_{off}\,. \tag{274}$$

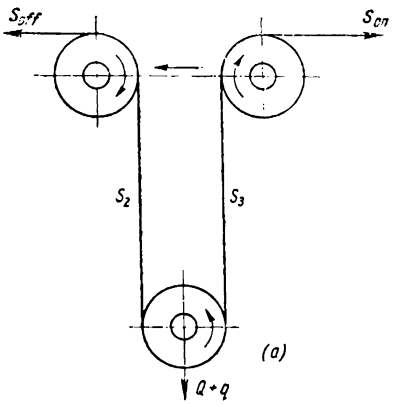

Fig. 215*a* shows a diagram of sheaves for a lifting rope. If we assume that $S_{off} \approx \frac{Q+q}{2}$, then the tension at various points of the rope will be

$$S_2 = S_{off}\,\varepsilon;\ S_3 = S_2\,\varepsilon;\ S_{on} = S_3\,\varepsilon$$

where ε—coefficient of resistance of the sheaves.

The maximum tension of the rope or chain for traversing the trolley is the sum of the resistance offered to the trolley motion W, rope tension S due to its sag and the resistance in the driving and guide sheaves.

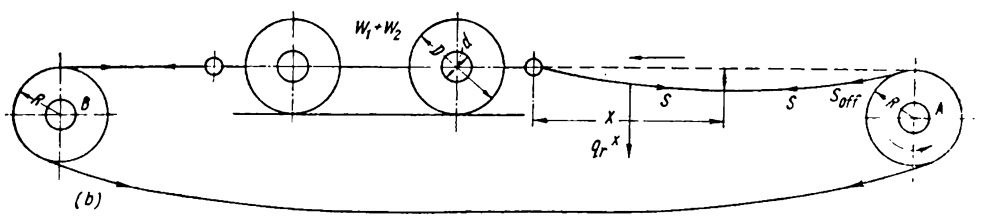

Fig. 215. Diagrams for designing the travelling mechanism of a rope-driven trolley

The tension of the rope or chain S due to its weight and sag f can be found from the condition of equality of moments (Fig. 215*b*):

$$S_f = q_r\,x\,\frac{x}{2}$$

whence

$$S = \frac{q_r\,x^2}{2f} \tag{275}$$

where q_r—weight per metre of rope or chain;
x—one half of the length of the sagging rope or chain (the maximum value x_{max} will be when the trolley is in one of the end positions);
f—safe sag of rope or chain usually taken as

$$f \approx \left(\frac{1}{100}\ \text{to}\ \frac{1}{200}\right) x_{max}.$$

When the trolley moves to the left (most unfavourable case for a driving sheave or sprocket A), the maximum tension S_{max} in the oncoming length of the rope or chain, taking into account the efficiency of idle sheave B, will be

$$S_{on} = \frac{W+S}{\eta_2}.$$

The moment on the rope driving sheave or sprocket required to move the trolley (when the tension of the running-off length of rope or chain $S_{off} = S$ and the peripheral force on the driving sheave or sprocket $P = S_{on} - S_{off}$, taking into account the efficiency of the driving sheave or sprocket) will be

$$M = \frac{(S_{on} - S_{off})\,R}{\eta_1} = \left(\frac{W+S}{\eta_1\eta_2} - \frac{S}{\eta_1}\right) R \tag{276}$$

where S_{on} and S_{off}—tensions of the oncoming and running-off lengths of rope or chain;

η_1—efficiency of the driving sheave or sprocket;

η_2—efficiency of the idle sheave (for a chain sprocket $\eta = 0.93$; for chain or rope sheave $\eta = 0.95$);

R—radius of the sprocket or sheave.

Moment M is used to determine the effort applied by the operator to the pull chain in a hand drive or the power of the electric motor. It will be interesting to note that force S considerably increases the tension of the rope or chain S_{on} and, conversely, little affects the moment necessary to revolve the driving sheave or sprocket since the difference $\frac{S}{\eta_1\eta_2} - \frac{S}{\eta_1}$ is a very small value.

Ropes and chains for traversing trolleys are checked for strength to withstand tension S_{on}.

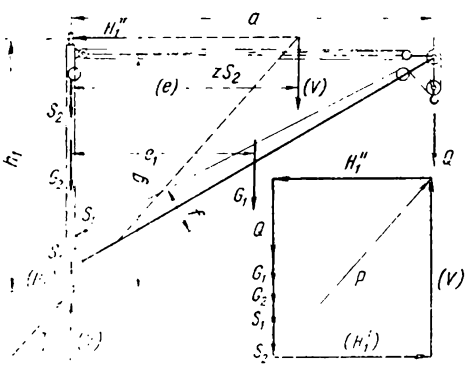

Fig. 216. Diagram for the design of a luffing mechanism operated by a pulley system

When the traversing distance is large rope drums are used as a rule instead of rope sheaves.

Luffing by Means of Rope Sheaves. Screw-driven mechanisms for luffing have the disadvantage of excessive wear of the thread in the nut, which is difficult to reveal when the crane operates. For this reason a crane boom is usually raised with the aid of rope sheaves.

Fig. 216 shows a diagram of the luffing mechanism of a derrick actuated by a pulley system. Fixed sheaves of the system, designed for a gain in force, are secured at the top of the mast and movable sheaves at the upper end of the boom. If the winch is located separate from the crane, the rope (running off the movable sheave) passes over one or two guide sheaves secured to the mast and is then wound around the winch lifting drum.

The tension of the boom luffing rope will reach its maximum value when the boom is in the lowered position (maximum outreach). If we denote by: Q—weight of the load being lifted at the maximum crane outreach a; G_1—weight of the boom; e_1—maximum distance from its centre of gravity to the slewing axis; S_1—tension in the lifting rope which will reduce the tension in the pulley system for luffing the boom (if the winch is erected on a fixed foundation); f—distance between the point of application of tension S_1 and the lower supporting point of the mast and g—the same distance for the luffing pulley, then the maximum total pull of the pulley system will be

$$Z_{max} = \frac{1}{g}(Qa + G_1e_1 + S_1f). \tag{277}$$

Depending on its load lifting capacity the pulley system is provided with $z = 2$ to 5 sheaves. When the pulley system efficiency is η_z the tension in the rope for luffing the boom will be

$$S_2 = \frac{Z_{max}}{(z+1)\eta_z} \tag{278}$$

where z—number of sheaves (disregarding guides for the rope).

As the boom is being raised, tension S_2 decreases and reaches its minimum value at the minimum outreach. This reduction in the pulling force will reduce the required torque.

A cone drum will help to achieve a constant motor torque.

Preference, however, is given to a cylindrical drum which is more convenient to manufacture.

When using the mechanism shown in Fig. 216, the load travels not only radially during raising or lowering but also a definite distance in a vertical direction. This undesirable lifting (or lowering) movement can be avoided by using a special design of luffing mechanism. Such mechanisms are employed mainly in portal cranes; when used in a derrick they may complicate the design. For this reason the lifting rope is usually taken up or run out to compensate for the lowering or raising of the load when the boom outreach is changed.

Luffing speed of the boom. If we denote by S (in metres) the path of the axles of the movable sheaves which corresponds to boom luffing from the lower to the upper position and by t—the time for luffing in minutes then the luffing speed of the boom at the point where the movable sheaves are fastened will be

$$v = \frac{S}{t} \text{ m/min.}$$

The speed of the rope on the drum is

$$v_{drum} = vi$$

where i—transmission ratio of the pulley system.

The power developed by the motor at steady motion can be found from the formula

$$N = \frac{S_2 v_{drum}}{60 \times 75\eta} \text{ hp} \qquad (279)$$

where v_{drum}—speed of rope on the drum in m/min;

η—efficiency of the intermediate mechanisms.

Moreover, the power of the motor should also be checked for luffing an unloaded boom.

CHAPTER XI

OPERATION OF HOISTING GEAR DURING TRANSIENT MOTION

A hoisting mechanism begins to operate at an established or steady speed when the operating device (drum, crane wheel or crane frame) reaches its assigned speed.

Each working movement of a crane comprises: the period of starting (acceleration), steady or established motion and stopping (braking). The first and last periods are distinguished by transient motion. Acceleration requires additional work to start the parts of the crane mechanisms and the load from rest; during stopping the additional work of the moving masses (inertia of movement) is absorbed by the brake. Hence, during acceleration the crane motor is loaded more than in steady motion. The design of brakes must also take into account the inertia forces.

1. DYNAMIC LOAD

If a body with a moment of inertia I revolves with a variable angular speed, the dynamic torque causing the change in the speed of the rotating parts will be

$$M_{dyn} = I\frac{d\omega}{dt}$$

where $\frac{d\omega}{dt}$ is the angular acceleration.

According to d'Alambert's principle, the motor torque is expressed by

$$M = M_{st} + M_{dyn} = M_{st} + I\frac{d\omega}{dt}$$

where M_{st}—moment of static resistance referred to the motor shaft. If the body picks up speed, then $\frac{d\omega}{dt} > 0$ and $M_{dyn} > 0$; on retardation $\frac{d\omega}{dt} < 0$ and $M_{dyn} < 0$.

The term "moment of gyration" will be very convenient for our purpose. If m and G are the mass and weight of a rotating body and ϱ and D are its radius and diameter of gyration, then

$$I = m\varrho^2 = \frac{GD^2}{4g}\ \text{kg-m-sec}^2$$

where $g = 9.81$ m/sec^2 is the acceleration of gravity.

The product GD^2 is known as the moment of gyration.

Hence,

$$M_{dyn} = \frac{GD^2}{4g}\frac{d\omega}{dt}. \qquad (280)$$

This formula can be used only for analysing a single revolving system. Ordinarily, each crane mechanism is a complex system incorporating both revolving links (at various angular speeds) and links in rectilinear motion. For this reason

if we wish to apply formula (280) the actual system should be replaced by an equivalent system which revolves at a certain single angular speed and performs the same action from the viewpoint of dynamics. For this purpose all movements are referred to the movement of a single link, usually the motor shaft, on the basis of constant kinetic energy, i.e., equality between the kinetic energies of the equivalent and the actual systems.

Taking in Fig. 217 only rotating links we can express this condition by the following equation:

$$\frac{I_{r.s}}{2}\omega^2 = \frac{I\omega^2}{2} + \frac{I_1\omega_1^2}{2} + \frac{I_2\omega_2^2}{2} + \ldots + \frac{I_n\omega_n^2}{2}. \qquad (281)$$

We shall use the following notation: $I_{r.s}$ and $(GD^2)_{r.s}$—moment of inertia and the moment of gyration of the equivalent system referred to the motor shaft; ω, I and GD^2—angular speed, moment of inertia and moment of gyration of the motor armature, clutch and other components on the motor shaft; $\omega_1, \omega_2, \ldots, \omega_n$; $I_1, I_2, \ldots, I_n$, $G_1D_1^2, G_2D_2^2, \ldots, G_nD_n^2$—angular speeds, moments of inertia and moments of gyration of gears, shafts and other rotating parts of the mechanism mounted on their respective shafts.

Introducing into our equation the respective moments of gyration and speeds we shall obtain from formula (281)

$$(GD^2)_{r.s} = GD^2 + G_1D_1^2\left(\frac{n_1}{n}\right)^2 + G_2D_2^2\left(\frac{n_2}{n}\right)^2 + \ldots + G_nD_n^2\left(\frac{n_n}{n}\right)^2. \qquad (282)$$

If we use the following designations for the transmission ratios:

$$i_1 = \frac{n}{n_1};\ i_2 = \frac{n}{n_2} \ldots;\ i_n = \frac{n}{n_n}$$

then

$$(GD)^2_{r.s} = GD^2 + \frac{G_1D_1^2}{i_1^2} + \frac{G_2D_2^2}{i_2^2} + \ldots + \frac{G_nD_n^2}{i_n^2}. \qquad (283)$$

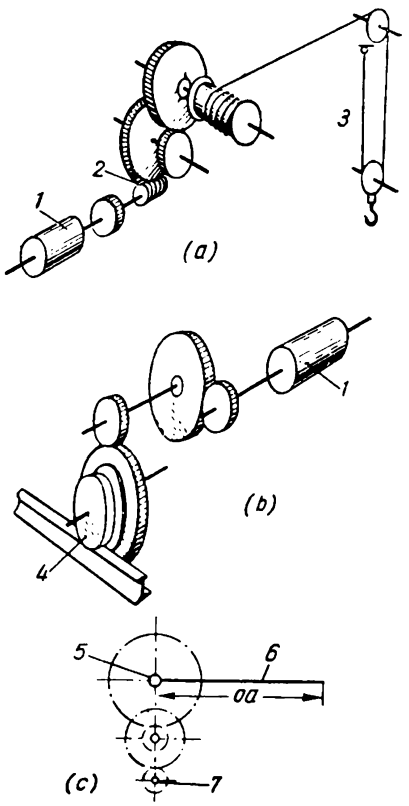

Fig. 217. Diagrams of mechanisms
a—hoisting, *b*—travelling *c*—slewing; *1*—electric motor armature, *2*—worm drive, *3*—pulley system, *4*—travelling wheel, *5*—slewing axis, *6*—boom, *7*—motor shaft

Since $i_n > i_2 > i_1$, the farther the link is removed from the motor shaft the less it will contribute to the moment of gyration. Parts mounted on the motor shaft contribute the greatest share.

Sometimes, to facilitate calculations, the effect produced by the rotating flywheel parts of the mechanism may be tentatively accounted for by taking a somewhat greater moment of gyration for the parts mounted on the motor shaft, i.e., it is assumed that

$$(GD^2)_{r.s} \approx \delta\, GD^2 \qquad (284)$$

where δ—1.1 to 1.25—coefficient accounting for the effect of the parts of the transmission mechanism;

GD^2—moment of gyration of the motor armature and coupling.

Let us now refer the rectilinear motion to the motor shaft. We shall denote the mass, weight and linear speed of the link in rectilinear motion (for example, the load in Fig. 217*a*) by m', G' and v; then the kinetic energy will be

$$\frac{m'v^2}{2} = \frac{(GD^2)_{r.rec}\omega^2}{4g \times 2}$$

where $(GD^2)_{r.rec}$ is an arbitrary moment of gyration of an equivalent system used instead of a rectilinear system.

The losses in the transmission mechanism which arise when dynamic power is transmitted are compensated for by the transmission mechanism efficiency η introduced into the formula. Therefore

$$\frac{m'v^2}{2\eta} = \frac{(GD^2)_{r.rec}\omega^2}{4g \times 2}. \tag{285}$$

On the other hand,

$$m' = \frac{G'}{g}; \omega = \frac{2\pi n}{60}.$$

From equation (285)

$$(GD^2)_{r.rec} = \frac{365G'v^2}{n^2\eta}. \tag{286}$$

Upon retardation the kinetic energy of the link in rectilinear motion is transmitted to the motor shaft and is partly absorbed in the drives. Therefore, when the mechanism is braked

$$\frac{m'v^2}{2}\eta = \frac{(GD^2)_{r.rec}\omega^2}{4g \times 2} \tag{287}$$

whence

$$(GD^2)_{r.rec} = \frac{365G'v^2}{n^2}\eta. \tag{288}$$

The following expression is obtained for the full moment of gyration of the equivalent system when the actual system is comprised of components with rectilinear motion and others with rotary motion:

$$(GD^2)_r = (GD^2)_{r.r} + (GD^2)_{r.rec}.$$

Hence, according to formula (280), the full dynamic torque for acceleration (or retardation) of the entire system with rotary parts and parts having rectilinear motion, as referred to the motor shaft, will be

$$M_{dyn} = \frac{(GD^2)_r}{4g}\frac{d\omega}{dt}.$$

Substituting here

$$\omega = \frac{2\pi n}{60}$$

we obtain

$$M_{dyn} = \frac{(GD^2)_r}{375}\frac{dn}{dt}. \tag{289}$$

This equation, known as the equation of motion, holds both for acceleration and retardation.

The motor torque in starting M_{mot} (both for hoisting and travelling mechanisms) will be used to overcome the static resistance and the inertia forces, i.e.,

$$M_{mot} = M_{st} + M_{dyn}. \tag{290}$$

The same method is used to determine the torque required to brake the hoisting mechanism (braking in load lowering)

$$M_{br} = M_{st} + M'_{dyn}.$$

Travelling mechanisms have a somewhat different relationship between the forces since during the braking action the moment of forces resisting motion M'_{st} acts opposite to the direction of rotation and helps the retarding action so that

$$M'_{dyn} = M'_{st} + M_{br}.$$

Hence

$$M_{br} = M'_{dyn} - M'_{st}.$$

Here: M_{br}—full (actual) braking torque comprising the electric braking torque and mechanical braking torque;

M'_{st}—moment of static resistance referred to the motor shaft;

M'_{st}—equals $71{,}620 \frac{N_{mot}}{n_{mot}}$ kg-cm where n_{mot} is the motor rpm;

N_{mot}—motor power developed at steady motion and equal to:

(a) for hoisting gear

$$N_{mot} = \frac{Qv}{75\eta} \text{ hp};$$

(b) for travelling gear

$$N_{mot} = \frac{Wv}{75\eta} \text{ hp}.$$

(Q—weight of the load being raised, in kg; W—resistance to motion, in kg; v—speed, in m/sec; η—full efficiency of the mechanism); M'_{st}—static torque on the braking shaft (in hoisting gear M'_{st}—moment created by the load, and in the travelling mechanism—the moment of forces resisting motion);

$$M'_{st} = 71{,}620 \frac{N_{br}}{n_{br}} \text{ kg-cm}$$

where n_{br}—speed of the braking shaft, in rpm;

N_{br}—static braking power equal to:

(a) for hoisting gear

$$N_{br} = \frac{Qv\eta}{75} \text{ hp};$$

(b) for travelling gear

$$N_{br} = \frac{Wv}{75\eta} \text{ hp.}^*$$

(η –efficiency of the mechanism up to the braking shaft; the other values as before); M_{dyn} and M'_{dyn} –dynamic torques in acceleration and retardation referred to the respective shafts (motor or brake shaft).

Considering that M_{st} = const independent of the speed and taking M_{mot} and M_{br} as constant values we obtain that M_{dyn} = const and M'_{dyn} = const. Then it follows from equation (289) that $\frac{dn}{dt}$ = const, i.e., the speed of the shaft increases with the time.

For starting $\frac{dn}{dt} = \frac{n}{t_s}$ and for braking $\frac{dn}{dt} = \frac{n}{t_{br}}$ where n is the maximum speed of the motor; t_s—starting time; t_{br}—braking time.

* When the wind pressure W_n exceeds the resistance due to friction forces W_{fr} (disregarding friction in the flanges of the travelling wheels), it is assumed that $W = W_n - W_{fr}$ and the efficiency η is transferred to the numerator.

We have from formula (289)

$$M_{dyn} = -\frac{(GD^2)_r}{375} \times \frac{n}{t} \tag{291}$$

in which case for starting $t = t_s$ and for braking $t = t_{br}$. Besides, for braking, we should substitute M'_{dyn} for M_{dyn}.

Then the starting time will be

$$t_s = \frac{(GD^2)_r n}{375\, M_{dyn}} \tag{292}$$

or, according to equation (290),

$$t_s = \frac{(GD^2)_r n}{375\, (M_{mot} - M_{st})}. \tag{293}$$

Recalling the preceding formulas we obtain the braking time: for hoisting gear

$$t_{br} = \frac{(GD^2)_r n}{375\, (M_{br} - M'_{st})}; \tag{294}$$

for travelling gear

$$t_{br} = \frac{(GD^2)_r\, n}{375\, (M'_{st} + M_{br})}. \tag{295}$$

On the basis of the earlier formulas the value of the dynamic torque in acceleration will be

$$M_{dyn} \approx \frac{\delta GD^2\, n}{375\, t_s} + \frac{0.975\, G'\, v^2}{n t_s\, \eta}. \tag{296}$$

Formulas (284), (288) and (291) provide an identical dynamic torque in retardation

$$M'_{dyn} \approx \frac{\delta GD^2 n}{375\, t_{br}} + \frac{0.975\, G'\, v^2 \eta}{n t_{br}}. \tag{297}$$

In these formulas M_{dyn} and M'_{dyn} are the dynamic torques in acceleration and retardation of the system as referred to the motor shaft, in kg-m; GD^2—moment of gyration due to the parts mounted on the motor shaft (usually the rotor and coupling), in kg-m^2; δ—coefficient accounting for the effect of the mass of the transmission mechanism ($\delta = 1.1$ to 1.25); n—speed of the motor shaft at steady motion, in rpm; G'—weight of the parts with rectilinear motion (full weight of the load in a hoisting gear or full weight of the crane (trolley) in the travelling gear), in kg; v—steady or established speed of the system in rectilinear motion (load, trolley, crane), in m/sec; η—full efficiency of the transmission mechanism; t_s and t_{br}—acceleration and braking time, in sec.

When t_s and t_{br} are reduced the dynamic torques increase in value.

After specifying time t_s and time t_{br} we can use formulas (296) and (297) to find the dynamic torques in starting and braking. To obtain the maximum average speed of the mechanism, the starting time t_s should comprise a small part of the full time of movement. It depends on the size of the parts being accelerated and on the final speed. For hoisting mechanisms and travelling mechanisms we may use average values of $t_s = 1.5$ to 5 sec; for bridge travelling mechanisms $t_s = 5$ to 8 sec; $t_{br} = 1$ sec is approximately correct for mechanisms with a lifting speed of $v < 12$ m/min and $t_{br} = 1.5$ sec for mechanisms with $v > 12$ m/min.

When the path s travelled by the mechanism in acceleration (or retardation) is given, the time t_s (or t_{br}) is determined from the length of this path and the final speed of motion v, i.e., $s = \frac{vt}{2}$. In this case the preceding formulas can be transformed as follows:

$$t_s \approx \frac{\delta GD^2 n}{375\, (M_{mot} - M_{st})} + \frac{0.975 G' v^2}{n\, (M_{mot} - M_{st})\, \eta}. \tag{298}$$

For hoisting gear

$$t_{br} \approx \frac{\delta GD^2 n}{375\,(M_{br} - M'_{st})} + \frac{0.975G'v^2\eta}{n(M_{br} - M'_{st})}. \tag{299}$$

For travelling gear

$$t_{br} \approx \frac{\delta GD^2 n}{375(M'_{st} + M_{br})} + \frac{0.975G'v^2\eta}{n(M'_{st} + M_{br})}. \tag{300}$$

Increased efficiency of the mechanisms requires that the times t_s and t_{br} should be at a minimum. For this reason motors for frequent starting are usually designed with a small moment of gyration.

To reduce the time t_s and t_{br} the maximum permissible values for M_{mot} and M_{br} should be assigned so that the motor can use its overload capacity to maximum advantage during acceleration and retardation. It should be noted, however, that an excessive starting torque in the travelling mechanism of a bridge, truck or trolley may cause the wheels to slip on the rails.

All the above equations hold only for constant acceleration and retardation, i.e., with a constant torque on the motor and a constant braking torque.

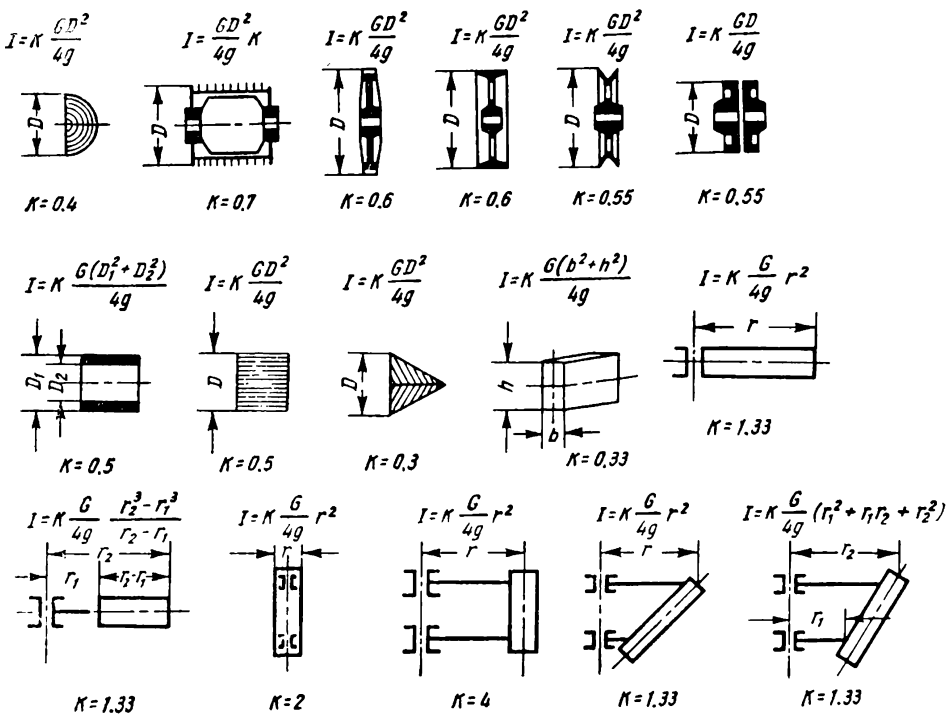

Fig. 218. Moments of inertia of various elements of mechanisms

Fig. 218 shows the moments of inertia of various rotating bodies and Table 39 lists the approximate values of the moments of inertia of couplings. The moments of gyration of electric motor rotors can be found in the respective catalogues.

Hoisting mechanisms should have retardation paths not above and braking coefficients not below the values indicated in Table 40.

Table 39

Approximate Values of Moments of Inertia of Couplings

Outer diameter, mm	Shaft diameter, mm	Hub length, mm	Rim width, mm	Weight, kg	Moments of inertia, kg-cm/sec²
150	30	120	60	10	0.003
200	40	160	80	20	0.01
250	50	200	100	40	0.03
300	60	240	120	70	0.08
400	70	280	140	140	0.28
500	80	320	160	250	0.78

Table 40

Path of Retardation and Braking Coefficients

Duty	Braking path, m	Braking coefficient β
Light	$s/120$	1.75
Medium	$s/100$	2.00
Heavy	$s/80$	2.5

Note: s—path in m travelled by the load per minute.

Table 41

Adhesion coefficient	Number of wheels braked		
	all	50%	25%
0.15	$\frac{v^2}{10,000}$	$\frac{v^2}{5,000}$	$\frac{v^2}{2,500}$
0.12	$\frac{v^2}{8,000}$	$\frac{v^2}{4,000}$	$\frac{v^2}{2,000}$

In travelling mechanisms the braking paths travelled by the truck or crane after the motor has been switched off should not be less than the values indicated in Table 41 (there should be no wheel slipping).

2. SELECTING THE MOTOR RATING AND DETERMINING BRAKING TORQUE FOR HOISTING MECHANISMS

The full torque developed by the motor in acceleration can be found from the formula

$$M_{mot} = M_{st} + M_{dyn}\,.$$

Two factors must be used as guidance for a correct determination of the required electric motor rating: heating and permissible overload. The safe short-term overload on a d-c motor depends on the permissible sparking across the commutator and is selected approximately at 200-300 per cent of the rated torque, i.e.,

$$M_{rated} = \frac{M_{max}}{2 \text{ to } 3} \tag{301}$$

where M_{rated}—rated torque of the motor;

M_{max}—maximum torque in acceleration and equal to M_{mot}.

The safe short-term overload on an a-c motor is conditioned by the stalling torque which should exceed the maximum torque; it is chosen approximately equal to 1.75-2 times the rated torque, i.e.,

$$M_{max} = (1.75 \text{ to } 2)M_{rated}. \tag{302}$$

More accurate safe values of motor overloads in acceleration can be found in the catalogues of the manufacturing plants.

The heating of the motor is caused by conversion of the losses arising during its operation into heat. Overheating damages insulation (charring) and reduces the life of the motor or may even completely disable it. For this reason, the motor rating is selected so that the temperature of the winding with an insulation especially susceptible to heating nowhere exceeds the safe limits under any operating conditions. On the other hand, if the temperature of the winding never reaches the maximum value the motor does not develop the full available power, i.e., it

is not being used to full capacity and its efficiency is reduced. This reduction in efficiency increases losses in a motor operating at incomplete load. In asynchronous motors there is also a decrease in the power factor.

Thus, an electric motor is to be selected by the static power requirements (at steady motion) $N_{st} = \dfrac{M_{st}n}{71{,}620}$ hp and is then to be checked for full torque during acceleration $M_{mot} = M_{max}$.

In internal combustion engine drives the starting torque should equal the rated value the engine develops.

In crane steam engines the starting torque is equal to 2-2.5 times the rated value.

The full (actual) braking torque M_{br} in hoisting mechanisms during braking can be found from the formulas

$$M_{br} = M'_{st} + M'_{dyn}$$

where

$$M'_{dyn} \approx \frac{\delta GD^2 n}{375 t_{br}} + \frac{0.975 G' v^2 \eta}{n t_{br}}$$

and

$$t_{br} \approx \frac{\delta GD^2 n}{375(M_{br} - M'_{st})} + \frac{0.975 G' v^2 \eta}{n(M_{br} - M'_{st})}.$$

3. DRIVE EFFICIENCY

The data on the efficiency of a mechanism or its elements indicated in reference books give the maximum value which corresponds to the rated load. The efficiency decreases when the loads are below rated.

Indeed, there may be two kinds of friction losses in the mechanism and its drives: constant (or idle run losses), independent of useful load, and variable which depend on the load. The latter losses are approximately proportional to the load; load variations do not affect the constant losses. Therefore, the efficiency η will drop as the load is decreased and may even reach the zero value in an idle run.

Hence, the features inherent to each machine require that the crane always operates under full load for, otherwise, harmful resistances will be noticeably increased in percentage to useful work.

4. SELECTING THE MOTOR RATING AND DETERMINING BRAKING TORQUE FOR TRAVELLING MECHANISMS

The required motor torque during acceleration and the braking torque during retardation in the travelling mechanisms of trucks, trolley hoists, overhead, cantilever, monorail and other cranes moving on runway rails can be found from the following formula:

$$M_{br} = M'_{dyn} - M'_{st} \tag{302a}$$

and also from formulas (290), (296), (297), (298) and (300).

The braking path s or run of a truck or crane after the motor has been switched off should be reduced to a minimum. However, to prevent slippage of the wheels it should not be less than the values indicated in Table 41. In determining the braking torque the resistance to motion is calculated without regard for the friction in the flanges of the travelling wheels.

For locomotive cranes the increase in the resistance due to the inertia forces during acceleration is accounted for by introducing an additional coefficient of resistance w_{in} ($w_{in} \sim 6$ kg/t) into formula (233).

Formulas (296) and (297) may be used to find the dynamic torque in acceleration and retardation of crawler and wheeled trackless travelling mechanisms.

In this case the braking path $s = \frac{vt}{2}$ is taken as: $s < 0.2$ m for $v < 5$ km/hr and $s < 0.3$ m for $v > 5$ km/hr.

The motor rating for travelling mechanisms is selected in the same way as for hoisting mechanisms.

5. SELECTING THE MOTOR RATING AND DETERMINING BRAKING TORQUE FOR SLEWING MECHANISMS

The required torque of the motor during acceleration and the braking torque during retardation are determined for crane slewing mechanisms by formulas (290) and (302*a*).

The static moments M_{st} and M'_{st} can be found from formula (303) by referring the respective moments of slewing resistance on the axis of the revolving part of the crane with a speed n_{cr} to the motor (or braking) shaft with a speed n_{mot} (or n_{br}):

$$M_{st} = M'_{st} = \frac{M_{\Sigma}}{i\eta} \tag{303}$$

where M_{Σ}—full moment of resistance to slewing with account taken of the wind pressure (for crane operation in the open) found from formulas (241), (250) and (254);

i—ratio of the transmission mechanism equal to

$$i = \frac{n_{mot}}{n_{cr}} \left(\text{or } i = \frac{n_{br}}{n_{cr}} \right);$$

η—drive efficiency.

In slewing mechanisms the effect of the inertia forces is quite considerable. Here account should be taken of the inertia of the load, revolving parts of the crane, counterweight and electric motor rotor as well as of the effect of the inertia of other parts of the drive.

The dynamic torque developed on the motor shaft during acceleration is

$$M_{dyn} = \frac{\delta GD^2 n_{mot}}{375 t_s} + (I_{load} + I_{cr} + I_{cw}) \frac{\pi n_{cr}}{30 t_s \eta i}. \tag{304}$$

The dynamic torque in retardation referred to the motor shaft is

$$M'_{dyn} \approx \frac{\delta GD^2 n_{mot}}{375 t_{br}} + (I_{load} + I_{cr} + I_{cw}) \frac{\pi n_{cr} \eta}{30 t_{br} i}. \tag{305}$$

In these formulas:

GD^2—moment of gyration from the parts mounted on the motor shaft (usually the rotor and coupling; see respective electric motor catalogues and Table 40), in kg-m^2;

δ—coefficient accounting for the effect of the mass of transmission mechanism parts ($\delta = 1.1$ to 2.5);

I_{load}, I_{cr}, I_{cw}—moments of inertia of the load, revolving part of the crane and the counterweight;

t_s—starting time$\sim$3 to 8 sec;

t_{br}—braking time, in sec, taken equal to

$$t_{br} = \frac{2n_t}{n_{cr}} 60$$

where n_{cr}—rpm of the revolving structure of the crane at steady motion;

n_t—fraction of one crane revolution from the moment the motor is switched off to the moment the mechanism stops completely. The values of n_t are as follows: for light-duty cranes $n_t < 1/24$ rev—15°; for medium-duty cranes $n_t < 1/18$ rev—20°; for heavy-duty cranes $n_t < 1/12$ rev—30°.

When the brake is not mounted on the motor shaft the dynamic torque M'_{dyn}, obtained from formula (305), should be referred to the motor shaft.

The motor rating required for crane slewing mechanisms is selected in the same way as for hoisting mechanisms.

6. SELECTING THE MOTOR RATING AND DETERMINING BRAKING TORQUE FOR JIB AND LUFFING MECHANISMS

When the outreach of a crane is changed by means of a rope-driven trolley the motor torque required during acceleration and the braking torque during retardation can be found from formulas (290), (302*a*), (296), (297), (298) and (300).

The braking path to stop the trolley is usually taken as $s \approx 0.25$ to 0.5 m.

In luffing mechanisms the motor torque required during acceleration and the braking torque during retardation are found from formulas (290) and (296) to (299), inclusive.

In these formulas G' is the full weight of the loaded boom and v—the speed of the centre of gravity of the loaded boom at steady motion.

The motor and brake of a luffing mechanism (of boom cranes) should be checked for maximum lifting capacity at various positions of the boom.

The required motor rating for jib and luffing mechanisms is selected in the same way as for hoisting mechanisms.

Example 1. Determine the required power ratings of the motors of an electric overhead travelling crane for the assembly shop of an engineering plant.

Given: Lifting capacity $Q = 5{,}000$ kg, span $L_{cr} = 14$ m, load lifting (or lowering) speed $v_{load} = 10$ m/min, trolley traverse speed $v_{trol} = 45$ m/min, crane travelling speed $v_{cr} = 100$ m/min, power supply—three-phase, 380 v, duty—medium (DF = 25 per cent).

Selecting a motor for the hoisting mechanism

1. The required static power of the motor is

$$N = \frac{Qv}{75\eta} \text{ or } N = \frac{5{,}000 \times 10}{75 \times 60 \times 0.8} = 13.8 \text{ hp.}$$

The efficiency η of the hoisting mechanism is assumed equal to 0.8 with three gear drives.

Let us consult catalogues of electric motors for the most suitable type; it will have the following characteristics: rated power $N_{rated} = 15$ hp, $n = 965$ rpm, permissible overload $\frac{M_{max}}{M_{rated}} = 2.5$, duty factor DF = 25 per cent, rotor moment of gyration $(GD^2)_{rot} = 0.78$ kg-m^2.

2. The static moment of resistance referred to the motor shaft is

$$M_{st} = 71{,}620 \frac{N}{n} = 71{,}620 \frac{13.8}{965} = 1{,}025 \text{ kg-cm} = 10.25 \text{ kg-m.}$$

3. We next determine the dynamic torque in starting referred to the motor shaft. We select a flexible coupling for the motor shaft with an external diameter of $D = 300$ mm. The moment of inertia of such a coupling (according to Table 39) will be approximately equal to $I = 0.03$ kg-m/sec^2 and the moment of gyration $(GD^2)_{coupl} = I \cdot 4g = 0.03 \times 4 \times 9.81 = 1.18$ kg-m^2; hence the moment of gyration from the rotor and coupling on the motor shaft will be

$$GD^2 = (GD^2)_{rot} + (GD^2)_{coupl} = 0.78 + 1.18 = 1.96 \text{ kg-m}^2.$$

The dynamic torque in starting is found from the formula

$$M_{dyn} = \frac{\delta GD^2 n}{375\, t_s} + \frac{0.975\, G' v^2}{n t_s \eta} = \frac{1.15 \times 1.96 \times 965}{375 \times 3} + \frac{0.975 \times 5{,}000 \times 10^2}{60^2 \times 965 \times 3 \times 0.8} = 1.99 \text{ kg-m}$$

where t_s—starting time (3 sec);

$G' = Q$—weight of the system in rectilinear motion (weight of the load being lifted).

4. The required motor torque in starting is

$M_{mot} = M_{st} + M_{dyn} = 10.25 + 1.99 = 12.24$ kg-m.

5. The rated torque of the motor is

$$M_{rated} = 716.2 \frac{N_{rated}}{n} = 716.2 \frac{15}{965} \sim 11.15 \text{ kg-m.}$$

6. Checking the motor for overload. The overload of the motor during starting ($M_{max} = M_{mot}$) is

$$\frac{M_{max}}{M_{rated}} = \frac{12.24}{11.15} \sim 1.1$$

which is much below the safe overload.

Selecting a motor for the trolley traversing mechanism

1. The resistance to motion is

$W = \beta (Q+G_0) w = 1.4 (5+2.7)23 \sim 248$ kg;

here G_0—weight of the trolley;

w—traction factor; for $D = 300$ mm and $d = 60$ mm w is equal to 23 kg/t.

2. The required static power of the motor is

$$N = \frac{Wv}{75\eta} = \frac{248 \times 75}{75 \times 60 \times 0.85} \sim 2.9 \text{ hp.}$$

The drive efficiency η is taken as 0.85 with two gear drives. The motor selected from the catalogue will have the following characteristics: rated power $N_{rated} = 4.1$ hp; speed $n = 930$ rpm; duty factor DF = 25 per cent, rotor moment of gyration $(GD^2) = 0.18$ kg-m^2.

The motor is checked for overload during the starting period in the same way as for crane travelling mechanisms.

Selecting a motor for the crane travelling mechanism

1. We determine the resistance to motion. The weight of the crane (with a length of span $L_{cr} = 14$ m) is taken equal to $G+G_0 = 15$ tons.

Determining the resistance to motion we obtain

$W = \beta (Q+G_0+G)w = 1.5 (5+15)18.5 \sim 555$ kg

where w—traction factor (at $D = 700$ mm and $d = 120$ mm w is equal to 18.5 kg/t).

2. Required static power of the motor.

We take the same motor as for the hoisting mechanism.

3. The static moment of resistance referred to the motor shaft is

$$M_{st} = 71{,}620 \frac{N}{n} = 71{,}620 \frac{14.5}{965} = 1{,}078 \text{ kg-cm} = 10.78 \text{ kg-m.}$$

4. The dynamic torque in starting referred to the motor shaft is

$$M_{dyn} = \delta \frac{GD^2 n}{375 t_s} + \frac{0.975 G' v^2}{n t_s \eta} = \frac{1.15 \times 1.96 \times 965}{375 \times 5} + \frac{0.975 \times 20{,}000 \times 100^2}{60^2 \times 965 \times 0.85} \sim 14.36 \text{ kg-m.}$$

Here G'—weight of the system in rectilinear motion (weight of loaded crane) equal to $G' = Q+G_0+G = 5+15 = 20$ tons $= 20{,}000$ kg.

5. The required motor torque in starting is

$$M_{mot} = M_{st} + M_{dyn} = 10.78+14.36 = 25.14 \text{ kg-m.}$$

6. Checking the motor for overload.

The overload of the motor in starting is

$$\frac{M_{max}}{M_{mot}} = \frac{25.14}{11.15} = 2.26,$$

a value below that specified by catalogues (2.5).

Example 2. Determine the braking torques for hoisting and travelling mechanisms of an electric overhead crane.

The data are the same as in Example 1.

Determining the braking torque of the hoisting mechanism.

1. Static moment developed by the load on the brake shaft.

When the brake is mounted on the motor shaft the static braking power will be

$$N_{br} = \frac{Qv\eta}{75} = \frac{5{,}000 \times 10 \times 0.8}{60 \times 75} \sim 8.9 \text{ hp.}$$

Hence, the static moment is

$$M'_{st} = 71{,}620 \frac{N_{br}}{n_{br}} = 71{,}620 \frac{8.9}{965} = 662 \text{ kg-cm} = 6.62 \text{ kg-m.}$$

2. The dynamic torque in braking referred to the brake shaft will be

$$M'_{dyn} = \frac{\delta GD^2 n}{375 t_{br}} + \frac{0.975 G' v^2 \eta}{n t_{br}} = \frac{1.15 \times 1.96 \times 965}{375 \times 1} + \frac{0.975 \times 5{,}000 \times 10^2 \times 0.8}{60^2 \times 965 \times 1} \sim$$

~ 5.91 kg-m.

3. The torque required for braking is

$$M_{br} = M'_{st} + M'_{dyn} = 6.62 + 5.91 = 12.53 \text{ kg-m.}$$

4. Checking the braking torque by means of the braking coefficient we obtain

$$M_{br} = M'_{st}\,\beta = 6.62 \times 2 = 13.24 \text{ kg-m}$$

where β—braking coefficient taken from Table 40 for medium duty (DF = 25 per cent).

For further calculations the actual braking torque M_{br} should have its largest value, i.e., $M_{br} = 13.24$ kg-m.

Determining the braking torque of the crane travelling mechanism

1. The resistance to motion disregarding friction of the travelling wheel flanges (without coefficient β) is

$$W = (Q+G_0+G)w = (5+15)\ 18.5 = 370 \text{ kg.}$$

2. Next we determine the static moment of the forces resisting motion as referred to the brake shaft.

When the brake is mounted on the motor shaft the static braking power will be

$$N_{br} = \frac{Wv}{75\eta} = \frac{370 \times 10}{60 \times 75 \times 0.85} \sim 9.7 \text{ hp.}$$

Hence, the static torque is

$$M'_{st} = 71{,}620 \frac{N_{br}}{n_{br}} = 71{,}620 \frac{9.7}{965} = 720 \text{ kg-cm} = 7.2 \text{ kg-m.}$$

3. The dynamic torque in braking as referred to the brake shaft is found as follows. We assume that half of the crane travelling wheels are braked; then the retardation path S should not be less than $S \geqslant \frac{v}{70} = 1.43$ m and the braking time will be

$$t = \frac{2S}{v} = \frac{2 \times 1.43 \times 60}{100} = 1.72 \text{ sec.}$$

We take $t_{br} = 2$ sec, thereby somewhat increasing the braking path S.

The dynamic torque in braking can be found from the formula

$$M'_{dyn} = \frac{\delta G D^2 n}{375\, t_{br}} + \frac{0.975 G' v \eta}{n t_{br}} = \frac{1.15 \times 1.96 \times 965}{375 \times 2} + \frac{0.975 \times 20{,}000 \times 100^2 \times 0.85}{60^2 \times 965 \times 2} =$$
$$= 26.7 \text{ kg-m.}$$

4. The torque required for braking will be

$$M_{br} = M'_{dyn} - M'_{st} = 26.7 - 7.2 = 19.5 \text{ kg-m.}$$

This actual braking torque M_{br} is used as the basis for designing the brake of the crane travelling mechanism.

CHAPTER XII

CRANE FRAME STRUCTURES (TRUSSES)

A crane frame carries all operating mechanisms, electrical equipment, motors and controlling gear. The frame sustains external dead load, live load, wind pressure (in exposed operation), inertia forces, etc., and transmits these forces either onto a fixed foundation or, through travelling wheels and runway rails, to the foundation or the supporting members of a building.

A crane frame should ensure adequate strength and stability of the entire construction. This means that the stresses in its separate elements should not exceed the safe values while the strains should be recoverable. Moreover, they should be so negligible that variable loads acting on the crane do not cause vibrations either in the frame as a whole or in its components.

Adequate rigidity of the crane structure is the prime requirement for dependable and faultless operation of all the working mechanisms. For this reason the design and solution of a crane framework should be done with great accuracy.

1. SUPERSTRUCTURES OF ROTARY CRANES WITH A FIXED RADIUS

Cranes with a Rotary Pillar. Diagrams of the superstructures of fixed cranes with a rotary pillar and a fixed radius are illustrated in Fig. 219.

Pivot pins are secured to both ends of the crane pillar; one is mounted in the lower support, provided with both thrust and radial bearings, and the other in the upper support with only a radial bearing. The theoretical height of the pillar is usually $h_1 = (0.5 \text{ to } 1.0)a$.

If we denote the weight of the load being raised by Q, the weight of the rotary boom by G_1 and the distance of its centre of gravity from the axis of rotation by e_1, the vertical reaction in the thrust bearing will be

$$V = Q + G_1$$

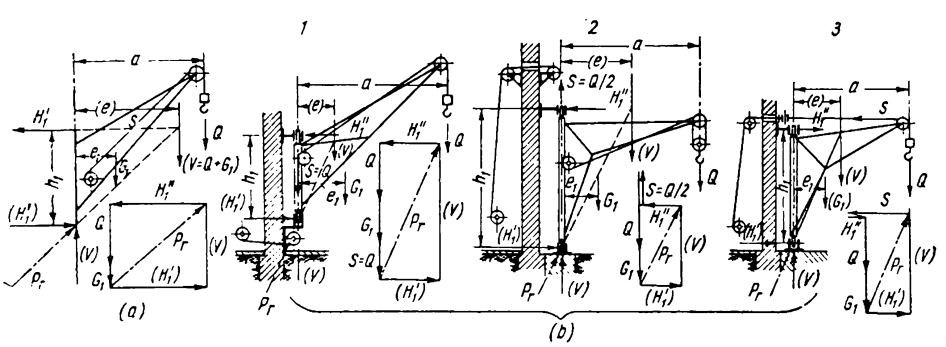

Fig. 219. Superstructures of rotary-pillar fixed radius cranes

and the horizontal reactions in the supports

$$H_1' = H'' = H_1 = \frac{1}{h_1}(Q_a + G_1 e_1). \tag{306}$$

The bearing reactions of the boom can also be found by graphical methods (Fig. 219*a*). For this purpose the line of force H'' is continued until it intersects the resultant of the vertical loads V, whose distance from the axis of rotation is

$$e = \frac{Qa + G_1 e_1}{Q + G_1},$$

and then the point of intersection is connected with the centre of the bottom support.

This will give us the direction of the resultant bearing force P_r of the lower support; the forces $V = Q + G_1$, H_1' and P_r are in equilibrium and form a force triangle in which H_1'' and P_r are determined. The vertical bearing reaction V and the lower horizontal reaction H_1' are also components of P_r.

If the hoisting gear is mounted on the boom (Fig. 219*a*), then the tension S of the lifting rope will be an internal force and may therefore be neglected in determining the bearing reactions of the boom. If the hoisting gear is separate from the revolving structure (Fig. 219*b*) rope tension will be an external force. In crane *1* the downward rope tension tends to increase the bearing pressure while in crane *2* the upward rope tension $S = \frac{Q}{2}$ decreases it. In crane *3* the rope tension reduces the upper horizontal bearing pressure H_1''.

Booms of light-duty rotary cranes are usually designed in the form of a triangle (Fig. 219*a* and *b-1*). For heavy-duty cranes and also when it is necessary to increase the head room at the lower end of the boom, arrangements such as those shown in Fig. 219*b-2* and *b-3* are employed.

The forces arising in the members are usually found graphically by plotting the Cremona force plan. In analysing rotary cranes with a small radius the boom weight is usually neglected and the forces arising in the members are determined as resulting only from the load being lifted. From the load, the bearing reactions in the boom will be (Fig. 220*a*)

$$V = Q;\ H' = H'' = Q\frac{a}{h}.$$

Since the tension of rope S leads to additional forces in the members it should be taken into consideration when determining the forces. If the load is suspended on one line of the rope, $S = Q$; in a pulley with two load-carrying parts $S = \frac{Q}{2}$.

To construct the Cremona force plan we should assume that the rope was cut through and that both tensions S needed for equilibrium of the system are applied at the upper guiding sheave of the boom and at the drum. The upper rope tension is added to the force from load Q to obtain resultant force R (Fig. 220*a*) which acts at the outer end of the boom. The bottom tension is distributed among the adjacent units of the pillar in the following proportion:

$$S' = S\frac{m_2}{m} \text{ and } S'' = S\frac{m_1}{m}.$$

The forces in the members are found from the Cremona force plan constructed after specifying the forces R, S' and S'' which act on the system (Fig. 220*a*).

For the superstructure shown in Fig. 220*b* the resultant R_1 of component forces S and Q at the outer end of the boom is found by the above method. The tensions S and S of the ropes on the sheave of intermediate member *4* will give the resultant

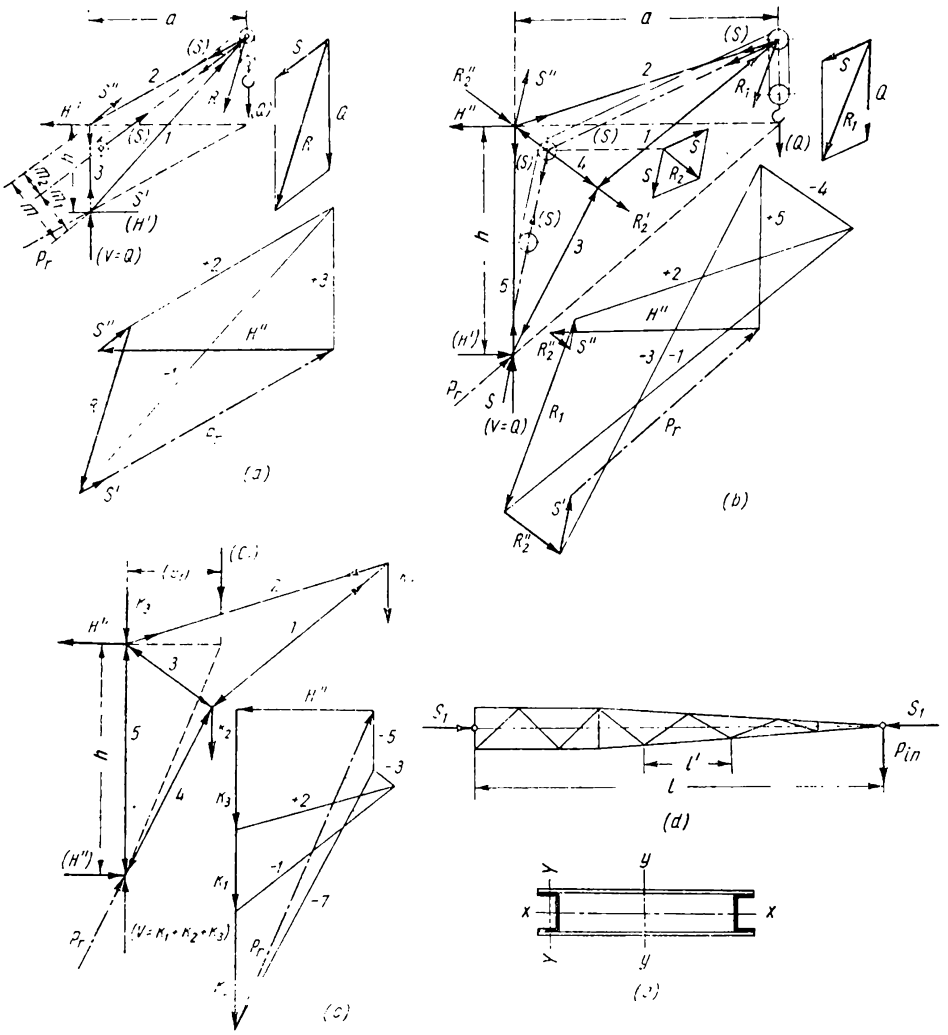

Fig. 220. Graphical solution of superstructures for rotary-pillar fixed-radius cranes

R_2 which is applied to the bearing parts of member *4* as R_2' and R_2'', in proportion to the arms. Force S on the drum is resolved into forces acting on the pillar parts (S' and S''). Forces R_1, R_2', R_2'', S' and S'' are used to construct the Cremona force plan and to find the stresses in the members due to the load and rope tension.

Fig. 220*c* also shows a diagram of stresses in the members due to the weight of the boom (it should be constructed to a larger scale than the diagram for the load weight). At first the weight of the boom and its resolution among the superstructure parts are specified tentatively. The actual stresses in the members are the sum of the forces from the dead and live loads.

In heavy cranes with a power-driven slewing mechanism the effect of the inertia forces is taken into account by the assumption that horizontal force $P_{in} \approx \frac{1}{10} Q$ is applied to the outer end of the boom. It is resisted by a horizontal truss (Fig. 220*d*) one half of which is subject to additional compression and the other—to tension.

Cranes with a Fixed Post. Let us examine by way of example a solid superstructure (Fig. 221) which is frequently employed for rotary pillar cranes without a counterweight. The advantage of this design is in the ample head room

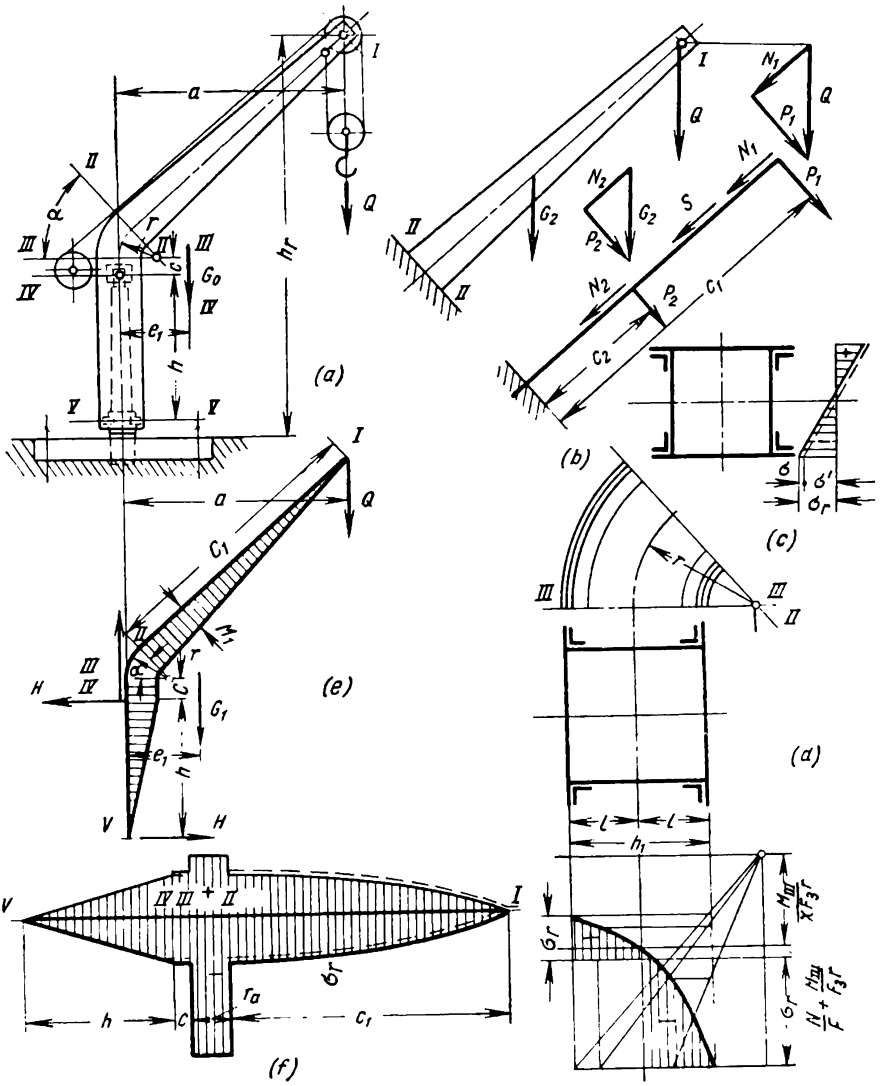

Fig. 221. Diagrams for the solution of a solid superstructure for a rotary crane

under the boom. The box girder is reinforced in its bent section by plates and in its straight sections by braces. The dimensions of the section are taken tentatively at first.

The stresses in sections *II-II*, *III-III* and *IV-IV* are determined as follows.

The upper inclined part is regarded as fixed (Fig. 221*b*) in section *II-II* (Fig. 221*a*). The weight of load Q is resolved into compressive force N_1 and bending force P_1 (the counteracting moment from rope tension S is usually neglected). To these values are added compressive force N_2 and bending force P_2 due to the weight of the superstructure G_2 (appraised tentatively).

The bending moment (disregarding dynamic correction factors) is

$$M_{II} = P_1 c_1 + P_2 c_2. \tag{307}$$

The normal force is

$$N_{II} = N_1 + N_2 + S. \tag{308}$$

The resultant unit stress (without the shearing force) is

$$\sigma_x = \pm \sigma' - \sigma = \pm \frac{M_{II}}{W_2} - \frac{N_{II}}{F_2} \tag{309}$$

where W_2 and F_2—the moment of resistance and the cross-sectional area in plane *II-II* (stress diagram, Fig. 221*c*).

The unit shearing stress is

$$\tau = \frac{P_1 + P_2}{F_2}. \tag{310}$$

The unit stress taking shear into account is

$$\sigma_{max} = \sqrt{(\sigma' + \sigma)^2 + 3\tau^2}. \tag{311}$$

Stress calculations of the bent middle part in section *III-III* (Fig. 221*a*) are made as for a curved beam. The bending moment $M_{III} = Qa + G_1e_1$. The normal force is $N_{III} = Q + G_1$. The resultant unit stress in the outer or inner fibres is

$$\sigma_{max} = -\frac{N_{III}}{F} + \frac{M_{III}}{F_3 r} \pm \frac{M_{III}}{\varkappa F_3 r} \frac{e}{r \pm e} \tag{312}$$

where r is the mean radius of beam curvature (Fig. 221*d*).

The value of $\varkappa$ is usually found by graphical methods. The upper sign in equation (312) refers to the outer fibres and the lower sign to the inner fibres. The unit stress varies along a hyperbola (Fig. 221*d*).

In section *IV-IV* in the straight lower part (Fig. 221*a*) moment $M_{IV} = M_{III}$. The normal force $N_{IV} = N_{III}$. The resultant unit stress is

$$\sigma_{max} = \pm \sigma' - \sigma = \pm \frac{M_{IV}}{W_4} - \frac{N_{IV}}{F_4}. \tag{313}$$

All cross-sections below section *IV-IV* are subject only to bending. The bending moment diagram of the beam is illustrated in Fig. 221*e* and the stress diagram in Fig. 221*f*.

2. SUPERSTRUCTURES OF ROTARY JIB CRANES AND ROTARY LUFFING-BOOM CRANES

Jib Cranes with a Trolley. A diagram of a jib crane which can be swung around in a complete circle and with a moving trolley is represented in Fig. 222*a*. The crane is provided with a counterweight to reduce the horizontal reactions on the supports.

The magnitude of the counterweight G_{cw} should be such that the horizontal bearing reactions with a fully loaded trolley at the maximum radius are the same in value as with an unloaded trolley at the minimum radius but opposite in direction, i. e.,

$$G_{cw} = \frac{(Q + G_0)a + 2G_1e_1 + G_0a_0}{2e_g}. \tag{314}$$

When a fully loaded trolley is at the outer end of the boom we shall have the following bearing reactions in the boom:

vertical reaction

$$V = Q + G_0 + G_1 + G_{cw},$$

horizontal reactions

$$H_1' = H_1'' = \frac{(Q + G_0)\,a + G_1e_1 - G_{cw}e_g}{h_1}. \tag{315}$$

In these formulas:

Q—weight of the load being lifted;

G_0—weight of the trolley;

G_1—weight of the boom.

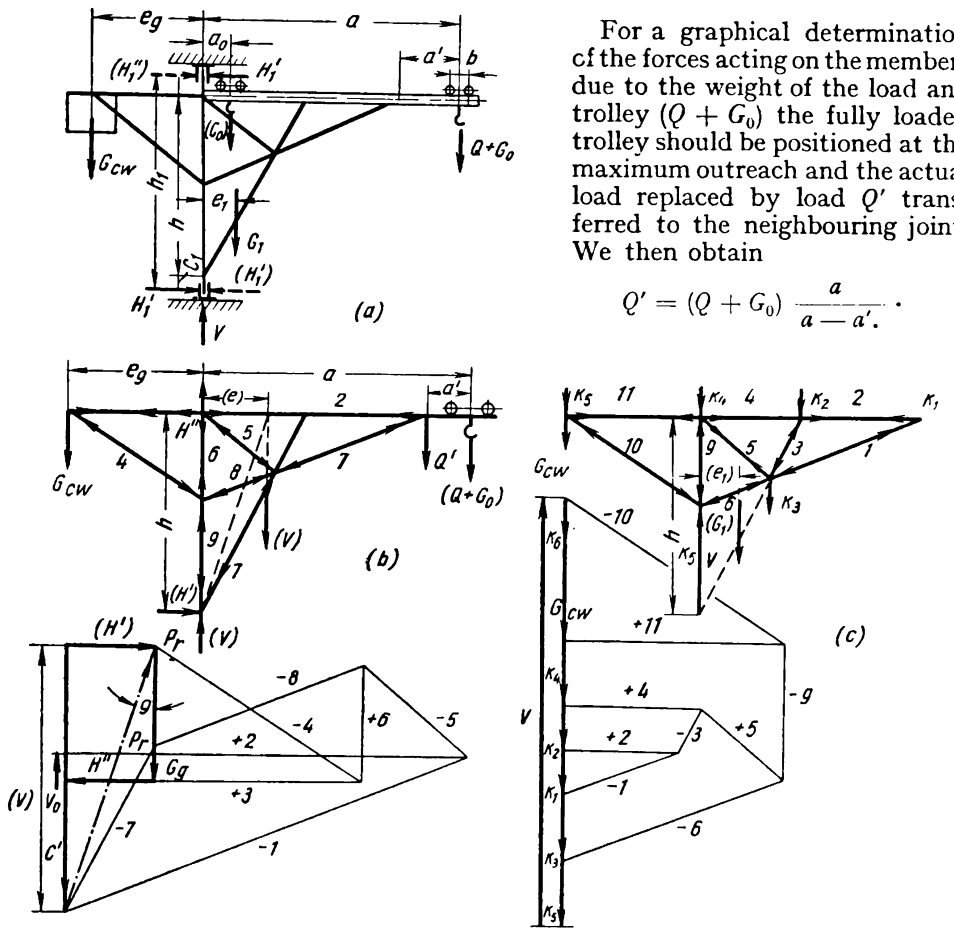

For a graphical determination of the forces acting on the members due to the weight of the load and trolley $(Q + G_0)$ the fully loaded trolley should be positioned at the maximum outreach and the actual load replaced by load Q' transferred to the neighbouring joint. We then obtain

$$Q' = (Q + G_0)\,\frac{a}{a - a'}.$$

Fig. 222. Graphical solution of a rotary jib crane superstructure in which the outreach is changed by a moving trolley

Forces Q' and G_{cw} are used to construct the Cremona force plan and to find the forces acting in the members due to the load and trolley (Fig. 222*b*).

The diagram for determining the forces due to the dead weight of the boom is constructed in the same way (Fig. 222*c*). Since in our crane the moment from the counterweight $G_{cw}\,e_g > G_1 e_1$ there will be no horizontal bearing pressure due to the dead weight of the boom.

Cranes with a Luffed Boom. Let us consider, by way of example, the revolving portion and the supporting members of a derrick crane (Fig. 223).

The forces acting in the boom and mast of such a crane can be easily found by graphical methods for the maximum radius (Fig. 223*a*). The weight of the boom G_1 and of the mast G_2 are transferred to the adjacent joints. Weight Q, force $\frac{G_1}{2}$ and the tensions in ropes S_1 and S_2 are combined at the end of the boom into resultant force R. Resultant forces R_1 and R_2 due to tensions S_1 and S_2 are distributed between the bottom and top joints of the mast as components R_1', R_1'', R_2' and R_2''. The Cremona force plan to find the stresses in the members is constructed from forces R, R_1', R_2', R_1'', R_2'', $\frac{G_1}{2}$, and $\frac{G_2}{2}$ (at the top and bottom).

The boom and the mast are subject to compression and bending. They are made of wood or rolled section steel. In the latter instance they have a square cross-section composed of four main angles connected in all planes by lattice bracing.

The mast of a derrick (Fig. 223*b*) is usually secured by two inclined supporting legs *11* and *12* at the top and by two horizontal members *13* and *14* at the bottom.

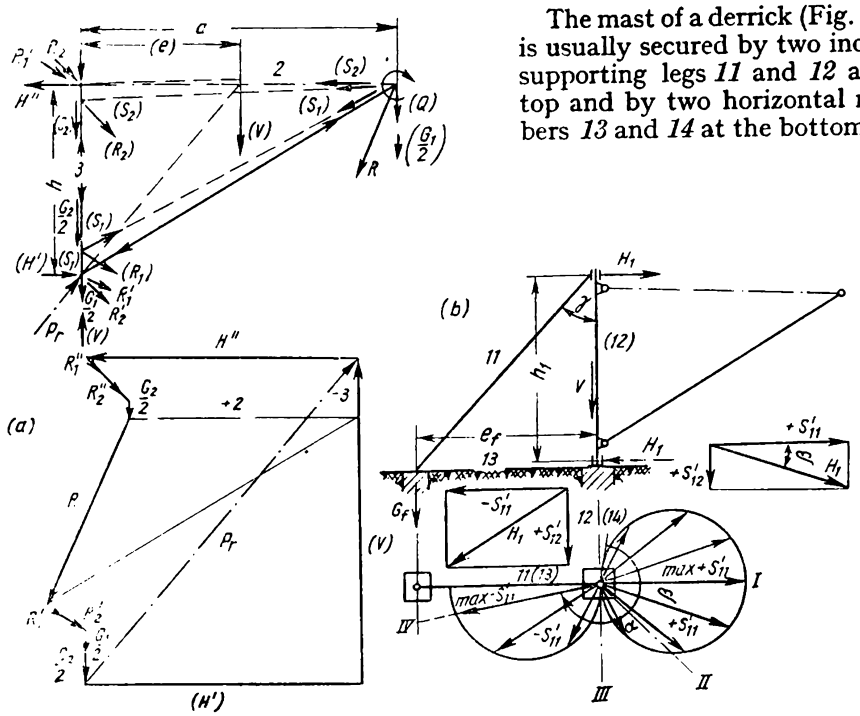

Fig. 223. Solution of the boom, mast and inclined braces of a derrick

When the boom is in position *I* ($\beta = 0$), leg *11* is loaded by the maximum force

$$+ S_{11}^{max} = + \frac{H_1}{\sin \gamma}$$

(leg *12* is not loaded). When the boom turns to the left of position *I*, the force acting on leg *11* decreases, being taken in part by leg *12* which in this case is subject to compression.

In position *II* (angle $\beta = 45°$) legs *11* and *12* carry the same load:

$$S_{11} = S_{12} = + H_1 \cos 45° \frac{1}{\sin \gamma}. \qquad (316)$$

In position *III*, if $\beta = 90°$, leg *11* is relieved of its load because leg *12* takes the entire horizontal force H_1. When $\beta > 90°$ leg *11* is subject to compression which will reach its maximum value in position *IV* ($\beta \approx 180°$)

$$- S_{11}^{max} = H_1 \sin (\beta - 90°) \frac{1}{\sin \gamma} \approx -1.0 \frac{H_1}{\sin \gamma}. \qquad (317)$$

The polar diagram (Fig. 223*b*) shows a curve representing the forces acting on leg *11* for the extreme positions of the boom limited by the angle α. The diagram for leg *12* will be similar to the one shown.

Horizontal members *13* and *14* are subject to compression or tension depending on the position of the boom. Member *13* is subject to maximum compressive stress in position *I*, that is, $S_{13}^{max} = -H_1$ and to maximum tensile stress in position *IV*, i. e.,

$$S_{13}^{max} = H_1 \sin (\beta - 90°) \approx + 1.0 H_1. \qquad (318)$$

If the bottom support of the mast transmits the horizontal bearing reaction directly to a concrete foundation, horizontal members *13* and *14* are dispensed

with. In this case the lower ends of legs *11* and *12* (each separately) are fastened by stay bolts to the concrete foundation. The upper pivot in a derrick which can be swung around in a full circle is not supported by legs *11* and *12* but is fastened rigidly by five or six steel guy ropes to the ground or to building columns. If we assume that of the six guy ropes two are stressed then the force applied to one guy rope will be equal to $\frac{H_1}{2\cos 30^\circ}$. But since the guy ropes are inclined at an angle of γ to the vertical, the actual design stress will be

$$S = \frac{H_1}{2\cos 30^\circ \sin\gamma}. \tag{319}$$

The actual margin of safety in the ropes should be at least five.

3. SUPERSTRUCTURES OF CANTILEVER CRANES

The supporting members of cantilever cranes are composed of two vertical travelling wheels which carry load due to the weight of crane, trolley and live load and two pairs of top and bottom horizontal bearing rollers which take the horizontal reactions from tipping moments (Fig. 224).

Fig. 224 shows the frame of a cantilever crane with an internal trolley and Fig. 225—that of a crane with an external trolley.

Full loads on the frame supports will be equal to (see Fig. 225):

the vertical bearing load is

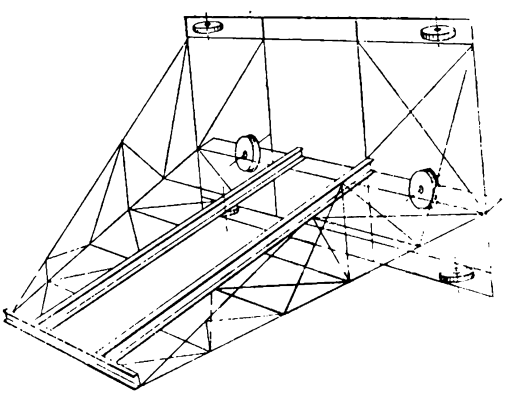

Fig. 224. Frame of a cantilever crane

$$V = Q + G_0 + G_1$$

where Q—weight of the load being lifted;
G_0—weight of the trolley;
G_1—weight of the crane without the trolley;

the horizontal bearing load is

$$H' = H'' = \frac{(Q + G_0)a + G_1 e_1}{h}. \tag{320}$$

Frames for cantilever cranes are manufactured in two modifications—with an external and internal trolley (running either on the top or bottom chord).

The constant load on the main girder of the frame (weight from dead load) comprises its own weight, half of the weight of the cross bracing and half of the weight of the platform structure with flooring. The other half of the weight of the cross bracing and flooring is carried by the auxiliary (side) girder.

The weight of the main girder, cross bracing and flooring is at first assumed tentatively by the comparison with available designs.

If we denote the load due to the girder weight by G_1 and the distance to its centre of gravity by e_1, then the reactions in the frame supports will be

$$V = G_1 \text{ and } H = G_1 \frac{e_1}{h}.$$

Assuming that load G_1 is uniformly distributed along the length of the girder we can find the forces acting on joints k_1 to k_6, inclusive, (Fig. 225*a*). When we

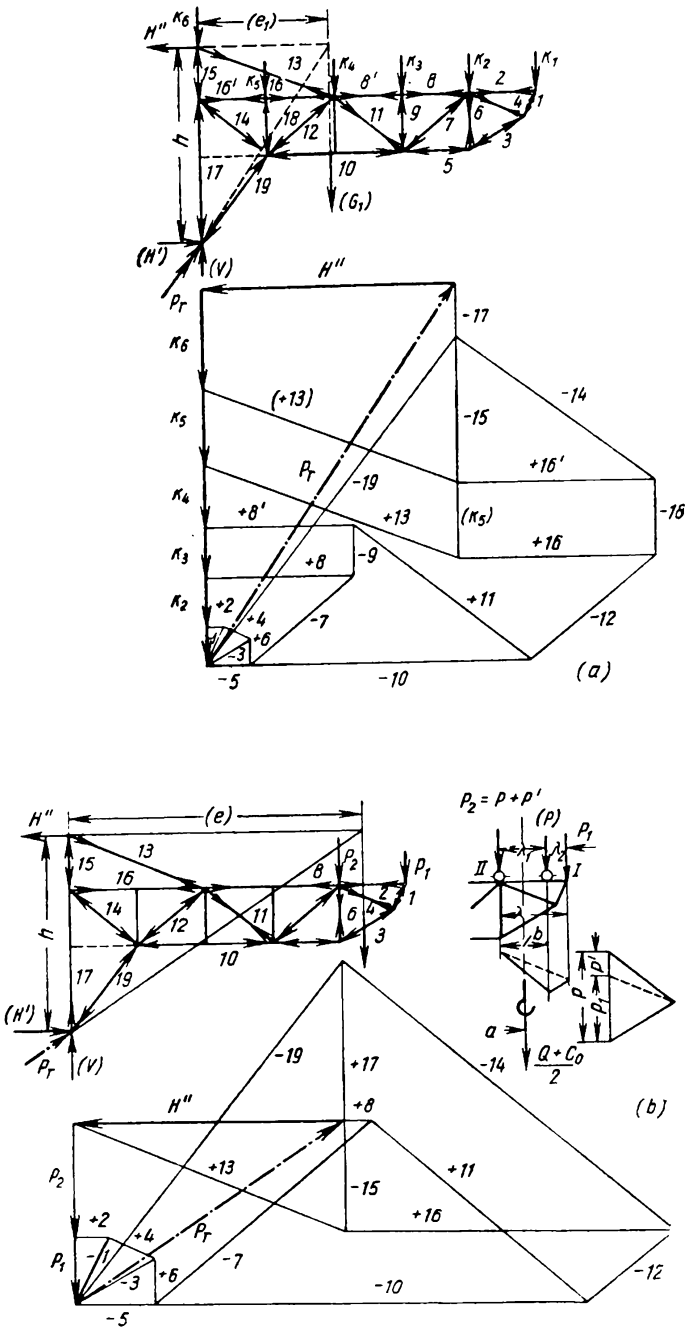

Fig. 225. Graphical solution of the main girders in a cantilever crane frame

know the forces at the joints we can find the stresses in the members, due to the weight of the girder, by constructing the Cremona force plan (Fig. 225*a*).

Stresses in the members due to a moving load (trolley and load). To find the maximum stress in the members we must construct several Cremona force plans for various positions of the load. At first the trolley is located at its extreme end position (maximum outreach *a*).

In this case the bearing reactions of two main girders will be

$$V = \frac{Q + G_0}{2} ; \quad H = \frac{Q + G_0}{2h} a = 2P \frac{a}{h}$$

where P is the load acting on one wheel of the trolley and is equal to

$$P \approx \frac{Q + G_0}{4} .$$

Force P is distributed between the adjacent joints (Fig. 225*b*); then in joints *I* and *II*

$$P_1 = P \frac{\lambda_1}{\lambda} ; \; P_2 = P + P' = P + P \frac{\lambda_2}{\lambda} .$$

Fig. 225*b* shows a Cremona force plan with the trolley at the maximum outreach. The members not designated in the diagram bear no stresses at all. The stresses due to the weight of the girder and the maximum stresses due to the moving load with the trolley at different positions are summed up.

The upper chord of the framework is subject to tension, and also to local bending due to the load of the trolley wheels. It is solved in the same way as the upper chord of the main girder of an overhead travelling crane (see below).

Most frequently the upper chord is designed in the form of one or two channel beams with a rail made of flat steel. The vertical members which are of secondary importance in the system decrease the panel length of the upper chord in respect to its resistance to local bending while for the lower chord, subject to compression, they decrease the length of the members subject to bending due to axial compression.

The side (auxiliary) girders of the framework are of the same construction as the main girder. Solution (by means of the Cremona force plan) is done only for constant load.

Cross bracing. When the crane is braked the framework is subject to bending due to the inertia forces from the loaded trolley stationed at maximum outreach. These inertia forces act parallel to the runway rails in a horizontal plane. As a rule, the horizontal force at maximum outreach *a* is assumed equal to

$$P_{in} = \frac{1}{10} (Q + G_0) .$$

The inertia forces of cantilever cranes are taken by horizontal trusses with cross bracing (Fig. 226). The vertical frame carrying the crane boom is provided with vertical and horizontal travelling and supporting wheels; the frame is made up of channel beams with diagonals. It should be sufficiently strong. A special check-up for strength should be applied to the girders with horizontal bearing rollers which take the reactions H_1' and H_1''.

Frame deflection. According to technical specifications, the deflection of cantilever crane framework at the maximum outreach should not exceed $\delta'' < \frac{1}{300} a$ (*a*—crane outreach).

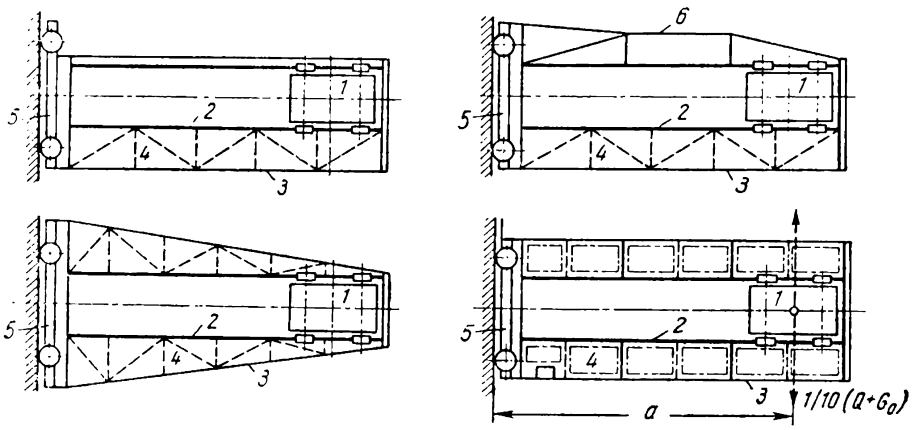

Fig. 226. Types of horizontal trusses of cantilever cranes
1—trolley, *2*—main girder, *3*—side (auxiliary) girder, *4*—cross bracing, *5*—vertical (travelling) frame, *6*—horizontal truss with braces

4. STRUCTURES OF OVERHEAD TRAVELLING CRANES

Depending on their lifting capacity and length of span the bridges of overhead travelling cranes are made up of plate girders (double-tees), trusses or box, double-web, girders.

Plate girders of overhead travelling cranes

The structure of an overhead travelling crane with plate girders is composed of two main longitudinal girders fastened at the ends to two cross girders which accommodate the travelling wheels. The other elements are auxiliary or side girders, cross bracing with a platform flooring and an operator's cab (these parts are not provided for all cranes with plate girders).

The main factors in the solution of plate girders are the safe unit bending stress and the permissible girder deflection. The vertical loads on the girders are: dead load (constant load) and the force exerted by the wheels of a trolley carrying the maximum load. The design dead weight of the main longitudinal girder of an overhead travelling crane is composed of the weight of the girder, one half the weight of the travelling mechanism (without wheels) and half the weight of the cross bracing and flooring (if such are on the crane).

Fig. 227 gives approximate values of the design dead weight of the main girders of electrically driven overhead travelling cranes with a lifting capacity from 5 to 50 tons and with a span from 10 to 30 metres.

Bending Moments and Lateral Forces due to Constant Load. If L (Fig. 228*a*) denotes the span of the main longitudinal girder in metres, G—its weight, i. e., constant load in tons uniformly distributed over the entire length of the span; q—dead weight in tons per running metre, then the bending moment at a distance x from the left support due to the dead weight will be

$$M_q = q\frac{L}{2}\,x - q\,\frac{x}{2} = q\,\frac{x}{2}(L-x) \text{ t-m.} \tag{321}$$

The maximum bending moment when $x = \frac{L}{2}$ is

$$M_q^{max} = q\frac{L^2}{8} = G\frac{L}{8} \text{ t-m.} \tag{322}$$

The curve of the bending moment will be a parabola plotted on length L with a maximum ordinate of M_q^{max} (Fig. 228*b*).

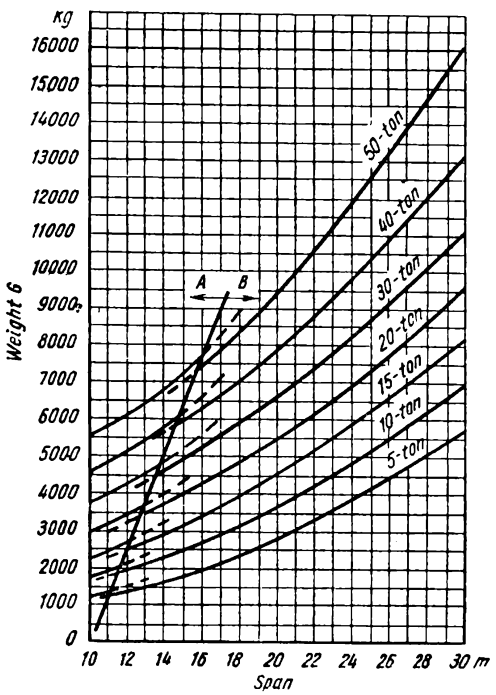

Fig. 227. Curves for approximate determination of the weight of the main longitudinal girders in overhead travelling cranes
A—plate girders, *B*—trusses

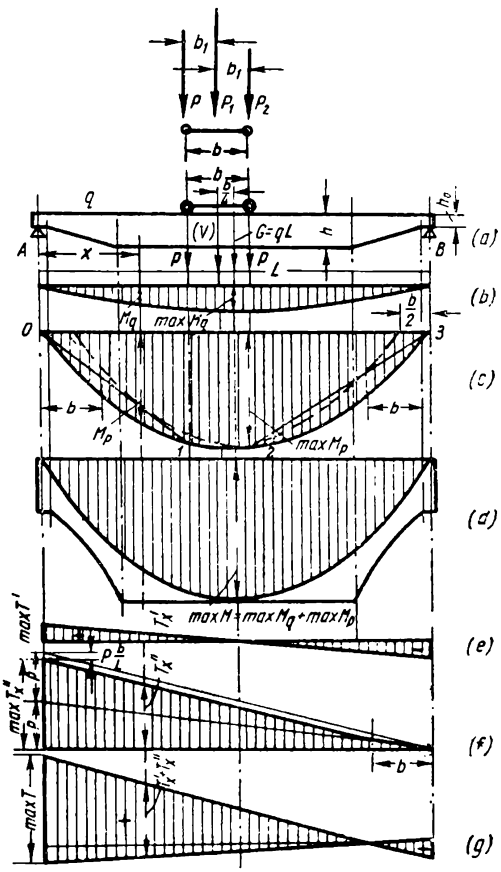

Fig. 228. Curves of moments and lateral forces for plate girders

The lateral force at a distance x from the left support is

$$T'_x = q\left(\frac{L}{2} - x\right) \text{ tons.} \tag{323}$$

The maximum lateral force on the right or left support at $x = 0$ will be

$$T'_{max} = \pm q\frac{L}{2} \text{ tons.} \tag{324}$$

The curve of lateral forces is shown in Fig. 228*e*.

Bending Moments and Lateral Forces due to Moving Load (Trolley and Load). When the weight of a loaded trolley is distributed uniformly on the wheels, the load acting on one wheel will be $P = \frac{Q + G_0}{4}$ where Q is the weight of the load carried and G_0—weight of the trolley.

It can be assumed in this case that the girder carries two identical loads P spaced at distance b (Fig. 228*a*). Then the bending moment in the section under the left wheel, stationed at distance x from the left support, will be

$$M_P = \frac{2P}{L}\left[\left(L - \frac{b}{2}\right) - x\right] x \text{ t-m.} \tag{325}$$

The maximum bending moment will be in the section at a distance $\frac{b}{4}$ from the middle of the girder span

$$M_p^{max} = \frac{P}{2L}\left(L - \frac{b}{2}\right)^2 \text{ t-m.} \tag{326}$$

The bending moment is distributed in the form of a parabola with the largest ordinate on length $\frac{L}{2} - \frac{b}{2}$ (Fig. 228*c*). The curve of moments for the most unfavourable position of the loads will be *0-1-2-3*; it is obtained from the plotting of two curves of moments—from the movement of the loads from the left to the right and from the right to the left.

The maximum bending moment is reduced as the distance between the wheels increases. If the distance between the wheels (for example, in hand trolleys) is small in respect to the length of the span we can assume with an accuracy sufficient for practical purposes that $b = 0$ and

$$M_p^{max} = P\,\frac{L}{2}.$$

If the trolley wheels are unequally loaded it can be assumed that two unequal loads P_1 and P_2 travel along the girder; then $V = P_1 + P_2$ is the resultant of both loads acting on the wheels and

$$b_1 = \frac{P_2\, b}{V} \quad \text{and} \quad b_2 = \frac{P_1\, b}{V}.$$

In this case the bending moment in the section under the left wheel, which is at a distance x from the left support, will be

$$M_p' = \frac{V}{L}\left[(L - b_1) - x\right]x \text{ t-m.} \tag{327}$$

The maximum bending moment under load P_1 at a distance $\frac{b_1}{2}$ from the middle of the girder is

$$M_p'^{max} = \frac{V}{4L}(L - b_1)^2 \text{ t-m.} \tag{328}$$

This expression is an equation of a parabola plotted on length $(L - b_1)$ with a maximum ordinate M_p^{max}.

The moments in the section under load P_2 at a distance x from the right support are determined in the same way, i. e.,

$$M_p'' = \frac{V}{L}[(L - b_2) - x]\,x \text{ t-m} \tag{329}$$

and

$$M_p''^{max} = \frac{V}{4L}(L - b_2)^2 \text{ t-m.} \tag{330}$$

Equation (330) is a parabola on the length $(L - b_2)$ with the ordinate $M_p''^{max}$.

For identical loads P and P the lateral force at a distance x from the left support (Fig. 228*f*) is

$$T_x'' = \frac{2P}{L}\left[\left(L - \frac{b}{2}\right) - x\right] \text{ tons.} \tag{331}$$

When $x = 0$ the maximum lateral force on the left support will be

$$T''_{max} = A = \frac{2P}{L}\left(L - \frac{b}{2}\right) = 2P - P\,\frac{b}{L} \text{ tons.} \tag{332}$$

The lateral force at a distance $(L - b)$ from the left support is

$$T_b'' = P\frac{b}{L} \text{ tons.} \tag{333}$$

With loads P_1 and P_2 the lateral force at a distance x will be

$$T_x^{P_1-P_2} = \frac{V}{L}[(L - b_1) - x] \text{ tons.} \tag{334}$$

When $x = 0$

$$T_{x(max)}^{P_1-P_2} = A = \frac{V}{L}(L - b_1) = (P_1 - P_2) - P_2\frac{b}{L} \text{ tons.} \tag{335}$$

The lateral force at a distance $(L - b)$ from the left support is

$$T_x = P_1\frac{b}{L}.$$

If we add together the curves of moments due to the action of the dead weight (Fig. 228*b*) and the moving loads (Fig. 228*c*) we shall obtain the resultant curve of moments (Fig. 228*d*)—hatched area. Multiplying the moments of resistance in the various cross-sections of the girder by the safe stress we shall get a curve illustrating the girder strength (curve of safe moments)—contour line in Fig. 228*d*. The resultant diagram of the lateral forces is shown in Fig. 228*g*.

Fig. 229 represents diagrams of moments M_p^{max} and M_q^{max} for the main longitudinal girders of overhead travelling cranes with lifting capacities from 5 to 50 tons and for spans from 10 to 30 metres.

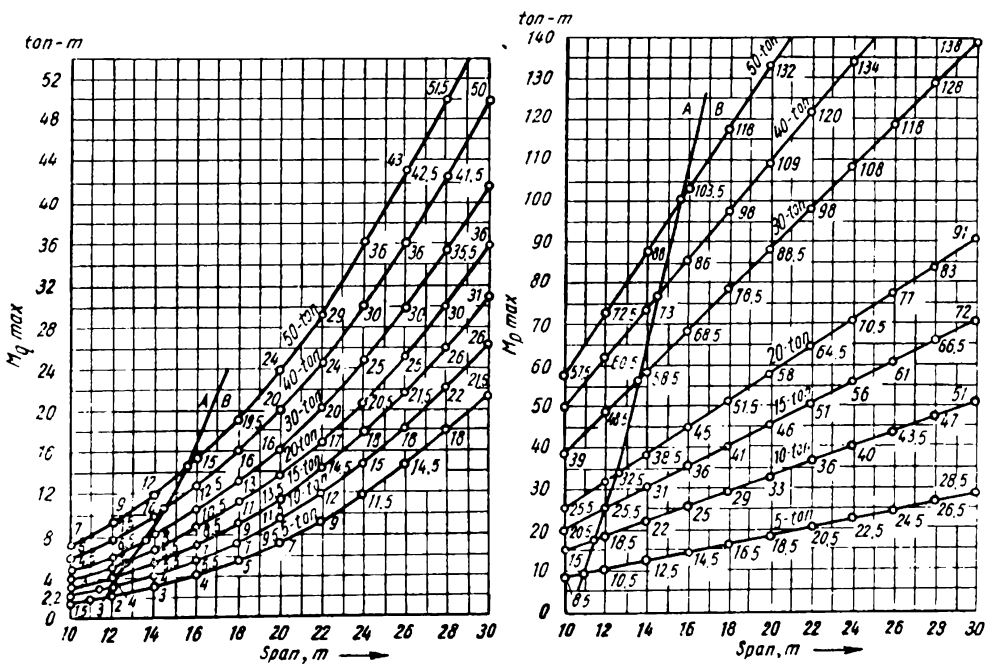

Fig. 229. Curves for approximate determination of the maximum moments due to constant (M_q^{max}) and moving (M_p^{max}) loads acting on the main longitudinal girders of overhead travelling cranes

A—plate girders, *B*—trusses

Unit stress due to bending moments

(a) From the main loads

$$\sigma = \frac{\psi M_q + \mu M_p}{W_{net}} < [\sigma] . \tag{336}$$

(b) From the main and additional loads

$$\sigma = \frac{\psi M_q + \mu M_p + \Sigma M_{add}}{W_{net}} < [\sigma] . \tag{337}$$

Unit stress from lateral forces

(a) From the main loads

$$\tau = \frac{[\psi T' + \mu T''] S_{gr}}{\delta I_{gr}} < [\tau] . \tag{338}$$

(b) From the main and additional loads

$$\tau = \frac{[\psi T' + \mu T'' + \Sigma T_{add}] S_{gr}}{\delta I_{gr}} < (\tau) . \tag{339}$$

The following notation is accepted in the preceding formulas:
σ—actual normal unit stress (in bending), in kg/cm²;
τ—actual tangential unit stress (in shear), in kg/cm²;
$[\sigma]$ and $[\tau]$—safe unit bending and shearing stresses, in kg/cm²;
ψ—dynamic coefficient for forces due to constant load;
μ—dynamic coefficient for forces due to moving load;
W_{net}—net section moment (without rivet holes);
ΣM_{add}—sum of the bending moments in the section due to additional loads;
S_{gr}—gross static moment in the corresponding part of the section (with rivet holes);
δ—thickness of the section wall;
I_{gr}—gross moment of inertia in respect to the main axis;
ΣT_{add}—sum of the lateral forces in the section due to additional loads.

Table 42 illustrates the values of coefficients ψ and Table 43—the values of coefficients μ.

Table 42

Dynamic Coefficients ψ for Forces due to the Constant Load

Type of crane	Duty	Crane travelling speed, m/min	Coefficient ψ
Hand driven	—	Up to 60	1.0
Power driven	Light	Up to 60	1.0
	Medium	Over 60	1.1
	Heavy		

Table 43

Dynamic Coefficients μ for Forces due to the Moving Load

Type of crane	Duty	Coefficient	Notes
Hand driven	—	1.0	
Power driven	Light	1.1	
	Medium	1.2	This group also includes foundry cranes
	Heavy	1.4	This group includes special cranes employed in metallurgical plants

The forces which arise in the metal structures of the crane under the action of constant loads should be reduced to actual forces by multiplying them by coefficient ψ which takes into account the dynamic effects of the moving structure and which depends on the travelling speed. In like manner coefficient μ is used to correct the forces due to a moving load.

Thus, the main loads in the structure are: dead weight, movable load and inertia load caused by the forces of acceleration of the structure together with the trolley and load.

Among the additional loads are: wind pressure, snow and ice, load due to temperature effects as well as the horizontal braking forces which appear along the bridge when the crane trolley is braked (assumed as 1/7 of the total forces exerted by all the driving wheels of the trolley), and across the bridge when the crane itself is braked [formulas (351) and (352)].

Deformation (Deflection) of Girders. Excessive deflection of the main girders causes the entire bridge to oscillate and unfavourably affects crane operation.

To keep the deflection within safe limits the main longitudinal girder should be sufficiently deep and possess an adequate moment of inertia.

In a girder with a constant moment of inertia I cm^4, the maximum deflection from its own weight (Fig. 230) will be

$$\delta' = \frac{G}{EI} \times \frac{5L^3}{384} \text{ cm} \tag{340}$$

where G—weight of the girder, in kg;

$E \approx 2{,}200{,}000$ kg/cm^2—modulus of elasticity.

The deflection due to moving loads can be determined on the assumption that two loads P and P (loads on the wheels of a loaded trolley) are located symmetrically in the middle of the crane (Fig. 230). Then we shall obtain with sufficient accuracy

$$\delta'' = \frac{P}{48\,EI}(L - b)\,[L^2 + (L + b)^2] \text{ cm}. \tag{341}$$

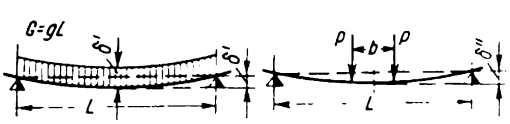

Fig. 230. Diagrams for calculating the deflection in the main girders of overhead travelling cranes

The full deflection will be

$$\delta = \delta' + \delta''.$$

Checking the Strength of the Lower Flanges on Monorail Tracks. In single-girder overhead cranes a hand or power-driven hoist is often designed to move on a rolled I-beam.

The lower flange of such a beam (Fig. 231) is subject to a bending down force. In calculations it is regarded as a plate rigidly fixed on one (long) side and with a load moving along the other free end. In this case the bending moment (per unit length) will be

$$M = 0.51P$$

where P—force exerted by a runner which in a four-wheel design will be

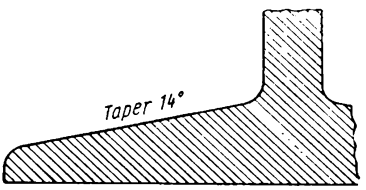

Fig. 231. Lower flange of an I-beam

$$P = \frac{Q + G_0}{4}$$

(G_0—weight of the movable hoist and Q—its lifting capacity).

Denoting the thickness of the flange by t, the section moment (per unit length) will equal

$$W = \frac{1t^2}{6} = \frac{t^2}{6}.$$

The stress in the flange will be

$$\sigma = \frac{3.05P}{t^2}.$$

Trusses of Overhead Travelling Cranes

Trusses are employed in overhead travelling cranes with spans of 12 metres and over. The depth of the truss (Fig. 232) is usually $h \approx (\frac{1}{12}$ to $\frac{1}{10})\,L$. The latticed framework may be either of triangular or diagonal design. The triangular version is more widespread.

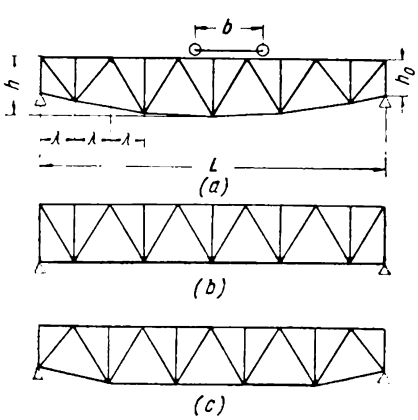

Fig. 232. Diagrams of trusses for overhead travelling cranes

A curved-chord truss (Fig. 232*a*) is superior to other designs due to smaller weight but the different lengths of the diagonals and verticals increase manufacturing costs.

A parallel-chord truss (Fig. 232*b*) is used mainly in cranes designed with an auxiliary trolley running along the lower chord. Such truss offers an advantage of uniform length of bracing members and is easy and inexpensive in manufacture. However, it is heavier than the preceding type.

Preference is usually given to a truss in which the lower flange is bevelled on both extreme panels (Fig. 232*c*). Such a design nullifies to a certain degree the shortcomings inherent to the first two types.

The depth of the truss ends h_0 depends on the height of the end cross beam and is

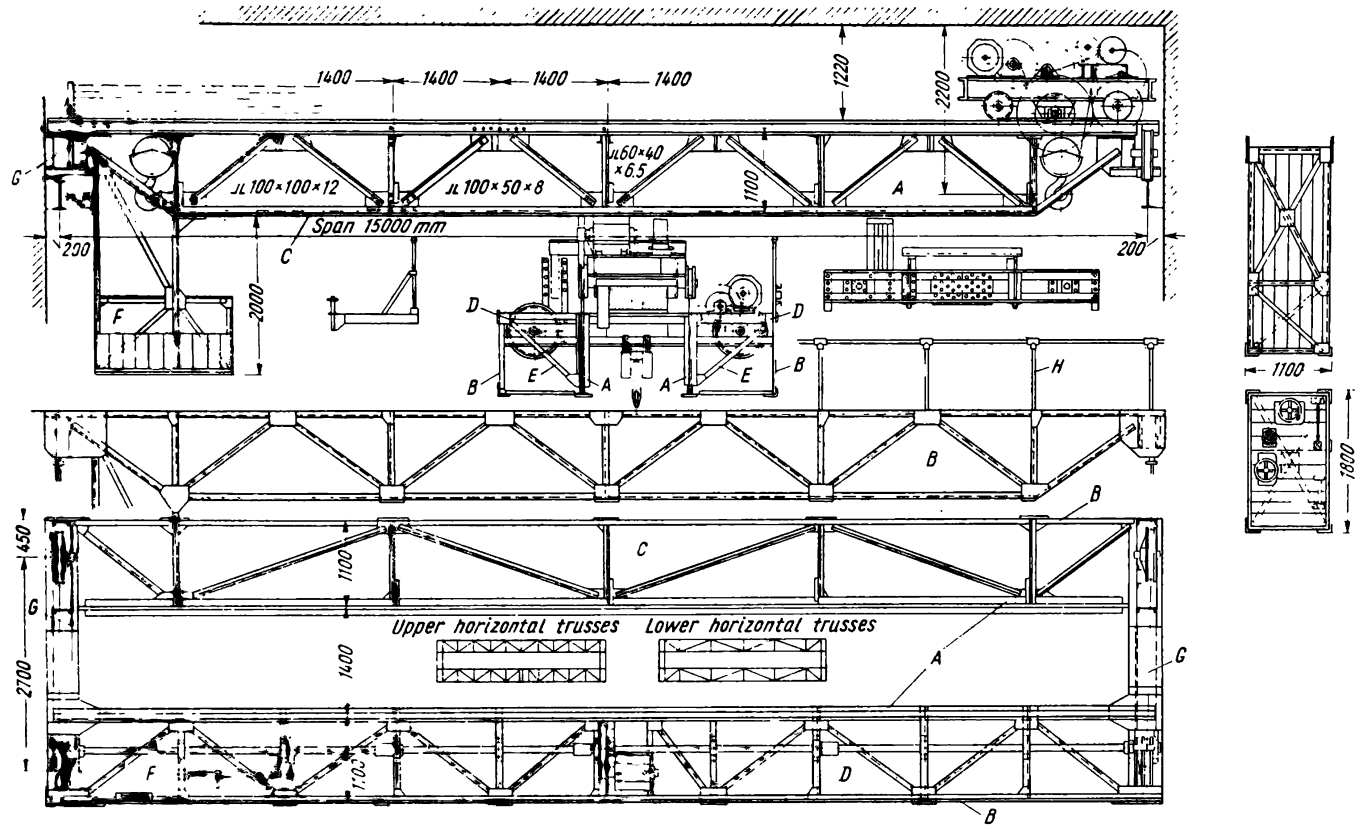

Fig. 233. Overhead travelling crane with a trussed structure

usually taken as $h_0 \approx$ (0.4 to 0.45) h. The width of the panel $\lambda \approx h$. Production considerations favour an even number of panels.

In a triangular design the auxiliary verticals serve only the purpose of decreasing by half the distance between the joints of the upper chord which experiences local bending from the load on the trolley wheels.

The structure of an overhead travelling crane is a complex spatial system (Fig. 233) which comprises the following elements: two main (internal) trusses A, two auxiliary or side (external) trusses B, two horizontal (wind) trusses C in the plane of the lower chords, two upper platform trusses D, two sets of cross bracings E, operator's cab F (suspended on one main and one auxiliary truss), railings H and end cross girders G.

The main trusses A take the load from the weight of the loaded trolley and transmit it through cross girders G and the travelling wheels to the crane runway rails. The side trusses B serve as secondary supporting members for the platform trusses D which carry the crane travelling mechanism. The horizontal trusses C, as well as the platform trusses, take the wind and inertia loads. Cross bracings E are provided to add stiffness to the box-shaped crane bridge.

The structure of an overhead travelling crane is analysed not as an integral spatial system but by an approximate method—by dividing it into a number of plane systems. This method, which has proved its worth in practice, helps to achieve a certain reserve of strength and stiffness of the entire structure.

The main trusses carry the maximum load and their solution requires greatest attention. The weight of one, most heavily loaded, main truss (on the side of the travelling mechanism) can be tentatively determined from the following empirical formulas:

for cranes with a lifting capacity of $Q = 5$ to 39 tons

$$G_{main} \approx 10\, Q_{tons}\, (L - 5) + 700 \text{ kg}; \tag{342}$$

for cranes with a lifting capacity of $Q = 40$ to 75 tons

$$G_{main} \approx 10\, Q_{tons}\, (L - 5) \text{ kg} \tag{343}$$

where L is the crane span, in metres.

The main truss carries the following loads:

1) constant load which includes the dead weight of the main truss, one half the weight of the platform truss with the flooring, one half the weight of the horizontal truss, one half the weight of the cross bracings (these loads are uniformly distributed over the entire truss length), one half the weight of the travelling mechanism (for more accurate calculations this load is distributed only among the three middle panel points of the truss), one half the weight of the operator's cab with electric gear (for more accurate calculations this load is distributed only among the two extreme panel points of the framework)*;

2) moving load from the weight of the trolley and load transmitted by the wheels to the main girder;

3) inertia loads which arise in braking the bridge with the trolley and load (account is taken only of the part of load bearing on the main truss);

4) local bending of the top or bottom chord from the direct load of the trolley wheels inside a panel;

5) wind pressure during exposed operation of the crane.

Stresses in the Truss Members due to Constant Load. The stresses in the members due to the truss weight can be easily determined graphically by constructing the Cremona force plan. The following should be taken into account when determining the total weight on the main truss from constant load:

1) weight of the main truss [formulas (342) and (343)];

* Sometimes calculations are done by a simplified method, assuming that the weight of the travelling mechanism and the operator's cab is distributed uniformly along the entire length of the girder.

2) weight of the horizontal truss $G_{hor} \approx \frac{1}{6} G_{main}$;

3) weight of the platform truss $G_{pl} \approx \frac{1}{8} G_{main}$ (without flooring);

4) weight of the flooring made usually of steel sheets with punched holes, so-called perforated steel

$$G_{fl} = Lb\delta\gamma k$$

where L—span, in mm;
b—width of the flooring, in mm;
δ—sheet thickness, in mm;
γ—specific weight of steel, in kg/dm³;
k—coefficient accounting for the punched holes in the flooring ~ 0.5*; the width of the flooring b is usually taken as 800-1,000-1,200 mm;

5) weight of cross bracings $G_{cr.br} \approx \frac{1}{30} G_{main}$;

6) weight of the travelling mechanism $G_{mech} \approx$ 700 to 1,300 kg for cranes with a lifting capacity up to 20 tons;

7) weight of the operator's cab with electric devices and the operator $G_{cab} \approx$ ≈1,000 to 1,500 kg.

Hence, the total weight of the main truss from the constant load will be

$$G = G_{main} + \frac{1}{2} G_{hor} + \frac{1}{2} (G_{pl} + G_{fl}) + \frac{1}{2} G_{cr.br} + \frac{1}{2} G_{mech} + \frac{1}{2} G_{cab} \qquad (344)$$

and the load borne by each joint or panel point of the framework will be

$$K = \frac{G}{n - 1} \qquad (345)$$

where n is the number of joints.

The two supporting end joints are considered as one joint since the load sustained by each is equal to half the load in the intermediate joints.

After drawing the truss diagram (to scale) and finding the load borne by the joints we proceed to construct the Cremona force plan which will by symmetrical if the operator's cab weight is assumed as distributed over the entire length of the girder.

Fig. 234 shows the Cremona force plan for the truss of an overhead travelling crane. Members 0_1 and 0_6 are unstressed.

In constructing this diagram we should take all the members in consecutive order (clockwise, for example). The forces acting on the joints and the bearing reactions are plotted in bold lines while the arrows indicate the direction of their action. The stresses in the members are denoted by thin lines and have no arrows on the diagram. The arrows are marked on the truss diagram in accordance with the force polygon. Each member is provided with two arrows: one from the force polygon of one

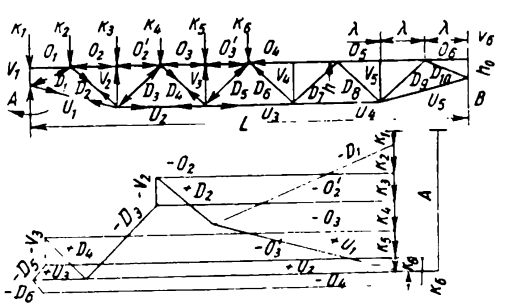

Fig. 234. Determining the stresses in the members of the truss due to constant load

* Perforated flooring is employed not only to reduce the weight of the entire structure but also to enable the crane operator to have a better view of the load grabbing device which otherwise may be in the shadow of the solid flooring since the main source of illumination is through skylights.

joint and the other from the force polygon of the second joint. If both arrows of a member, for example, in the lower chord (Fig. 234), are directed away from the joints, then the member will be in tension; if they go towards the joints the member (for example, in the upper chord) will be in compression. Tension and compression are denoted by plus and minus signs, respectively. The stresses in the members due to the dead weight obtained from the diagram are set down in the respective column of the summary table.

Stresses in the Truss Members due to Moving Load. A moving load (load on the trolley wheels from its weight and the weight of the carried load) subjects the upper chord of the main girder to compression and the lower chord to tension. Depending on the position of the trolley the diagonals are subjected to either tension or compression.

The verticals in a triangular lattice truss (see Fig. 232) are always in compression. The position of the trolley at which individual members are subject to maximum stress can be found as follows. When the trolley is moved from the left to the right support and its left wheel is located consecutively over joints *II*, *III*, . . . to *IX*, each time two members are subject to maximum stress (indicated in Fig. 235 by thick and thin lines for tensile or compressive forces, respectively). Diagonals D_1, D_3, etc., with the trolley in these positions, experience maximum compression and diagonals D_2 and D_4 maximum tension.

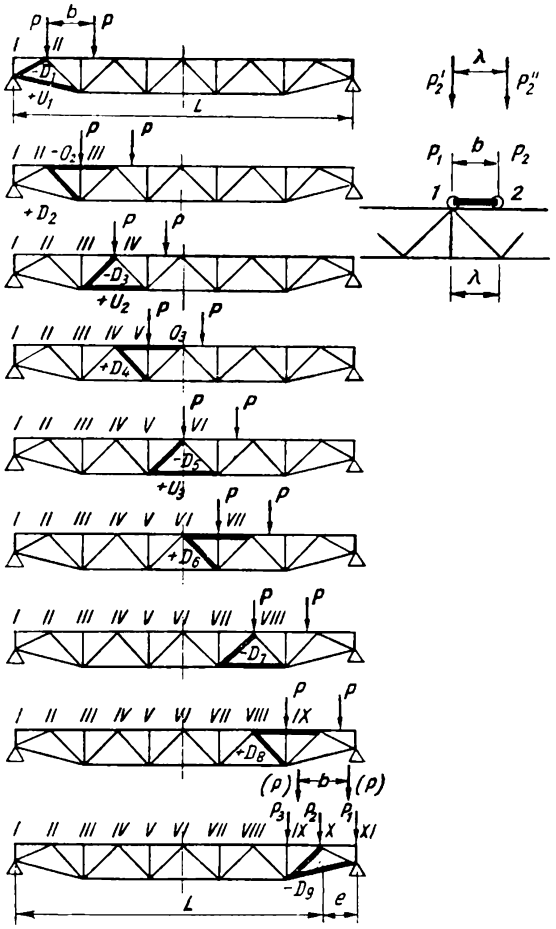

Fig. 235. Determining the maximum stresses in the members of the main girder due to moving load

When the trolley, moving to the right, reaches the middle of the span, diagonals D_6 (D_5) and D_8 (D_7) are subjected to maximum tension and diagonals D_7 (D_4)—maximum compression. If the distance between the trolley wheels exceeds the length of the panel, even the most unfavourable position of the load has no effect on maximum compression of $D_5(D_2)$.

To obtain the compressive stress in member D_9 (D_2) when $b>\lambda$, the loaded trolley should be positioned on the zero panel *e* and the wheel load should be replaced by three forces P_1-P_2-P_3 acting on joints *XI*, *X* and *IX*.

The maximum stresses in the members of the upper and lower chords due to a moving load are determined by finding the bending moments for all joints of the truss, when the trolley travels from the left to the right and from the right to the left, with the aid of a funicular polygon or by means of influence lines.

The second method will be examined in more detail.

If the distance between the trolley wheels is $b \leqslant \lambda$ wheel *1* is placed on the front joint and forces P_2' and P_2'' of wheel *2* are determined for the adjacent joints according to the moment equation. When $b<\lambda$ the actual trolley is replaced

by an imaginary one in which the distance between the wheels is λ and the loads on the wheels are $P+P_2'$ and P_2''; when $b>\lambda$ the imaginary trolley will have three axles at distances λ and the loads on the wheels will be P_1, P_2' and P_2'' (Fig. 235).

After the moving loads have been determined proceed to construct influence lines of the moments. For this purpose first plot to scale a diagram of the truss (Fig. 236), draw a horizontal line at the bottom equal to the length of the span

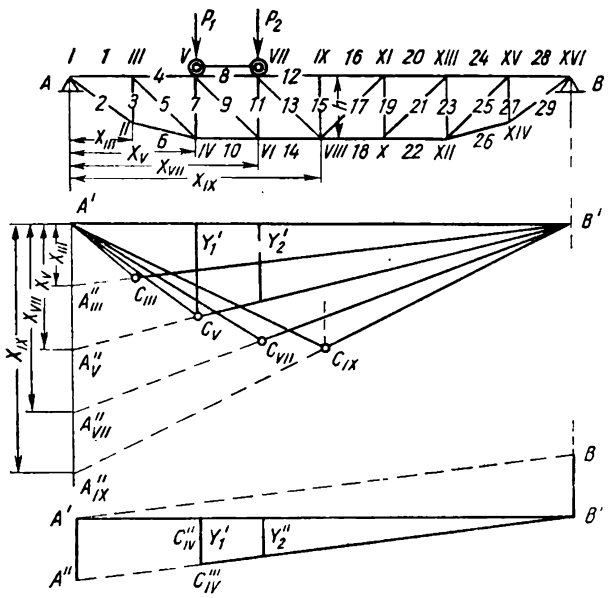

Fig. 236. Construction of influence lines

and plot on the vertical line perpendicular to it ordinates corresponding to various positions of the trolley. Points A''_{III}, A''_{V}, etc., are connected by straight lines with point B'; the contour obtained will depict the influence lines of the moments.

The maximum moment, for instance for joint IV (Fig. 236), is determined by placing the trolley over it in the most unfavourable position. After that joint IV is projected on line $A''_{V}B'$ to obtain point C_V which is connected by a straight line with point A'; the moment in joint IV will be equal to

$$M_{IV} = Py'_1 + P_2y'_2. \tag{346}$$

The same method is used to find the moments in the other joints.

The stresses in the chords are found by dividing the moment in the joint opposite to the triangle of the truss by the shortest distance from the member to the joint, i.e.,

$$S_4 = \frac{M_{IV}}{h}. \tag{347}$$

If we construct the influence lines of lateral forces we can find the stresses in the inclined braces. This is done as follows. To find the lateral force for joint IV, for example, the load is stationed in the most unfavourable position. Then, perpendicular to straight line AB (which is equal to the truss span) (Fig. 236), line $A'A''=1$ is plotted downwards from point A' and line $B'B''=1$ upwards from point B'. Point A is connected with point B'' and point A'' with point B', after which a vertical line is drawn through joint IV to obtain line $C''_{IV}C'''_{IV}=y''_1$

The lateral force will be

$$T_{IV} = Py_1'' + P_2y_2''. \tag{348}$$

The same method is used to find lateral forces for the other joints.

The stresses in the inclined braces are determined with the help of a Cremona force plan constructed for a truss when the reaction of the left support is $A = 1$ ton.

For this purpose the right penultimate joint is correspondingly loaded. The stresses in the inclined braces will be

$$S = F\frac{T}{1{,}000} \tag{349}$$

where F—stress in the inclined brace obtained from the Cremona force plan for $A = 1$ ton;

T—lateral force in the joint (most unfavourable).

The trolley wheel loads lead to only compressive stresses in the verticals.

If $b = \lambda$ or $b > \lambda$ (see Fig. 232*a*), then the stress in the vertical will be $S = P_1$; if $b < \lambda$, then

$$S = P_1 + P_2\frac{\lambda - b}{\lambda}. \tag{350}$$

The values of the stresses in the members due to the moving load are noted down in the respective column of the summary table.

Additional Stresses in the Truss Members due to Crane Braking. The upper chord is also subject to bending forces in a horizontal plane due to the braking forces of the moving parts of a loaded crane. The force from the inertia of the parts reaches its maximum when the crane travelling wheels are suddenly braked.

If we denote the weight of the load being lifted by Q, weight of the trolley by G_0, weight of the crane (without the trolley) by G in kg, acceleration of gravity by g ($g = 9.81$ m/sec^2) and the coefficient of friction between the travelling wheel and the rail by μ ($\mu \approx 0.2$) and if one half of the crane wheels are braked we shall obtain

$$\frac{Q + G_0 + G}{g}a = \frac{Q + G_0 + G}{2}\mu$$

where retardation will be

$$a = \mu\frac{g}{2}.$$

The inertia force of the trolley mass acting on the truss in a horizontal plane will be

$$P_{in} = \frac{Q + G_0}{4}a;$$

$$P_{in} = \frac{1}{10}(Q + G_0)\text{kg}. \tag{351}$$

Since this force is transmitted to the rails of both main girders, each upper chord and its horizontal stiffening frames take (through the cross bracing) one half of the inertia forces. The maximum bending moment will occur at a distance $\frac{b}{4}$ from the middle of the span. The moment equation [formula (326)] should be complemented with the value of the horizontal force exerted by one wheel on one truss

$$P'_{in} = \frac{1}{10} \times \frac{Q + G_0}{4}.$$

Hence the maximum horizontal bending moment will be

$$M_{hor}^{max} = \frac{P'_{in}}{2L}\left(L - \frac{b}{2}\right)^2 \text{ kg-cm.} \tag{352}$$

Unit Stresses in the Truss Members

Checking for tension or compression:
(a) due to the action of the main loads

$$\sigma = \frac{\psi S_q + \mu S_p}{F_{net}} < [\sigma]; \tag{353}$$

(b) due to the action of the main and additional loads

$$\sigma = \frac{\psi S_q + \mu S_p + \Sigma S_{add}}{F_{net}} < [\sigma]. \tag{354}$$

Checking for stability (in compression):
(a) due to the action of the main loads

$$\sigma = \frac{\psi S_q + \mu S_p}{\varphi F_{gr}} < [\sigma]; \tag{355}$$

(b) due to the action of the main and additional loads

$$\sigma = \frac{\psi S_q + \mu S_p + \Sigma S_{add}}{\varphi F_{gr}} < [\sigma]. \tag{356}$$

Checking for lateral bending and compression:
(a) due to the action of the main loads

$$\sigma = \frac{\psi S_q + \mu S_p}{F_{net}} + \frac{\mu M_p}{W_{net}} < [\sigma]; \tag{357}$$

(b) due to the action of the main and additional loads

$$\sigma = \frac{\psi S_q + \mu S_p + \Sigma S_{add}}{F_{net}} + \frac{\mu M_p + \Sigma M_{add}}{W_{net}} < [\sigma]. \tag{358}$$

Checking for stability:
(a) due to the action of the main loads

$$\sigma = \frac{\psi S_q + \mu S_p}{\varphi F_{gr}} + \frac{\mu M_p}{W_{gr}} < [\sigma]; \tag{359}$$

(b) due to the action of the main and additional loads

$$\sigma = \frac{\psi S_q + \mu S_p + \Sigma S_{add}}{\varphi F_{gr}} + \frac{\mu M_p + \Sigma M_{add}}{W_{gr}} < [\sigma]. \tag{360}$$

In checking stability (bending due to axial compression) the value of coefficient φ is taken for the flexibility of the member in the bending plane from Table 44.

Table 44

Coefficients φ by Which Safe Stresses are to be Reduced in Bending due to Axial Compression of Centrally Loaded Truss Members

Flexibility of member γ	Coefficient φ for steel	Flexibility of member γ	Coefficient φ for steel	Flexibility of member γ	Coefficient φ for steel
0	1.00	70	0.81	140	0.36
10	0.99	80	0.75	150	0.32
20	0.96	90	0.69	160	0.29
30	0.94	100	0.60	170	0.26
40	0.92	110	0.52	180	0.23
50	0.89	120	0.45	190	0.21
60	0.86	130	0.40	200	0.19

The flexibility of the member is found from the formula

$$\gamma = \frac{l}{\sqrt{\frac{I_{gr}}{F_{gr}}}} \tag{361}$$

where I_{gr}—gross moment of inertia of the section of the member;
F_{gr}—gross sectional area of the member;
l—length of the member.

The flexibility of the member should not exceed:

(a) 120—for members of chords and end braces of the truss in compression;

(b) 150—for other members of the main truss in compression and also for a chord in tension;

(c) 200—for other members of the main truss in tension;

(d) 200—for members of auxiliary trusses in compression;

(e) 250—for other members of auxiliary trusses.

The following notation is used in formulas (353) to (360), inclusive:

ψ—dynamic coefficient for forces due to constant load (see Table 42);

S_q—force due to constant load;

μ—dynamic coefficient for forces due to moving load (see Table 43);

S_p—force due to moving load;

M_p—bending moment due to local bending in the upper chord resulting from the trolley wheel loads (Fig. 237), found from the formula

$$M_p = P_1 \frac{\lambda}{6}, \tag{362}$$

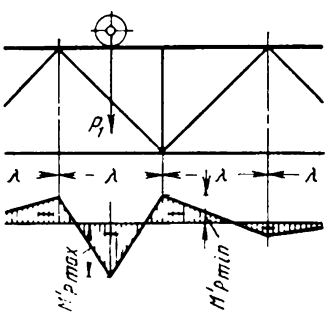

Fig. 237. Diagram of moments due to local bending of the upper chord resulting from the trolley wheel loads

F_{net}—net sectional area of the member (without rivet holes);

F_{gr}—gross sectional area of the member (with rivet holes);

W_{net}—net section moment of the member;

W_{gr}—gross section moment of the member;

ΣS_{add}—summary force due to additional loads*;

ΣM_{add}—summary moment due to additional loads*;

$[\sigma]$—safe stress.

The additional load due to crane braking is taken by the cross-section (Fig. 238) or the horizontal truss situated between the main and side trusses (Fig. 239). If (in the absence of a horizontal truss) the flooring of sheet steel is considered to take this load then the stress in the horizontal plane in the outer fibres can be determined from the moment by equation (352).

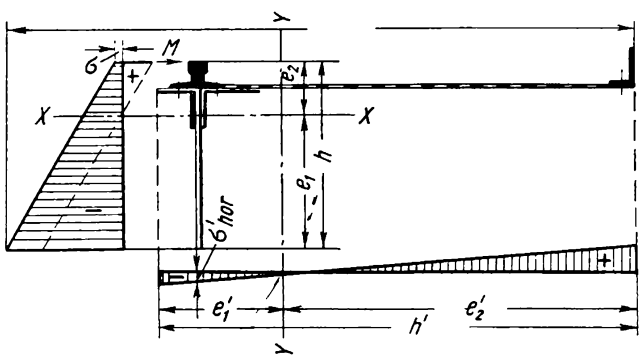

Fig. 238. Diagram for solving the upper chord of a truss with flooring

* The additional loads are: wind pressure, snow and ice, load due to temperature effects and the horizontal braking forces arising both along the bridge when crane trolleys are braked (assumed equal to 1/7 of the summary load of all travelling wheels of the trolley), and across the bridge when the crane itself is braked.

The moments of resistance (Fig. 238) are

$$W'_1 = \frac{I_y}{e'_1}; \qquad W'_2 = \frac{I_y}{e'_2}.$$

Since the sheet steel flooring is perforated its cross-section is regarded as useful only by 50 per cent.

Depending on the direction of crane movement the stresses in the horizontal plane are alternately either compression or tensile stresses. If the inertia force of the parts is taken by the horizontal truss (Fig. 239) we should distribute the

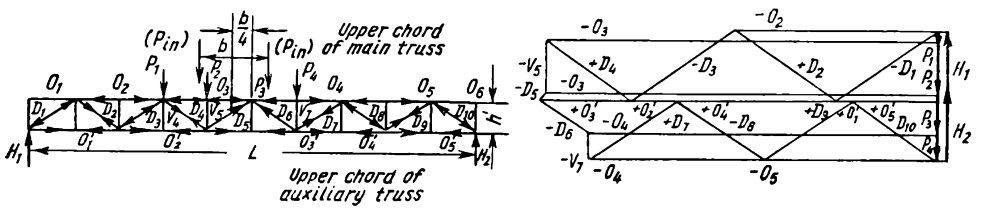

Fig. 239. Determining the stresses in the members of the horizontal truss due to crane braking

load on the trolley wheels P_{in} to the adjacent joints, determine the horizontal reactions H_1 and H_2 and construct the Cremona force plan (Fig. 239). It is used to find additional stresses in the members of the upper chord which are compressive for the accepted direction of crane movement. Additional stress $\sigma_{hor} = -\frac{S_{hor}}{F_{net}}$ is added to the maximum stress due to vertical compressive forces to find [see formulas (354) to (360), inclusive] the maximum stress in the upper chord (the lower chord is subject to tension only).

Deflection of Trusses and Camber. As has been noted above the deflection of trusses due to the maximum load being raised and the weight of trolley should not exceed $\sigma'' < \frac{1}{700} L$ where L—length of the truss span.

The deflection of latticed trusses of overhead travelling bridges can be determined to an accuracy within 10 per cent from the formula

$$\delta'' \approx 1.2 \frac{40ML^2}{384\varepsilon I_m} \tag{363}$$

where M—design moment due to the moving load in kg-cm;

L—span in cm;

$$I_m = (F_{up} + F_{low}) \frac{h^2}{4}$$

(h—depth of truss, in cm, and F_{up} and F_{low}—gross sectional areas of the upper and lower chords, in sq cm); ε—modulus of elasticity; 1.2—coefficient to account for the deformation of the inclined braces.

So-called camber is sometimes imparted to a latticed truss to pretension the members. The camber of the middle joint is usually taken equal to the safe deflection. The camber of other joints follows a parabola.

Let us consider by way of example the truss of an electric overhead travelling crane (Fig. 240) with the following characteristics: span L = 24,000 mm, number of panels n = 10, length of panel λ = 2,400 mm, depth of truss h = 2,400 mm, maximum camber f_{max} = 24 mm = $\frac{1}{1,000} L$.

Let us describe a circle with a radius equal to f_{max} = 24 mm (Fig. 240) and divide one-quarter of the circle into equal angles according to the number of panels (in our case into five angles of 18°). Let us now drop perpendiculars, which

will be the sought-for ordinates of the cambered joints, from the points where the radii intersect the circle. The following values can be obtained to scale: $y_1 = 7.5$ mm, $y_2 = 14$ mm, $y_3 = 19.5$ mm, $y_4 = 23$ mm and $y_5 = 24$ mm.

The lower chord of the truss is cambered along the same curve but beginning usually from the second joint since the trusses are fastened to the cross supporting beams of the bridge very rigidly and over a considerable length (by means of large gusset plates). Moreover, the camber is eliminated between *O* and joint *2* on the lower chord where the operator's cab is accommodated.

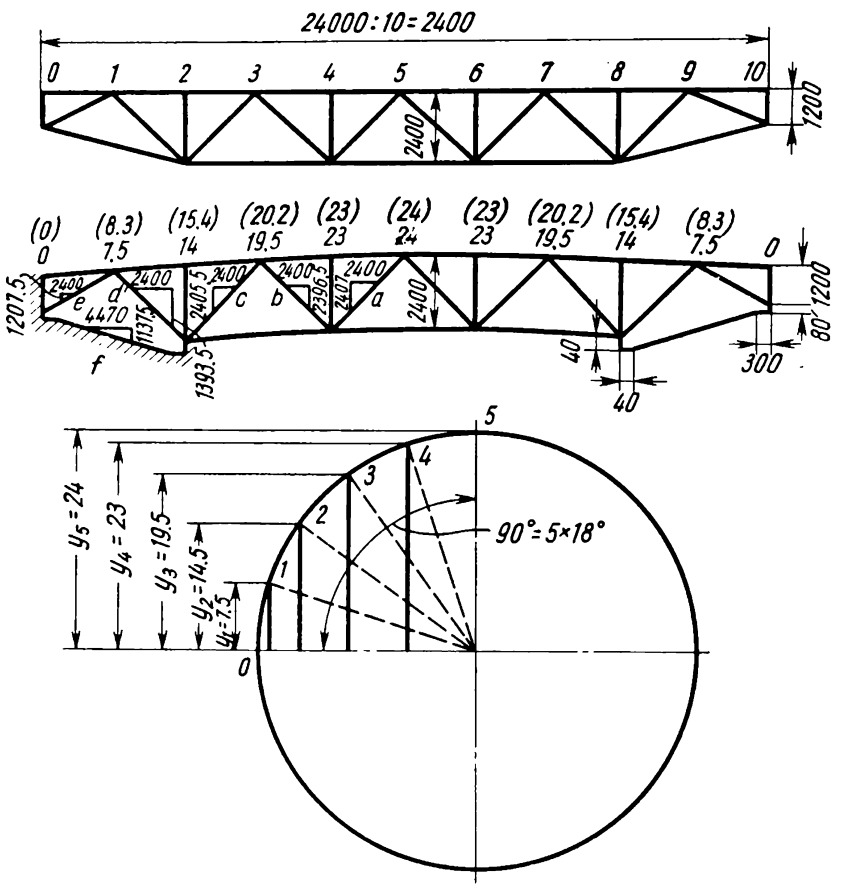

Fig. 240. Graphical determination of truss camber

Like the main trusses, the auxiliary (side) trusses of an overhead travelling crane bridge are cambered; but this camber is calculated by other methods taking into account the truss design and the section of members. A cambered crane bridge has diagonals of varying length in view of which the individual members (chord and diagonals) are pretensioned.

The lengths of members (mainly diagonals) are determined at the manufacturing plant by the following method (Fig. 240). Diagonal *a:* joint *5* is above joint *4* by 1 mm, hence the length of the diagonal can be found from the right triangle with the sides 2,401 and 2,400 mm. Diagonal *b:* joint *3* is below joint *4* by 3.5 mm, hence the sides of the right triangle will be equal to 2,396.5 and 2,400 mm, etc., i. e., diagonal *c*—2,405.5 and 2,400 mm, diagonal *d*—2,393.5 and 2,400 mm, diagonal *l*—1,207.4 and 2,400 mm.

We have pointed out above that for practical reasons no camber is imparted to member *f* of the lower chord. Therefore, the supporting strut and chord *f*, includ-

ing the shoulder shown in Fig. 240, are depicted by the overall lines of the truss (hatched line in Fig. 240). The remainder of the truss is represented in a distorted form with account taken of the camber along the lines of the centres of gravity of the members. This explains the formation of shoulders with sizes 40×40 mm in joints *2* and *8*; they are obtained by joining the contour lines with the lines of the centres of gravity of the truss members excluding the supporting strut and chord *f*. The figures in the brackets (Fig. 240) indicate accurately calculated magnitudes of camber.

Today almost all Soviet plants manufacturing overhead travelling cranes have turned to double-web welded designs of bridges (Podyemnik, Uralmash, Kirov plants, etc.). A general view of an overhead travelling crane with double-web girders is represented in Fig. 241.

Example. Design a truss for an electric overhead travelling crane.

Given: Lifting capacity $Q = 5{,}000$ kg; span $L = 15$ m; duty—medium (DF = 25 per cent).

1. Constant load. The weight of the main truss is

$$G_{main} = 10\, Q_{tons}\, (L_{metres} - 5) + 700 \text{ kg} = 10 \times 5\, (15-5) + 700 = 1{,}200 \text{ kg}.$$

The full load taken by the main truss (without the weight of the travelling mechanism and operator's cab) is

$$G = G_{main} + \frac{1}{2} G_{hor} + \frac{1}{2} (G_{pl} + G_{fl}) + \frac{1}{2} G_{cr.br} =$$

$$= 1{,}200 + \frac{1}{2} 200 + \frac{1}{2} (150+200) + \frac{1}{2} 40 = 1{,}495 \text{ kg}.$$

The load acting on each joint of the truss is

$$K = \frac{G}{n-1} = \frac{1{,}495}{13-1} = 125 \text{ kg}.$$

The additional load on the three middle joints due to the weight of the travelling mechanism is

$$K_1 \approx \frac{\frac{1}{2} G_{mech}}{3} = \frac{1}{2} \times \frac{1{,}200}{3} = 200 \text{ kg}.$$

The additional load on two extreme left joints due to the weight of the operator's cab is

$$K_2 = \frac{\frac{1}{2} G_{cab}}{2} = \frac{1}{2} \times \frac{1{,}000}{2} = 250 \text{ kg}.$$

The length of panel $\lambda = 1{,}250$ mm.

The reactions in the supports due to constant load are

$$A = \frac{G}{2} + \frac{1}{2} 3 K_1 + K_2 + K_2 \frac{L-\lambda}{L} = \frac{1{,}495}{2} + \frac{1}{2} 3 \times 200 +$$

$$+ 250 + 250 \frac{15-1.25}{15} = 1{,}527 \text{ kg};$$

$$B = \frac{G}{2} + \frac{1}{2} 3 K_1 + K_2 \frac{\lambda}{L} = \frac{1{,}495}{2} + \frac{1}{2} 3 \times 200 + 250 \frac{1.25}{15} = 1{,}068 \text{ kg}.$$

The obtained values of the reactions in the supports are used to construct a vertical polygon of forces and the Cremona force plan to determine the stresses in the members due to constant load (Fig. 242).

2. Moving load. The load on a trolley wheel is

$$P = \frac{Q+G_0}{4} = \frac{5{,}000 + 2{,}200}{4} = 1{,}800 \text{ kg}.$$

(The weight of the trolley is assumed equal to $G_0 \approx 2{,}200$ kg.)

The moving loads with a trolley wheel-base of $b = 950$ mm (Fig. 242*a*) are

$$P_1 + P_2' = P + P \frac{\lambda - b}{\lambda} = 1{,}800 + 1{,}800 \frac{1{,}250-950}{1{,}250} = 2{,}230 \text{ kg};$$

$$P_2'' = P \frac{b}{\lambda} = 1{,}800 \frac{950}{1{,}250} = 1{,}370 \text{ kg}.$$

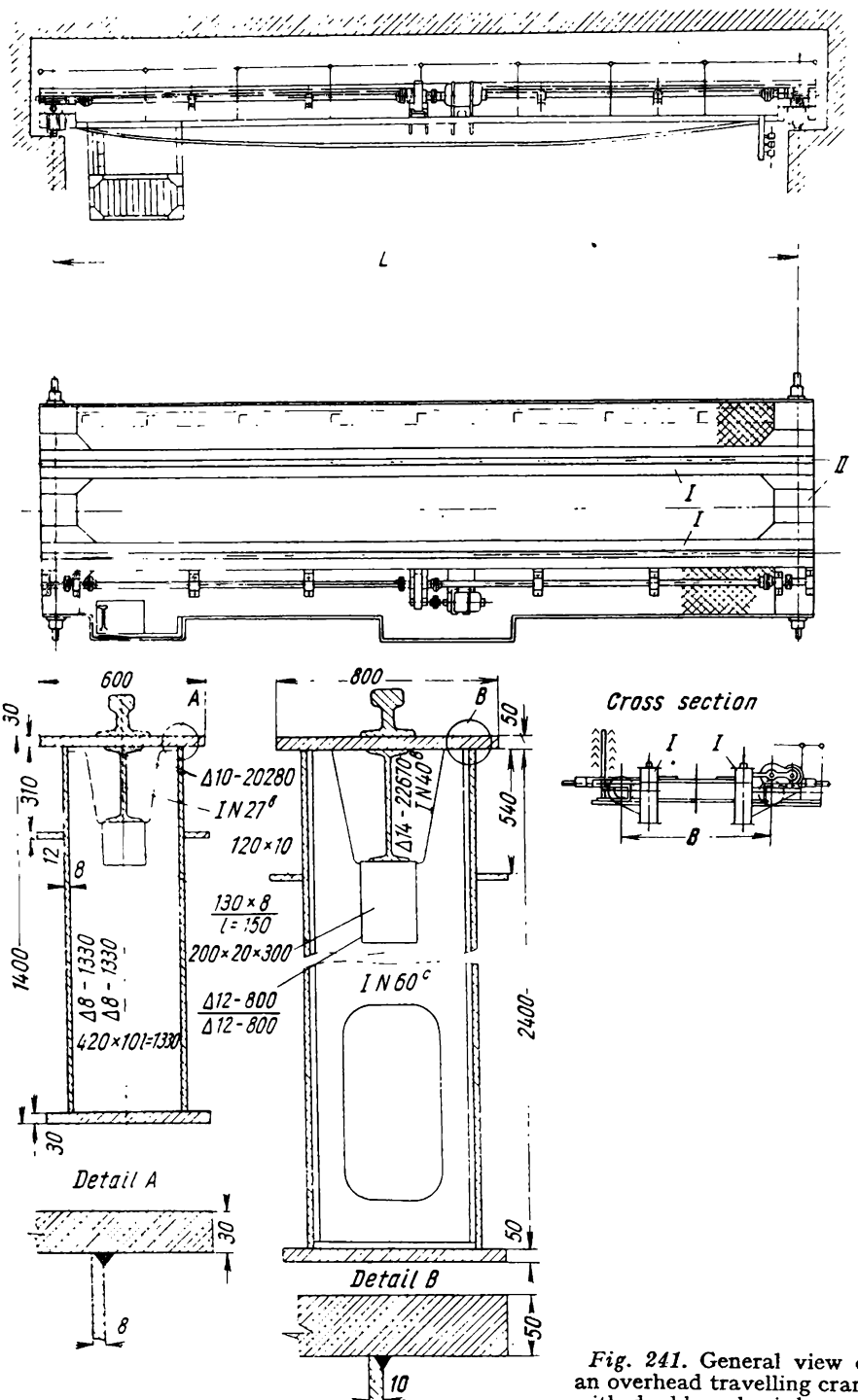

Fig. 241. General view of an overhead travelling crane with double-web girders

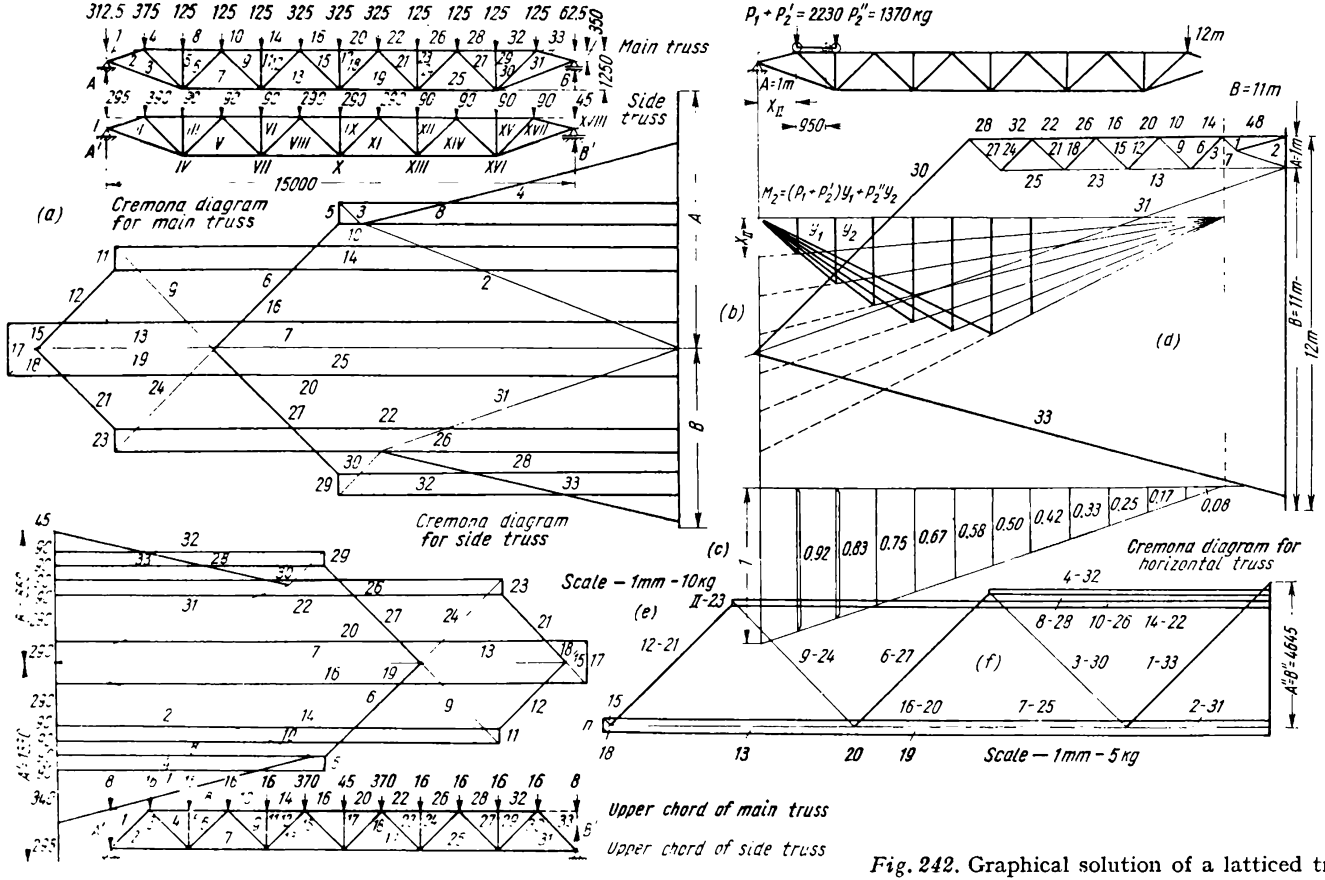

Fig. 242. Graphical solution of a latticed truss

After making these calculations, plot moment and lateral force influence lines (Fig. 242*b* and *c*) whose values are given in Table 45. Then find the stresses in the chords and inclined braces. These stresses can be found from the Cremona force plan with $A = 1$ ton (Fig. 242*d*).

Table 45

Moments and Lateral Forces from Moving Load

Joints	Ordinates for determination of moments		Moment M, kg-m	Ordinates for determination of lateral force		Lateral force T, kg
	y'_1, m	y'_2, m		y''_1	y''_2	
I	0	0	0	1	0.92	3,490
II	1.18	1.1	4,140	0.92	0.83	3,190
III-IV	2.15	1.9	7,450	0.83	0.75	2,880
V	2.85	2.5	9,800	0.75	0.67	2,590
VI-VII	3.35	2.9	11,400	0.67	0.58	2,285
VIII	3.6	3.1	12,300	0.58	0.50	1,975
IX-X	3.75	3.1	12,650	0.50	0.42	1,690
XI	3.75	3.1	12,300	0.42	0.33	1,390
XII-XIII	3.35	2.9	11,400	0.33	0.25	1,080
XIV	2.85	2.5	9,800	0.25	0.17	790
XV-XVI	2.15	1.9	7,450	0.17	0.08	490
XVII	1.18	1.1	4,140	0.08	0	180
XVIII	0	0	0	0	0	0

3. The unit stress in the most heavily loaded members of the main truss. These are members *15* and *20* of the upper chord. The unit stress in them is

$$\sigma = \frac{\varphi S_q + \mu S_p + \sum S_{add}}{\varphi F_{gr}} + \frac{\mu M_p + \sum M_{add}}{W_{gr}} =$$

$$= \frac{1.1 \times 4{,}310 + 1.2 \times 10{,}200 + 2{,}150}{0.8 \times 15.36 \times 2} + \frac{1.2 \times 37{,}500 + 0}{57.7 \times 2} = 1{,}100 \text{ kg/cm}^2$$

where $M_p = P_1 \frac{\lambda}{6} = 1{,}800 \frac{125}{6} = 37{,}500$ kg-cm and $\varphi = 0.87$;

$$\lambda = \frac{l}{\sqrt{\frac{I_{gr}}{F_{gr}}}} = \frac{125}{\sqrt{\frac{155.4}{30.72}}} = 55.$$

The preceding calculations permit us to use two No. 12 channel beams for the upper chord of the truss.

The lower chord (members *13* and *19*—two angles $60 \times 60 \times 8$ mm).

The unit stress in the members of the lower chord is

$$\sigma = \frac{\varphi S_q + \mu S_p}{F_{net}} = \frac{1.1 \times 4{,}120 + 1.2 \times 9{,}850}{15.35} = 107 \text{ kg/cm}^2$$

where $F_{net} = 0.85$, $F_{gr} = 0.85 \times 9.03 \times 2 = 15.35$ (accounting for the weakening of the section by rivet holes).

The inclined braces (member *6*—two angles $50 \times 50 \times 6$ mm).

The unit stress in the inclined braces is

$$\sigma = \frac{\varphi S_q + \mu S_p}{\varphi F_{gr}} = \frac{1.1 \times 1{,}130 + 1.2 \times 4{,}020}{0.75 \times 11.38} = 1{,}180 \text{ kg/cm}^2$$

where $\varphi = 0.45$;

$$\lambda = \frac{l}{\sqrt{\frac{I_{gr}}{F_{gr}}}} = \frac{180}{\sqrt{\frac{26.2}{11.38}}} = 120.$$

The struts are likewise made of two angles $50 \times 50 \times 6$ mm since the stresses in them do not exceed those in the inclined braces.

The unit stresses in the members of the main truss are quite safe for steel 2.

Fig. 242*e* shows a Cremona force plan for solving the side truss and Fig. 242*d*—one for the horizontal truss. The values of the stresses in these trusses are summarised in Table 46.

Table 46

Parts of truss	Member No.	Main truss: Moment due to moving load, kg-m	Main truss: Arm of moment due to moving load, m	Main truss: Stress due to constant load, kg	Main truss: Stress due to moving load, kg	Main truss: Stress F for $A = 1$ ton, kg	Main truss: Lateral force T, kg	Main truss: Summary stresses due to constant and moving loads, kg	Side truss: Stress in members due to constant load, kg	Horizontal truss: Stresses due to inertia forces in braking the crane, kg
Upper chord	1	7,450	1.55	—2,100	— 4,000			— 6,900	—1,630	— 640
	4	7,450	1.25	—2,180	— 5,950			— 8,130	—1,670	— 900
	8	7,450	1.25	—2,180	— 5,950			— 8,130	—1,670	— 900
	10	11,400	1.25	—3,610	— 9,100			—12,710	—2,770	—1,720
	16	12,650	1.25	—4,310	—10,200			—12,710	—2,770	—1,720
	20	12,650	1.25	—4,310	—10,200			—14,510	—3,330	—2,150
	20	12,650	1.25	—4,310	—10,200			—14,510	—3,330	—2,150
	22	11,400	1.25	—3,610	— 9,100			—12,710	—2,730	—1,720
	26	11,400	1.25	—3,610	— 9,100			—12,710	—2,730	—1,720
	28	7,450	1.25	—2,180	— 5,950			— 8,130	—1,630	— 900
	32	7,450	1.25	—2,180	— 5,950			— 8,130	—1,630	— 900
	33	7,450	1.55	—1,970	— 4,800			— 6,770	—1,450	— 640
Lower chord	2	4,140	0.70	+2,190	+ 5,900			+ 8,090	+1,680	+ 455
	7	9,800	1.25	+2,980	+ 7,800			+10,780	+2,270	+1,330
	13	12,300	1.25	+4,130	+ 9,850			+13,980	+3,180	+2,120
	19	12,300	1.25	+4,130	+ 9,850			+13,980	+3,180	+2,120
	25	9,800	1.25	+2,980	+ 7,800			+10,780	+2,270	+1,330
	31	4,140	0.70	+2,030	+ 5,900			+ 7,930	+1,500	+ 455
Struts	5			— 140				— 2,370	— 90	— 16
	11			— 140				— 2,370	— 90	— 16
	17	0	0	— 340	— 2,230			— 2,570	— 290	— 45
	23			— 140				— 2,370	— 90	— 16
	29			— 140				— 2,370	— 90	— 16
Inclined braces	3			+ 200	+ 1,915	+ 600	3,190	+ 2,115	+ 140	+ 620
	6			—1,130	— 4,020	—1,400	2,880	— 5,150	— 840	— 600
	9			+ 920	+ 3,760	+1,400	2,590	+ 4,680	+ 710	+ 550
	12			— 730	— 3,200	—1,400	2,285	— 3,930	— 590	— 550
	15	0	0	+ 250	+ 2,760	+1,400	1,975	+ 3,010	+ 200	+ 25
	18			+ 250	— 2,360	—1,400	1,690	— 2,110	+ 200	+ 25
	21			— 710	+ 1,890	+1,400	1,350	+ 1,180	— 590	— 550
	24			+ 910	— 1,510	—1,400	1,080	— 600	+ 720	+ 550
	27			—1,110	+ 1,100	+1,400	790	— 10	— 870	— 600
	30			+ 390	— 4,750	—9,700	490	— 4,360	+ 310	+ 620

4. Deflection of the main truss due to the moving load [formula (363)]

$$\delta'' = 1.2\,\frac{40ML^2}{384\,EI_m} = 1.2\,\frac{40\times 1{,}265{,}000\times 1{,}500^2}{384\times 2.1\times 10^6\times 190{,}000} = 0.9\text{ cm}.$$

The calculated moment due to the moving load will be

$$M = \frac{P}{2L}\left(L-\frac{b}{2}\right)^2 = \frac{1{,}800}{2\times 1{,}500}\left(1{,}500-\frac{95}{2}\right)^2 = 1{,}265{,}000\text{ kg-cm}$$

and the moment of inertia of the two chords of the truss

$$I_m = (F_{up} + F_{low})\,\frac{h^2}{4} = (15.36\times 2\times 9.03\times 2)\,\frac{125^2}{4} = 190{,}000\text{ cm}^4.$$

According to engineering inspection rules, the deflection should not exceed

$$\delta'' = \frac{1}{700}L = \frac{1}{700}\,1{,}500 = 2.14\text{ cm}.$$

Hence, the deflection $\delta'' = 0.9$ cm we have obtained is quite permissible.

CHAPTER XIII

STABILITY OF CRANES

Any crane should be stable in any position in operation and irrespective of its dead and live loads.

Some types of cranes require no special check-up for stability, for example, cranes in which the supporting members are so arranged as to preclude completely tipping over.

On the other hand, checking for stability is obligatory for stationary rotary cranes with a fixed pillar or turntable, all kinds of travelling rotary cranes (locomotive, crawler, truck- and tractor-mounted, etc.) and all gantry and semigantry cranes, load transfer bridges, tower and portal cranes, etc.

1. STABILITY OF STATIONARY ROTARY CRANES WITH A FIXED PILLAR SECURED IN THE FOUNDATION

Fig. 243 shows a rotary crane with a fixed pillar erected on a foundation. The counterweight for such cranes is usually selected so that its moment completely equalises the moment from the crane weight and one half of the load moment. In this case the load on the central pillar will be the same for a loaded and unloaded crane. The bottom, usually tapered, end of the fixed pillar is fitted into a steel (Fig. 244) or cast-iron (Fig. 245) star-shaped foundation plate. The plate is fastened to the foundation by stay bolts. Hence, the crane tends to tip together with the massive foundation.

To select the proper size of the foundation we must know not only the margin of stability of the crane but also the properties of the soil which can often sustain only very small unit pressures. As a rule, the foundation is designed with a square base and its size is initially specified tentatively. The foundation is manufactured from concrete or stone with a specific weight of 2-1.6 t/m^3.

We shall use the following notation:

α—coefficient taking into consideration the crane test overload (usually, $\alpha = 1.25$);

Q—weight of load;

G_1—weight of the revolving part of the crane (without the counterweight);

G_{cw}—counterweight;

G_2—weight of the pillar and foundation plate;

G_f—weight of the foundation.

Then, the resultant of all the vertical forces of a crane carrying full load will be

$$V_s = \alpha Q + G_1 + G_{cw} + G_2 + G_f .$$

The crane retains stability as long as the distance e_s between this resultant force and the axis of rotation is less than one half the width of the foundation,*

* The wind pressure and inertia loads are usually disregarded here since, in practice, the stability for these cranes is taken with a large margin of safety.

$$e_s = \frac{\alpha Q a + G_1 e_1 - G_{cw} e_g}{\alpha Q + G_1 + G_{cw} + G_2 + G_f} < \frac{b}{2}. \tag{364}$$

When the crane carries no load

$$V = G_1 + G_{cw} + G_2 + G_f \ ;$$

$$e'_s = \frac{G_{cw} e_g - G_1 e_1}{G_{cw} + G_1 + G_2 + G_f} < \frac{b}{2}. \tag{365}$$

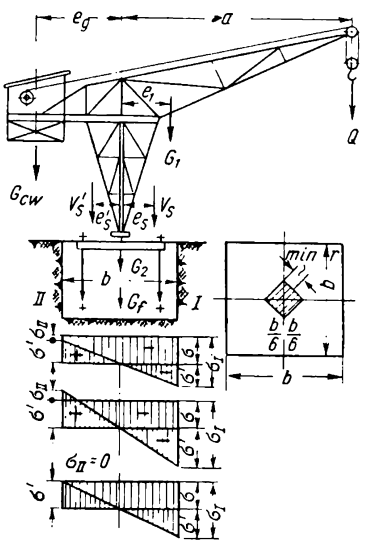

Fig. 243. Diagram of a stationary rotary crane with a fixed pillar

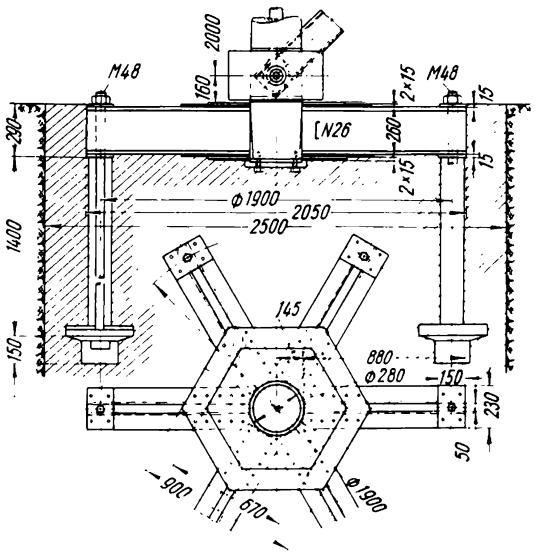

Fig. 244. Foundation plate made of steel channels

Unit Pressure Between the Foundation and the Ground. The unit compressive stress from force V_s, i. e., $\sigma = \frac{V_s}{b^2}$ is distributed uniformly over the entire bearing surface of the foundation. This stress is also complemented by a bending stress due to the eccentric application of the resultant V_s, so that

$$\sigma' = \frac{M}{W} = \pm \frac{6 V_s e}{b^3} \tag{366}$$

Both kinds of stresses for edges *I* and *II* should be summed algebraically. We thus obtain the following resultant stresses:

edge *I*

$$\sigma_I = -\frac{V_s}{b^2} - \frac{6 V_s e_s}{b^3}; \tag{367}$$

edge *II*

$$\sigma_{II} = -\frac{V_s}{b^2} + \frac{6 V_s e_s}{b^3}. \tag{368}$$

Since the foundation can transmit only compressive stresses, the unit pressure on edge *II* should be $\sigma > +\sigma'$. This will be true when resultant V_s passes inside the core (Fig. 243), i. e., when $e_s < \frac{b}{6}$.

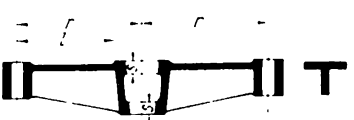

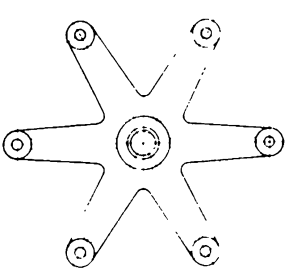

Fig. 245. Cast-iron foundation plate

The following safe bearing pressures may be recommended:
σ_{safe} = 10 to 15 kg/cm² for rocky ground;
σ_{safe} = 5 to 8 kg/cm² for clinker and gravel;
σ_{safe} = 2 to 3 kg/cm² for coarse-grained sandy soil.

If the ground can bear only a small load (deposited sand, wet clay, marl, etc.) the foundation must be reinforced by artificial means.

Foundation Plate. The foundation plate has the form of a star. For light-duty cranes the plates are cast from grey iron (see Fig. 245), more powerful cranes require plates made of channel or I-beams (see Fig. 244). In designing, the dimensions of plates are first assumed tentatively and are then checked for strength. The plate hub securing the tapered end of the pillar should be sufficiently massive and rigid.

The hub of a foundation plate is subject to the action of a couple of forces $H_0h_0 = Hh$ (see Fig. 202). Since the length of arm h_0 is small, the forces H_0 are quite large and require a sufficiently large bearing surface between the pillar and the hub hole.

The unit pressures are

$$\sigma' = \frac{H_o}{sD'} \text{ and } \sigma'' = \frac{H_o}{sD''}$$

where D' and D''—maximum and minimum diameters of the fitted-in taper of the pillar;
s—thickness of sheets or the bearing part of the plate.

The lugs of cast-iron plates are usually tee-shaped and subject to bending forces. The critical cross-section in a cast-iron plate is at the hub and in plates of rolled sections—at the gusset plates. The moment of resistance of the lugs at the critical cross-section can be found from the formula

$$W = V\left(\frac{2e}{nr} + \frac{1}{n}\right)\frac{e}{[\sigma_{bend}]} \tag{369}$$

where V—resultant of the weight of the load and the weight of the revolving part of the crane together with the counterweight equalling $V = Q + G_1 + G_{cw}$;
e—distance between resultant V and the axis of rotation;
n—number of bolts.

Stay Bolts. If we assume that the tensile stress in the bolts caused by the overturning moment of the crane is taken by only two bolts on the side opposite to the boom then the design force Z on the two bolts can be found from the equation of moments relative to the right-hand bolt (Fig. 245)

$$Q(a - r) + G_1(e_1 - r) - G_{cw}(e_g + r) - G_2 r - Z2r = 0,$$

whence the force acting on two stay bolts will be

$$Z = \frac{Q}{2}\left(\frac{a}{r} - 1\right) + \frac{G_1}{2}\left(\frac{e_1}{r} - 1\right) - \frac{G_{cw}}{2}\left(\frac{e_g}{r} + 1\right) - \frac{G_2}{2}. \tag{370}$$

2. STABILITY OF STATIONARY ROTARY CRANES WITH A TURNTABLE

Fig. 246 gives a diagram of a crane with a turntable. The counterweight for such cranes should be selected so that the resultant of all the vertical forces both in a loaded and unloaded crane is inside the bearing or balance edges *I* and *II*.

Let us denote by:
α—coefficient accounting for possible crane overloading (for example, during tests). Usually $\alpha = 1.25$;
Q—weight of the load;
a—crane outreach;

G_1—weight of the revolving part of the crane (without counterweight);
e_1—arm of force G_1 relative to the axis of rotation;
G_{cw} and e_g—counterweight and its length of arm.
Then, the resultant force for a fully loaded crane will be

$$V = \alpha Q + G_1 + G_{cw}.$$

The point of application of force V should lie behind the front balance edge. In this case

$$e = \frac{\alpha Q a + G_1 e_1 - G_{cw} e_g}{\alpha Q + G_1 + G_{cw}} < e_r. \qquad (371)$$

In an unloaded crane the resultant $V_0 = G_{cw} + G_1$ should lie in front of the rear balance edge *II*. Then,

$$e_0 = \frac{G_{cw} e_g - G_1 e_1}{G_{cw} + G_1} < e_r. \qquad (372)$$

Account should also be taken of the area acted on by wind pressure W and inertia loads. When the margin of stability is not high (a frequent feature in cranes with a turntable), these additional loads will tend to tip the crane over. This will be prevented by the central pivot which will take the load due to the difference of moments.

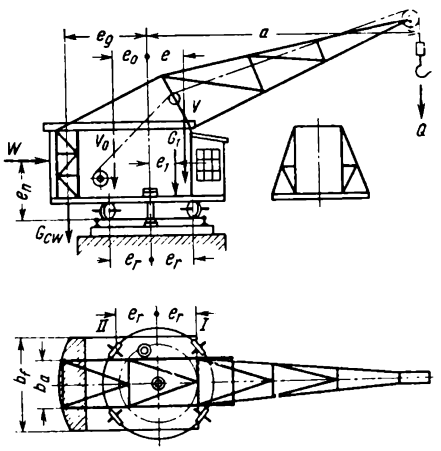

Fig. 246. Diagram for checking the stability of a stationary crane with a turntable

3. STABILITY OF TRAVELLING ROTARY CRANES

All travelling boom cranes (locomotive, crawler, truck-mounted, etc.) should possess adequate stability to prevent them from tipping over.

The coefficient of forward or load stability, i.e., the ratio of the moment relative to the balance line of all the forces acting on the crane, except for the working load, taking into consideration all possible additional loads (wind, snow, inertia forces and the effect of the maximum safe gradient), to the moment created by the working load relative to the same balance line should not be less than 1.15.

When only the maximum working load is acting (disregarding all additional loads) the coefficient of load stability should not be less than 1.4.

The coefficient of backward stability (in the direction opposite to the boom) of these cranes when there is no working load, or the coefficient of unloaded-crane stability, i.e., the ratio of the moment relative to the balance line due to the weight of all crane parts located from this line towards the bearing area to the moment due to the weight of all crane parts arranged on the other side of the balance line, taking into consideration all possible additional tipping loads (wind, snow, inertia forces and the effect of the maximum safe gradient) should also be not less than 1.15. In this case, the resultant of all forces acting on the crane should be inside the bearing area and at a distance from the balance line in a direction opposite to the boom of not less than 0.15 of the minimum distance between the bearing points of the area.

The numerical values of the coefficients of the load and unloaded-crane stability should be determined with the boom perpendicular to the balance line (disregarding the effect of the rail clamps) by the formulas given below.

Notes: 1. In determining the numerical value of the coefficient of unloaded-crane stability the boom is assumed to be positioned at the minimum outreach; the outriggers, jacks and anchoring devices available on the crane should be omitted from calculations.

2. The water level in the steam boiler should be taken at its highest point if the location of the boiler is liable to reduce crane stability; in the opposite case the water level should be at the lowest point.

3. The fuel and water tanks and fuel bunkers should be regarded as completely filled if their arrangement may detract from crane stability; otherwise they should be considered empty.

The following formula can be used to find the numerical value of the load stability coefficient

$$K_1 = \frac{G\left(c + b - h_0 \sin\alpha\right) - \frac{Qv}{gt}\left(a - b\right) - W_1\varrho_1 - W_2\varrho_2 - \frac{Qn^2\,ah}{900 - n^2H}}{Q\,(a - b)}. \quad (373)$$

In this formula:

K_1—coefficient of load stability;

G—weight of crane, in kg;

c—distance from the crane centre of gravity to its axis of rotation, in metres (Fig. 247);

h_0—distance from the crane centre of gravity to a plane passing through the points of the bearing outline, in metres;

b—distance between the crane axis of rotation and the balance line, in metres;

Q—weight of the maximum working load, in kg;

g—acceleration of gravity, equal to 9.81 m/sec^2;

v—load lifting speed, in m/sec; if the design provides for free descent of load the speed is taken at $1.5v$;

t—braking time, in sec;

a—distance between the crane axis of rotation and the centre of gravity of a suspended maximum working load, in metres, in a crane standing on a horizontal surface;

W_1—wind force acting on the crane wind area in a direction parallel to the plane on which the crane is standing in accordance with respective Soviet Standards, in kg;

ϱ_1—distance between the line of wind pressure and the balance line, in metres;

W_2—wind force acting on the wind area of a suspended maximum working load in the same direction according to respective Soviet Standards, in kg;

$\varrho_2 = h$;

n—crane slewing rpm;

h—distance between the boom head and a plane passing through the balance line, perpendicular to the axis of the crane rotation, in metres;

H—distance between the boom head and the centre of gravity of the suspended load at its lowest position (the load is assumed to be at ground level), in metres;

α—angle of the crane inclination or the road gradient; taken as 3° for locomotive and truck-mounted cranes operating without outriggers (jacks) and also for crawler cranes; and as 1°30′ for locomotive and truck-mounted cranes with outriggers (jacks). The numerical value of the coefficient of unloaded-crane stability is calculated from the following formula

$$K_2 = \frac{G_1\,(b - c_1 - h_1 \sin\alpha) - W_1\varrho_1}{G_2\,(c_2 - b + h_2 \sin\alpha)} \quad (374)$$

where K_2—coefficient of unloaded-crane stability;

G_1—weight of all parts of the crane located towards the bearing area relative to the tipping line and with the boom in the extreme upper idle position (against the stop), in kg;

b—distance between the axis of the crane rotation and the balance line, in metres (Fig. 247b);

h_1—distance between the centre of gravity of all crane parts located towards the bearing area relative to the balance line and the axis of crane rotation with the boom in the same position, in metres;

G_2—weight of all crane parts located outside the bearing area, on the other side of the balance line and with the boom in the same position, in kg;

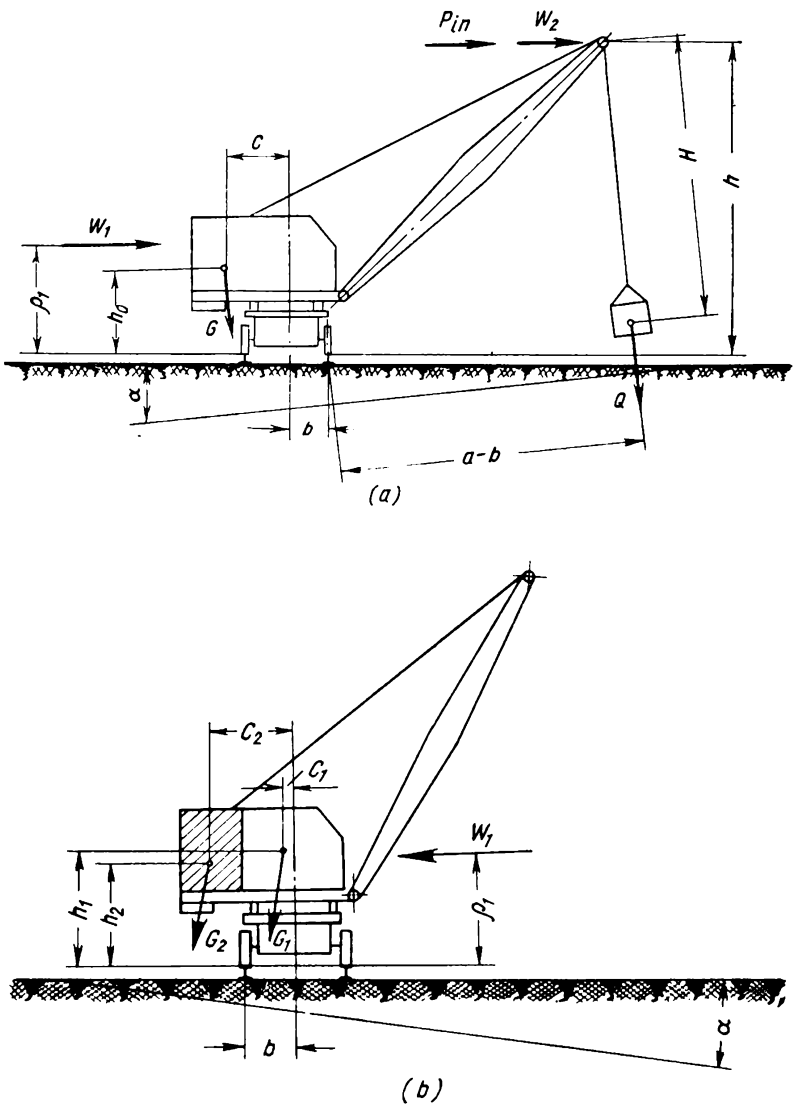

Fig. 247. Diagram for checking the stability of a travelling boom crane
a—crane carrying full load, *b*—crane carrying no load

c_2—distance between the centre of gravity of all crane parts located outside the bearing area and the axis of crane rotation with the boom in the same position, in metres;

h_2—distance between the centre of gravity of all crane parts located outside the bearing area and a plane passing through the edge points of the bearing area and with the boom in the same position as above, in metres;

W_1—wind force acting in a direction parallel to the plane supporting the crane on the crane wind area, according to the respective Soviet Standards, and with the boom in the same position, in kg;

a_1—distance between the line of wind force W_1 and the balance line;

α—angle of crane inclination (or road gradient), in degrees.

In determining the coefficient of load stability [formula (373)] the following most unfavourable conditions should be taken into account:

1) lifting of the maximum load to the maximum outreach;
2) ground gradient towards the load;
3) wind pressure towards the load;
4) inertia forces when the load is braked;
5) centrifugal forces when the crane is slewed.

The following conditions should be taken into account in determining the coefficient of unloaded-crane stability [formula (374)]:

1) minimum boom radius with the load removed;
2) ground gradient towards the counterweight;
3) wind pressure to the side of tipping.

4. STABILITY OF SEMIGANTRIES

Let us assume (Fig. 248) that with the trolley in an extreme position the direction of the forces due to the weight of the load Q and trolley G_0 will pass exactly through the bottom runway rail. Then, denoting the weight of the truss by G_1 and the inertia force in braking the trolley by G_{in}, we obtain the distance between the resultant V (equal to $V=Q+G_0+G_1$) and the axis of the supporting rail

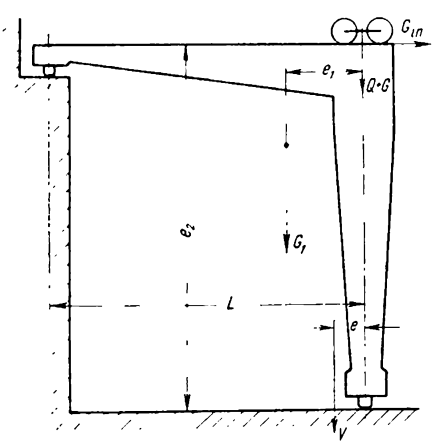

Fig. 248. Diagram for checking the stability of a semigantry crane

$$e = \frac{G_1 e_1 - G_{in} e_2}{G + G_0 + G_1} \qquad (375)$$

and the margin of stability is

$$\psi = \frac{L}{L - e}.$$

The safe value is $\psi < 1.35$.

Semigantry (as well as gantry) cranes should also be checked for stability along the crane runway track, taking into consideration the wind pressure and the inertia loads developed when the crane is being braked.

PART THREE

ELEVATORS

1. CAGE ELEVATORS

Cage elevators (also called lifts) are intended exclusively for vertical lifting of freight and passengers in a cage which moves on rigid guide rails. They find an extensive application in industrial enterprises, department stores and dwelling houses.

Cage elevators are classified as freight or passenger lifts. Freight elevators are further subdivided into freight elevators proper, goods-passenger (with an attendant) and light-duty goods elevators (for food and commercial enterprises). The type of drive employed classifies them as electric (Figs 249 and 250), hydraulic and hand-operated (Fig. 251). Electrically driven elevators are the most popular type.

The travel speed of freight elevators ranges from 0.1 to 1.5 m/sec. Ordinary passenger lifts travel at a speed of 0.5 to 3.5 m/sec.

The main data of passenger and freight electric elevators conform to State Standards.

Passenger lifts are usually available in capacities of 0.25 to 1.5 tons; freight elevators can handle from 0.25 to 15 tons while light-duty goods elevators—from 50 to 100 kg.

An electrical cage elevator comprises the following main parts (Fig. 249): cage or car, self-supporting guide rails, shaftway, counterweight, suspension gear, hoisting machine, safety devices and electric controls.

Gages. The cage, or car, accommodates freight or passengers. It should be entirely enclosed and provided with doors on one or two sides for exit. The cage must be solid, light and simple in design. Passenger elevators may have the following approximate weight:

Capacity (number of passengers)	2	3	4	5	6
Weight of cage, kg	250	275	300	350	400

The weight of the cage of freight elevators can be found from the following equations:

$$G_{cage} = 300 + 100\ F \text{ for } Q = 500 \text{ kg},$$
$$G_{cage} = 300 + 125\ F \text{ for } Q = 1{,}000 \text{ kg},$$
$$G_{cage} = 300 + 150\ F \text{ for } Q = 1{,}500 \text{ kg}$$

where F is the floor area, in sq m and Q—capacity, in kg.

Passenger cars are usually designed with a pleasant interior trim, with a ceiling, a floor and a door. An allowance of 0.5 to 0.3 sq m per passenger is the usual basis for figuring car capacity while the height is not less than 2.2 metres.

The frame of freight cages is manufactured from channel beams and angle steel and the walls and floor from wood or checkered steel. The cages should be sufficiently rigid to withstand deformation due to shocks liable to arise in loading. The exit can be either completely open or provided with a sliding door. One design of a freight elevator cage with an open exit is shown in Fig. 252

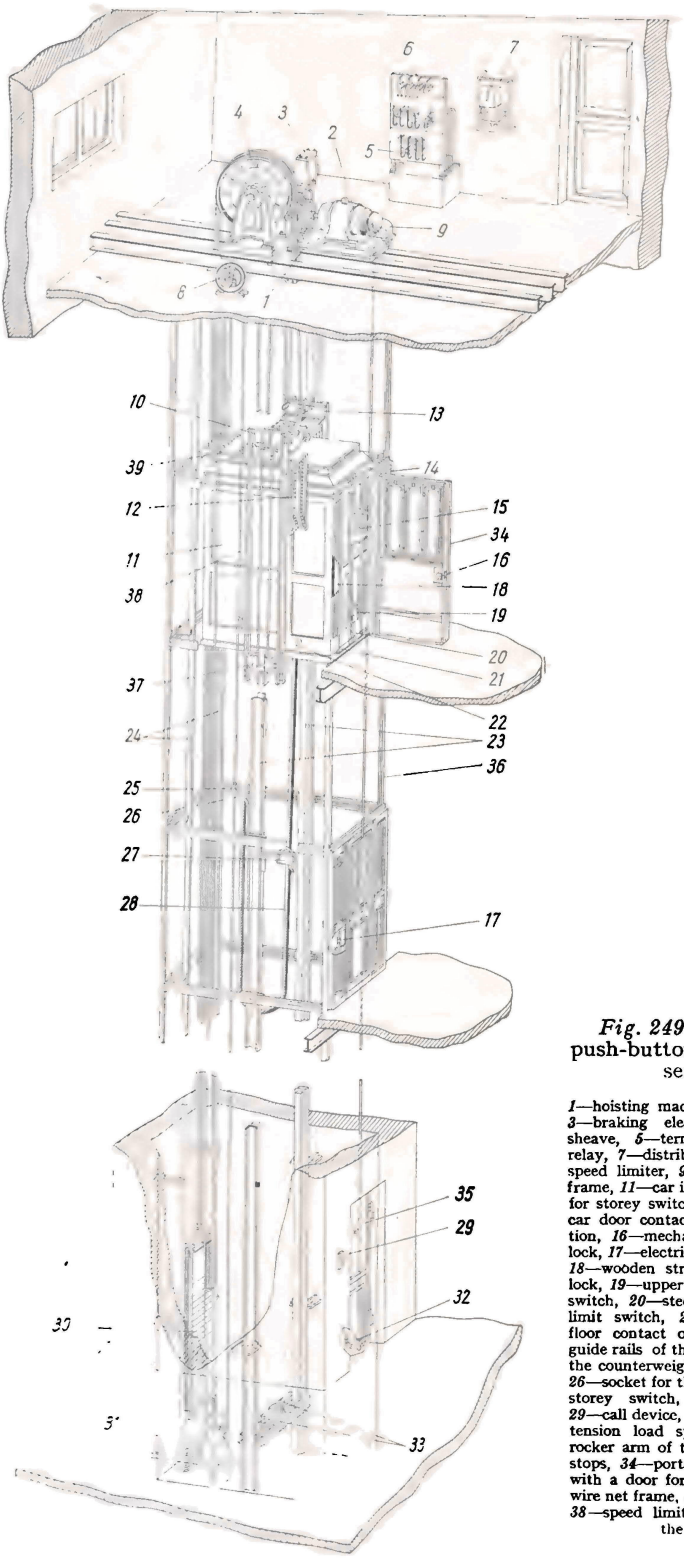

Fig. 249. Diagram of a push-button-controlled passenger lift

1—hoisting machine, *2*—electric motor *3*—braking electromagnet, *4*—driving sheave, *5*—terminal panel, *6*—storey relay, *7*—distribution switchboard, *8*—speed limiter, *9*—limit switch, *10*—car frame, *11*—car interior, *12*—tripping bar for storey switches, *13*—equaliser, *14*—car door contact, *15*—push-button station, *16*—mechanical part of the door lock, *17*—electrical part of the door lock, *18*—wooden strike block for the door lock, *19*—upper rocker arm of the limit switch, *20*—steel tripping bar for the limit switch, *21*—car threshold, *22*—floor contact of the car, *23*—wooden guide rails of the car, *24*—guide rails for the counterweight, *25*—terminal boards, *26*—socket for the suspension cable, *27*—storey switch, *28*—suspension cable, *29*—call device, *30*—counterweight, *31*—tension load speed limiter, *32*—lower rocker arm of the limit switch, *33*—car stops, *34*—portal with door, *35*—block with a door for a blind shaftway, *36*—wire net frame, *37*—safety catch wedges, *38*—speed limiter rope, *39*—tie-rod to the safety catch

The size of a freight cage is selected from the unit pressure exerted on the floor

$$q = \frac{Q}{F} .$$

For small loads q is taken from 200 to 300 kg/cm², for large loads q=600 to 800 kg/cm²; in this case the floor area should be at least 1 sq m.

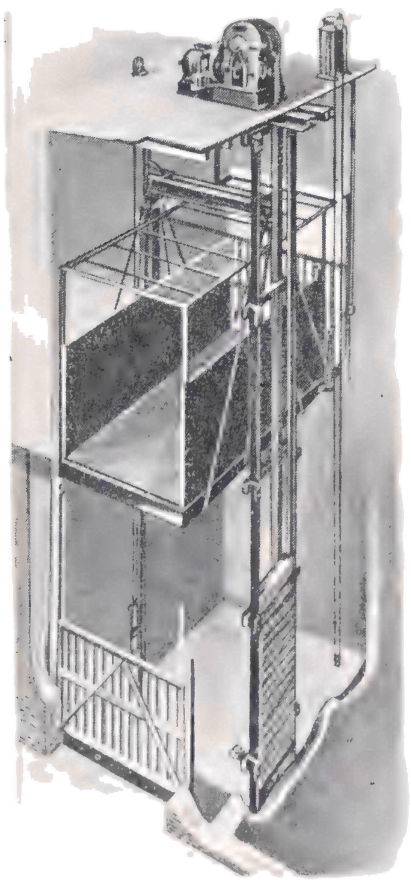

Fig. 350. Electrically driven freight cage elevator

Fig. 251. Hand-operated freight cage elevator

Guiding Devices. The cage, or car, travels in the shaftway on fixed guide rails for which purpose the upper and lower ends of the car frame are provided on both sides with two guides whose profile conforms to that of the guide rails.

Fig. 253 illustrates different designs of cage guides, viz.:

a –a conventional guide for a freight elevator comprising two angles which slide along a square wooden rail;

b guide for passenger lifts with a coil spring which holds the end member of the guide against the rail; the guides are depressed at narrow places between the two rails thereby preventing misalignment of the cage;

c—a hinged guide for a special tee rail.

Guide rails or bars are made of rolled steel sections (angles, tees, double-tees or of wooden beams and are secured on two opposite sides of the shaftway.

Wooden guide rails should be impregnated with creosote to protect them against moisture and other atmospheric effects. The rails should be regularly greased. The losses due to friction in the guide rails are taken from 5 to 10 per cent of the weight of the moving parts. The guide rails are fastened to the shaftway frame of passenger lifts at each storey and of freight elevators at 3 to 5 metre intervals. Fig. 254*a* to *i*, inclusive, shows how guide rails can be fastened to the building walls or the shaftway frame.

In designing guide rails and their fastenings it should be borne in mind that during engagement with the safety catch, when the ropes break, besides the weight of the loaded cage, they must withstand the impact caused by the absorption of the kinetic energy of the falling cage. The shorter the braking path of the cage during retardation, the greater will be the force of impact. The kinetic energy due to the weight of the cage G kg with a load Q is

$$\frac{mv^2}{2} = \frac{Q + G_{cage}}{2g} v^2$$

where v—travel speed, in m/sec;

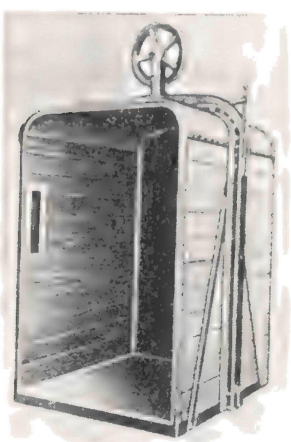

Fig. 252. Cage of a freight elevator

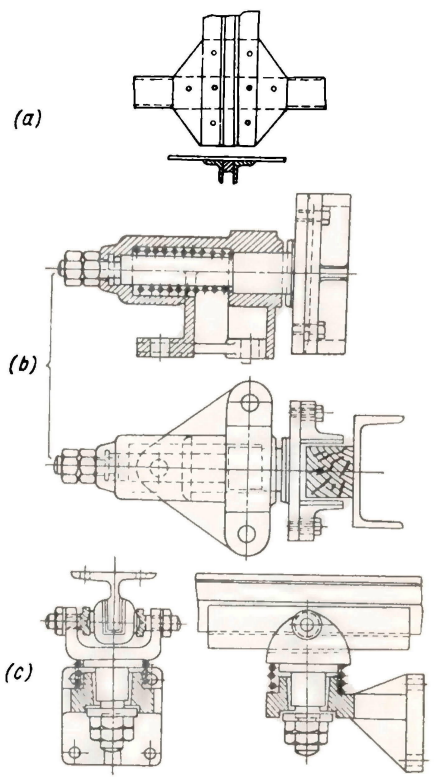

Fig. 253. Guides of an elevator cage

g—acceleration of gravity equal to $g \approx 9.81$ m/sec².

The braking path is assumed equal to 5-10 cm. The calculations are based on the assumption that the engagement of the safety catch with the rails causes a force in each rail over path s which increases from 0 to R_{max} according to a straight-line relationship. The work performed by force $2R_{max}$ (with two rails) over path s will be $\frac{1}{2} \times 2R_{max}s$.

The general equation of work can then be expressed as follows:

$$\frac{Q + G_{cage}}{2g} v^2 + (Q + G_{cage})\, s = \frac{1}{2}\, 2R_{max}\, s.$$

Hence the force acting along one guide rail will be

$$R_{max} = \left(1 + \frac{v^2}{2gs}\right)(Q + G_{cage}). \qquad (376)$$

Elevator Shaftways. A shaftway is the space in which the cage travels. Besides the cage, the shaftway contains guide rails, counterweight, rope sheaves and a hoisting machine.

The dimensions of a shaftway cross-section are assigned so as to ensure free travel of the cage. The dimensions of shaftways and machine rooms of the elevators are standardised.

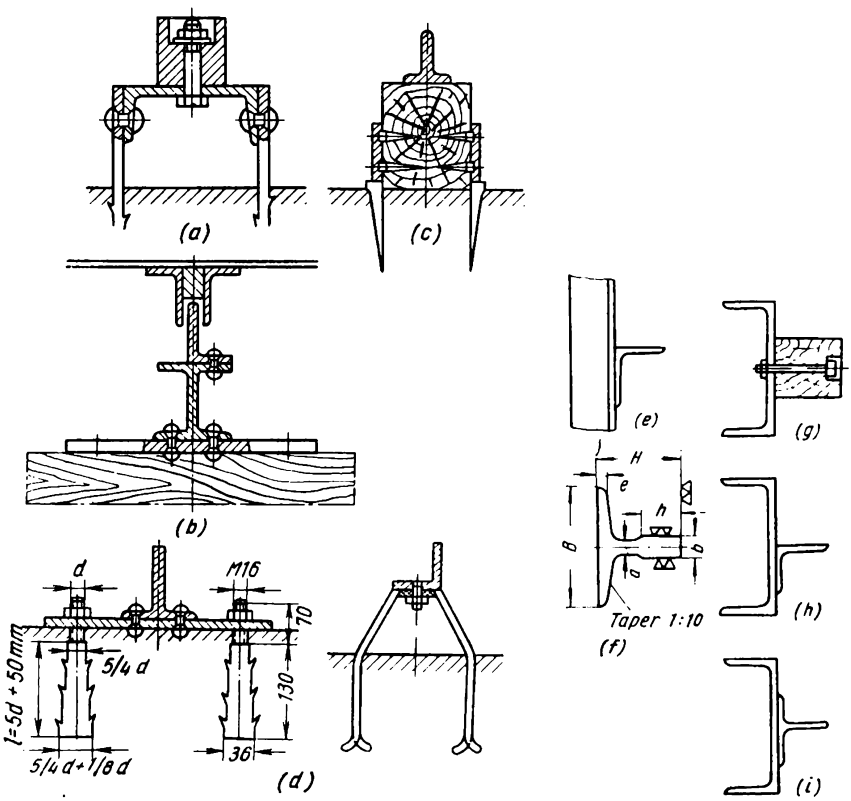

Fig. 254. Fastening of guide rails of cage elevators

The frames of shaftways for both passenger and freight elevators may vary in design and shape as well as in the kind of materials from which they are made. However, under all conditions, shaftways must have an adequate strength, preclude fire hazards and provide general safety.

Shaftways of external elevators are usually designed with a metal frame (channel and angle steel) which is secured reliably by stay bolts on a concrete foundation. The shaftway doors, linings and wire netting should meet all the safety precaution requirements.

Fig. 255 shows a frame of a metal shaftway of a freight elevator.

Elevator Counterweights. To relieve load on the hoisting machine the weight of the cage is counterbalanced with an additional load—a counterweight which is connected by ropes with the cage (Fig. 256*a*), with the drum of the hoisting machine (Fig. 256*b*) or with both simultaneously (Fig. 256*d*). At the present time preference is given to the second method. Sometimes two counterweights are provided (Fig. 256*c*): one for balancing the weight of the cage and the other for balancing a certain portion of the load.

The weight of the counterweight shown in the diagrams in Fig. 256*a*, *b*, *c* and

G_{cw} is usually assumed equal to the weight of the cage plus 0.4 to 0.5 of the maximum load, i.e.,

$$G_{cw} = G_{cage} + 0.5Q. \tag{377}$$

If we denote by P the effort which must be exerted in raising or lowering a loaded or empty cage (disregarding harmful losses), taking into consideration the counterweight according to formula (377), then this effort will be

for raising a loaded cage $P = +0.5Q$
for lowering a loaded cage $P = +0.5Q$
for raising an empty cage $P = +0.5Q$
for lowering an empty cage $P = +0.5Q$

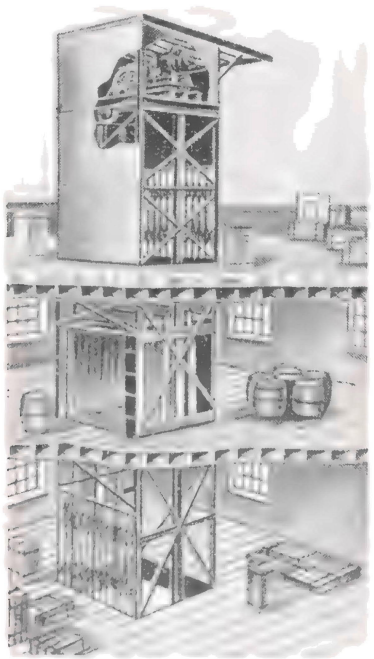

Fig. 255. Shaftway frame of a freight cage elevator

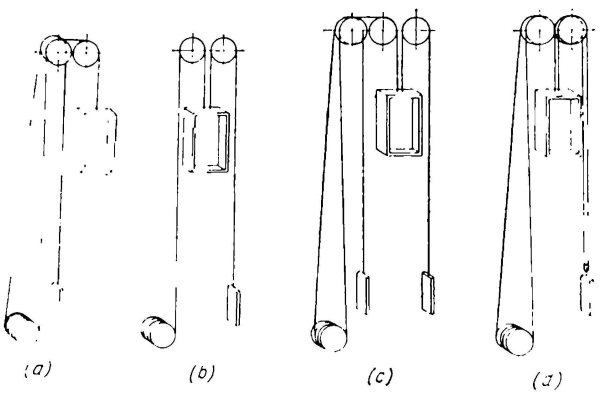

Fig. 256. Reeving of cages and counterweights in elevators operated by drum-type hoisting machines

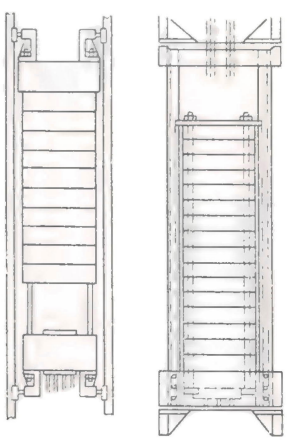

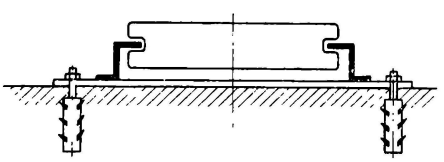

Fig. 257. Counterweights of cage elevators

The counterweight is composed of grey iron castings because a sectional design facilitates weight regulation and simplifies assembly. The shape of the counterweight (plan view) should be such as to utilise the shaftway section to the best advantage. Both the counterweight and the cage should slide in guide rails arranged over the entire height of the shaftway (Fig. 257).

Suspension Gear. Parallel or cross laid wire ropes are the flexible lifting appliances by which the cage is suspended.

The ropes for cages and counterweights can be selected by assuming the following safety values: 8 for freight elevators (with drum-type hoisting machines), 10 (with driving sheave hoisting machines) and from 12 to 14 for passenger lifts.

Depending on the type and speed of the elevator the ratio of the drum diameter D to the rope diameter d should not be less than $\frac{D}{d} > 35$ to 40 while $\frac{D}{d} > 50$ can be recommended for the driving sheave.

To make an effective use of ropes of a smaller diameter the cage and counterweight are suspended on two, four or six ropes. Uniform distribution of the load on all the ropes is achieved by employing a lever-type suspension crosspiece, as shown in Fig. 258*a*.

Not infrequently, hoisting machines with driving sheaves employ a springed suspension of the separate ropes (Fig. 258*b*); however, it is difficult to attain uniform load on all the ropes by this method.

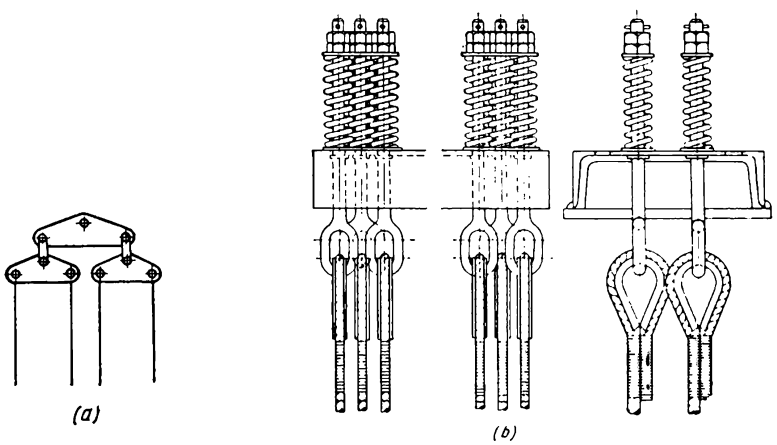

Fig. 258. Suspensions for the equalising ropes

The ropes require guide sheaves (depending on the mode of suspension of the cage and counterweight). The sheaves should be mounted so that the fleet angle α_{max} of the running-on rope does not exceed the safe value $\left(\tan \alpha_{max} \approx \frac{1}{10}\right)$.

Elevator Hoisting Machines. Cage elevators employ drum-type and driving sheave hoisting machines. In the former design the rope supporting the cage is secured on the drum and winds around its surface; in the latter design the rope runs over the sheave which drives it by the force of friction. Hoisting machines with driving sheaves are more widespread because they can be used for any lifting heights and because they are more compact in size. Moreover, since the driving sheave does not provide for a positive linkage between the cage and hoisting machine the limit switch, which is a regular feature in drum-type hoisting machines, can be dispensed with.

Hoisting machines of the second type are also effective for yet another reason. The traction force of driving sheaves ceases to act if a descending cage encounters an obstacle; in this case (due to a sharp slackening of the running-off part), the sheave will slip in the rope. Any chance stoppage of cages operated by drum-type hoisting machines may lead to a serious breakdown since the drum continues to rotate and will wind off slack rope which forms a free loop. As soon as the cause of the stoppage is eliminated the cage will drop down until it is stopped by the rope. This impact may break the rope.

Application of driving sheave hoisting machines has drastically reduced the number of accidents due to rope failure.

Drum-type hoisting machines intended for cage elevators differ from general-purpose machines mainly by a smaller size (due to the use of a worm drive) and also by the provision of special safety devices.

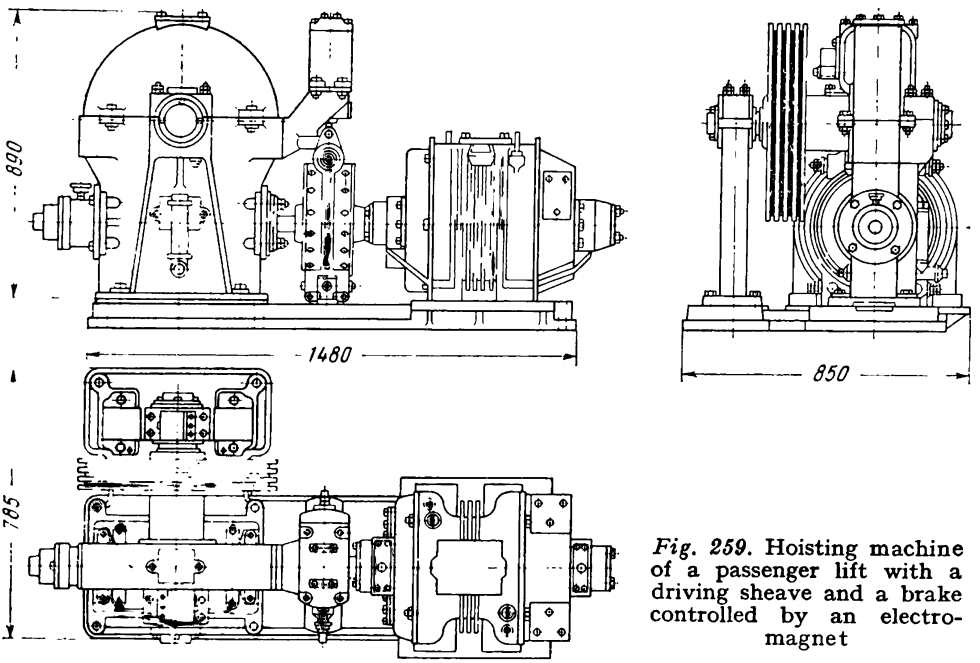

Fig. 259. Hoisting machine of a passenger lift with a driving sheave and a brake controlled by an electromagnet

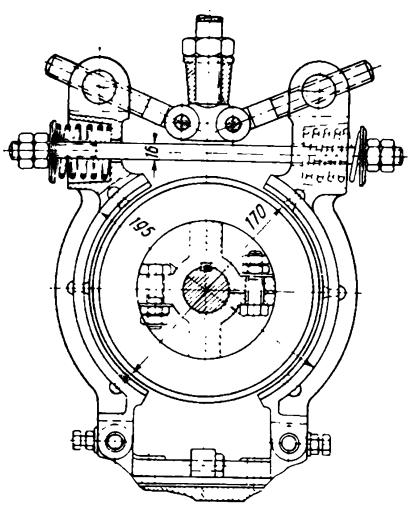

Fig. 260. Double shoe brake controlled by an electromagnet

A driving sheave hoisting machine for passenger lifts is shown in Fig. 259. This machine employs a double shoe brake controlled by an electric magnet (Fig. 260).

Driving sheaves are cast of grey iron. Annular grooves for the ropes should not be machined at all in order not to remove the harder outer layer of metal. This increases the wear resistance of the sheave.

Fig. 261 shows variously shaped grooves of driving sheaves. Vee grooves (Fig. 261*a*) change their shape during operation and acquire the form shown in Fig. 261*b*. Subsequently, they tend to assume a shape of an ordinary semicircular groove. However, wear to this extent is usually avoided since a sheave with a semicircular groove is not able to transmit the designed peripheral force due to the reduced coefficient of friction and the rope begins to slip on the sheave. Experiments and observations have shown that the best results are obtained not with an ordinary semicircular groove (Fig. 261*c*) but with a groove having a rectangular undercut (Fig. 261*d*). Wear of this last type of groove does not affect the coefficient of friction between the sheave and the rope.

Specific Features of Driving Sheave Hoisting Machine Design. The desired life of the sheave is the basis for establishing the safe unit pressure between the rope and groove. The sheave groove is impaired because of abrasion on its walls which depends on the slipping and elastic movement of the rope. The greater the speed of rope movement and the greater the number of cycles the elevator performs per unit of time, the more intensive the wear will be. Experiments have established magnitudes of safe unit pressures for driving sheaves (semicircular grooves with a rectangular undercut) shown in Fig. 261*e*. Here curves *1* and *3* refer to elevators with a highly intermittent duty. The values of unit pressures (in the diagram) refer to cross laid ropes and in practice they never exceed $p_{max} = 100$ kg/cm² for passenger lifts and $p_{max} = 110$ kg/cm² for freight elevators. For parallel laid ropes the unit pressures can be increased approximately by 25 per cent if the same maximum values, as for cross laid ropes, are adhered to.

The tractive capacity of the sheave groove depends on its shape; for example, the tractive capacity of a semicircular undercut groove depends on the central angle of the undercut β (Fig. 261*d*).

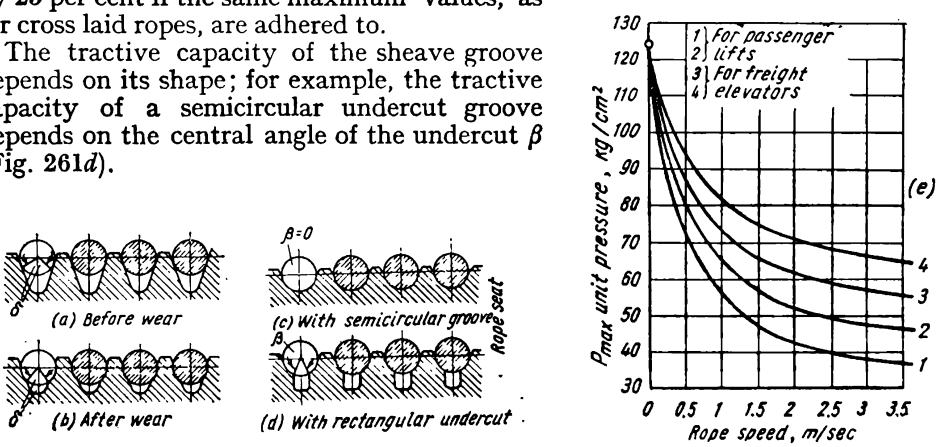

Fig. 261. Profiles of driving sheaves and their safe unit pressures
1 and *2*—for passenger lifts, *3* and *4*—for freight elevators

The expression $e^{\mu\alpha}$ is known as the pull factor of various grooves; here μ is the referred coefficient of friction and α is the angle of contact between the rope and sheave in radians. Experimental data provide the following values of μ for different angles of undercut β.

β =	0°	30°	60°	90°	100°	110°	120°	130°
μ =	0.107	0.117	0.137	0.173	0.192	0.216	0.246	0.289

To determine the size of the groove we must know the ratio between the tensions of the oncoming (S_{on}) and running-off (S_{off}) parts of the rope during the period of transient motion.

In an elevator where the hoisting machine is arranged on top (machines with driving sheaves) the numerical values of permissible acceleration and retardation (a) are determined and established by experimental methods. The following should be accepted as average values:

v, m/sec	0.75	1.0	1.5	2.0	2.5	3.0	3.5
a, m/sec²	0.65	0.85	1.15	1.4	1.65	1.88	2.1

The ratio $\frac{S_{on}}{S_{off}}$ during the period of acceleration and retardation can be expressed approximately by the following formula:

$$\left(\frac{S_{on}}{S_{off}}\right)_{st}\left(\frac{g+a}{g-a}\right) = \left(\frac{S_{on}}{S_{off}}\right)_{dyn} \tag{378}$$

where g—acceleration of gravity;

S_{on}—tension in the oncoming part of the rope;
S_{off}—tension in the running-off part of the rope.

The specified values of $\left(\frac{S_{on}}{S_{off}}\right)_{st} = e^{\mu\alpha}$, which depend on the static load on the ends of the rope running over the sheave and the speed of the cage, are used, with the aid of the alignment chart (Fig. 262), to find the angle of contact α, taking into consideration the coefficient of acceleration $\left(\frac{g+a}{g-a}\right)$ as well as the angle of undercut β or the vee angle δ (in vee grooves). Besides, the alignment chart can be used to find the value of the referred coefficient of friction μ.

The alignment chart shows examples in which these values are determined for $\left(\frac{S_{on}}{S_{off}}\right)_{st} = 1.325$ and a speed of $v = 2$ m/sec (points A, B, C, C' and C'') at sheave angles of contact $\alpha = 180°$, 150° and 130°.

To avoid excessive wear the safe load on each rope should be checked according to the following formula:

$$S = dDp_{max}\frac{\pi - \beta - \sin\beta}{8\cos\frac{\beta}{2}} \tag{379}$$

where d—rope diameter, in cm;
D—driving sheave diameter, in cm;
p_{max}—maximum safe unit pressure, in kg/cm².

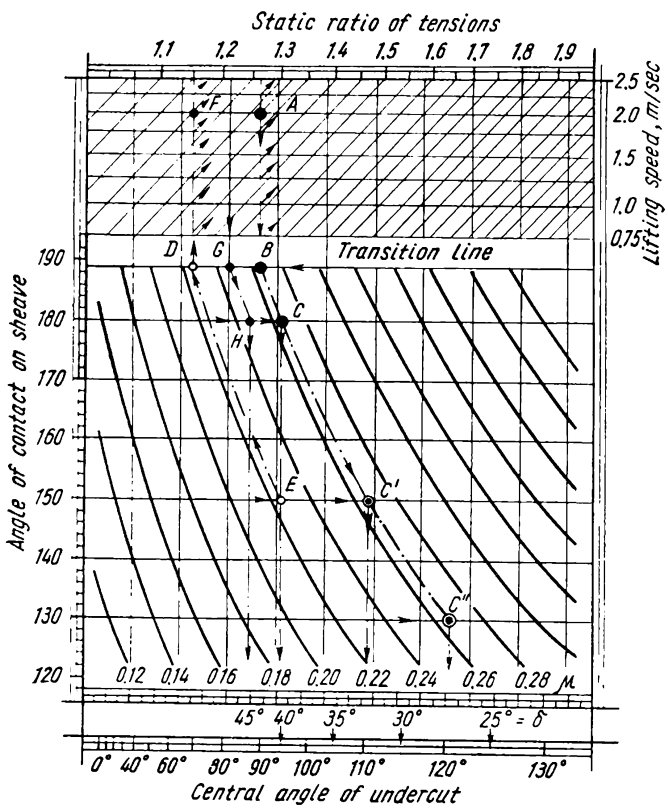

Fig. 262. Alignment chart for selecting the shape of driving sheave grooves

To prolong rope life the minimum number of ropes should be

$$n = \frac{Q + G_{cage}}{S}$$

for the cage and

$$n = \frac{G_{cw}}{S}$$

for the counterweight.

The required static power developed by the motor intended for a cage elevator can be found from the formula

$$N_{st} = \frac{(Q + G_{cage} - G_{cw})\, v}{75\eta} \qquad (380)$$

where η—total efficiency of the elevator equal to

$$\eta = \eta_{hm}\, \eta_g\, \eta_{sh}\,.$$

Here η_{hm}—efficiency of the hoisting machine;
η_g—efficiency of the guide sheaves;
η_{sh}—efficiency of deflecting sheaves.

Safety Devices of Elevators. The cages of all elevators should be provided with special safety devices—catches—which stop the cage automatically when the lifting ropes break or slacken.

There are many designs of safety catches equipped with eccentrics, wedges, clamping rollers, knives and smooth braking surfaces. The latter devices which tightly engage the guides along the entire length of contact are most efficient in operation.

The catches stop the cage when one or all supporting ropes break simultaneously, when one of the ropes is more tensioned than the others, when all ropes slacken at the same time, and when the descending speed becomes excessive.

In all these cases a specially provided device should also automatically switch off the hoisting machine. The safety catch mechanism should not be accessible to unauthorised persons and requires careful maintenance. To operate instantaneously the mechanism should be simple in design and its harmful resistance should be negligible.

The catches are usually operated by the power developed by a spring, the weight of the cage or counterweight or the force of compressed air.

Fig. 263 shows a safety device manufactured by the Podyemnik Plant. It consists of safety catches and a speed limiter. The safety catch wire rope *7*, tensioned by roller *15* with weight *16*, passes over the groove of the speed limiter sheave *4*. The ends of the wire rope are secured on plate *6* which is hinge-jointed to arm *8* on the car roof. When the car speed is normal wire rope *7* travels with it and sheave *4* rotates. If the ropes break the speed of the car as well as that of the wire rope and the sheave increases. When the speed reaches 140 per cent of the rated value weights *W1* and *W2* fastened at points *0* on the sheave are spread apart and by means of arms *1* and *3* shift arm *5* into the position shown by the dash line. In this case rollers *R1* and *R2* drop into the narrowing gap between blocks *B1* and *B2* of the sheave and stationary body *2* of the limiter and brake the sheave which wedges the tensioned rope and stops it. Since the car continues downwards arm *8* and axle *9* turn clockwise. At the same time forks *12* provided on both sides of the car raise up wedges X_1 and X_2 (a pair of wedges on each side) which slide along fixed blocks *13* mounted on the car roof. The serrated inner surfaces of the wedges grip guide rails *14* on both sides, the cage is retarded and remains suspended from the guide rails. Simultaneously, strap *10* presses against pin *11* which opens the corresponding contacts. This will brake and stop the hoisting machine motor.

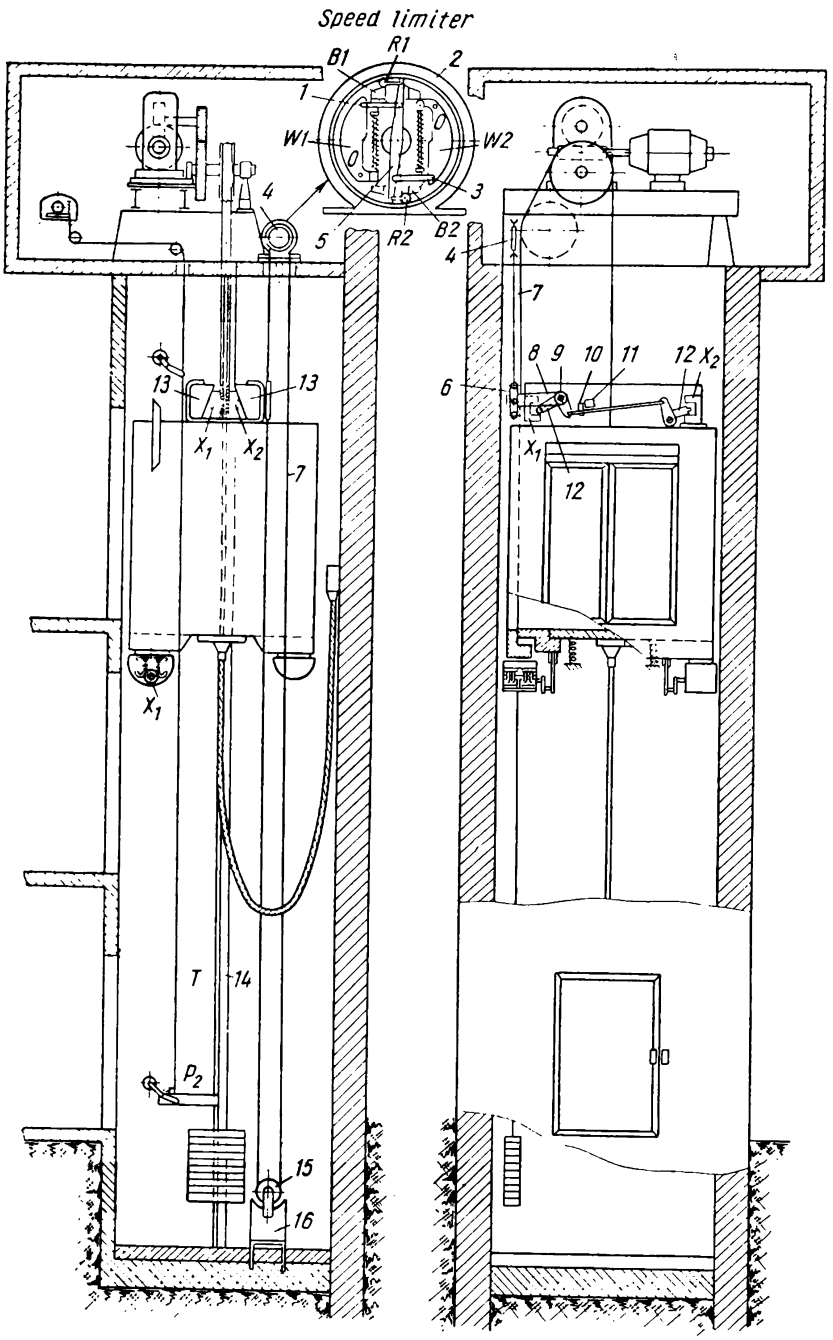

Fig. 263. Passenger lift with a safety catch manufactured by the Podyemnik Plant

2. PORTABLE AIR-OPERATED HOISTS

Portable air-operated hoists have the same applications as other types of hoists.

Fig. 264, illustrates the design of the air-operated hoist manufactured by the Uralmash Plant with a capacity of 500 kg and a lifting height of 1,150 mm.

Cylinder *9* is a piece of seamless steel tube closed on both ends with cast-iron covers. Attached to top cover *2* is shackle *1* by which the hoist is suspended. Bottom cover *3* is provided at the bottom with a cylindrical projection with thread for a nut. Gland *4*, which can be tightened by means of a gland bushing and nut when required, is inserted into the cylindrical bore of the bottom cover. The gland prevents the escape of compressed air from the cylinder to the atmosphere through the hole in the cover for the rod. The cylinder covers are tied together by bolts *18*.

A threaded hole for the rod is provided in the centre of cast-iron piston *5*. Cup *6* which is held against the cylinder walls by spring *8* is secured on the piston with a cast-iron ring. The flat part of the cup is attached to the piston by screws *7*. Lifting hook *19* is suspended from the lower end of the piston rod.

The starting mechanism has the following design. The cast-iron body *15* of the starting valve is attached to the bottom cover with screws. Rotary pin *16* with square shanks passes through the centre of the valve. Fitted on one shank is starting arm *17* controlled by two pull chains and on the other—flat valve member *13* enclosed by a lid. The lid contains conical spring *12* which presses the valve member against body *15*.

The following ducts are provided in the valve body: for admitting compressed air through a safety valve under the valve member (vertical duct), for admitting compressed air from under the valve member into the bottom part of the cylinder and for discharging the used air into the atmosphere. The lower part of the cylinder can be connected by means of the valve either to the compressed air supply or to the atmosphere. The starting arm is held by spring *10* in a position in which the lower part of the cylinder remains closed; therefore, the load can be raised or lowered only by pulling on one of the pull chains.

Device Preventing Dropping of the Load When the Hose Is Damaged. On its way to the valve the compressed air passes through safety valve *11* mounted in a threaded hole of the starting valve body. Sleeves and a special head with a spring holding it against the hole in the sleeve are inserted into the safety valve between the infeed pipe and the starting valve body.

When the pressure in the air pipe is normal the head is in the bottom position and admits compressed air to the starting valve. A pressure drop in the infeed pipe will cause a return flow of compressed air from the cylinder which shifts the head into the upper position and closes the hole in the sleeve; thus, the load suspended from the hook will not fall even if the supply hose is damaged or broken.

Device for Adjusting Descending Speed. This device comprises screw *14* with a locknut located at the bottom of the starting valve body. The screw can be turned to achieve the desired speed of discharge of the used air from under the piston and, therefore, the required speed of load descent.

3. STACKERS

Stackers find their principal application in warehouses for tiering and stocking of unit loads in stacks. They can also be used for certain loading operations.

The stackers may be of either manually propelled or self-propelled design. Fig. 265 illustrates a stacker produced by the Krasny Metallist Plant.

The guide wheels of a cantilever platform run along guiding uprights. The hoisting mechanism comprises a drum, worm drive, double shoe brake with electromagnetic controls and an electric motor with starting devices. The hoisting

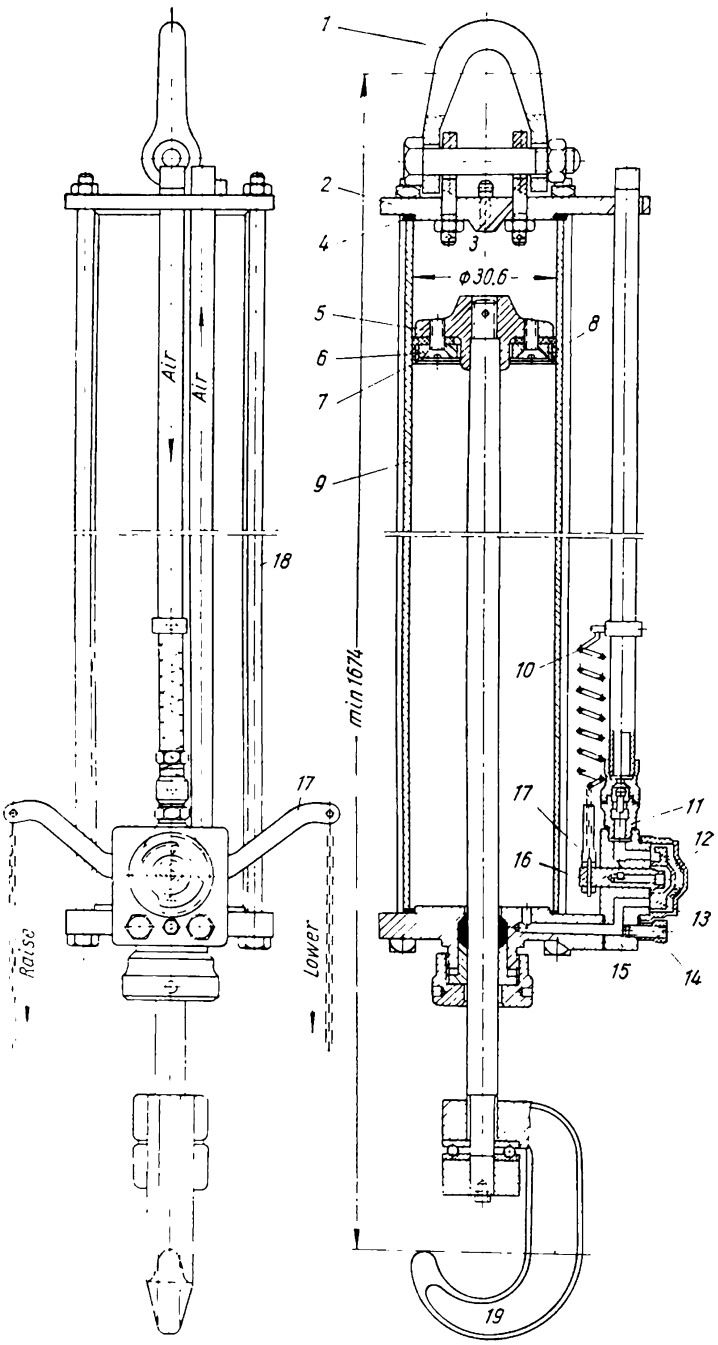

Fig. 264. Portable air-operated hoist manufactured by the Uralmash Plant

mechanism is provided with a limit switch to stop the platform at the extreme positions.

Safety catches prevent load drop in case the ropes fail. During transportation the frame is folded by means of a screw with a handwheel (Fig. 265) (to permit the machine to pass through doorways). The stacker is mounted on rubber-tyred wheels and is propelled manually. The motor is supplied through a cable plugged into a socket at the site of operation.

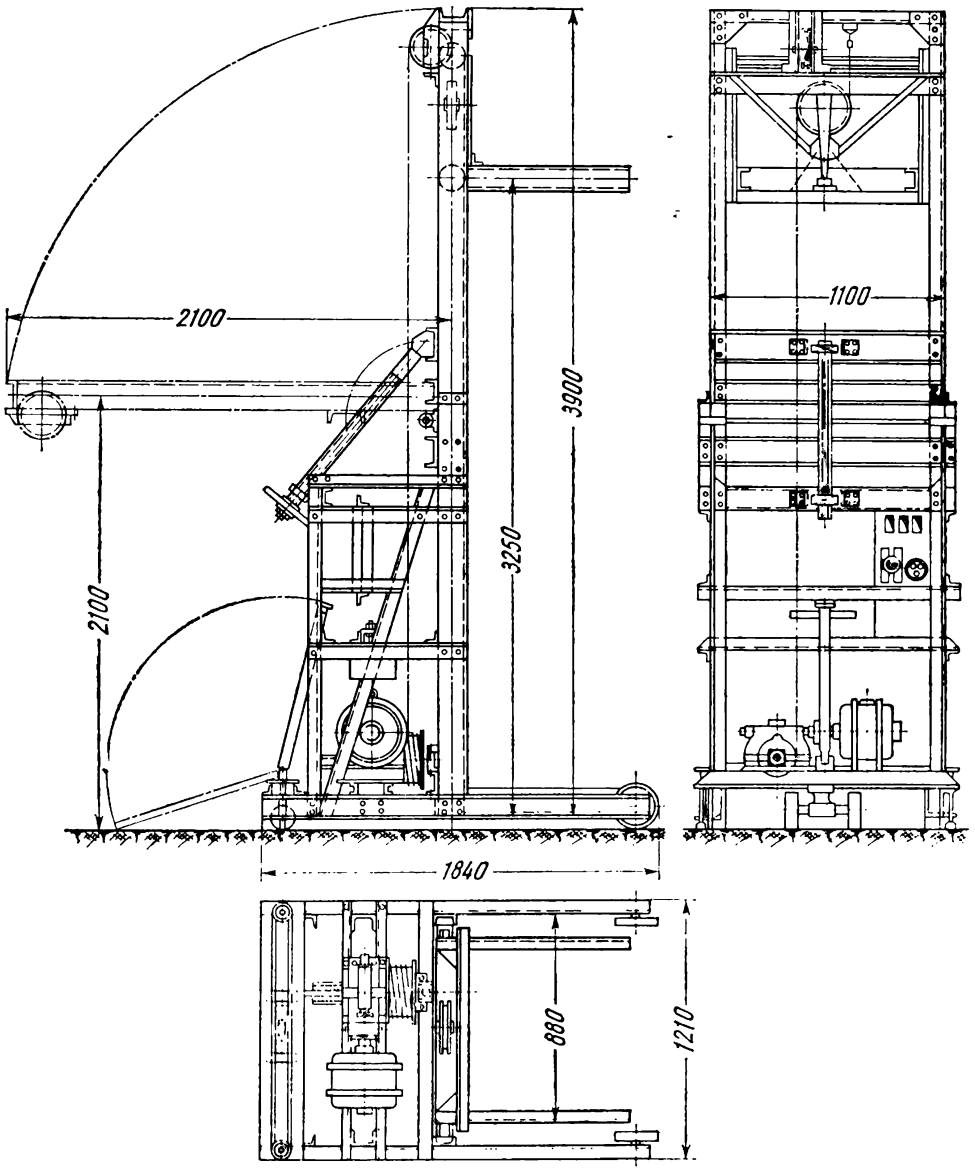

Fig. 265. Stacker manufactured by the Krasny Metallist Plant

Apart from an electrically driven hoisting mechanism stackers can be also designed with an air or hydraulic drive and for light duty even with a manually operated hoisting mechanism.

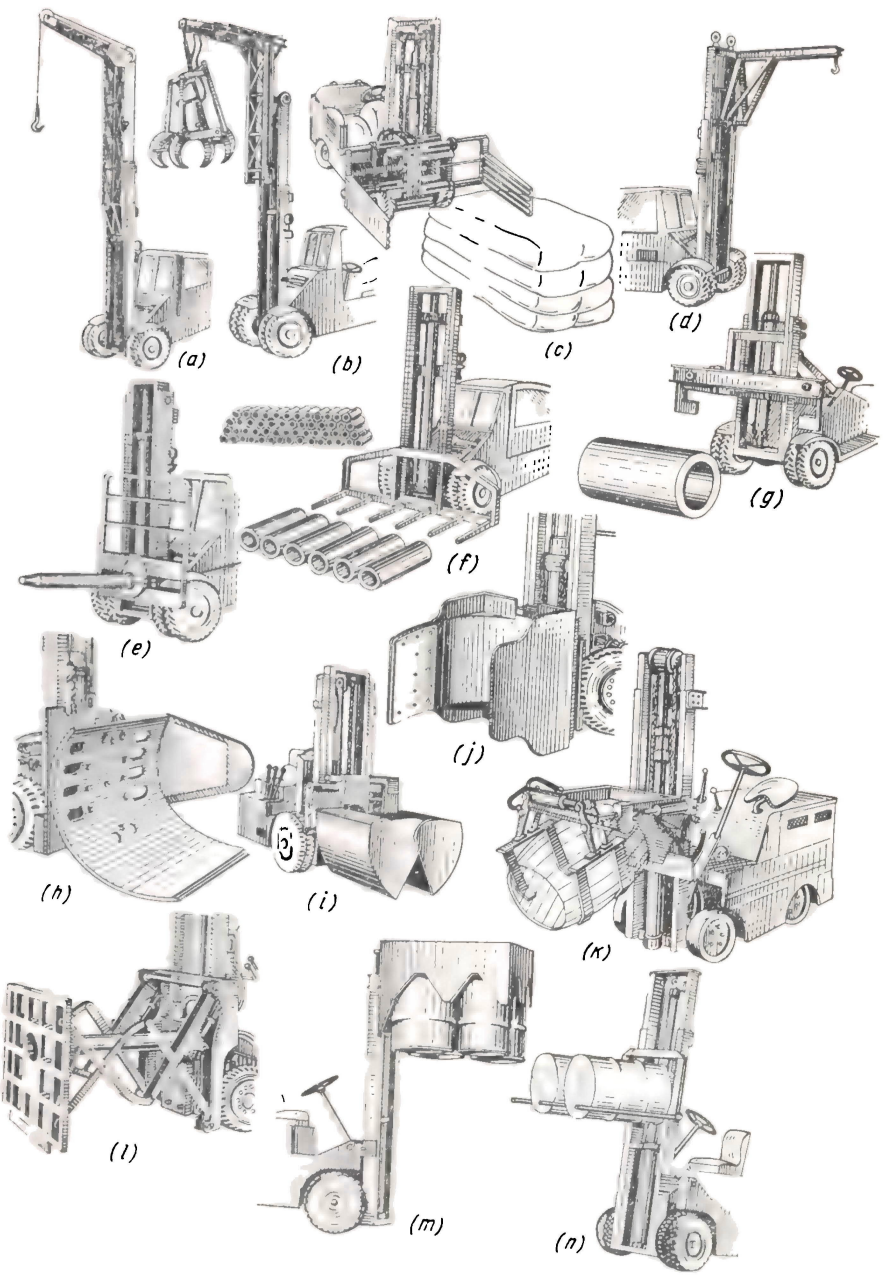

Fig. 266. Replaceable equipment

a—truck with boom, *b*—hydraulic log handler, *c*—hydraulic bale clamp, *d*—crane attachment, *e*—ram for handling hollow-centre loads (railway wheels, gears, automobile tyres), *f*—forks for small concrete and ceramic pipe, *g*—grip for large concrete pipe, *h*—grab for positioning rolls vertically, *i*—bulk load grab, *j*—clamp attachment for vertical rolls, *k*—barrel handler, *l*—universal load pusher

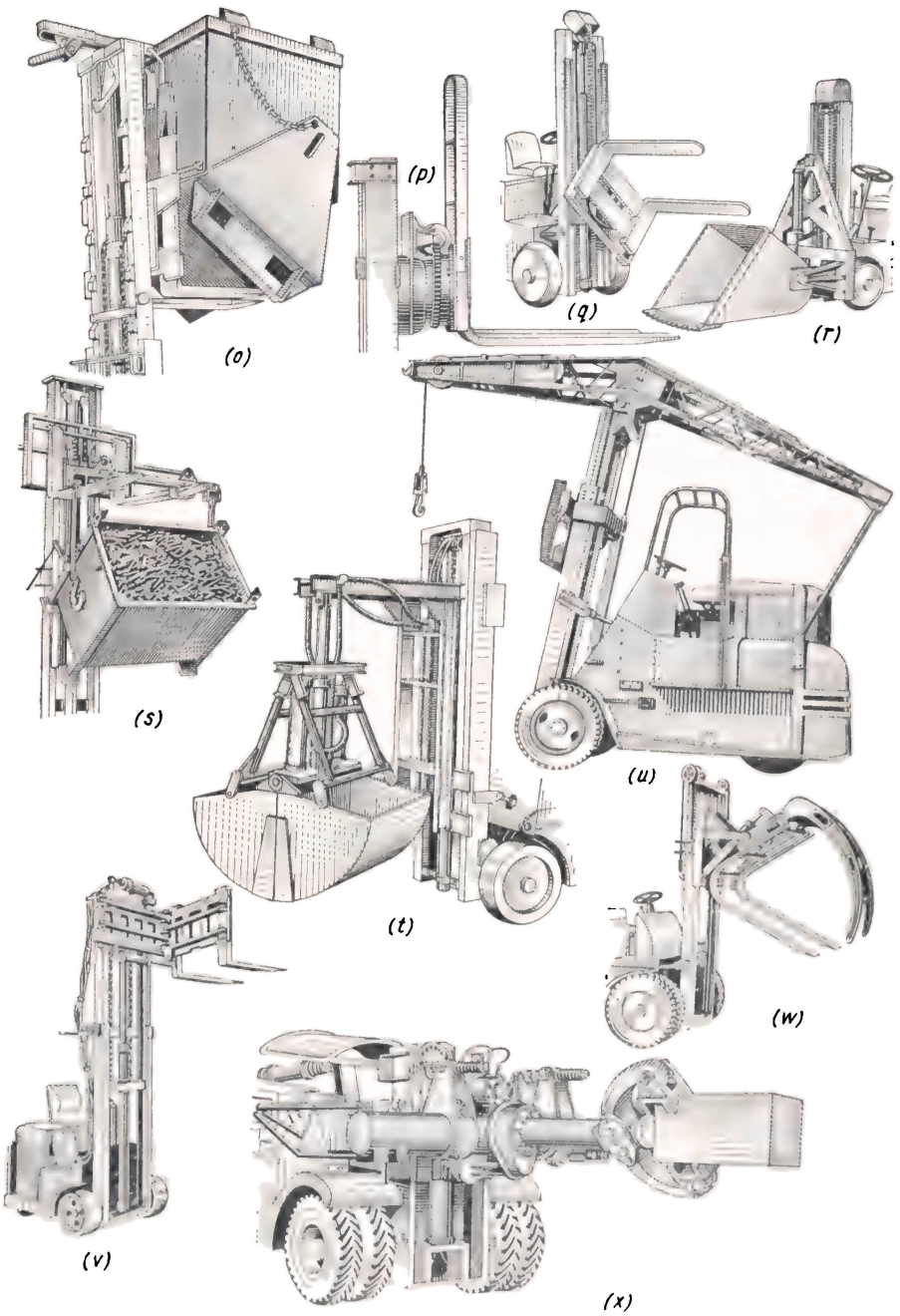

of forked stacker trucks

with a ram, *m*—four-drum carrier, *n*—horizontal drum handling device, *o*—self-dumping chip hopper, *p*—vertical turning mechanism, *q*—revolving forks, *r*—scoop attachment, *s*—gravity shovel, *t*—clamshell bucket, *u*—boom-mounted on the moving frame, *v*—high lift fork truck, *w*—grab for mining timber and logs, *x*—hydraulic clamps for hot billets

The capacity of stackers usually ranges from 250 to 1,000 kg with a lifting height of up to 5 metres.

A recent development are self-propelled stackers mounted either on universal power trucks (so-called electric, or motor trucks) or on special wheels utilising a number of standard automobile units and parts. Their capacity seldom exceeds 5 tons with an elevation of up to 5 metres.

Self-propelled stackers are manufactured with different handling devices which conform to the shape of the load being lifted.

Fig. 266 illustrates various modifications of forked stacker trucks.

APPENDIX

TYPICAL DESIGNS OF MATERIALS HANDLING EQUIPMENT

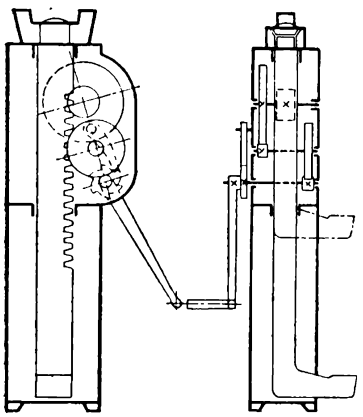

1. Rack-and-pinion jack

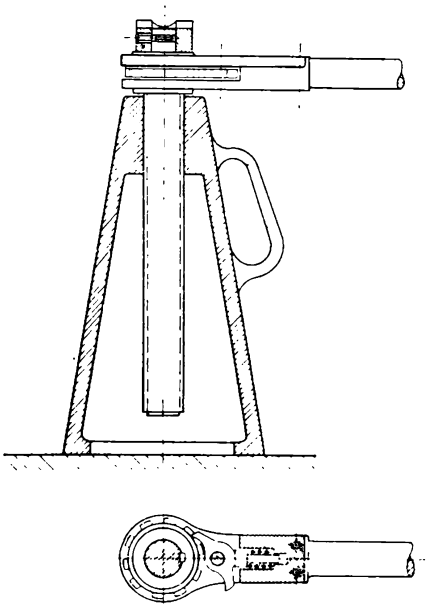

2. Screw jack

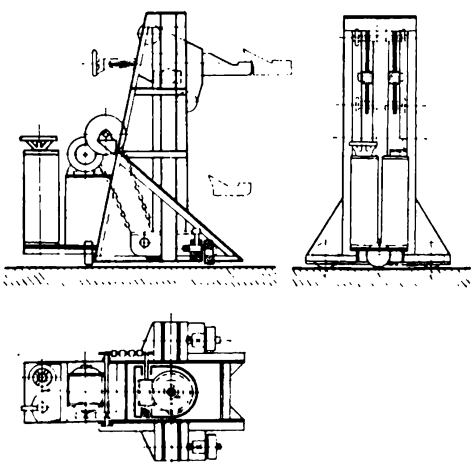

3. Travelling electric jack

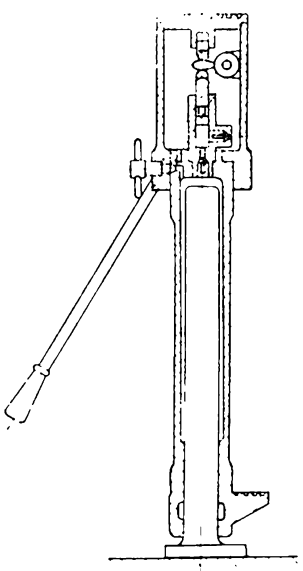

4 Lever jack

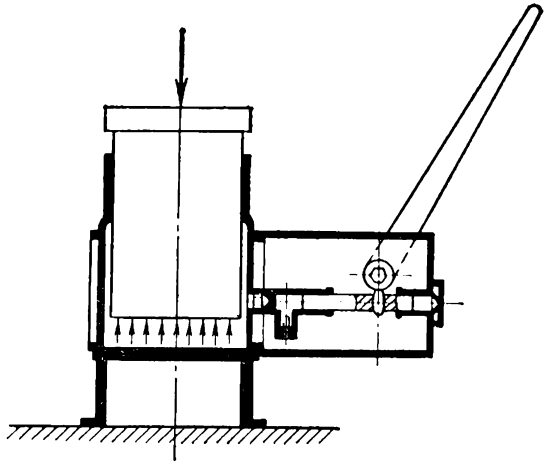

5. Hydraulic jack

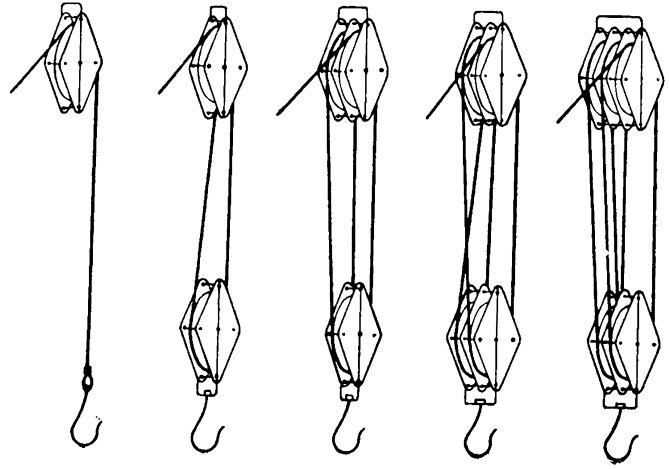

6. Rope pulleys

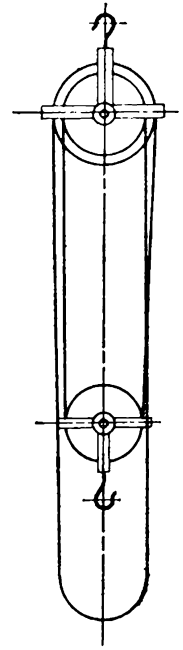

7. Differential chain pulley

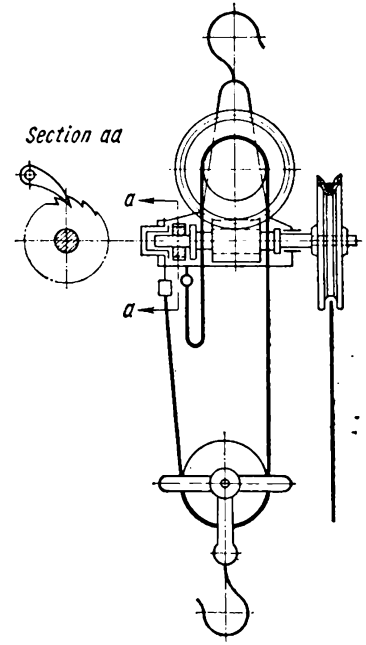

8. Portable worm-gar hand hoist

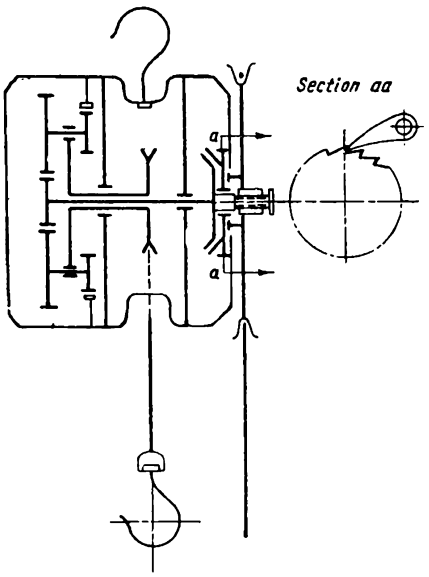

9. Portable spur-geared hand hoist

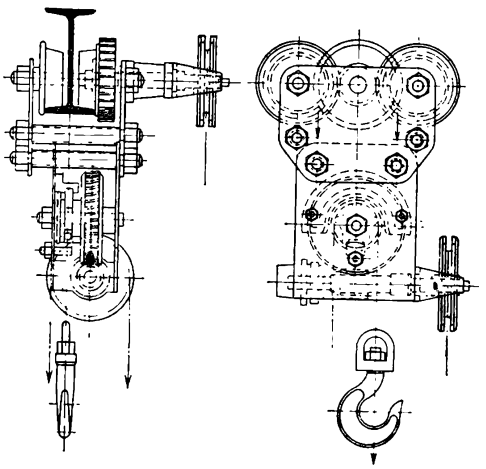

10. Hand worm-geared trolley hoist

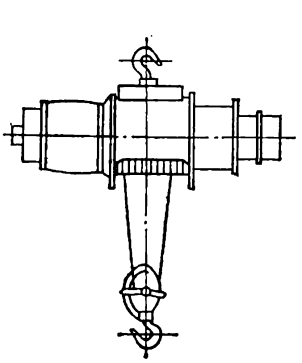

11. Portable power-operated hoist

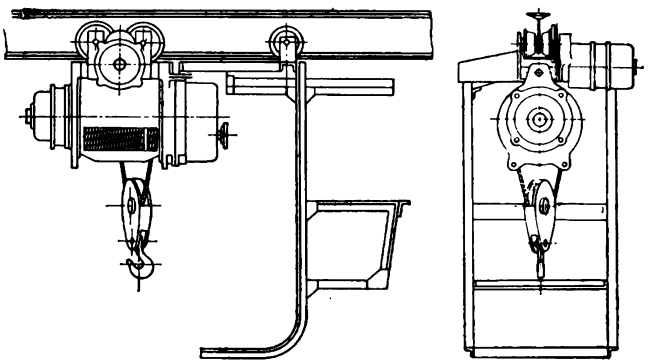

12. Travelling electric hoist

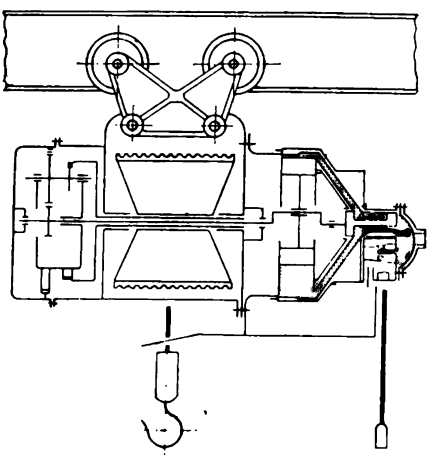

13. Travelling air-operated hoist

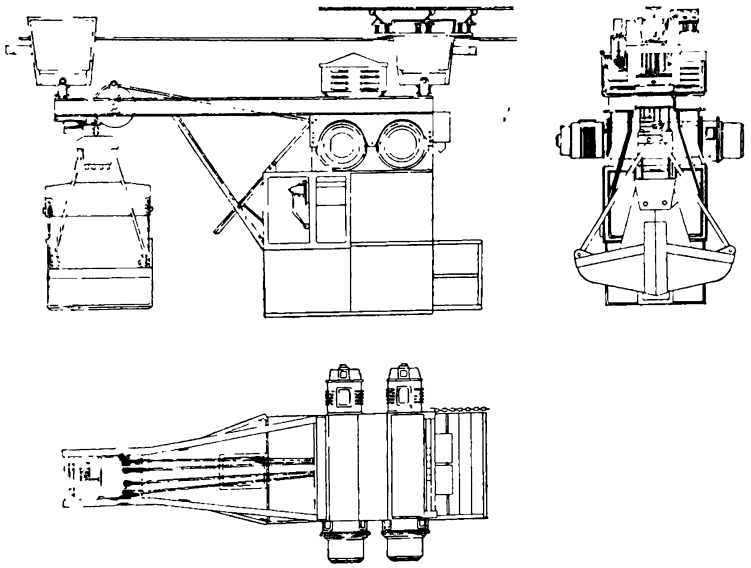

14. Monorail telpher

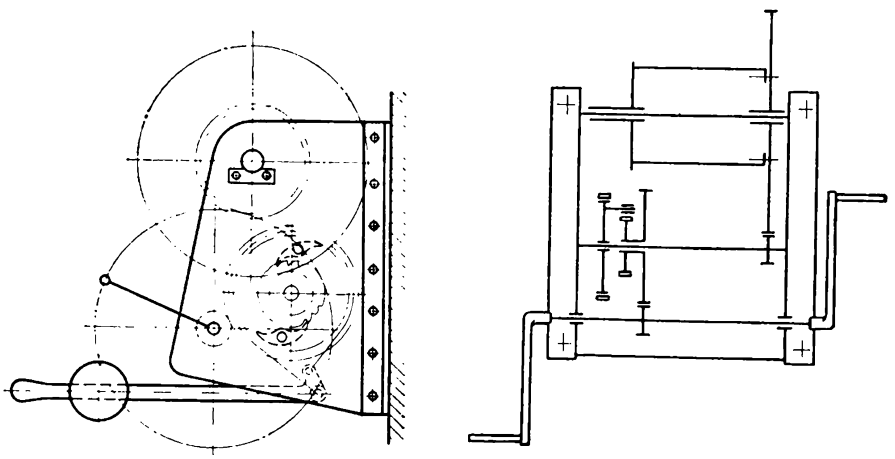

15. Wall-mounted hand winch

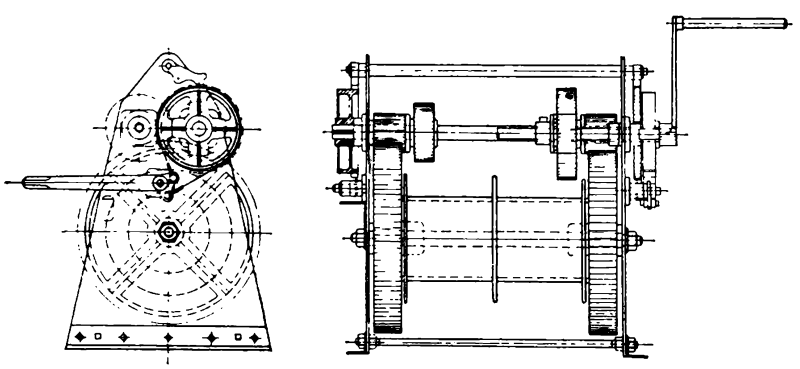

16. Double-drum hand winch

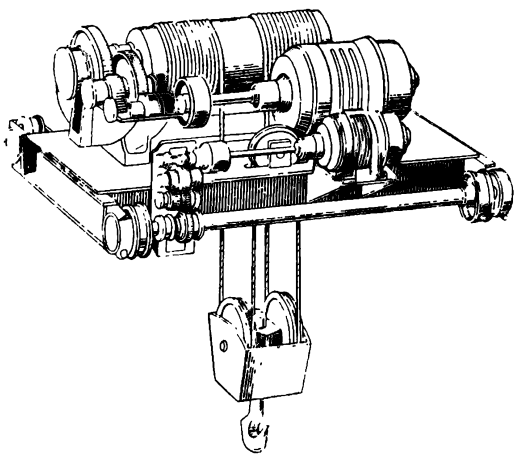

17. Crane trolley

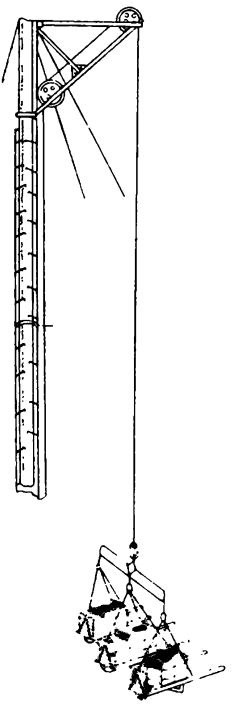

18. Guyed boom crane

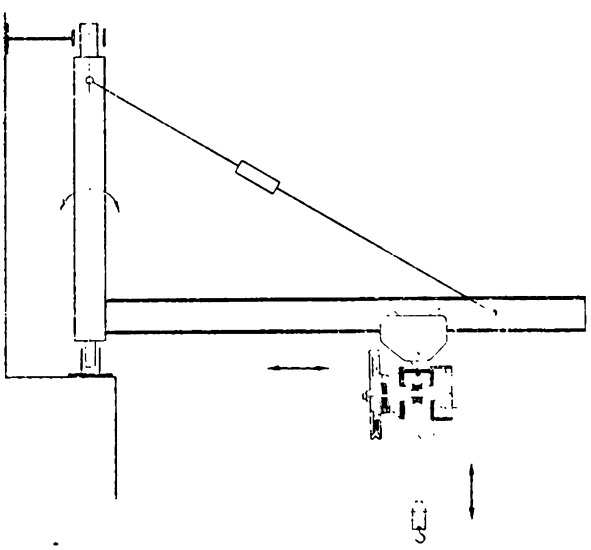

19. Wall jib crane

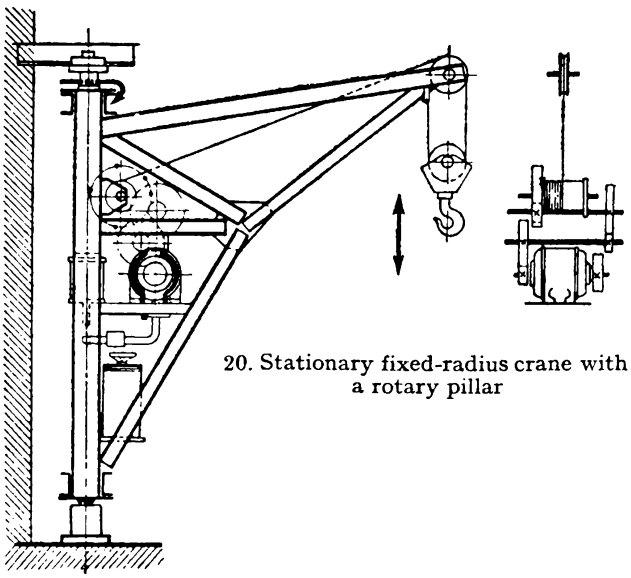

20. Stationary fixed-radius crane with a rotary pillar

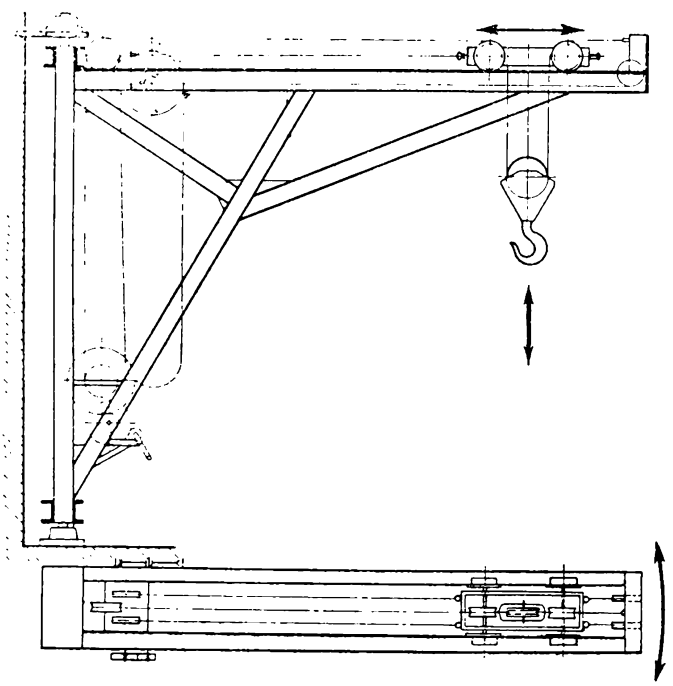

21. Stationary jib crane with a rotary pillar

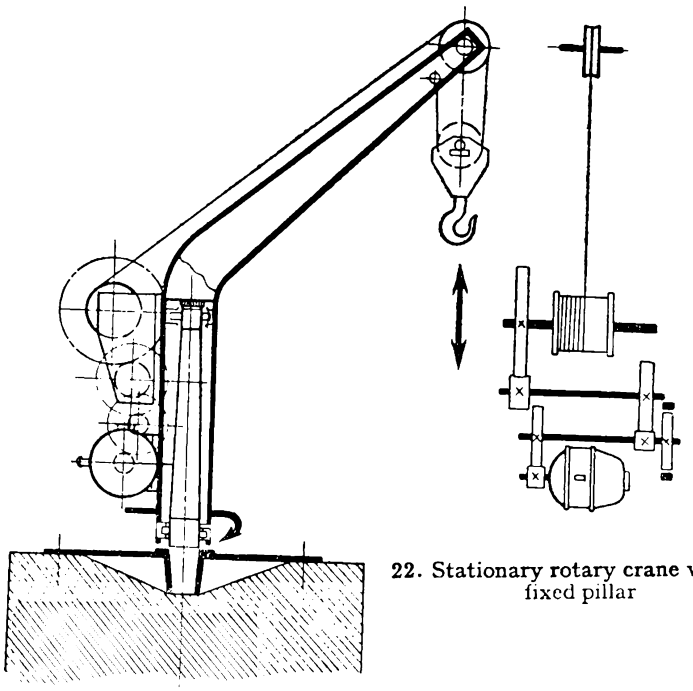

22. Stationary rotary crane with a fixed pillar

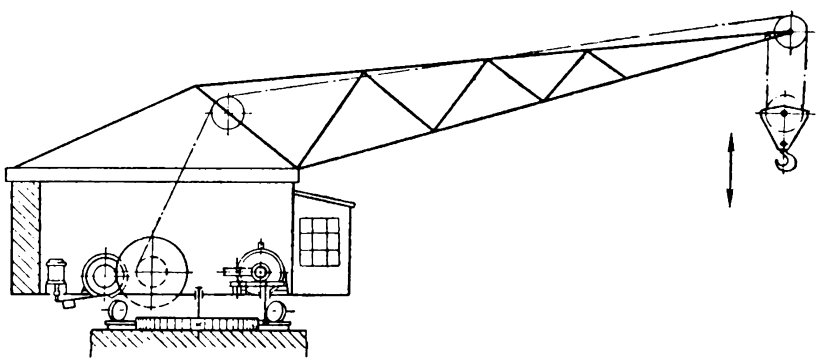

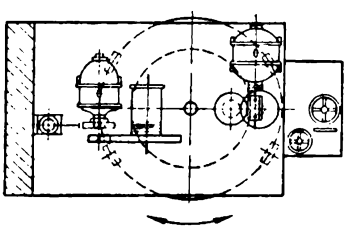

23. Stationary crane with a turntable

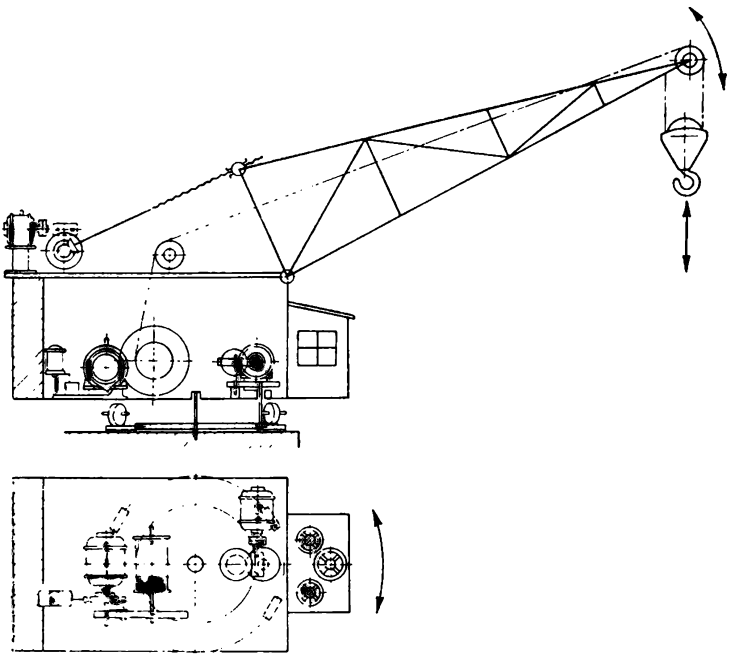

24. Stationary turntable crane with a luffing boom

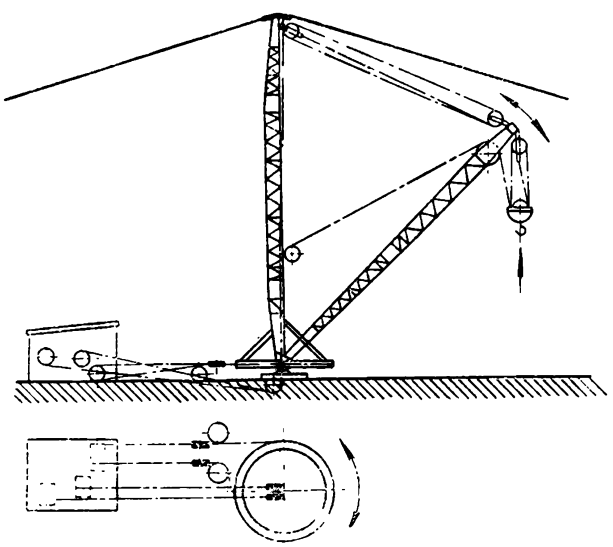

25. A-frame derrick

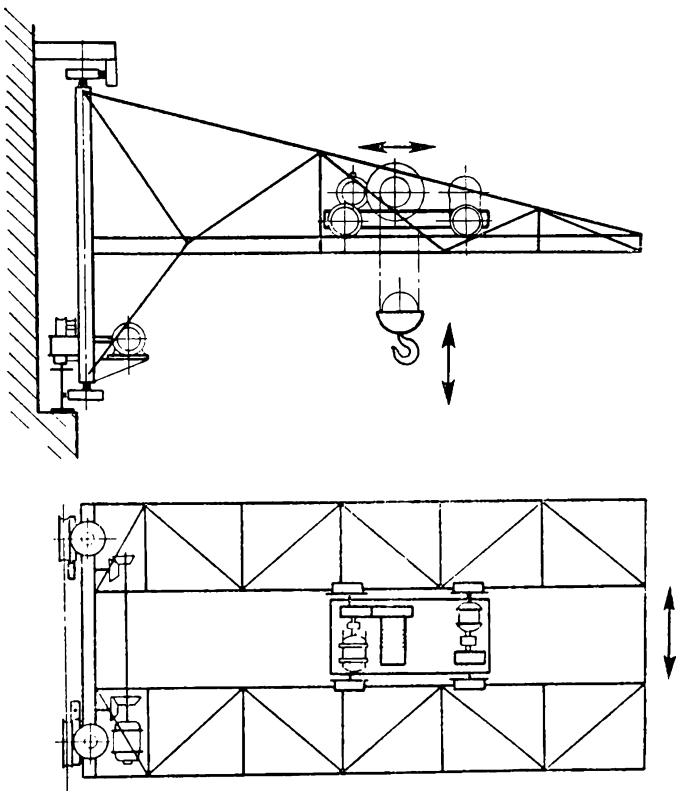

26. Cantilever jib crane

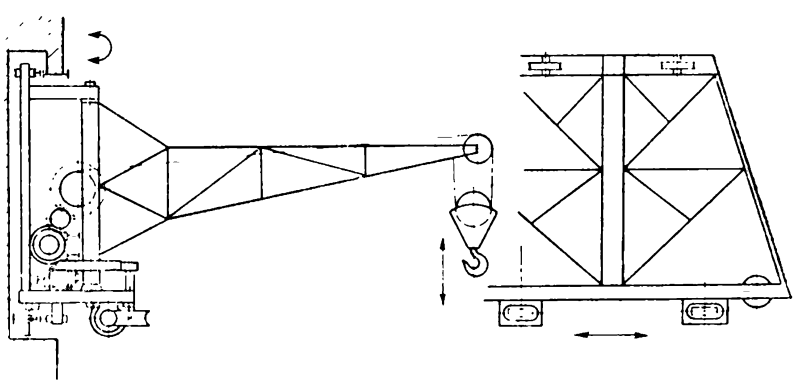

27. Cantilever crane with an upper rotary boom

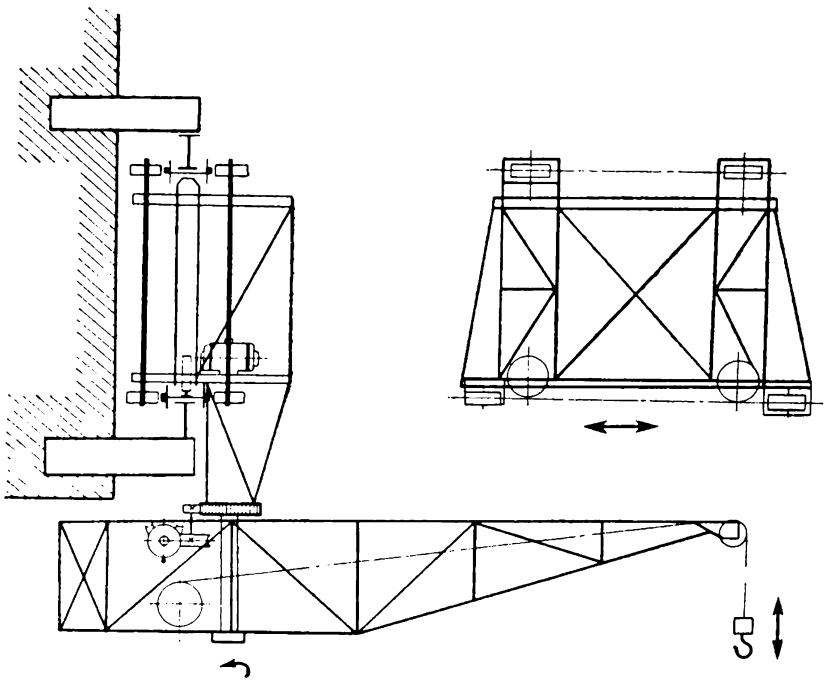

28. Cantilever crane with a lower rotary boom

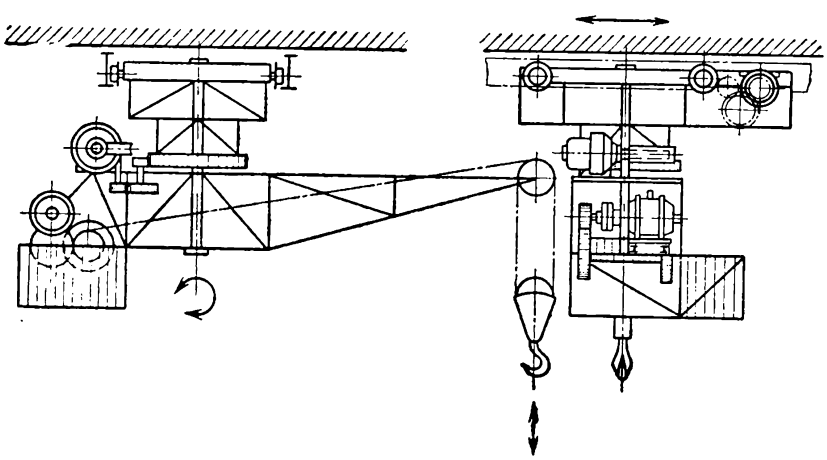

29. Ceiling-mounted crane

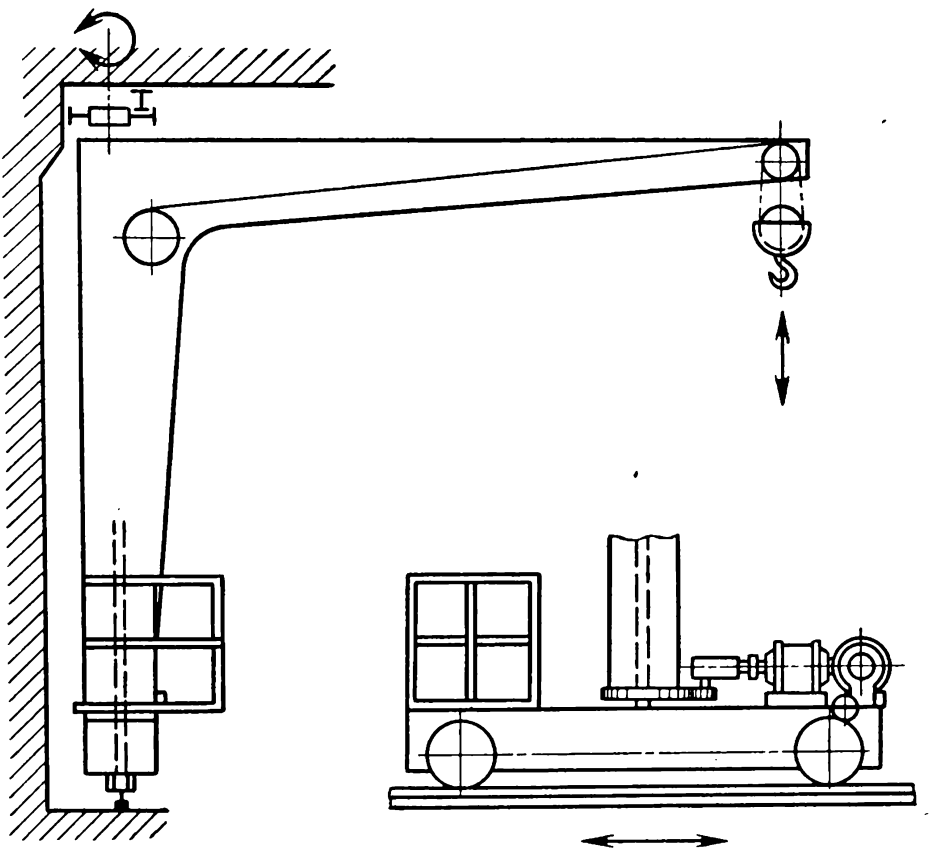

30. Monorail crane

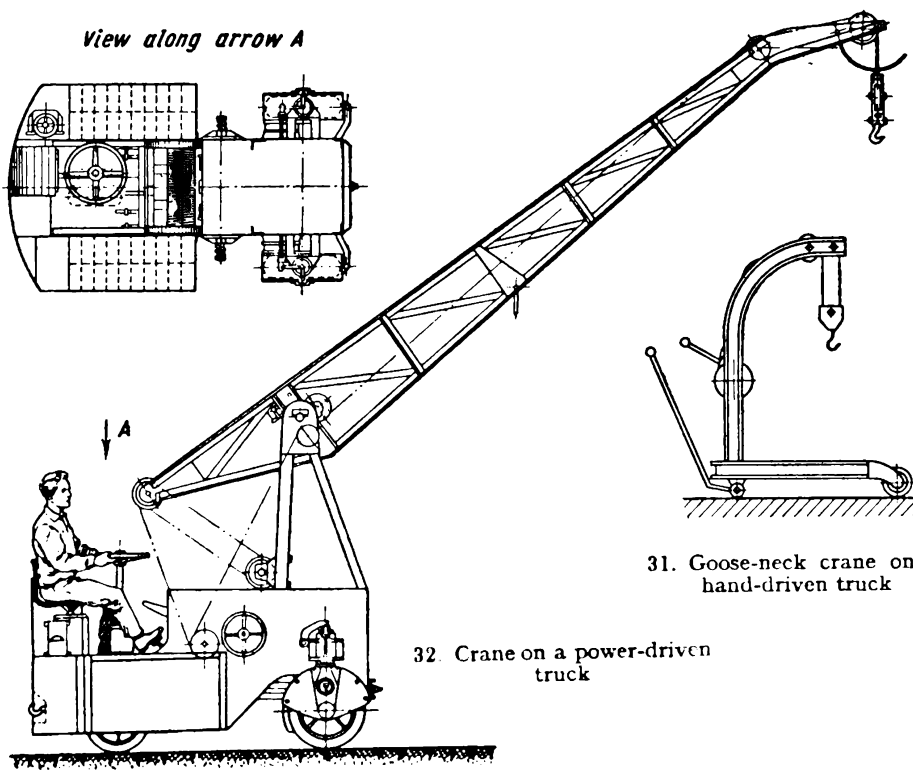

31. Goose-neck crane on a hand-driven truck

32. Crane on a power-driven truck

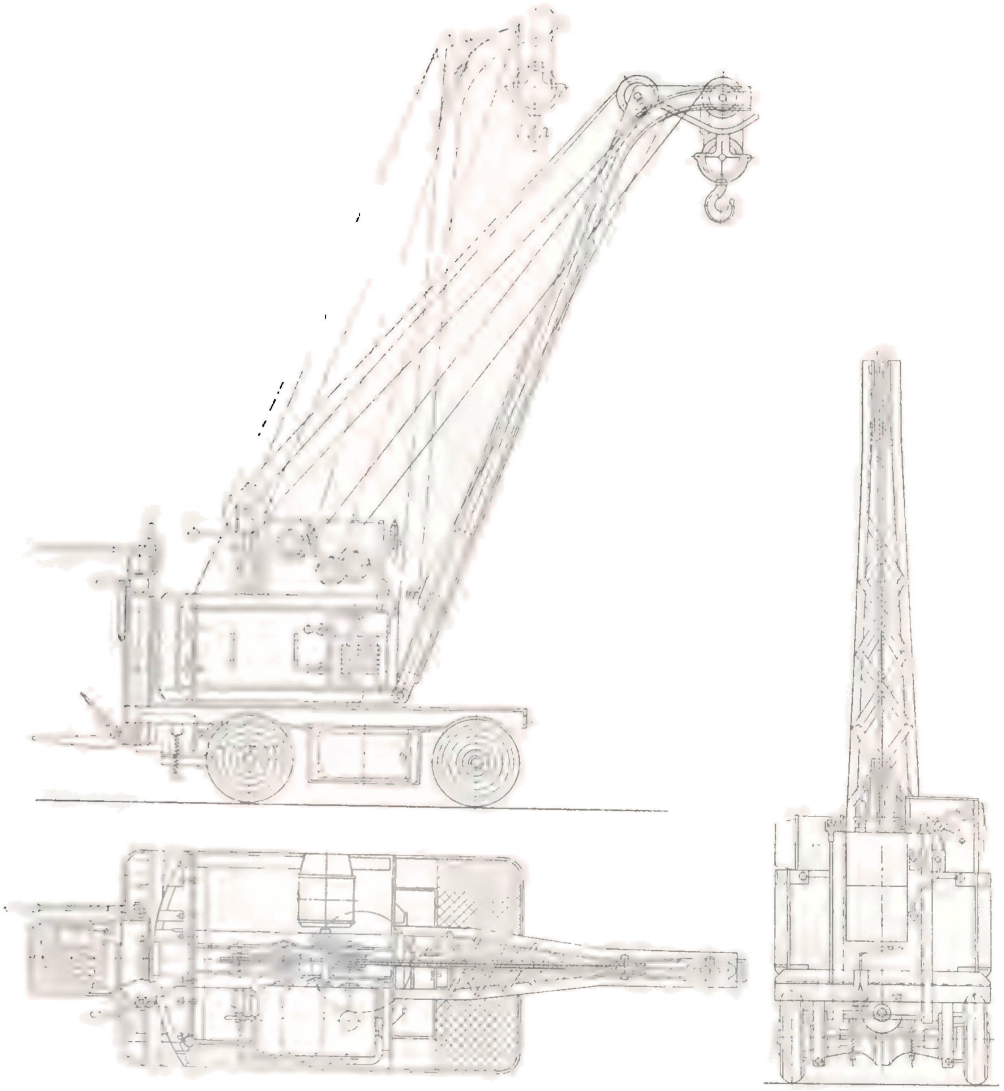

33. Crane on a universal power-driven truck

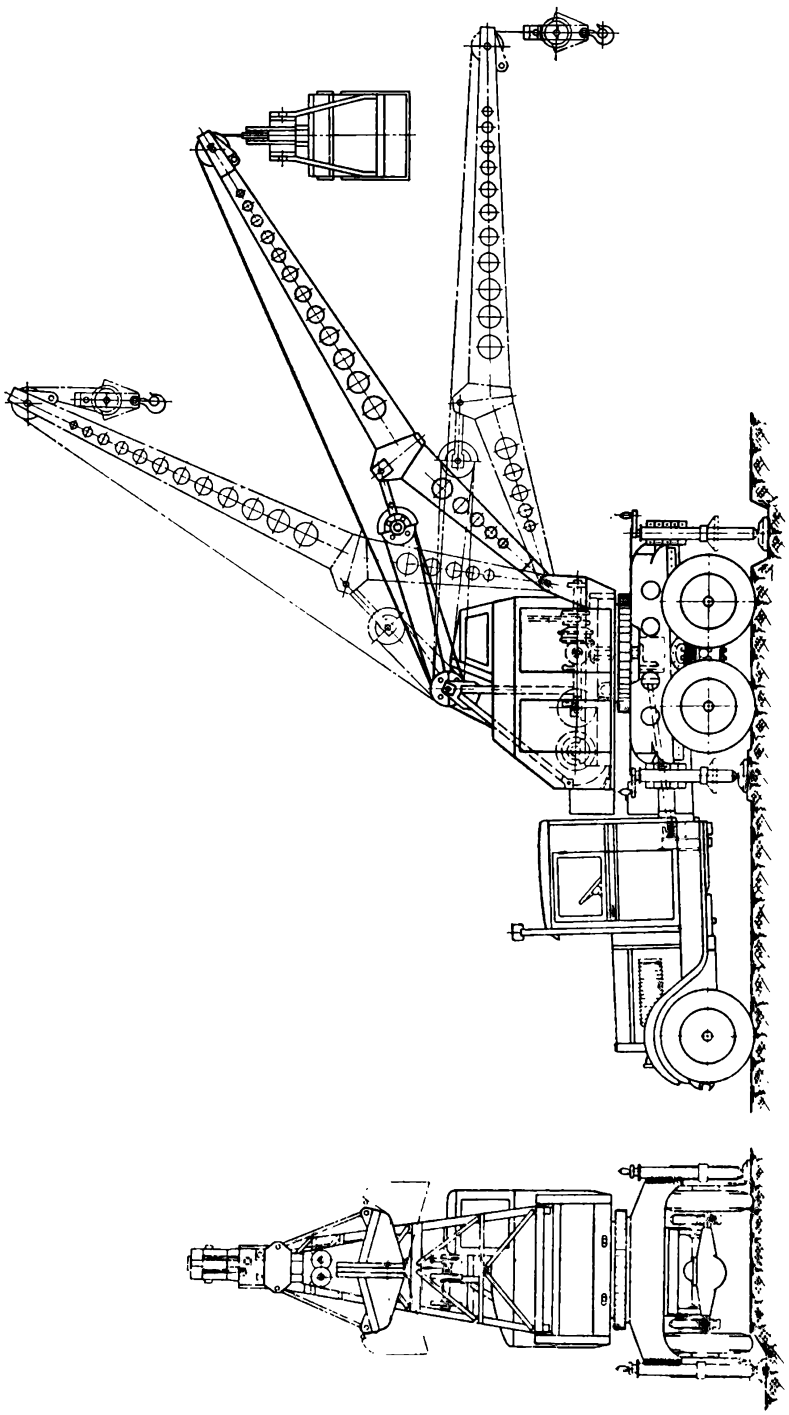

34. Truck-mounted crane

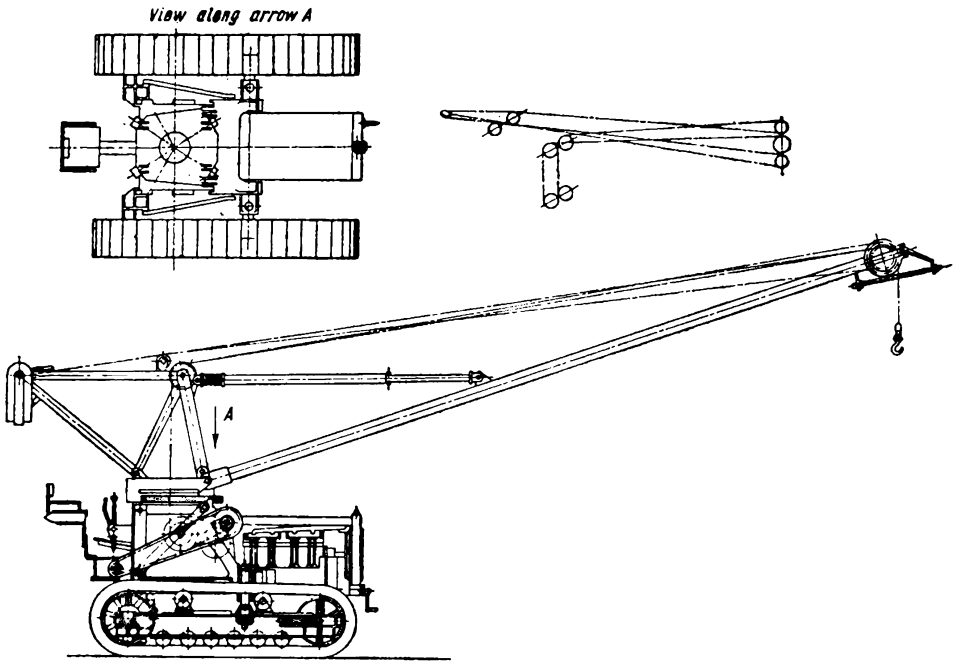

35. Tractor-mounted crane

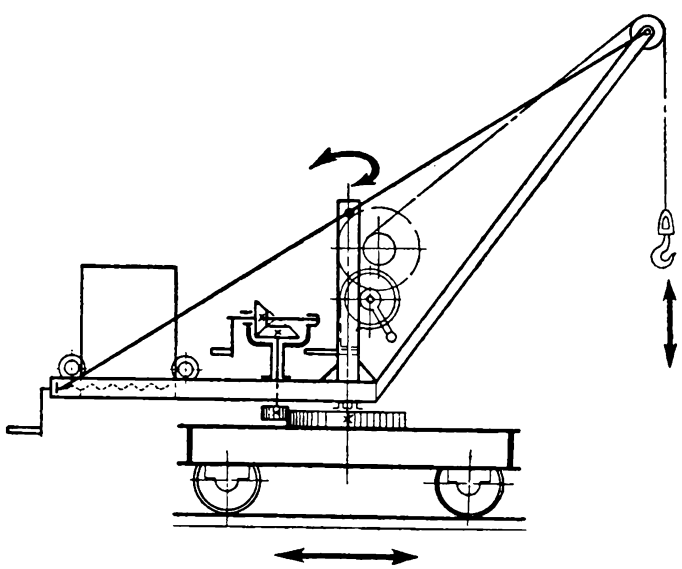

36. Hand-driven railway crane

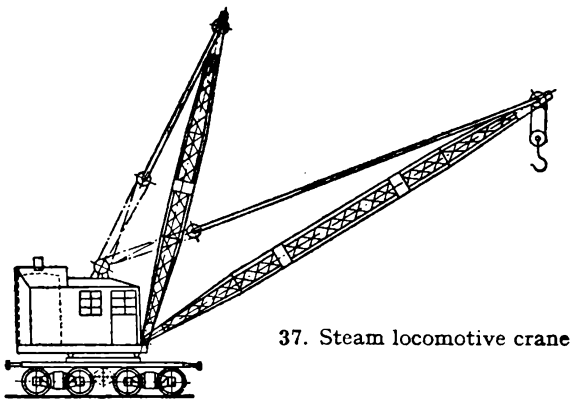

37. Steam locomotive crane

38. Crawler-mounted crane

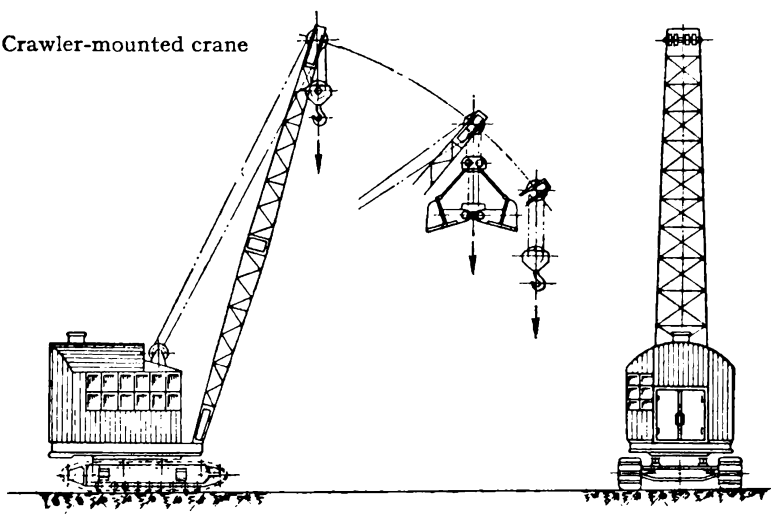

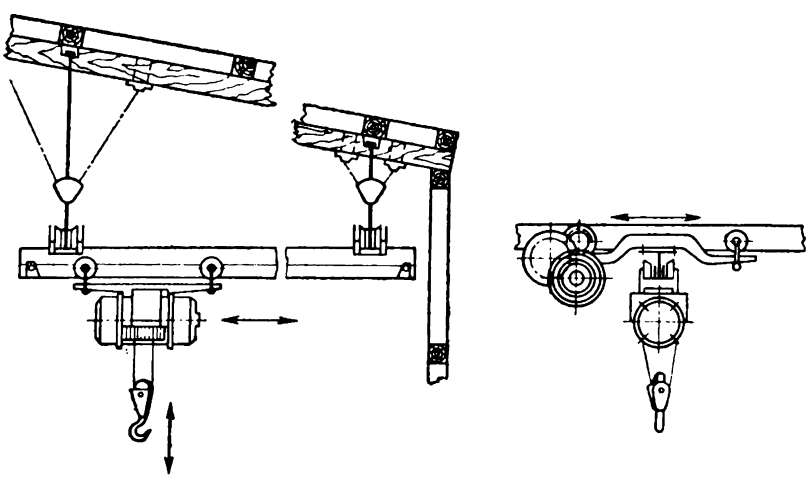

39. Girder crane

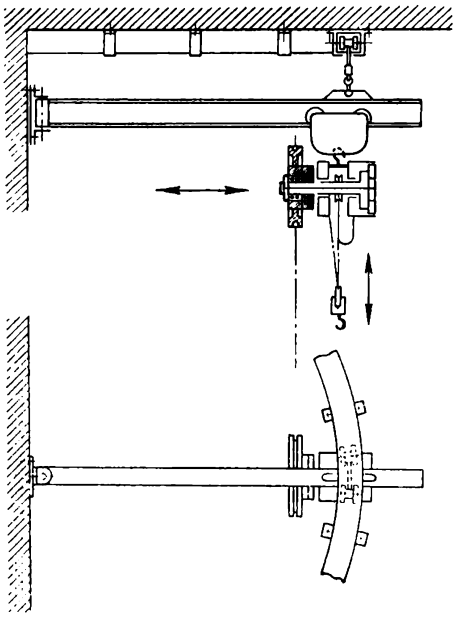

40. Rotary girder jib crane

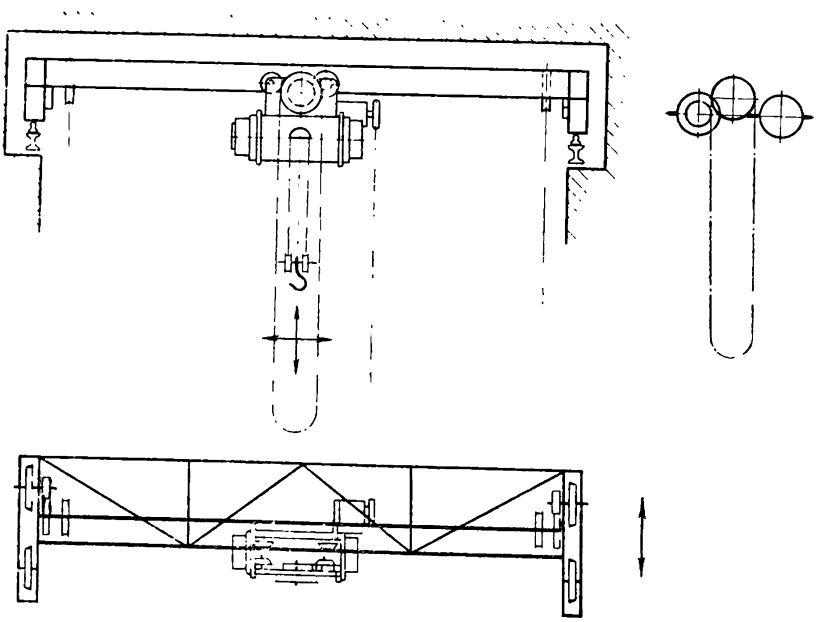

41. Single-girder overhead travelling crane

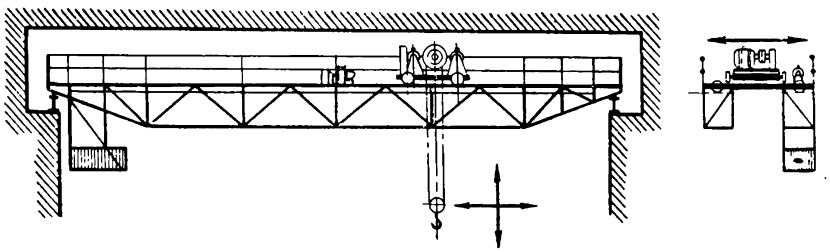

42. Double-girder overhead travelling crane with a top-running trolley

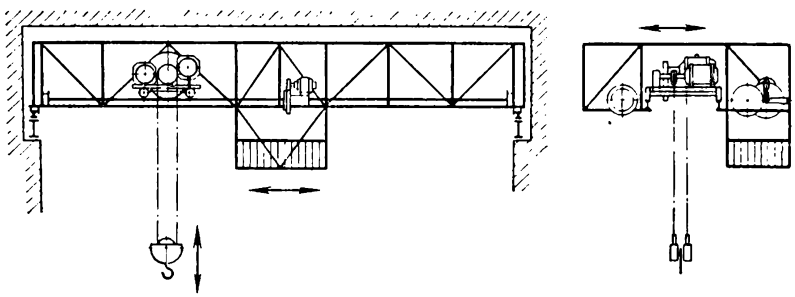

43. Double-girder overhead travelling crane with an underrunning trolley

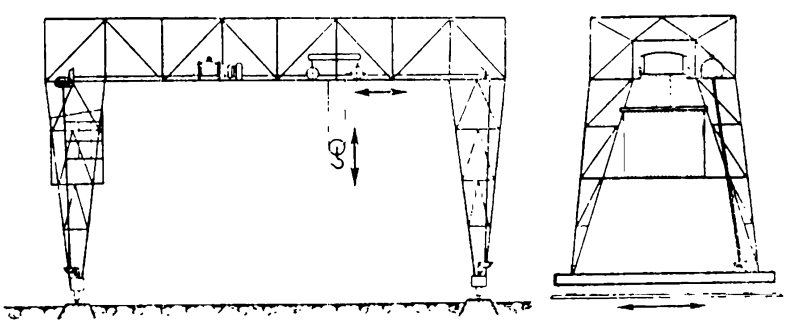

44. Gantry crane

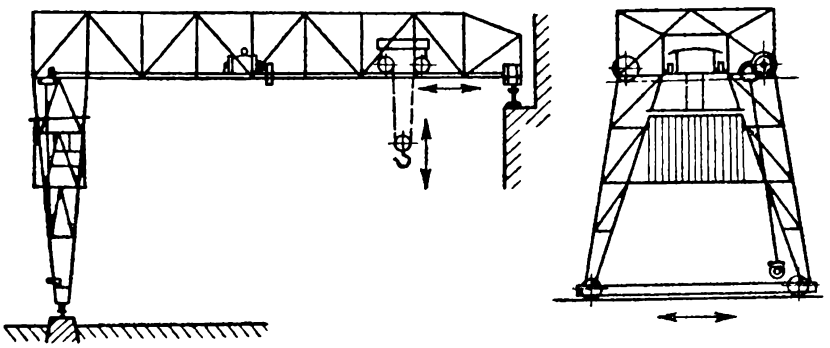

45. Semigantry crane

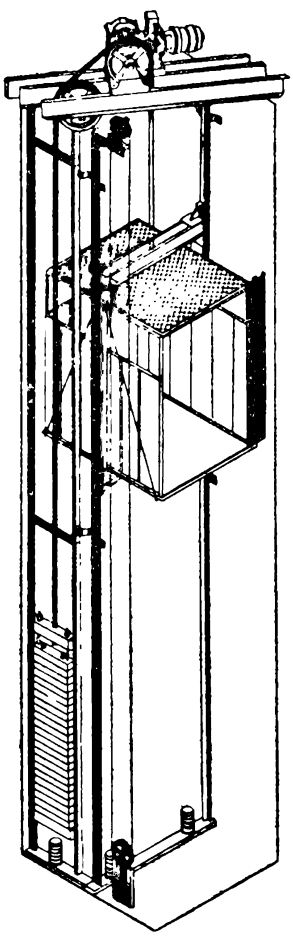

46. Elevator

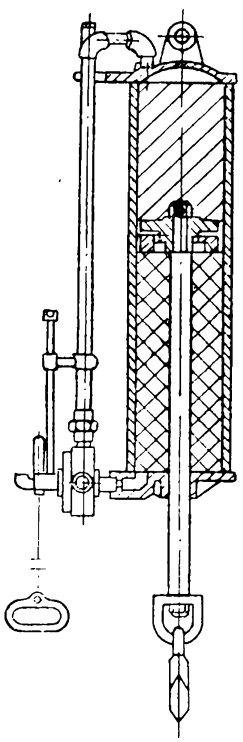

47. Portable air-operated hoist

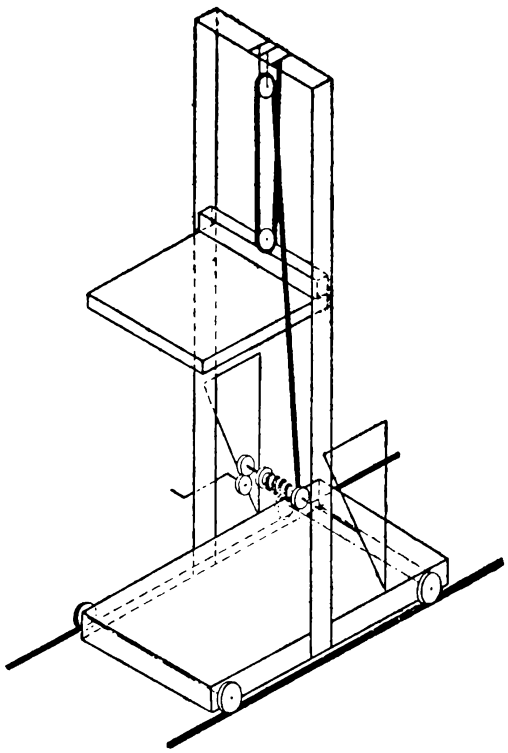

48. Manually-propelled stacker

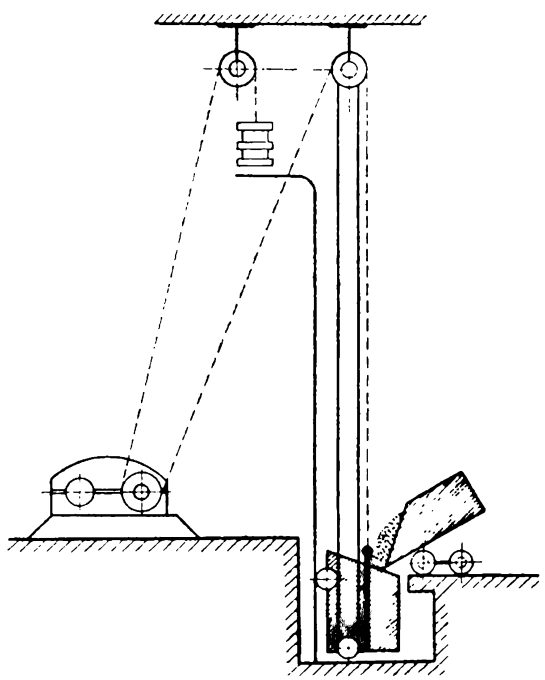

49. Vertical skip elevator

TO THE READAR

Peace Publishers would be glad to have your opinion of the translation and the design of the book.

Please send all suggestions to 2. Pervy Rizhsky Pereulok, Moscow, U.S.S.R.

Printed in the Union of Soviet Socialist Republics